In Silico Design and Biological Evaluation of Benzofused Polyamides Targeting G-Quadruplex DNA Structures

Rahman, A.k.m Azadur

Awarding institution:
King's College London

In Silico Design and Biological Evaluation of Benzofused Polyamides Targeting G-Quadruplex DNA Structures

A dissertation submitted in partial fulfilment of the requirements for the degree of

Doctor of Philosophy

A.K.M Azadur Rahman

Institute of Pharmaceutical Science

School of Biomedical Science

King's College London

Supervisors

Professor David E. Thurston

Dr Khondaker Miraz Rahman

June 2016

Dedicated to the quote

I know that I am intelligent,
Because I know that I know nothing

-Socrates

Plagiarism Statement

This thesis describes research work conducted in King's College London, University of London between 2012 and 2016 under the supervision of Professor David E. Thurston and Dr Khondaker Miraz Rahman. I declare that the research work done and described in this thesis is original and the parts of this work which have been conducted by other researchers are clearly mentioned. I also certify that I have written all the text herein and have supported this thesis with suitable citations which have already appeared in publications from different scientific journals.

Signature---------- Date----------

Acknowledgements

I would like to express my deep sense of gratitude to Professor David E. Thurston for his guidance in carrying out my research and for his support, compassion and encouragement which has helped me to overcome all the difficulties I have faced during the course of my thesis work.

I would like to express my profound thanks to Dr Khondaker Miraz Rahman for his day-to-day supervision, realistic and valuable suggestions and important direction towards completing my research work. I am sincerely grateful to him for his guidance in this field of research.

I am grateful to Dr Paul J M Jackson for his continuous support and suggestions regarding this project. I would also like to express my gratitude to him along with Mr. Meir Toui Tou for carrying out molecular modelling studies.

I am indebted and thankful to Amrit Varsha (visiting researcher) for her kind help in carrying out the biological evaluation of the synthesized molecules.

I am highly grateful to Kazi Sharmin Nahar, Simon.J. Teague, Rashedul Islam, Mohammad Kaisarul Islam, Nicolas Veillard, George Procopiou, Fabrizio Minicone, Julia Mantaj, Mark Laws, David Corcoran, Pietro Picconi, Sandra Luengo Arratta, Ilona Pysz, Louise Soh, Jennifer Auer, Paolo Andriollo, Christopher Chamberlain and Emad Sadeghian.

I would like to thank Dr. Sukhvinder Bansal for his valuable guidelines in designing this project as my postgraduate co-ordinator.

I would like to express special gratitude to the funding agency The Ministry of Science and ICT, Government of People's Republic of Bangladesh.

I acknowledge all my memories of my father Abdul Latif Akanda; they make me happy even when I am facing difficulties.

Finally, I would like to thank my family memebers, especially my wife Umme Salma Jannatul Ferdous Lina who felt the burden of supporting me whilst carrying out my project. I offer my love to my son AKM Zahid bin Azad Kathak, my little daughter Onugga Azad Nritto and my mother Rojina Akhter. They were always there to encourage me when I was facing hard times.

Important Abbreviations

A-T	Adenine-Thymine
bp	Base Pairs
CD	Circular Dichroism
C-G	Cytosine-Guanine
cDNA	Complementary DNA
COSY	Correlation Spectroscopy
d	Doublet
DCM	Dichloromethane
dd	Double of doublets
DIC	1,3-Diisopropylcarbodiimide
DMF	*N, N´*-Di-methyl formamide
DMSO	Dimethyl Sulfoxide
DNA	Deoxyribonucleic acid
DS	Double Stranded
dt	Doublet of triplets
ΔTm	Increment in melting temperature
EDTA	Ethylene diamine tetra acetic acid
EI-MS	Electrospray Ionization Mass Spectrometry
EtoAc	Ethyl Acetate
FAM	6-carboxyfluorescein
FID	Fluorescent Intercalator displacement
FRET	Fluorescence Resonance Energy Transfer
HOBt	1-Hydroxybenzotriazole
HPLC/MS	High performance Liquid Chromatography/Mass Spectrometry
HRMS	High Resolution Mass Spectroscopy
hTERT	Human Telomerase Reverse Transcriptase
HT	Human Telomere
IC_{50}	Half maximal inhibitory concentration
IR	Infra-red
Im	Imidazole
kDA	Kilo Dalton
kbp	Kilo base pairs
LCMS	Liquid Chromatography Mass Spectrometry
MD	Molecular Dynamics
MeCN	Acetonitrile
MeOH	Methanol
µL	Micro litre
µm	Micro meter
µM	Micro molar
MS	Mass Spectrometry
mRNA	Messenger RNA
MW	Molecular Weight
NADPH	Nicotinamide Adenine Dinucleotide Phosphate
NCI	National Institute of Cancer.
NH3-MeOH	2M Ammonia (NH3) in MeOH

NMR	Nuclear Magnetic Resonance
NSE	Nuclear Sensitive Element
Pd	Palladium
POT1	Protection of Telomeres-1
RNA	Ribonucleic acid
RT	Room Temperature
TERT	Telomerase Reverse Transcriptase
TGF-β	Transforming Growth Factor Beta
TLC	Thin Layer Chromatography
Tm	Melting Temperature
UV	Ultraviolet

Abstract

Guanine-rich nucleic acids can fold into distinctive four-stranded G-quadruplex structures which are found in telomeric DNA repeats as well as in sequences in the promoter and other regulatory regions of genes, especially those involved in cellular proliferation. Small molecules that can selectively bind and stabilize the G-quadruplex structure have become of significant interest to researchers, and are gaining momentum as a possible new class of anticancer agents.

This project was based on a previously reported series of novel biaryl polyamides with significant selectively toward G-quadruplexes compared to duplex DNA, and with modest selectivity between different quadruplex types. Using a distamycin scaffold as a starting point, biaryl building blocks were introduced in place of pyrroles to switch preference from duplex to quadruplex DNA. This alteration in shape ensured that the molecules had low affinity for duplex DNA while increasing their interaction with a G-quadruplex structure since the ligands have similar 3D structures. The main aim of this project was to modify the structure of the previously reported biaryl polyamides (with the help of a molecular modelling based approach) through the incorporation of benzofused building blocks to improve their affinity for G-quadruplexes, while further reducing their affinity for duplex DNA, thereby enhancing their selectivity for quadruplex DNA.

A small, focused benzofused-polyamide library (18 molecules) was initially synthesized and evaluated for the ability of members to stabilize G-quadruplex structures using a FRET-based DNA thermal denaturation assay and molecular dynamics (MD) simulations. However, these compounds failed to stabilize the F21T (human telomeric G-quadruplex), c-Kit quadruplexes and Bcl-2 quadruplexes, and MD simulations suggested that the shape of the molecules required further modification to facilitate quadruplex interaction. A second library of molecules (43 in total) was then designed and synthesized using a molecular modelling-based approach. In this series, the shape of the polyamide fragment was changed, while retaining the original scaffold, by introducing benzofused moieties with 3,5-substitutions. Evaluation of these molecules in the same FRET assay showed a notable increase in stabilization of the F21T quadruplex for many library members. For example, compounds **4.93** and **4.71** stabilized

the quadruplex by 15°C and 17°C, respectively (at 1 μM concentration), while showing insignificant affinity for duplex DNA. Moreover a third set of benzofused polyamides (9 in total) has been synthesized by the addition of two consecutive benzofused moieties instead of three consecutive benzofused moieties for the ideal length of G-quadruplex DNA targeting ligand molecules. These molecules were also evaluated by the same FRET-based DNA thermal denaturation assay. The overall data showed that benzofused polyamides made of three consecutive benzofused moieties had a specific curvature which improved their G-quadruplex interacting capacities compared to those with two consecutive benzofused moieties.

Cytotoxicity studies were undertaken on MDA-MB-231 and HeLa cell lines and some library members are active at the low micromolar level. Molecule **4.45** has emerged as a lead compound, possessing a cytotoxicity of 40nM in MDA-MB-231.

Given their low molecular weight (between 422-646 Daltons), reasonable water solubility and good cellular penetration properties compared to other known G-quadruplex inhibitors which are mostly non-drug-like, molecules of this type have the potential to be developed into both reagents that can probe DNA structure and into novel quadruplex-targeting therapeutic agents.

Contents

List of Figures

List of Figures

Chapter 2

List of Figures

Chapter 3

List of Figure

Chapter 4

List of Table

Chapter 1

List of Table

Chapter 2

List of Table

Chapter 3

List of Table

Chapter 4

Chapter 1: Introduction

1.1 Cancer

Cancer is a term that applies to a group of multiple diseases. It is a malignant disease caused by alteration of normal cells due to genetic mutations. These genetic mutations may either be inherited or be originated by inaccurate DNA replication and chromosomal division or by various physiological, chemical and environmental factors. These permanent aberrations, either in a single DNA base or in a chromosomal fragment, ultimately lead to the divergent functions of a gene. Thus cells lose control of their proliferation, resulting in abnormal growth. This uncontrolled growth is likely to localise at the early stage of cancer. As cell division continues, the cellular mass is no longer fixed in its origin, but rather forms tumours which occupy neighbouring cellular spaces and share nutrients to make new blood vessels from pre-existing vessels through the process of angiogenesis. They invade nearby parts of the body [1] and also start to spread throughout the body through the lymphatic and cardiovascular pathways, and can eventually prove fatal **(Figure-1.1)**.

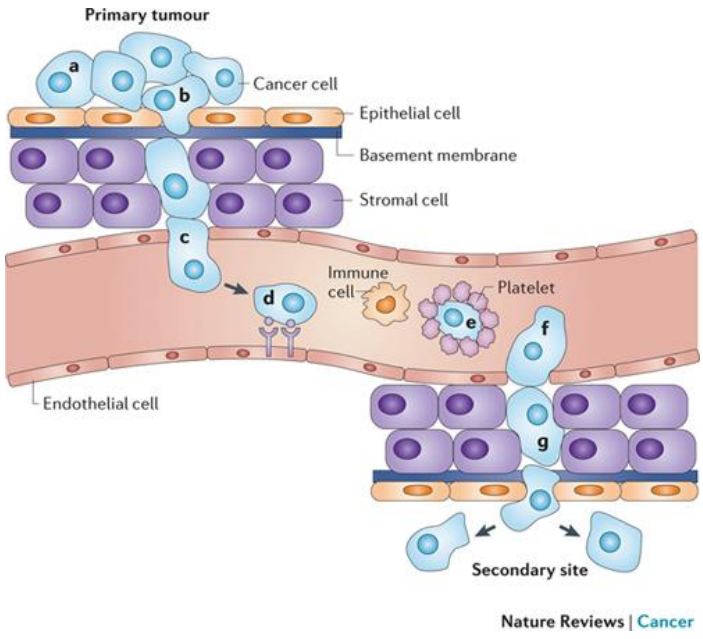

Figure 1.1: Diagram representing the growth and spread of cancer cells. Malignant cells spread away from their origin to the secondary site through the blood and lymph system. [taken from Schroeder A, Heller DA, Winslow MM, Dahlman and JE, Pratt GW. Nat. Rev. Cancer. 12(2012):39-50] [2].

Indeed, almost 90 percent of cancer-related deaths are due to the tumour spreading to secondary sites by a process called metastasis [3]. Cancers are named mostly according to their origins including the types of cells and organs from where they start to get malignant phenotypes.

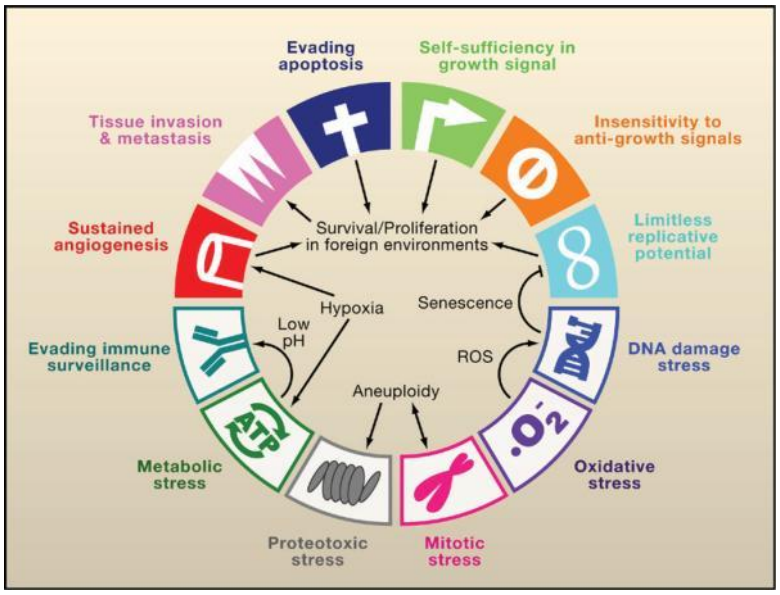

Figure 1.2: The illustration of the classical hallmarks of cancer cells: autonomous cell proliferatin, escaping from apoptosis, angiogenesis, metastasis etc. In fact these are the major distinguishing characteristics of malignant cells from normal cells. [taken from Dey I, Rath PC. BBRC. 327(2005):276-86] **[4].**

Malignant cells usually have some distinguishing characteristics, familiar as the phenotypic hallmarks of cancers **(Figure-1.2)**. These mainly include autonomous replication and proliferation, restriction to cytostatic and apoptotic signal, induction of neighbouring tissue invasion, metastasis and angiogenesis [4].

1.1.1 Treatment of Cancer

There are many therapies including surgery, chemotherapy, radiation treatment, stem cell transplant and targeted therapy developed to fight cancer, but it is hard to get rid of completely. For example, surgery and chemotherapy are not capable of abolishing all of the cancerous cells and these are potentially harmful to normal cells as well. In addition, cancer cells can continue their proliferation if even a few of them remain in the area of origin and some of them may gain resistance to cytotoxic agents and thereby escape apoptosis [5]. Thus in most

cases, therapies help to prolong the life expectancy of a cancer patient rather than (instead of) acting as a total cure. An effective medication can be rationalized by considering early accurate diagnosis and choosing an appropriate therapy. Indeed, current research places the emphasis on cell biology, genetics and biotechnology to understand the molecular mechanisms involved in tumorigenesis. However, it is necessary to take the advances in distinguishing the characteristics of cancer cells from normal cells and to know the genetic changes happening in cancer in order to develop a fruitful strategy for anticancer therapeutics.

1.1.2 Cancer Chemotherapy

Chemotherapy began to be used as a cancer therapy in the early stages of the 20th century. The idea came from World War 2; the naval forces that were exposed to nitrogen mustard surprisingly developed reduced white blood cell counts. However, chemotherapy is one of the most preferable treatments to tackle any type of cancer. Recently a significant number of chemotherapeutic agents have been screened out based on their cytotoxic efficacy. They can be prescribed alone or be combined with other therapies like radiation, surgery, hormone or immune therapies to make them more effective than a single agent. They kill the cancer cells by either arresting cell division or through DNA/RNA damage so that cells can't divide anymore and ultimately die. They are of different types due to their modes of action and target sites. For example, methotrexate and vinca alkaloids kill the cells belonging to a particular part of the cell cycle; on the other hand, platinum derivatives are non-specific and have a cytotoxic effect in both proliferating and resting phases. However, chemotherapy is limited in its action. It mainly targets the fast growing cells, thus chemotherapeutics don't have enough of an effect on cancer cells of resting phase and restraint to play any positive role on tumour progression and metastasis. In addition, they may kill normal cells as well. It is better to adjust the chemotherapeutic dose to minimise this harmful effect on normal cells and side effects like bone marrow suppression, alopecia, mucositis, nausea and vomiting [6].

A better understating of gene and protein expression patterns is supposed to help to identify the cancer-specific targets like enzymes, receptors or specific molecular targets expressed abnormally in cancer cells compared to normal cells.

1.1.3 DNA as a Molecular Target in Cancer Therapeutics

Mutated or damaged DNA is usually repaired by the normal cellular machinery. If a cell fails to repair a genetic abnormality, it results in cellular death through apoptosis or programmed cell death. In a malignant neoplasm, the damaged DNA remains unrepaired in the cancer cell, and the cell doesn't die but instead proliferates further to generate new cells with the same faulty DNA as the first one. DNA and the processes concerning it have long been considered to be targets for cancer chemotherapeutics.

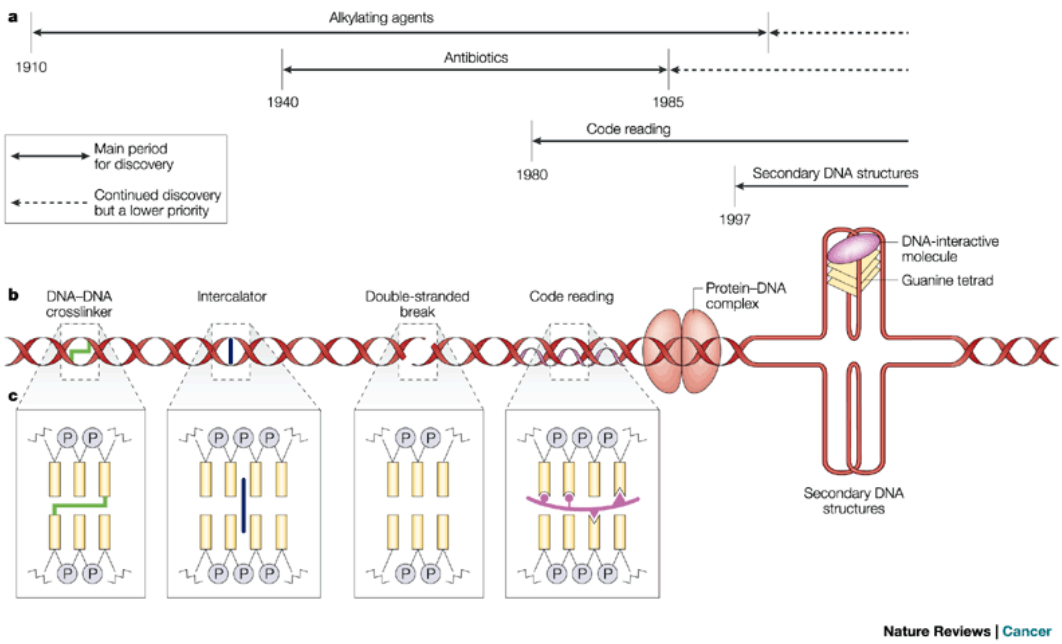

Figure-1.3: (a) Represents the periodic road map for discovery and research of chemical drugs (i.e. DNA interacting agents) like alkylating agent, targeting DNA molecules.

(b) Shows the various conformational modifications within DNA molecules due to the interaction of ligand molecules including crosslinking, intercalating and double strand breaking agents.

(c) Illustrates the different types of structural modifications of DNA in detail [taken from Hurley LH. Natural Reviews Cancer. 2 (2002):188-200] [7].

Alkylating agents including nitrogen mustards and triazines function in any phase of the cell cycle and are widely used against many cancers such as leukaemia, multiple myeloma, sarcoma and lymphoma. They directly damage DNA by alkylating guanine nucleotides within the DNA helix.

They usually interact non-specifically and some of them can close down tumorigenesis by cross linking guanine bases between two complementary DNA strands. These DNA strands cannot be uncoiled and be separated due to the cross linkage. As a consequence, the DNA cannot undergo replication and cell stops further cell division. Because of their non-specificity, they are harmful to normal cells as well.

Targeting a specific sequence of DNA or higher order DNA structures, like minor and major grooves or G-quadruplexes, with small-molecules can result in distortion or cleavage of the DNA and this can inhibit gene transcription, translation and/or other cellular processes specifically within tumour cells [8]. More recently, the G-quadruplex secondary structure is attracting scientific interest as it represents a new and special architecture as a target for DNA interactive ligand molecules. These secondary structures are more frequently present in guanine-rich sequences, especially in the single-stranded 3' overhang of telomeres and in promoter regions of various oncogenes like C-myc, BCL-2, c-kit etc. Thus G-quadruplexes may be better targets against which to design drugs to control transcription in malignant neoplasms [7].

1.1.4 DNA Structure

Deoxyribonucleic acid (DNA), a passive library of genetic information, is a polymer comprised of nucleotides which are linked to one another by phosphodiester linkages **(Figures 1.4 and 1.5)**. As the 2′ position of ribose sugar does not have an OH group, it is called deoxyribonucleic acid (DNA). Two complementary strands are paired together to make a double helical structure and this configuration is supported by hydrogen bonding between the purine and pyrimidine bases of both the anti-parallel chains. The 'double helix model` was established by James Watson (b. 1928), Francis Crick (1916–2004), Maurice Wilkins (1916–2004), who were jointly awarded the Nobel Prize in

Physiology or Medicine in 1962. Together, they developed the idea that the fundamental unit of base-sugar-phosphate is an appropriate building block for a three dimensional helix [9].

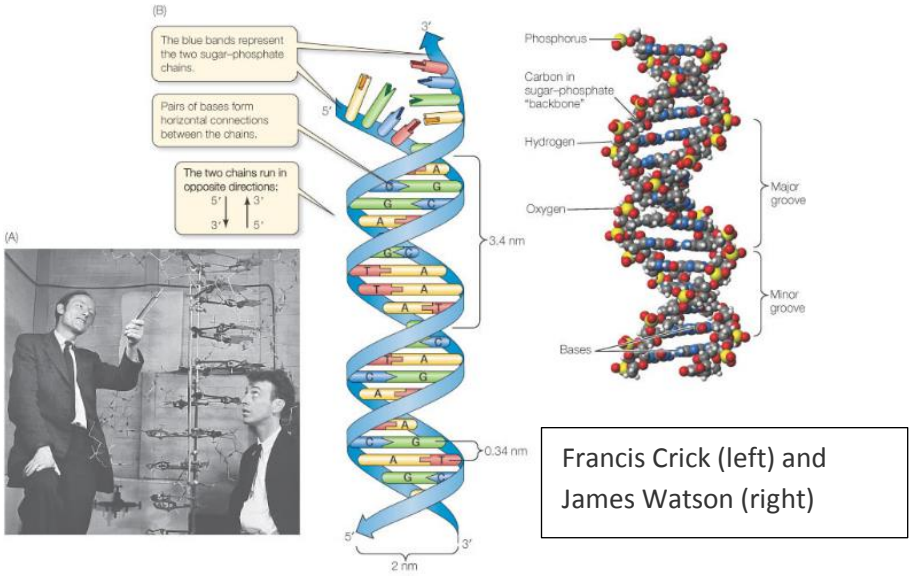

Figure 1.4: Diagram showing the double helical structure of DNA and the Watson-Crick base paring between purine and pyrimidine bases. It also illustrates the strand directions and the major and minor groove within the helical structure. [taken from *The Science of Biology*. 8th edition, 2008, W.H. Freeman]

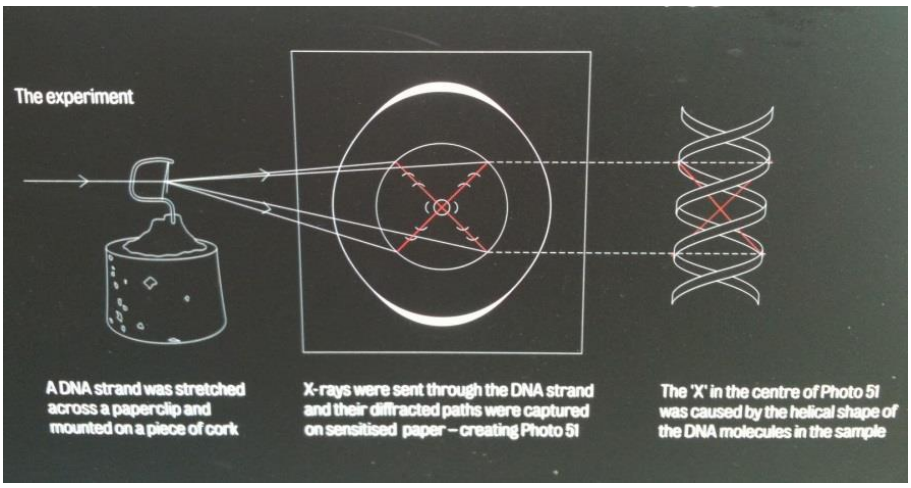

Figure 1.5: Diagram showing the X-ray diffraction studies of DNA done by Maurice Wilkins and Rosalind Franklin [taken from King's College London Archive Project Blog, 15 October 2010]

Detailed structural studies show that DNA has two grooves in its backbone, called major and minor grooves. These are due to the different arrangements of nucleotides in opposite directional complementary sequences. Nitrogen and oxygen atoms are pointed inward toward the helix in major grooves, whereas in minor grooves these atoms are pointed outward. These geometrical patterns make them different in size. Major grooves are larger (about 240° in angle) and wider compared to the minor grooves (about 120° in angle) **(Figure 1.6)**. Thus major grooves can accommodate a pair of water molecules, unlike minor grooves. Major grooves are also an easy way for DNA binding proteins to bind duplex DNA.

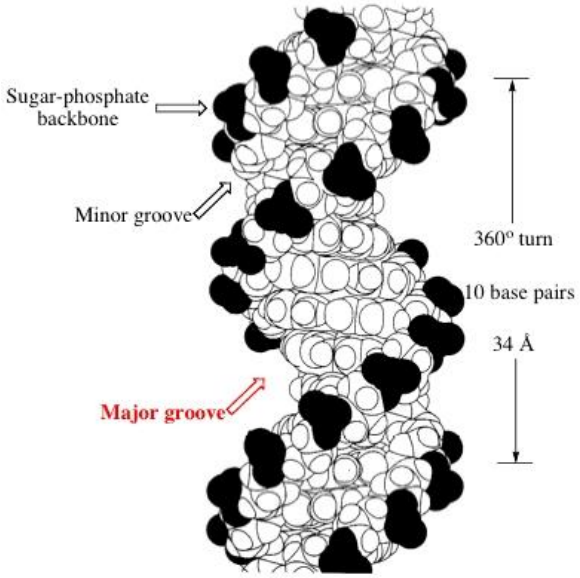

Figure 1.6: Major and minor grooves of DNA with sugar-phosphate backbone. The major groove is about two times wider than the minor groove present in the right handed duplex DNA [taken from UCLA Chemistry Illustrated Glossary of Organic Chemistry]

DNA is a polymer of nucleotides consisting of a deoxyribose, a nitrogenous base and a phosphate group. The bases are of two types: purines and pyrimidines. Six-membered and five-membered nitrogenous rings are fused together to form a purine base. On the other hand, pyrimidines consist of a six-membered nitrogen-containing ring [10].

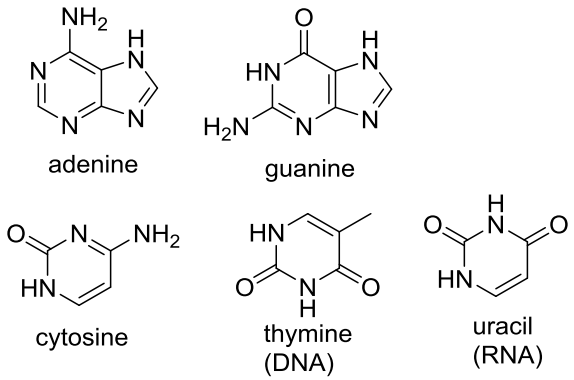

Figure 1.7: Structures of the purine (i.e. adenine and guanine) and pyrimidine (i.e. cytosine, thymine and uracil) bases that constitute DNA and RNA.

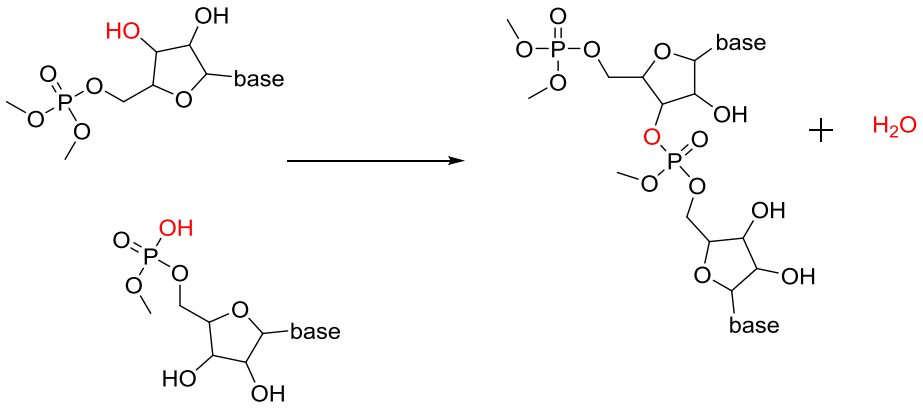

Figure 1.8: The phosphodiester bond formation between two consecutive nucleotides within a helical structure of DNA strand. Nucleotides are linked together through phosphodiester linkages.

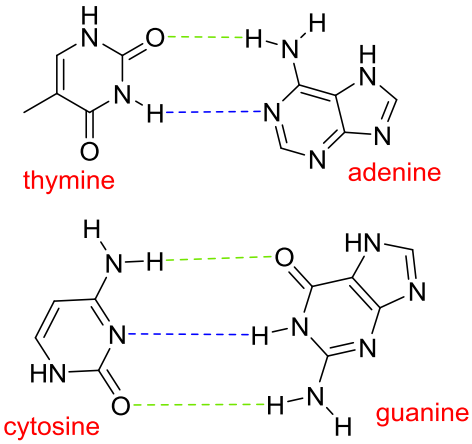

Figure 1.9: Diagram showing the hydrogen bonding between base pairs of complementary DNA strands. Adenine residue forms two hydrogen bonds with thymine base and cytosine residue forms three hydrogen bonds with guanine base.

The two complementary strands within the double helical structure of DNA are associated with each other *via* hydrogen bonding between the nitrogenous bases. Hydrogen bonds can be formed in two ways: between amine and carbonyl groups (green in **Figure 1.9**) or between amine and imine groups (blue in **Figure 1.9**). Adenine forms two hydrogen bonds with thymine and cytosine forms three hydrogen bonds with guanine residues **(Figure 1.9)**. The stability of the double helical structure is further enhanced by hydrogen bonds between the bases and water molecules around the helix. Moreover, the hydrophobic interactions and π-π stacking interactions among the bases play an important role in stabilising the double helix [11].

1.1.5 Different Forms of DNA

It is believed that DNA can be found in three conformations; A-form, B-form and Z-form DNA. The most common one is B-form DNA, the conformation proposed by Watson and Crick. A double helix composed of two anti-parallel and complementary right-handed strands which are wound around each other and remain together through hydrogen bonds between nucleotides of each strands. A-form DNA is similar to the most common form (B-form) of DNA, but short in size and, unlike B-form, its base pairs are not perpendicular to the DNA axis. The third form of DNA, Z-form, is totally different in terms of helical orientation. It has left-handed helical structures and is exclusively found in negatively supercoiled DNA.

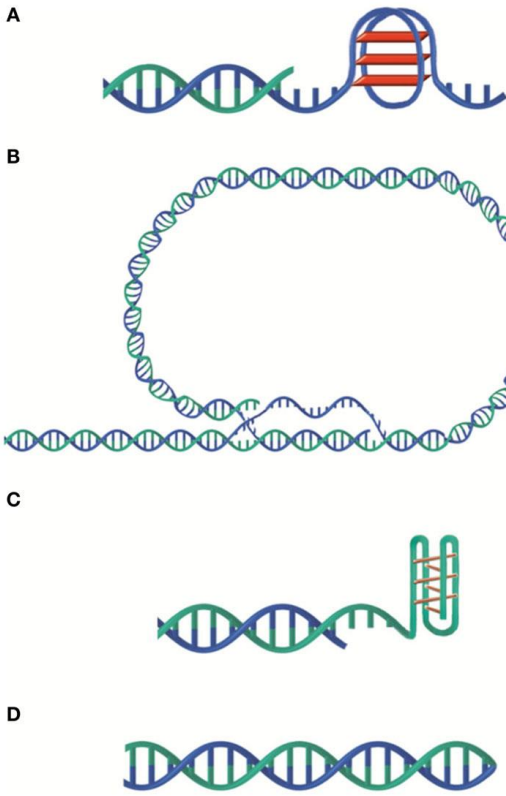

Figure 1.10: (A) Intramolecular G-quadruplex, a secondary structure formed by by hoogsteen hydrogen bonding among the guanine residues, each of which comes from one of the four g-tracts of DNA strand.
(B) t-loop formation, usually telomeric DNA associates with some telomeric associated protein collectively called sheterin and form T shaped loop to protect the telomeric end of a chromosome.
(C) I-motif, a secondary structure which is rich in cytosine residues can form i-motif by hydrogen bonding among the cytosine residues.
(D) Hairpin end formed by G-C pairing. Blue and green represent the G-rich and C-rich stretches of DNA respectively
[Taken from Gilson E, Giraud-Panis M-J and Pisano S, Frontiers in Oncology. 3(2013)] [12].

Besides, A-, B- and Z-form double helices, DNA can exist in various structures because of different orientations, helical pieces and number of residues per turn which ultimately can change the structure of DNA. Although canonical B-DNA is considered to be a most common form, detailed analysis shows it does not have straight, monotonous, uniform structures. The structural modifications of DNA are due to the presence of various types of sequences within a DNA sequence. Sometimes DNA may form triple helices, I-motifs or four strands may arrange together to form secondary structures **(Figure 1.10)**.

Some of these structures are favourable and some are unfavourable in nature due to steric hindrance, but still special types of DNA are found to participate in different cellular processes. For example, sequences like inverted repeats, palindromic repeats, mirror repeats, direct repeats and homo purine-homo pyrimidine G-rich or A-T rich regions favour formation of unusual conformations [13].

1.1.6 Triplex DNA

A triple DNA helix can form at some points of a canonical double helical DNA sequence through the accommodation of a third strand within its major groove. The three complementary helices are twisted together around a common axis to form a special conformation under certain biological conditions.

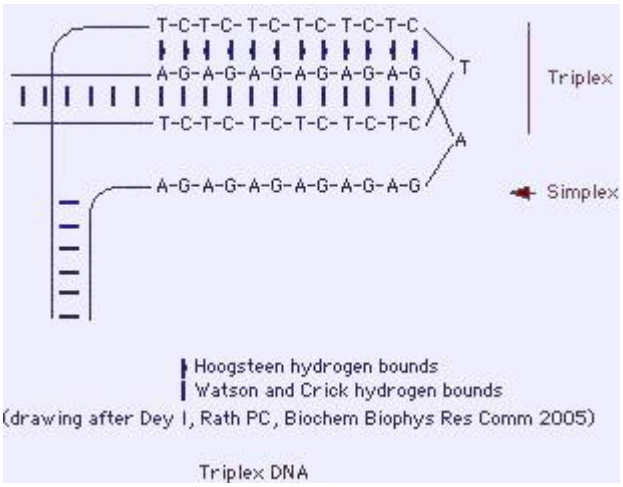

Figure 1.11: Formation of triplex DNA from two duplex DNA strands. [taken from Dey I, Rath PC. Biochem Biophys Res Comm. 327(2005):276-86.] [14].

Triple helical DNA can also be formed from the interactions of two duplex DNA strands, where third strand may come from one of these two dsDNA strand. A dsDNA strand especially rich in guanine (G) and adenine (A) purines nucleotides can often incorporate a third strand to make triplex DNA **(Figure 1.11)**.

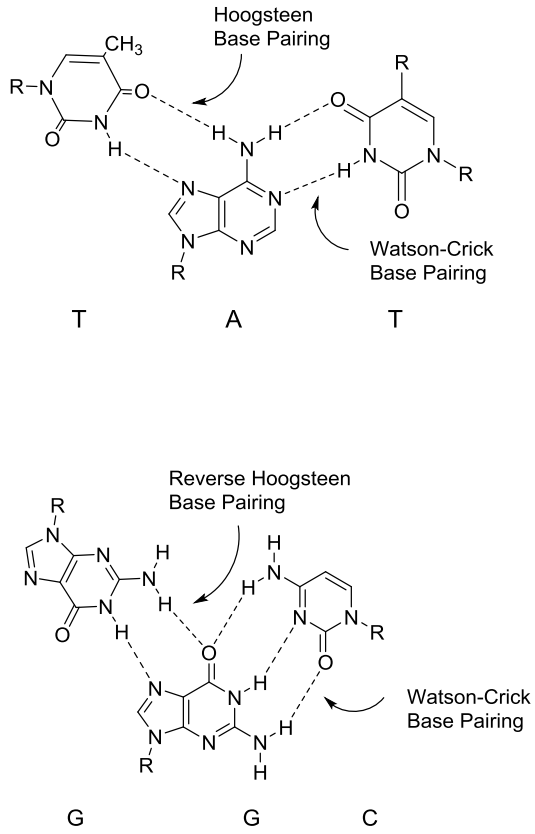

Figure 1.12: The mechanism of the Hoogsteen bonds and Watson-Crick base pairing between guanine, cytosine, adenine and thymine found in triple helix DNA.

Although purine bases forming hydrogen bonds are involved in Watson-Crick base pairing, they still have two additional hydrogen-bonding sites in their major groove: N-7 and O-6 for guanine residues, N-7 and 6-N for adenine residues. Therefore, besides the Watson-Crick hydrogen bonds, they can also make Hoogsteen bonds with cytosine (C) and thymine (T) residues of the complementary sequence of a third strand **(Figure 1.12)**.

The cytosine residues of the third strand need to get protonated to recognize the complementary guanine residues of the duplex DNA. Thus the triplex DNA can be formed only at low pH. The triple helix is comparatively less stable than dsDNA; this is because of electrostatic repulsion between the negatively charged phosphate groups on the backbones of the three strands. Bivalent cations like Mg^{2+} can minimise this electrostatic repulsion and stabilise the triplex DNA. However, the formation of the triplex structure does not interfere with specificity, transcription and translation of dsDNA.

1.1.7 G-Quadruplexes

DNA not only acts as a passive storage of genetic information, but is also reported to take part significantly in biological processes. Besides the Watson-Crick duplex, DNA can transiently adopt secondary structures. DNA sequences especially rich in guanine residues can tetramerize to form a four-stranded architecture which can be stabilized by monovalent and bivalent cations like Na^+, K^+ or Mg^{2+}. DNA may also make a special framework which is structurally and functionally different from that of DNA and of RNA **(Figure 1.13)**.

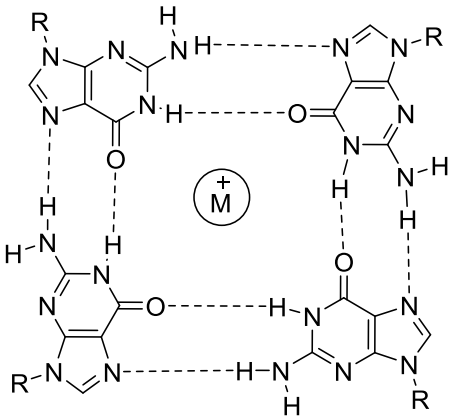

Figure 1.13: Diagram showing Hoogsteen hydrogen bonding among the guanine residues in a G-quadruplex quartet. A monovalent cation is incorporated with carbonyl (C-6) oxygen atoms of guanine bases within tetrads.

These monovalent alkali metal cations effectively help to form and stabilize the quadruplex structure through coordination with the carbonyl (C-6) oxygen atoms of guanine bases within tetrads. In every quadruplex, a single alkali metal ion sits at the central point between the tetrads, passing through the core of the G-quartets.

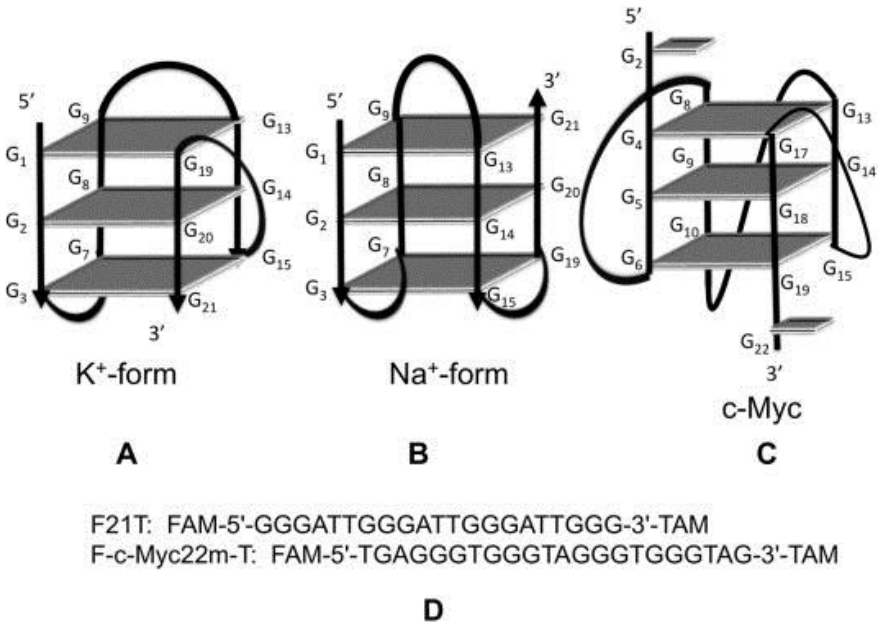

Figure 1.14: Topological view of (A) human telomeric G-quadruplex stabilized by a potassium cation (K^+);

(B) Telomeric G-quadruplex with anti-parallel strands in the presence of sodium (Na^+);

(C) The parallel G-quadruplex of c-Myc sequence (c-Myc);

(D) G-quadruplex forming telomeric and c-Myc promoter oriented sequences labelled with chromophores FAM and TAM at both ends [taken from Schoonover M, Kerwin SM. Bioorganic & Medicinal Chemistry. 24(2012):6904-18.] [15].

The four guanine residues of a G-tetrad are arranged in a rotationally symmetric fashion to make a planar platform and thereby self-associate through Hoogsteen hydrogen bonding rather than Watson-Crick base-pairing **(Figures 1.13 and 1.14)** [16]. G-quartets stack together *via* π- π interactions [17].

1.1.8 Sequence and Topology of Different G-Quadruplexes

Guanine bases of a G-tetrad can orient together either in *syn* or *anti* glycosidic conformations. NMR and crystallographic studies of various G-quadruplexes have revealed their diverse topologies.

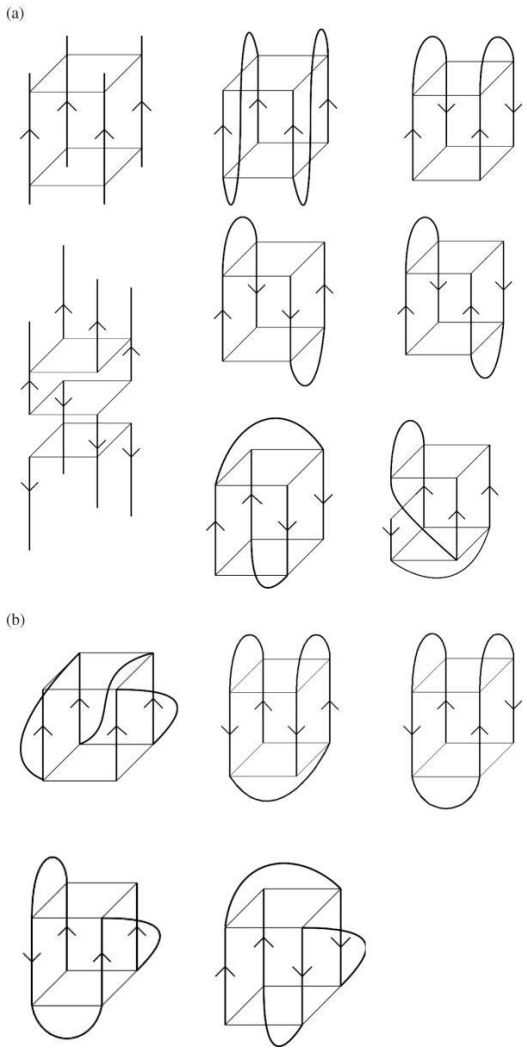

Figure 1.15: (a) The various topologies of bimolecular and tetramolecular quadruplexes with different directions of the DNA stands and diferrent connecting loops types. (b) The multiple possible ways to form unimolecular quadruplexes, giving different topological conformations [taken from Burge S, Parkinson GN, Hazel P, Todd AK, Neidle S. Nucleic Acids Res .34(2006):5402-15.] [18].

G-quadruplex complexes are found to be formed by either a single (unimolecular), two (bimolecular) or four (tetra molecular) different DNA strands [19]. These variations in possible combinations of DNA strands, strand directions, loop lengths and sequence contexts are also responsible for the topological diversity of different G-quadruplexes **(Figure 1.15)**. Conformational dissimilarity due to particular folding patterns and loop types makes each particular type of G-quadruplex a unique drug-interacting cavity [19, 20].

Quadruplex structures can also be varied because of their stand polarities/directions and loop types. Loops do not always connect the strands aggregated together to make a quadruplex in the same way.

Categorically, four types of loops are found to be present in G-quadruplex structures. The most common is the propeller type and the other three are lateral, diagonal and V-shaped type loops, respectively **(Figure 1.16)**.

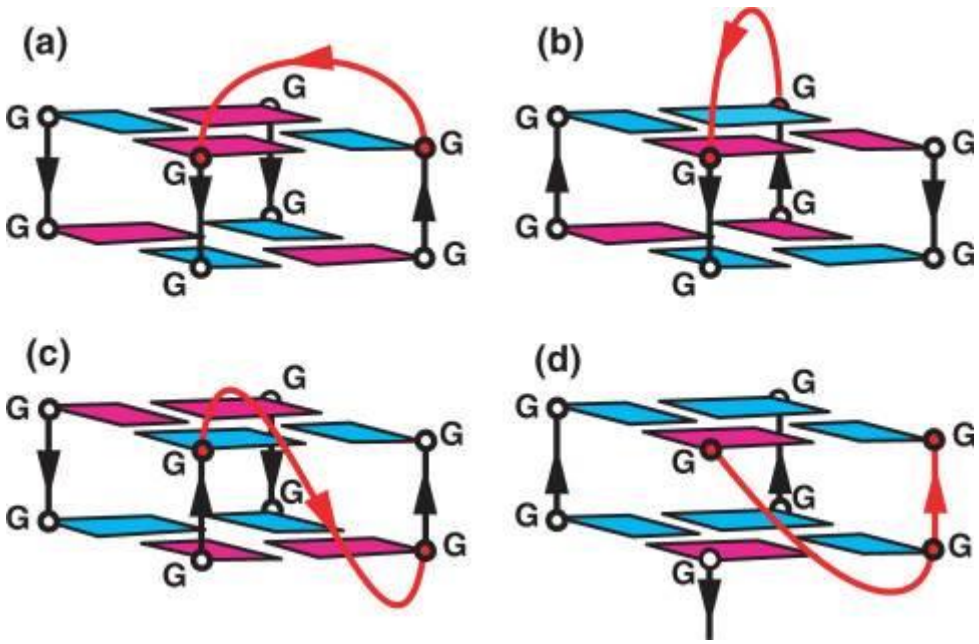

Figure 1.16: (a) Lateral type connecting two adjacent and anti-parallel strands , (b) Diagonal type, , joins the opposite anti-parallel strands as lateral loop connect (c) Propeller type connecting two adjacent and parallel strands and (d) V-shaped type loops connect two adjacent g-tracts [taken from Patel DJ, Phan AT, Kuryavyi V. Nucleic Acids Res. 35 (2007):7429-55] [21].

Adjacent and parallel strands are linked together *via* a loop connecting the top G-tetrad to the bottom G-tetrad, forming a propeller type loop [22]. On the other hand, lateral loop types connect between the two anti-parallel adjacent strands *via* linking the top G-tetrad of one strand to the top G-tetrad of another strand [23]. Diagonal loops are a third type of antiparallel loop, joining the opposite anti-parallel strands as lateral loop connect [24]. V-shaped loops make a connection between two consecutive quartets *via* a guanine residue, but unlike the other guanine residues present in G-tracts, this residue has no further connection with other guanine residues immediately before or after it [25].

A G-quadruplex can be defined in a generalized form as a structure originating from the stacking of at least two G-tetrads. G-quadruplexes of four G-tracts (tetra molecular) with tetrad guanines adopting anti-glyosidic conformations are most commonly parallel-stranded. Oligonucleotide sequences forming a potential unimolecular G-quadruplex have already been formulated as shown below.

$$G_mX_nG_mX_oG_mX_pG_m$$

Here 'm' indicates the number of guanine units in each G-tract, which in turn participate directly in Hoogsteen hydrogen bonding to connect with the guanine nucleotides of the three other G-tracts. 'X_n', 'X_o' and 'X_p' represent any combination of different nucleotide residues, forming a loop type [26].

1.1.9 G-Quadruplex Sequence Occurrences and their Significance as Antitumour Targets

G-quadruplex-forming sequences are reported to be present throughout the human genome, which includes exons, introns, and untranslated regions of genes, promoter sequences and gene deserts, amongst others. As many as 5,713,900 possible potential quadruplex sequences have been reported by the Ensemble database (V20 NCBI assembly 34c) survey to be present in the human genome [27]. According to bioinformatics and molecular sequence analysis reports, G-quadruplexes are found to be overexpressed in some particular regions of the genome, especially in the single-stranded overhang DNA of telomeres and in the nuclease hyper sensitive element (NHE) of promoter regions of several oncogenes [28]. G-quadruplexes are also highly expressed within cancer-affected cells in regions of genomic damage, like translocation hot-spots [29], [30].

These structures can also originate from the guanine-rich part of messenger RNA (mRNA), ribosomal DNA (rDNA) and thrombin-binding aptamer (TBA) [31]. Recently, the existence of a G-quadruplex within the 5′ untranslated region (UTR) of RNA has also been reported [32].

However, the enzyme telomerase appears to be highly expressed in tumours and plays a significant role in proliferation of cancer cells, controlling oncogene

transcription[33, 34]. A number of studies have reported that G-quadruplex formation on telomeres prevents telomere extension as they inhibit telomerase by displacing it from the telomere. Thus G-quadruplexes are gaining prominence as anti-cancer targets because of their genetic context and antineoplastic potential[35-37].

1.1.10 Telomere Structure and Function

Telomeres are often likened to the protective plastic caps at both ends of a shoelace **(Figure 1.17)**. They protect the ends of human chromosomes from deterioration or from fusion with neighbouring chromosomes.

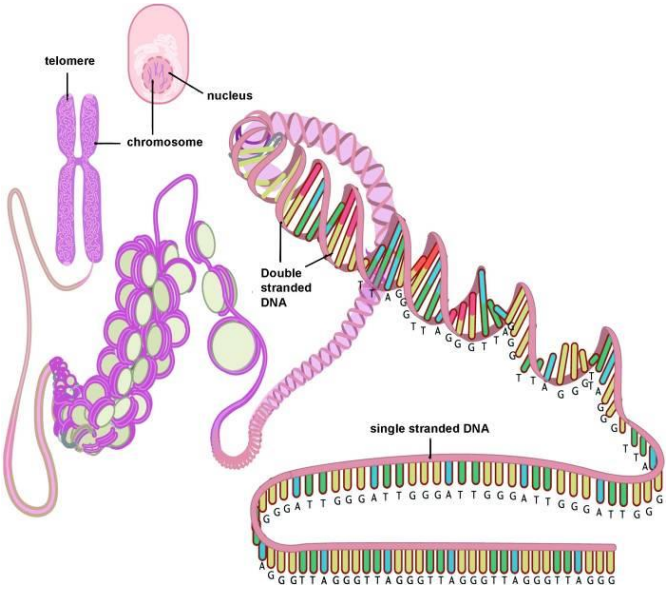

Figure 1.17: Diagrammatic representation of telomeric structure with a single-stranded overhang at the end of a chromosome in the nucleus. [taken from Wong LSM, van der Harst P, de Boer RA, Huzen J, van Gilst WH, van Veldhuisen DJ.**Heart Fail Rev**. 15(2010):479-86.] [38].

If cell division were to take place without telomeres, a loss of DNA bases from the chromosomal ends would occur along with a potentially lethal loss of genetic information [39].

Across different species, telomeres can reach a length of approximately 15,000 base pairs and contain regions of highly conserved repetitive sequences. In humans, telomeres may extend to 15-20 kb in length at birth and have reduced to approximately 8-10 kb in adults. Because of the end replication problem, telomeres get shorter in size with each cell division. DNA synthesis goes in the

5′-3′ direction, as it requires the 3′-OH group from the template strand to add free nucleotides. The RNA primer used in starting the DNA replication provides a 3′-OH group and a complementary strand to run the lagging strand synthesis. Then, after as the RNA is removed shortly after DNA synthesis starts, the 5′ end of the lagging strand is placed inside of the utmost 3′ end of the complementary template strand and there is nothing for this piece to attach to. Thus the last section of the lagging strand cannot be synthesized, and after several cycles of replication, DNA molecules ultimately get shorter and smaller, causing the end replication problem. Thus the capacity of human cells to divide is limited and the number of cell divisions before the cells enter into senescence is called the Hay flick limit [40].

The 3' single stranded overhang DNA of telomeres has guanine-rich tandem repeats of d $(TTAGGG)_n$ sequences. The average length of this single-stranded overhang is 150 nucleotides and these stretches of DNA are prone to adopt a four-stranded G-quadruplex [21]. This unimolecular secondary conformation is supported by monovalent cations and Hoogsteen hydrogen bonding between four guanine residues from each of the four G-tracts. The DNA strand is folded in such a way that four guanine residues of four tandem repeats (i.e. a G-tract) are close enough together in the same plane to make hydrogen bonds among themselves and form a G-tetrad. Two or more G-tetrads are then stacked together to form a G-quadruplex. This special secondary conformation then inhibits the enzyme telomerase. This enzyme complex helps to maintain the telomere length by synthesizing and adding telomeric DNA repeats and thereby protecting the DNA from becoming shortened during cell division. Telomerase inhibition through the G-quadruplex formation ultimately inhibits cellular growth and makes cells ready to enter apoptosis.

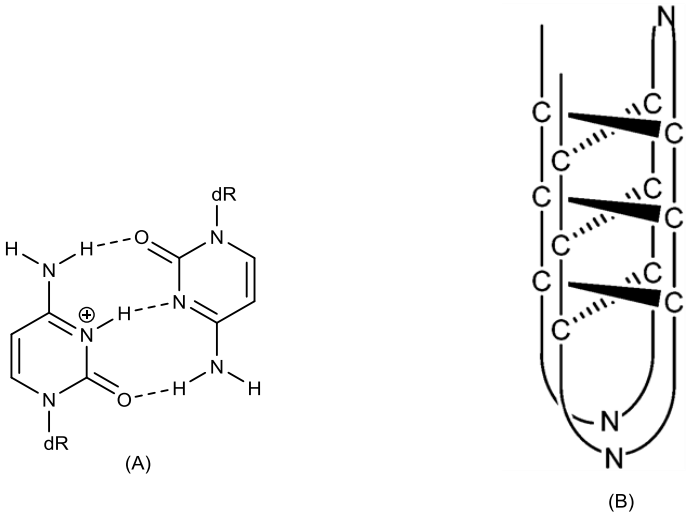

Figure 1.18 : (A) Cytosine-cytosine base pairing and (B) i-motif formation through base pairing between c-rich tracts; N indicates any nucleotides [taken from Gurung SP, Schwarz C, Hall JP, Cardin CJ, Brazier JA. Chem com. 51(2015):5630-2] [41].

Thus these G-quadruplexes formed within telomeres are potential therapeutic targets for anti-cancer drugs [42]. Besides this 3' single-stranded overhang, double-stranded telomeric DNA is found to be incorporated into several telomeric proteins. Telomeric DNA in association with these proteins favours formation of G-quadruplexes[43]. On the other hand, telomeric DNA has been shown to prefer duplex DNA over quadruplex and i- motif DNA in the absence of these proteins [44].

Like the 3' overhang, the telomeric duplex is also rich in $(TTAGGG/CCCTAA)_n$ repeats. Thus the complementary G-rich strand makes a secondary G-quadruplex whereas the other complementary C-rich strand also makes a four stranded architecture which is supported and organised by the cytosine-cytosine base pairings **(Figure 1.18)**.

A limited number of detailed structural reports on quadruplexes of topological diversity exist to date [45]. Among those, crystallographic analyses of telomeric quadruplexes have been reported and a few oncogene promoter-oriented G-quadruplexes have also been reported using NMR spectroscopy.

Crystallography of both intra- and intermolecular human telomeric quadruplexes (12 and 22 mer sequences shown in **Figure 1.19**) unveil a totally different folding conformation and topology type **(Figure 1.20)** [22].

1) d (TAGGGTTAGGGT)

2) d [AGGG(TTAGGG)$_3$]

Figure 1.19: 12 and 22 mer sequences of telomeric quadruplexes [46, 47].

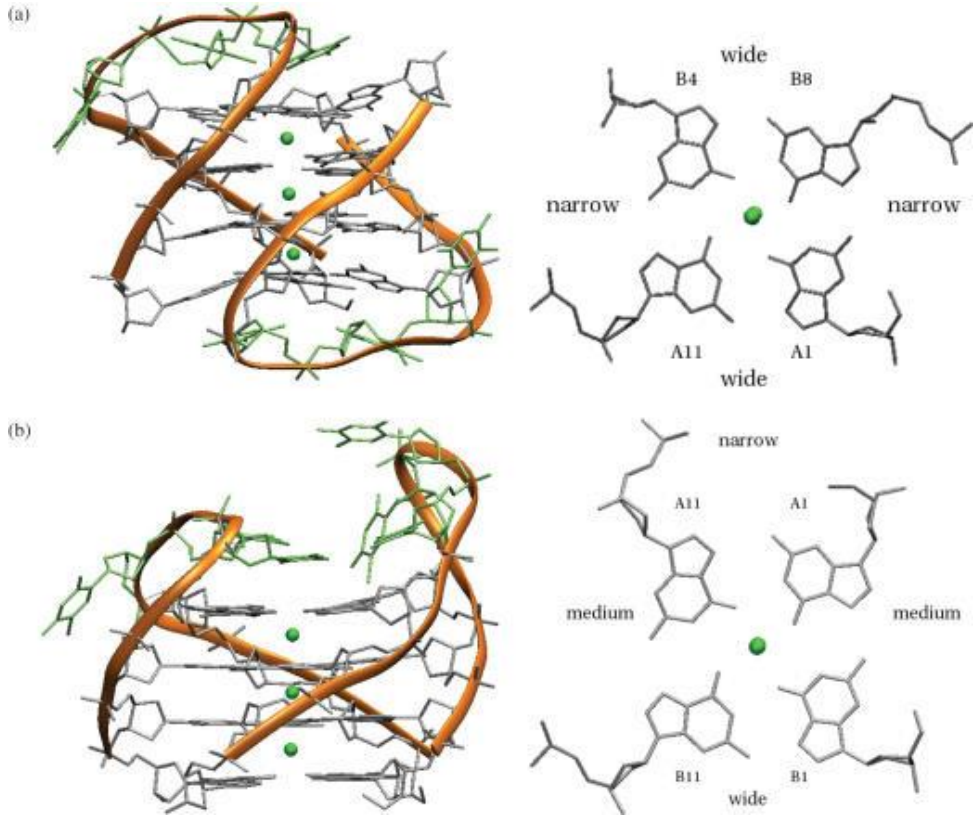

Figure 1.20: Crystallographic view of the two bimolecular G-quadruplex-sequences d($G_4T_3G_4$). Alkali metal ions (green) are appeared to be incorporated with the oxygen atoms of guanine residues within tetrads.

a) Two visualisations of head-to-tail G-quadruplexes. b) Two visualisations of head-to-head G-quadruplexes. [taken from Burge S, Parkinson GN, Hazel P, Todd AK, Neidle S. Quadruplex DNA: Nucleic Acids Res . 34(2006):5402-15.] [26]

.

1.1.11 Targeting G-Quadruplexes in Gene Promoters

A structure-specific monoclonal antibody targeting G-quadruplexes has been engineered and the existing G-quadruples, either of DNA or RNA, have also been visualised [48],[49]. In 1990, G-quadruplexes were reported to be first seen at the ends of eukaryotic telomeres [50]. Later, Hurley and co-workers revealed a potential G-quadruplex structure within the nuclease hypersensitive element III_1 ($NHEIII_1$) of the promoter of the c-*myc* oncogene, and they further showed that putative G-quadruplex formation induced by a sequence-targeting small ligand molecule caused the transcriptional repression of c-*myc* [51]. Further studies have reported G-quadruplex-forming sequences are also in the promoter sequences of other oncogenes like c-*kit* [52], KRAS [53], bcl-2 [54] and VEGF [55] .

In general, it is now thought that nuclease hypersensitive element III_1 ($NHEIII_1$) in the promoter regions of most genes contain more guanine-rich quadruplex forming sequences relative to the rest of the genome, meaning G-quadruplex structures can be one of the regulatory factors affecting the expression of genes; they are linked to the processes of replication, transcription and recombination of DNA. In addition, these transiently-formed structures are more frequently expressed at sites of primary tumours relative to in normal tissues [56]. Thus many G-quadruplex-containing gene promoters have been reported to date [57] and are reported to be highly connected with many diseases [48], including cancer [58], diabetes [59] and cardiovascular diseases [60].

Table 1.1: The base sequences, topology and loop length of C-MYC, KIT1 and BCL-2 promoter-oriented G-quadruplexes [61] [62].

Gene	Sequence	Topology	Loop	PDB ID	Ref
MYC	$d[TGAG_3TG_2TGAG_3TG_4A_2G_2$	Parallel	3' P	2A5P	[63]
KIT1	$d[AG_3AG_3CGCTG_3AG_2AG_3]$	Parallel	2' P	2O3M	[63]
BCL-2	$D[G_3CGCG_3AG_3A_2T_2G_3CG_3]$	Mixed: parallel and anti-parallel	2' L	2F8U	[54]

The discovery of G-quadruplex formation in oncogenic promoter sequences and their subsequent role in vital cellular processes, especially in transcription, may herald a new era in the development of targeted anti-cancer therapies [20].

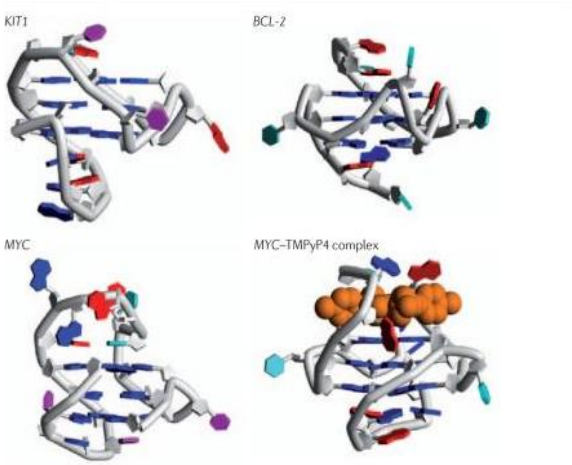

Figure 1.21: The topological conformations of G-quadruplexes belonging to the Myc, Kit and BCL-2 gene promoters and the Myc-TMPyP4 complex [64] through NMR studies [taken from Balasubramanian S, Hurley LH, Neidle S. Nat. Rev. drug Disco.24(2011):261-75.] [20].

The folding patterns of G-quadruplexes in gene promoter regions are not similar to those of telomeric G-quadruplexes **(figure-1.21)** [65]. Promoter-oriented G-quadruplexes are primarily influenced by the duplex nature of genomic DNA [63]. On the other hand, the telomeric G-quadruplex is more frequently found to form on the 3'-end single-stranded overhang of a telomere.

1.1.12 G-quadruplex Sequences Present in C-kit Promoter

c-kit, a proto-oncogene encoding a transmembrane protein with tyrosine kinase activity, plays an important role as a cell surface receptor for cytokines to regulate cellular surveillance, proliferation and haematopoiesis [66]. In response to Kit ligands like KITLG/SCF (stem cell growth factors), tyrosine kinase phosphorylates several regulatory proteins like PIK3R1 (phosphoinositide-3-kinase, a regulatory subunit-1) and PLCG1 (phospholipase C, Gamma 1) amongst others, thereby ultimately activating the signalling pathway through the phosphorylating capacity of the c-kit gene product. This in turn involves the phosphorylation of transcription factors including STAT1 and STAT2 [67]. The 5' flanking region of the human c-kit gene is rich in guanine and cytosine nucleotides [68]. Putative G-quadruplex-forming G-rich tracts have already been recognized in the promoter region of the c-kit gene [62]. One of these sequences, d(5'-GGG AGG GCG CTG GGA GGA GGG-3'), called c-kit-1, is reported to be

located 87bp ahead of transcriptional start site. The second quadruplex-forming sequence, d(5'-GGG CGG GCG CGA GGG AGG GG-3') known as c-kit-2 has been identified in a site of core promoter activity [62, 69]. G-quadruplex-forming sequences and their occurrence in the regulatory region of the c-kit gene make them target sites for gastro intestinal tumour therapy [70].

The d (5'-AGGG AGG GCG CTG GGA GGA GGG-3') DNA sequence of the c-kit oncogene forms a four-stranded G-quadruplex architecture, as confirmed by the combined efforts of NMR and circular dichroism spectroscopy [52, 63]. Guanine-rich tracts arrange together to have an intramolecular G-quadruplex structure in the presence of K^+ ions, thereby giving a distinct topological structure with four loops including two propeller loops formed separately by nucleotide residues A5 and C9. Residues C11 and U12 together make another loop and a relatively long stem loop is formed of nucleotide residues A16-G17-G18-A19-G20 **(Figure 1.22)**.

It has been reported that alkali metal ions like K^+, Na^+ and Li^+ take part in stabilising G-quadruplexes [71-75]. On the other hand, Mg^{2+} ions have been reported to destabilize human telomeric G-quadruplexes [76]. Interestingly, promoter-based G-quadruplexes are stabilised by Mg^{2+} ions [77]. In addition to K^+ ions, two Mg^{2+} ions appear to be included within the loops of G-quadruplex-A.

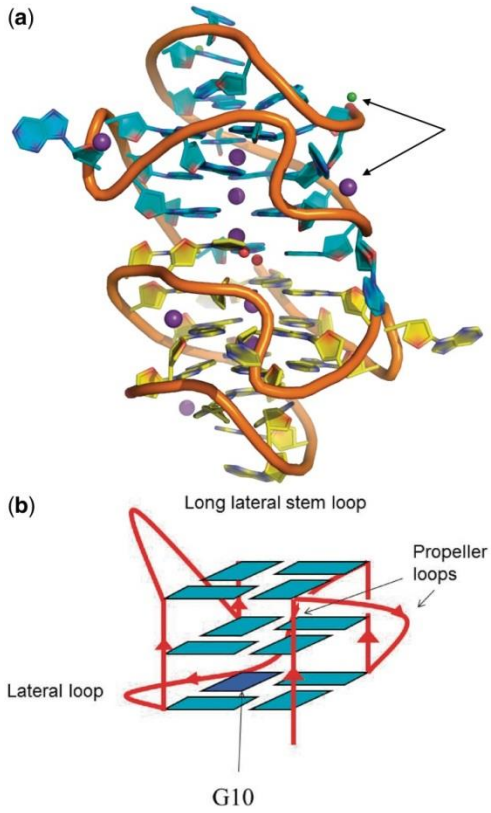

Figure 1.22: (a) A model presentation of two asymmetric and independent c-kit quadruplexes (blue coloured A and yellow coloured B). Violet and green coloured balls (indicated by arrows) symbolize K^+ and Mg^{2+} ions, respectively. (b) The c-kit G-quadruplex topology with a non-G-tract guanine residue (G10) [taken from Wei D, Parkinson GN, Reszka AP, Neidle S. Nucleic Acids Res. 40 (2012):4691-700] [78].

In addition to the G-tracts available for the formation of the G-quadruplex, an isolated non-G-tract guanine is thought to participate [79]. Crystallographic analysis of c-kit-1 also reveals that the two independently formed asymmetric quadruplexes (A and B) appear to be stacked upon each other and arranged in a head to head fashion, allowing the incorporation of water molecules into the structure [78]. Therefore, this distinct conformational feature of c-kit oriented G-quadruplexes makes them attractive as anticancer-specific therapeutic targets for ligand molecules.

1.1.13 G-quadruplex Sequences Present in Bcl-2 Promoter

Bcl-2 was first identified as an anti-apoptotic gene [80]. As many as 25 Bcl-2 genes have already been found to be present in human chromosomes. Bcl-2 proto-oncogenes encode a family of proteins which control mitochondrial outer membrane permeability (MOMP) and can either be pro-apotopic (including Bax, BAD, Bak and Bok) or anti-apoptopic (including Bcl-2 proper and Bcl-w) [81]. However, the proportional balance between these anti-functional proteins partly defines the cellular vulnerability towards entering apoptosis [82]. Bcl-2 proto-oncogenes were first discovered at the breakpoint of chromosome 14, linked to B-cell lymphoma-related bcl-2 gene translocation to chromosome 18 [83].

Bcl-2 proteins can trigger apoptosis by either inducing pro-apoptotic factors or repressing anti-apoptotic factors. They instigate the release of apoptogenic factors like cytochrome c into the cytosol which in turn facilitate the process of apoptosis through the activation of caspases [84]. On the other hand, anti-apoptotic Bcl-2 proteins may inhibit apoptosis possibly by inhibiting the pro-apoptotic Bax, BAD,Bak, Bok etc[85]. However, the upregulated Bcl-2 gene plays an important role in the development of many of common cancers and has also been reported to have resistance to conventional cancer therapies. Bcl-2 proteins are also found to coordinate signalling systems to inhibit cell proliferation and cell death[86-88].

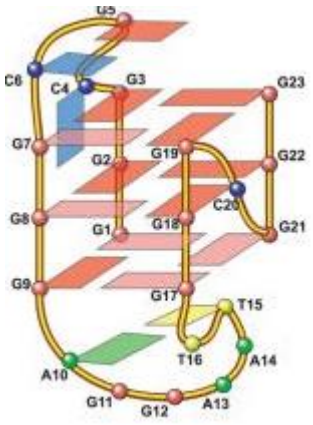

Figure 1.23: Simplistic diagram of the folding pattern of G-tracts in Bcl-2 quadruplexes. Red and blue coloured boxes indicate guanine residues with *anti* and *syn* configurations, respectively [taken from Raghavan SC, Swanson PC, Wu X, Hsieh CL, Lieber MR. Nature. 428(2004):88-93.] [89].

Guanine-rich regions upstream of the Bcl-2 promoter can potentially form G-quadruplexes and thereby play an important role in regulating Bcl-2 transcription. Quadruplexes can also be formed within the G-rich stretches of chromosomal translocations[83, 89]

A novel folding pattern gives the unimolecular G-quadruplexes of the Bcl-2 gene a unique conformation. An intramolecular quadruplex is built through the association of both parallel and antiparallel G-tracts to form two lateral and one propeller-type loops [54]. Three nucleotides (C-G-C) in the non-G-tract region make a lateral loop. Another non-G-tract stretch of seven nucleotides (A-G-G-A-A-T-T) forms a relatively bigger lateral loop. A single nucleotide C connects three consecutive G-tetrads and makes a propeller-type loop **(Figure 1.23)**. These loops make a similar, but not identical, topology to that seen for the 22 nucleotide-long telomeric quadruplex[42, 90]. This special topological feature emphasizes the significance of G-quadruplexes of the Bcl-2 gene as targets for small ligand molecules in the field of cancer therapeutics.

1.1.14 G-quadruplex Sequences Present in STAT-3 Gene

The Signal Transducer and Activator of Transcription 3 (STAT-3) gene encodes a family of proteins acting as transcriptional activators involved in intracellular signalling pathways, and thereby plays a substantial role in many cellular processes [91].

It has already been reported that STAT-3 is constitutively active in various human cancers and mutated STAT-3 inhibits apoptosis and stimulates cell proliferation, angiogenesis, invasion and metastasis. Thus the suppression of STAT-3 activation through the stabilisation of G-quadruplexes at its downstream flanking region is believed to be a favourable target in the field of anticancer therapy [92].

The STAT-3 G-quadruplex, of sequence d(5'-G_3CTG_3GATG_3GAG_3GG-3'), has a different type of topological conformation due to its sequence and folding pattern. Recently, STAT-3 G-quadruplex folding patterns have been studied using a combination of CD spectroscopy and molecular modelling. Loop isomers 3:2:2 and 3:3:1 have already been considered as potential G-quadruplex conformations [93].

1.1.15 Therapeutic Significance of Promoter-Oriented G-quadruplex Sequences

As anticancer targets, promoter G-quadruplexes has increased in therapeutic significance during the last decade. Small molecules capable of selectively targeting and interacting with to stabilise the G-quadruplex motif are receiving significant interest and gaining momentum as a possible new class of anticancer agents. In particular, a number of small ligand molecules have already been reported to inhibit transcription of some oncogenes by forming and stabilizing G-quadruplexes.

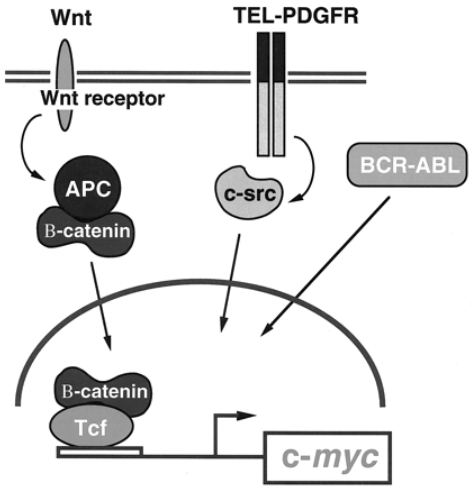

Figure 1.24: c-myc gene operating as a central oncogenic switch for oncogenes and the tumour suppressor APC (adenomatous polyposis coli) [taken from Dang CV. Molecular and Cell Biology. January 19(1999):1-11.] [94].

For example, transcriptional repression of the MYC proto-oncogene, which is overexpressed in up to 80% of solid tumours, has already been reported [95].The Myc gene is found to be mutated in many malignancies such as breast cancer, which makes Myc constitutively expressed. This ultimately upregulates the expression of numerous genes, such as the genes involving cell proliferation, and ultimately develops into cancer **(Figures 1.24, 1.25)**. A number of publications provide evidence in support of the presence of parallel-stranded G-quadruplexes upstream of the P1 and P2 promoters of c-MYC [96].

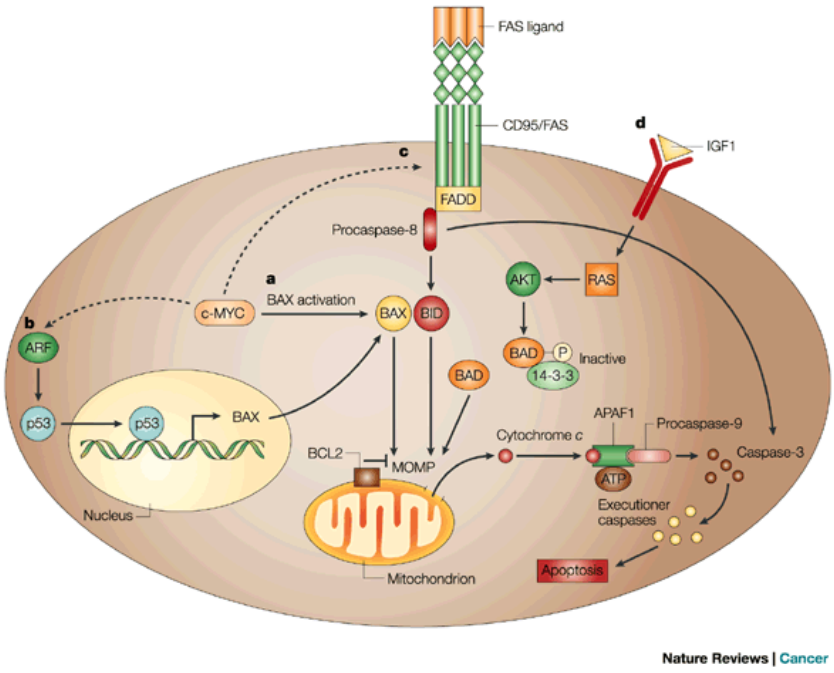

Figure 1.25: Diagram showing c-MYC sensitization of a cell to a number of pro-apoptotic stimuli. C-Myc may induce apoptosis in three possible ways via activating either BAX or p53 or FAS. Apoptosis can be blocked by antiapoptotic factor BCl-2 XL and BCL-2 proper via blocking the release of cytochrome c from the outer mitochondrial membrane [taken from Stella Pelengaris1 MKAtaGE. Nature Reviews Cancer October 2(2002):764-76 [97]].

Cytochrome c is released from mitochondria into the cytosol in response to the induction of c-MYC; this may be due to the induction of BAX, a pro-apoptotic molecule [98-101] (a). Active BAX then alters membrane pores, causing mitochondrial-outer-membrane permeabilization (MOMP)[101, 102]. The apoptosome is formed by cytochrome attaching together with procaspase-9 and apoptotic protease-activating factor 1 (APAF1)[103]. This formation is then complexed with dATP and ultimately activates the downstream caspase pathways involving caspase-3, degrading cell components. C-MYC may induce apoptosis in an alternative p53/ARF pathway involving tumour suppressor protein p53 activation *via* ARF, leading to BAX (b) transcription[104]. An apoptotic signal may pass through the FAS ligand binding with prototype death receptor CD95. It is then further combined with an intracellular adaptor protein FADD (FAS-associated death domain) (c) and ultimately enters into the main caspase pathway *via* activation of caspase-8 **(Figure 1.25)**. C-Myc-mediated apoptosis can be blocked by anti-apoptotic proteins such as BCL-2 or BCL-XL in a

pathway involving IGF-1 receptor (d). Binding of IGF-1 to its receptor leads to activation of RAS and AKT kinase[105]. Pro-apoptotic protein BAD is activated by phosphorylation and subsequently segregated and inactivated by cytosolic 14-3-3 proteins[106]. BAX may be sequestered and cytochrome c release blocked by BCL2 and BCL-XL [107].

1.1.16 G-quadruplex-Stabilizers as Anti-Cancer Agents

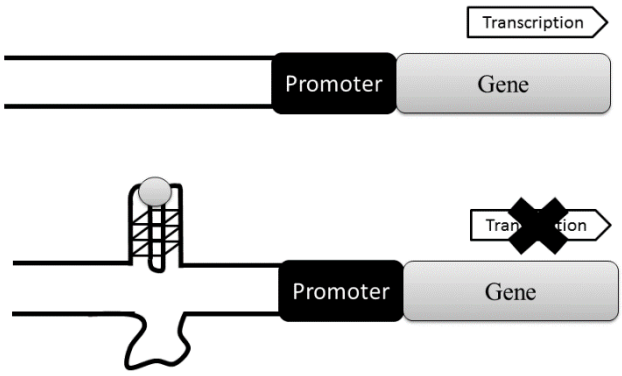

Figure 1.26: Diagram illustrating the effect of promoter-oriented G-quadruplex targeting ligands on transcription. The stabilisation of promoter oriented G-quadruplex with a ligand molecules blocks the transcription of a gene [taken from Ma D-L, Ma VP-Y, Leung K-H, He H-Z, Chan DS-H, Zhong H-J: (2013):01-24.] [28].

G-quadruplex-stabilizing ligands can modulate transcription [108] and thereby play a major role in proliferation **(Figure-1.26)**. An anthraquinone derivative **(Figure 1.27)** was one of the very first small ligand molecules reported to interact with G-quadruplex structures in telomeres [109].

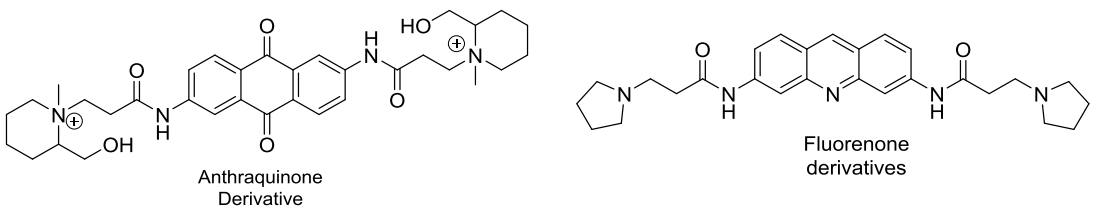

Figure 1.27: Structures of G-quadruplex-targeting ligands; anthraquinone derivatives and fluorenone derivatives.

In fact it had been developed to target duplex and triplex DNA, but was observed to inhibit the enzyme telomerase (EC_{50}=23 μM) *via* a mechanism involving the binding of G-quadruplex DNA [110].

A series of structurally-similar molecules including fluorenones **(Figure 1.27)** and acridines[111, 112] have been developed on the basis of the molecular motif of anthraquinones[113]. On the other hand, TMPyP4 was the first reported c-myc G-quadruplex stabilizer that could inhibit c-Myc expression [114]. Recently, a number of other c-myc G-quadruplex-interacting ligand molecules have been reported. For example, quindoline and berberine derivatives [115] and trisubstituted isoalloxazines [116], cationic porphyrins [114], BRACO-19, Piper, RHPS4 and Quarfloxin **(figure 1.28)** [117] all show notable interference with oncogenic transcription *in vitro*. Quarfloxin, designed by Cylene Pharmaceuticals, entered clinical phase-II trials having been reported to interact with G-quadruplexes *in vivo* [28].

Trisubstituted acridine (AS1410, with a very similar structure to that of BRACO-19) has been found to exert cytotoxic effects in two cancer cell lines including breast (MCF7) and lung (A549) at sub-cytotoxic concentrations[118, 119]. It has also shown a synergistic action while combining with even a low dose of cis-platin[120].

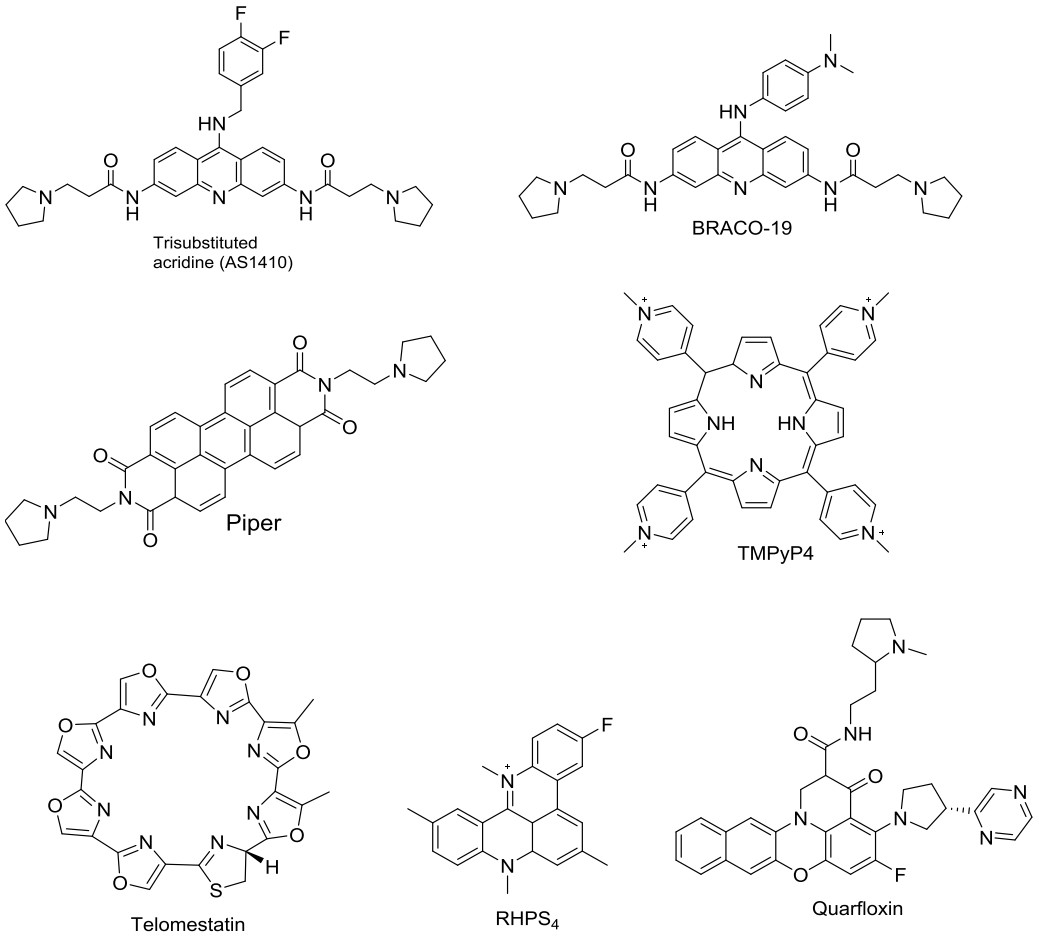

Figure 1.28: Structures of some classical G-quadruplex-interacting ligands with their planar and polycyclic aromatic cores [117].

1.1.17 BRACO-19

3, 6, 9-trisubstituted acridine is considered to be the most telomeric G-quadruplex-interacting ligand amongst all other acridine derivatives reported [121]. In fact, the molecular structure of BRACO-19 was designed carefully through computer modelling to target telomeric quadruplexes; it can fit in three grooves in addition to sitting/stacking on to the terminal G-tetrads of the target G-quadruplex architecture[121]. Therefore, it is found to provide a significantly high degree of stabilisation. Although it has no a significant cytotoxic effect on cancer cells, it has been shown to have a great inhibitory impact on the enzyme telomerase [36] by displacing it from telomeres, which ultimately produces a number of biological responses including the onset of a senescence phenotype, telomere shortening, the induction of chromosomal end-to-end fusions [122], uncapping of telomeres and reduced expression of human telomerase reverse

transcriptase (hTERT) [123]. BRACO-19 was found to be a highly active agent against various cancer cell lines *in vivo*.

In fact, extensive studies of BRACO-19 both *in vitro* and *in vivo* helped to develop telomeric G-quadruplexes as valid targets for anti–cancer therapy. However, *in vivo* studies reported that BRACO-19 has rapid and significant anti-tumour effects and it shows remarkable tumour regression in human uterus carcinoma UXF1138L xenograft models[123]. Although BRACO-19 has a number of anti-tumour activities, its entry into the cell membrane is a limitation. This restriction on membrane permeability gives it therapeutic value to be an anti-cancer drug [124]. Acridines have been structurally modified [125-128] further to get a new promising and drug-like lead compound, BSG-17, which has entered pre-clinical trials as an anti-tumour agent.

1.1.18 PIPER

PIPER is one of the most potent perylene diimides, shown to bind with G-quadruplex DNA through a π-π stacking interaction with the terminal G-tetrad as demonstrated by NMR studies[129]. Further experiments using single-stranded and duplex DNA showed that PIPER is complexed with duplex DNA, limiting its selectivity to G-quadruplexes. Later, PIPER was found to stabilize the secondary architecture of G-quadruplexes by preventing the unwinding of it through the inhibition of G-quadruplex-specific helicases Sgs1 and T-ag [130]. This result led to further ligand development through a number of studies involving side chain optimisation, resulting in new analogues targeted to improve their telomerase inhibitory potentials[131-133]. The biological evaluation of these newly-synthesized analogues is not extensively aimed at scrutinising them to produce a drug-like molecule, which may be a major drawback in the future development of PIPER as a potent anti-cancer agent.

1.1.19 TMPyP4

Cationic porphyrins like TMPyP4 are commonly chosen to use as G-quadruplex ligands [134]. The ligand TMPyP4 was first reported to interact with DNA 40 years ago; it has since been shown to be a G-quadruplex ligand [135, 136] with significant interaction; its four cationic side chains were reported to interact with each of

the four grooves of G-quadruplexes [136]. Since then, the DNA-interacting capacity of this ligand has been widely assessed and it has been found to have a high level of affinity toward G-quadruplex DNA with poor selectivity [137-139]. However, sometimes it might be peculiar to show extraordinary responses such as the unfolding of quadruplexes in both d(CGG) repeats [140] or antithrombin aptamer [141] and RNA sequences r(CGG) repeats [142]. Interestingly, this ligand has interactions with the wide variety of quadruplexes and shows binding ability toward duplex DNA [143], RNA, triplex DNA [144] and DNA-RNA hybrids [145]. Thus it is still extensively studied and analysed to investigate its interactive mode and capacities towards the different forms of DNA [146]. Interestingly, crystallographic studies revealed that TMPyP4 did not stack to the G-tetrads, but rather intercalate into or stack to base pairs formed by the DNA loops [147]. This finding was found to be consistent with the previous evidence of its poor selectivity towards quadruplexes with respect to duplex DNA [137, 138]. However, TMPyP4 and its analogues were found to exhibit their cytotoxic effects against a number of cancer cell lines with IC_{50} values of more than 50μM [136, 148, 149]. Moreover, they were also shown to downregulate c-MYC [114] and *k-ras* genes [51].

1.1.20 Telomestatin

Unlike chemically-synthesized BRACO-19 and TMPyP-4, telomestatin was first extracted from the bacterium *Streptomyces anulatus 3533-sv4* [150, 151]. It has been reported to be the most potent telomerase inhibitor to date. It was identified as a G-quadruplex ligand based on its unique cyclic aromatic structure, resembling the G-quartet plane, which was established by molecular modelling studies [152]. It is shown to interact with both intra- and intermolecular G-quadruplexes with about 70 times more affinity than for duplex DNA. Telomestatin has been proved to be a prolific anticancer agent in a number of cancer cell lines. It inhibits cellular growth through inhibition of telomerase, shortening the telomere, displacing telomerase associated proteins POT1 and TRF2 from telomerase and facilitating apoptosis, causing cell death [153, 154]. However, it is challenging to synthesize this ligand chemically [155]. A good number of structurally similar and related molecules have been studied in order to try and reproduce its potency as a G-quadruplex ligand [156-158].

1.1.21 $RHPS_4$

A five-ring-containing polycyclic acridine, $RHPS_4$ was first reported by Gowan's group as a potent telomerase inhibitor and has been shown to interact with G-quadruplexes by stacking at the end of the G-quadruplex in vitro [159]. Subsequently, it was demonstrated to exhibit acute cellular cytotoxicity upon exposure of 21NT breast cancer and A431 vulval cancer cells with a significant reduction of telomerase activity at low concentrations. It has also been shown to reduce the cell growth in a number of melanoma cell lines by targeting the enzyme telomerase. However, further studies have suggested that the anti-proliferating effect of $RHPS_4$ was not due to the telomerase shortening but rather a dysfunction of telomerase with an alteration of telomeric capping [160]. This, in turn, causes the interruption of the cell cycle, senescence, apoptosis and telomeric fusions. *In vivo* studies have showed that $RHPS_4$-exposed MCF-7 cells appear to be more sensitive to a combination therapy such as the combination of $RHPS_4$ with taxol or doxorubicin [161]. This combinatory effect was thought to be caused by the enhanced telomerase dysfunction [162, 163].

A large number of ligands targeting G-quadruplexes have already been reported to date. These molecules have been primarily designed through the rational drug design technique [164, 165]. The common feature of all these G-quadruplex interacting ligands is that they have extended planar functionalized polycyclic aromatic systems (Table 1.1). They can be categorized into two classes: putative groove binders [166] and end polycyclic aromatic chromophores. The second class is composed of cationic porphyrins (e.g. TMPyP4), anthraquinones or perylenes.

Polycyclic ring systems within these ligand types are assumed to provide more π-π stacking interactions with the terminal quartet of G-quadruplexes. Many of them appear to have a positively charged cationic side chain so that they can interact with the phosphate backbone of G-quadruplexes. Thus most of the drug design process is based on targeting the π-π interactions [134] and introducing moieties to interact with the DNA backbone (for example, amidic tails) [121]. One example of this is the design of the porphyrin TMPyP4.

Although these ligands molecules can have a higher interactivity toward their target sequence G-quadruplex, they are mostly non-drug like and deviate from

the Lipinski Rule of Five concerning potential for oral bioavailability [167, 168]. This is due to their planar surfaces, high molecular weights (~600 or above), lipophilicity and (for some) their significant charge and poor water solubility [169].

1.1.22 Quarfloxin

To date, CX-3543 or itarnafloxin (generally known as quarfloxin) is the only G-quadruplex ligand from the large number studied to have progressed to phase II clinical evaluation for therapeutic values against malignancies such as neuroendocrine tumours [170 171]. This G-quadruplex-targeting ligand helps to move nucleolin from the nucleolus to the nucleoplasm through redistribution of it. This specifically breaks the nucleolin-G-quadruplex entity and thereby inhibits Pol I transcription to facilitate apoptosis [172, 173].

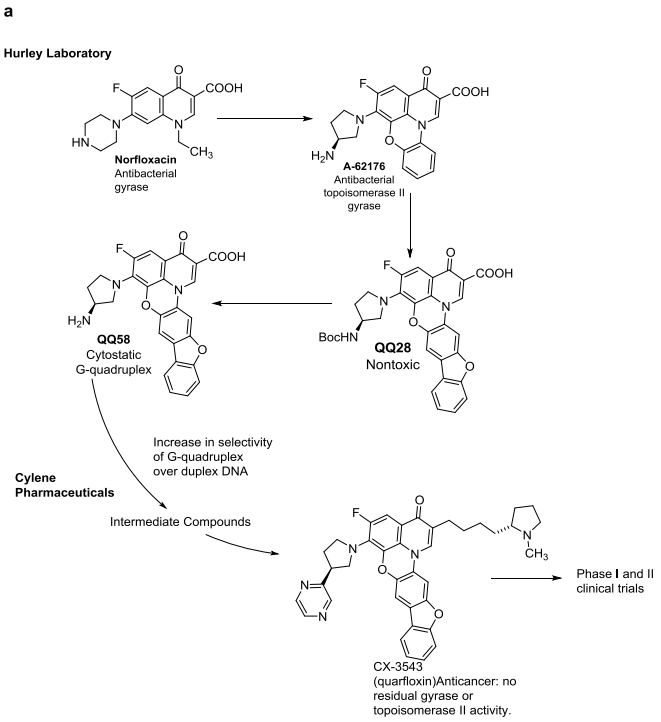

Figure 1.29: The synthesis and clinical progression of quarfloxin. This is the only molecule developed by Hurley and coworkers, enter into the phase-II clinical trails. [taken from Shankar Balasubramanian LHH, and Stephen Neidle. Nature Reviews Drug Discovery. April10(2011): 261-75.] [58].

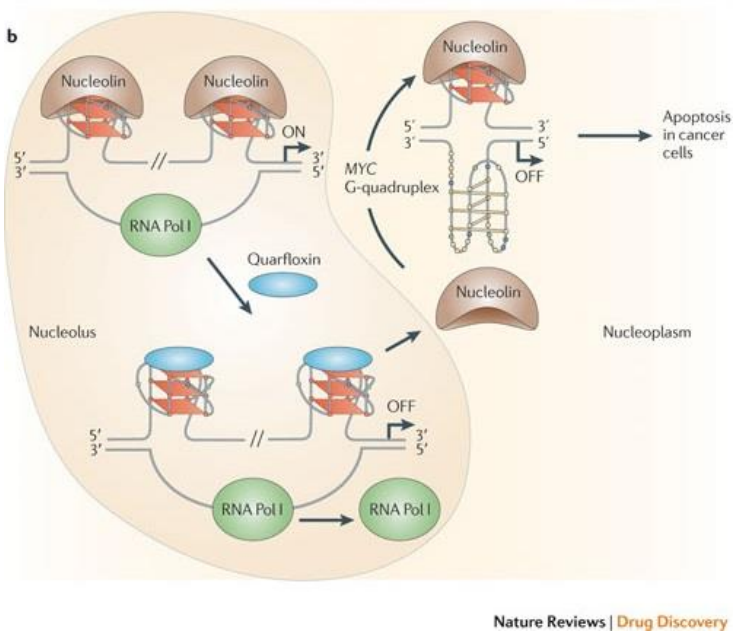

Figure 1.30: Diagram illustrating the proposed mechanism of action of quarfloxin upon the redistribution of transcription coactivator nucleolin into the nucleoplasm [taken from Shankar Balasubramanian LHH, and Stephen Neidle. Nature Rev Drug Disco. (2011): 261-75.] [58]

After penetrating the nucleus, quarfloxin dissociates nucleolin from the G-quadruplex. Therefore, nucleolin gets redistributed within the nucleoplasm which in turn triggers the process of apoptosis and ultimately inhibits tumour growth **(Figure 1.30)** [28].

1.1.23 Other G-quadruplex-Targeting Agents Reported

Many other G-quadruplex-targeting potential ligands **(Figure 1.31)** have already been developed to date. These include triazine derivatives, shown to be potent inhibitors of telomerase with cytotoxic activity at sub-cytotoxic concentrations [174, 175], diamidoanthraquinones such as GSU1051, found to show a different degree of selectivity and potency towards G-quadruplexes [109], 2,6-pyridine dicarboxylate derivatives such as 360A[176], shown to bind telomeres *in vivo* [177], and the phenanthroline analogue EDL35 [178] and isoalloxazines [35], shown to inhibit *c-kit* expression. Many of these ligand molecules are presently in different preclinical stages and some are likely to enter into clinical use.

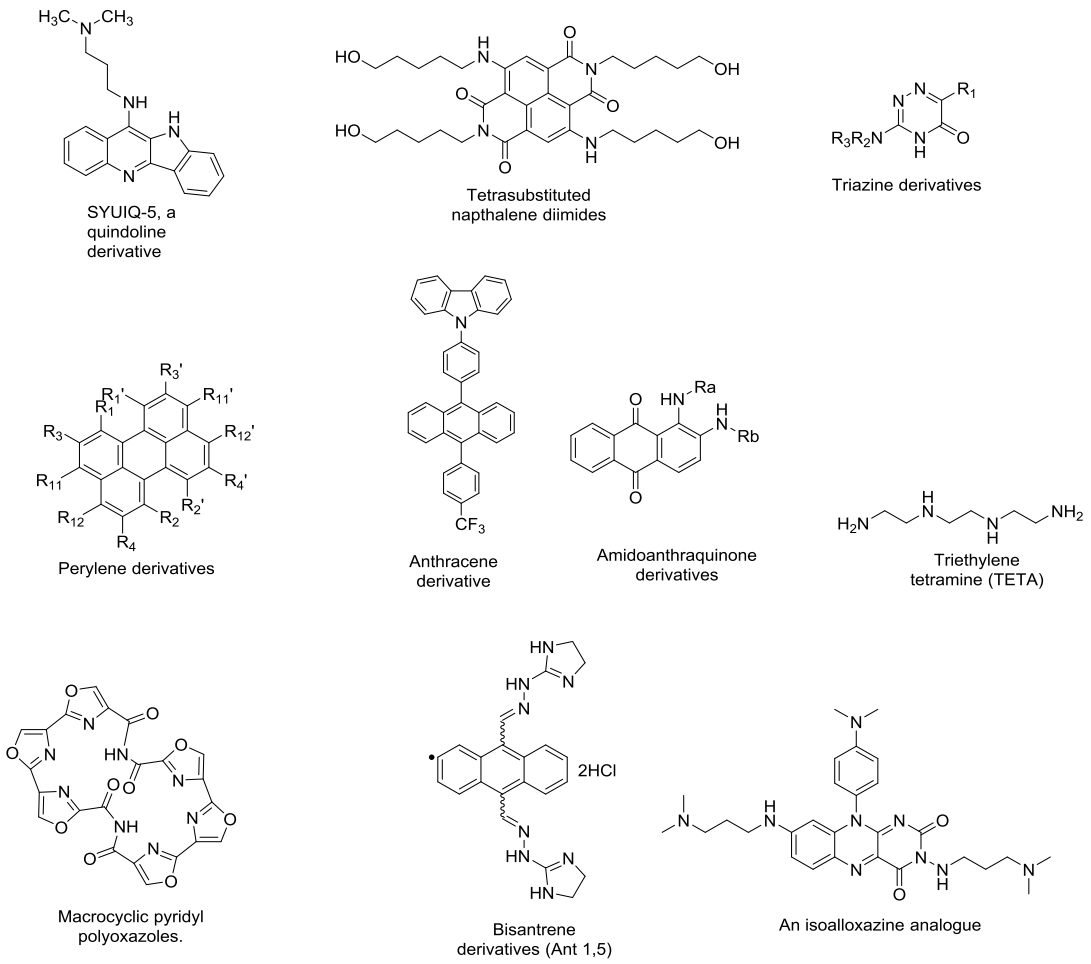

Figure 1.31: Structures of some G-quadruplex-interacting compounds.

However, newly developed rational and drug-like molecules are being reported regularly with relevance to the G-quadruplex area of nucleic acid research. Recently published reviews on this issue provide important insights into G-quadruplex ligands[179, 180].

SYUIQ-05, a quindoline derivative, is reported as a c-myc-oriented G-quadruplex targeting ligand. Unlike other ligands, it has shown insignificant interaction with human telomeric G-quadruplexes. Therefore, it was found to inhibit cancer cell proliferation through selective binding with quadruplexes formed within the G-rich NHEIII1 (Nuclear hypersensitive element) of the promoter region of c-myc [181, 182]. It has been reported to induce apoptosis and cancer cell senescence[183-186].

Tetrasubstituted naphthalene diimides have been reported to be highly active and selective ligands for G-quadruplexes, especially for human telomeric and c-kit-2 G-quadruplexes [187]. They induce G-rich sequences to form G-quadruplex

structures with parallel loops and have been shown to prevent hPOT1 and topoisomerase IIIα from binding telomeres [188]. They also appear to inhibit telomerase in MCF7 cells [118]. They are highly cytotoxic in a number of cancer cell lines with IC_{50} values of ~0.1 µM.

Anthracene derivatives have been found to bind with telomeric quadruplexes, impairing telomere function, inhibiting cancer cell proliferation and promoting senescence [189].

Both amidoanthraquinone and perylene derivatives have been reported to be telomeric G-quadruplex-binding ligands and thereby they inhibit telomerase with the inhibition of cancer cell proliferation[190-192].

Macrocyclic pyridyl polyoxazoles are reported to be selective ligands for G-quadruplexes over duplex DNA [193, 194].

Triethylene tetramine (TETA) has been reported to interrupt telomerase function by inhibiting human telomerase reverse transcriptase (hTERT) expression and promoting tumour cell senescence[195, 196].

Bisantrene, synthesized from an anthracene derivative through the substitution of two side chains (4, 5-dihydro-1H-imidazol-2-yl-hydrazonic groups) at the 1 and 5 or 1 and 7 positions of the aromatic ring, has been reported to bind G-quadruplexes on telomeres and inhibit telomerase [189, 197].

A tetra-substituted naphthalene-diimine derivative (MM41) **(Figure 1.32)** has been reported as a strong ligand, targeting BCL-2, k-RAS1 and k-RAS1 gene promoter-oriented G-quadruplexes, as it shows significant ΔTm values of 26.4 °C, 22.5 °C and 19.8°C, respectively, from FRET experiments.

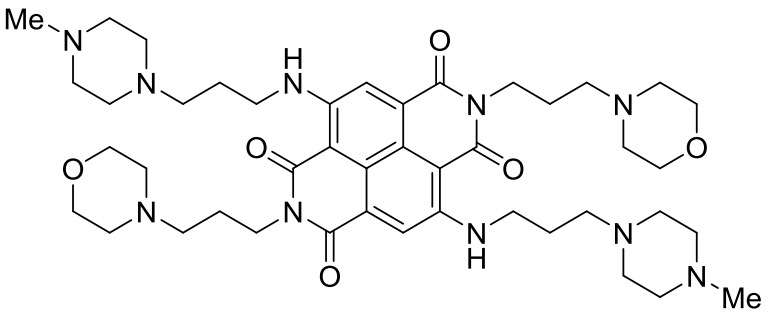

Figure 1.32: The structure of MM41.

This ligand molecule is found to have significant *in vivo* anti-tumour potential against the MIA PaCa-2 pancreatic cancer xenograft model [198].

Distamycin A, a polyamide chemical compound, is being used as an anti-cancer drug [199]. This drug prefers A-T rich minor grooves as this groove proves a narrow space to achieve tight contact and strong van der Waal's interactions. However, distamycin alters the DNA conformation by changing structural dimensions within the particular part of the minor groove, in turn hampering the interaction of transcription factors, and ultimately altering genetic control [200].

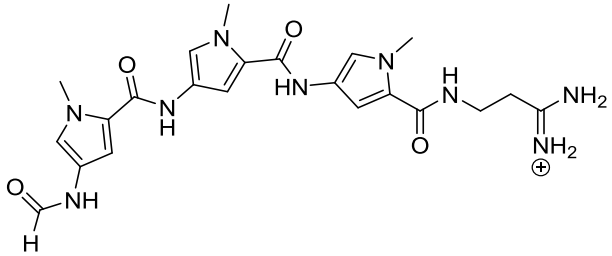

Figure 1.33: Structure of Distamycin A.

Recent NMR studies show that distamycin A **(Figure 1.33)** also has binding affinity towards G-quadruplexes and stacks upon the terminal plane of G-quadruplex conformations. They either interact as a dimer with two of the four grooves of the quadruplex or two molecules of distamycin A sit over each of the two G-tetrads planes [201].

Stephen Neidle's group reported that the pyrrole group's (specially 2,5 bi-substituted pyrrole group) inclusion within the distamycin A structure increases its affinity towards quadruplexes. They synthesized a number of polyamides by linking pyrrole rings based on the distamycin A molecules. Subsequently, they evaluated those molecules through the FRET melting assay. Few of these structurally modified molecules displayed a higher affinity for G-quadruplex DNA over duplex DNA than that of distamycin A [202].

Recently, the Thurston/Rahman Group has reported a new set of G-quadruplex selective acyclic bi-aryl polyamides based on a distamycin motif **(Figure 1.34)** [203]. They replaced pyrroles by introducing biaryl building blocks to switch preference to quadruplex DNA from duplex DNA, using the distamycin scaffold

as a molecular backbone. G-quadruplex ligands of this novel class showed a high degree of selectivity towards quadruplex DNA over duplex DNA.

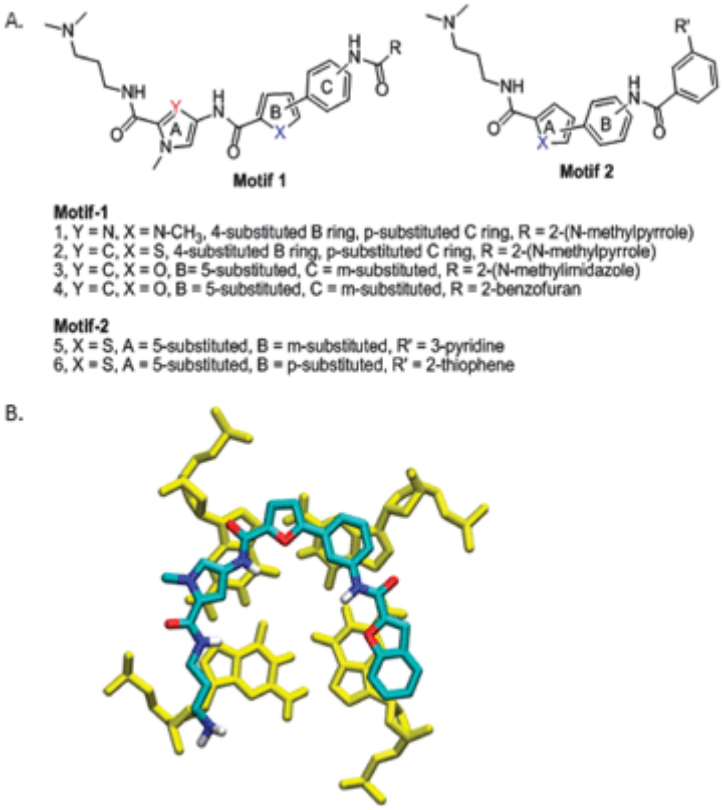

Figure 1.34: A) Structures of the biaryl polyamides synthesized by the Thurston/Rahman Group [203]. B) Crystal structure based on the molecular model of compound 4, which is shown to interact to the terminal G-tetrad (yellow) of a human intramolecular telomeric quadruplex–ligand complex, shows the distinguishing U shape of the biaryl polyamides [taken from Rahman KM, Reszka AP, Gunaratnam M, Haider SM, Howard PW, Fox KR. Chem comm. 27(2009):4097-9.] [203].

Those ligands with relatively large aromatic ring systems can be used as a rational scaffold to attempt to make molecules with improved affinity for quadruplex DNA while retaining selectivity. The design strategy is to change or introduce different functional groups and phenyl rings to target a particular type of quadruplex [203].

More recently, the Thurston/Rahman Group has identified 13 different drug-like chemical scaffolds by screening three different NCI chemical libraries **(Figure 1.35)** [117].

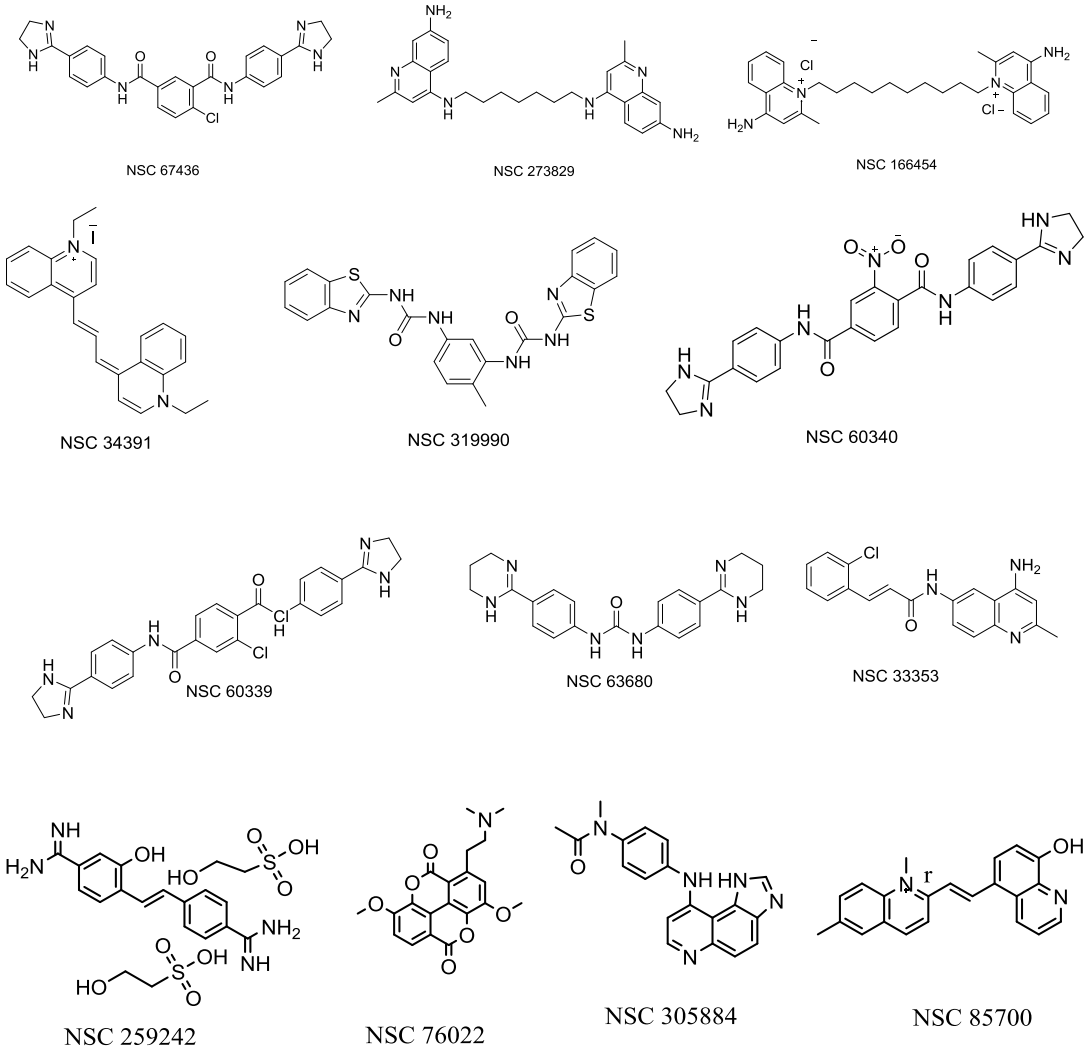

Figure 1.35: Structures of the thirteen compounds of diverse chemical structure with selective telomeric G-quadruplex-binding activity discovered by the Thurston/Rahman Group.

These compounds were screened from a total of 2307 structurally diverse molecules and evaluated through a FRET-based melting assay. These compounds showed notable binding affinity towards telomeric G-quadruplex sequences and it should prove possible to modify them to enhance their affinity for different quadruplex sequences.

Molecules, especially 1, 3-phenylene-bisbenzothiazole-urea (NSC 319990), a reported Chemokine Receptor 2 (CCR2) antagonist, are shown to be more selective stabilisers of telomeric G-quadruplex structures. It achieves 22.7°C stabilisation of the same at 1 µM concentration. Therefore, it could be a target scaffold to achieve structural modification with different benzofused building blocks for optimum activity [204].

In fact, a good number of molecules interacting with DNA have already been reported, having benzofused rings in their structures. Some of them are discussed below.

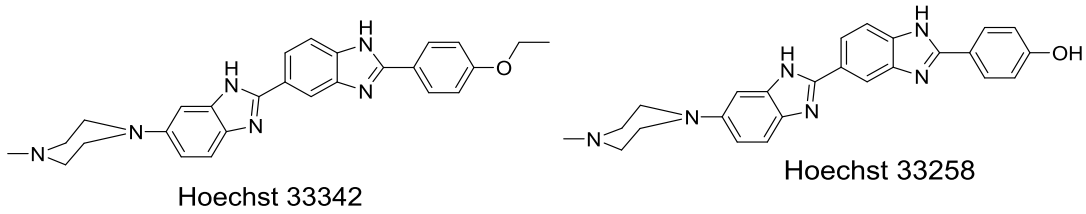

Figure 1.36: Structures of Hoechst 33342 and Hoechst 33358.

Hoechst stains, particularly Hoechst 33258 and Hoechst 33342 **(Figure 1.36)**, are blue fluorescent dyes used for staining DNA in emission or excitation spectra[205, 206]. These minor groove-targeting fluorescent compounds have two benzofused rings (benzimidazole rings) linked to one another. These flat molecules preferentially bind to AT base pairs and stabilise target DNA through hydrogen bonds, Van der Waals and electrostatic interactions [207].

A lot of structural modification on Hoechst 33258 has already been done to tune its activity towards specific DNA sequences[208, 209]. Maji *et al*. (2013) reported that they synthesized molecules based on Hoechst 33258.

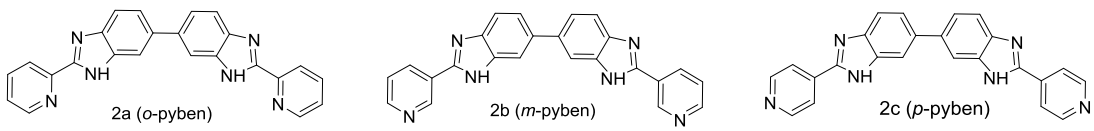

Figure 1.37: Structures of three isomers 2a (o-pyben), 2b (*m*-pyben) and 2c (*p*-pyben).

They replaced the phenolic group and piperazine residue at both ends of Hoechst 33258 with *p*-pyben, *m*-pyben and *o*-pyben, respectively, to achieve positional isomers. The molecules they synthesized, named (2a), (2b) and (2c) **(Figure 1.37)**, are found to show selectivity towards telomeric G-quadruplexes over duplex DNA [210].

Novel indole derivatives, including bis-indole carboxamide and a derivative containing pyridine, **(Figure 1.38)** have been reported to interact with G-quadruplex sequences.

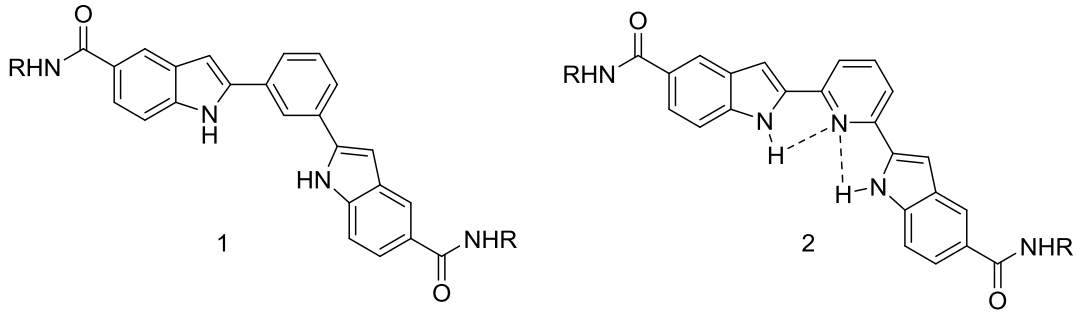

Figure 1.38: Structures of cationic bis-indole derivatives 1 and 2.

These molecules appear to exhibit a high stabilization capsid against F21T, c-kit-1, c-kit2 and c-myc quadruplex sequences [211].

1.1.24 Biological Consequences of G-quadruplex-Targeting Ligands

Ligands interacting with G-quadruplex DNA are shown to give biological responses *in vivo*; in some cases they are supported by *in vitro* observations as well. There are a number of biological effects including anti-proliferative activities at sub-cytotoxic concentrations in various cancer cell lines, inhibition of telomerase, induction of senescence and apoptosis, telomere shortening, chromosomal end-to-end fusion and DNA damage responses. Many cancer xenografts with various models have been found to show anti-tumour activity of individual ligands and in combination with other anticancer drugs. Initially, these activities shown by using different ligands were explained on the basis of telomerase inhibition, but now it is believed that the antitumor activity is not only due to the telomerase inhibition; the binding of the ligands to telomeres and the

subsequent telomere uncapping are also thought to be responsible for these biological effects.

Recently, it has been evident that telomerase plays an independent role in maintaining telomere length during the process of tumorigenesis [212]. In fact, telomerase at high expression levels is well connected with the development of cancer. Differences in both the telomeric lengths of cancer or normal cells and the levels of telomerase activity could both be particular indications for the selective toxicity effects of particular G-quadruplex ligand molecules *in vivo*. G-quadruplex ligands are found to inhibit the expression of several oncogenes[20, 213].

Human telomerase reverse transcriptase (hTERT) is highly expressed in cancer cells. It has been shown that oncogene c-myc-encoded transcription factors play a direct role in the upregulation of telomerase activity in cancer cells, as they stimulate expression of hTERT among others genes. The reduced telomerase activity due to G-quadruplex ligand binding could be correlated with reduced expression of oncogenes like c-myc [214].

Biological evaluations are suggesting that G-quadruplex ligands are mainly dual-action molecules. The main mode of action is still thought to be the inhibition of telomerase activity. On the other hand, some other biological responses implicate an inhibitory role of G-quadruplex ligands in the transcription of particular genes. These different findings have attracted research into ligands molecules which can discriminate between various G-quadruplex-forming sequences with different topologies within the human genome, with the aim of developing a more selective G-quadruplex ligand to act on a specific oncogene for the induction of selective biological responses.

1.1.25 Design of New G-quadruplex Stabilizer

Hurley and co-workers first reported the potential binding of cationic porphyrin TMPyP4 with telomeric G-quadruplexes in 1998 [215]. They proposed that TMPyP4 has an appropriate size and shape to stack with the G-tetrads in order to stabilise quadruplex DNA after obtaining the structural and conformational information of the telomeric G-quadruplex through UV and NMR spectroscopy

studies. They investigated the G-quadruplex stabilizing capacity of TMPyP4 through several techniques and they also evaluated a large number of TMPyP4 analogues and completed a SAR study to elucidate the mechanism of action and to identify the lead porphyrin TMPyP4. This lead molecule has been reported to be an effective inhibitor of human telomerase in HeLa cell extract. Accordingly, porphyrin TMPyP4 showed an IC_{50} of 6.5 ±1.4 µM [215].

Another promising method to design G-quadruplex stabilizing ligands is molecular docking**.** It is a computer-assisted drug design technique to visualise three dimensional features and evaluate newly-proposed drugs within their receptors. It informs about effective binding between ligand and receptor and at the same time helps to choose a rational molecule from a molecular library to fit with a specific topological conformation of diversified G-quadruplexes. The overall selection process involves several steps **(figure 1.39)** [28].

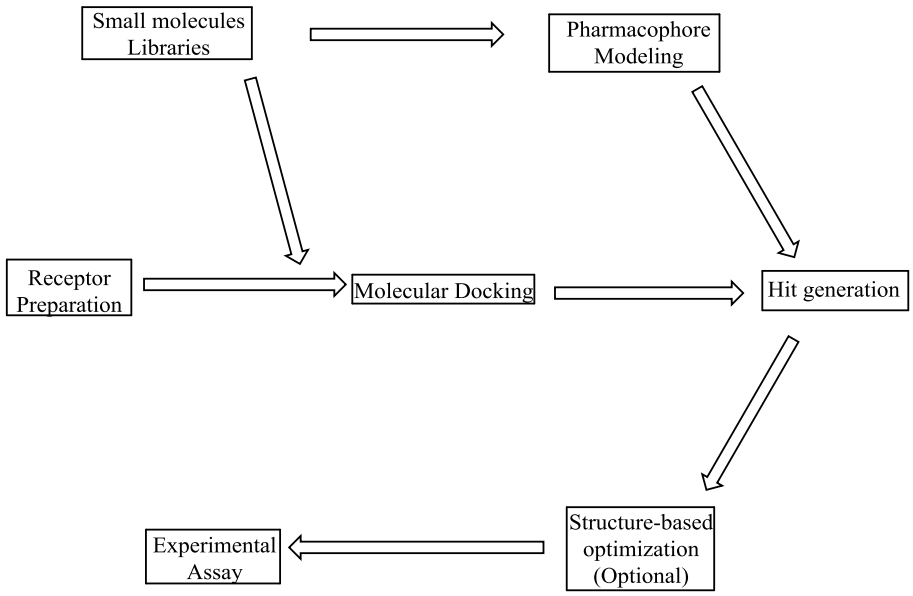

Figure 1.39: Sequential drug design process using a molecular docking system [28].

This process has been successfully used to develop G-quadruplex-binding ligands. The following body of work contains a combined process whereby molecular docking and rational design have both been used to develop a library of ligands specific for certain types of quadruplex.

1.2 Biophysical Evaluation of G-quadruplex-Targeting Ligands

There are many biophysical methods used to study the mode and the interaction capacity of ligands molecules towards G-quadruplex secondary structures. Experimental methods, especially different spectroscopic approaches, are widely used for biophysical evaluation of different chemically synthesized G-quadruplex ligand molecules. Some of these techniques are described below in short [216].

1.2.1 Circular Dichroism Spectroscopy

Circular Dichroism (CD) spectroscopy has long been used to study for G-quadruplex structure types and their interactions with targeted ligand molecules. Its capacity to show structural signals based on the conformational differences of the target makes this method an efficient technique in the field of modern biochemistry. The conformational changes observed upon binding of specific ligands can be monitored by this method through the measurement of absorption differences between left-handed and right-handed polarized light. Zero CD intensity shows in the absence of regular structure. Initially, zero CD intensity shows as there no regular structure to monitor, but a specific conformation/structure produces both positive and negative signals in a spectrum. Therefore, it is widely used for the structural analysis of proteins and nucleic acids. Any changes including temperature, salt concentration and pH can significantly modify the DNA secondary structure and this modification exhibits particular signals in the absorption spectrum. It is also useful to know the binding mode and affinity of a ligand molecule [217-219].

1.2.2 UV/Fluorescence Technique

UV or fluorescence spectroscopy is a simple technique used to study the interaction of G-quadruplexes with their corresponding ligand molecules. It gives changes in the intensity and wavelength of the G-quadruplex absorption/emission signals upon the addition of the ligand molecules. Ligand

molecules in free form in solution show well-characterised absorption bands in the visible region. As the drug molecules soon complex with the secondary structure, it causes a maximum shift of this band. Therefore this method is an easy approach to determine the degree of ligand affinity toward G-quadruplex structure. However, these techniques can be used for both qualitative and quantitative analyses, like stoichiometry and binding constants of ligand molecules with DNA[146, 220].

DNA secondary structure stabilization by a specific ligand molecule can also be measured through thermal studies where UV absorbance of different temperatures is monitored at a certain wavelength.

1.2.3 Isothermal Titration Calorimetry

Isothermal Titration Calorimetry (ITC) is used for the direct measurement of thermodynamic characteristics such as binding affinity constant, enthalpy and stoichiometry of interaction between the G-quadruplex DNA and ligands. ITC can measure the heat either released or absorbed during DNA-ligand interactions. By measuring this heat, it is possible to characterise the total thermodynamic profile of a DNA-ligand interaction in a solution. The heat values represent the molar ratio between ligand and G-quadruplex and thereby provide a parameter to know the degree of interaction of ligand toward G-quadruplex. This technique has the capacity to allow direct comparison of a large number of ligand molecules like TMPyP4 and acridine in order to study their interaction capacity with G-quadruplex secondary structures[221, 222].

1.2.4 DNA Footprinting

A method which is used for determining the selectivity and interacting capacity of a ligand binding with a target DNA sequence *in vitro*, DNA footprinting involves the target sequence containing radiolabelled DNA fragment being first incubated with the ligand. It is then allowed to be digested with the enzyme DNase I. DNase I is widely chosen as it can bind with the minor groove and break the phosphodiester bonds of the DNA template. This enzyme cuts the DNA in a random manner, but the sequence bound by ligand remains

protected. The resulting fragments are subjected to polyacrylamide gel electrophoresis (PAGE) for separating into different bands. The gel is then visualised by phosphor imager screen. The specific ligand-bound part of the target DNA can be identified by the absence of fragments corresponding to the cleavage of DNA in that region. This is also a simple method to investigate whether a ligand can selectively bind to a specific sequence of DNA [223].

1.2.5 Equilibrium Dialysis

It is a simple and convenient method to evaluate the interacting capacity and sequence selectivity of a G-quadruplex-targeting ligand molecule. This process involves two chambers separated by a selectively semi-permeable membrane which allows only ligand but not G-quadruplex to pass through. G-quadruplex DNA of known concentrations is placed in each of these two chambers. The ligand molecules can easily pass from their own chamber to the other chamber, while the G-quadruplex is retained in its chamber[224, 225]. Therefore, ligand molecules move freely between these two chambers and they are supposed to interact with the target G-quadruplex in the other chamber.

The ultimate concentration of free ligand molecules becomes the same in both chambers at the equilibrium stage. If the ligand molecules bind with the G-quadruplex, the ligand concentration will be higher in the G-quadruplex chamber. Thus the concentrations of ligands can be varied with their respective affinities towards their target G-quadruplex DNA. The concentrations of free and DNA-bound ligand are required to determine the equilibrium binding constant. One of the major advantages of this tool is to measure the low affinity of a ligand molecule which is not detectable by other methods available.

1.2.6 Nuclear Magnetic Resonance

Nuclear Magnetic Resonance has been used for studying the capacity of a ligand molecule to bind with a target G-quadruplex. It provides a distinguishing set of NMR signals in the proton spectrum upon the binding of the ligand with the G-quadruplex. It can also explain the conformational changes that occur due to G-quadruplex-ligand complex formation [226].

1.2.7 Mass Spectrometry

Mass spectroscopy is a common tool used to determine the interacting characteristics between ligands and DNA molecules. The electrospray ionization technique can determine the mass of both the G-quadruplex and a G-quadruplex–ligand complex as this approach allows minimum fragmentation of the biomolecules, which ultimately helps to reveal the stoichiometry of the G-quadruplex-ligand complex [227-230].

1.2.8 Voltammetric Methods

The electrochemical voltammetric approach is also used to investigate the interacting capacity of a ligand toward its target G-quadruplex sequences. Data obtained from the voltammetric method helps to determine the binding constant (K) and binding site size of the target sequence. The binding site size suggests the binding area in terms of the number of base pairs covered by the ligand molecules. Electroactive species are excited by the application of voltage, which then increases the electric current. The intensity of the electric flow depends on the concentration of species under study. Ligands molecules with binding capacity for DNA reduce the current flow and also reduce the diffusion rate [231, 232].

1.2.9 Viscosimetry Titration

Binding of a ligand to the target DNA changes the viscosity of the DNA solution. The relative specific viscosity coming from the change in the viscosity of the DNA solution upon addition of the ligand molecules can be used to study ligand binding affinity. A ligand which intercalates or electrostatically binds to a target DNA sequence causes conformational distortion in that DNA molecule, which ultimately increases DNA length. Therefore, the titration of duplex DNA with interacting ligands causes an increase of relative viscosity; it is because of the presence of more intercalating agents at the site of base pairs throughout of the target sequence. On the other hand, ligands with less intercalating activity cause no changes of DNA solution viscosity in aqueous state [233, 234].

1.2.10 Melting Experiment

The melting experiment is based on the relative melting temperatures of both ligand-bound DNA and the unbound DNA molecules. It is a specific temperature at which fifty percent of DNA is denatured and takes a single stranded form. Generally ligands have a tendency to stabilize the DNA secondary structure. Thus DNA which is bound with a ligand molecule is found to melt at a higher temperature relative to the unbound DNA. Therefore, higher affinity of a ligand for the DNA results in a higher melting temperature of the ligand-bound DNA. The melting experiment can be monitored by a number of techniques like UV, CD or fluorescence spectroscopy [235].

1.3 FRET-based DNA Melting Assay

Fluorescence Resonance Energy Transfer (FRET) technology is extensively used to evaluate the interacting capacity of ligands towards specific secondary DNA structures like G-quadruplexes by measuring an increase in nucleic acid melting temperature (ΔTm) [236]. The difference between the Tm of the ligand-bound structure and the T_m of the unbound DNA is termed the ΔTm parameter [237]. One strand of an oligonucleotide is labelled with FAM (fluorescein) as a fluorescence donor and complementary strand (or other end of heparin) is labelled with TAMRA as an acceptor [238]. The intensity of the FAM fluorescence upon excitation by heating is then measured as a function of temperature [239].

1.3.1 Principle of FRET

FRET is a fluorescence-based spectroscopic method with distance information based on structural changes of a molecular complex. It is based on the non-radiative energy passing between molecules over long distances (10-80°A). The donor molecule absorbs photons and then transfers the energy gained to the acceptor molecule. The transfer of this energy needs to satisfy two factors: proximity and compatibility. The 'Förster distance' or R_0 (also called the Förster radius, R representing the distance between the donor and acceptor chromophores) is defined as the characteristic distance between donor and acceptor chromophores within which the non-radiative energy transfer is

possible. It is usually within 10 - 80 ^{0}A. At the same time, the absorbance spectrum of the acceptor molecule needs to overlap with the emission spectrum of the donor molecule. This donor fluorophore can only then directly excite an acceptor fluorophore which ultimately emits energy at a new wavelength. Thus activation of the acceptor fluorophore can be detected by emitted energy at a new wavelength. Target DNA sequence and a ligand are associated together to make a stable complex with lower energy. The interacting affinities of different ligands toward target DNA sequence are assessed by the changes in their stabilisation through their corresponding melting temperatures. FRET results have been shown to correlate with results from UV melting profiles. Melting curves following the melting process of DNA-ligand complexes represent the corresponding melting temperatures (ΔTm) against various ligands of different concentrations. The changes in the melting temperatures due to the DNA bound ligands can be measured with respect a melting temperature of respective control DNA [240].

A G-quadruplex-forming oligonucleotide (for example, human telomeric F21T sequence) can be labelled with the two fluorescent probes; one is a donor and the other an acceptor **(Figure 1.40)**.

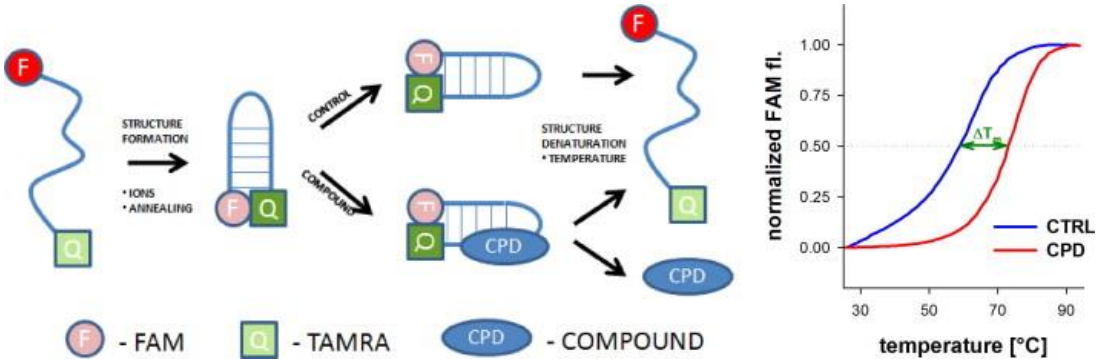

Figure 1.40: Schematic diagram of the experimental determination of the stabilizing effect of a G-quadruplex-binding ligand using FRET Technology.
[taken from Renčiuk D, Zhou J, Beaurepaire L, Guédin A, Bourdoncle A, Mergny J-L. 57(2012):122-8.] [237].

1.3.2 Advantages of the FRET Assay

The FRET technique of DNA melting processes has a couple of advantages over other traditional techniques like CD or UV spectroscopy [241]. FRET-based measurement is a relatively rapid and cheap process to implement, applicable to fluorescent derivatives of any molecular system and is an automatable process that requires a very small amount of DNA sample to monitor the melting process with high precision and accuracy. FRET-based assays with specificity for human DNA have been successfully adopted in a high-throughput format resulting in the rapid measurement of the quadruplex stabilisation potential of synthetic ligands. In contrast, both CD and UV spectroscopy require high concentrations of oligonucleotides, resulting in high costs and their measurements cannot easily be conducted in a high-throughput format. Moreover, the change in absorbance in the UV method is small in comparison with the large signal changes observed in the FRET fluorescence technique. FRET is also a more sensitive technique to determine the stability of a DNA by the means of melting temperature [242].

1.4 Aim of the Current Study

The diversity in shape and nature of G-quadruplex structures could be used to enhance selectivity to a particular type. In particular, analysis and exploitation of the different grooves and loops that are present in different types of G-quadruplex DNA, like Telomeric, *c-kit-1*, *c-kit-2*, and Bcl-2 G-quadruplexes, has not yet been undertaken in a systemic manner from a drug design perspective.

However, the overall goal of this project is to exploit the recent structural information available on human telomeric, bcl-2 and *c-kit* oncogenic DNA quadruplexes to achieve guidelines for the discovery of a novel set of quadruplex-specific small-molecule ligands. Based on the promising quadruplex-selectivity observed for the reported biaryl polyamides [203], the first objective was to synthesize libraries of novel ligands based on this template that could have potentially enhanced selectivity and binding affinity for quadruplex versus duplex DNA, and selectivity for quadruplexes of different types within the specific oncogene sequences. This should provide greater understanding of structure-activity relationships for molecules of this type.

The specific objectives are as follows:

- Synthesise novel benzofused polyamide ligands by replacing the 5-membered heterocycles and central biaryl ring with different benzofused groups using solution phase chemistry.
- Evaluation of the new molecules using the FRET-based DNA thermal denaturation assay (including duplex competition) and also circular dichroism (CD) spectroscopy for determining their affinity and selectivity for a number of different G-quadruplex sequences including the c-Myc quadruplex.
- Evaluation of the novel ligands for cytotoxicity against a panel of relevant tumour cell lines such as MDA-MB-231(Triple negative breast cancer cell line), HeLa (Cervical cancer cell line) etc.
- A longer term objective of the project is to select a suitable candidate ligand for evaluation in a human tumour xenograft mouse model of a specific cancer type associated with the oncogenic quadruplex being targeted. Ligands with antitumor activity in this model may be selected for further preclinical studies with a view for progression to phase-I clinical trials.

Chapter 2: Results and Discussion

2.1. Introduction

A new set of G-quadruplex-selective acyclic biaryl polyamides based on a distamycin motif **(Figure 2.1)** [203] has already been reported by the Thurston/Rahman Group. They replaced pyrroles by introducing biaryl building blocks to switch preference to quadruplex DNA over duplex, using the distamycin scaffold as a molecular backbone. G-quadruplex ligands of this novel class showed a high degree of selectivity towards quadruplexes like HT4, C-kit-1 and C-kit-2 G-quadruplexes over duplex DNA.

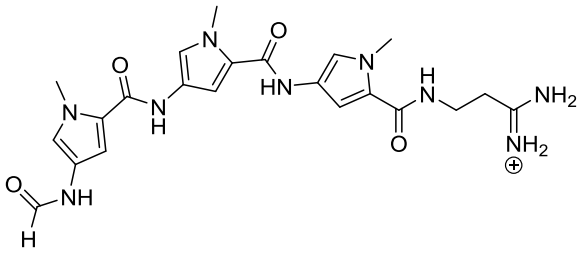

Figure 2.1: Structure of Distamycin A.

The Thurston/Rahman Group has also previously identified 13 different drug-like chemical scaffolds by screening three different NCI chemical libraries. They screened those compounds out from a total of 2307 structurally different molecules and they evaluated them through the technique of FRET-based DNA melting assay. These compounds showed notable binding affinity towards telomeric G-quadruplex sequences. It is possible to modify their structures with the help of molecular modelling and bio-physical assay to enhance their affinity towards different quadruplex sequences.

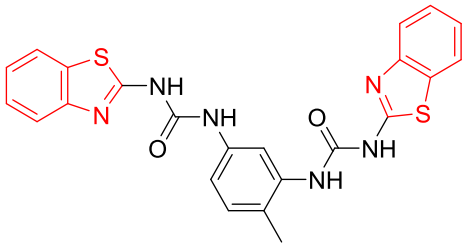

NSC 319990

Figure 2.2: Structure of 1, 3-phenylene-bisbenzothiazole-urea (NSC 319990) with benzofused rings (red).

Molecules, especially 1,3-phenylene-bisbenzothiazole-urea (NSC 319990) **(Figure 2.2)**, a reported Chemokine Receptor 2 (CCR2) antagonist, are shown to be more selective stabilisers of telomeric G-quadruplex structure. It does 22.7°C stabilisation of the same at 1 µM concentration. Therefore it could be target scaffold to get a structural modification with the different benzofused building blocks for optimum activities [204].

In fact a good numbers of molecules interacting DNA have already been reported, having benzofused rings in their structures. Some of them are discussed below-

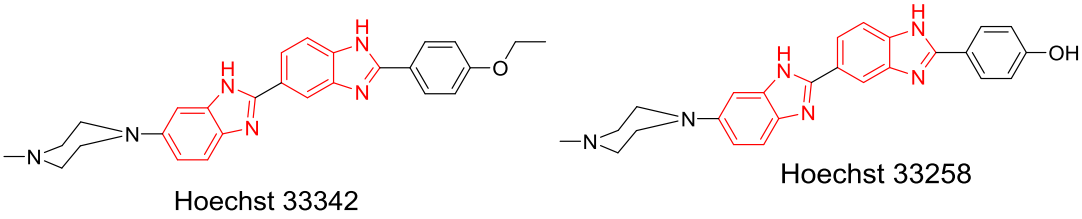

Figure 2.3: Molecular structures of Hoechst 33342 and Hoechst 33358. Benzofused rings are shown as red.

Hoechst stains particularly Hoechst 33258 and Hoechst 33342 **(Figure 2.3)** are blue fluorescent dye, being used for staining DNA in emission or excitation spectra [205, 206]. These minor groove targeting fluorescent compounds having two benzofused rings (benzimidazole rings) linked one after another. These flat faced molecules preferentially bind to the AT base pairs and stabilize the target DNA by forming hydrogen bonds, Vander Walls and electrostatic interactions[207].

A lot of structural modification on Hoechst 33258 has already been done to tune its activity towards specific DNA sequences interested[208, 209]. Maji *et al*. 2013 reported that they synthesized few molecules basing Hoechst 33258.

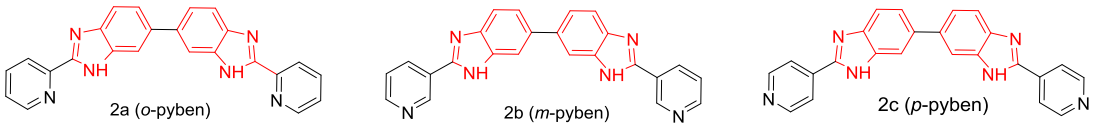

Figure 2.4: Three isomers 2a (o-pyben), 2b (*m*-pyben) and 2c (*p*-pyben). Benzofused rings are shown as red.

They replaced the phenolic group and piperazine residue at both ends of Hoechst 33258 with *p*-pyben, *m*-pyben and *o*-pyben respectively to have the positional isomers. The molecules they synthesized named (2a), (2b) and (2c) **(Figure 2.4)** are found to show the selectivity towards telomeric G-quadruplex over duplex DNA [210].

In 2008 Dash and his group has also reported by the synthesis of novel indole derivatives including bis-indole carboxamide and a derivative containing pyridine to target G-quadruplex sequences **(Figure 2.5)**.

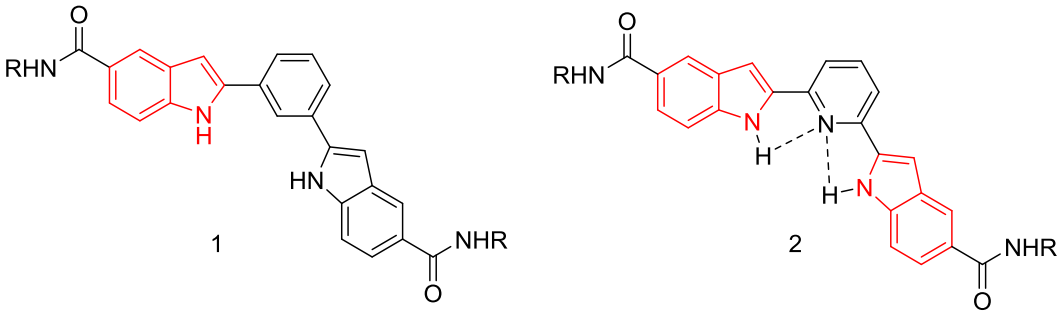

Figure 2.5: Cationic bis-indole derivatives 1 and 2 Benzofused rings are shown as red.

They evaluated these ligands through FRET-based melting analysis. These molecules appear to exhibit high stabilization capacity against F21T, c-kit-1, c-kit2 and c-myc quadruplex sequences [211].

Therefore, a novel class of biaryl polyamides developed by the Rahman and Thurston group was taken as a template and benzofused building blocks of different types were chosen to make another new class of molecules which were assumed to be more potent and drug-like G-quadruplex ligands.

2.1.1 Rational Design of Benzofused Polyamide Synthesis

A number of different benzofused polyamides were synthesized based on biaryl polyamide as a structural motif. A benzofused building block was initially

coupled with a tertiary amine tail through an amide coupling reaction. Then two other consecutive benzofused carboxylic acids were coupled in a same way to synthesize a benzofused polyamide. Benzofused units were incorporated in place of the pyrrole and furan rings of biaryl polyamide motif **(Figure 2.6)**.

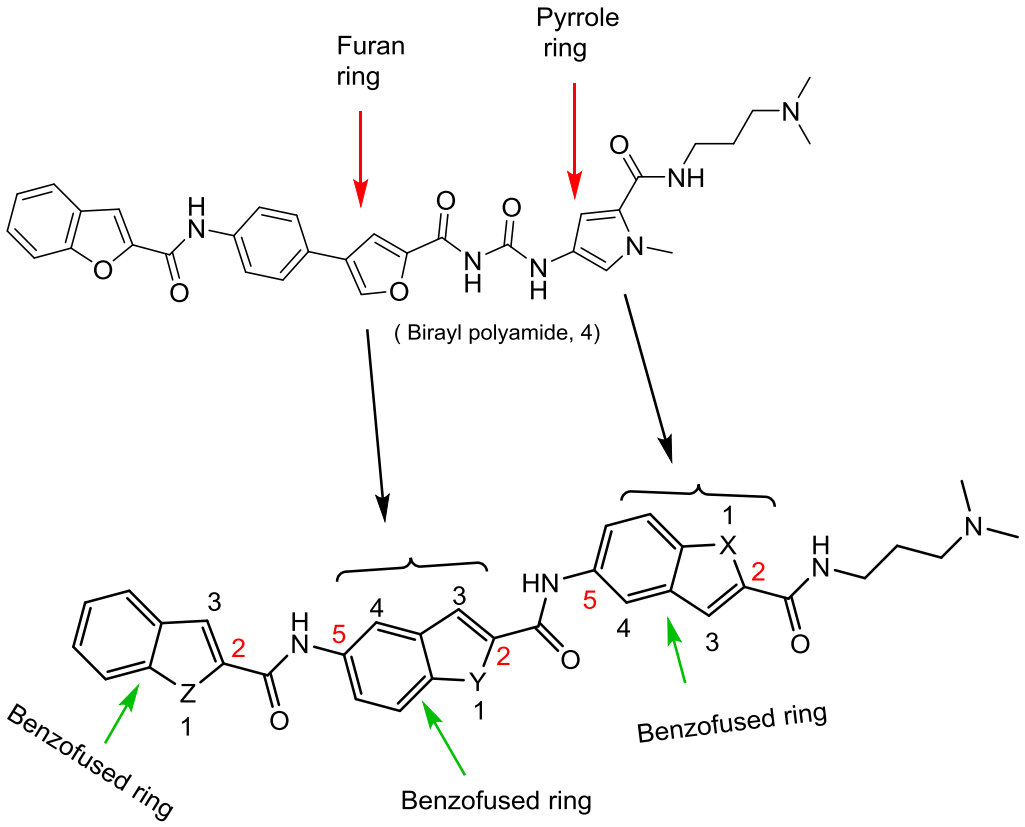

Figure 2.6: Benzofused building blocks incorporated in place of the pyrrole and furan rings of biaryl polyamide, 4 motifs.

The idea is that the inclusion of more aromatic ring systems within biaryl polyamides is supposed to provide more π electrons to achieve improved π-π interaction between the G-quartet and polycyclic ring system of the ligand molecules **(Figure 2.6)**.

2.2 Rational Approaches and Strategies for Designing Different Libraries

As many as 10 libraries of benzofused polyamides were designed and synthesized throughout the project period. FRET-based DNA melting assays and Molecular Modelling and Molecular Dynamics (MD) Studies on the molecules of a previous synthesized library provided the guidelines for

designing the structural motifs of the next libraries. These rational strategies helped to achieve better G-quadruplex interacting molecules**.**

2.2.1 Design and Rationale of Library-1A Molecules

At the beginning of this project, a set of benzofused polyamides (8 in total) were synthesized by adding three consecutive 5-nitro-benzofused-2-carboxylic acid units through the HOBt-DIC mediated amide coupling reaction with a tertiary amino tail *via* the N^1,N^1-dimethylpropane-1,3-diamine building block. This followed the 5′-2′ substitution reaction. A structural motif of these molecules is shown below **(Figure 2.7)**.

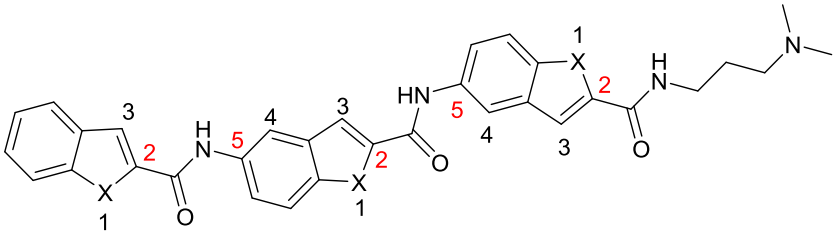

Figure 2.7: The basic chemical scaffold for 5'-2' substituted benzofused polyamides; X= O or N or S.

2.2.2 Design and Rationale of Library-1B Molecules

As the molecules belonging to **library-1A** did not show any significant interaction towards any of the G-quadruplex sequences used in the FRET-based analysis, a similar set of molecules (10 in total) were synthesized with structural modifications through the replacement of the tails and the functional groups at the third benzofused ring; these formed **library-1B**.

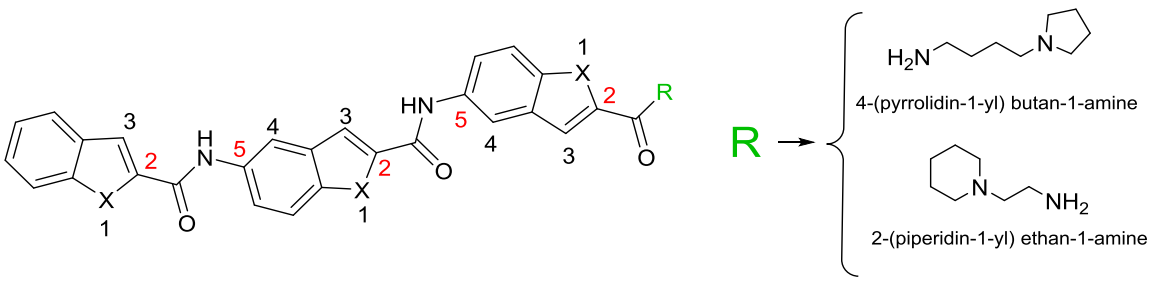

Figure 2.8: The basic chemical scaffold for 5'-2' substituted benzofused polyamides; X = O or N or S and R represents the tertiary amine tails including 4-(pyrrolidin-1-yl) butan-1-amine and 2-(piperidin-1-yl) ethan-1-amine.

These modifications were done to investigate whether these molecules gave any improved interaction towards G-quadruplex DNA types. A structural motif of these molecules is shown below **(Figure 2.8)**.

2.2.3 Design and Rationale of Library-2 Molecules

As the molecules belonging to both **library-1A** and **1B** did not show a significant interaction with G-quadruplex DNA types, a set of new molecules (9 molecules in total) were synthesized with the help of molecular modelling studies **(Figure 2.21, 2.22 in sections 2.5).** Here, a 5-nitro-benzofused-3 carboxylic acid was included as a second building block instead of 5-nitro-benzofused-2-carboxylic acid so that ligand molecules would have relatively more curvature in their structures compared to the **library-1** ligand molecules. Commercially available 5-nitro-indole-3-carboxylic acid was introduced as the second building block through the 5′-3′ substitution instead of 5′-2′ substitution as used for synthesizing **library-1A** and **1-B** molecules. The structural motif of this library is shown below **(Figure 2.9)**.

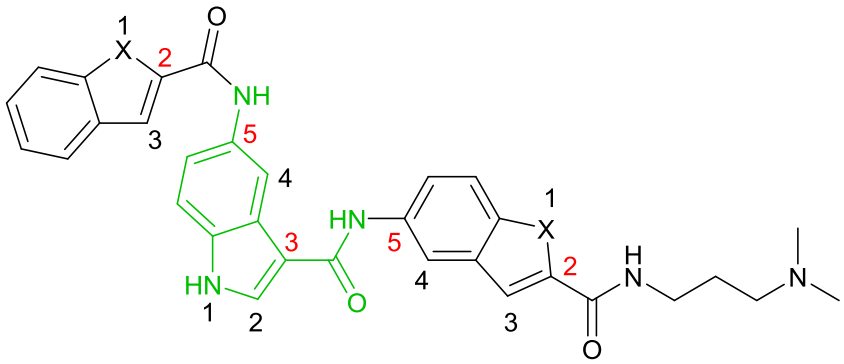

Figure 2.9: The basic chemical scaffold for **library-2** molecules; X= O or N or S.

2.2.4 Design and Rationale of Library-3A Molecules

As the introduction of curvature within the **library-2** molecules made the benzofused polyamides more potent towards the G-quadruplexes used, it encouraged the development of another library of molecules with enhanced curvature within the same scaffold. Therefore, two sets of molecules were synthesized by including two consecutive molecules of the 5-nitro-benzofused-3- carboxylic acid unit in a benzofused polyamide structure in two different fashions. A first set of molecules was synthesized by coupling two consecutive

5-nitro-indole-3-carboxylic acids followed by termination with four different benzofused acids **(Figure 2.10 (A))**. A second set of molecules was then synthesized by starting with a 5-nitro-benzofused-2-carboxylic acid, which was then immediately coupled with 5-nitroindole-3-carboxylic acid and terminated with four different benzofused-3-carboxylic acids **(Figure 2.10 (B))**.

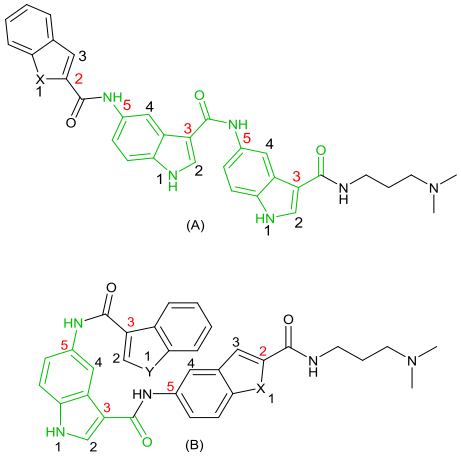

Figure 2.10: The basic chemical scaffolds for **library-3A** molecules. (A) and (B) represent each set of molecules within this library. Here X = O, N, S.

2.2.5 Design and Rationale of Library-3B Molecules

This library was aimed at investigating the effect of an electron-withdrawing nitro-group at the terminal indole unit. Therefore the **library-3A** molecules were modified by keeping the nitro group of the terminal 5-nitro-indole-3-carboxylic acid unit without changing the shape of the molecules. The structural motif of **library-3B** is shown **(Figure 2.11).**

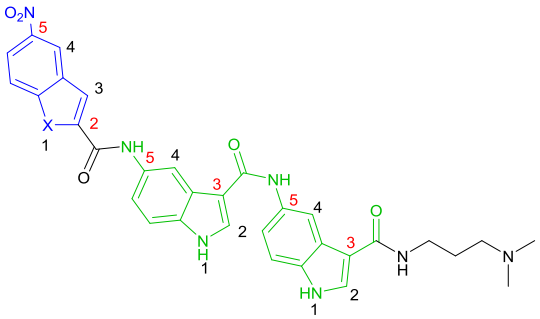

Figure 2.11: Structural motif of **library-3B** molecules. Here X = O, S, N.

As one (**4.77**) of the compounds **(Figure 2.39)** in this library showed a significantly higher interaction with G-quadruplex sequence types, that

benzofused polyamide (**4.77**) was taken as a lead ligand for further structural modifications through a structure-activity relationship (SAR) study. The structure-activity relationship (SAR) was done with various possible modifications of the shape, tail types and functional groups attached to the terminal building block as shown on the structural motif.

It was found that the electron-withdrawing nitro group plays a positive role in enhancing the ligand-G-quadruplex interaction and at the same time it was apparently found that the indole is comparatively better than any other type of nitro-benzofused-acid building blocks used. The most curved molecule was found to be the most interactive towards G-quadruplex types as shown in the FRET-based DNA melting assay.

2.2.6 Design and Rationale of Library-4A Molecules

Molecular docking studies of molecules containing three consecutive 5'-3' benzofused moieties (for example, **4.93**) **(Figure 2.39)** suggested that the inclusion of a third 5'-3'-substituted benzofused moiety should enhance G-quadruplex stabilisation to a small degree compared to two 5'-3'-substituted benzofused moieties (for example, **4.77**) **(Figure 2.39)**.

A new library of molecules containing four different benzofused polyamides was synthesized to investigate the relevance of the electron-withdrawing NO_2 group to the activity of the most active compound **4.93**. The common structural motif of **library-4A** molecules is shown here **(Figure 2.12)**.

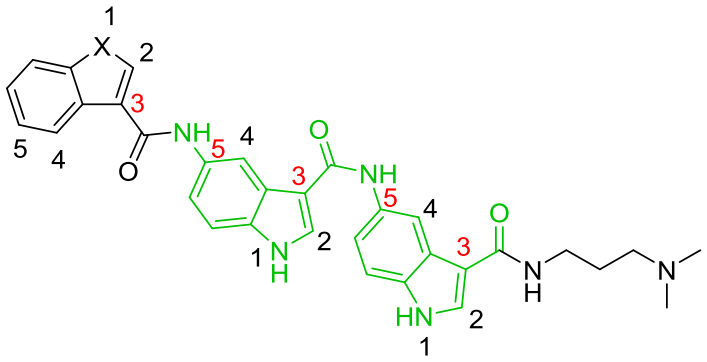

Figure 2.12: The basic chemical scaffold for **library-4A** molecules. Here X = O, N, S.

2.2.7 Design and Rationale of Library-4B Molecules

Here, the most interactive lead ligand **4.93** was optimised through tertiary amine tail modifications. Therefore, a set of molecules was synthesized by structural modification of lead compound through the substitution of the N^1, N^1-dimethylpropane-1,3-diamine tail with different tails including 3-(piperidin-1-yl)propan-1-amine, 3-(pyrrolidin-1-yl)propan-1-amine, 3-(4-methylpiperazin-1-yl)propan-1-amine and 3-morpholinopropan-1-amine tails, respectively.

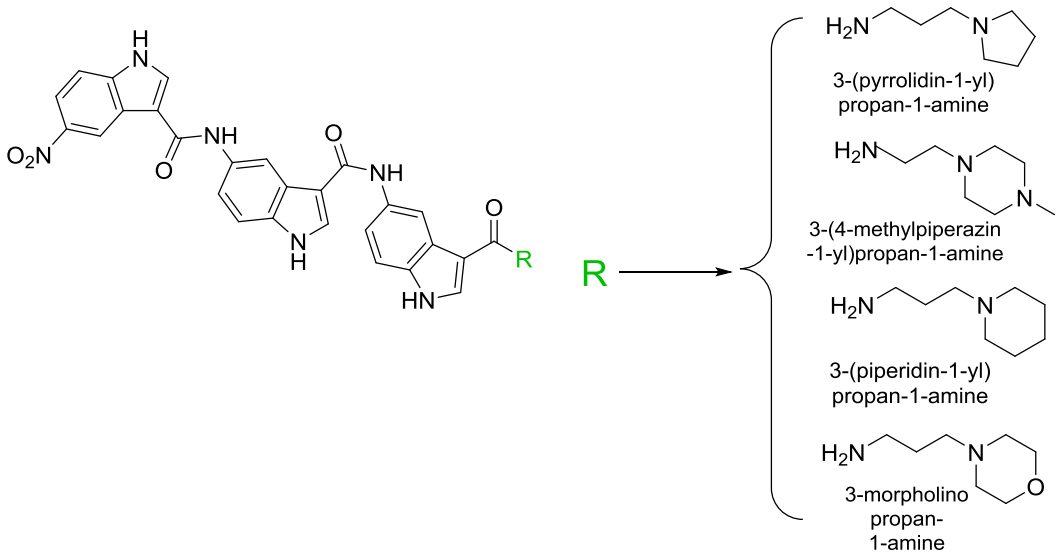

Figure 2.13: The chemical scaffold for 5′-3′ substituted benzofused polyamides for **Library-4B**. Here, R represents the tertiary amine tails including 3-(pyrrolidin-1-yl) propan-1-amine, 3-(4-methylpiperazin-1-yl) propan-1-amine and 3-(piperidin-1-yl) propan-1-amine and 3-morpholinopropan-1-amine.

2.2.8 Design and Rationale of Library-4C Molecules

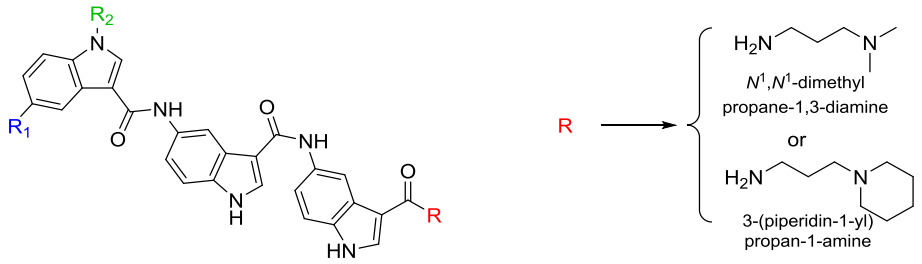

Here, R_1 = CN, Cl, $–OCH_3$, $-NH_2$, etc. and R_2=$–CH_3$, functional groups.

Figure 2.14: The structural motif of **Library-4C**.

Here, the functional groups attached to the terminal benzofused unit of the lead compound **4.93** were optimised. Thus a set of molecules was made by structural modification of **4.93** through the substitution of nitro-groups with different functional groups **(Figure 2.14)**.

2.2.9 Design and Rationale of Library-4D Molecules

Here a set of molecules were synthesized through the replacement of indole with indazole rings to investigate the preference between indole and indazole as a chemical scaffold for G-quadruplex ligands. The structural motif is given below **(Figure 2.15)**.

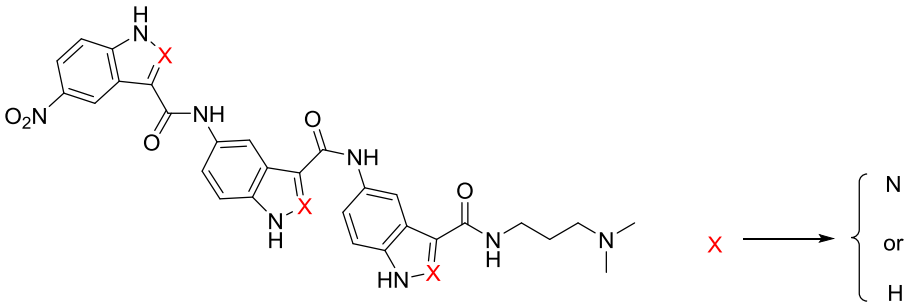

Figure 2.15: The structural motif of **Library-4D** molecules.

2.2.10 Design and Rationale of Library-5 Molecules

Two sets of molecules were made by using commercially available 5-nitro-indole-3-carboxylic acid and 5-nitro-indazole-3-carboxylic acid building blocks targeting the shape of lead molecule **4.93 (Figure 2.71)**. This library was designed with an aim to check whether benzofused polyamides of three consecutive benzofused units were better interactive ligands over benzofused polyamides of two consecutive benzofused units. The structural motif of **Library-5** is show below **(Figure 2.16).**

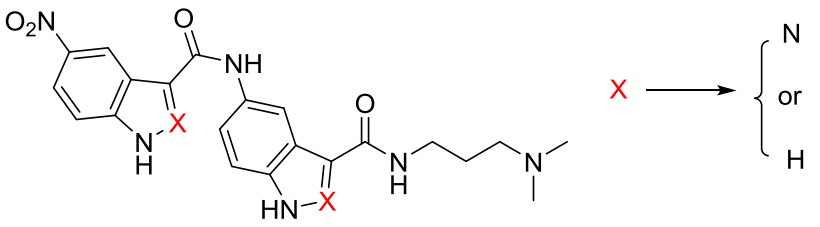

Figure 2.16: The structural motif of **Library-5** molecules.

Library-1A

2.3 Synthetic Scheme for Library-1A Molecules

A set of 8 molecules **(Figure 2.18)** were synthesized by 5′-2′ substitution of benzofuran and benzothiophene building block types. A nitro-benzofused acid was initially coupled with a N1, N1-dimethylpropane-1,3-diamine tail to make an amide. Then two consecutive benzofused acids were coupled one after another through amide coupling reactions to make benzofused polyamides **(Figure 2.17)**.

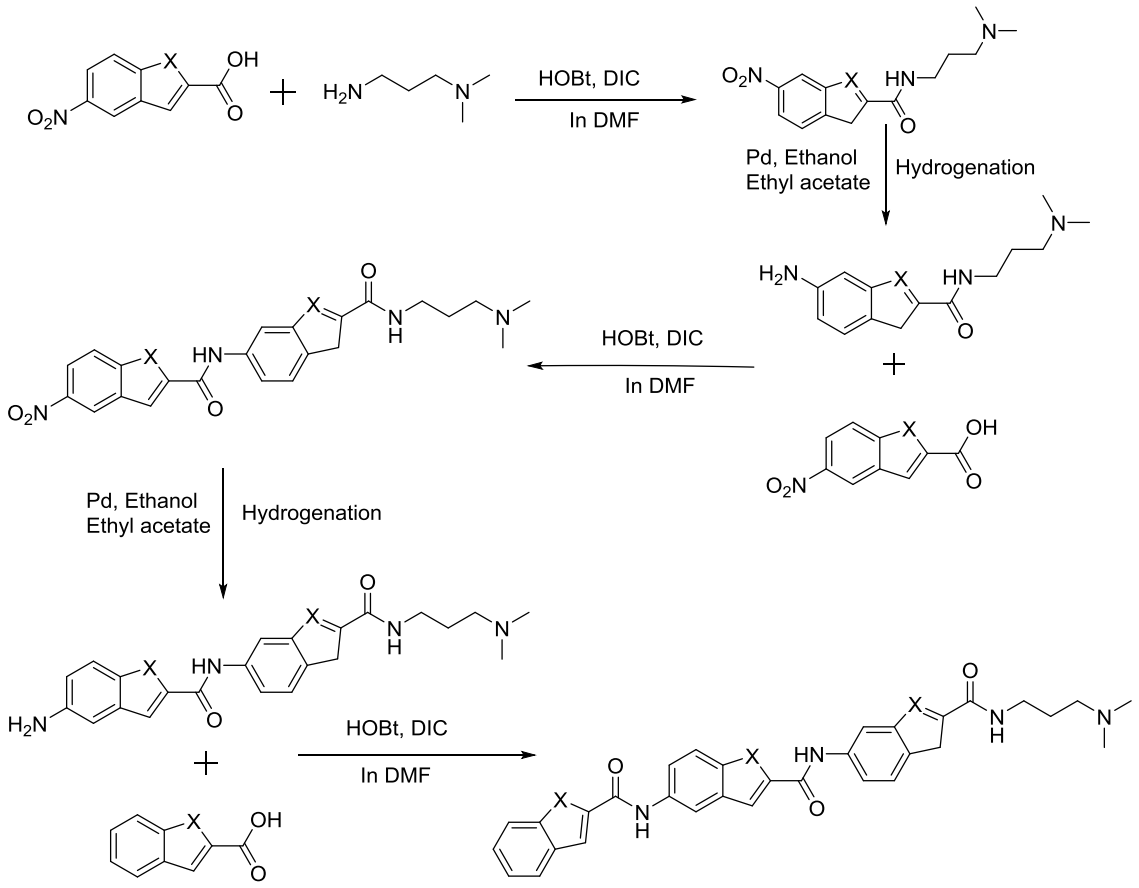

Figure 2.17: Synthetic scheme of **Library-1A** molecules. Here X= O or N or S.

Initially the acid (1.2 eq.) was dissolved in DMF (5 mL for 100 mg of starting material) in a round bottom flask fitted with a magnetic stirrer. Then DIC (1.75 eq.) and HOBt (2.0 eq.) were added to the acid (1.0 eq.) and this mixture was allowed to stir at room temperature for the formation of the ester from the acid. The amine (1 eq.) was added to the mixture and the mixture allowed stirring until the reaction was complete, as indicated by TLC or LCMS. Finally the

reaction mixture was applied to a conditioned SCX-2 cartridge and the resultant product was purified by the 'Catch and Release' method (described in the section '**Methods and Materials**' of Chapter 3).

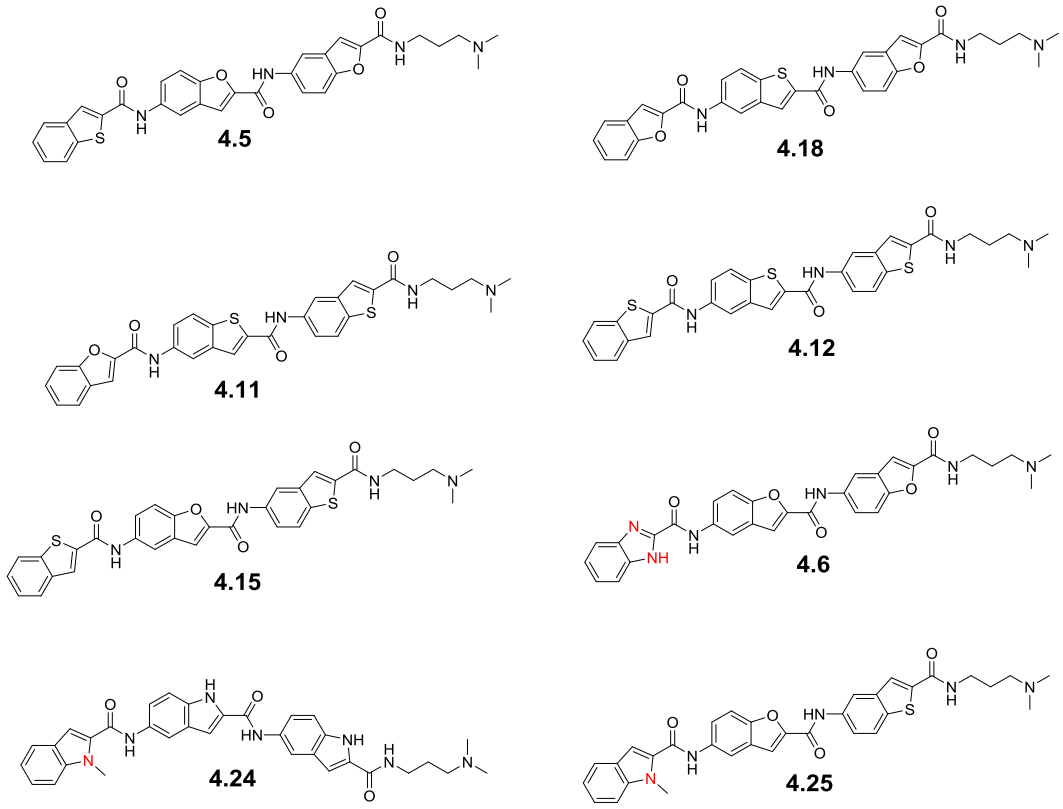

Figure 2.18: Structures of benzofused polyamides of **library-1A** molecules.

2.3.1 Characterisation of Library-1A Benzofused Polyamides through Various Spectroscopic Techniques

The benzofused polyamides of this library were purified and fully characterized by different spectroscopic techniques including mass spectrometry, both ^{1}H and ^{13}C NMR, and IR techniques (described in the '**Experimental**' section of Chapter 4). Compounds were primarily identified by LCMS and confirmed using high resolution mass spectroscopy (HRMS) **(Table 2.1)**. Finally the characterised compounds were evaluated by a FRET-based DNA melting assay.

Table 2.1: HRMS data for **library-1A** molecules

Number	Compound code	Theoretical mass	Observed mass $[M+H]^+$
1	**4.5**	580.1780	581.1851
2	**4.18**	580.1780	581.1851
3	**4.11**	596.1552	597.1625
4	**4.12**	612.1324	613.1395
5	**4.15**	596.1552	597.1625
6	**4.6**	564.2121	565.2187
7	**4.24**	575.2645	576.2714
8	**4.25**	593.2097	594.2169

2.3.2 Purity Analysis of Benzofused Polyamides Synthesized

The purity of the benzofused polyamides of this library was checked by two different HPLC methods with two different retention times. Both methods were carried out on a Waters Alliance 1695 HPLC Pump with water and acetonitrile comprising the mobile phases. The Waters 996 PDA start wavelength was 210 nm for the 10 minute method (Method A), with a start wavelength of 220 nm and end wavelength of 500 nm for the 5 minute method (Method B) **(Table 2.2)**.

Table 2.2: Purity data for **library-1A** observed by LCMS

Number	Compound code	Purity	
		Method A (10 min)%	Method B (5 min)%
1	**4.5**	100	100
2	**4.18**	100	100
3	**4.11**	100	100
4	**4.12**	100	100
5	**4.15**	100	100
6	**4.6**	91	89.09
7	**4.24**	100	100
8	**4.25**	100	100

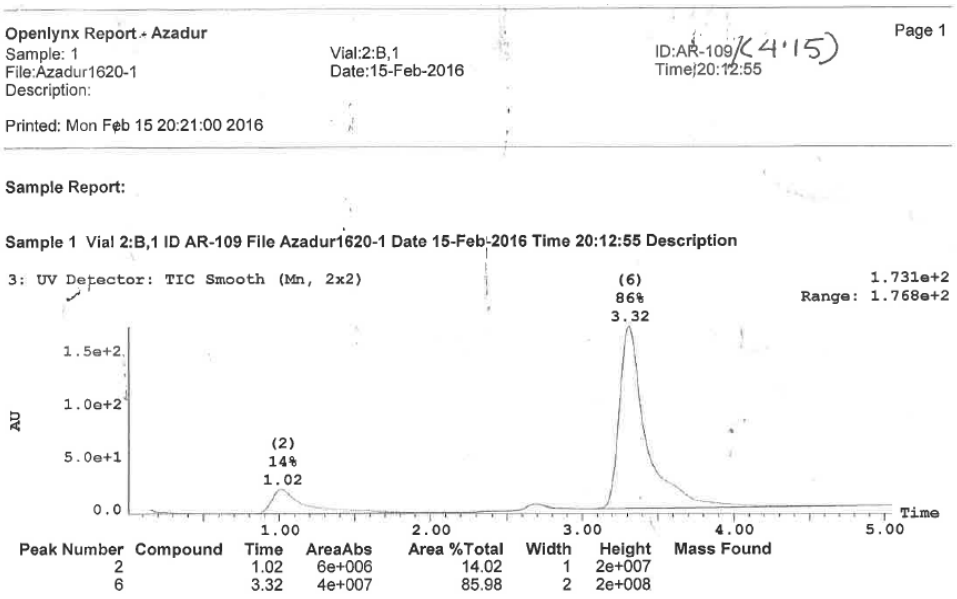

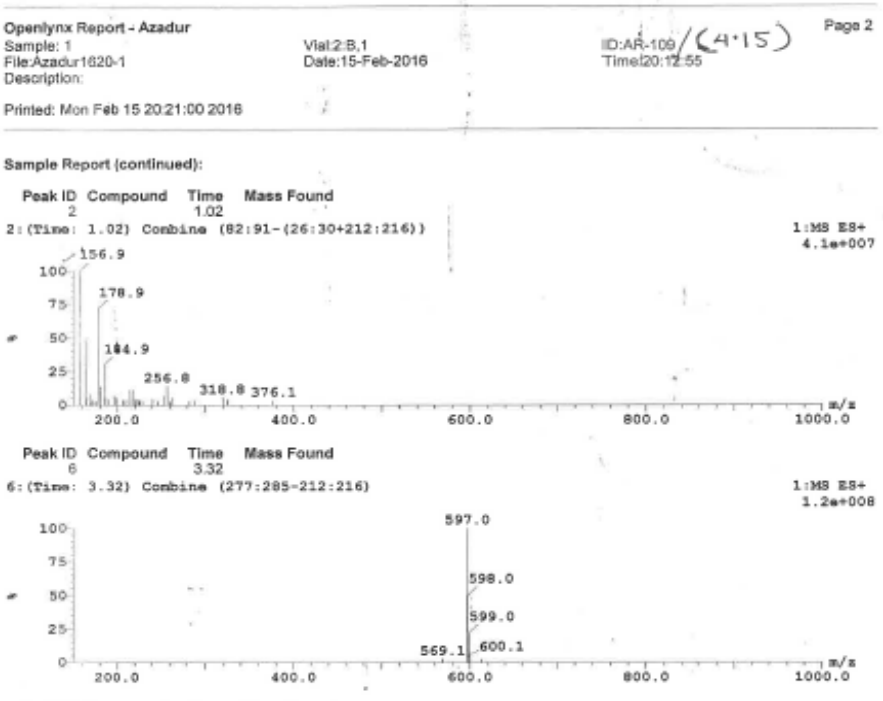

Figure 2.19: Example of an adapted LCMS profile of **Library-1A** compound **4.15**

Table 2.3: G-quadruplex and duplex DNA stabilization by ligands of **library-1A** in FRET melting experiments at concentrations of 5, 2 and 1 µM respectively (the data are means of three technical repeats)

Compounds	Quadruplex types	ΔT_m(°C) ±(s/d)		
		5 µM	2 µM	1 µM
4.5	F21T	0.2±0.21	0.2±0.14	0.0±0.26
	C-kit-1	1.6±0.15	0.9±0.15	1.1±0.20
	C-kit-2	1.5±0.05	1.1±0.49	1.2±0.43
	BCL-2	1.6±0.60	1.5±0.15	1.3±0.15
	Duplex DNA	0.0±0.15	0.0±0.20	0.0±0.17
4.18	F21T	7.0±0.07	2.0±0.36	0.8±0.05
	C-kit-1	3.8±0.26	1.8±0.26	1.6±0.45
	C-kit-2	9.7±0.25	3.8±0.11	2.4±0.26
	BCL-2	5.7±0.1	0.9±0.30	0.6±0.35
	Duplex DNA	1.2±0.11	0.0±0.06	0.0±0.11
4.11	F21T	6.3±0.11	4.7±0.15	2.8±0.23
	C-kit-1	3.5±0.11	1.3±0.20	0.9±0.37
	C-kit-2	8.4±0.30	3.8±0.25	2.5±0.35
	BCL-2	0.8±0.17	0.9±0.16	0.7±0.32
	Duplex DNA	0.0±0.05	0.0±0.25	0.0±0.24
4.12	F21T	1.8±0.05	0.6±0.1	0.7±0.2
	C-kit-1	1.3±0.45	0.7±0.49	0.5±0.39
	C-kit-2	4.1±0.17	1.9±0.45	1.4±0.30
	BCL-2	1.5±0.25	1.2±0.20	1.2±0.25
	Duplex DNA	0.0±0.12	0.0±0.15	0.0±0.07

Table 2.4: DNA Stabilization by ligands of **library-1A** in FRET at concentrations of 5, 2 and 1 µM respectively (the data are means of three technical repeats)

Compounds	Quadruplex	ΔT_m(°C) ±(s/d)		
		5 µM	2 µM	1 µM
4.15	F21T	20.1±0.28	3.6±0.20	2.2±0.25
	C-kit-1	3.1±0.41	1.4±0.30	0.2±0.49
	C-kit-2	9.2±0.25	3.8±0.05	2.3±0.30
	BCL-2	17.5±0.26	1.8±0.37	0.2± 0.32
	Duplex DNA	0.0±0.11	0.0±0.06	0.0±0.07
4.6	F21T	20±0.32	4.0±0.12	2.0±0.35
	C-kit-1	1.5±0.25	1.3±0.20	1.1±0.17
	C-kit-2	5.0±0.30	2.5±0.11	1.8±0.25
	BCL-2	5.7±0.60	2.2±0.28	1.2±0.057
	Duplex DNA	0.0±0.10	0.0±0.21	0.0±0.16
4.24	F21T	0.8±0.20	0.4±0.31	0.3±0.12
	C-kit-1	1.3±0.40	1.0±0.65	0.7±`0.35
	C-kit-2	3.8±0.45	2.0±0.30	1.3±0.25
	BCL-2	1.2±0.05	0.5±0.25	0.3±0.17
	Duplex DNA	0.0±0.12	0.0±0.07	0.0±0.21
4.25	F21T	2.8±0.34	2.5±0.27	1.3±0.25
	C-kit-1	3.7±0.35	1.5±0.36	1.1±0.36
	C-kit-2	9.4±0.51	3.9±0.28	2.1±0.30
	BCL-2	13±0.32	2.7±0.26	1.5±0.25
	Duplex DNA	0.0±12	0.0±0.05	0.0±0.05

FRET data analysis **(Table 2.3 and 2.4)** showed that only **4.11**, **4.15** and **4.6** had moderate but significant interaction with telomeric F21T sequences and C-kit-2 G-quadruplex sequences. These ligands provided 2.8°C, 2.2°C and 2.0°C stabilisation against telomeric F21T sequences and 2.5°C, 2.3°C and 1.8°C against C-kit-2 G-quadruplex sequences at 1 µM concentrations but they did not show notable interaction with C-kit-1 or Bcl-2 G-quadruplex sequences.

In contrast, **4.5**, **4.18**, **4.12**, **4.24** and **4.25** showed insignificant interaction against all the G-quadruplex sequences used except **4.18** and **4.25** against C-kit-2 sequence as they provide stabilisations of 2.4°C and 2.1°C respectively.

It was observed that some of the molecules, including **4.15** and **4.6**, show significant interactions at higher concentrations (i.e. 5 µM) but suddenly lose their stabilisation capacities at lower concentrations (1, 2 µM). These molecules are assumed to form dimers at higher concentrations (5 µM) and that dimer may interact with the terminal quartet of G-quadruplex architectures. As soon as molecular density goes down at subsequent lower concentrations (1, 2 µM), the melting temperatures fall sharply (for example, ΔTm=3.6°C and 2.2°C for 4.15°C against F21T respectively). This means molecular density is not high enough for dimer formation at low concentrations.

However, all of these ligands are specific toward G-quadruplex sequences as none of these molecules have shown any interaction with duplex DNA.

2.3.3: Key Observations on Library-1A and Library-1B Molecules

A number of conclusions can be drawn from the FRET-based DNA thermal denaturation assays conducted on the **library-1A** molecules.

- These compounds showed insignificant interaction with the F21T (human telomeric G-quadruplex), C-kit-1, C-kit-2 and Bcl-2 G-quadruplexes.
- The inclusion of either a benzofuran or benzothiophene building block in the structure of these molecules does not make any notable difference.
- Linear molecules, especially **4.15** and **4.6**, are assumed to form dimers at higher concentrations (5 µM) and these dimers may interact with the terminal quartets of G-quadruplex architectures.

Library-1B

2.4 Synthetic Scheme of Library-1B Molecules

As a whole, the benzofused polyamides of **library 1-A** were not capable of achieving significant interaction with the G-quadruplex DNA types used. At the same time, the alteration of building block types at their respective positions didn't result in impressive ΔTm values. This means the activity of these ligands was not depend on either the benzofuran or benzothiophene building block types.

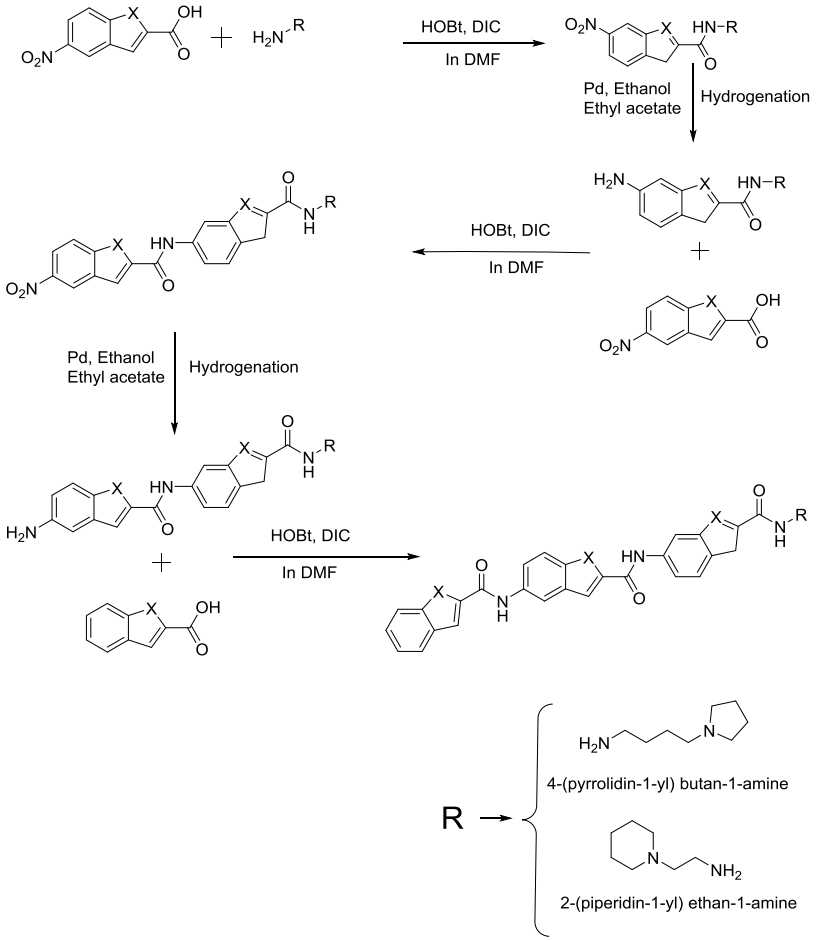

Figure 2.20: Synthetic scheme of **Library-1B** molecules. Here X = O or N or S and R represents the tertiary amine tails including 4-(pyrrolidin-1-yl) butan-1-amine and 2-(piperidin-1-yl) ethan-1-amine.

Therefore, further structural modifications using different tail types were done to design **library-1B (Figure 2.20)** in order to investigate whether different tail types may have any additional effect on the ligand-quadruplex DNA interaction. A nitro-benzofused acid was initially coupled with tail types 4-(pyrrolidin-1-yl) butan-1-amine and 2-(piperidin-1-yl) ethan-1-amine, respectively. Then two

consecutive benzofused acids were coupled further through amide coupling reactions to get benzofused polyamides. This library was comprised of 9 molecules in total (**Figure 2.19**).

Initially, the acid (1.2 eq.) was dissolved in DMF (5 mL for 100 mg of starting material) in a round bottom flask fitted with a magnetic stirrer. Then DIC (1.75 eq.) and HOBt (2.0 eq.) were added to the acid (1.0 eq.) and this mixture was allowed to stir at room temperature for the formation of the ester from the acid.

The amine (1 eq.) was added to the mixture and the mixture allowed to stir until the reaction was complete, as indicated by TLC or LCMS. Finally the reaction mixture was applied to a conditioned SCX-2 cartridge and the resultant product was purified by the 'Catch and Release' method (described in the section '**Method and Materials**' of Chapter 3).

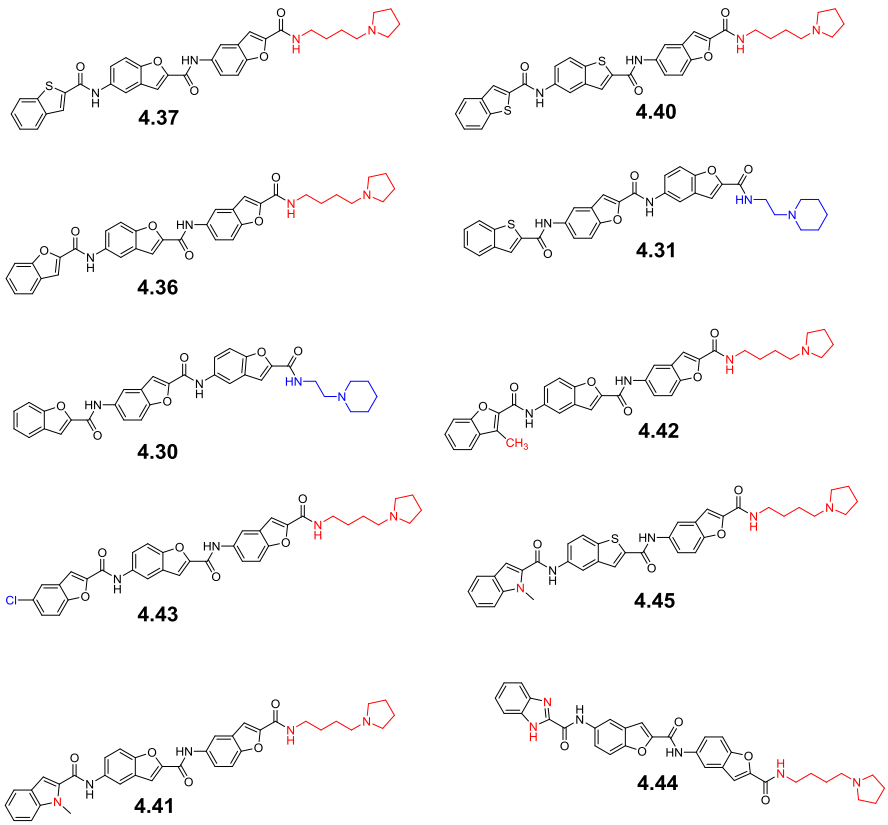

Figure 2.21: Structures of the **library-1B** molecules.

2.4.1 Characterisation of Benzofused Polyamides through Various Spectroscopic Techniques

The benzofused polyamides of **library-1B** were purified and fully characterized by different spectroscopic techniques including mass spectrometry, both ^{1}H and ^{13}C NMR, and IR techniques (described in the **Experimental** section of Chapter

4). Compounds were primarily identified by LCMS and confirmed using high resolution mass spectroscopy (HRMS) **(Table 2.5 and 2.6)**. Finally these well characterised compounds were evaluated by FRET based DNA melting assay.

Table 2.5: HRMS data for **library-1B** molecules

Number	Compound code	Theoretical mass	Observed mass $[M+H]^+$
1	**4.37**	620.2093	621.2155
2	**4.40**	636.1865	637.1934
3	**4.36**	604.2322	605.2401
4	**4.31**	606.1937	607.2010
5	**4.30**	590.2165	591.2244
6	**4.42**	618.2478	619.2544
7	**4.43**	638.1932	639.2006
8	**4.45**	633.2410	634.2473
9	**4.41**	617.2638	618.2708
10	**4.44**	604.2434	605.2511

2.4.2 Purity Analysis of Benzofused Polyamides Synthesized

The purity of the benzofused polyamides of this library was checked by two different HPLC methods with two different retention times. Both methods were carried out on a Waters Alliance 1695 HPLC Pump with water and acetonitrile comprising the mobile phases. The Waters 996 PDA start wavelength was 210 nm for the 10 minute method (Method A), with a start wavelength of 220 nm and end wavelength of 500 nm for the 5 minute method (Method B) **(Tables 2.5 and 2.6)**.

Table 2.6: Purity data for **library-1B** observed by LCMS

Number	Compound code	Purity	
		Method A(10 min)%	Method B(5 min)%
1	**4.37**	91	89.09
2	**4.40**	100	100
3	**4.36**	100	100
4	**4.31**	94	100
5	**4.30**	100	100
6	**4.42**	100	100
7	**4.43**	100	100
8	**4.45**	100	100
9	**4.41**	100	94.37
10	**4.44**	100	100

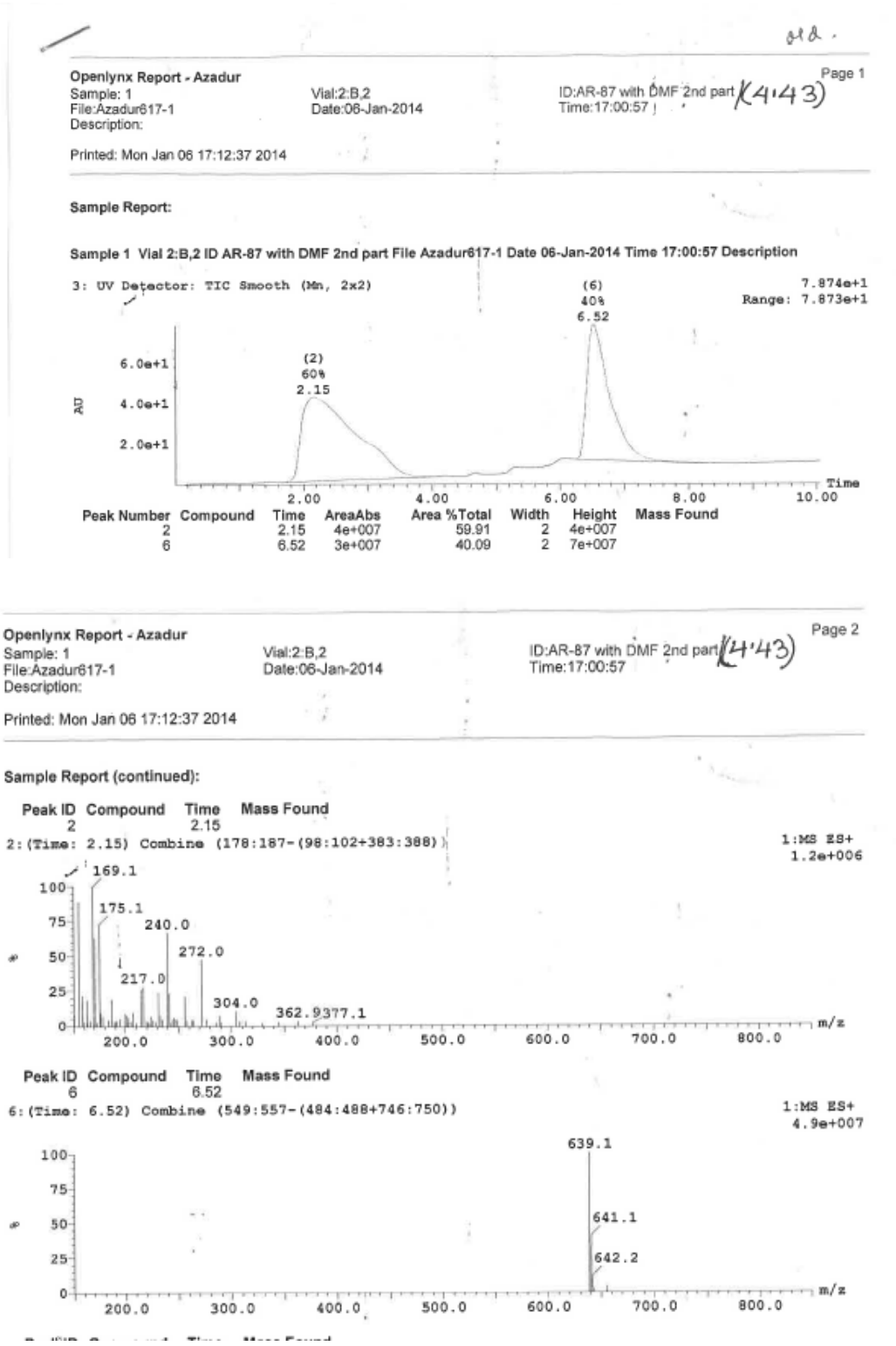

Figure 2.22: Example of an adapted LCMS profile of **Library-1B** compound **4.43**

Table 2.7: G-quadruplex and duplex DNA stabilization by ligands of **library-1B** in FRET melting experiments at concentrations of 5, 2 and 1 μM respectively (the data are means of three technical repeats)

Compounds	Quadruplex types	ΔT_m(°C) ±(s/d)		
		5 μM	2 μM	1 μM
4.37	F21T	18.1±0.21	1.8±0.31	1.1±0.23
	C-kit-1	2.4±0.15	1.5±0.35	1.2±0.23
	C-kit-2	4.7±0.20	2.8±0.11	1.9±0.40
	BCL-2	5.1±0.36	2.5±0.20	2.1±0.20
	Duplex DNA	0.0±0.20	0.0±0.11	0.0±0.07
4.40	F21T	4.1±0.3	2.5±0.13	1.9±0.7
	C-kit-1	1.8±0.26	0.6±0.07	0.5±0.21
	C-kit-2	5.4±0.20	2.8±0.26	2.1±0.17
	BCL-2	2.8±0.40	1.3±0.25	1.4±0.45
	Duplex DNA	0.0±0.07	0.0±0.2	0.0±0.04
4.36	F21T	9.3±0.23	2.8±0.13	1.8±0.16
	C-kit-1	3.4±0.15	2.2±0.15	1.5±0.3
	C-kit-2	5.7±0.1	2.8±0.11	2.2±0.15
	BCL-2	4.7±0.34	2.9±0.11	2.7±0.41
	Duplex DNA	0.0±0.06	0.0±0.21	0.0±0.25
4.31	F21T	0.5±0.32	0.7±0.12	0.6±0.24
	C-kit-1	0.8±0.15	0.9±0.20	0.8±0.32
	C-kit-2	2.0±0.47	1.1±0.17	0.8±0.05
	BCL-2	1.9±0.20	1.5±0.30	1.5±0.05
	Duplex DNA	0.0±0.16	0.0±0.21	0.0±0.2

Table 2.8: G-quadruplex and duplex DNA stabilization by ligands in FRET melting experiments at concentrations of 5, 2 and 1 μM respectively (the data are means of three technical repeats)

Compounds	Quadruplex types	ΔT_m(°C) ±(s/d)		
		5 μM	2 μM	1 μM
4.30	F21T	1.2±0.20	0.5±0.27	0.3±0.31
	C-kit-1	0.9±0.20	1.0±0.15	0.4±0.10
	C-kit-2	2.1±0.20	1.2±0.36	0.9±0.17
	BCL-2	1.7±0.20	0.5±0.30	0.6±0.15
	Duplex DNA	0.0±0.15	0.0±0.34	0.0±0.06
4.42	F21T	4.6±0.20	0.9±0.05	0.4±0.05
	C-kit-1	2.9±0.10	1.1±0.32	0.3±0.26
	C-kit-2	6.1±0.11	2.0±0.30	0.9±0.45
	BCL-2	3.9±0.10	1.3±0.14	0.3±0.14
	Duplex DNA	0.0±0.06	0.0±0.20	0.0±0.21
4.43	F21T	5.1±0.11	2.3±0.41	1.0±0.12
	C-kit-1	1.1±0.20	0.6±0.10	0.7±0.20
	C-kit-2	4.3±0.35	1.9±0.20	1.4±0.20
	BCL-2	2.9±0.23	1.7±0.32	1.4±0.05
	Duplex DNA	0.0±0.31	0.0±0.24	0.0±0.07
4.45	F21T	4.1±0.21	1.9±0.23	0.6±0.11
	C-kit-1	3.9±0.25	1.2±0.15	1.3±0.15
	C-kit-2	7.3±0.40	3.7±0.15	2.7±0.21
	BCL-2	6.8±0.14	1.6±0.10	1.5±0.26
	Duplex DNA	0.0±0.06	0.0±0.12	0.0±0.16
4.41	F21T	3.1±0.11	2.5±0.32	0.3±0.21
	C-kit-1	2.5±0.34	1.3±0.15	1.0±0.20
	C-kit-2	3.8±0.35	1.8±0.30	1.5±0.20
	BCL-2	3.5±0.32	1.9±0.45	1.6±0.47
	Duplex DNA	0.0±0.32	0.0±0.25	0.0±0.10
4.44	F21T	12.1±0.31	3.7±0.18	2.3±0.12
	C-kit-1	3.7±0.32	1.8±0.14	1.5±0.15
	C-kit-2	6.1±0.30	2.9±0.32	2.2±0.40
	BCL-2	7.8±0.20	3.7±0.31	2.9±0.21
	Duplex DNA	0.0±0.31	0.0±0.13	0.0±0.12

Molecules (except **4.44**) mentioned in this section **(Table 2.7 and 2.8)** did not show any significant interaction with G-quadruplex sequences. Thus tail replacement does not make a notable improvement of the interacting capacity of ligand molecules. However, although the ΔTm values were not significant, it is notable that the ligands (**4.37**, **4.40** and **4.36**) possessing 4-(pyrrolidin-1-yl) butan-1-amine tail showed better interacting ability than those molecules (**4.31** and **4.30**) possessing 2-(piperidin-1-yl) ethan-1-amine tails. **4.37** provided 1.1°C, 1.2°C, 1.9°C and 2.1°C stabilisation; **4.40** provided stabilisations of

1.9°C, 0.5°C, 2.1°C and 1°C; **4.36** provided 1.8°C, 1.5°C, 2.2°C and 2.7°C stabilisation; **4.31** provided 0.6°C, 0.8°C, 0.8°C and 1.5°C stabilisation; **4.30** provided 0.3°C, 0.4°C, 0.9°C and 0.6°C stabilisation at 1 µM concentration against F21T, C-kit-1, C-kit-2 and Bcl-2 G-quadruplex sequences respectively.

This stabilisation indicates the superiority of the 4-(pyrrolidin-1-yl) butan-1-amine tail over the 2-(piperidin-1-yl) ethan-1-amine tails. On other hand, **4.37** and **4.40** are nearly identical in their interactions toward G-quadruplexes. This further indicates that the activity of these molecules does not depend on either the benzothiophene or benzofuran building blocks types.

Two similar molecules attached with the preferred 4-(pyrrolidin-1-yl) butan-1-amine tail were made to get an idea of whether any kind of substitution in these structures may have an extra effect. **4.42** and **4.43** were synthesized in the form of **4.36** with the exception of a substitution at the terminal building block. **4.42** possessed the substitution of an electron-pushing methyl (-CH_3) group and **4.43** possessed an electron-pulling chloride (Cl^-) group.

Melting temperatures of these two molecules were not more impressive than those of **4.36**. This means these substitutions may not have a positive effect on ligand activity. But it is assumed that the electron-pulling group (chloride group) may have an enhancing effect on G-quadruplex interactivity of the benzofused-polyamide structure; **4.43** showed stabilisation of 1.0°C, 0.7°C, 1.4°C and 1.4°C at 1 µM concentration against F21T, C-kit-1, C-kit-2 and Bcl-2 G-quadruplex sequences respectively, which is insignificantly better than **4.42**, which itself provided ΔTm values of a 0.4°C, 0.3°C, 0.9°C and 0.3°C at 1 µM concentration against F21T, C-kit-1, C-kit-2 and Bcl-2 G-quadruplex sequences. This difference of melting temperatures between **4.43** and **4.42** provides a preliminary idea that electron-pushing groups like methyl (CH_3-) group may reduce the interacting capacity of a ligand, whereas electron-pulling group like chloride (Cl^-) enhance the interacting capacity of ligands towards G-quadruplex DNA. These ideas helped to guide further ligand synthesis. **4.44** is slightly more interactive than any other molecules of this library, as it provided 2.3°C,1.5°C, 2.2°C C and 2.9°C stabilisation at 1 µM concentration against F21T, C-kit-1, C-kit-2 and Bcl-2 G-quadruplex sequences, which is insignificantly better than any other members of this library. Therefore, it was assumed that the inclusion of

nitrogen-contacting building blocks (i.e. Imidazole) may allow the formation of hydrogen bonds with the guanine residues of quadruplex DNA and thereby enhance ligand interacting capacity with G-quadruplex structures to a certain extent.

It was observed that some of the molecules, including **4.15**, **4.6** and **4.37**, were found to show significant interaction at higher concentrations (5 µM) but suddenly lose their stabilisation capacities at lower concentrations. These unexpected higher melting temperatures (for example, 18.1°C for **4.37**) were assumed to be contributed by the cooperative binding of these molecules at high concentrations (5 µM). A dimer of **4.37** may stack together over the terminal quartet of a G-quadruplex. As soon as molecular density goes down at lower concentrations (1, 2 µM), the melting temperatures fall sharply (ΔTm=1.8°C and 1.1°C, respectively). This means the molecular density is not great enough to make a dimer at low concentrations of **4.37**.

2.4.3: Key Observations on Library-1A and Library-1B Molecules

- These compounds showed insignificant interaction with the F21T, C-kit-1, C-kit-2 and Bcl-2 G-quadruplexes.
- The inclusion of either a benzofuran or benzothiophene building block in the structure of these molecules does not make any notable difference.
- N1, N1-dimethyl propane-1, 3-diamine and 4-(pyrrolidin-1-yl) butan-1-amine are comparatively better than 2-(piperidin-1-yl) ethan-1-amine as tails in benzofused-polyamides.
- Inclusion of N-containing benzofused rings may increase the stabilising capacity of benzofused polyamides.
- Electron-pulling groups like chloride group (Cl^-) attached to a benzofused ring is better than electron-pushing groups like methyl group (-CH3) in conferring activity upon the ligand molecules.

2.5 Molecular Modelling of Benzofused Polyamides of Library-1A and 1-B as G-quadruplex Stabilising Agents

Molecular modelling studies were undertaken in an effort to rationalise the poor FRET binding results obtained for the **Library 1** molecules.

Molecular docking experiments were undertaken on the human telomeric quadruplex F21T (PDB ID 3CDM). It was immediately evident from visual analysis that 5'-2' substituted benzofused moieties do not have the appropriate curvature to stack on the quadruplex interface.

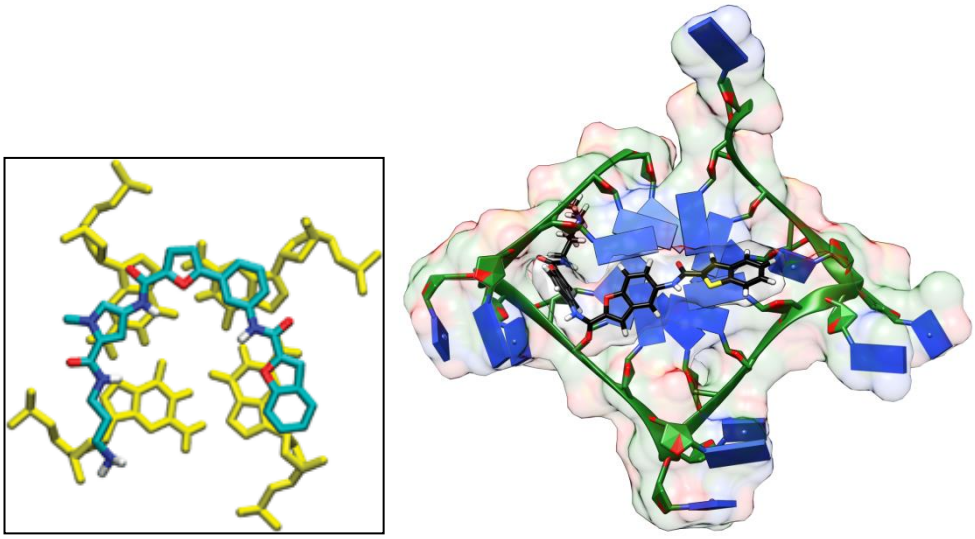

Figure 2.23: Molecular model of the G-quadruplex-interactive biaryl polyamide (left panel) showing the curvature of the molecule, which assists the stabilisation of DNA. **Library-1** molecules (e.g., **4.5**, black sticks, right panel) do not possess the same curvature, and therefore cannot stabilise quadruplex DNA.

*Molecular Modelling Studies were carried out by Dr. Paul Jackson and Mr. Meir Touitou.

Traditional quadruplex inhibitors such as quarfloxacin and the small molecule biaryl polyamides are composed of fused rings and possess a specific curvature which enables them to stack on the quadruplex interface **(Figure 2.21). Library-1** molecules, on the other hand, are linear in structure. For example, molecular models of **4.5** (containing benzothiophene and benzofuran building blocks) show that the molecule does not stack effectively on the quadruplex interface, thereby producing few non-covalent interactions **(Figure 2.21)**.

FRET binding results also suggest that the introduction of nitrogen-containing benzofused groups (i.e., indole and benzimidazole) does not enhance binding to the quadruplex interface. Although indole, and particularly benzimidazole, contain nitrogen groups capable of forming H-bonding interactions, and therefore interacting with amine groups of guanines in the quadruplex, FRET binding results suggest that the presence of these moieties does not alter the binding capability of the molecule. This is reflected in docking results where nitrogen-containing molecules possess similar binding energies to sulphur and oxygen-containing compounds. For example **4.15** containing both benzothiophene and benzofuran, and **4.6** containing benzimidazole and benzofuran groups both have similar GBSA binding energies (i.e., -66.29kcal/mol and -69.25kcal/mol respectively), thereby suggesting that the introduction of nitrogen does not affect binding to the DNA. This is reflected in visual analysis of the docked models where the nitrogens of the indole and benzimidazole moieties do not form H-bonds with the quadruplex structure. H-bonds are absent, presumably, due to the lone pairs of the nitrogens not being in the appropriate orientation to interact with quadruplex DNA. Furthermore, the replacement of the amidic tail of the molecule with a variety of amine tails has little effect on the binding of the series of molecules to DNA, and this is reflected in GBSA binding calculations. For example, binding calculations are similar to other members of **Library-1**, where GBSA scores are in the region of -60kcal/mol (e.g., in the case of **4.30** and **4.43**, binding energies are -59.83kcal/mol and -68.54kcal/mol respectively).

It is evident from modelling analysis that shape-based factors are critical in affecting interactivity of benzofused polyamides with G-quadruplex DNA. When compared with the highly interactive biaryl polyamide produced by Rahman *et al* (**Figure 2.21,** left panel), there is a distinct difference in curvature of both sets of

molecules. In order to enhance quadruplex binding, it is recommended that the 5'-2' substituted central benzofused moiety is replaced with a 5'-3' substituted benzofused moiety. Such a substitution is likely to enhance curvature of the molecule and increase binding with the quadruplex structure through efficient stacking on the G-tetrad **(Figure 2.22)**.

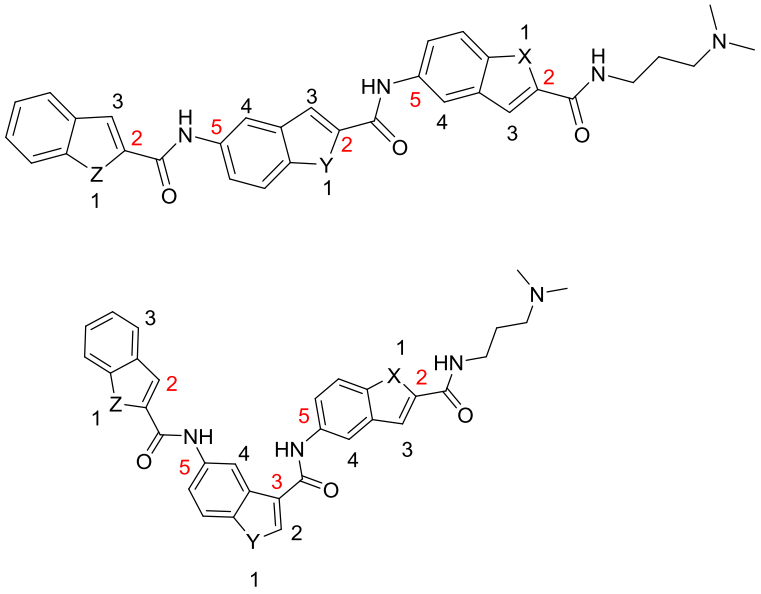

Figure 2.24: Schematic of **Library-1A and 1B** molecules (top) and proposed modification to generate **Library-2** molecules (bottom).

Library-2

2.6 Synthetic Scheme for Library-2 Molecules.

As the molecules belonging to **library-1A** and **library-1B** did not show significant interaction with G-quadruplex DNA types, a set of new molecules (9 molecules in total) were synthesized **(Figure 2.24)** with the help of molecular modelling studies (**Figure 2.21**). Here, a 5-nitro-benzofused-3-carboxylic acid was included as a second building block instead of 5-nitro-benzofused-2-carboxylic acid so that ligand molecules would have relatively more curvature in their structures compared to **library-1A** and **1B** ligand molecules. Commercially available 5-nitro-indole-3-carboxylic acid was introduced at the middle of the benzofused polyamide **(Figure 2.23)**.

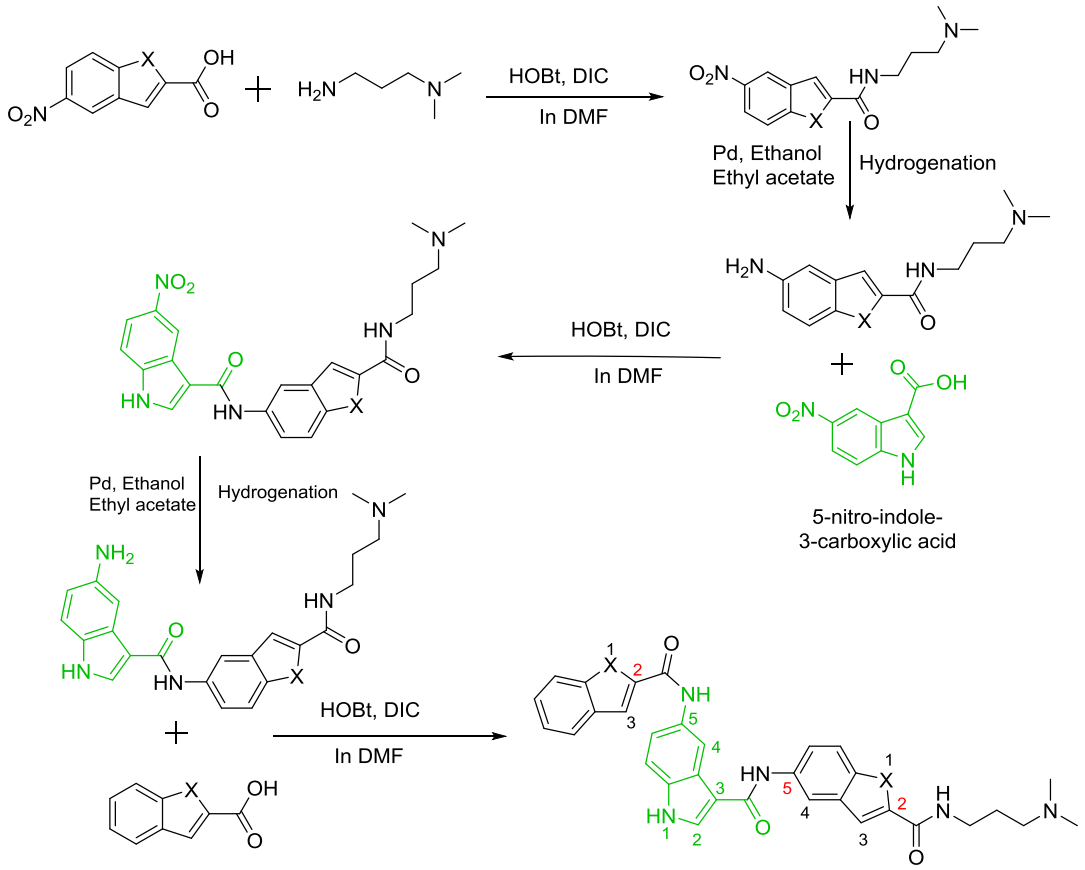

Figure 2.25: Synthetic Scheme of **Library-2** molecules. Here X = O or N or S. 5-nitro-benzofused-3-carboxylic acid was used as a second building block, as shown as green.

Initially the acid (1.2 eq.) was dissolved in DMF (5 mL for 100 mg of starting material) in a round bottom flask fitted with a magnetic stirrer. Then DIC (1.75

eq.) and HOBt (2.0 eq.) were added to the acid (1.0 eq.) and this mixture was allowed to stir at room temperature for formation of the ester from the acid. The amine (1 eq.) was added to the mixture and the mixture allowed for stirring until the reaction was complete, as indicated by TLC or LCMS. Finally the reaction mixture was applied to a conditioned SCX-2 cartridge and the resultant product was purified by the 'Catch and Release' method (described in the section '**Method and Materials**' of Chapter 3).

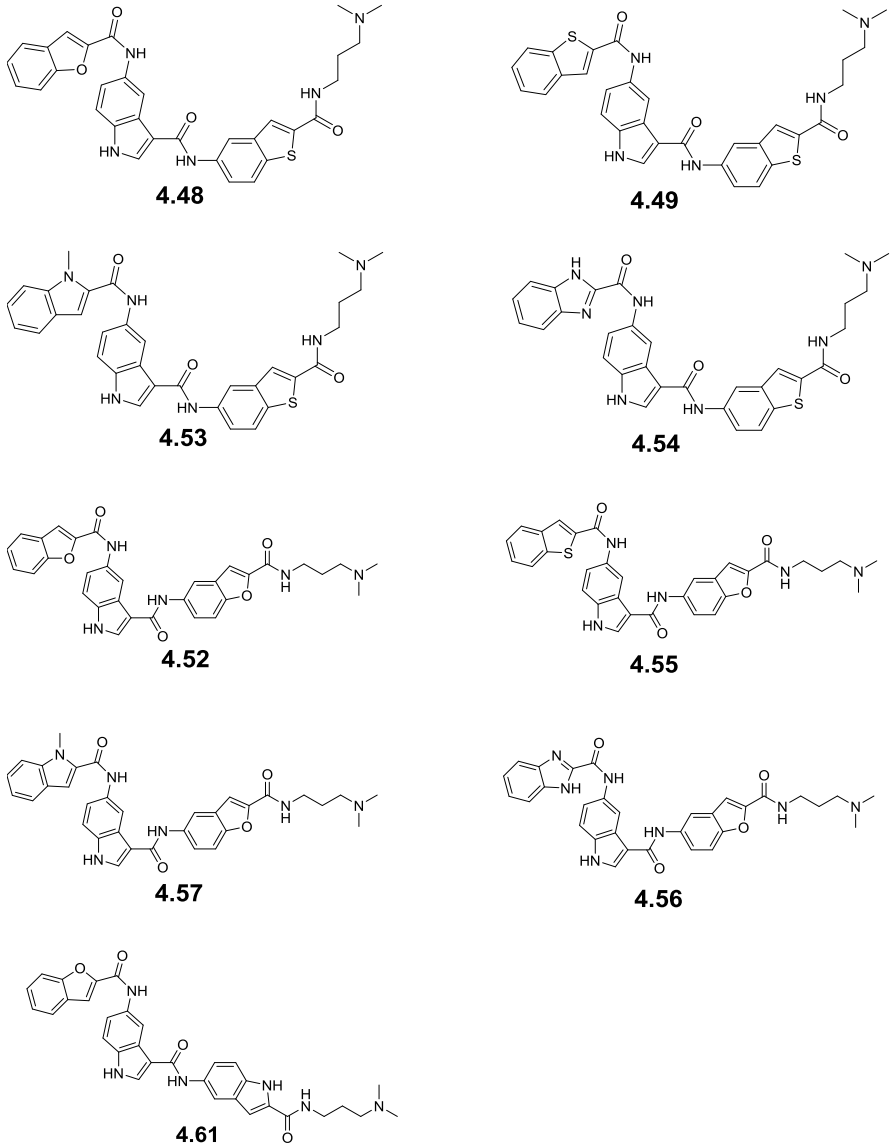

Figure 2.26: Structures of the molecules in **library-2**

2.6.1 Characterisation of Benzofused Polyamides through Various Spectroscopic Techniques

Molecules of **library-2** were purified and fully characterized by different spectroscopic techniques including mass spectrometry, both ^{1}H and ^{13}C NMR, and IR techniques (described in the **Experimental** section of Chapter 4). Compounds were primarily identified by LCMS and confirmed using high resolution mass spectroscopy (HRMS) **(Table 2.9)**.

Table 2.9: HRMS data for **library-2** molecules

Number	Compound code	Theoretical mass	Observed mass $[M+H]^+$
1	**4.48**	579.1940	580.2000
2	**4.49**	595.1712	596.1771
3	**4.53**	592.2257	593.2314
4	**4.54**	579.2053	580.2113
5	**4.52**	563.2169	564.2230
6	**4.55**	579.1940	580.2003
7	**4.57**	576.2485	577.2544
8	**4.56**	563.2281	564.2340
9	**4.61**	562.2329	563.2387

2.6.2 Purity Analysis of Benzofused Polyamides Synthesized

The purity of the benzofused polyamides of this library was checked by two different HPLC methods with two different retention times. Both methods were carried out on a Waters Alliance 1695 HPLC Pump with water and acetonitrile comprising the mobile phases. The Waters 996 PDA start wavelength was 210 nm for the 10 minute method (Method A), with a start wavelength of 220 nm and end wavelength of 500 nm for the 5 minute method (Method B) **(Table 2.10)**.

Table 2.10: Purity data for **library-2** molecules as observed by HPLC

Number	Compound code	Purity	
		Method A (10 min)%	Method B (5 min)%
1	**4.48**	100	100
2	**4.49**	100	100
3	**4.53**	100	100
4	**4.54**	100	100
5	**4.52**	100	100
6	**4.55**	91	89.09
7	**4.57**	100	100
8	**4.56**	100	100
9	**4.61**	100	100

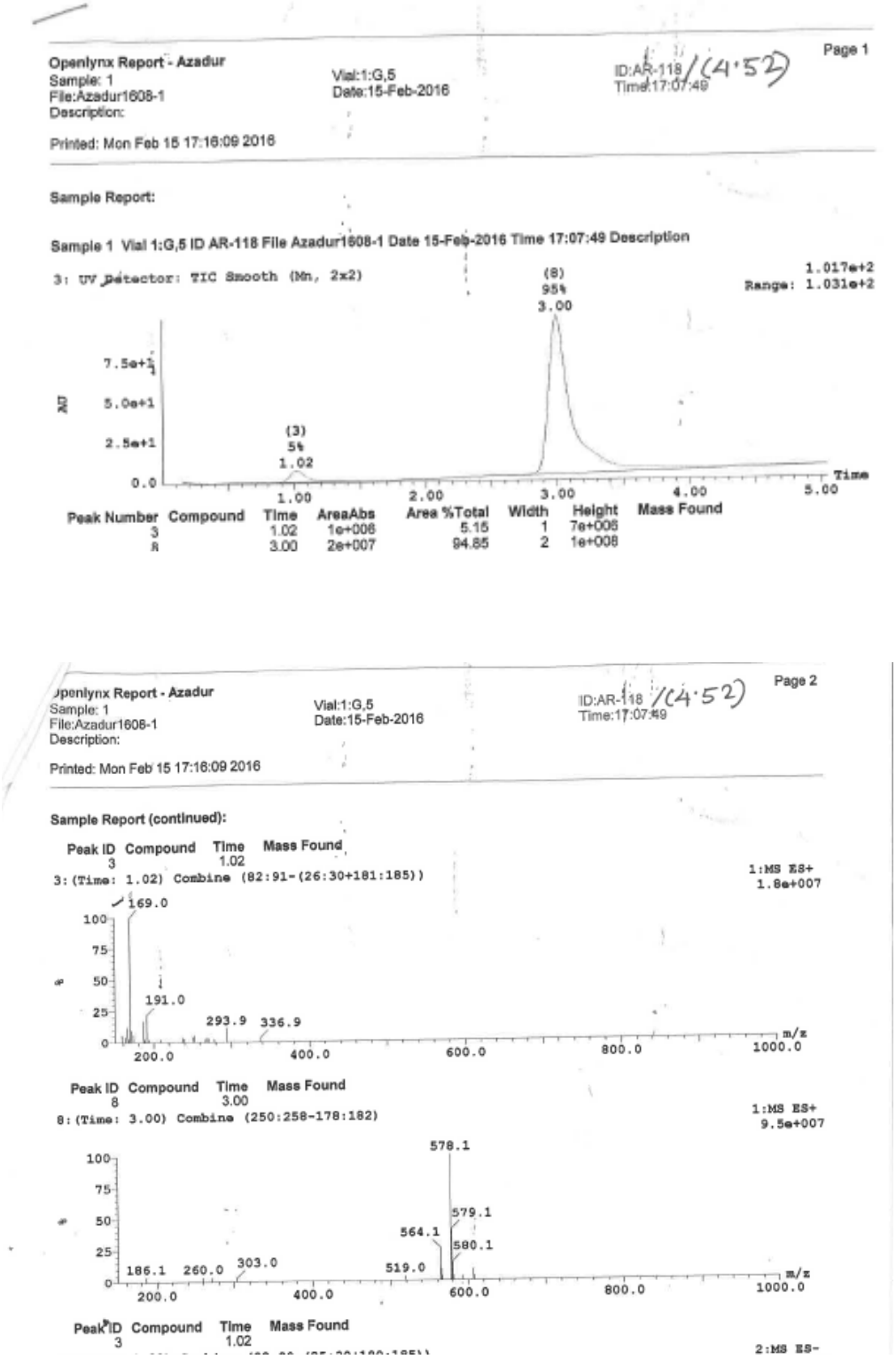

Figure 2.27: Example of an adapted LCMS profile of **Library-2** compound **4.52**

Table 2.11: G-quadruplex and duplex DNA stabilization by ligands in FRET melting experiments at concentrations of 5, 2 and 1 μM respectively (the data are means of three technical repeats)

Compounds code	Quadruplex types	ΔT_m(°C) ±(s/d)		
		5 μM	2 μM	1 μM
4.48	F21T	14.3±0.23	6.6±0.20	3.0±0.21
	C-kit-1	19.2±0.15	13.1±0.17	9.6±0.05
	C-kit-2	16.2±0.28	9.2±0.23	6.9±0.05
	BCL-2	13.9±0.20	9.1±0.28	8.4±0.10
	Duplex DNA	0.0±0.15	0.0±0.05	0.0±0.21
4.49	F21T	14.6±0.20	7.5±0.14	3.4±0.34
	C-kit-1	13.1±0.25	10.4±0.36	9.9±0.21
	C-kit-2	17.2±0.23	11.7±0.05	11.0±0.20
	BCL-2	12.3±0.15	5.6±0.20	5.3±0.20
	Duplex DNA	0.0±0.23	0.0±0.21	0.0±0.35
4.53	F21T	13.8±0.07	8.3±0.23	4.3±0.11
	C-kit-1	14.6±0.17	11.4±0.37	8.2±0.45
	C-kit-2	16.4±0.25	10.3±0.20	9.5±0.15
	BCL-2	13.6±0.45	7.0±0.20	4.6±0.34
	Duplex DNA	0.0±0.10	0.0±0.21	0.0±0.26
4.54	F21T	17.0±21	10.4±017	5.5±0.13
	C-kit-1	20.8±0.20	15.1±0.10	12.0±0.40
	C-kit-2	19.6±0.15	12.2±0.30	8.9±0.37
	BCL-2	18.9±0.36	12.0±0.20	9.3±0.23
	Duplex DNA	0.0±0.24	0.0±0.20	0.0±0.25

Here, **4.48** provided 3.0°C, 9.6°C, 6.9°C and 8.4°C stabilisation, **4.49** provided 3.4°C, 9.9°C, 11.0 °C and 5.3°C stabilisation, **4.53** provided 4.3°C, 8.2°C, 9.5°C and 4.6°C stabilisation and **4.54** provided 5.5°C, 12.0°C, 8.9°C and 9.3°C stabilisation at 1 μM concentrations against F21T, C-kit-1, C-kit-2 and Bcl-2 G-quadruplex sequences respectively.

FRET data analysis showed that, as a whole, the introduction of curvature within the **library-1A** and **1B** molecules significantly improved ligand interactivity with all G-quadruplex sequences used. **4.54** was found to be the most active member of this library, possibly due to the extra nitrogen atom of its terminal imidazole ring. This additional electronegative nitrogen may form a hydrogen bond with an amine, carbonyl or imine group of the G-quadruplex DNA or it may provide an electronic interaction within the ligand molecule which may reinforce the π-π stacking interaction.

Table 2.12: G-quadruplex and duplex DNA stabilization by ligands in FRET melting experiments at concentrations of 5, 2 and 1 μM respectively (the data are means of three technical repeats)

Compound code	Quadruplex types	ΔT_m(°C) ±(s/d)		
		5 μM	2 μM	1 μM
4.52	F21T	6.22±0.41	3.5±0.24	2.4±0.37
	C-kit-1	13.1±0.23	8.5±0.25	7.8±0.15
	C-kit-2	18.0±0.15	10.3±0.40	8.1±0.36
	BCL-2	14.8±0.40	8.3±0.35	5.6±0.36
	Duplex DNA	0.0±0.17	0.0±0.14	0.0±0.22
4.55	F21T	12.2±0.11	7.1±0.14	5.0±0.32
	C-kit-1	15.6±0.26	11.1±0.1	10.7±0.10
	C-kit-2	15.8±0.30	9.7±0.30	6.7±0.28
	BCL-2	11.9±0.15	5.7±0.26	3.2±0.26
	Duplex DNA	0.0±0.12	0.0±0.23	0.0±0.31
4.57	F21T	10.6±0.10	5.0±0.07	3.9±0.21
	C-kit-1	11.8±0.15	7.8±0.05	3.3±0.26
	C-kit-2	18.2±0.37	8.8±0.25	8.1±0.37
	BCL-2	9.3±0.20	5.7±0.46	3.6±0.23
	Duplex DNA	0.0±0.14	0.0±0.12	0.0±0.17
4.56	F21T	17.2±0.23	10.7±0.41	6.6±0.12
	C-kit-1	12.5±0.17	9.8±0.25	8.7±0.15
	C-kit-2	20.6±0.15	14.1±0.15	10.6±0.05
	BCL-2	14.9±0.17	8.3±0.32	6.4±0.37
	Duplex DNA	0.0±0.32	0.0±0.21	0.0±0.27
4.61	F21T	18.0±0.20	7.4±0.13	5.2±0.34
	C-kit-1	14.4±0.10	8.8±0.10	7.4±0.32
	C-kit-2	18.1±0.45	11.4±0.20	7.7±0.30
	BCL-2	13.9±0.15	7.6±0.17	4.7±0.30
	Duplex DNA	0.0±0.14	0.0±0.21	0.0±0.15

Here, introduction of curvature improved the interacting capacity of ligand molecules in an apparently similar pattern to the first set **(Table 2.11)**. Although these molecules were composed differently, as they start with a benzothiophene and end with the same benzothiophene building block instead of a benzofuran as in the previous set, they were nearly identical in their stabilisation capacities. This further indicated that the effect of these two different benzofused ring types (benzothiophene and benzofuran) were very similar. In more detail, it was found that molecules of this type interacted equivalently with F21T (human telomeric quadruplex) and Bcl-2 G-quadruplexes. They were more active toward C-kit-1 and relatively better

toward C-kit-2 G-quadruplexes. **4.56** is likely to be the most interactive library member, again possibly due to the imidazole ring as previously discussed.

It is interesting to note that although **4.61** was equivalent to **4.52**, it provided relatively higher melting temperatures of 5.2°C, 7.4°C, 7.7°C and 4.7°C stabilisation at 1 µM concentration against F21T, C-kit-1, C-kit-2 and Bcl-2 G-quadruplex sequences respectively. This indicated the preference of indole building blocks over either benzofuran or benzothiophene building blocks with regard to G-quadruplex interacting capacities.

Two equivalent molecules from each of the libraries (for example, **4.15** and **4.18** of **library-1** can be compared directly with **4.49** and **4.52** of **library-2**) were taken and their FRET data subsequently analysed to evaluate the introduction of curvature.

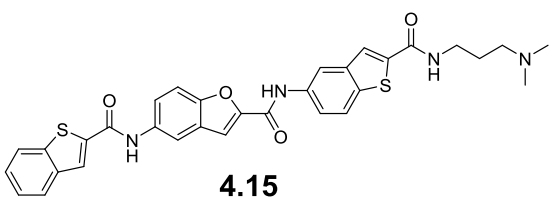

4.15

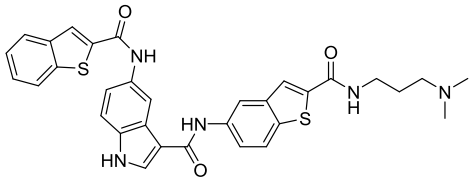

4.49

Figure 2.28: Structures of **4.15** and **4.49** from **library-1** and **library-2** respectively.

Table 2.13: Comparative FRET data analysis between **4.15** and **4.49** (the data are means of three technical repeats)

Quadruplex types	ΔT_m(°C)±(s/d)					
	4.15	**4.49**	**4.15**	**4.49**	**4.15**	**4.49**
	5 µM	5 µM	2 µM	2 µM	1 µM	1 µM
F21T	20.1±0.28	14.6±0.20	3.6±0.2	7.5±0.14	2.2±0.25	3.4±0.34
C-kit-1	3.1±0.41	13.1±0.25	1.4±0.30	10.4±0.36	0.2±0.49	9.9±0.21
C-kit-2	9.2±0.25	17.2±0.23	3.8±0.05	11.7±0.05	2.3±0.30	11.0±0.20
BCL-2	17.5±0.26	12.3±0.15	1.8±0.37	5.6±0.20	0.2± 0.32	5.3±0.20
Duplex DNA	0.0±0.11	0.0±0.23	0.0±0.06	0.0±0.21	0.0±0.07	0.0±0.35

Here, **4.49** provided 3.4°C, 9.9°C, 11.0°C and 5.3°C stabilisation at 1 µM concentration against F21T, C-kit-1, C-kit-2 and Bcl-2 G-quadruplex sequences,

respectively. In contrast, **4.15** provided 2.2°C, 0.2°C, 2.3°C and 0.2°C stabilisation at 1 µM concentration against F21T, C-kit-1, C-kit-2 and Bcl-2 G-quadruplex sequences, respectively. This difference in ΔTm values implicates the enhanced curvature in the improved interactivity of the ligands with the G-quadruplex sequences. Both of these molecules showed a similar degree of G-quadruplex stabilisation from higher to lower concentrations for all of the G-quadruplex sequences used. However, **4.15** showed a higher degree of stabilisation (ΔTm=20.1°C) at 5 µM for human telomeric G-quadruplex. This was higher even than **4.49** (ΔTm=14.6°C). These unexpected higher melting temperatures were assumed to be contributed by cooperative binding of **4.15** at high concentration. A dimer of **4.15** may stack together over the terminal quartet of G-quadruplexes. As soon as molecular density decreases at subsequent lower concentrations (1, 2 µM), the melting temperatures fall sharply (ΔTm=3.6 °C and 2.2 °C, respectively). This means the molecular density is not sufficient to make a dimer at low concentrations of **4.15**.

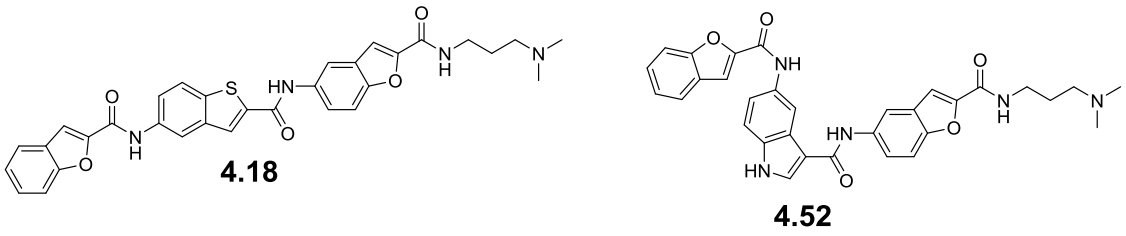

Figure 2.29: Structures of **4.18** and **4.52**

Table 2.14: Comparative FRET data analysis between **4.18** and **4.52** (the data are means of three technical repeats)

Quadruplex types	ΔT_m(°C)±(s/d)					
	4.18	**4.52**	**4.18**	**4.52**	**4.18**	**4.52**
	5 µM	5 µM	2 µM	2 µM	1 µM	1 µM
F21T	7.0±0.07	6.22±0.41	2.0±0.36	3.5±0.24	0.8±0.05	2.4±0.37
C-kit-1	3.8±0.26	13.1±0.23	1.8±0.26	8.5±0.25	1.6±0.45	7.8±0.15
C-kit-2	9.7±0.25	18.0±0.15	3.8±0.11	10.3±0.40	2.4±0.26	8.1±0.36
BCL-2	5.7±0.1	14.8±0.40	0.9±0.30	8.3±0.35	0.6±0.35	5.6±0.36
Duplex DNA	1.2±0.11	0.0±0.17	0.0±0.06	0.0±0.14	0.0±0.11	0.0±0.22

Here, **4.18** and **4.52** followed the same pattern of stabilising capacities as for **4.15** and **4.49**. **4.52** gave 2.4°C, 7.8°C, 8.1°C and 5.6°C stabilisation at 1 µM

concentration against F21T, C-kit-1, C-kit-2 and Bcl-2 G-quadruplex sequences, respectively. In contrast, **4.18** provided 0.8°C, 1.6°C, 2.4°C and 0.6°C stabilisation at 1 μM concentration against F21T, C-kit-1, C-kit-2 and Bcl-2 G-quadruplex sequences, respectively. Therefore, it was further evident that the introduction of curvature made the aryl-polyamides more potent towards G-quadruplexes used. However, **4.49** and **4.52** were more active towards C-kit-2 compared to the other sequences. The pattern of activation against F21T and BCL-2 quadruplex sequences was nearly equivalent.

2.6.3 Key Observations Based on the Overall FRET Data Analysis of Library-2 Molecules

- Introduction of curvature in the benzofused polyamide structural motif through the 5′-3′ substitution enhanced the stabilising capacity of the benzofused polyamides toward G-quadruplex DNA.

2.7 Molecular Modelling of Library-2 Molecules

It is evident from biophysical studies that the introduction of a 5'-3' substituted moiety instead of a 5'-2'-substituted moiety has a considerable effect on the binding of triaryl benzofused molecules to quadruplex DNA. For example, in the case of **4.18** and **4.52** (**Figure: 2.24**), stabilisation is enhanced by 6-7 $^{\circ}$C in the case of c-kit-1 and c-kit2, and an increase in 2-3°C in other quadruplexes such as F21T.

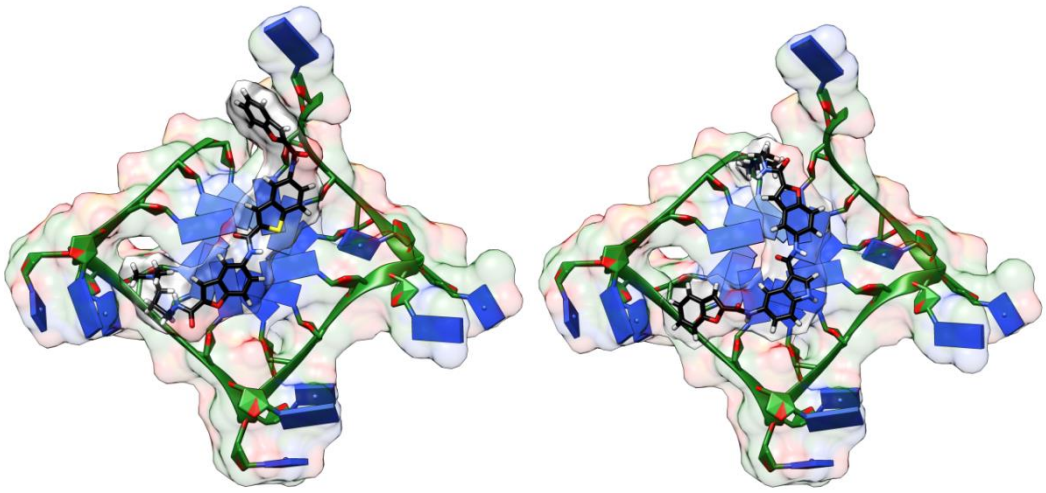

Figure 2.30: Molecular model of **4.18** (left panel) and **4.52** (right panel) bound to the telomeric F21T G-quadruplex illustrating the difference in accommodation of a **Library 1** molecule (**4.18**) and **Library 2** molecule (**4.52**). In the case of **4.52** (black sticks), three benzofused molecules are capable of orienting directly over guanine bases (blue nucleotide objects), thereby enhancing stabilisation. In the case of **4.18**, only two benzofused moieties are capable of inducing G-quadruplex stabilisation.

Molecular modelling studies suggest that this increase in binding affinity occurs due to increased stacking on the quadruplex interface. This is particularly evident in docking studies of the human telomeric quadruplex (PDB ID 3CDM), where **4.52** stacks effectively on the quadruplex interfaces and enhances interaction through pi-pi interactions, whereby **4.18** does not **(Figure 2.27)**. This is supported by GBSA calculations which suggest that **4.18** has an affinity of -67.11kcal/mol, whereas **4.52** has a considerably enhanced binding affinity of -75.35kcal/mol. Interestingly, a significant selective enhancement of stabilisation of both c-kit-1 and c-kit2 was observed over other quadruplexes. Although

crystal or NMR structures of the c-kit-1 and c-kit2 sequences used in the biophysical study were not available, and therefore relevant docking studies could not be undertaken, it is likely that differences in the topologies of c-kit-1 and c-kit2 allowed greater accommodation of **Library-2** molecules over **Library-1**.

Preliminary docking studies also suggested that the introduction of further 5'-3'-substituted benzofused moieties to the polyamide core instead of 5'-2'-benzofused moieties should enhance binding further **(Fig. 2.28),** and this was explored in **Library 3A**.

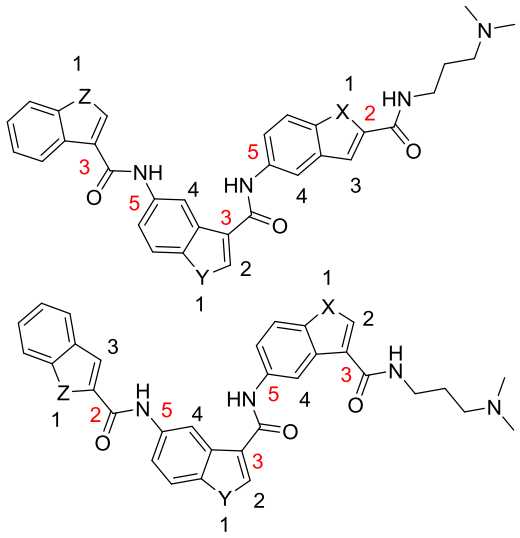

Figure 2.31: Schematic of **Library-2** molecules (top) and proposed modification to generate **Library-3** molecules (bottom).

Library-3A

2.8 Synthetic Scheme for First Set of Library-3A Molecules

As evaluated by the DNA modelling studies (**Figure 2.27** and **Figure 2.28**), it was suggested to introduce further curvature within the **library-2** ligand molecules. Thus a set of new molecules (7 in total) were synthesized **(Figure 2.31)** by replacing the 1st building block of the **library-2** molecules (5-nitro benzofused-2-carboxylic acid) with 5-nitro benzofused-3-carboxylic acid). Thus the final benzofused polyamides were hoped to have more curvature compared to those of **library-2**. Two sets of molecules were synthesized by including two molecules of 5-nitro-benzofused-3- carboxylic acids in benzofused polyamide structures in two different fashions. The first set of molecules was made by the coupling of two consecutive 5-nitro-indole-3-carboxylic acids followed by termination with four different benzofused acids **(Figure 2.29)**. The second set of molecules was made by starting with a 5-nitro-benzofuran-2-carboxylic acid which was immediately coupled with 5-nitroindole-3-carboxylic acid and terminated with different benzofused-3 carboxylic acids **(Figure 2.30)**.

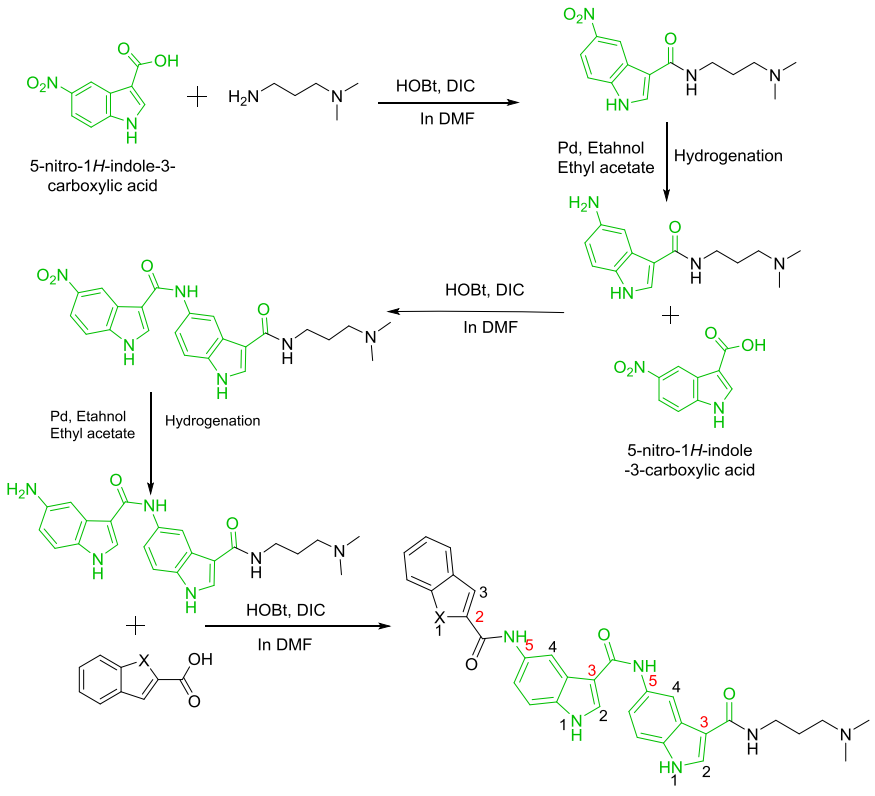

Figure 2.32: The synthetic reaction scheme for the first set of **library-3A** molecules. Here, X = O or N or S.

Initially, the acid (1.2 eq.) was dissolved in DMF (5 mL for 100 mg of starting material) in a round bottom flask fitted with a magnetic stirrer. Then DIC (1.75 eq.) and HOBt (2.0 eq.) were added to the acid (1.0 eq.) and this mixture was allowed to stir at room temperature for formation of the ester from the acid. The amine (1 eq.) was added to the mixture and the mixture allowed stirring until the reaction was complete, as indicated by TLC or LCMS. Finally the reaction mixture was applied to a conditioned SCX-2 cartridge and the resultant product was purified by the 'Catch and Release' method (described in the section '**Methods and Materials**' of Chapter 3).

2.8.1 Synthetic Scheme for Second Set of Library-3A Molecules

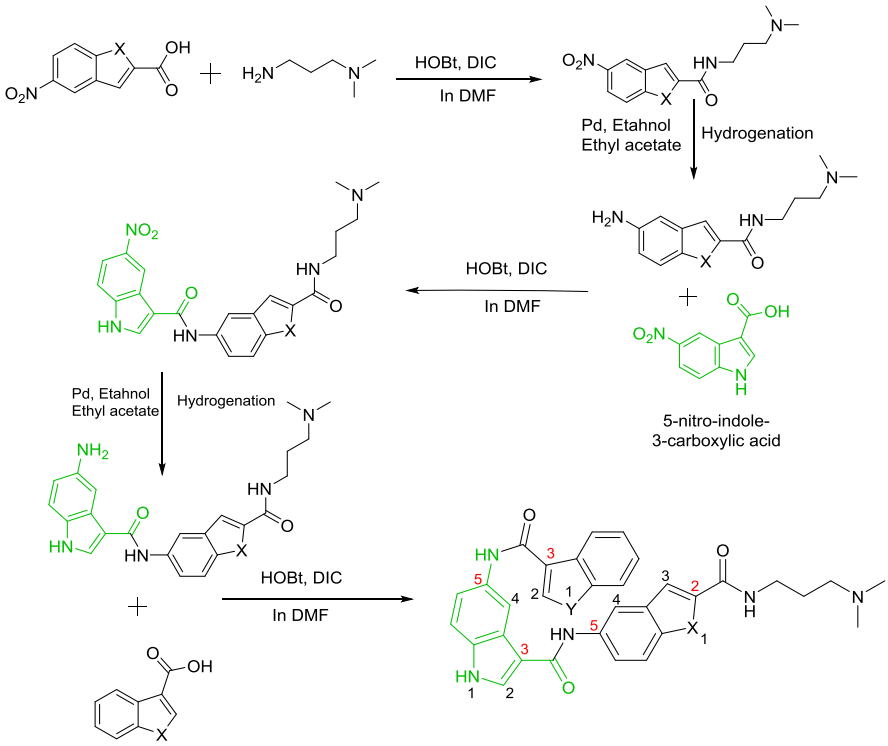

Figure 2.33: The synthetic reaction scheme for the second set of **library-3A** molecules. Here X = O or N or S.

Initially the acid (1.2 eq.) was dissolved in DMF (5 mL for 100 mg of starting material) in a round bottom flask fitted with a magnetic stirrer. Then DIC (1.75 eq.) and HOBt (2.0 eq.) were added to the acid (1.0 eq.) and this mixture was allowed to stir at room temperature for formation of the ester from the acid. The amine (1 eq.) was added to the mixture and the mixture allowed stirring until the reaction was complete, as indicated by TLC or LCMS. Finally the reaction

mixture was applied to a conditioned SCX-2 cartridge and the resultant product was purified by the 'Catch and Release' method (described in the section '**Methods and Materials'** of Chapter 3).

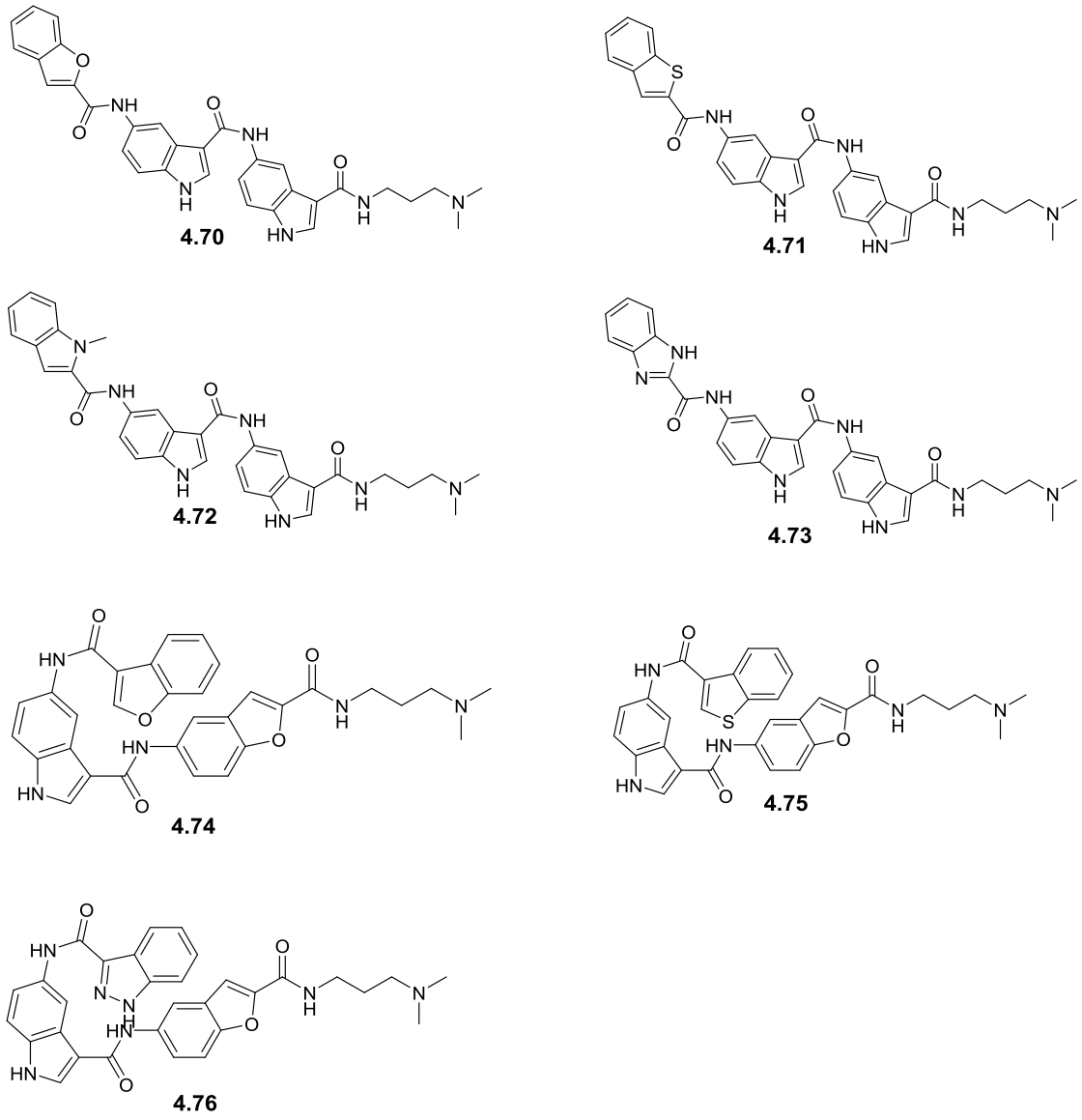

Figure 2.34: Structures of the **library-3A** molecules.

2.8.2 Characterisation of Library-3A Molecules through Various Spectroscopic Techniques

The benzofused polyamides of **library-3A** were purified and fully characterized by different spectroscopic techniques including mass spectrometry, both ^{1}H and ^{13}C NMR, and IR techniques (described in the '**Experimental**' section of

Chapter 4). Compounds were primarily identified by LCMS and confirmed using high resolution mass spectroscopy (HRMS) **(Tables 2.15 and 2.16)**.

Table 2.15: HRMS data for **library-3A** molecules

Number	Compound code	Theoretical mass	Observed mass $[M+H]^+$
1	**4.70**	562.2329	563.2388
2	**4.71**	578.2100	579.1430
3	**4.72**	575.2645	576.2703
4	**4.73**	562.2441	563.2502
5	**4.74**	563.2169	564.2228
6	**4.75**	579.1940	580.2000
7	**4.76**	563.2281	564.2344

2.8.3 Purity Analysis of Benzofused Polyamides Synthesized

The purity of the benzofused polyamides of this library was checked by two different HPLC methods with two different retention times. Both methods were carried out on a Waters Alliance 1695 HPLC Pump with water and acetonitrile comprising the mobile phases. The Waters 996 PDA start wavelength was 210 nm for the 10 minute method (Method A), with a start wavelength of 220 nm and end wavelength of 500 nm for the 5 minute method (Method B) **(Table 2.15 and 2.16)**.

Table 2.16: Purity data for **library-3A** as observed by HPLC

Number	Compound code	Purity	
		Method A(10 min)%	Method B(5 min)%
1	**4.70**	100	100
2	**4.71**	100	100
3	**4.72**	93	94
4	**4.73**	100	100
5	**4.74**	100	100
6	**4.75**	91	89.09
7	**4.76**	100	100

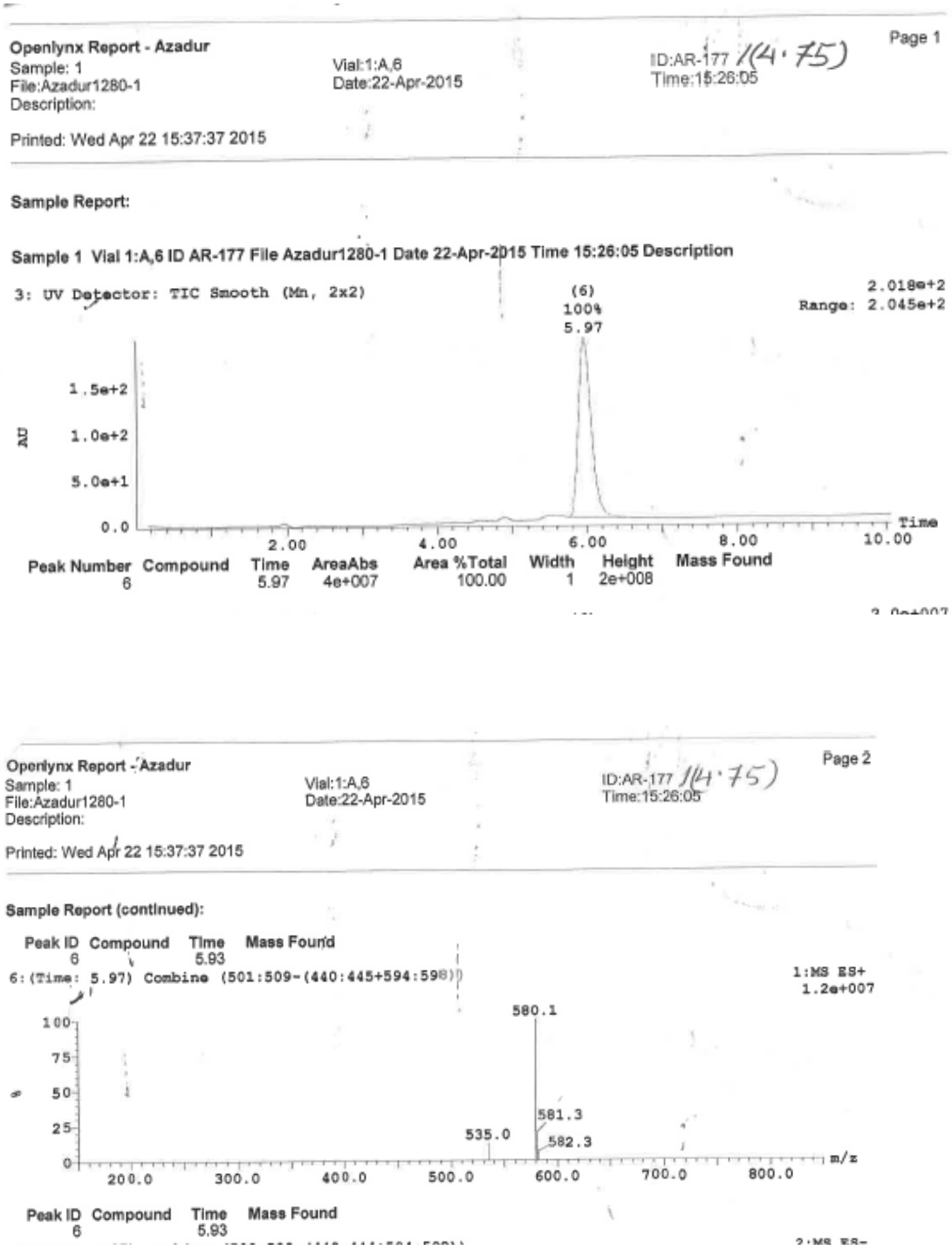

Figure 2.35: Example of an adapted LCMS profile of **Library-3A** compound **4.75**

Table 2.17: G-quadruplex and duplex DNA stabilization by ligands of **library-3A** in FRET melting experiments at concentrations of 5, 2 and 1 μM respectively (the data are means of three technical repeats)

Compounds	Quadruplex	ΔT_m(°C) ±(s/d)		
		5 μM	2 μM	1 μM
4.70	F21T	13.6±0.37	8.6±0.23	4.89±0.11
	C-kit-1	14.2±0.28	10.7±0.28	9.2±0.34
	C-kit-2	18.3±0.15	11.4±0.11	8.6±0.26
	BCL-2	15.7±0.23	10.4±0.20	7.4±0.20
	Duplex DNA	0.0±0.11	0.0±0.23	0.0±0.25
4.71	F21T	17.7±0.2	9.3±0.07	7.2±0.14
	C-kit-1	23.0±0.35	18.3±0.05	15.1±0.17
	C-kit-2	17.7±0.26	11.8±0.15	8.3±0.32
	BCL-2	15.5±0.26	8.9±0.23	5.9±0.14
	Duplex DNA	0.0±0.11	0.0±0.37	0.0±0.11
4.72	F21T	9.4±0.17	4.2±20	2.6±0.14
	C-kit-1	12.3±0.17	8.4±0.15	6.8±0.32
	C-kit-2	12.8±0.37	7.2±0.17	5.8±0.30
	BCL-2	10.2±0.11	5.3±0.32	4.2±0.20
	Duplex DNA	0.0±0.23	0.0±0.12	0.0±0.31
4.73	F21T	11.5±0.21	7.6±0.34	6.0±0.23
	C-kit-1	15.0±0.0	11.7±0.20	9.7±0.25
	C-kit-2	17.6±0.23	11.4±0.05	8.8±0.11
	BCL-2	15.8±0.05	10.4±0.25	7.8±0.36
	Duplex DNA	0.0±0.32	0.0±0.26	0.0±0.34

All the molecules belonging to this library showed significant interaction with the different G-quadruplex sequences used. **4.70** provided 4.89°C, 9.2°C, 8.6°C and 7.4°C stabilisation, **4.71** provided a 7.2°C, 15.1°C, 8.3°C and 5.9°C stabilisation, **4.72** provided 2.6 °C, 6.8 °C, 5.8 °C and 4.2 °C stabilisation and **4.73** provided 6.0°C, 9.7°C, 8.8°C and 7.8°C stabilisation at 1 μM concentrations against F21T, C-kit-1, C-kit-2 and Bcl-2 G-quadruplex sequences, respectively. It is notable that **4.71** showed a significantly higher degree of stabilisation against the C-kit-1 quadruplex sequence. Thus **4.71** is nearly specific to the C-kit-1 G-quadruplex sequence.

Table 2.18: G-quadruplex and duplex DNA stabilization by ligands of **library-3A** in FRET melting experiments at concentrations of 5, 2 and 1 μM respectively (the data are means of three technical repeats)

Compounds	Quadruplex types	ΔT_m(°C) ±(s/d)		
		5 μM	2 μM	1 μM
4.74	F21T	16.2±0.12	10.2±0.20	5.2±0.23
	C-kit-1	17.0±0.05	13.9±0.35	11.4±0.26
	C-kit-2	22.2±0.28	15.7±0.40	12.5±0.35
	BCL-2	17.1±0.15	11.7±0.28	10.0±0.15
	Duplex DNA	0.0±0.12	0.0±0.07	0.0±0.11
4.75	F21T	17.7±0.13	10.6±0.12	7.8±0.31
	C-kit-1	17.8±0.36	15.4±0.25	12.8±0.11
	C-kit-2	24.4±0.05	18.4±0.30	14.6±0.10
	BCL-2	18.7±0.10	13.5±0.25	10.0±0.20
	Duplex DNA	0.0±0.41	0.0±0.14	0.0±0.07
4.76	F21T	21.3±0.33	15.2±0.41	12.0±0.11
	C-kit-1	22.4±0.11	18.2±0.11	15.6±0.50
	C-kit-2	22.0±0.11	17.5±0.05	13.6±0.25
	BCL-2	19.3±0.11	13.6±0.15	9.9±0.10
	Duplex DNA	0.0±0.1	0.0±0.23	0.0±0.11

The second set of molecules showed similar interactions to the first set. Here, **4.74** provided 5.2°C, 11.4°C, 12.5°C and 10.0°C stabilisation, **4.75** provided 7.8°C, 12.8 °C, 14.6°C and 10.0°C stabilisation and **4.76** provided 12.0°C, 15.6°C, 13.6°C and 9.9°C stabilisation at 1 μM concentrations against F21T, C-kit-1, C-kit-2 and Bcl-2 G-quadruplex sequences, respectively. **4.76** was relatively more active towards G-quadruplex sequences. This is possibly due to the extra nitrogen atom of the terminal benzimidazole building block. However, when compared to the molecules from both libraries (**library-2** and **library-3**) with equivalent melting temperatures, it would be more convenient to investigate the effect of the introduction of additional curvature within the ligand molecules.

FRET data comparison between **library-2** and **library-3A** clearly identified a distinguishing feature. Two equivalent molecules (**4.52** and **4.49** from **library-2** compared with **4.70** and **4.71** from **library-3A**) were taken from both libraries to compare directly for the effects of curvature. **4.70** started with an indole building block instead of benzofuran as in **4.52**. In contrast, **4.71** started with an indole building block instead of benzothiophene as in **4.49**.

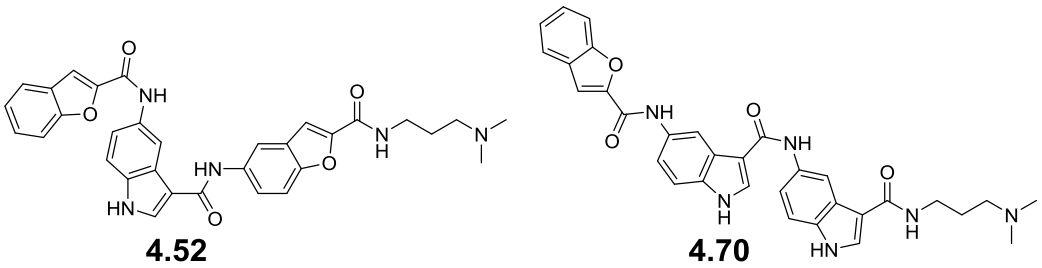

4.52 **4.70**

Figure 2.36: Structures of **4.52** and **4.70**.

Table 2.19: Direct comparison between the equivalent molecules of **library-2** and **library-3A** (the data are means of three technical repeats)

Quadruplex types	ΔT_m(°C) ±(s/d)					
	4.52	**4.70**	**4.52**	**4.70**	**4.52**	**4.70**
	5 µM	5 µM	2 µM	2 µM	1 µM	1 µM
F21T	6.22±0.41	13.6±0.37	3.5±0.24	8.6±0.23	2.4±0.37	4.89±0.11
C-kit-1	13.1±0.23	14.2±0.28	8.5±0.25	10.7±0.28	7.8±0.15	9.2±0.34
C-kit-2	18.0±0.15	18.3±0.15	10.3±0.40	11.4±0.11	8.1±0.36	8.6±0.26
BCL-2	14.8±0.40	15.7±0.23	8.3±0.35	10.4±0.20	5.6±0.36	7.4±0.20
Duplex DNA	0.0±0.17	0.0±0.11	0.0±0.14	0.0±0.23	0.0±0.22	0.0±0.25

FRET data analysis of the benzofused polyamides of **library-2** and **library-3A** showed a clear difference in melting temperatures (ΔT_m). The introduction of a second 5′-3′-benzofused moiety moderately improved the interacting capacity of the polyamides. This could be explained by the comparison of ΔTm values of two equivalent molecules (i.e. **4.70** from **library-3A** and **4.52** from **library-2**)**. 4.70** showed comparatively more stabilising capacity than **4.52**; **4.52** provided 2.4°C, 7.8°C, 8.1°C and 5.6°C stabilisation, whereas **4.70** provided 4.9°C, 9.2°C, 8.6°C and 7.4°C stabilisation at 1 µM concentrations against F21T, C-kit-1, C-kit-2 and Bcl-2 G-quadruplex sequences, respectively. This suggested that the introduction of more curvature made the ligands more potent. In addition, **4.52** and **4.70** both showed a nearly identical pattern of stabilisation towards the different G-quadruplex sequence types tested against.

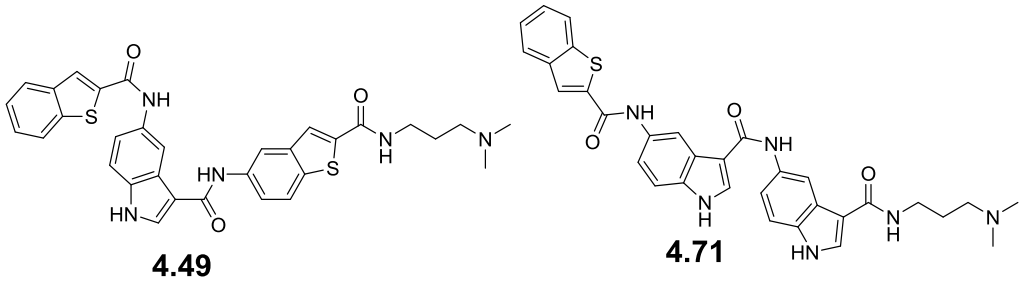

Figure 2.37: Structures of equivalent molecules **4.49** and **4.71**.

Table 2.20: Direct comparison between the equivalent molecules of **library-2** and **library-3A** (the data are means of three technical repeats)

Quadruplex types	ΔT_m(°C) ±(s/d)					
	4.49	**4.71**	**4.49**	**4.71**	**4.49**	**4.71**
	5 µM	5 µM	2 µM	2 µM	1 µM	1 µM
F21T	14.6±0.20	17.7±0.2	7.5±0.14	9.3±0.07	3.4±0.34	7.2±0.14
C-kit-1	13.1±0.25	23.0±0.35	10.4±0.36	18.3±0.05	9.9±0.21	15.1±0.17
C-kit-2	17.2±0.23	17.7±0.26	11.7±0.05	11.8±0.15	11.0±0.20	8.3±0.32
BCL-2	12.3±0.15	15.5±0.26	5.6±0.20	8.9±0.23	5.3±0.20	5.9±0.14
Duplex DNA	0.0±0.23	0.0±0.11	0.0±0.21	0.0±0.37	0.0±0.35	0.0±0.11

4.49 and **4.71** also showed the same pattern of stabilisation as **4.52** and **4.70**. **4.71** was found to show comparatively more stabilisation capacity than **4.49**; **4.49** provided 3.4°C, 9.9°C, 11.0°C and 5.3°C stabilisation at 1 µM concentration against F21T, C-kit-1, C-kit-2 and Bcl-2 G-quadruplex sequences, respectively, whereas **4.71** provided 7.2°C, 15.1°C, 8.3°C and 5.9°C stabilisation at 1 µM concentration against F21T, C-kit-1, C-kit-2 and Bcl-2 G-quadruplex sequences, respectively.

These obseravations are suggesting an idea that the introduction of more curvature within the benzofused polyamides results in a greater stabilisation capacity of the ligand molecules. In addition, **4.52** and **4.70** followed a similar pattern of stabilizing capacities toward the different G-quadruplex sequence types tested.

These molecules of **library-3A** were supposed to interact differently as they include four different benzofused ring types; however, all of them are following a nearly similar pattern of activities. This infers that first and second consecutive indole rings might be an interaction capacity-determining factor for these ligand molecules.

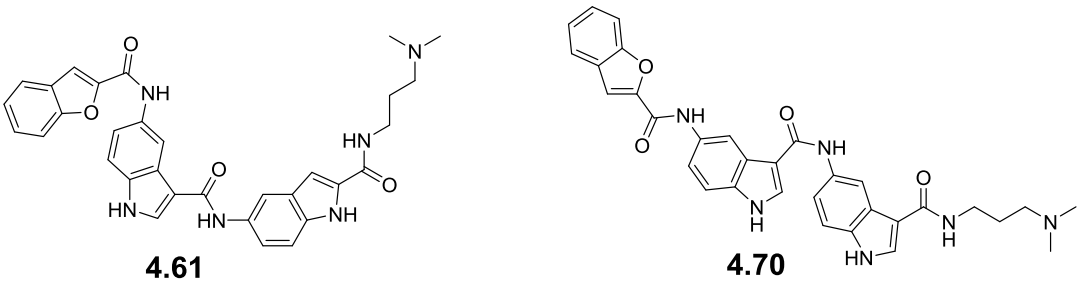

4.61 **4.70**

Figure 2.38: Structures of **4.61** and **4.70**.

Table 2.21: Direct comparison between first and second degree curvature of molecules starting with two consecutive indole rings (the data are means of three technical repeats)

Quadruplex types	ΔT_m(°C) ±(s/d)					
	4.61	**4.70**	**4.61**	**4.70**	**4.61**	**4.70**
	5 µM	5 µM	2 µM	2 µM	1 µM	1 µM
F21T	18.0±0.20	13.6±0.37	7.4±0.13	8.6±0.23	5.2±0.34	4.89±0.11
C-kit-1	14.4±0.10	14.2±0.28	8.8±0.10	10.7±0.28	7.4±0.32	9.2±0.34
C-kit-2	18.1±0.45	18.3±0.15	11.4±0.20	11.4±0.11	7.7±0.30	8.6±0.26
BCL-2	13.9±0.15	15.7±0.23	7.6±0.17	10.4±0.20	4.7±0.30	7.4±0.20
Duplex DNA	0.0±0.14	0.0±0.11	0.0±0.21	0.0±0.23	0.0±0.15	0.0±0.25

Here, it was found that **4.70** interacts with G-quadruplex sequences more strongly than **4.61**; **4.61** provided 5.2°C, 7.4°C, 7.7°C and 4.7°C stabilisation at 1 µM concentration against F21T, C-kit-1, C-kit-2 and Bcl-2 G-quadruplex sequences, respectively, whereas **4.70** provided 4.89°C, 9.2°C, 8.6°C and 7.4°C stabilisation at 1 µM concentration against the same G-quadruplex sequences. This result indicated that **4.61** may be the best ligand out of the library in providing G-quadruplex stabilisation, and supports the notion that the curvature of the ligand molecules contributes towards an enhanced stabilisation of G-quadruplex.

2.8.4 Key Observations from the Overall Library-3A FRET Melting Data Analysis

- Introduction of curvature strongly correlates with increases in the stabilisation capacity of ligand molecules.
- A second degree of curvature is better than a first degree of curvature.
- Indole, rather than the benzothiophene or benzofuran building blocks, appears to be the best scaffold for making more potent ligands.

2.9 Molecular Modelling Study of Library-3A Molecules

Molecular docking studies of the molecules synthesised in **Library-3A** support predictions made during analysis of **Library-2** molecules. In general, the introduction of a second 5'-3'-benzofused moiety enhanced stabilisation of each quadruplex structure. This likely occurs due to an enhanced shape-fit of the molecule with DNA. For example, in the case of **4.61** and **4.70** (**Figure: 2:24** and **2.31**, **Table: 2.12** and **2.17**) (which have identical benzofused content and only differ by benzofused substitution pattern), G-quadruplex stabilisation was increased by up to 2.7°C at 1 μM concentration in the case of BCL-2. Although this increase is not as substantial as the increase observed between **Libraries 1** and **2**, the increase is nonetheless significant. This difference is reflected in binding energies calculated for **4.61** and **4.70** (-74.54kcal/mol and -76.5 kcal/mol, which suggest that **4.70** should enhance G-quadruplex stabilisation to a greater extent than **4.61 (Figure 2.35)**.

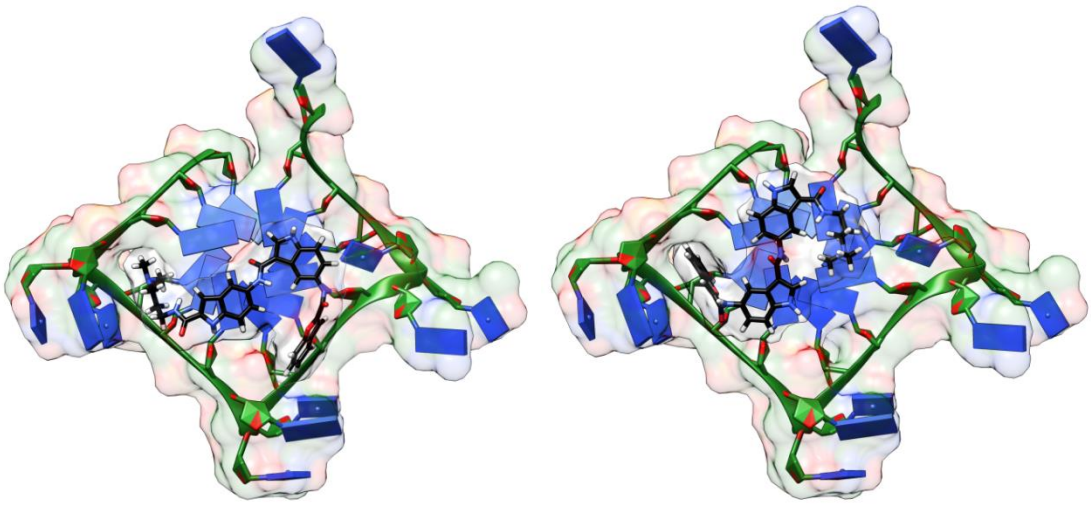

Figure 2.39: Molecular model of **4.61** (left panel) and **4.70** (right panel) bound to the telomeric F21T G-quadruplex illustrating the difference in accommodation of a **Library 2** molecule (**4.61**) and **Library 3** molecule (**4.70**). In the case of **4.61** (black sticks), two benzofused molecules are capable of orienting directly over guanine bases (blue nucleotide objects), thereby enhancing stabilisation. In the case of **4.70**, two benzofused moieties are capable of interacting with the G-quadruplex, but appear to stack directly over the G tetrad. The amidic tail of the molecule also appears to interact with DNA to some degree, thereby enhancing stabilisation.

Library-3B

2.10 Synthesis of Library-3B Molecules by the Structural Modification of Library-3A Molecules

Initially, 4 molecules **(Figure 2.37)** were synthesized and evaluated to investigate the effect of an electron-withdrawing nitro group on the terminal indole unit of **library-3A** molecules. Then 5 more molecules **(Figure 2.37)** were synthesized further for a structure activity relationship (SAR) of **4.77** through modification of the shape of **4.77**. Here, 5-nitro-benzofused-2-carboxylic acid was chosen to be a capping acid instead of benzofused-3-carboxylic acid in order to observe the effect of a nitro group on the G-quadruplex interactive capacities of the ligand molecules.

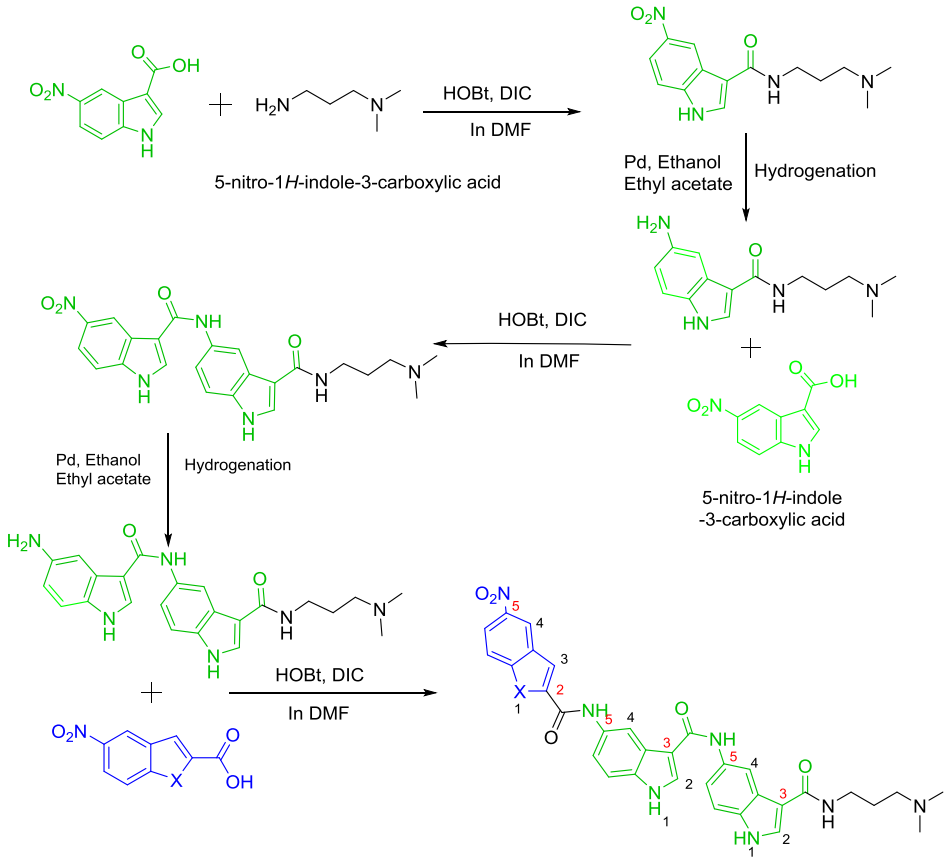

Figure 2.40: Synthetic scheme of **library-3B** molecules. Here X = O or N or S.

Two consecutive 5-nitro-indole-3 carboxylic acids were coupled one after another and then this intermediate was capped with four different 5-nitro-benzofused-2-carboxylic acids to get final ligands with the same shape as the **library-3A** molecules **(Figure 2.36)**. In addition to this, **4.80**, an equivalent

molecule of **4.77**, was synthesized to investigate the relative effects of indole and indazole as terminal capping acids.

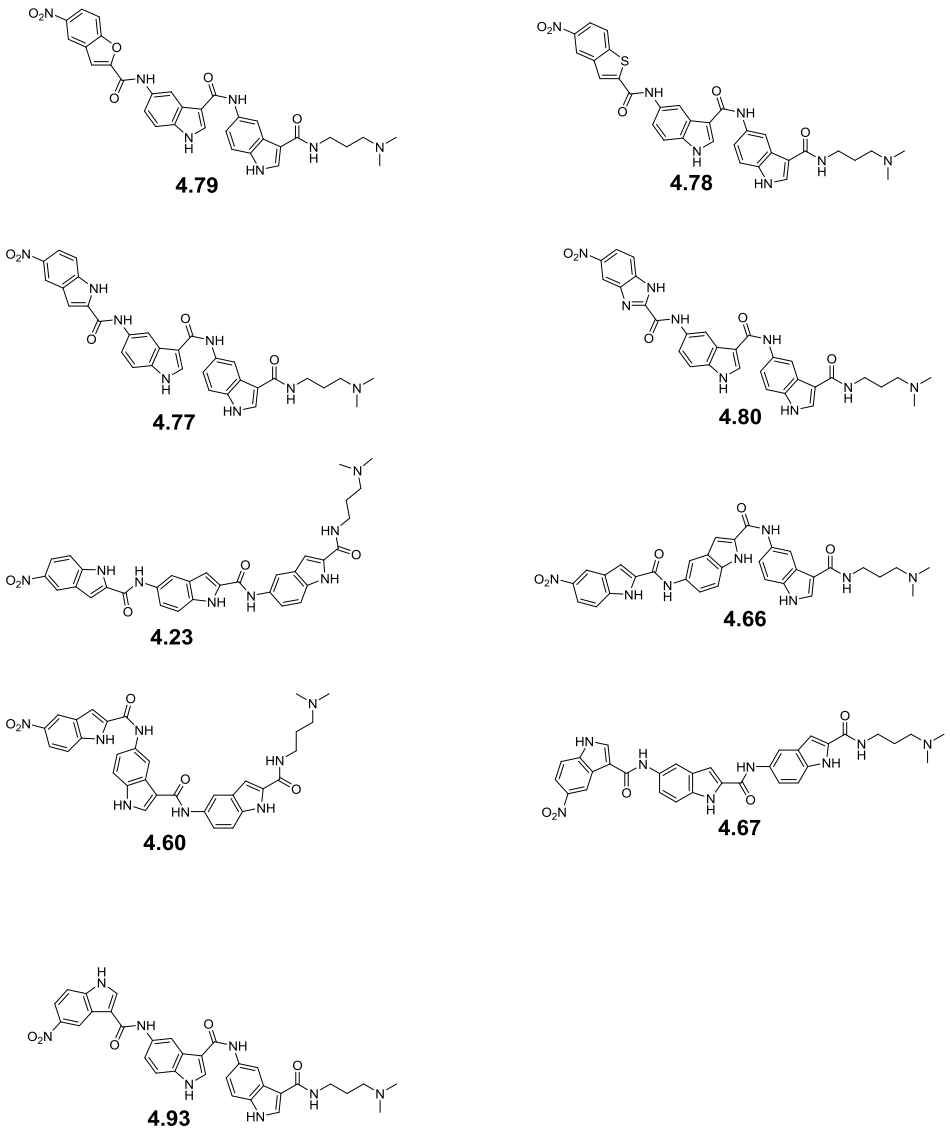

Figure 2.41: Structures of **library-3B** molecules.

Initially the acid (1.2 eq.) was dissolved in DMF (5 mL for 100 mg of starting material) in a round bottom flask fitted with a magnetic stirrer. Then DIC (1.75 eq.) and HOBt (2.0 eq.) were added to the acid (1.0 eq.) and this mixture was allowed to stir at room temperature for formation of the ester from the acid. The amine (1 eq.) was added to the mixture and the mixture allowed to stir until the reaction was complete, as indicated by TLC or LCMS. Finally the reaction mixture was applied to a conditioned SCX-2 cartridge and the resultant product was purified by the 'Catch and Release' method (described in the section '**Methods and Materials**' of Chapter 3).

2.10.1 Characterisation of Benzofused Polyamides through Various Spectroscopic Techniques

The benzofused polyamides of **library-3B** were purified and fully characterized by different spectroscopic techniques including mass spectrometry, both ^{1}H and ^{13}C NMR, and IR techniques (described in the '**Experimental**' section of Chapter 4). Compounds were primarily identified by LCMS and confirmed using high resolution mass spectroscopy (HRMS) **(Table 2.22 and 2.23)**.

Table 2.22: HRMS data for **library-3B** molecules

Number	Compound code	Theoretical mass	Observed mass $[M+H]^+$
1	**4.79**	607.2179	608.2244
2	**4.78**	623.1951	624.2017
3	**4.77**	606.2339	607.2396
4	**4.80**	607.2292	608.2362
5	**4.23**	606.2339	607.2405
6	**4.66**	606.2339	607.2398
7	**4.60**	606.2339	607.2400
8	**4.67**	606.2339	607.2399
9	**4.93**	606.2339	607.2402

2.10.2 Purity Analysis of Benzofused Polyamides Synthesized

The purity of the benzofused polyamides of this library was checked by two different HPLC methods with two different retention times. The Waters 996 PDA start wavelength was 210 nm for the 10 minute method (Method A), with a start wavelength of 220 nm and end wavelength of 500 nm for the 5 minute method (Method B) **(Table 2.22 and 2.23)**.

Table 2.23: Purity data for **library-3B** molecules as observed by HPLC

Number	Compound code	Purity	
		Method A (10 min)%	Method B (5 min)%
1	**4.79**	100	100
2	**4.78**	100	100
3	**4.77**	100	100
4	**4.80**	100	100
5	**4.23**	100	100
6	**4.66**	100	100
7	**4.60**	100	100
8	**4.67**	100	100
9	**4.93**	100	100

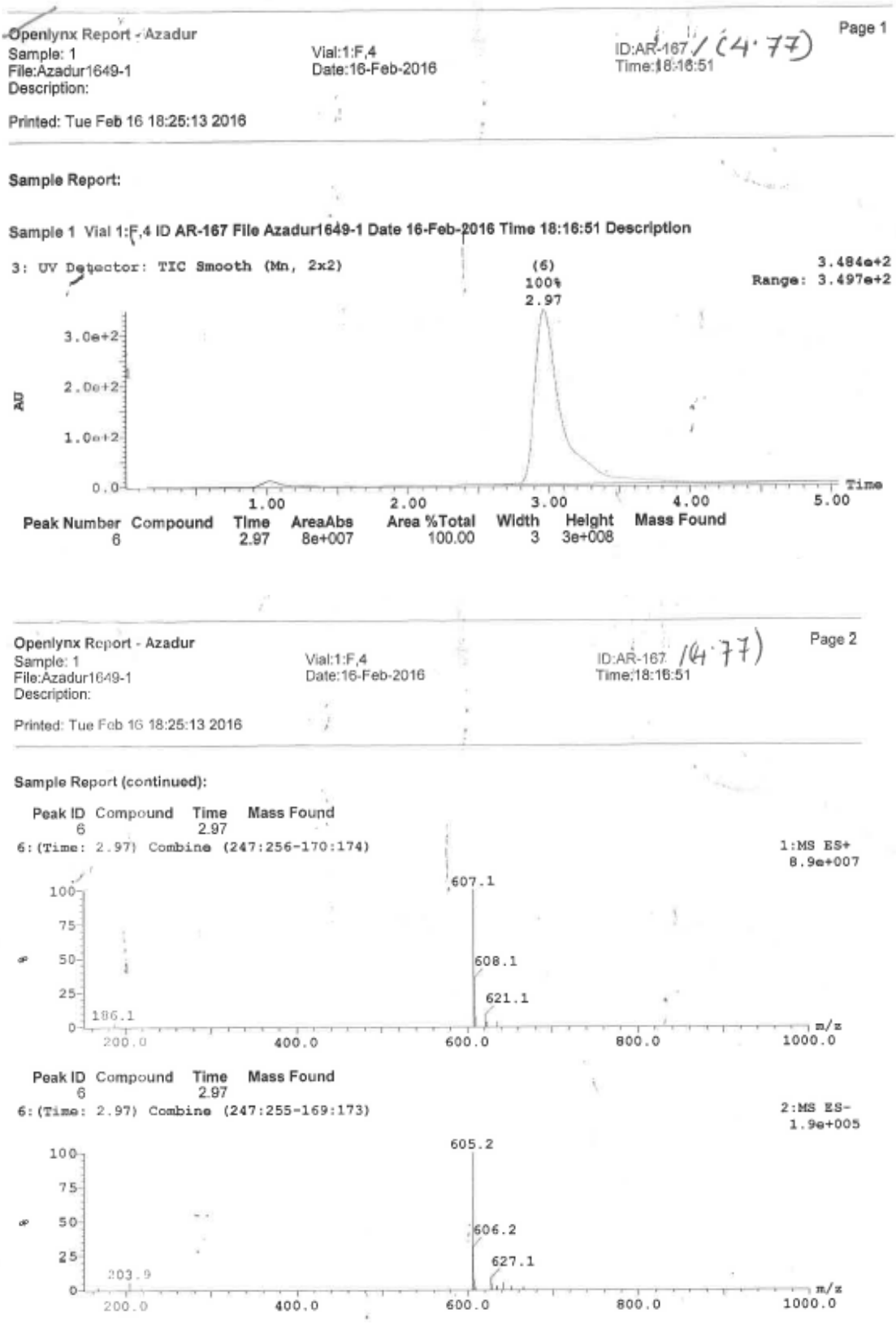

Figure 2.42: Example of an adapted LCMS profile of **Library-3B** compound **4.77**

Table 2.24: G-quadruplex and duplex DNA stabilization by ligands in FRET melting experiments at concentrations of 5, 2 and 1 μM respectively (the data are means of three technical repeats)

Compound code	Quadruplex	ΔT_m(°C) ±(s/d)		
		5 μM	2 μM	1 μM
4.79	F21T	15.8±0.23	9.9±0.21	6.0±0.20
	C-kit-1	19.5±0.35	12.8±0.34	9.2±0.20
	C-kit-2	19.3±0.20	14.8±0.36	11.2±0.40
	BCL-2	22.9±0.07	11.4±0.35	7.7±0.24
	Duplex DNA	0.0±0.32	0.0±0.21	0.0±0.43
4.78	F21T	18.8±0.12	11.6±0.23	8.8±0.07
	C-kit-1	21.6±0.07	14.8±0.28	11.7±0.35
	C-kit-2	27.0±0.32	15.8±0.15	13.0±0.32
	BCL-2	23.9±0.05	14.7±0.10	10.5±0.15
	Duplex DNA	1.0±0.23	0.0±0.12	0.0±0.07
4.77	F21T	21.7±0.26	15.6±0.07	12.2±0.23
	C-kit-1	24.5±0.40	16.7±0.26	14.4±0.35
	C-kit-2	27.8±0.36	17.9±0.21	14.7±0.26
	BCL-2	30.8±0.21	15.7±0.28	12.1±0.25
	Duplex DNA	1.0±0.12	0.0±0.1	0.0±0.23
4.80	F21T	12.7±0.24	8.4±0.16	4.8±0.21
	C-kit-1	16.2±0.20	11.6±0.32	7.6±0.15
	C-kit-2	22.1±0.20	15.0±0.34	10.2±0.26
	BCL-2	18.6±0.41	10.7±0.40	7.7±0.11
	Duplex DNA	0.0±0.23	0.0±0.31	0.0±0.12

From this FRET data analysis, it is very clear that the introduction of a nitro group enhances the interactive capacities of ligand molecules. This could be explained in a number of possible ways, including hydrogen bond formation between the nitro group and amino, imine or carbonyl groups from guanine residues of the G-quartet, the nitro group potentially recruiting potassium ions which could help to stack the quartet together, or the nitro group providing additional electronic interactions.

However, it is more convenient to evaluate the effect of the nitro group's inclusion by comparing between equivalent molecules of **library-3A** and **library-3B.**

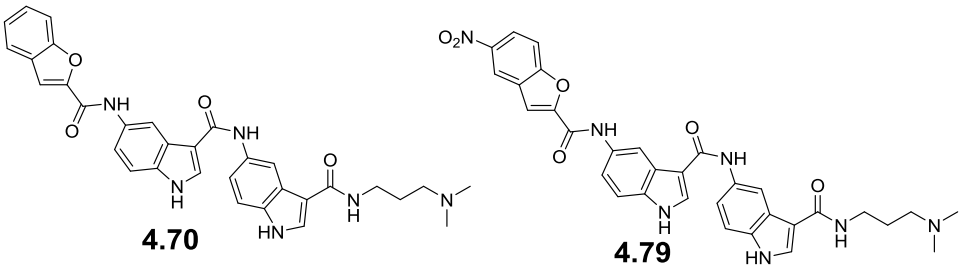

Figure 2.43: Structures of **4.70** and **4.79**.

Table 2.25: Comparative G-quadruplex and duplex DNA stabilization between ligands **4.70** and **4.79** in FRET melting experiments at concentrations of 5, 2 and 1 µM respectively (the data are means of three technical repeats)

Quadruplex types	ΔT_m(°C) ±(s/d)					
	4.70	**4.79**	**4.70**	**4.79**	**4.70**	**4.79**
	5 µM	5 µM	2 µM	2 µM	1 µM	1 µM
F21T	13.6±0.37	15.8±0.23	8.6±0.23	9.9±0.21	4.89±0.11	6.0±0.20
C-kit-1	14.2±0.28	19.5±0.35	10.7±0.28	12.8±0.34	9.2±0.34	9.2±0.20
C-kit-2	18.3±0.15	19.3±0.20	11.4±0.11	14.8±0.36	8.6±0.26	11.2±0.40
BCL-2	15.7±0.23	22.9±0.07	10.4±0.20	11.4±0.35	7.4±0.20	7.7±0.24
Duplex DNA	0.0±0.11	0.0±0.32	0.0±0.23	0.0±0.21	0.0±0.25	0.0±0.43

Here, **4.79** is shown to have a better interacting capacity compared to the equivalent ligand **4.70**, since **4.70** provided 4.89°C, 9.2°C, 8.6°C and 7.4°C stabilisation at 1 µM concentration against F21T, C-kit-1, C-kit-2 and Bcl-2 G-quadruplex sequences, respectively, whilst **4.79** provided 6.0°C, 9.2°C, 11.2°C and 7.7°C stabilisation at 1 µM concentration against the same G-quadruplex sequences, respectively. Thus the molecules terminating with benzofuran did not show a significant difference in their melting temperatures even though they have an electron-withdrawing nitro group in their structures.

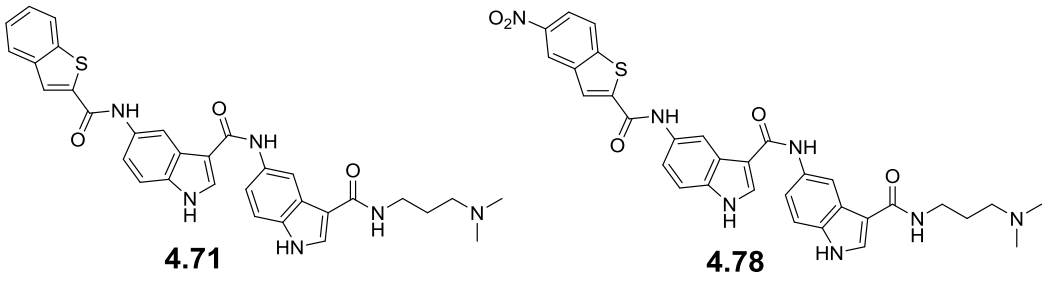

Figure 2.44: Structures of equivalent molecules **4.71** and **4.78**.

Table 2.26: Comparative FRET data analysis between **4.71** and **4.78** (the data are means of three technical repeats)

Quadruplex types	ΔT_m(°C) ±(s/d)					
	4.71	**4.78**	**4.71**	**4.78**	**4.71**	**4.78**
	5 µM	5 µM	2 µM	2 µM	1 µM	1 µM
F21T	17.7±0.2	18.8±0.12	9.3±0.07	11.6±0.23	7.2±0.14	8.8±0.07
C-kit-1	23.0±0.35	21.6±0.07	18.3±0.05	14.8±0.28	15.1±0.17	11.7±0.35
C-kit-2	17.7±0.26	27.0±0.32	11.8±0.15	15.8±0.15	8.3±0.32	13.0±0.32
BCL-2	15.5±0.26	23.9±0.05	8.9±0.23	14.7±0.10	5.9±0.14	10.5±0.15
Duplex DNA	0.0±0.11	1.0±0.23	0.0±0.37	0.0±0.12	0.0±0.11	0.0±0.07

Here, **4.71** provided 7.2°C, 15.1°C, 8.3°C and 5.9°C stabilisation at 1 µM concentration against F21T, C-kit-1, C-kit-2 and Bcl-2 G-quadruplex sequences, respectively, and **4.78** provided 8.8°C, 11.7°C, 13.0°C and 10.5°C stabilisation at 1 µM concentration against the same G-quadruplex sequences. Both of them were found to be equally interactive towards G-quadruplex sequences. Moreover, **4.71** had a tendency to be a partially specific toward C-kit-1 and c-kit-2. On the other hand, **4.78** tended to show a partial specificity toward-kit-2 rather than C-kit-1. However, like **4.70** and **4.79**, the molecules terminating with nitro group-containing thiophenes did not possess significantly improved melting temperatures.

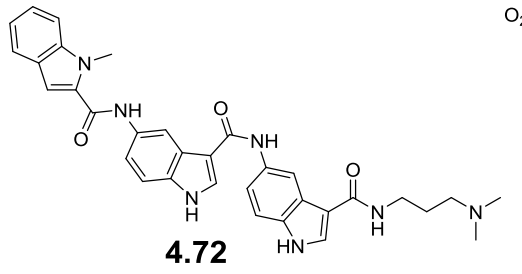

4.72

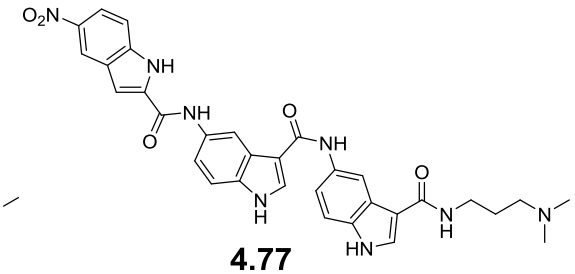

4.77

Figure 2.45: Structures of **4.72** and **4.77**.

Table 2.27: Comparative FRET data analysis between **4.72** and **4.77** molecules (the data are means of three technical repeats)

Quadruplex types	ΔT_m(°C) ±(s/d)					
	4.72	**4.77**	**4.72**	**4.77**	**4.72**	**4.77**
	5 µM	5 µM	2 µM	2 µM	1 µM	1 µM
F21T	9.4±0.17	21.7±0.26	4.2±20	15.6±0.07	2.6±0.14	12.2±0.23
C-kit-1	12.3±0.17	24.5±0.40	8.4±0.15	16.7±0.26	6.8±0.32	14.4±0.35
C-kit-2	12.8±0.37	27.8±0.36	7.2±0.17	17.9±0.21	5.8±0.30	14.7±0.26
BCL-2	10.2±0.11	30.8±0.21	5.3±0.32	15.7±0.28	4.2±0.20	12.1±0.25
Duplex DNA	0.0±0.23	1.0±0.12	0.0±0.12	0.0±0.1	0.0±0.31	0.0±0.23

Here, **4.77** provided relatively higher melting temperatures of 12.2°C, 14.4°C, 14.7°C and 12.2°C stabilisation at 1 µM concentration against F21T, C-kit-1, C-kit-2 and Bcl-2 G-quadruplex sequences, respectively. On the other hand, an equivalent molecule **4.72** lacking the nitro group provided 2.6°C, 6.8°C, 5.8°C and 4.2°C stabilisation at 1 µM concentration against F21T, C-kit-1, C-kit-2 and Bcl-2 G-quadruplex sequences, respectively. Here, unlike with the benzofuran or benzothiophene, the molecules with nitro-indole groups had significantly higher melting temperatures compared to the equivalent ligands without the nitro group. Therefore, it is evident that the electron-withdrawing nitro group plays a positive role in improving the G-quadruplex interacting capacity of these ligands.

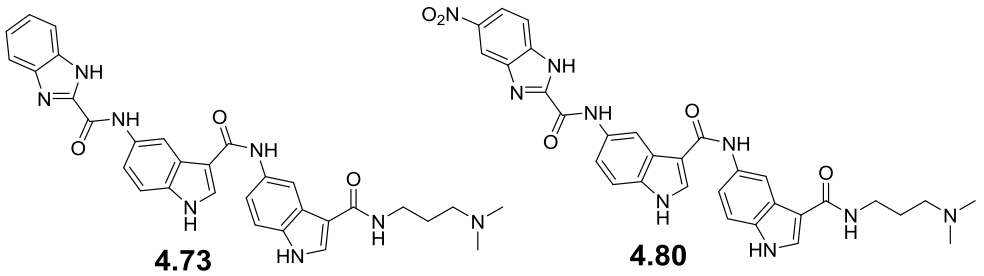

Figure 2.46: Structures of **4.73** and **4.80**.

Table 2.28: Comparative FRET data analysis between **4.73** and **4.80** (the data are means of three technical repeats)

Quadruplex types	ΔT_m(°C) ±(s/d)					
	4.73	**4.80**	**4.73**	**4.80**	**4.73**	**4.80**
	5 µM	5 µM	2 µM	2 µM	1 µM	1 µM
F21T	11.5±0.21	12.7±0.24	7.6±0.34	8.4±0.16	4.8±0.21	6.0±0.23
C-kit-1	15.0±0.0	16.2±0.20	11.7±0.20	11.6±0.32	7.6±0.15	9.7±0.25
C-kit-2	17.6±0.23	22.1±0.20	11.4±0.05	15.0±0.34	10.2±0.26	8.8±0.11
BCL-2	15.8±0.05	18.6±0.41	10.4±0.25	10.7±0.40	7.7±0.11	7.8±0.36
Duplex DNA	0.0±0.32	0.0±0.23	0.0±0.26	0.0±0.31	0.0±0.12	0.0±0.34

The overall data analysis showed that **4.77** was better than any other members of this library. Therefore **4.77** was taken to be a lead benzofused polyamide for a subsequent structure activity relationship (SAR) study.

It was possible to find a preferred building block by comparing the two equivalent molecules **4.80** and **4.77** (both of them are structurally equivalent with the exception of their terminal building block types).

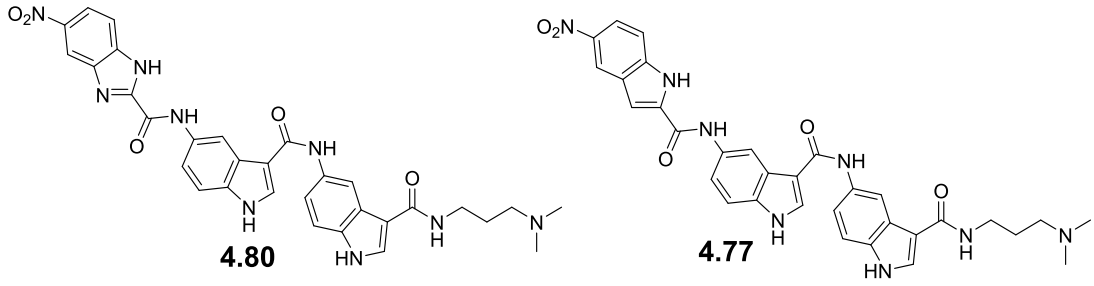

Figure 2.47: Structures of equivalent molecules **4.80** and **4.77**.

Table 2.29: Comparative FRET data analysis between **4.80** and **4.77** (the data are means of three technical repeats)

Quadruplex types	ΔT_m(°C) ±(s/d)					
	4.80	**4.77**	**4.80**	**4.77**	**4.80**	**4.77**
	5 µM	5 µM	2 µM	2 µM	1 µM	1 µM
F21T	12.7±0.24	21.7±0.26	8.4±0.16	15.6±0.07	6.0±0.23	12.2±0.23
C-kit-1	16.2±0.20	24.5±0.40	11.6±0.32	16.7±0.26	9.7±0.25	14.4±0.35
C-kit-2	22.1±0.20	27.8±0.36	15.0±0.34	17.9±0.21	8.8±0.11	14.7±0.26
BCL-2	18.6±0.41	30.8±0.21	10.7±0.40	15.7±0.28	7.8±0.36	12.1±0.25
Duplex DNA	0.0±0.23	1.0±0.12	0.0±0.31	0.0±0.1	0.0±0.34	0.0±0.23

4.77 provided relatively high melting temperature of 12.2°C, 14.4°C, 14.7°C and 12.2°C stabilisation at 1 µM concentration against F21T, C-kit-1, C-kit-2 and Bcl-2 G-quadruplex sequences, respectively, whilst an equivalent **4.80** provided relatively low ΔTm values of 6.0°C, 9.2°C, 11.2°C and 7.7°C stabilisation at 1 µM concentration against the same G-quadruplex sequences, respectively. It was very clear from the overall data analysis that for the molecules belonging to **library-3B**, **4.77** is a more highly G-quadruplex-interactive molecule than **4.80**, even though **4.80** possessed a terminal nitro-benzimidazole group instead of the nitro-indole seen in **4.77**. This indicated that indole was a better group compared to any of the other building blocks used. At the same time, **4.77** could be rationally considered to be a lead ligand for all of G-quadruplex sequences used, for further optimisation in order to get a more potent ligand.

2.10.3 Structure Activity Relationship of Lead Ligand 4.77

4.77 showed significantly interaction with G-quadruplex sequences; therefore this was taken as a lead ligand for further structural modifications. A structural activity relationship (SAR) was done including modifications of the shape (**Figure 2.37, Table 2.30**), tail types **(Figure 2.55, Table 2.42)** and functional groups **(Figure 2.57, Table 2.45)** attached to the terminal indole group.

Table 2.30: G-quadruplex and duplex DNA stabilization by ligands **(4.23, 4.66, 4.60, 4.67, 4.77 and 4.93)** in FRET melting experiments (the data are means of three technical repeats)

Compound Code	Quadruplex type	ΔT_m(°C) ±(s/d)		
		5 µM	2 µM	1 µM
4.23	F21T	0.5±0.13	0.4±0.34	0.3±0.17
	C-kit-1	0.8±0.2	0.1±0.35	0.4±0.23
	C-kit-2	1.9±0.20	0.7±0.15	0.03±0.23
	BCL-2	0.8±0.36	0.3±0.20	0.5±0.34
	Duplex DNA	0.0±0.15	0.0±0.11	0.0±0.14
4.66	F21T	0.6±0.11	0.3±0.32	0.3±0.37
	C-kit-1	10.5±0.25	0.8±0.26	0.3±0.20
	C-kit-2	6.1±0.30	1.3±0.20	1.0±0.30
	BCL-2	5.1±0.25	1.8±0.12	1.3±0.15
	Duplex DNA	1.0±0.34	0.0±0.21	0.0±0.07
4.60	F21T	18.2±0.05	7.4±0.07	5.7±0.21
	C-kit-1	18.6±0.15	14.3±0.05	11.5±0.25
	C-kit-2	21.7±0.15	14.0±0.26	10.9±0.20
	BCL-2	17.8±0.15	9.4±5.34	6.6±0.11
	Duplex DNA	0.0±0.27	0.0±0.11	0.0±0.31
4.67	F21T	5.6±0.21	2.5±0.41	1.5±0.15
	C-kit-1	10.2±0.20	5.3±0.36	3.1±0.23
	C-kit-2	11.0±0.11	5.7±0.20	4.1±0.35
	BCL-2	17.3±0.36	4.1±0.36	2.2±0.26
	Duplex DNA	1.0±0.10	1.0±0.10	0.0±0.360.05
4.93	F21T	21.0±0.17	15.9±0.28	12.6±0.26
	C-kit-1	27.7±0.30	22.1±0.35	17.6±0.28
	C-kit-2	21.3±0.23	14.8±0.20	11.4±0.32
	BCL-2	25.4±0.30	17.8±0.14	13.5±0.20
	Duplex DNA	0.0±0.05	0.0±0.05	0.0±0.05

Here, **4.23** did not show any interaction with the G-quadruplex types used, as seen before for similar molecules belonging to **library-1**. This 5'-2' substituted

molecule was structurally the same as the molecules of **library-1**. Its FRET data further verified that of the **library-1** molecules and indicated that 5'-2' substituted ligands do not have sufficient curvature in their structures to fit into G-quartets. However, **4.66**, a molecule with a first degree of curvature, showed very minor interaction with G-quadruplexes, similar to that of **4.23**. This indicated that the introduction of curvature at the beginning of a ligand through 5'-3' substitution started to change the shape correctly so that the molecule could fit into the G-quartet. Whereas **4.60** provided 5.7°C, 11.5°C, 10.9°C and 6.6 °C stabilisation at 1 µM concentration against F21T, C-kit-1, C-kit-2 and Bcl-2 G-quadruplex sequences, respectively, **4.67** showed 1.5°C, 3.1°C, 4.1°C and 2.2°C stabilisation at 1 µM concentration against the same G-quadruplex sequences. It had better interaction with G-quadruplexes than **4.66**, meaning that the 5'-3' substitution at the terminal gave molecules comparatively better shapes with which to interact than for the same substitution at the beginning of the ligand. However, the sudden change in the melting temperatures for **4.60**, **4.23**, **4.66** and **4.67** suggested that a 5'-3' substitution in the middle of a ligand can help to give a molecule a better shape with which to fit onto the G-quadruplex. **4.77**, a molecule of second degree curvature, showed a more significant interaction with all types of G-quadruplex sequences used as it provided 12.2°C, 14.4°C, 14.7°C and 6.0°C stabilisation at 1 µM concentration against F21T, C-kit-1, C-kit-2 and Bcl-2 G-quadruplex sequences, respectively. These high interactions were assumed to be due to the introduction of more curvature within the structure of this molecule. Finally, the most curved molecule, **4.93**, a molecule of the third degree of curvature, was made to complete all possible shapes based on structural modifications of **4.77**. **4.93** provided ΔTm of 12.6°C, 17.6°C, 11.4°C and 13.5°C stabilisation at 1 µM concentration against F21T, C-kit-1, C-kit-2 and Bcl-2 G-quadruplex sequences, respectively. It was obvious that **4.93** was a better interactive ligand than **4.77**, thus **4.93** was taken as a new lead for further structure activity relationship analysis.

2.10.4 Key Observations made from the Comparative FRET Data Analysis of Library-3B Molecules

- Electron-withdrawing groups (such as the NO_2 group) enhance the interacting capacity of benzofused polyamides towards G-quadruplex DNA.
- Indole is comparatively better than any other types of nitro-benzofused-acid building blocks for the enhancement of G-quadruplex interactivity.
- Compound **4.93** was taken as a new lead for further structure activity relationship studies.

2.11 Shape-Based Assessment of 4.93 Analogues

Four directly equivalent analogues of **4.77** were assessed using molecular docking studies in order to establish a rationale behind the enhanced stabilisation of libraries 2, 3 and 4 relative to **library 1**. The four chosen molecules contain the same skeleton (i.e., three indole rings and tail), and differ only by shape. **4.23** (containing three 5'-2' substituted indoles) has a GBSA score of -66.48 kcal/mol, which is the lowest calculated binding affinity. Visual analysis of the docked complex suggests that the molecule is not positioned appropriately on the G-quadruplex for interaction, relative to the highly interactive biaryl polyamide (**Figure 2.43** left and right panel), thereby providing a rationale behind its poor quadruplex stabilisation and FRET binding results.

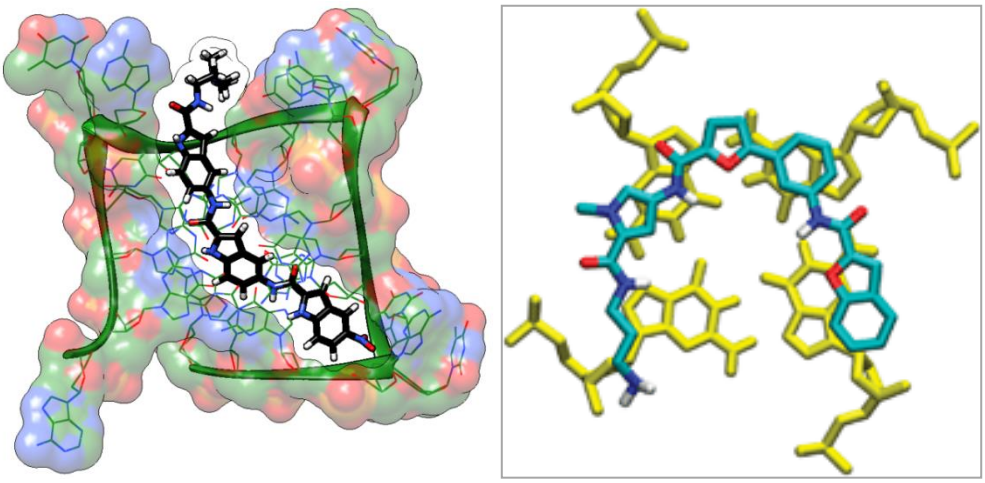

Figure 2.48: Left Panel **4.23** (black) docked on the G-quadruplex interface of the Human telomeric quadruplex (PDB ID: 3CDM). The molecule is too straight

in nature to bind to the full tetrad. Right Panel shows molecular model of G-quadruplex-interacting U-shaped biaryl polyamide (blue) based on distamycin A motif docked on the Human telomeric quadruplex (yellow).

Energy calculations also suggest that **4.60**, **4.77** and **4.93** (**Library- 2, 3** and **4** respectively) have enhanced binding over **4.23**. In particular, **4.93** has the greatest calculated binding affinity (-77.20kcal/mol), and this molecule possesses three 5'-3' substituted indole groups. Our hypothesis suggests that increasing curvature (*i.e.,* introducing a greater number of 5'-3' substituted benzofused building blocks) should increase DNA binding, and this is reflected in the enhanced ΔT_m of 17°C at 1 μM observed for **4.93**. **4.77** has a similarly high ΔT_m (*i.e.,* 16 °C at 1 μM), and has a GBSA score which is greater than -70 kcal/mol. **4.60**, which has one 5'-3' substituted indole group, has a GBSA score of -76.81 kcal/mol and ΔT_m of 10°C. Visual analysis of the docked molecules shows reasons behind their enhanced stabilisation, relative to **4.23**. For instance, in the case of **4.60**, the introduction of a 5'-3' substitution to the central indole **(Figure 2.44)**, orients the ligand over the central G-tetrad, thereby inducing stabilisation of the quadruplex. A similar observation can be made with **4.77** and **4.93** (**Figure 2.45 and Figure 2.46**), whereby the introduction of greater curvature allows the molecules to capture a greater area of the quadruplex.

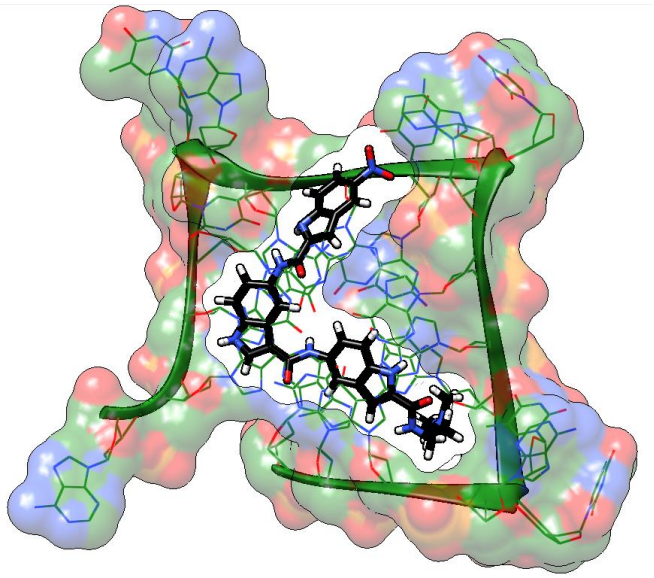

Figure 2.49: 4.60 (black) docked on the G-quadruplex interface of the Human telomeric quadruplex (PDB ID: 3CDM). The molecule has a curved shape, and is therefore capable of enhancing binding to the quadruplex structure.

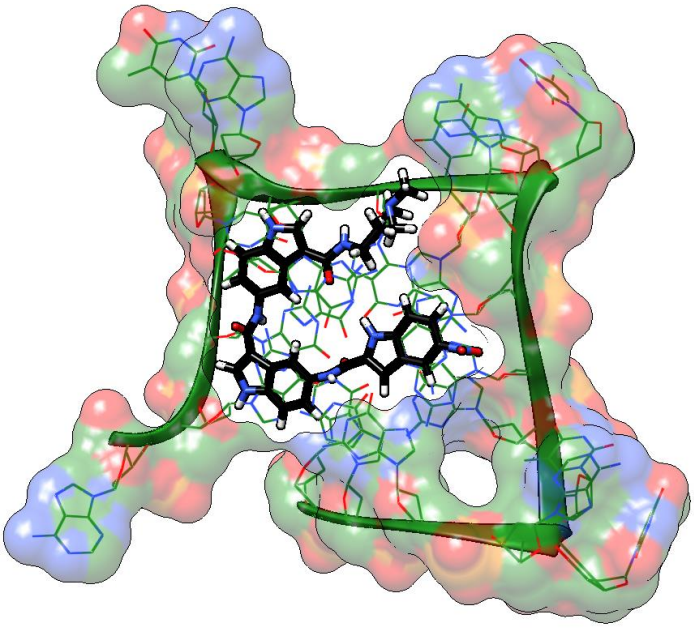

Figure 2.50: 4.77 (black) docked on the G-quadruplex interface of the Human telomeric quadruplex (PDB ID: 3CDM). The molecule has a more enhanced curvature than **4.23** and **4.60** and is therefore capable of stabilising the G-quadruplex structure to a greater extent.

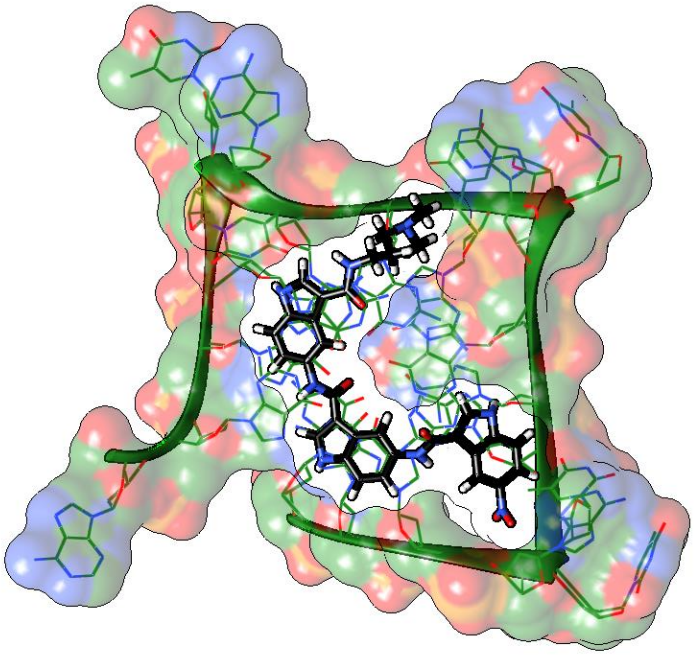

Figure 2.51: Molecular model of **4.93** (black sticks) binding to the G-quadruplex interface. It can be seen that the three benzofused components of the molecule stack directly over the G-tetrad, thereby stabilising the quadruplex. The presence of 5'-3'-substituted to benzofused building blocks help to create a sufficient shape of molecule to maximise interaction.

Table 2.31: Molecule names, structures, GBSA scores (kcal/mol) and FRET melting temperatures for **4.23**, **4.60**, **4.77** and **4.93**.

Compound code	Degree of curvature	Structure	GBSA score (kcal/mol)	ΔTm(°C)±0.5°C		
				5 µm	2 µm	1 µm
4.23	Linear	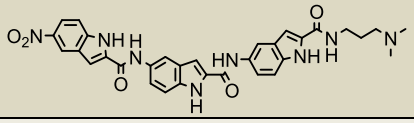	-66.48	1	0	0
4.60	First degree of curveture	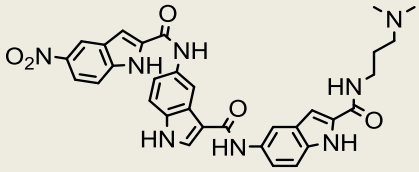	-76.81	19	14	10
4.77	second degree of curveture	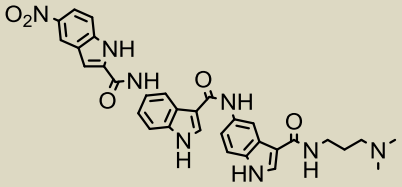	-70.20	24	16	15
4.93	Thirds degree of curveture	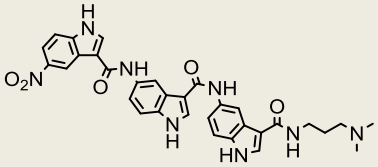	-77.20	27	22	17

It is evident from molecular docking results that a clear shape-based rationale for enhanced DNA stabilisation can be established. The introduction of a 5'-3'-substituted indole as the second of three amide-linked benzofused building blocks (instead of a 5'-2'-substituted indole) can dramatically enhance binding of the triaryl scaffold to the quadruplex. Introduction of further 5'-3'-substituted benzofused moieties (for example, in the case of **4.77** and **4.93**) can further enhance stabilisation, and this occurs due to the presence of aryl structures in an appropriate orientation to induce quadruplex stabilisation.

Library-4A

2.12 Synthetic Scheme for Library-4A Molecules

The molecular docking studies of molecules containing three consecutive 5'-3' benzofused moieties (for example, **4.93**) suggested that the inclusion of a third 5'-3'-substituted benzofused moiety should enhance G-quadruplex stabilisation to a small degree compared to two 5'-3'-substituted benzofused moieties (for example, **4.77**).

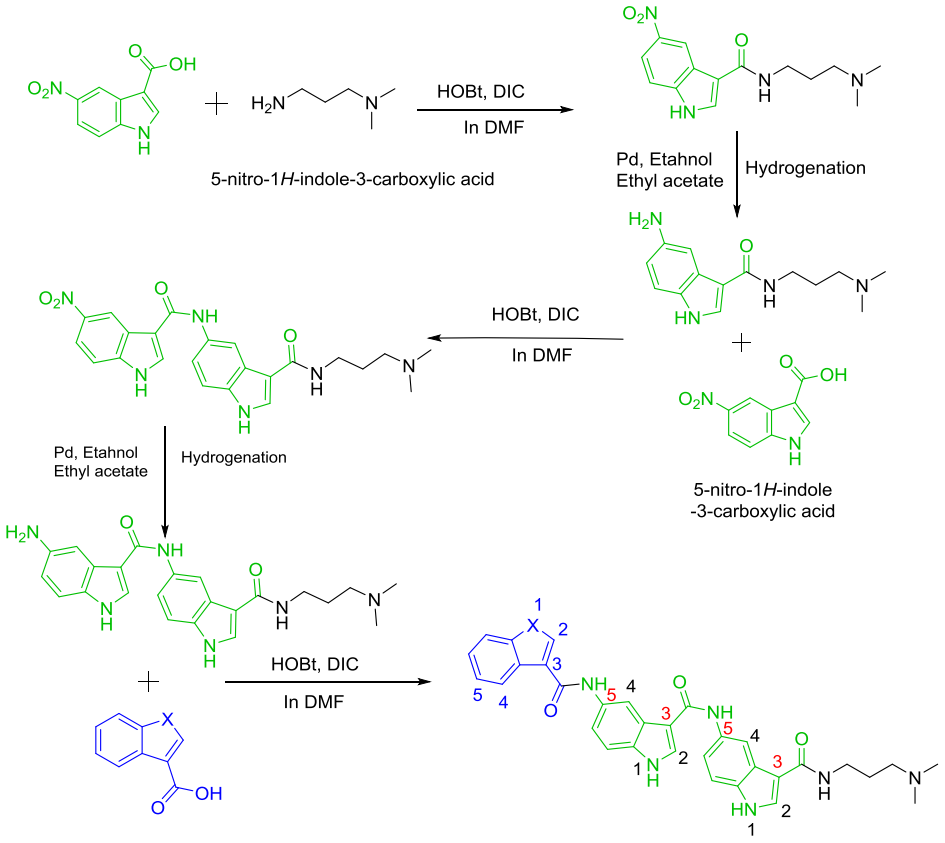

Figure 2.52: Synthetic scheme of **library-4A** molecules. Here X = O, N, S.

A new library of molecules containing four different benzofused polyamides was synthesized to investigate the relevance of the electron-withdrawing NO_2 group to the activity of the most active compound **4.93**. The synthesised molecules were capped with a benzofused building block containing a carboxylic acid in the 3' position only, instead of a 5-nitro-3-carboxylic acid benzofused building block as found in **4.93**, to assess this factor. At the same time, the equivalent molecules from **library-3A** and **library-4A** were directly compared to investigate the effect of structural curvature within their structures to provide the interactive

capacity towards G-quadruplexes. This would provide a guideline for finding the right degree of curvature to fit into G-quadruplex architecture.

Initially, the acid (1.2 eq.) was dissolved in DMF (5 mL for 100 mg of starting material) in a round bottom flask fitted with a magnetic stirrer. Then DIC (1.75 eq.) and HOBt (2.0 eq.) were added to the acid (1.0 eq.) and this mixture was allowed to stir at room temperature for formation of the ester from the acid. The amine (1 eq.) was added to the mixture and the mixture allowed for stirring until the reaction was complete, as indicated by TLC or LCMS. Finally the reaction mixture was applied to a conditioned SCX-2 cartridge and the resultant product was purified by the 'Catch and Release' method (described in the section '**Methods and Materials**' of Chapter 3).

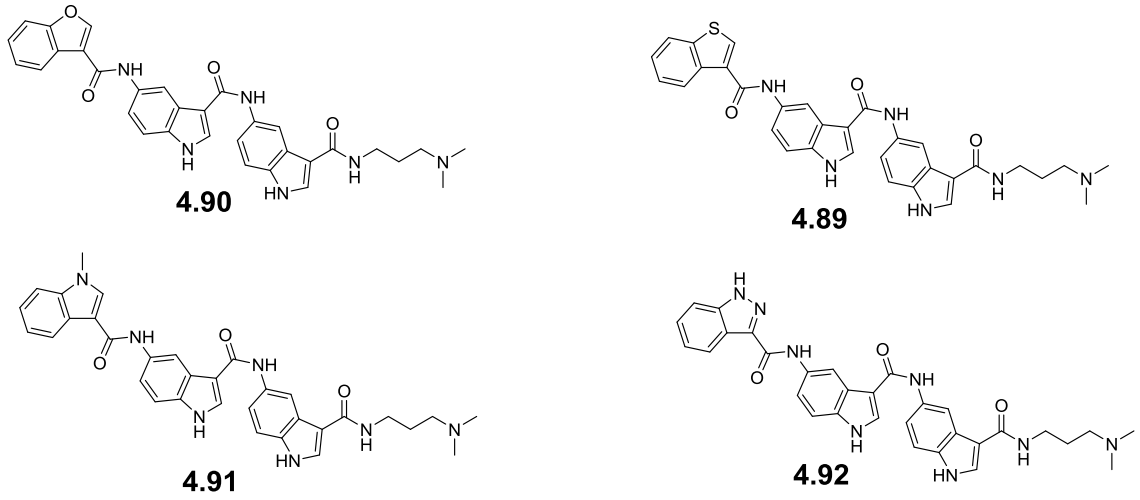

Figure 2.53: Structures of the **library-4A** molecules.

2.12.1 Characterisation of Benzofused Polyamides through Various Spectroscopic Techniques

Benzofused polyamides of this library were purified and fully characterized by different spectroscopic techniques including mass spectrometry, both ^{1}H and ^{13}C NMR, and IR techniques (described in the **Experimental** section of Chapter 4). Compounds were primarily identified by LCMS and confirmed using high resolution mass spectroscopy (HRMS) **(Table 2.32 and 2.33)**.

Table 2.32: HRMS data for **library-4A** molecules

Number	Compound code	Theoretical mass	Observed mass $[M+H]^{+}$
1	**4.90**	562.2329	563.2388
2	**4.89**	578.2100	578.2100
3	**4.91**	575.2645	576.2703
4	**4.92**	562.2441	563.2498

2.12.2 Purity Analysis of Benzofused Polyamides Synthesized

The purity of the benzofused polyamides of this library was checked by two different HPLC methods with two different retention times. Both methods were carried out on a Waters Alliance 1695 HPLC Pump with water and acetonitrile comprising the mobile phases. The Waters 996 PDA start wavelength was 210 nm for the 10 minute method (Method A), with a start wavelength of 220 nm and end wavelength of 500 nm for the 5 minute method (Method B) **(Table 2.32 and 2.33)**.

Table 2.33: Purity data for **library-4A** molecules as observed by HPLC

Number	Compound code	Purity	
		Method A (10 min)%	Method B (5 min)%
1	**4.90**	100	95
2	**4.89**	100	95
3	**4.91**	100	88
4	**4.92**	100	100

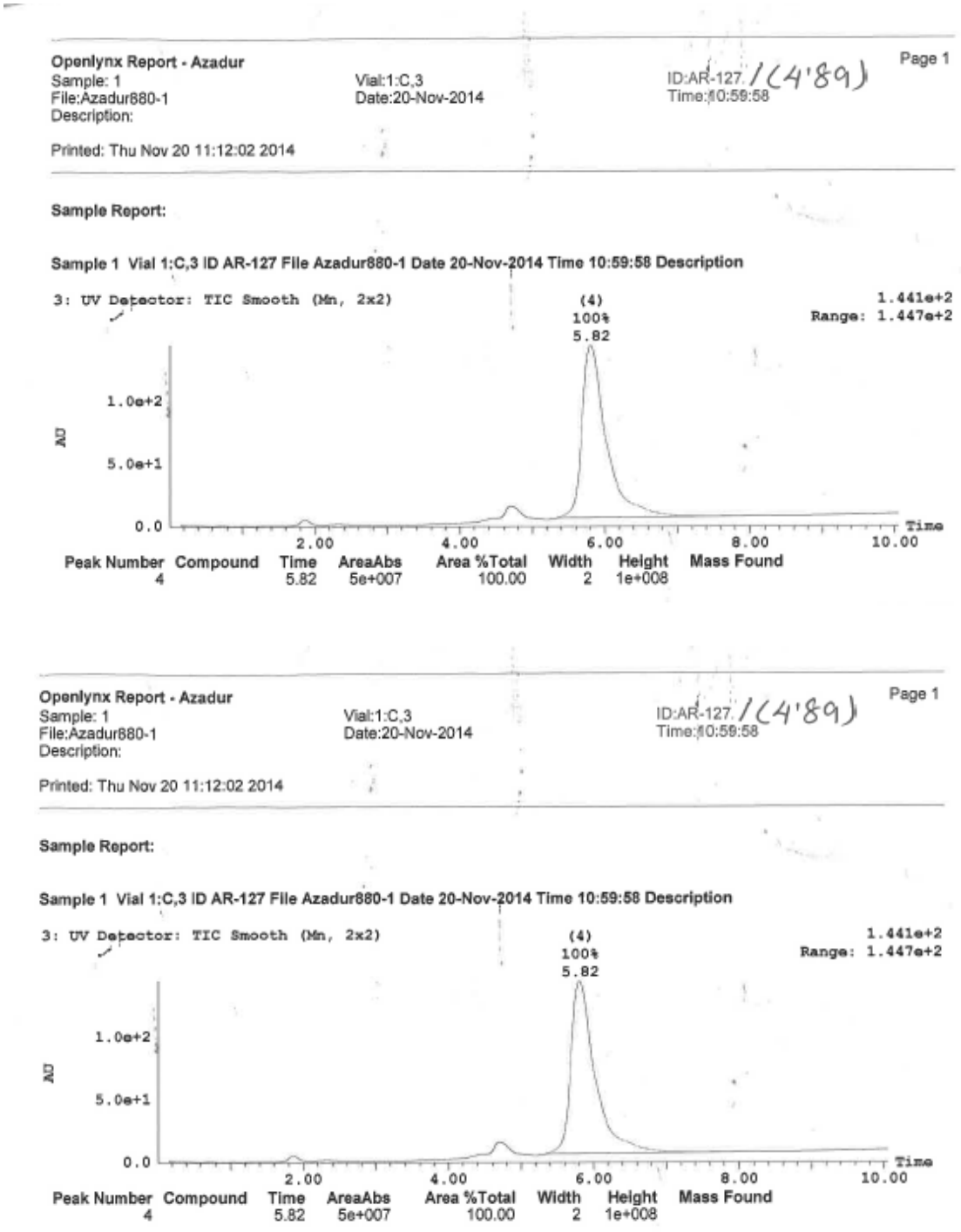

Figure 2.54: Example of an adapted LCMS profile of **Library-4A** compound **4.89**

Table 2.34: G-quadruplex and duplex DNA stabilization by **library-4A** molecules in FRET melting experiments at concentrations of 5, 2 and 1 µM respectively (the data are means of three technical repeats)

Compounds	Quadruplex type	ΔT_m(°C) ±(s/d)		
		5 µM	2 µM	1 µM
4.90	F21T	8.8±0.07	5.2±0.20	3.2±0.12
	C-kit-1	13.1±0.20	8.7±0.2	4.9±0.25
	C-kit-2	14.8±0.05	7.8±0.23	6.2±0.28
	BCL-2	13.4±0.36	7.4±0.15	4.2±0.11
	Duplex DNA	0.0±0.12	0.0±0.15	0.0±0.08
4.89	F21T	8.6±0.10	5.1±0.05	3.5±0.20
	C-kit-1	12.0±0.20	7.7±0.20	5.9±0.20
	C-kit-2	13.2±0.20	7.7±0.25	5.3±0.15
	BCL-2	11.2±0.2	6.0±0.35	3.6±0.21
	Duplex DNA	0.0±0.12	0.0±0.15	0.0±0.18
4.91	F21T	10.9±0.13	6.7±0.22	2.9±0.14
	C-kit-1	15.2±0.30	9.9±0.17	8.2±0.25
	C-kit-2	17.2±0.15	11.6±0.05	8.9±0.10
	BCL-2	16.3±0.20	10.4±0.23	7.5±0.14
	Duplex DNA	0.0±0.17	0.0±0.32	0.0±0.31
4.92	F21T	17.2±0.21	10.7±0.21	9.3±0.05
	C-kit-1	20.4±0.20	17.1±0.11	15.7±0.17
	C-kit-2	22.1±0.15	15.9±0.26	13.4±0.36
	BCL-2	22.4±0.10	13.4±0.11	10.3±0.30
	Duplex DNA	0.0±0.29	0.0±0.34	0.0±0.16

Here, all of the molecules except **4.92** were found to be moderately interactive towards the different G-quadruplex sequence types. **4.92** provided 9.3°C, 15.7 °C, 13.4°C and 10.3°C stabilisation at 1 µM concentration against F21T, C-kit-1, C-kit-2 and Bcl-2 G-quadruplex sequences, respectively. This significant activity of **4.92** was due to the effect of the additional nitrogen atom of the terminal indazole building block as previously discussed.

The effect of an electron-withdrawing nitro group on the interaction capacity of benzofused polyamides towards G-quadruplex DNA can be shown by the direct comparison of the equivalent molecules **4.93** from **library-3B** and **4.91** from **libaray-4A.** A clear difference in the melting temperatures was observed.

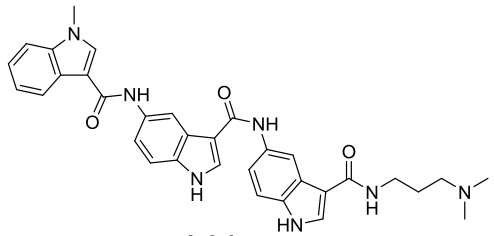

4.91

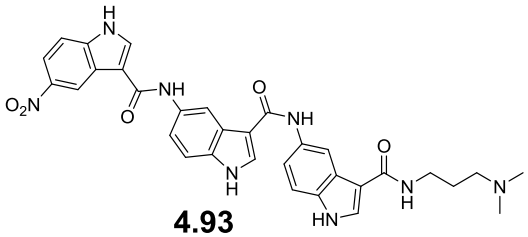

4.93

Figure 2.55: Structures of **4.91** and **4.93**.

Table 2.35: Direct comparison between molecules **4.91** and **4.93** of **library-4A** and **library-3B**, respectively (the data are means of three technical repeats)

Quadruplex types	ΔT_m(°C) ±(s/d)					
	4.91	**4.93**	**4.91**	**4.93**	**4.91**	**4.93**
	5 µM	5 µM	2 µM	2 µM	1 µM	1 µM
F21T	10.9±0.13	21.0±0.17	6.7±0.22	15.9±0.28	2.9±0.14	12.6±0.26
C-kit-1	15.2±0.30	27.7±0.30	9.9±0.17	22.1±0.35	8.2±0.25	17.6±0.28
C-kit-2	17.2±0.15	21.3±0.23	11.6±0.05	14.8±0.20	8.9±0.10	11.4±0.32
BCL-2	16.3±0.20	25.4±0.30	10.4±0.23	17.8±0.14	7.5±0.14	13.5±0.20
Duplex DNA	0.0±0.17	0.0±0.05	0.0±0.32	0.0±0.05	0.0±0.31	0.0±0.05

4.91 provided 2.9°C, 8.2°C, 8.9°C and 7.5°C stabilisation at 1 µM concentration against F21T, C-kit-1, C-kit-2 and Bcl-2 G-quadruplex sequences, respectively, whereas **4.93,** a nitro group-containing benzofused polyamide, provided 12.6°C, 17.6°C, 11.4°C and 13.5°C stabilisation at 1 µM concentration against F21T, C-kit-1, C-kit-2 and Bcl-2 G-quadruplex sequences, respectively. Thus it was obvious that **4.93** was more interactive towards all types of G-quadruplex sequences used than **4.91**.

Two other molecules (**4.90** and **4.89**) were not as interactive as **4.93** towards G-quadruplex DNA, although they have the same degree of curvature in their structure. This observation also supports the positive impact of an electron-withdrawing nitro group at the terminal benzofused unit on interaction ability with G-quadruplex DNA.

It was important to compare the equivalent molecules from **library-3A** and **library-4A** to investigate the effect of structural curvature on their G-quadruplex interactive capacities - it would provide guidelines for finding the right degree of curvature to fit into G-quadruplex architecture. **4.70**, a member of **library-3A**

(with a second degree of curvature) was equivalent to **4.90** (with a third degree of curvature), a member of **library-4A**, and the two are directly comparable.

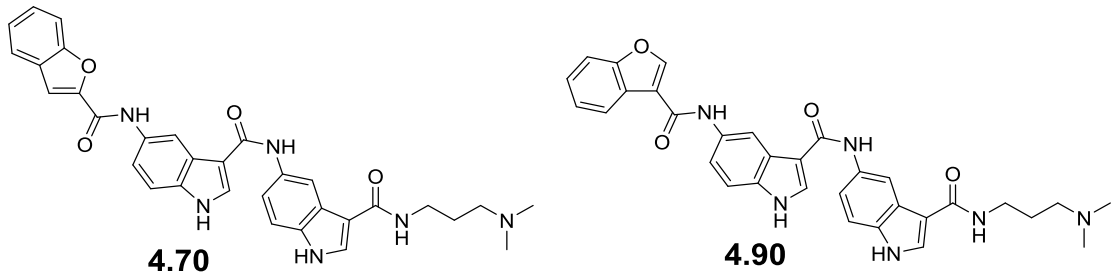

Figure 2.56: Structures of **4.70** and **4.90**.

Table 2.36: Direct comparison between molecules **4.70** and **4.90** of **library-3A** and **library-4A**, respectively (the data are means of three technical repeats)

Quadruplex types	ΔT_m(°C) ±(s/d)					
	4.70	**4.90**	**4.70**	**4.90**	**4.70**	**4.90**
	5 µM	5 µM	2 µM	2 µM	1 µM	1 µM
F21T	13.6±0.37	8.8±0.07	8.6±0.23	5.2±0.20	4.89±0.11	3.2±0.12
C-kit-1	14.2±0.28	13.1±0.20	10.7±0.28	8.7±0.2	9.2±0.34	4.9±0.25
C-kit-2	18.3±0.15	14.8±0.05	11.4±0.11	7.8±0.23	8.6±0.26	6.2±0.28
BCL-2	15.7±0.23	13.4±0.36	10.4±0.20	7.4±0.15	7.4±0.20	4.2±0.11
Duplex DNA	0.0±0.11	0.0±0.12	0.0±0.23	0.0±0.15	0.0±0.25	0.0±0.08

Here, **4.90** provided 3.2°C, 4.9°C, 6.2°C and 4.2°C stabilisation and **4.70** provided 4.89°C, 9.2°C, 8.6°C and 7.4°C stabilisation at 1 µM concentration against F21T, C-kit-1, C-kit-2 and Bcl-2 G-quadruplex sequences, respectively. This result suggested that these two molecules were approximately equivalent to each other with regards to interaction with G-quadruplex DNA.

Similarly, molecules **4.71** and **4.89** from **library-3A** and **library-4A**, respectively, are also directly comparable.

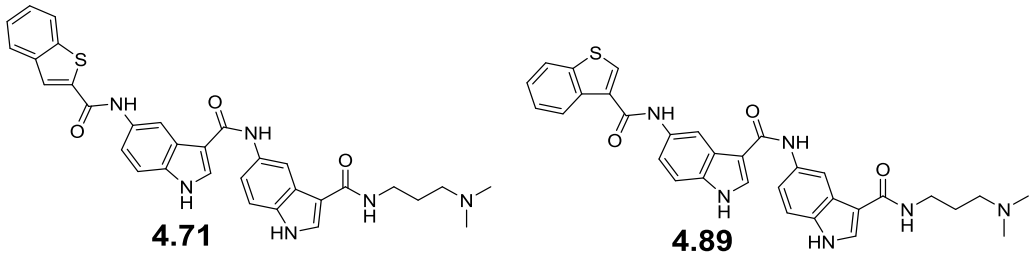

Figure 2.57: Structures of equivalent molecules **4.71** and **4.89**.

Table 2.37: Direct comparison between **4.71** and **4.89** of **library-3** and **library-4**, respectively (the data are means of three technical repeats)

Quadruplex type	ΔT_m(°C) ±(s/d)					
	4.71	**4.89**	**4.71**	**4.89**	**4.71**	**4.89**
	5 µM	5 µM	2 µM	2 µM	1 µM	1 µM
F21T	17.7±0.2	8.6±0.10	9.3±0.07	5.1±0.05	7.2±0.14	3.5±0.20
C-kit-1	23.0±0.35	12.0±0.20	18.3±0.05	7.7±0.20	15.1±0.17	5.9±0.20
C-kit-2	17.7±0.26	13.2±0.20	11.8±0.15	7.7±0.25	8.3±0.32	5.3±0.15
BCL-2	15.5±0.26	11.2±0.2	8.9±0.23	6.0±0.35	5.9±0.14	3.6±0.21
Duplex DNA	0.0±0.11	0.0±0.12	0.0±0.37	0.0±0.15	0.0±0.11	0.0±0.18

Here, **4.89** provided 3.5°C, 5.9°C, 5.3°C and 3.6°C stabilisation and **4.71** provided 7.2°C, 15.1°C, 8.3°C and 5.9°C stabilisation at 1 µM concentration against F21T, C-kit-1, C-kit-2 and Bcl-2 G-quadruplex sequences, respectively.

Molecules **4.72** and **4.91** from **library-3A** and **library-4A**, respectively, are also directly comparable.

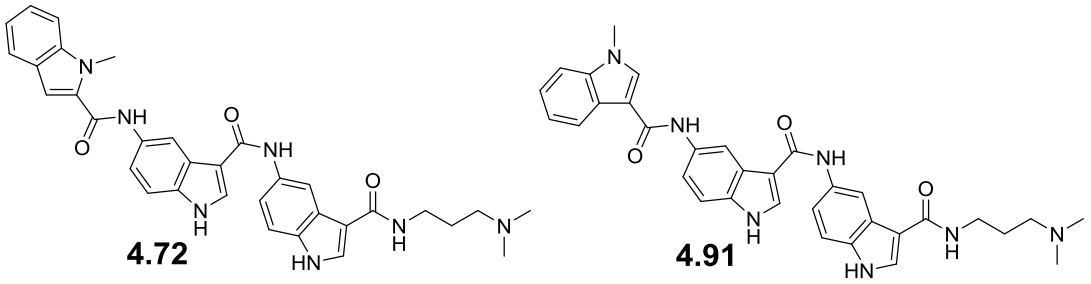

Figure 2.58: Structures of **4.72** and **4.91**.

Table 2.38: Direct comparison between equivalent molecules **4.72** and **4.91** of **library-3A** and **library-4A**, respectively (the data are means of three technical repeats)

Quadruplex type	ΔT_m(°C) ±(s/d)					
	4.72	**4.91**	**4.72**	**4.91**	**4.72**	**4.91**
	5 µM	5 µM	2 µM	2 µM	1 µM	1 µM
F21T	9.4±0.17	10.9±0.13	4.2±20	6.7±0.22	2.6±0.14	2.9±0.14
C-kit-1	12.3±0.17	15.2±0.30	8.4±0.15	9.9±0.17	6.8±0.32	8.2±0.25
C-kit-2	12.8±0.37	17.2±0.15	7.2±0.17	11.6±0.05	5.8±0.30	8.9±0.10
BCL-2	10.2±0.11	16.3±0.20	5.3±0.32	10.4±0.23	4.2±0.20	7.5±0.14
Duplex DNA	0.0±0.23	0.0±0.17	0.0±0.12	0.0±0.32	0.0±0.31	0.0±0.31

4.91 provided 2.9°C, 8.2°C, 8.9°C and 7.5°C stabilisation whilst **4.72** provided 2.6°C, 6.8°C, 5.8°C and 4.2°C stabilisation at 1 µM concentration against F21T, C-kit-1, C-kit-2 and Bcl-2 G-quadruplex sequences, respectively. **4.91** (relatively more curved) was found to be more G-quadruplex interactive than the equivalent molecule **4.72** (relatively less curved)**.** This observation suggested that the inclusion of a third 5'-3'-substituted benzofused moiety should enhance G-quadruplex stabilisation to a small degree compared to two 5'-3'-substituted benzofused moieties **(Figure 2.39)**.

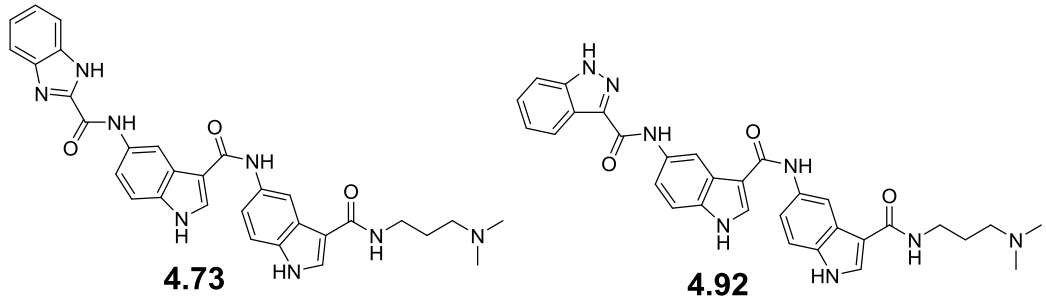

Figure 2.59: Structures of the equivalent molecules **4.73** and **4.92**.

Table 2.39: Direct comparison between equivalent molecules **4.73** and **4.92** of **library-3** and **library-4**, respectively (the data are means of three technical repeats)

Quadruplex types	ΔT_m(°C) ±(s/d)					
	4.73	**4.92**	**4.73**	**4.92**	**4.73**	**4.92**
	5 µM	5 µM	2 µM	2 µM	1 µM	1 µM
F21T	11.5±0.21	17.2±0.21	7.6±0.34	10.7±0.21	6.0±0.23	9.3±0.05
C-kit-1	15.0±0.0	20.4±0.20	11.7±0.20	17.1±0.11	9.7±0.25	15.7±0.17
C-kit-2	17.6±0.23	22.1±0.15	11.4±0.05	15.9±0.26	8.8±0.11	13.4±0.36
BCL-2	15.8±0.05	22.4±0.10	10.4±0.25	13.4±0.11	7.8±0.36	10.3±0.30
Duplex DNA	0.0±0.32	0.0±0.29	0.0±0.26	0.0±0.34	0.0±0.34	0.0±0.16

4.92, with a third degree of curvature, provided 9.3°C, 15.7°C, 13.4°C and 10.3°C stabilisation and the equivalent **4.73**, a molecule with a second degree of curvature, provided a 6.0°C, 9.7°C, 8.8°C and 7.8°C stabilisation at 1 µM concentration against F21T, C-kit-1, C-kit-2 and Bcl-2 G-quadruplex sequences, respectively. It is evident that **4.92** had more significant interactions due to having an extra electronegative nitrogen atom in the terminal indazole ring.

2.12.3 Key Observations from Library-4A

- Results from **library 4A** suggest that an electron-withdrawing nitro group at the terminal benzofused building block enhances G-quadruplex stabilisation considerably.
- The molecules made of three consecutive indole units with a third degree of curvature are assumed to fit nicely within the G-quadruplex to provide more interaction than the molecules of the same unit with a second degree of curvature in their structure.

Library-4B

2.13 Synthetic Scheme for Library-4B Molecules

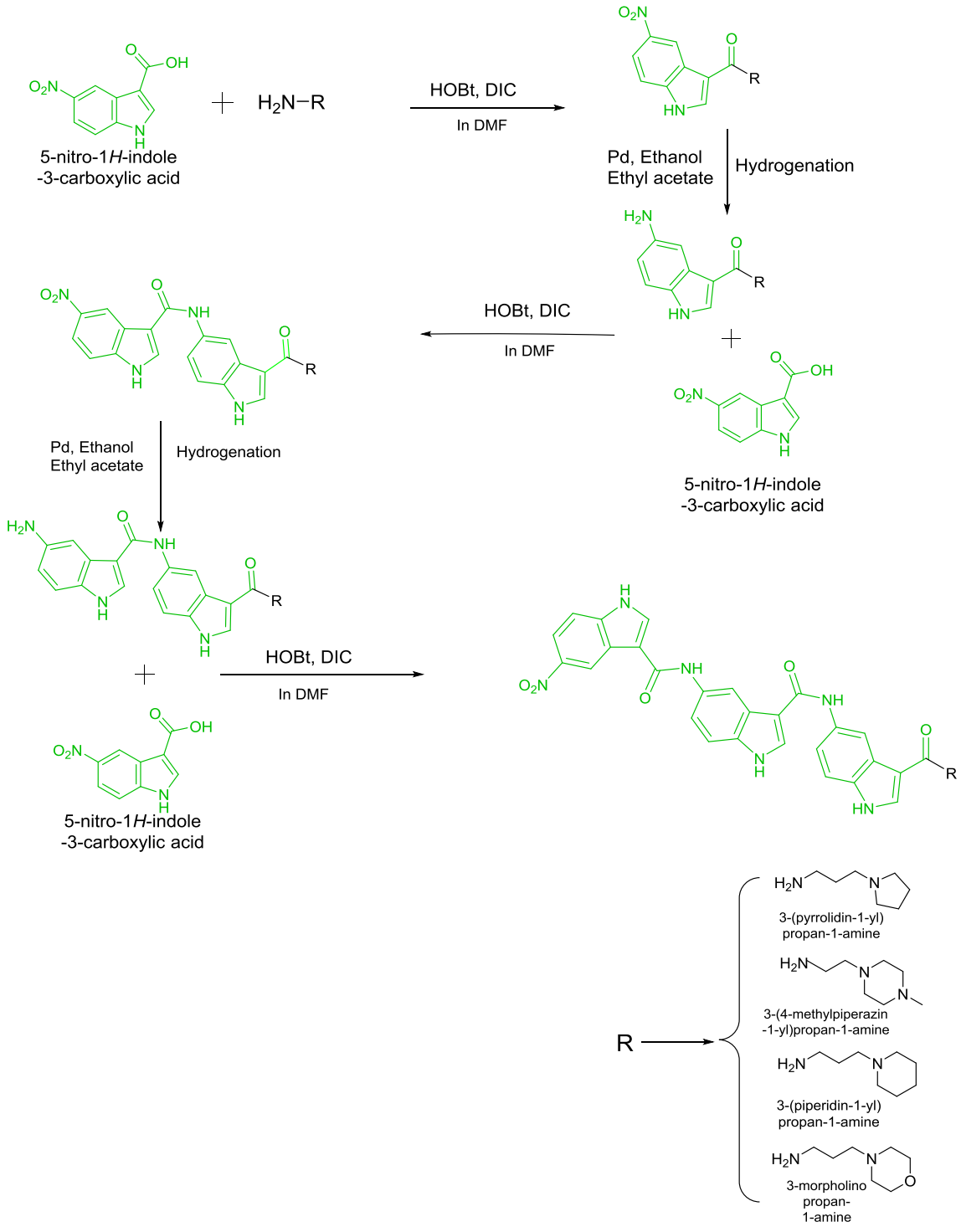

Figure 2.60: Synthetic scheme of **library-4B** molecules.

A set of molecules (4 in total) was next synthesized for the structure activity relationship of **4.93** through the modification of the tertiary amine tails initially

attached through an amide coupling reaction. These structural modifications of **4.93** were done by the substitution of the N1, N1-dimethylpropane-1,3-diamine tail with different tails including 3-(piperidin-1-yl)propan-1-amine, 3-(pyrrolidin-1-yl)propan-1-amine, 3-morpholinopropan-1-amine and 3-(4-methylpiperazin-1-yl)propan-1-amine

Initially the acid (1.2 eq.) was dissolved in DMF (5 mL for 100 mg of starting material) in a round bottom flask fitted with a magnetic stirrer. Then DIC (1.75 eq.) and HOBt (2.0 eq.) were added to the acid (1.0 eq.) and this mixture was allowed to stir at room temperature for formation of the ester from the acid. The amine (1 eq.) was added to the mixture and the mixture allowed to stir until the reaction was complete, as indicated by TLC or LCMS. Finally the reaction mixture was applied to a conditioned SCX-2 cartridge and the resultant product was purified by the 'Catch and Release' method (described in the section '**Methods and Materials**' of Chapter 3).

Four molecules with the highest curvature were synthesized to investigate the effect of tertiary tail types on interaction with G-quadruplex DNA. Here, ligands were synthesized by using different tails.

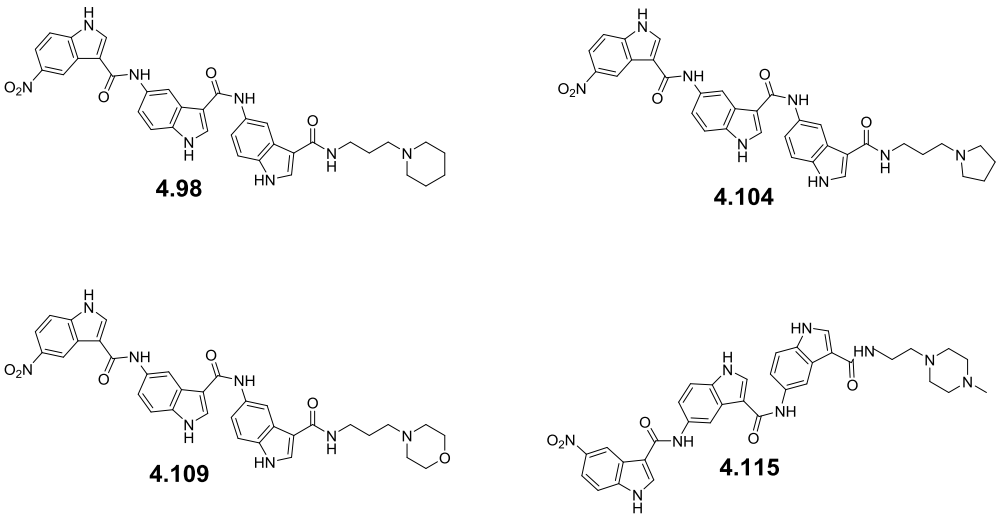

Figure 2.61: Structures of **library-4B** molecules with different tails.

2.13.1 Characterisation of Benzofused Polyamides through Various Spectroscopic Techniques

Benzofused polyamides of **library-4B** were purified and fully characterized by different spectroscopic techniques including mass spectrometry, both ^{1}H and ^{13}C NMR, and IR techniques (described in the **Experimental** section of Chapter 4). Compounds were primarily identified by LCMS and confirmed using high resolution mass spectroscopy (HRMS) **(Table 2.40 and 2.41)**.

Table 2.40: HRMS data for **library-4B** molecules

Number	Compound code	Theoretical mass	Observed mass $[M+H]^{+}$
1	**4.98**	646.2652	647.2709
2	**4.104**	632.2496	633.2557
3	**4.109**	648.2445	649.2513
4	**4.115**	661.2761	662.2820

2.13.2 Purity Analysis of Benzofused Polyamides Synthesized

The purity of the benzofused polyamides of this library was checked by two different HPLC methods with two different retention times. Both methods were carried out on a Waters Alliance 1695 HPLC Pump with water and acetonitrile comprising the mobile phases. The Waters 996 PDA start wavelength was 210 nm for the 10 minute method (Method A), with a start wavelength of 220 nm and end wavelength of 500 nm for the 5 minute method (Method B) **(Table 2.41 and 2.42)**.

Table 2.41: Purity data for **library-4B** molecules as observed by HPLC

Number	Compound code	Purity	
		Method A (10 min)%	Method B (5 min)%
1	**4.98**	100	100
2	**4.104**	100	100
3	**4.109**	100	92
4	**4.115**	100	100

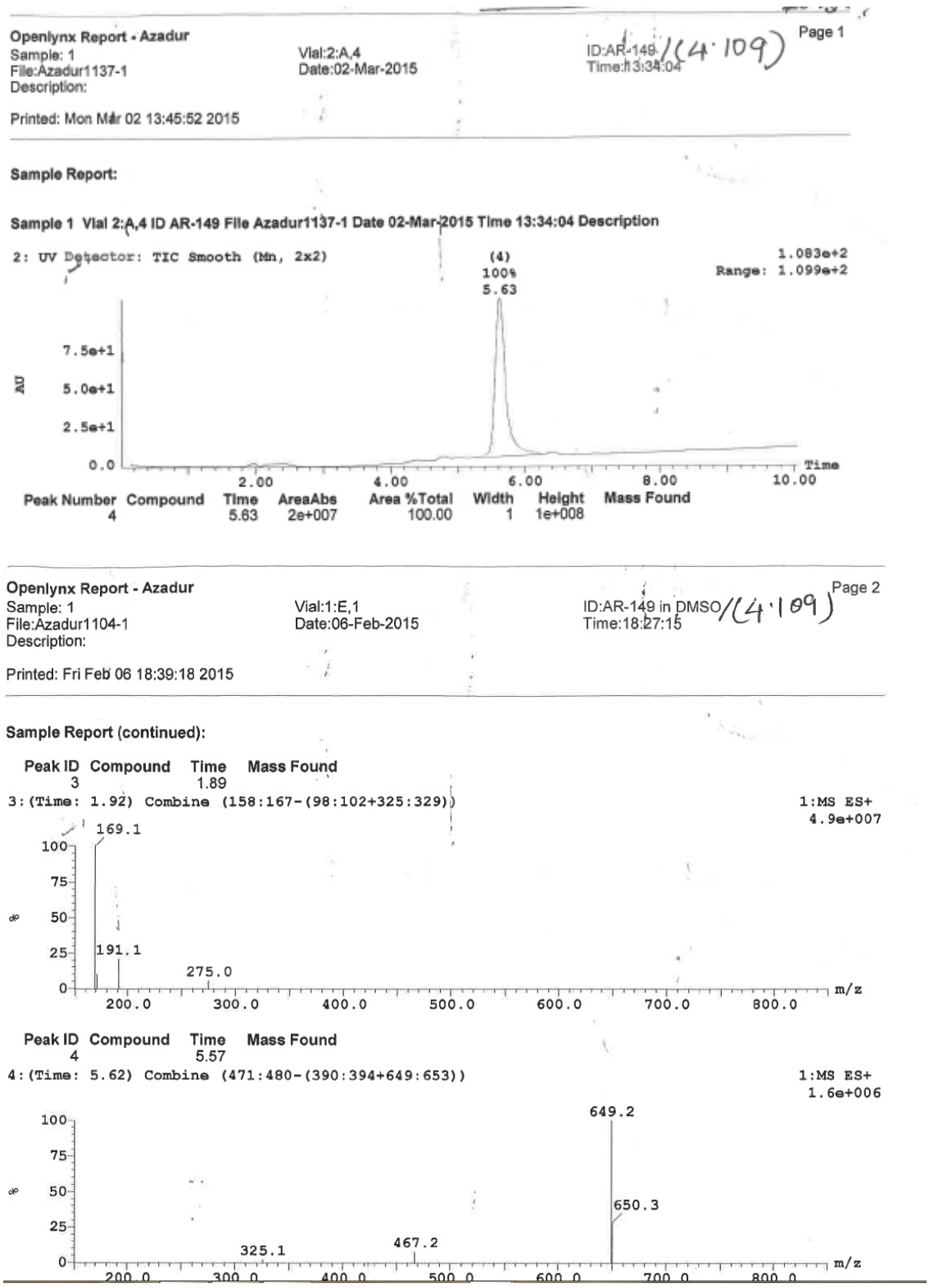

Figure 2.62: Example of an adapted LCMS profile of **Library-4B** compound **4.109**

Table 2.42: G-quadruplex and duplex DNA stabilization by **library-4B** ligands in FRET melting experiments at concentrations of 5, 2 and 1 µM respectively (the data are means of three technical repeats)

Compounds	Quadruplex types	ΔT_m(°C) ±(s/d)		
		5 µM	2 µM	1 µM
4.98	F21T	18.0±0.11	10.0±0.31	5.0±0.43
	C-kit-1	23.8±0.23	18.7±0.24	15.5±0.32
	C-kit-2	20.5±0.15	13.9±0.17	11.3±0.21
	BCL-2	22.1±0.24	13.0±0.15	9.6±0.22
	Duplex DNA	0.0±0.20	0.0±0.26	0.0±0.23
4.104	F21T	16.3±0.11	9.6±0.20	4.8±0.15
	C-kit-1	21.3±0.30	14.5±0.21	12.2±0.26
	C-kit-2	20.4±017	14.2±0.12	11.1±0.27
	BCL-2	17.9±0.42	11.6±0.05	7.8±0.20
	Duplex DNA	0.0±0.12	0.0±0.11	0.0±0.13
4.109	F21T	11.6±0.14	7.0±0.15	5.3±0.06
	C-kit-1	14.9±0.17	10.4±0.27	9.1±0.07
	C-kit-2	10.3±0.19	6.7±0.11	4.7±0.22
	BCL-2	11.6±0.11	7.0±0.42	5.6±0.21
	Duplex DNA	0.0±0.32	0.0±0.27	0.0±0.34
4.115	F21T	18.2±0.13	10.7±0.21	6.9±0.15
	C-kit-1	22.1±0.06	16.9±0.16	13.9±0.23
	C-kit-2	21.1±0.07	12.6±0.06	11.6±0.27
	BCL-2	20.9±0.20	13.2±0.37	10.8±0.08
	Duplex DNA	0.0±0.25	0.0±0.17	0.0±0.05

4.98 provided 5.9°C, 15.5°C, 11.3°C and 9.6°C stabilisation; **4.104** provided 4.8°C, 12.2°C, 11.1°C, 7.8°C stabilisation; **4.99** provided 5.3 °C, 9.1 °C, 4.7°C 5.6°C stabilisation; and **4.115** provided 6.9°C,13.9°C,11.6°C, 10.8°C stabilisation at 1 µM concentration against F21T, C-kit-1, C-kit-2 and Bcl-2 G-quadruplex sequences, respectively. None of them showed better interaction with F21T, C-kit-1 and C-kit-2 than **4.93** (12.6°C, 17.6°C and 11.4°C stabilisation at 1 µM concentration, respectively). **4.93** was most active towards F21T compared to the other G-quadruplex sequences, while the rest of the ligand molecules showed only moderate activity towards the F21T G-quadruplex. **4.98**, **4.104** and **4.115** were equivalent in their interactions with C-kit-1, C-kit-2 and Bcl-2 sequences and **4.115** showed better interactivity towards Bcl-2 G-quadruplexes than the rest of the molecules. **4.109** showed comparatively less interactivity towards all of the sequences used. The overall data analysis concluded that the N1, N1-dimethylpropane-1, 3-diamine tail

provides a better interactive entity within the ligand molecules than any other tails types used. It is noticeable that the tail 3-morpholinopropan-1-amine is not sufficient to provide interactive capacity for ligand molecules, since **4.109** is not as interactive as the other ligands. This may be due to the less electronegative oxygen atom in place of more electronegative nitrogen atom as in the other ligands, or it may be due to the presence of an electron-withdrawing oxygen atom within the cyclic system of this tail; this oxygen atom may attract the electron cloud and increase the electronegativity on the nitrogen atom which could ultimately hamper the electrostatic balance.

2.13.3 Key Observations from Library-4B

- The tertiary amine tail n N1, N1-dimethylpropane-1,3-diamine is comparatively better than other tails, including 3-(piperidin-1-yl)propan-1-amine, 3-(pyrrolidin-1-yl)propan-1-amine, 3-morpholinopropan-1-amine and 3-(4-methylpiperazin-1-yl)propan-1-amine, at providing the interactive capacity of a ligand molecule towards G-quadruplex DNA.

Library-4C

2.14 Synthetic Scheme for Library-4C Molecules.

Here, a set of four molecules (**Figure 2.57**) were made by the structural modification of **4.93** through the substitution of the nitro group with different functional groups for the optimisation of the interacting capacity of the lead ligand **4.93**.

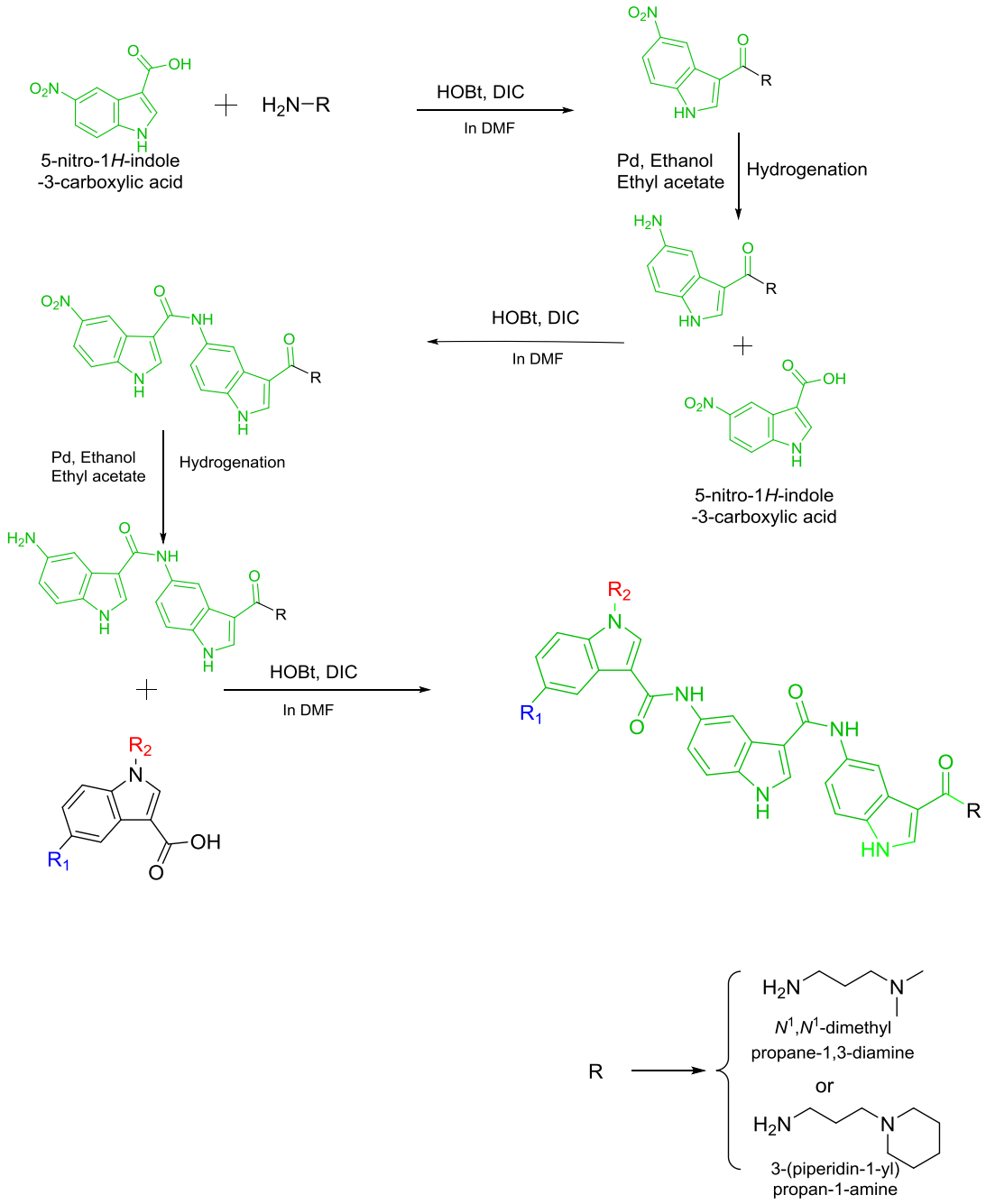

Figure 2.63: Synthetic scheme of **library-4C** molecules. Here, R_1 = CN, Cl, –OCH_3, -NH_2 etc. and R_2 = –CH_3, functional groups.

Initially the acid (1.2 eq.) was dissolved in DMF (5 mL for 100 mg of starting material) in a round bottom flask fitted with a magnetic stirrer. Then DIC (1.75 eq.) and HOBt (2.0 eq.) were added to the acid (1.0 eq.) and this mixture was allowed to stir at room temperature for formation of the ester from the acid. The amine (1 eq.) was added to the mixture and the mixture allowed to stir until the reaction was complete, as indicated by TLC or LCMS. Finally the reaction mixture was applied to a conditioned SCX-2 cartridge and the resultant product was purified by the 'Catch and Release' method (described in the section '**Methods and Materials**' of Chapter 3).

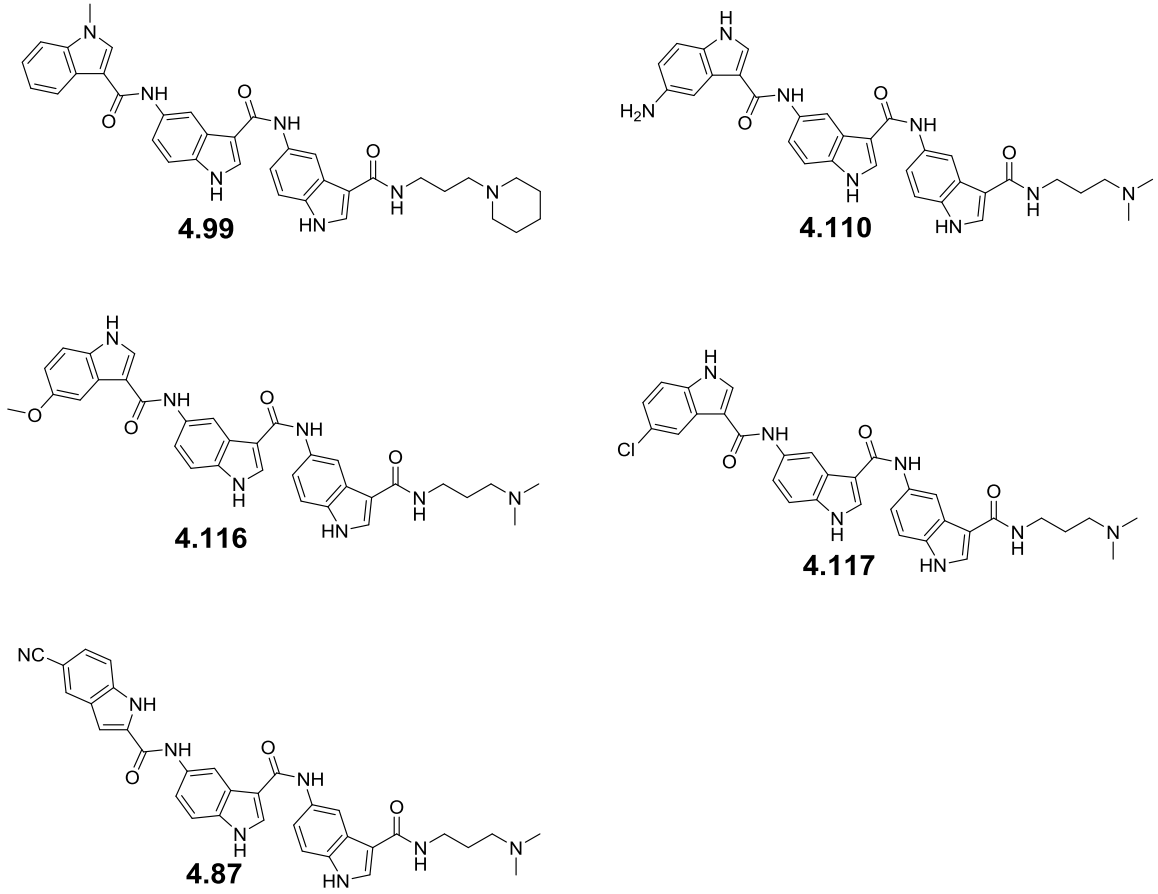

Figure 2.64: Structure of **library-4C** molecules.

2.14.1 Characterisation of Benzofused Polyamides through Various Spectroscopic Techniques

The benzofused polyamides were purified and fully characterized by different spectroscopic techniques including mass spectrometry, both ^{1}H and ^{13}C NMR, and IR techniques (described in the **Experimental** section of Chapter 4).

Compounds were primarily identified by LCMS and confirmed using high resolution mass spectroscopy (HRMS) **(Table 2.43 and 2.44)**.

Table 2.43: HRMS data for **library-4C** molecules

Number	Compound code	Theoretical mass	Observed mass $[M+H]^+$
1	**4.99**	615.2958	616.3023
2	**4.110**	576.2597	577.2668
3	**4.116**	591.2594	592.2662
4	**4.117**	595.2092	596.2165
5	**4.87**	586.2441	587.2508

2.14.2 Purity Analysis of Benzofused Polyamides Synthesized

The purity of the benzofused polyamides of this library was checked by two different HPLC methods with two different retention times. Both methods were carried out on a Waters Alliance 1695 HPLC Pump with water and acetonitrile comprising the mobile phases. The Waters 996 PDA start wavelength was 210 nm for the 10 minute method (Method A), with a start wavelength of 220 nm and end wavelength of 500 nm for the 5 minute method (Method B) **(Table 2.43 and 2.44)**.

Table 2.44: Purity data for **library-4C** molecules as observed by HPLC

Number	Compound code	Purity	
		Method A (10 min)%	Method B (5 min)%
1	**4.99**	100	94.2
2	**4.110**	100	100
3	**4.116**	88	93
4	**4.117**	91	100
5	**4.87**	100	100

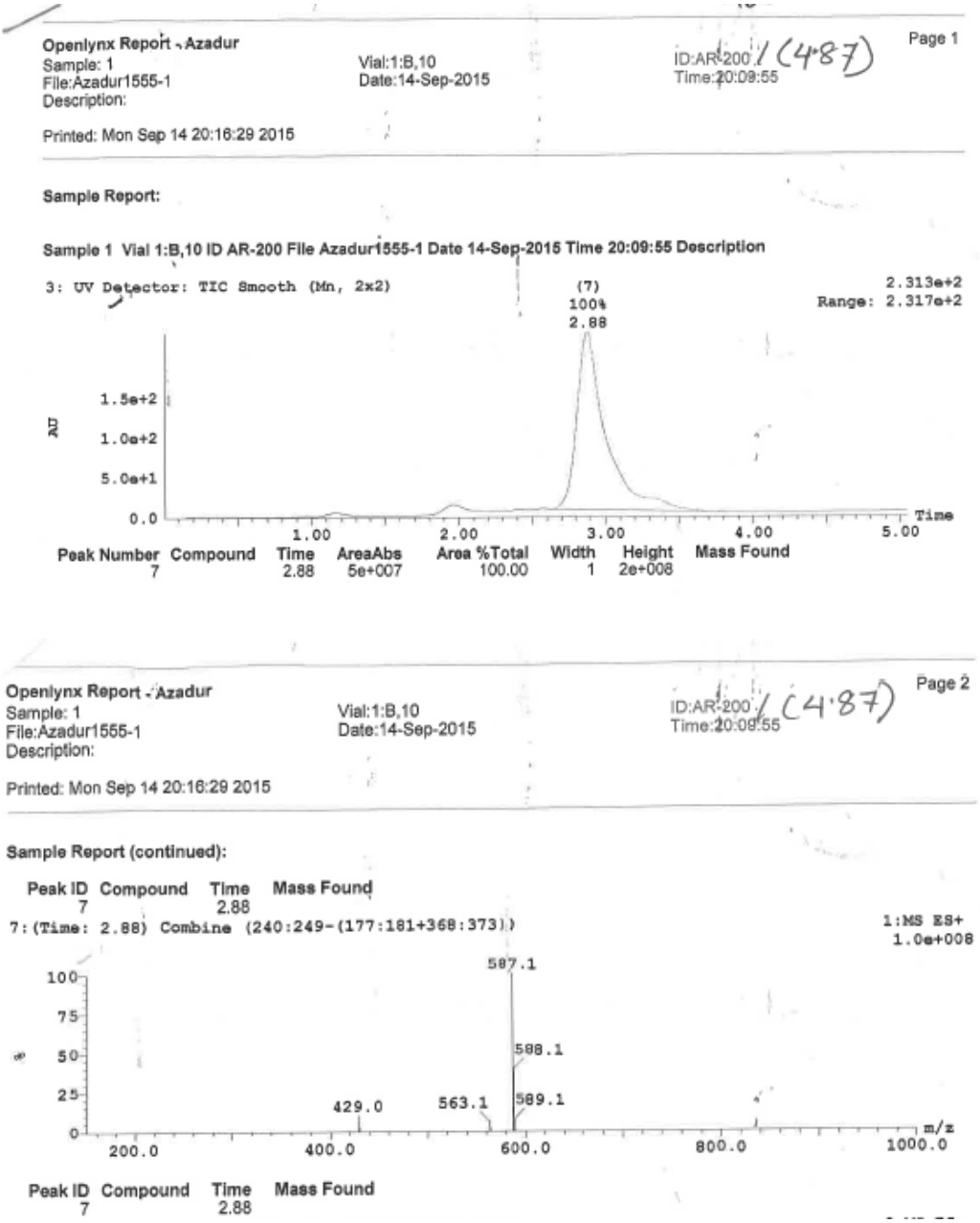

Figure 2.65: Example of an adapted LCMS profile of **Library-4C** compound **4.87**

Table 2.45: G-quadruplex and duplex DNA stabilization by ligands in FRET melting experiments at concentrations of 5, 2 and 1 μM respectively (the data are means of three technical repeats)

Compounds	Quadruplex types	ΔT_m(°C) ±(s/d)		
		5 μM	2 μM	1 μM
4.110	F21T	7.0±0.21	3.6±0.14	2.1±0.10
	C-kit-1	12.3±0.07	7.8±0.20	5.2±0.17
	C-kit-2	13.3±0.20	8.2±0.17	6.1±0.20
	BCL-2	13.3±0.31	8.2±0.32	5.8±0.32
	Duplex DNA	0.0±0.35	0.0±0.21	0.0±0.41
4.116	F21T	14.2±0.41	9.2±0.31	6.8±0.12
	C-kit-1	18.5±0.12	13.5±0.06	10.4±0.27
	C-kit-2	21.1±0.32	16.4±0.29	12.8±0.25
	BCL-2	21.4±0.15	15.6±0.34	12.0±0.05
	Duplex DNA	1.0±0.14	0.0±0.21	0.0±0.31
4.117	F21T	12.1±0.15	4.5±0.15	2.9±0.22
	C-kit-1	15.8±0.20	7.2±0.26	4.4±0.12
	C-kit-2	17.8±0.14	10.6±0.12	7.6±0.32
	BCL-2	16.8±0.17	9.5±0.16	5.1±0.41
	Duplex DNA	0.0±0.32	0.0±0.07	0.0±0.36
4.87	F21T	16.0±0.37	10.0±0.12	6.4±0.27
	C-kit-1	18.0±0.24	9.8±0.17	2.9±0.10
	C-kit-2	22.2±0.25	15.1±0.14	11.6±0.17
	BCL-2	20.8±0.11	11.9±0.15	8.1±0.20
	Duplex DNA	0.0±0.00	0.0±0.10	0.0±0.05

No compound in this group was as good as **4.93** at interacting with the F21T and C-kit-1 G-quadruplex sequences. **4.110** showed moderate interaction with all types of G-quadruplex used, providing 2.1°C, 5.2°C, 6.1°C and 5.8°C stabilisation against F21T, C-kit-1, C-kit-2 and Bcl-2 G-quadruplex sequences, respectively. **4.117** only slightly improved the stabilisation with respect to **4.110**. On the other hand, **4.116** and **4.87** provided comparatively better stabilisation than that of **4.110** or **4.117**; **4.116** provided 10.4°C, 12.8°C and 12.0°C stabilisation at 1 μM concentration against C-kit-1, C-kit-2 and Bcl-2 G-quadruplex sequences respectively, but did not show any significant stabilisation against the F21T G-quadruplex. In contrast, **4.87** provided 11.6°C and 8.1°C stabilisation at 1 μM concentration against C-kit-2 and Bcl-2 G-quadruplex sequences, respectively, and provided 6.4°C and 2.9°C stabilisation at 1 μM concentration against F21T and C-kit-1 G-quadruplex sequences respectively. Thus **4.87** is assumed to be more specific to the C-kit-2 sequence.

From the overall data analysis, it is concluded that electron-withdrawing nitro groups can enhance the interaction between ligands and G-quadruplexes.

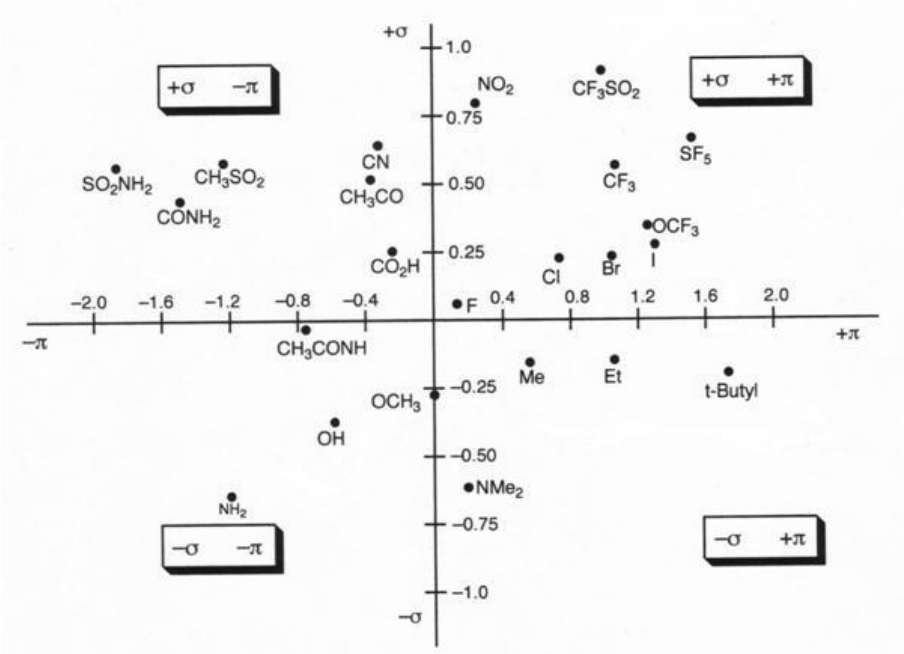

Figure 2.66: Craig plot representing σ constants versus π values of aromatic substituent groups

(http://medchem4410.up.n.seesaa.net/medchem4410/image/110926.jpg?d=a1)

At the same time the comparative FRET data analysis of the different benzofused polyamides in this group suggested that electron-withdrawing groups like chloride groups (-Cl) for **4.117** and cyanide groups (-CN) for **4.87** appeared to enhance the interacting capacity whereas electron-donating groups like methyl groups (-CH_3) for **4.99,** methoxy groups (-O-CH_3) for **4.116** and amino groups (-NH_2) for **4.110** appeared to reduce the interacting capacity of benzofused polyamides (**Table 2.45** and **Table 2.46**). Moreover, it is interesting to note that the comparatively more electron-withdrawing cyanide group (-CN) group-containing **4.87** provided more stabilisation than the less electron-withdrawing chloride group-containing **4.117** (**Figure 2.58**)**.** Similarly, electron-donating groups like methyl and methoxy appeared to reduce the interacting capacity of benzofused polyamides in proportion to their electron donating power (**Figure 2.58)**.

2.14.3 Introduction of Electron-Donating Group

Interestingly, the molecule **4.99** was made in the form of **4.98** to further verify the nitro group effect previously detailed. Here, the effect of nitro group was observed by using a 3-(piperidin-1-yl) propan-1-amine tail instead of a N1, N1-dimethylpropane-1,3-diamine tail with which this effect had already been observed.

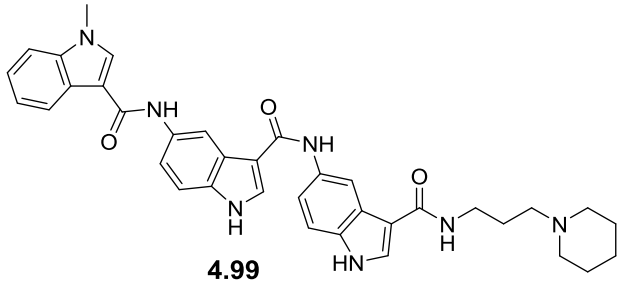

4.99

Figure 2.67: Structure of **4.99**.

Table 2.67: G-quadruplex and duplex DNA stabilization by ligand **4.99** in FRET melting experiments at concentrations of 5, 2 and 1 µM respectively (the data are means of three technical repeats)

Compounds	Quadruplex types	ΔT_m(°C) ±(s/d)		
		5 µM	2 µM	1 µM
4.99	F21T	7.2±0.11	3.9±0.17	1.3±0.21
	C-kit-1	11.5±0.17	7.9±0.11	1.0±0.16
	C-kit-2	14.0±0.18	8.9±0.35	6.5±0.25
	BCL-2	11.6±0.07	6.0±0.21	4.4±0.31
	Duplex DNA	0.0±0.23	0.0±0.05	0.0±0.06

4.99 provided 1.3 °C, 1.0 °C, 6.5 °C and 4.4 °C stabilisation at 1 µM concentration against F21T, C-kit-1, C-kit-2 and Bcl-2 G-quadruplex sequences, respectively. These values clearly distinguish the effect of nitro groups, as **4.98** provided 5.9 °C, 15.5 °C, 11.3 °C and 9.6 °C stabilisation at 1 µM concentration against F21T, C-kit-1, C-kit-2 and Bcl-2 G-quadruplex sequences, respectively. Thus this further indicated that unlike electron-withdrawing groups, electron-donating groups like methyl (-CH3) groups play a negative role in the interaction of ligand molecules with G-quadruplex sequences.

Library-4D

2.15 Synthetic sScheme for Library-4D Molecules.

A set of molecules (**Figure 2.59**) was synthesized through the replacement of indole with indazole rings by mirroring the structures of **4.77** and **4.93** in order to verify the relative abilities of indole or indazole in providing interaction capacity for the ligand towards G-quadruplex DNA.

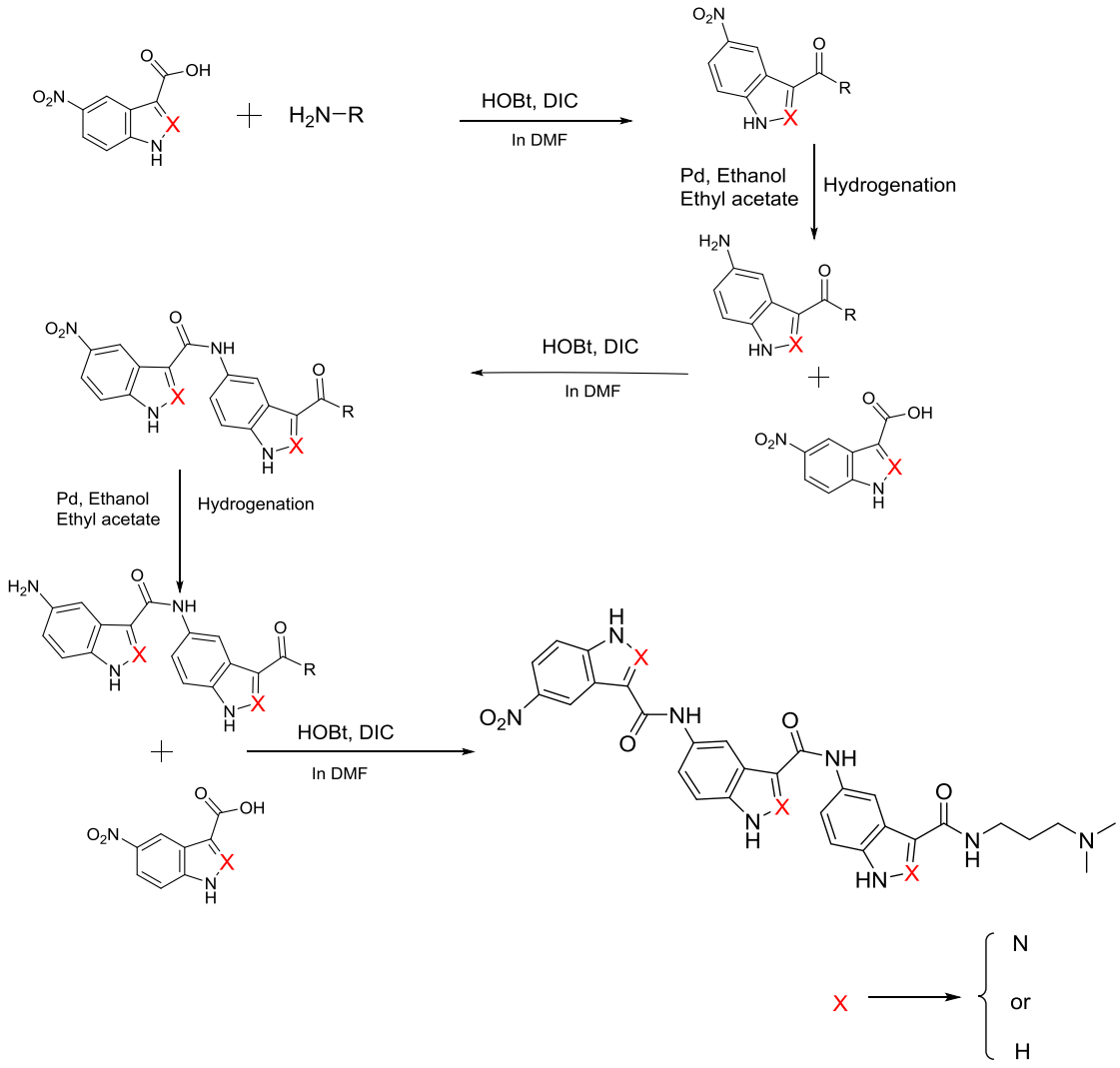

Figure 2.68: Synthetic scheme of **library-4D** molecules.

Initially the acid (1.2 eq.) was dissolved in DMF (5 mL for 100 mg of starting material) in a round bottom flask fitted with a magnetic stirrer. Then DIC (1.75 eq.) and HOBt (2.0 eq.) were added to the acid (1.0 eq.) and this mixture was allowed to stir at room temperature for formation of the ester from the acid. The amine (1 eq.) was added to the mixture and the mixture allowed stirring until the reaction was complete, as indicated by TLC or LCMS. Finally the reaction

mixture was applied to a conditioned SCX-2 cartridge and the resultant product was purified by the 'Catch and Release' method (described in the section '**Methods and Materials**' of Chapter 3).

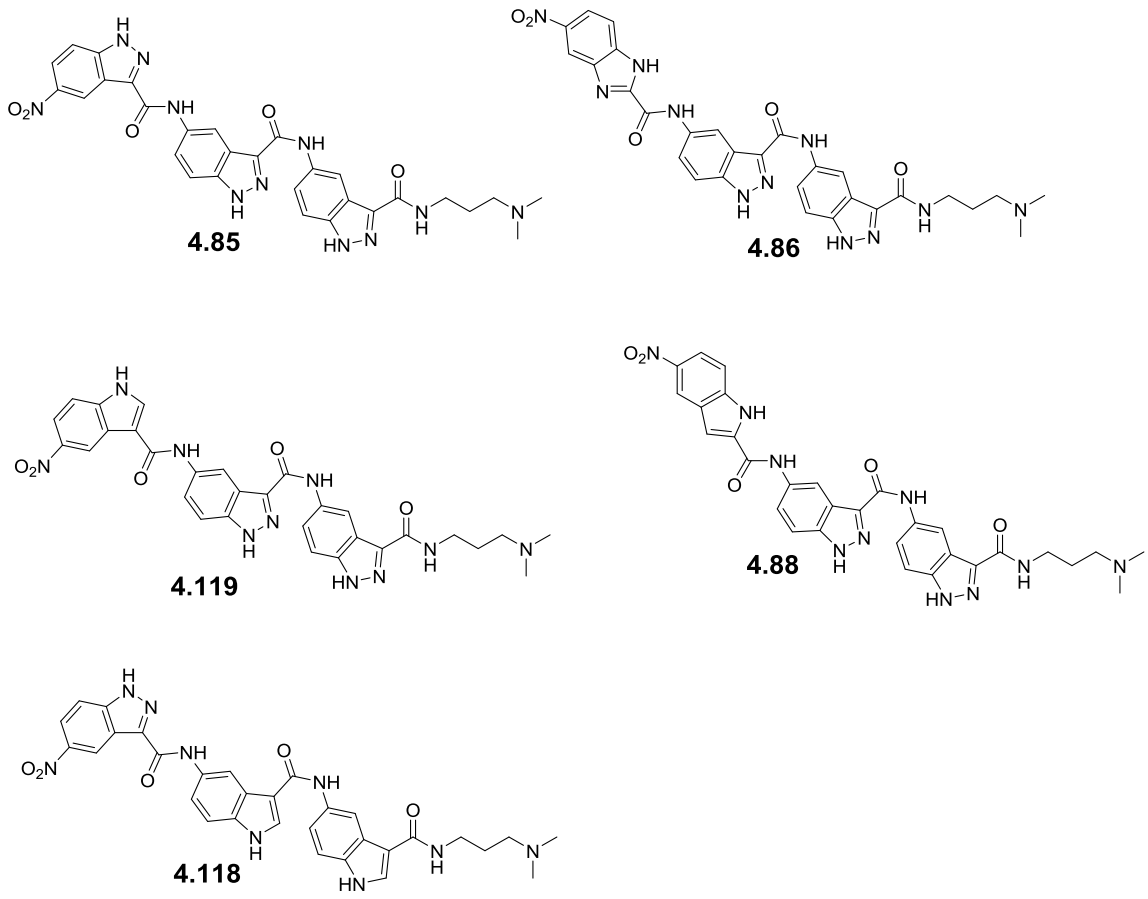

Figure 2.69: Structure of **library-4D** molecules.

2.15.1 Characterisation of Benzofused Polyamides through Various Spectroscopic Techniques

These benzofused polyamides were purified and fully characterized by different spectroscopic techniques including mass spectrometry, both ^{1}H and ^{13}C NMR, and IR techniques (described in the **Experimental** section of Chapter 4). Compounds were primarily identified by LCMS and confirmed using high resolution mass spectroscopy (HRMS) **(Table 2.47 and 2.48)**.

Table 2.47: HRMS data for **library-4D** molecules

Number	Compound code	Theoretical mass	Observed mass $[M+H]^+$
1	**4.85**	609.2197	610.2264
2	**4.86**	609.2197	610.2258
3	**4.119**	608.2244	609.2318
4	**4.88**	608.2244	609.2317
5	**4.118**	607.2292	608.2354

2.15.2 Purity Analysis of Benzofused Polyamides Synthesized

The purity of the benzofused polyamides of this library was checked by two different HPLC methods with two different retention times. Both methods were carried out on a Waters Alliance 1695 HPLC Pump with water and acetonitrile comprising the mobile phases. The Waters 996 PDA start wavelength was 210 nm for the 10 minute method (Method A), with a start wavelength of 220 nm and end wavelength of 500 nm for the 5 minute method (Method B) **(Table 2.48)**.

Table 2.48: Purity data for **library-4D** molecules as observed by HPLC

Number	Compound code	Purity	
		Method A(10 min)%	Method B(5 min)%
1	**4.85**	100	100
2	**4.86**	100	100
3	**4.119**	100	92
4	**4.88**	91	100
5	**4.118**	100	100

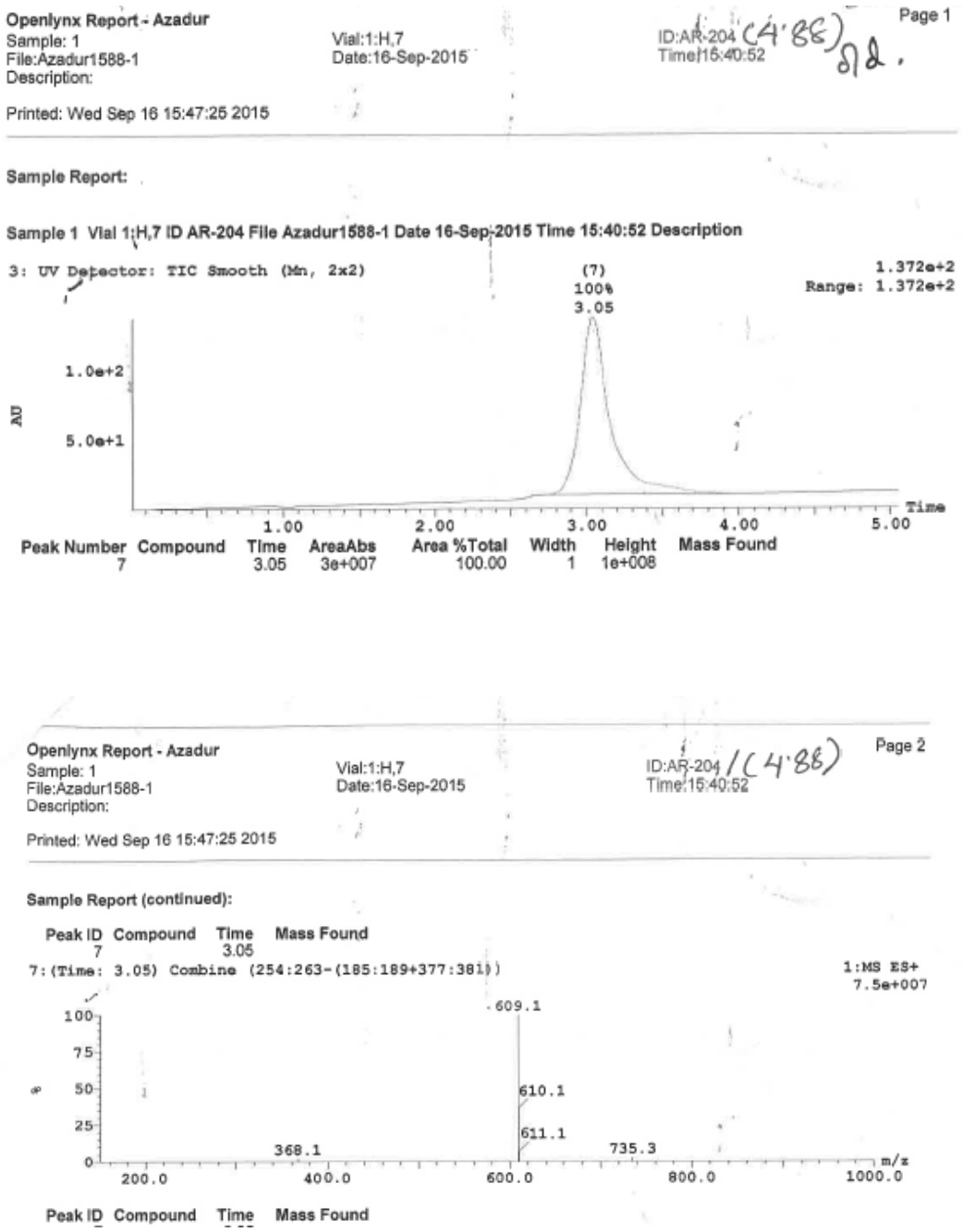

Figure 2.70: Example of an adapted LCMS profile of **Library-4D** compound **4.88**

Two molecules of benzofused polyamides were synthesized by the coupling of three consecutive, commercially available 5-nitro-indazole-3-carboxylic acid equivalents to produce molecules including **4.93** and **4.77** in order to investigate the promise of indole within the chemical scaffold.

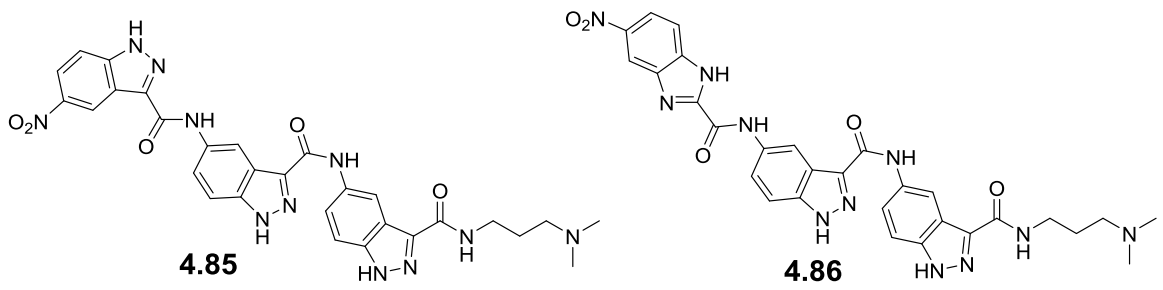

Figure 2.71: Structure of equivalent molecules **4.85** and **4.86**.

Table 2.49: G-quadruplex and duplex DNA stabilization by ligands **4.85** and **4.86** in FRET melting experiments at concentrations of 5, 2 and 1 µM respectively (the data are means of three technical repeats)

Compounds	Quadruplex types	ΔT_m(°C) ±(s/d)		
		5 µM	2 µM	1 µM
4.85	F21T	11.0±0.21	4.3±0.15	1.4±0.32
	C-kit-1	11.8±0.31	8.0±0.20	4.4±0.42
	C-kit-2	17.9±0.11	10.7±0.25	8.2±0.26
	BCL-2	20.8±0.31	7.8±0.33	4.7±0.12
	Duplex DNA	0.0±0.16	0.0±0.31	0.0±0.20
4.86	F21T	14.8±0.30	10.5±0.11	8.0±0.06
	C-kit-1	16.9±0.12	13.1±0.36	9.9±0.32
	C-kit-2	21.7±0.04	16.6±0.7	13.1±0.21
	BCL-2	19.9±0.14	13.5±0.20	8.5±0.20
	Duplex DNA	0.0±0.12	0.0±0.17	0.0±0.06

4.85 (structurally equivalent to **4.93**) provided 1.4°C, 4.4°C, 8.2 °C and 4.7°C stabilisation at 1 µM concentration against F21T, C-kit-1, C-kit-2 and Bcl-2 G-quadruplex sequences, respectively. These ΔTm values were significantly less than those of **4.93**, which indicated that benzofused polyamides made of three consecutive indole units **(4.93)** were preferable over benzofused polyamides made of three consecutive indazole units **(4.85)**. However, **4.85** seemed to be specific to the C-kit-2 G-quadruplex sequence. **4.86** (structurally equivalent to **4.77**) provided 8.0°C, 9.9°C, 13.1°C and 8.5°C stabilisation at 1 µM concentration against F21T, C-kit-1, C-kit-2 and Bcl-2 G-quadruplex sequences respectively, thus **4.86** showed significantly more stabilising capacity than **4.85**. This difference in melting temperature is possibly due to the formation of intramolecular hydrogen bonds between proximal amine and imine groups of the indazoles in the middle and terminal positions of **4.85**. In contrast, in **4.86** the terminal building block is 5'-2' substituted rather than 5'-3' substitution as in

4.85, making the amine and imine groups of **4.86** too far from each other, so that these groups can only form hydrogen bonds with the guanine residues of the G-quadruplex sequences rather making an intramolecular hydrogen bond as in **4.85.**

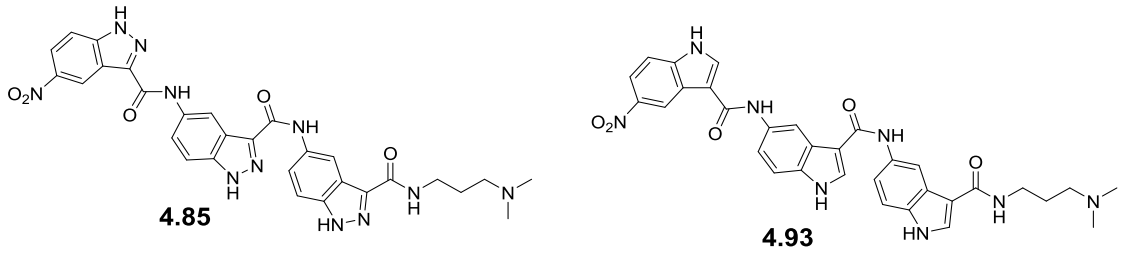

Figure 2.72: Structures of equivalent molecules **4.85** and **4.93**.

Table 2.50: Comparative stabilising abilities of the equivalent molecules **4.85** and **4.93** (the data are means of three technical repeats)

Quadruplex types	ΔT_m(°C) ±(s/d)					
	4.85	**4.93**	**4.85**	**4.93**	**4.85**	**4.93**
	5 µM	5 µM	2 µM	2 µM	1 µM	1 µM
F21T	11.0±0.21	21.0±0.17	4.3±0.15	15.9±0.28	1.4±0.32	12.6±0.26
C-kit-1	11.8±0.31	27.7±0.30	8.0±0.20	22.1±0.35	4.4±0.42	17.6±0.28
C-kit-2	17.9±0.11	21.3±0.23	10.7±0.25	14.8±0.20	8.2±0.26	11.4±0.32
BCL-2	20.8±0.31	25.4±0.30	7.8±0.33	17.8±0.14	4.7±0.12	13.5±0.20
Duplex DNA	0.0±0.16	0.0±0.05	0.0±0.31	0.0±0.05	0.0±0.20	0.0±0.05

Here, **4.85** (structurally equivalent to **4.93**) provided 1.4°C, 4.4°C, 8.2 °C and 4.7°C stabilisation at 1 µM concentration against F21T, C-kit-1, C-kit-2 and Bcl-2 G-quadruplex sequences, respectively. On the other hand, **4.93** provided 12.6°C, 17.6°C, 11.4°C and 13.5°C stabilisation at 1 µM concentration against F21T, C-kit-1, C-kit-2 and Bcl-2 G-quadruplex sequences, respectively.

From this DNA melting assay comparison, it is evident that **4.93** had far greater stabilisation capacity than **4.85** for all the G-quadruplex sequences used, reflecting the greater applicability of indole. Even though **4.86** showed a significantly higher activity, it did not have a better stabilisation capacity than **4.77**.

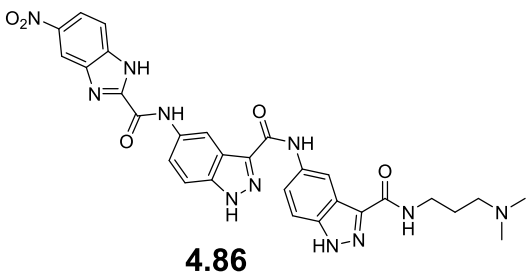

4.86

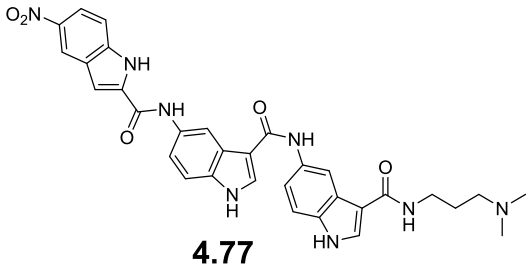

4.77

Figure 2.73: Structures of equivalent molecules **4.86** and **4.77**.

Table 2.51: Comparative stabilising abilities between equivalent molecules **4.86** and **4.77** (the data are means of three technical repeats)

Quadruplex types	ΔT_m(°C) ±(s/d)					
	4.86	**4.77**	**4.86**	**4.77**	**4.86**	**4.77**
	5 µM	5 µM	2 µM	2 µM	1 µM	1 µM
F21T	14.8±0.30	21.7±0.26	10.5±0.11	15.6±0.07	8.0±0.06	12.2±0.23
C-kit-1	16.9±0.12	24.5±0.40	13.1±0.36	16.7±0.26	9.9±0.32	14.4±0.35
C-kit-2	21.7±0.04	27.8±0.36	16.6±0.7	17.9±0.21	13.1±0.21	14.7±0.26
BCL-2	19.9±0.14	30.8±0.21	13.5±0.20	15.7±0.28	8.5±0.20	12.1±0.25
Duplex DNA	0.0±0.12	1.0±0.12	0.0±0.17	0.0±0.1	0.0±0.06	0.0±0.23

Here, **4.86** (structurally equivalent to **4.77**) provided 8.0°C, 9.9°C, 13.1°C and 8.5°C stabilisation at 1 µM concentration against F21T, C-kit-1, C-kit-2 and Bcl-2 G-quadruplex sequences, respectively. On the other hand, **4.77** provided 12.2°C, 14.4°C, 14.7°C and 12.1°C stabilisation at 1 µM concentration against F21T, C-kit-1, C-kit-2 and Bcl-2 G-quadruplex sequences, respectively.

From this DNA melting assay comparison, it is evident that **4.77** had a greater stabilisation capacity than **4.86** for all the G-quadruplex sequences used, further reflecting the superiority of the indole building block in this application.

2.15.3 Structural Modifications of 4.85 and 4.86

Although the benzofused polyamides made of three consecutive indazole carboxylic acids did not have show interactions towards the G-quadruplex DNAs than **4.93** and **4.77**, they showed significant improved melting temperatures. Therefore there is a possibility that structural modifications of **4.85** and **4.86**, specifically capping with 5-nitro-indole-3-carboxylic acid and 5-nitro-indole-2-carboxylic acid, may improve their interactive capacity.

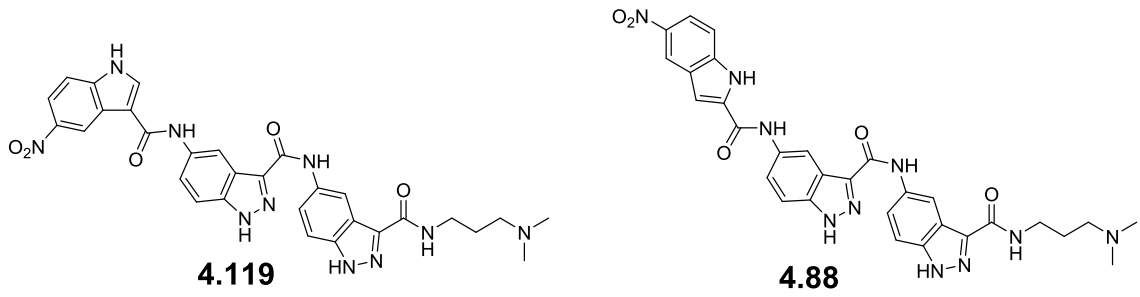

Figure 2.74: Structures of **4.119** and **4.88**.

Table 2.52: Comparative G-quadruplex and duplex DNA stabilization between ligands **4.119** and **4.88** (the data are means of three technical repeats)

Compounds	Quadruplex types	ΔT_m(°C) ±(s/d)		
		5 µM	2 µM	1 µM
4.119	F21T	17.8±0.17	14.8±0.26	13.0±0.35
	C-kit-1	18.2±0.13	14.2±0.23	11.1±0.21
	C-kit-2	20.4±0.23	17.8±0.24	16.4±0.32
	BCL-2	18.1±0.26	14.1±0.05	10.8±0.13
	Duplex DNA	0.0±0.1	0.0±0.05	0.0±0.11
4.88	F21T	12.1±0.2	8.1±0.20	6.1±0.11
	C-kit-1	10.8±0.27	6.1±0.36	2.6±0.23
	C-kit-2	18.9±0.15	14.6±0.20	12.8±0.18
	BCL-2	15.3±0.23	8.8±0.20	7.1±0.34
	Duplex DNA	0.0±0.11	0.0±0.10	0.0±0.20

Here, **4.119** (structurally equivalent to **4.85** and **4.93**) provided 13.0°C, 11.1°C 16.4°C and 10.8°C stabilisation at 1 µM concentration against F21T, C-kit-1, C-kit-2 and Bcl-2 G-quadruplex sequences, respectively. **4.88** (structurally equivalent to **4.86** and **4.77**) provided 6.1°C, 2.6°C, 12.8°C and 7.1°C stabilisation at 1 µM concentration against F21T, C-kit-1, C-kit-2 and Bcl-2 G-quadruplex sequences, respectively. It is notable that **4.88** was more specific towards the C-kit-2 sequence. Therefore, it is evident that indole in place of indazole improved the stabilisation capacity of the ligands and the third degree of curvature is preferable for fitting into the terminal quartet of the G-quadruplex sequence types. The higher activity of **4.119** was assumed to be because the distance between the nitrogen atoms of indazole and the terminal indole unit is far enough to avoid the intramolecular hydrogen bonding as assumed for **4.85**.

The comparative melting data analysis indicates the preference of the indole over indazole building block at the terminal point of the ligands.

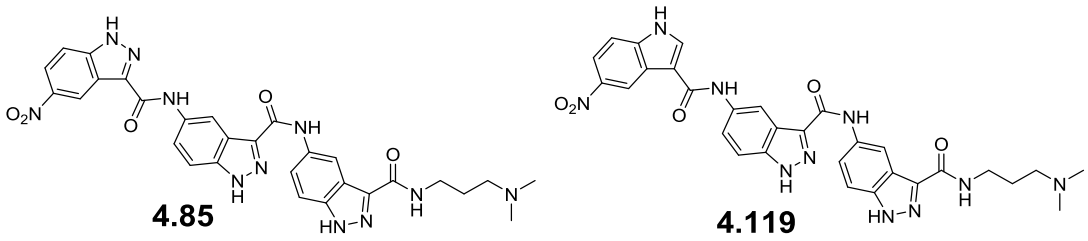

Figure 2.75: Structures of semi-equivalent molecules **4.85** and **4.119**.

Table 2.53: FRET data comparison between **4.85** and **4.119** (the data are means of three technical repeats)

Quadruplex types	ΔT_m(°C) ±(s/d)					
	4.85	**4.119**	**4.85**	**4.119**	**4.85**	**4.119**
	5 µM	5 µM	2 µM	2 µM	1 µM	1 µM
F21T	11.0±0.21	17.8±0.17	4.3±0.15	14.8±0.26	1.4±0.32	13.0±0.35
C-kit-1	11.8±0.31	18.2±0.13	8.0±0.20	14.2±0.23	4.4±0.42	11.1±0.21
C-kit-2	17.9±0.11	20.4±0.23	10.7±0.25	17.8±0.24	8.2±0.26	16.4±0.32
BCL-2	20.8±0.31	18.1±0.26	7.8±0.33	14.1±0.05	4.7±0.12	10.8±0.13
Duplex DNA	0.0±0.16	0.0±0.1	0.0±0.31	0.0±0.05	0.0±0.20	13.0±0.35

Here, **4.85** (structurally equivalent to **4.119**, only with exception of the terminal building block) provided 1.4°C, 4.4°C, 8.2°C and 4.7°C stabilisation at 1 µM concentration against F21T, C-kit-1, C-kit-2 and Bcl-2 G-quadruplex sequences, respectively. In contrast, **4.119** provided 13.0°C, 11.1°C, 16.4°C and 10.8°C stabilisation at 1 µM concentration against the same G-quadruplex sequences, respectively. Therefore, it is further evident that the indole, especially at the terminal position, is better than the benzimidazole building block at providing significant G-quadruplex stabilisation capacity.

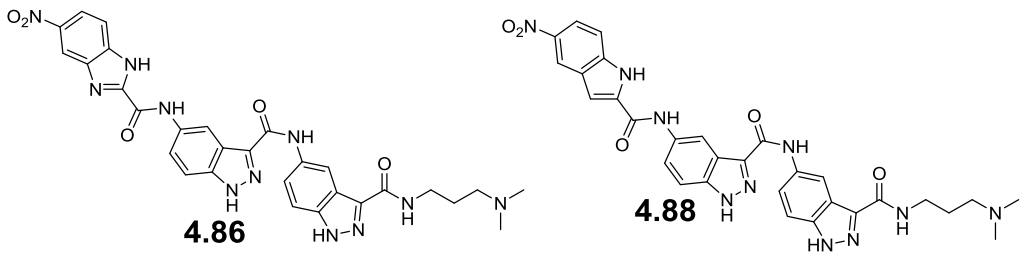

Figure 2.76: Structures of **4.86** and **4.88**.

Table 2.54: FRET data comparison between equivalent molecules **4.86** and **4.88** (the data are means of three technical repeats)

Quadruplex types	ΔT_m(°C) ±(s/d)					
	4.86	**4.88**	**4.86**	**4.88**	**4.86**	**4.88**
	5 µM	5 µM	2 µM	2 µM	1 µM	1 µM
F21T	14.8±0.30	12.1±0.2	10.5±0.11	8.1±0.20	8.0±0.06	6.1±0.11
C-kit-1	16.9±0.12	10.8±0.27	13.1±0.36	6.1±0.36	9.9±0.32	2.6±0.23
C-kit-2	21.7±0.04	18.9±0.15	16.6±0.7	14.6±0.20	13.1±0.21	12.8±0.18
BCL-2	19.9±0.14	15.3±0.23	13.5±0.20	8.8±0.20	8.5±0.20	7.1±0.34
Duplex DNA	0.0±0.12	0.0±0.11	0.0±0.17	0.0±0.10	0.0±0.06	0.0±0.20

Here, **4.86** (structurally equivalent to **4.88,** only with the exception of the terminal building block) provided 8.0°C, 9.9°C, 13.1°C and 8.5°C stabilisation at 1 µM concentration against F21T, C-kit-1, C-kit-2 and Bcl-2 G-quadruplex sequences, respectively. By comparison, **4.88** provided 6.1°C, 2.6°C 12.8°C and 7.1°C stabilisation at 1 µM concentration against F21T, C-kit-1, C-kit-2 and Bcl-2 G-quadruplex sequences, respectively. Both of them showed equivalent ΔTms against the sequences used, but it is notable that **4.119** showed better interaction than **4.88**, since **4.119** provided 13.0°C, 11.1°C, 16.4°C and 10.8°C stabilisation at 1 µM concentration against F21T, C-kit-1, C-kit-2 and Bcl-2 G-quadruplex sequences, respectively. Therefore, it is evident that third degree curved molecules of this type show more interactive capacity than their second degree curved equivalents.

Since a terminal indole in place of an indazole makes a ligand more potent, a molecule (**4.118** in the form of **4.119**) was made by replacing indazole with another indole in the middle.

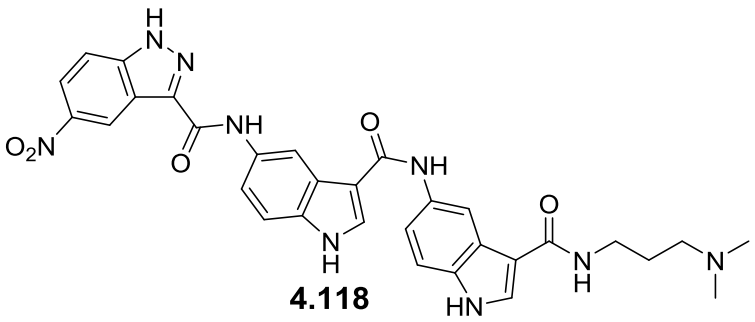

4.118

Figure 2.77: Structure of **4.118**.

Table 2.55: G-quadruplex and duplex DNA stabilization by ligand **4.118** in FRET melting experiments at concentrations of 5, 2 and 1 μM respectively (the data are means of three technical repeats)

Compounds	Quadruplex types	ΔT_m(°C) ±(s/d)		
		5 μM	2 μM	1 μM
4.118	F21T	15.1±0.21	12.2±0.11	10.2±0.16
	C-kit-1	18.6±0.07	14.8±0.12	10.7±0.27
	C-kit-2	19.3±0.35	16.1±0.38	13.9±0.23
	BCL-2	26.4±0.31	15.9±0.06	12.2±0.27
	Duplex DNA	0.0±0.17	0.0±0.20	0.0±0.20

Here, **4.118** (structurally equivalent to **4.119** and **4.93**) provided 10.2°C, 10.7°C, 13.9°C and 12.2°C stabilisation at 1 μM concentration against F21T, C-kit-1, C-kit-2 and Bcl-2 G-quadruplex sequences, respectively. By comparison, **4.119** provided 13.0°C, 11.1°C 16.4°C and 10.8°C stabilisation at 1 μM concentration against F21T, C-kit-1, C-kit-2 and Bcl-2 G-quadruplex sequences, respectively. Although **4.118** showed comparatively better activity towards Bcl-2 G-quadruplex, **4.119** showed stabilising capacity for the other G-quadruplex types used. This indicated that the molecules made of consecutive indole building blocks were more potent with regard G-quadruplex interaction. These two molecules were equivalent in their G-quadruplex stabilising capacities. Finally, the most active molecules from this library were compared with lead ligand **4.93**.

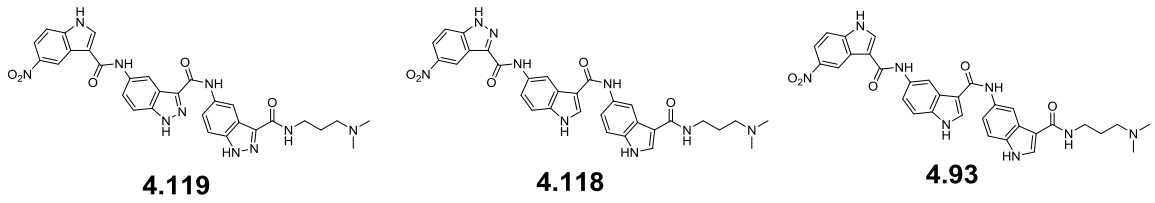

Figure 2.78: Structures of **4.119**, **4.118** and **4.93**.

Table 2.56: Comparative FRET data analysis between ligands **4.119**, **4.118** and **4.93** (the data are means of three technical repeats)

Quadruplex types	ΔT_m(°C) ±(s/d)								
	5 µM			2 µM			1 µM		
	4.119	**4.118**	**4.93**	**4.119**	**4.118**	**4.93**	**4.119**	**4.118**	**4.93**
F21T	17.8±0.1	15.1±0.2	21.0±0.17	14.8±0.2	12.2±0.1	15.9±0.2	13.0±0.35	10.2±0.16	12.6±0.26
C-kit-1	18.2±0.1	18.6±0.0	27.7±0.30	14.2±0.2	14.8±0.1	22.1±0.3	11.1±0.21	10.7±0.27	17.6±0.28
C-kit-2	20.4±0.2	19.3±0.3	21.3±0.23	17.8±0.2	16.1±0.3	14.8±0.2	16.4±0.32	13.9±0.23	11.4±0.32
BCL-2	18.1±0.2	26.4±0.3	25.4±0.30	14.1±0.0	15.9±0.0	17.8±0.1	10.8±0.13	12.2±0.27	13.5±0.20
Duplex DNA	0.0±0.1	0.0±0.17	0.0±0.05	0.0±0.05	0.0±0.20	0.0	0.0±0.11	0.0±0.20	0.0

Here, **4.93** is a better ligand for providing stabilisation towards all of the G-quadruplex sequences; the only exception is for c-kit-2. **4.93** provided 12.6 °C, 17.6°C and 13.5°C stabilisation at 1 µM concentration against F21T, C-kit-1 and Bcl-2 G-quadruplex sequences, respectively; **4.118** and **4.119** showed greater melting temperatures (ΔTm=13.9 $^{\circ}$C) and (ΔTm=12.2 $^{\circ}$C) against the C-kit-2 sequence. **4.119** had a greater stabilising capacity towards C-kit-2 than **4.118** and **4.93**; therefore it is evident that **4.93** is the ultimate lead ligand against F21T, C-kit-1 and Bcl-2 G-quadruplex sequences respectively. **4.93** is most active towards F21T compared to the other G-quadruplex sequences. In fact the ligands **4.119**, **4.118** and **4.93** are interact equivalently and significantly with G-quadruplex DNA types. Thus these molecules can be used as structural scaffolds for further modification to achieve better G-quadruplex-targeting, drug-like ligands. Although indazole at certain positions of the benzofused polyamide structure improves the ligand's G-quadruplex interactivity, evidence from a variety of experiments previously discussed has established indole as a better benzofused unit which has a positive impact on the interaction of benzofused polyamides with G-quadruplex DNA by enhancing the stabilising capacity of the former.

Library-5

2.16 Synthetic Scheme for Library-5 Molecules

Library-5 was comprised of 9 compounds **(Figure 2.70)**. Two sets of molecules were made by using commercially available 5-nitro-indole-3-carboxylic acid and 5-nitro-indazole-3-carboxylic acid building blocks by following the structural motif of lead molecule **4.93**. These molecules were synthesized with the aim to check whether benzofused polyamides with three consecutive building blocks are better G-quadruplex-interactive ligands than benzofused polyamides with two consecutive building blocks.

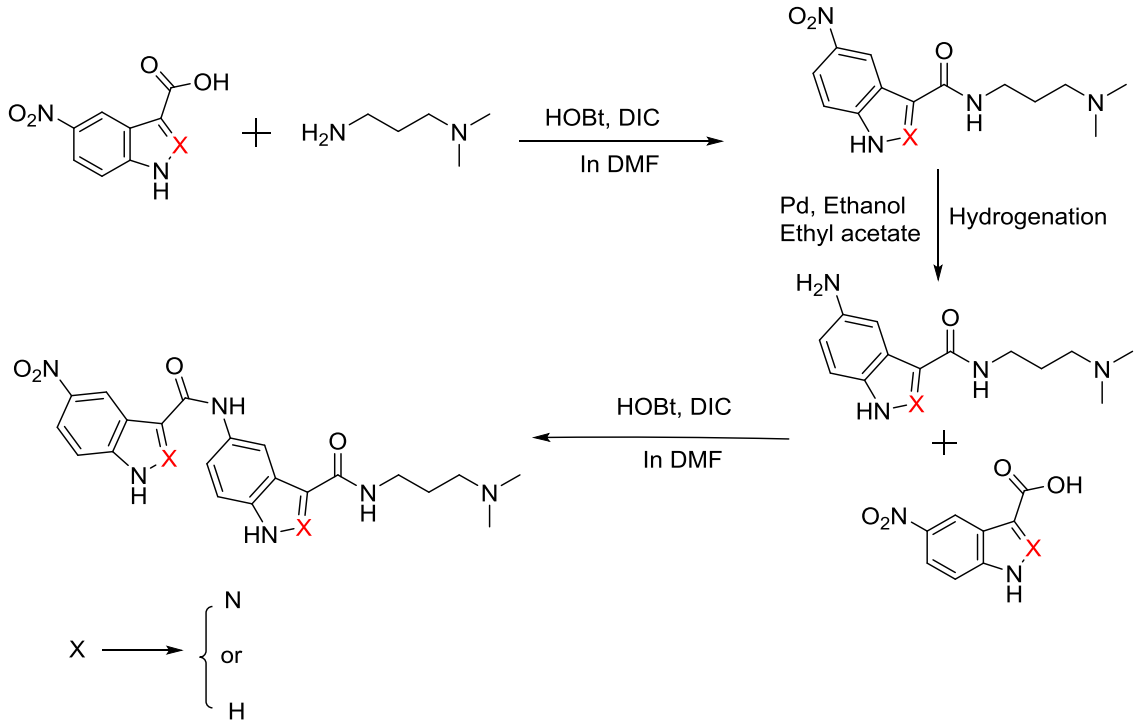

Figure 2.79: Synthetic scheme of **library-5** molecules.

Initially the acid (1.2 eq.) was dissolved in DMF (5 mL for 100 mg of starting material) in a round bottom flask fitted with a magnetic stirrer. Then DIC (1.75 eq.) and HOBt (2.0 eq.) were added to the acid (1.0 eq.) and this mixture was allowed to stir at room temperature for formation of the ester from the acid. The amine (1 eq.) was added to the mixture and the mixture allowed to stir until the reaction was complete, as indicated by TLC or LCMS. Finally the reaction mixture was applied to a conditioned SCX-2 cartridge and the resultant product

was purified by the 'Catch and Release' method (described in the section '**Methods and Materials**' of Chapter 3).

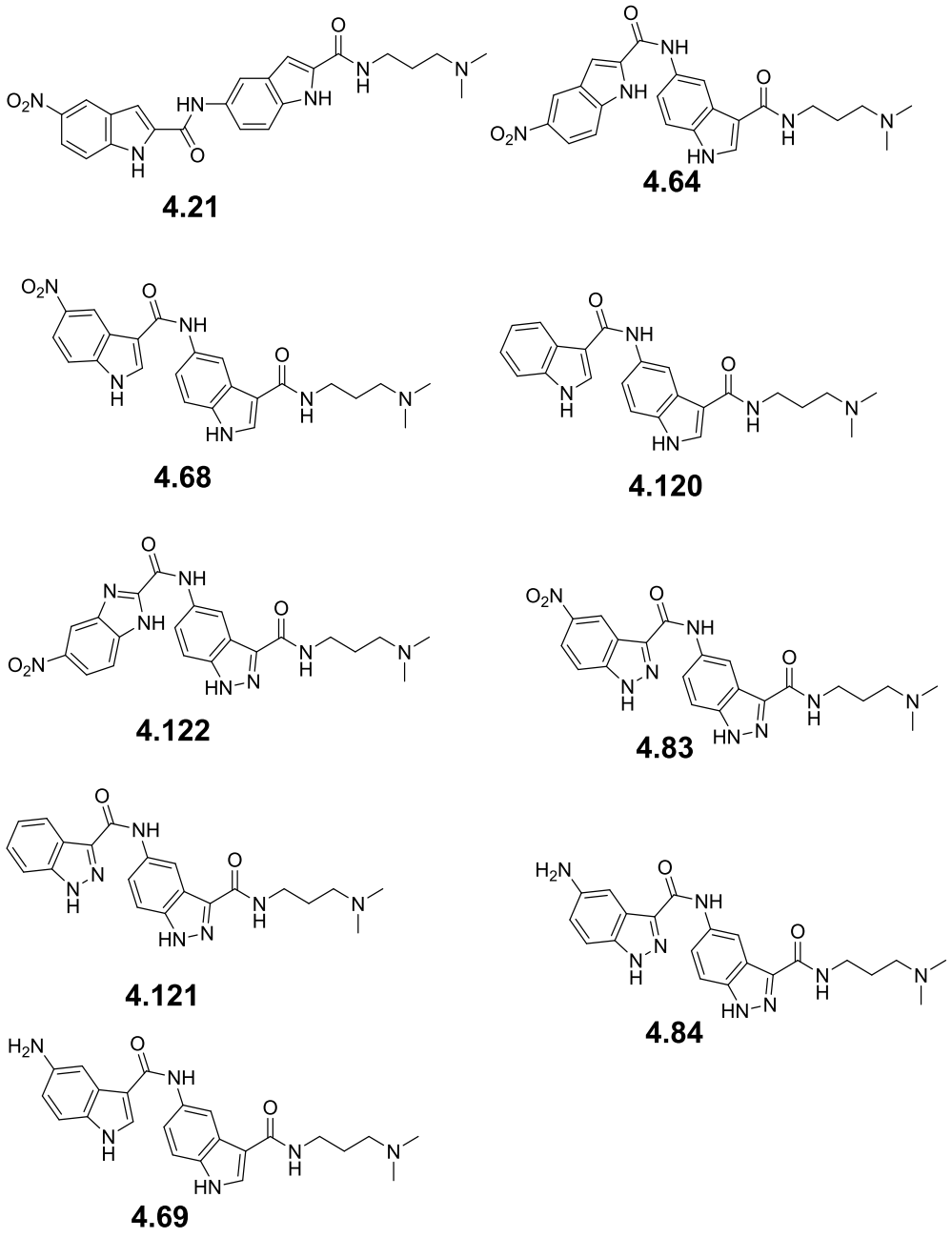

Figure 2.80: Structures of **library-5** molecules.

2.16.1 Characterisation of Benzofused Polyamides through Various Spectroscopic Techniques

Library-5 is comprised of 9 compounds. These benzofused polyamides were purified and fully characterized by different spectroscopic techniques including

mass spectroscopy, both ^{1}H and ^{13}C NMR, and IR techniques (see **Experimental** section in Chapter 4). Compounds were primarily identified by LCMS and confirmed using high resolution mass spectroscopy (HRMS) **(Table 2.57 and 2.58)**.

Table 2.57: HRMS data for **library-5** molecules

Number	Compound code	Theoretical mass	Observed mass $[M+H]^+$
1	**4.21**	448.1859	449.1924
2	**4.64**	448.1859	449.1925
3	**4.68**	448.1859	449.1926
4	**4.120**	403.2008	404.2072
5	**4.122**	450.1764	451.1835
6	**4.83**	450.1764	451.1826
7	**4.121**	405.1913	406.1980
8	**4.84**	420.2022	421.2095
9	**4.69**	418.2117	419.2182

2.16.2 Purity Analysis of Benzofused Polyamides Synthesized

The purity of the benzofused polyamides of **library-5** was checked by two different HPLC methods with two different retention times. Both methods were carried out on a Waters Alliance 1695 HPLC Pump with water and acetonitrile comprising the mobile phases. The Waters 996 PDA start wavelength was 210 nm for the 10 minute method (Method A), with a start wavelength of 220 nm and end wavelength of 500 nm for the 5 minute method (Method B) **(Tables 2.3 and 2.4)**.

Table 2.58: Purity data for **library-5** molecules as observed by HPLC

Number	Compound code	Purity	
		Method A (10 min)%	Method B (5 min)%
1	**4.21**	100	100
2	**4.64**	100	100
3	**4.68**	100	92
4	**4.120**	100	100
5	**4.122**	100	100
6	**4.83**	100	100
7	**4.121**	100	100
8	**4.84**	92	87
9	**4.69**	100	100

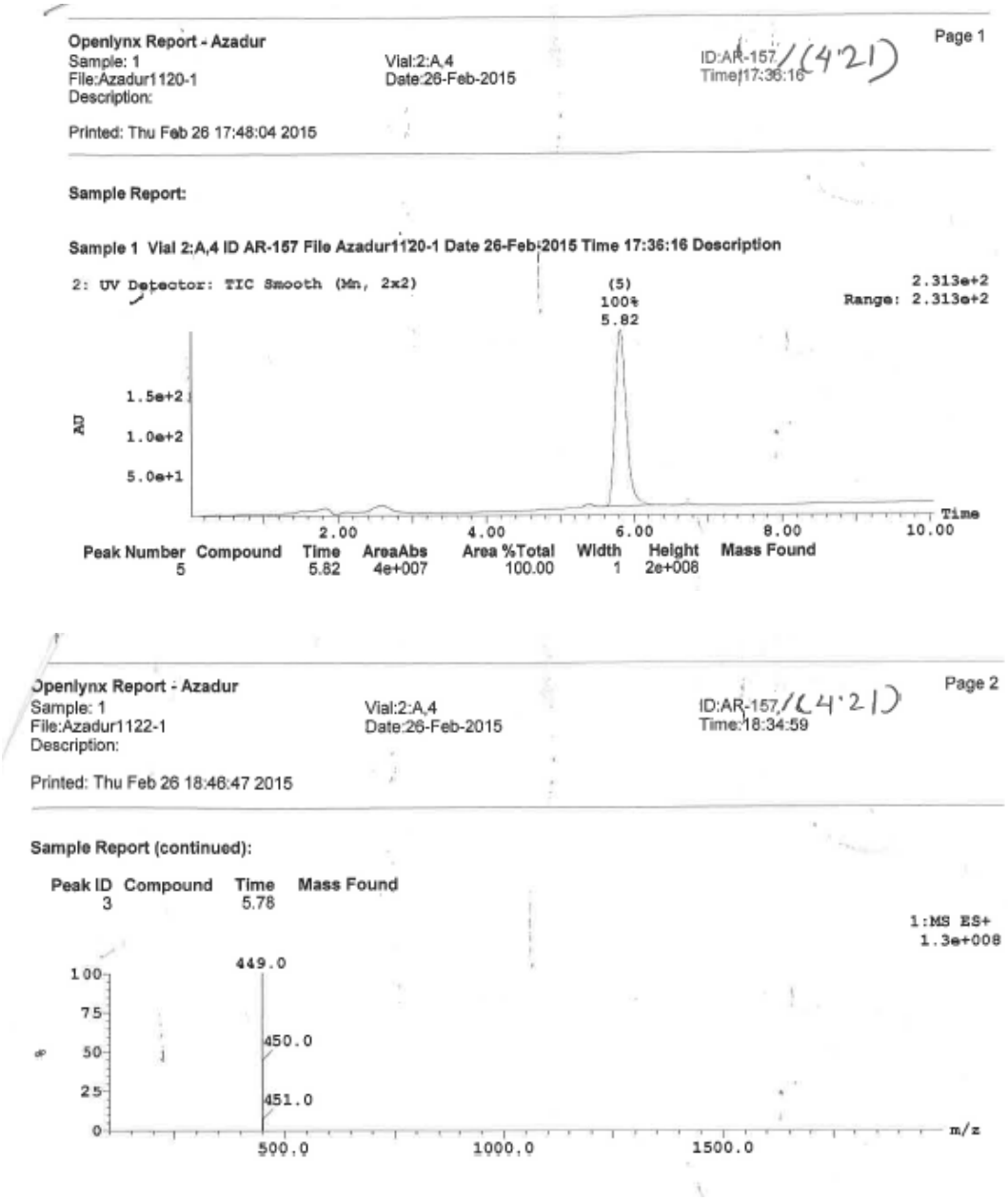

Figure 2.81: Example of an adapted LCMS profile of **Library-5** compound **4.21**

Table 2.59: G-quadruplex and duplex DNA stabilization by ligands in FRET melting experiments at concentrations of 5, 2 and 1 μM respectively (the data are means of three technical repeats)

Compounds	Quadruplex types	ΔT_m(°C) ±(s/d)		
		5 μM	2 μM	1 μM
4.21	F21T	3.4±0.11	1.3±0.27	0.5±0.30
	C-kit-1	6.2±0.27	3.1±0.29	1.5±0.07
	C-kit-2	10.8±0.32	5.7±0.21	3.4±0.22
	BCL-2	7.7±0.30	3.9±0.21	2.8±0.15
	Duplex DNA	0.0±0.26	0.0±0.15	0.0±0.18
4.64	F21T	4.8±0.25	2.5±0.28	1.2±0.11
	C-kit-1	8.7±0.13	5.9±0.23	3.7±0.26
	C-kit-2	14.2±0.11	9.4±0.14	7.0±0.16
	BCL-2	9.7±0.28	6.1±0.31	3.6±0.05
	Duplex DNA	0.0±0.6	0.0±0.17	0.0±0.27
4.68	F21T	10.0±0.13	6.5±0.35	3.9±0.18
	C-kit-1	13.3±0.38	10.2±0.42	7.3±0.45
	C-kit-2	15.7±0.11	12.2±0.17	9.1±0.41
	BCL-2	12.8±0.15	8.8±0.20	5.9±0.12
	Duplex DNA	0.0±0.23	0.0±0.18	0.0±0.28
4.120	F21T	2.3±0.31	0.9±0.25	0.4±0.17
	C-kit-1	4.9±0.33	2.8±0.15	1.6±0.06
	C-kit-2	7.7±0.12	5.4±0.27	3.7±.010
	BCL-2	3.9±0.16	1.8±0.20	1.3±0.11
	Duplex DNA	0.0±0.11	0.0±0.10	0.0±0.27

Here, **4.21**, a 5'-2' substituted benzofused polyamide of two consecutive 5-nitro indole-2-carboxylic acids, provided 0.5°C, 1.5°C 3.4°C and 2.8°C stabilisation at 1 μM concentration against F21T, C-kit-1, C-kit-2 and Bcl-2 G-quadruplex sequences, respectively. **4.64** (a first degree curved molecule), a 5'-3' and 5'-2' substituted benzofused polyamide of two consecutive 5-nitro indole-3-carboxylic acids and 5-nitro indole-2-carboxylic acid, showed a marginally better G-quadruplex sequence interacting capacity with 1.2°C, 3.7°C, 7.0°C and 3.6°C stabilisation at 1 μM concentration against F21T, C-kit-1, C-kit-2 and Bcl-2 G-quadruplex sequences, respectively. This difference in melting temperatures suggests that the introduction of curvature by the 5′-3′ substitution makes a ligand more potent towards the G-quadruplex sequences used in this study. This is further justified by FRET data of second degree curved molecule **4.68**, made through the 5'-3' substitution of consecutive 5-nitro-indole-3-carboxylic acids, which showed 3.9°C, 7.3°C, 9.1°C and 5.9°C stabilisation at 1 μM

concentration against F21T, C-kit-1, C-kit-2 and Bcl-2 G-quadruplex sequences, respectively.

It is necessary to investigate the effect of nitro group of a ligand molecule. Therefore, **4.120** was made by following the shape of **4.68**, capped with indole-3-carboxylic acid instead of 5-nitro-indole-3-carboxylic acid. The melting temperatures against the different G-quadruplex types suddenly decreased as it provided stabilisation of 0.4°C, 1.6°C, 3.7°C and 1.3°C at 1 µM concentration against F21T, C-kit-1, C-kit-2 and Bcl-2 G-quadruplex sequences, respectively. This means the nitro group must play a positive role in increasing the stabilising capacity of these ligands.

A molecule in the form of **4.68** with an electron-donating amino group rather an electron-withdrawing nitro group would be expected to enhance the interaction capacity of ligand molecules.

A molecule was made by reducing the nitro group of **4.68** and was assessed by FRET melting assay to investigate further the effects of the nitro group.

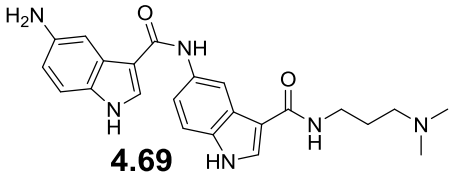

4.69

Figure 2.82: Structure of **4.69**.

Table 2.60: G-quadruplex and duplex DNA stabilization by ligand **4.69** in FRET melting experiments at concentrations of 5, 2 and 1 µM respectively (the data are means of three technical repeats)

Compounds	Quadruplex types	ΔT_m(°C) ±(s/d)		
		5 µM	2 µM	1 µM
4.69	F21T	3.0±0.41	1.7±0.22	1.0±0.18
	C-kit-1	4.8±0.13	2.9±0.33	0.7±0.16
	C-kit-2	7.7±0.15	5.1±0.42	3.6±0.07
	BCL-2	6.5±0.23	3.6±0.13	1.9±0.21
	Duplex DNA	0.0±0.15	0.0±0.15	0.0±0.11

It is evident that the reduced form of the nitro group reduces the stabilisation capacity of **4.68** as the melting temperatures were decreased to 1.0°C, 0.7°C, 3.6°C and 1.9°C stabilisation at 1 µM concentration against F21T, C-kit-1, C-kit-

2 and Bcl-2 G-quadruplex sequences respectively. However, it would be easier to visualise the effect of the nitro group by the direct comparison of the stabilisation capacities of both **4.68** and **4.69** in a same table.

Table 2.61: Comparison of G-quadruplex and duplex DNA stabilization of ligands **4.69** and **4.68** in FRET melting experiments at concentrations of 5, 2 and 1 µM, respectively (the data are means of three technical repeats)

Quadruplex type	ΔT_m(°C) ±(s/d)					
	4.69	**4.68**	**4.69**	**4.68**	**4.69**	**4.68**
	5 µM	5 µM	2 µM	2 µM	1 µM	1 µM
F21T	3.0±0.41	10.0±0.13	1.7±0.22	6.5±0.35	1.0±0.18	3.9±0.18
C-kit-1	4.8±0.13	13.3±0.38	2.9±0.33	10.2±0.42	0.7±0.16	7.3±0.45
C-kit-2	7.7±0.15	15.7±0.11	5.1±0.42	12.2±0.17	3.6±0.07	9.1±0.41
BCL-2	6.5±0.23	12.8±0.15	3.6±0.13	8.8±0.20	1.9±0.21	5.9±0.12
Duplex DNA	0.0±0.15	0.0±0.23	0.0±0.15	0.0±0.18	0.0±0.11	0.0±0.28

As shown above, **4.68**, a 5'-3' substituted benzofused polyamide with a terminal nitro group, provided 3.9°C, 7.3°C, 9.1°C and 5.9°C stabilisation at 1 µM concentration against F21T, C-kit-1, C-kit-2 and Bcl-2 G-quadruplex sequences respectively, far better than **4.69**, a 5'-3' substituted benzofused polyamide with the terminal amino group, which showed stabilisation of 1°C, 0.7°C, 3.6°C and 1.9°C at 1 µM concentration against the same G-quadruplex sequences respectively.

The overall FRET data analysis of this library of molecules suggests the following conclusions-

- Most curved molecules potentially have a greater stabilisation capacity to interact with G-quadruplex sequences. This result resembles the findings as found for the structure activity relationship of **4.93**.
- Electron-withdrawing groups (for example, nitro groups) play a positive role in improving the G-quadruplex-interactive properties of a ligand molecule.

Table 2.62: G-quadruplex and duplex DNA stabilization by ligands in FRET melting experiments at concentrations of 5, 2 and 1 µM respectively (the data are means of three technical repeats)

Compounds	Quadruplex types	ΔT_m(°C) ±(s/d)		
		5 µM	2 µM	1 µM
4.122	F21T	7.3±0.25	3.9±0.15	1.8±0.25
	C-kit-1	8.5±0.20	6.6±0.24	3.9±0.14
	C-kit-2	16.4±0.11	11.8±0.10	8.1±0.23
	BCL-2	13.8±0.31	8.4±0.37	5.1±0.12
	Duplex DNA	0.0±0.1	0.0±0.05	0.0±0.2
4.83	F21T	17.1±0.17	13.3±0.05	10.6±0.15
	C-kit-1	17.4±0.05	13.2±0.21	11.8±0.07
	C-kit-2	23.5±0.11	18.7±0.17	15.8±0.17
	BCL-2	21.1±0.20	16.2±0.23	12.8±0.15
	Duplex DNA	0.0±0.05	0.0±0.07	0.0±0.05
4.121	F21T	10.6±0.20	7.2±0.25	5.1±0.25
	C-kit-1	13.0±0.23	9.5±0.14	7.1±0.33
	C-kit-2	15.0±0.34	11.7±0.18	9.3±0.16
	BCL-2	12.5±0.16	9.4±0.35	6.5±0.37
	Duplex DNA	0.0±0.10	0.0±0.10	0.0±0.46
4.84	F21T	8.7±0.20	4.8±0.10	2.6±0.18
	C-kit-1	13.0±0.32	9.0±0.15	6.6±0.15
	C-kit-2	15.3±0.23	9.7±0.34	7.9±0.27
	BCL-2	12.6±0.14	6.9±0.16	2.9±0.26
	Duplex DNA	0.0±0.11	0.0±0.10	0.0±0.05
4.69	F21T	3.0±0.05	1.7±0.11	1.0±0.2
	C-kit-1	4.8±0.14	2.9±0.17	0.7±0.15
	C-kit-2	7.7±0.20	5.1±0.41	3.6±0.45
	BCL-2	6.5±0.16	3.6±0.18	1.9±0.13
	Duplex DNA	0.0±0.05	0.0±0.05	0.0±0.20

As the indole derivatives did before, the above table illustrates the strong correlation between the interactive ability of ligands and both their shape and the presence electron-withdrawing groups in their structures.

4.122, a 5'-3' and 5'-2' substituted benzofused polyamide formed of 5-nitro indazole-3-carboxylic acid and 5-nitro indazole-2-carboxylic acid, showed G-quadruplex sequence interacting capabilities of 1.8 °C, 3.9 °C, 8.1 °C and 5.1 °C at 1 µM concentration against F21T, C-kit-1, C-kit-2 and Bcl-2 G-quadruplex sequences, respectively, whereas the most curved molecule **4.83**, a 5'-3' and 5'-3' substituted benzofused polyamide of two consecutive indazole-3-carboxylic acids, showed G-quadruplex sequence stabilisation of 10.6°C, 11.8°C, 15.8°C and 12.8°C at 1 µM concentration against the same G-

quadruplex sequences. The significant difference in the melting temperatures of each suggests again that the most curved ligands have better shapes with which to fit into G-quadruplex sequences.

Now it is necessary to investigate the effect of the nitro group of the ligand molecules. Therefore, **4.121** was made by following the shape of **4.83**, but capped with indazole-3-carboxylic acid instead of 5-nitro-indole-3-carboxylic acid. Melting temperatures against the different G-quadruplex types suddenly decreased as it provided stabilisation of 5.1°C, 7.1°C, 9.3°C and 6.5°C at 1 µM concentration against F21T, C-kit-1, C-kit-2 and Bcl-2 G-quadruplex sequences, respectively. This means the nitro group must play a positive role in increasing the stabilising capacity of these ligands.

Making of a molecule in the form of **4.83** with an electron-donating amino group rather than an electron-withdrawing nitro group helped to investigate the effect of the nitro group.

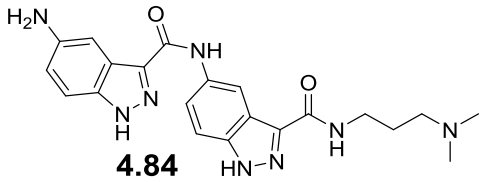

4.84

Figure 2.83: Structure of **4.84**.

Here, it was evident that the reduced form of the nitro group clearly reduced the stabilisation capacity of **4.83** as the melting temperatures decreased. However, it is easier to visualise the effect of the nitro group by directly comparing the stabilisation capacities of both **4.83** and **4.84** in one table.

Table 2.63: Comparative FRET data analysis between the equivalent molecules **4.83** and **4.84** (the data are means of three technical repeats)

Quadruplex types	ΔT_m(°C) ±(s/d)					
	4.84	**4.83**	**4.84**	**4.83**	**4.84**	**4.83**
	5 µM	5 µM	2 µM	2 µM	1 µM	1 µM
F21T	8.7±0.20	17.1±0.17	4.8±0.10	13.3±0.05	2.6±0.18	10.6±0.15
C-kit-1	13.0±0.32	17.4±0.05	9.0±0.15	13.2±0.21	6.6±0.15	11.8±0.07
C-kit-2	15.3±0.23	23.5±0.11	9.7±0.34	18.7±0.17	7.9±0.27	15.8±0.17
BCL-2	12.6±0.14	21.1±0.20	6.9±0.16	16.2±0.23	2.9±0.26	12.8±0.15
Duplex DNA	0.0±0.11	0.0±0.05	0.0±0.10	0.0±0.07	0.0±0.05	0.0±0.05

Here, **4.83**, a 5'-3' and 5'-3' substituted benzofused polyamide of two consecutive 5-nitro indazole-3-carboxylic acids, showed G-quadruplex sequence stabilisation of 10.6°C, 11.8°C, 15.8°C and 12.8°C stabilisation at 1 µM concentration against F21T, C-kit-1, C-kit-2 and Bcl-2 G-quadruplex sequences, respectively, which are far better than those of **4.84**, a 5'-3' substituted benzofused polyamide with the terminal amino group, which showed stabilisation of 2.6°C, 6.6°C, 7.9°C and 2.9°C at 1 µM concentration against the same G-quadruplex sequences.

2.16.3 Comparative Study between Benzofused Polyamides of Two and Three Consecutive 5-Nitro-indazole-3-carboxylic acids respectively

The pair of equivalent molecules **4.68** and **4.93** are directly comparable to each other.

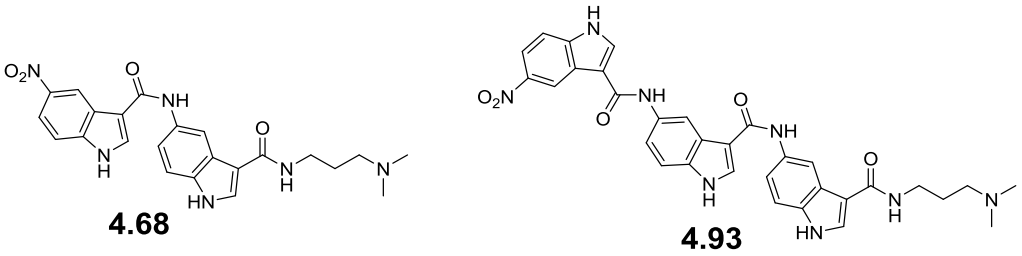

Figure 2.84: Structures of **4.68** and **4.93**.

Table 2.64: Comparative G-quadruplex and duplex DNA stabilization between ligands **4.68** and **4.93** in FRET melting experiments at concentrations of 5, 2 and 1 µM respectively (the data are means of three technical repeats)

Quadruplex types	ΔT_m(°C) ±(s/d)					
	4.68	**4.93**	**4.68**	**4.93**	**4.68**	**4.93**
	5 µM	5 µM	2 µM	2 µM	1 µM	1 µM
F21T	10.0±0.13	21.0±0.17	6.5±0.35	15.9±0.28	3.9±0.18	12.6±0.26
C-kit-1	13.3±0.38	27.7±0.30	10.2±0.42	22.1±0.35	7.3±0.45	17.6±0.28
C-kit-2	15.7±0.11	21.3±0.23	12.2±0.17	14.8±0.20	9.1±0.41	11.4±0.32
BCL-2	12.8±0.15	25.4±0.30	8.8±0.20	17.8±0.14	5.9±0.12	13.5±0.20
Duplex DNA	0.0±0.23	0.0±0.05	0.0±0.18	0.0±0.05	0.0±0.28	0.0±0.05

Here, the most potent tri- and bi-aryl benzofused polyamides were taken to compare their melting temperatures against the G-quadruplex sequences used. It is evident that **4.93** (which provided ΔTms of 12.6°C, 17.6°C, 11.4°C and

13.5°C stabilisation at 1 µM concentration against F21T, C-kit-1, C-kit-2 and Bcl-2 G-quadruplex sequences, respectively) showed a significantly higher degree of stabilisation than **4.68** (which showed 3.9°C, 7.3 °C, 9.1°C and 5.9°C stabilisation at 1 µM concentration against the same G-quadruplex sequences).

Another pair of equivalent molecules, **4.83** and **4.119**, are directly comparable to each other.

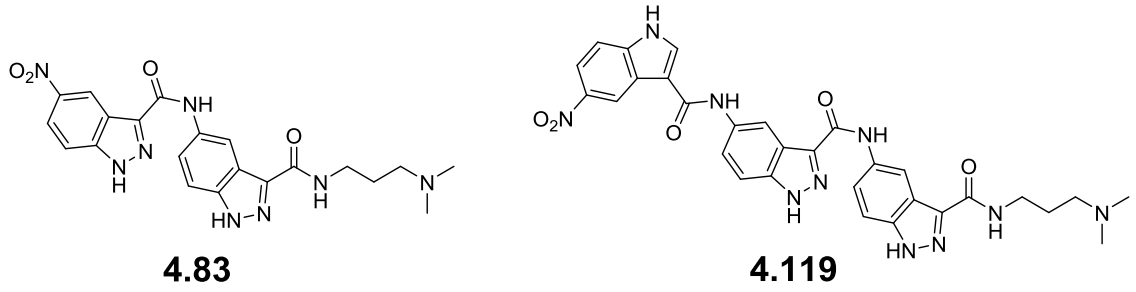

4.83 **4.119**

Figure 2.85: Structures of **4.83** and **4.119**.

Table 2.65: Comparative G-quadruplex and duplex DNA stabilization between ligands **4.83** and **4.119** in FRET melting experiments at concentrations of 5, 2 and 1 µM respectively (the data are means of three technical repeats)

Quadruplex types	ΔT_m(°C) ±(s/d)					
	4.83	**4.119**	**4.83**	**4.119**	**4.83**	**4.119**
	5 µM	5 µM	2 µM	2 µM	1 µM	1 µM
F21T	17.1±0.17	17.8±0.17	13.3±0.05	14.8±0.26	10.6±0.15	13.0±0.35
C-kit-1	17.4±0.05	18.2±0.13	13.2±0.21	14.2±0.23	11.8±0.07	11.1±0.21
C-kit-2	23.5±0.11	20.4±0.23	18.7±0.17	17.8±0.24	15.8±0.17	16.4±0.32
BCL-2	21.1±0.20	18.1±0.26	16.2±0.23	14.1±0.05	12.8±0.15	10.8±0.13
Duplex DNA	0.0±0.05	0.0±0.1	0.0±0.07	0.0±0.05	0.0±0.05	0.0±0.11

Here, **4.83** (which showed G-quadruplex sequence stabilisation of 10.6°C, 11.8°C, 15.8°C and 12.8°C at 1 µM concentration against F21T, C-kit-1, C-kit-2 and Bcl-2 G-quadruplex sequences, respectively) is nearly equivalent to **4.119** (provided 13.0°C, 11.1°C, 16.4°C and 10.8°C stabilisation at 1 µM concentration against the same G-quadruplex sequences) with regards to their interactions towards the different G-quadruplex sequences. Thus there are opportunities to optimise this benzofused polyamide scaffold through both structural and functional group modifications.

An overall data comparison of these ligands suggests that benzofused polyamides made of three consecutive 5'-3' substituted nitro indole carboxylic acids have a significantly higher ability to interact with and stabilise G-quadruplex sequences than benzofused polyamides of two consecutive nitro indole carboxylic acids. On the other hand, benzofused polyamides made of three consecutive 5'-3' substituted nitro indazole carboxylic acids have almost equivalent abilities to interact with G-quadruplex sequences types to benzofused polyamides of two consecutive nitro indazole carboxylic acids.

2.17 Conclusions Based on the FRET Data Analysis of the Benzofused Polyamides of Libraries 1-5.

Using a distamycin scaffold as a starting point, different types of benzofused building blocks were introduced in place of pyrroles with the help of a rational molecular modelling approach to improve the affinity of benzofused polyamides for G-quadruplexes while further reducing their affinity for duplex DNA in order to enhance their selectivity for quadruplex versus duplex DNA.

A series of benzofused polyamides (18 molecules in total) (**Library-1A** and **Library-1B**) were initially synthesized through the 5′-2′ substitution of amide coupling reactions using different nitro-benzofused-carboxylic acids as building blocks and they were subsequently evaluated by FRET-based DNA thermal denaturation assays. However, these compounds failed to stabilize the G-quadruplexes as much as expected. Though the molecules of **library-1A** and **1B** did not show significant interaction capacities toward G-quadruplex DNA types, the detailed FRET data analysis (i.e. ΔTm values) of individual molecules provided some of the following preliminary ideas which in turn helped to design a new set of molecules.

- Molecules including **4.15**, **4.6** and **4.37** were found to show significant interaction at higher concentrations (5 μM) but they suddenly lost their stabilisation capacities at subsequent lower concentrations. These unexpected higher melting temperatures (for example, **4.37** provided 18.1°C for F21T) were assumed to be contributed to by cooperative

binding of this molecule at high concentrations (5 µM). A dimer of **4.37** may stack together over the terminal quartet of G-quadruplexes. As soon as molecular density decreases at the subsequent lower concentrations (i.e. 2 and 1 µM), the melting temperatures fall sharply (ΔTm=1.8 °C and 1.1 °C, respectively). This means the molecular density of this molecule is not sufficient to make a dimer at low concentrations of **4.37 (Tables 2.3, 2.4** and **2.7)**.

- **4.44** was slightly more interactive than any other molecules, as it provided stabilisation of 2.3°C, 1.5°C, 2.2°C and 2.9°C at 1 µM concentration against F21T, C-kit-1, C-kit-2 and Bcl-2 G-quadruplex sequences, respectively **(Table 2.8)**. Thus it was assumed that the inclusion of nitrogen-containing building blocks (i.e. imidazole) may allow the possibility of hydrogen bond formation with guanine residues of the quadruplex and thereby enhance the ligand capacity to interact with the G-quadruplex structure to a certain extent.

- Two structurally equivalent molecules (**4.42** and **4.43**) were synthesized to investigate whether an electron-withdrawing (Cl^-) or donating group ($-CH_3$) on the 3rd building block could have any impact on their interacting capacities towards G-quadruplexes. Though the melting temperatures of these two molecules were not impressive, the minor differences between the ΔTm values of these two molecules suggested that an electron-withdrawing functional group may have a enhancing impact on their G-quadruplex-interacting capacities; **4.43** showed stabilisation of 1.0°C, 0.7°C, 1.4°C and 1.4°C at 1 µM concentration against F21T, C-kit-1, C-kit-2 and Bcl-2 G-quadruplex sequences, respectively, which was insignificantly better than that of **4.42** (provided ΔTm values of 0.4°C, 0.3°C, 0.9°C and 0.3°C at 1 µM concentration against F21T, C-kit-1, C-kit-2 and Bcl-2 G-quadruplex sequences, respectively) (**Table 2.8**).

The benzofused polyamides of **library-1A** and **library-1B** were assumed to have more π-π interactions with terminal G-quartets than previously reported biaryl polyamides[117, 203] but this was not reflected in the FRET-based DNA melting assay. Therefore molecular modelling studies were done on **library-1A**

and **1B** molecules to rationalise their poor FRET-based meting temperatures (ΔTm) with the aim of designing a chemical scaffold for a series of **library-2** benzofused polyamides. Molecular docking experiments were undertaken on the human telomeric quadruplex F21T (PDB ID 3CDM) (**Section 2.5**).

Molecular modelling of the G-quadruplex-interactive biaryl benzofused polyamide helps assess the curvature of molecules (left panel of **Figure 2.21)**, which assists in the stabilisation of DNA by covering the terminal quartet. **Library-1** molecules (e.g., **4.5**) do not possess the requisite curvature, and therefore cannot cover the central core of the G-quadruplex DNA to stabilise quadruplex DNA **(Figure 2.21)**. They are linear in structure. For example, molecular models of **4.5** (containing benzothiophene and benzofuran building blocks) showed that the molecule does not stack effectively on the quadruplex interface, thereby producing few non-covalent interactions **(Figure 2.21).** These studies recommended that the 5'-2' substituted central benzofused moiety be replaced with a 5′-3' substituted benzofused moiety to introduce curvature within the benzofused polyamide molecules **(Figure 2.22).** Therefore a set of new molecules (**library-2**) was synthesized by including 5-nitro-benzofused-3-carboxylic acid as a second building block instead of 5-nitro-benzofused-2-carboxylic acid through 3′-5′ substitution. Commercially available 5-nitro-indole-3-carboxylic acid was introduced in the middle of the polyamides.

FRET data analysis of **library-2** molecules clearly indicated that the introduction of curvature within benzofused polyamides dramatically improves their interacting capacity towards different G-quadruplex DNA used. Equivalent molecules from each of the libraries (i.e. **4.18** of **library-1** can be compared directly with **4.52** of **library-2**) were taken and their FRET data subsequently analysed to evaluate the impact of the introduction of curvature on their stabilization capabilities. **4.18** provided 0.8°C, 1.6°C, 2.4°C and 0.6°C stabilisation; in contrast, the relatively curved **4.52** showed 2.4 °C, 7.8 °C, 8.1°C and 5.6°C stabilisation at 1 μM concentration against F21T, C-kit-1, C-kit-2 and Bcl-2 G-quadruplex sequences respectively (**Table 2.11 and 2.12**).

Molecular modelling of **4.18** (**library-1** molecule) and **4.52** (**library-2** molecule) bound to the telomeric F21T G-quadruplex illustrated the difference in the accommodation of **library 1** molecules (**4.18**) and **library 2** molecules (**4.52**). In

the case of **4.52**, three benzofused molecules are capable of orienting directly over guanine bases, thereby enhancing stabilisation (**Figure 2.27)**.

Preliminary docking studies also suggested that the introduction of further 5'-3'-substituted benzofused moieties to the polyamide core instead of 5'-2'-benzofused moieties should enhance binding further **(Fig. 2.28),** and this was explored in **library 3A**.

Here, a set of new molecules (**library-3A**) were synthesized by introducing 5-nitro-indole-3-carboxylic acid in place of 5-nitro-benzofused-2-carboxylic acid either at the first or third building block positions of the **library-2** molecules. Thus the final benzofused polyamides had more curvature compared to those of **library-2**.

In general, the introduction of a second 5'-3'-benzofused moiety enhanced G-quadruplex stabilisation. This is likely to have occured due to an enhanced shape-fit of the molecule within G-quadruplex DNA. FRET data analysis of the benzofused polyamides of **library-2** and **library-3A** showed a clear difference in melting temperatures (ΔT_m) between the two. The introduction of second 5'-3'-benzofused moiety moderately improves the interacting capacity of polyamides. This can be explained through the comparison of ΔTm values of two equivalent molecules - for example, **4.70** from **library-3A** and **4.52** from **library-2**. **4.70** showed comparatively more stabilising capacity than **4.52**; the latter provided 2.4°C, 7.8°C, 8.1°C and 5.6°C stabilisation whilst the former provided 4.9°C, 9.2°C, 8.6°C and 7.4°C stabilisation at 1 µM concentration against F21T, C-kit-1, C-kit-2 and Bcl-2 G-quadruplex sequences, respectively (**Tables 2.12, 2.17**). This suggested that the introduction of additional curvature makes the ligand more potent. In addition, **4.52** and **4.70** both follow a nearly identical pattern of stabilisation towards the different G-quadruplex sequences used. However, molecular modelling of **library-3A** molecules suggested that the introduction of 5′-3′ substitution in the second of three consecutive building blocks (i.e. (5′-2′)-(5′-3′)-(5′-2′)) is more critical for the enhanced G-quadruplex stabilisation compared to the introduction of two 3′-5′ substitutions (i.e. (5′-3′)-(5′-3′)-(5′-2′) or (5′-2′)-(5′-3′)-(5′-3′)) as seen in **library-2** and **library-3**, respectively. Docking studies of the **library-3A** benzofused polyamides (such as **4.70**) also suggested that the two 3′-5′ substituted benzofused moieties are

capable of interacting with the G-quadruplex, but appear to stack directly over the G tetrad (**Section 2.9**, **Figure 2.35**). The amidic tail of the molecule also appears to interact with DNA to some degree, thereby enhancing stabilisation. Therefore the curvature of **library-3A** molecules was taken as a molecular scaffold to investigate the electron-withdrawing nitro group at the 5′ position of the terminal building block, as it was observed from the previous **library-1** molecules (i.e. **4.42**) that an electron-withdrawing functional group may have a positive impact on G-quadruplex interacting capacities. Therefore, a set of molecules (**library-3B**) were made through the modification of **library-3A** molecules by introducing a nitro group at the 5′ position of third building block. The synthesised molecules were capped with four different 5-nitro-3-carboxylic acid benzofused building blocks instead of benzofused building blocks containing a carboxylic acid in the 3' position only (**Figure 2.37)**.

FRET data analysis suggested that the introduction of nitro group enhanced the interactive capacities of ligand molecules. This could be rationalised a number of ways, including by the formation of a hydrogen bond formation between nitro group of the ligand and amino, imine or carbonyl groups of the guanine residues of the G-quartet, by the potentially ability of the nitro group to recruit potassium ions which could help to stack the quartet together, or through possible electronic interactions provided by the addition of the nitro group.

However, it is more convenient to evaluate the effect of nitro group inclusion by comparing between equivalent molecules of **library-3A** and **library-3B**. For example, **4.79** (a molecule of **Library-3B**) evidently showed better interacting capacity compared to the equivalent ligand **4.70** (a molecule of **library-3A**), since **4.70** provided 4.89°C, 9.2°C, 8.6°C, 7.4°C stabilisation and **4.79** provided 6.0°C, 9.2°C, 11.2°C and 7.7°C stabilisation at 1 µM concentration against F21T, C-kit-1, C-kit-2 and Bcl-2 G-quadruplex sequences, respectively. Similarly, the other equivalent molecules, including **4.78**, **4.77** and **4.80** (molecules of **library-3B**), showed nearly the same pattern of interaction compared to their equivalent molecules, **4.71**, **4.72** and **4.73**, respectively. **4.77** showed a significant stabilising capacity for G-quadruplex DNA, providing stabilisation of 12.2 $^{\circ}$C, 14.4 $^{\circ}$C, 14.7 $^{\circ}$C and 12.2 $^{\circ}$C stabilisation at 1 µM concentration against F21T, C-kit-1, C-kit-2 and Bcl-2 G-quadruplex sequences, respectively. It is also notable that **4.77** is a more G-quadruplex interacting

benzofused polyamide than any other structurally equivalent molecules of **library-3B**. Even the molecule **4.80,** which was capped with an additional nitrogen atom-containing benzimidazole, provided relatively low ΔTm values of 6.0°C, 9.2°C, 11.2°C and 7.7°C stabilisation at 1 μM concentration against F21T, C-kit-1, C-kit-2 and Bcl-2 G-quadruplex sequences, respectively (**Tables 2.17, 2.24**). Thus it is evident that indole is preferable as a third building block to enhance the stabilising capacity of ligands relative to the other benzofused building blocks tested.

Therefore **4.77** was rationally considered to be a lead ligand for all of the G-quadruplex sequences used and, accordingly, this specific polyamide was subjected to structural modifications *via* a structure-activity relationship to get a more potent ligand. Four additional molecules, including **4.23**, **4.66**, **4.60**, **4.67** and **4.93**, were synthesized with all possible shape modifications of **4.77** through changing the degree of curvature within their structures. It was observed that the linear molecule **4.23**, made of three consecutive 5-nitro-indole-2-caboxylic acids (through the three consecutive 5′-2′ substitutions (i.e.(5′-2′)-(5′-2′)-(5′-2′)), showed minimum G-quadruplex interactions (i.e. 0.3°C, 0.4 °C, 0.03°C and 0.5°C stabilisation at 1 μM concentration against F21T, C-kit-1, C-kit-2 and Bcl-2 G-quadruplex sequences, respectively) compared to any other molecules which had been selected for SAR. The subsequent molecules with increasing degrees of curvature because of 5′-3′ substitutions were found to be increasingly more interactive towards G-quadruplex DNA. For example, relatively curved molecules **4.66** (i.e. (**5′-3′**)-(5′-2′)-(5′-2′)), **4.60** (i.e.(5′-2′)-(**5′-3′)-(**5′-2′)) and **4.67** (i.e. (5′-2′)-(5′-2′)-(**5′-3′**)), with 5’-3’ substitutions of 5-nitro-benzofused-3-carboxylic acid at different positions of nitro-benzofused polyamides, showed relatively more interacting capacities than the relatively linear **4.23** molecule (**Table 2.30**). However, it is notable that the molecule **4.60**, with a 3′-5′ substitution at the middle, showed the most significant ΔTm values (5.7°C, 11.5°C, 10.9°C and 6.6°C stabilisation at 1 μM concentration against F21T, C-kit-1, C-kit-2 and Bcl-2 G-quadruplex sequences, respectively) among the molecules with a single 3′-5′ substitution as in **4.66** and **4.67** (i.e. at the first or third of three consecutive building blocks). This supported the previous observations (as seen in the comparative analysis of **library-2** and **library-3A** molecules) that the introduction of 5′-3′ substitution in the second of three

consecutive building blocks (i.e. (5′-2′)-(5′-3′)-(5′-2′)) is more critical for enhanced G-quadruplex stabilisation.

Accordingly, a molecule **4.77** (i.e. (5′-3′)-(5′-3′)-(5′-2′)) was found to be more interactive than the less curved **4.60** (i.e. (5′-2′)-(5′-3′)-(5′-2′)). Finally, molecule **4.93** (i.e. (5′-3′)-(5′-3′)-(5′-3′)), with the highest degree of curvature because of three consecutive 5′-3′ substitution of 5-nitro-indole-3-carboxylic acids, was found to show a more significant interaction towards G-quadruplex DNA than that of **4.77**; **4.93** provided 12.6°C, 17.6°C, 11.4°C and 13.5°C stabilisation at 1 µM concentration against F21T, C-kit-1, C-kit-2 and Bcl-2 G-quadruplex sequences, respectively (**Table 2.30**). This is strong evidence for the idea that the greater the degree of curvature, the greater the interactions towards G-quadruplex DNA, and this trend can be simplified as **4.93>4.77>4.60>4.23** (**Figure 2.76**). Finally, this structure-activity relationship (SAR) was then rationalised by the shape-based assessment of **4.93** analogues (**Section 2.11**) (i.e. the molecular modelling studies of benzofused polyamides **4.23** (Figure 2.43), **4.60** (Figure 2.44), **4.77** (Figure 2.45) **and 4.93** (**Figure 2.46**) (**Table 2.31**)).

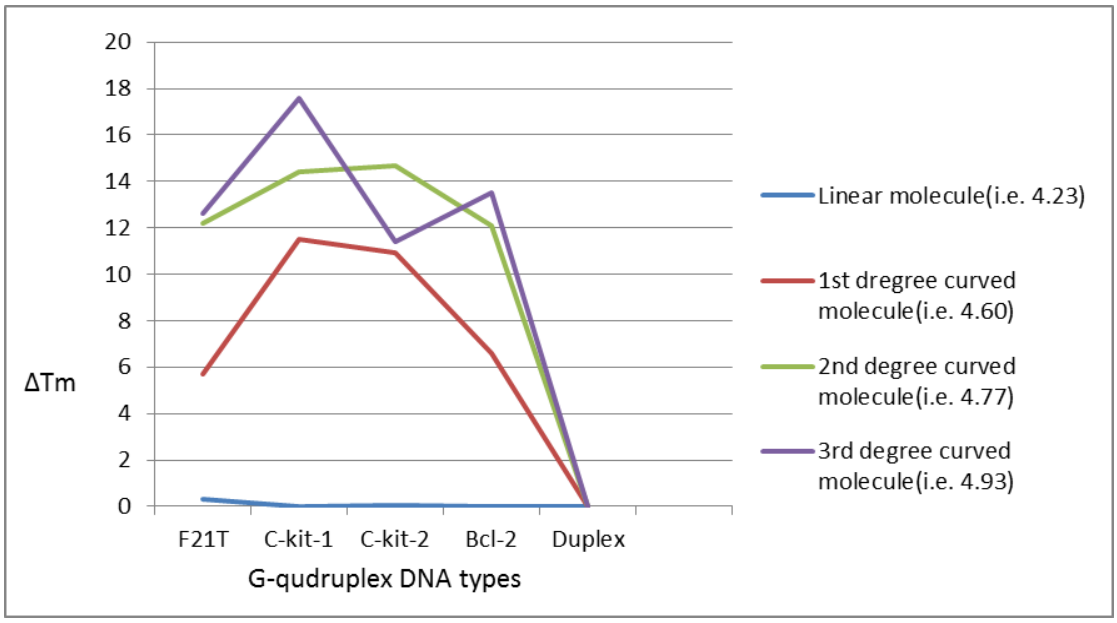

Figure 2.86: Graph of the relationship between degree of curvature and ΔTm values for different G-quadruplex DNA.

A new library of molecules (**library-4A**) containing four different benzofused polyamides was synthesized to investigate the relevance of the electron-

withdrawing NO_2 group to the activity of the most active compound **4.93**. The synthesised molecules were capped with a benzofused building block containing a carboxylic acid in the 3' position only, instead of a 5-nitro-3-carboxylic acid benzofused building block as found in **4.93**, to further assess this factor. At the same time, the equivalent molecules from **library-3A** and **library-4A** were directly compared to investigate the effect of structural curvature within their structures on interactive capacity towards G-quadruplexes. All of these molecules except **4.92** were found to be moderately interactive towards the different G-quadruplex sequence types; **4.92** provided 9.3°C, 15.7°C, 13.4°C and 10.3°C stabilisation at 1 µM concentration against F21T, C-kit-1, C-kit-2 and Bcl-2 G-quadruplex sequences respectively (**Table 2.34**). The significant activity of **4.92** is due to the effect of the additional nitrogen atom of the terminal indazole building block, as discussed previously.

The effect of the nitro group can be evaluated by the direct comparison of molecules **4.91** and **4.93** of **library-4A** and **library-3B,** respectively. The molecule **4.91,** without a nitro group, provided 2.9°C, 8.2°C, 8.9°C and 7.5°C stabilisation, whereas the molecule **4.93** containing nitro group provided 12.6°C, 17.6°C, 11.4°C and 13.5 °C stabilisation at 1 µM concentration against F21T, C-kit-1, C-kit-2 and Bcl-2 G-quadruplex sequences, respectively. Thus it is obvious that **4.93** is more interactive towards G-quadruplex sequences of all types used than **4.91**. Therefore it is strongly evident that the nitro group play an important role in the improvement of ligand interacting capacities (**Table 2.30** and **2.34**).

Direct comparison between equivalent molecules **4.72** and **4.91** of **library-3A** and **library-4A** evaluate the effect of additional curvature due to the introduction of third benzofused (i.e. as **4.91**) building block through the 5′-3′ substitution. **4.91** provided 2.9°C, 8.2°C, 8.9°C and 7.5°C stabilisation while the equivalent **4.72** provided 2.6°C, 6.8°C, 5.8°C and 4.2°C stabilisation at 1 µM concentration against F21T, C-kit-1, C-kit-2 and Bcl-2 G-quadruplex sequences respectively (**Table 2.38**). Thus molecule **4.91** (the more curved of the two) was found to be more G-quadruplex interactive than **4.72** (less curved)**.** This observation suggests that the inclusion of a third 5'-3'-substituted benzofused moiety should enhance G-quadruplex stabilisation to a small degree compared to two 5'-3'-substituted benzofused moieties **(Figure 2.52)**.

Hence the most interactive compound **4.93** was then taken as a new lead for further structure-activity relationship studies. Accordingly, new sets of molecules were synthesized through the modification of the tertiary amine tails (i.e **library-4B**) and functional groups (i.e **library-4C**) attached with the third benzofused building block of **4.93.** A total of 4 molecules (i.e **library-4B**) were synthesized through the replacement of the N1, N1-dimethylpropane-1,3-diamine tertiary amine tail of **4.93.** These molecules included **4.98**, with a tail of 3-(piperidin-1-yl) propan-1-amine, **4.104**, with a tail of 3-(pyrrolidin-1-yl)propan-1-amine, **4.109**, with a tail of 3-morpholinopropan-1-amine, and **4.115**, with a tail of 3-(4-methylpiperazin-1-yl)propan-1-amine.

FRET data analysis showed that these four molecules with different tails did not show the stabilising capacity like **4.93** showed. For example, **4.98** provided 5.9°C, 15.5°C, 11.3°C and 9.6°C stabilisation, whereas **4.93** provided 12.6°C, 17.6°C and 11.4°C stabilisation at 1 µM concentration. This suggested that the N1, N1-dimethylpropane-1, 3-diamine tail was better than any other tails used in improving the interacting capacities of benzofused polyamides.

Library-4C molecules were synthesized (**Figure 2.57**) by the structural modification of **4.93** through the substitution of the nitro group with different functional groups for optimisation of the interacting capacity of lead ligand **4.93**.

Molecules, including **4.99** with a methyl group ($-CH_3$), **4.110** with an amino group ($-NH_2$), **4.116** with a methoxy group ($-O-CH_3$), **4.117** with a chloride group (-Cl) and **4.87** with cyanide group (-CN), did show moderate interactions but not as significant as for **4.93.** For example, **4.110** provided 2.1°C, 5.2°C, 6.1°C and 5.8°C stabilisation, whereas **4.93** provided 12.6°C, 17.6°C and 11.4°C stabilisation at 1 µM concentration (**Table 2.45**). This suggests that the electron pulling nitro group is essential for improving the interacting capacity of benzofused polyamides.

At the same time, the comparative FRET data analysis among the different benzofused polyamides in this group suggested that electron-withdrawing groups, like the chloride group (-Cl) for **4.117** and cyanide group (-CN) for **4.87**, appeared to enhance interacting capacity whereas electron-donating groups like methyl groups ($-CH_3$) for **4.99,** methoxy groups ($-O-CH_3$) for **4.116** and amino groups ($-NH_2$) for **4.110**, appeared to reduce the interacting capacity of

benzofused polyamides (**Tables 2.45 and 2.46**). Moreover, it is interesting that the comparatively more electron-withdrawing cyanide group-containing **4.87** provided more stabilisation than the relatively less electron-withdrawing chloride group-containing **4.117 (Figure 2.58)**. Similarly, electron-donating group-containing ligands, like **4.99** and **4.116**, follow an equivalent degree of reduction in interacting capacity according to the strength of their electron-donating group (**Figure 2.58)**.

Since **4.92** of **library-4A** showed more significant interaction (i.e 9.3°C, 15.7°C, 13.4°C and 10.3°C stabilisation at 1 µM concentration against F21T, C-kit-1, C-kit-2 and Bcl-2 G-quadruplex sequences, respectively) (**Table 2.34**). compared to the other library members (i.e. molecules which have been capped with indole, such as **4.91**, benzofuran, such as **4.90**, and benzothiophine-3 carboxylic acids, such as **4.89**, respectively), it is necessary to verify the effect of indazole over indole in improving the interacting capacity of benzofused polyamides of three consecutive nitro-benzofused-acids. Therefore, a set of 5 molecules (**Library-4D**) (**Figure 2.61**) were synthesized through the replacement of indole with indazole rings by following the structures of **4.77** and **4.93** to verify the preference of either indole or indazole in providing interacting capacity of ligand towards G-quadruplex DNA. Benzofused polyamidse of three consecutive indazole units were supposed to provide a significant interaction but the FRET data analysis on the equivalent molecules **4.85** (i.e. molecule of three consecutive indazole units) and **4.93** (i.e. a molecule of three consecutive indole units) showed that **4.85** is less G-quadruplex interactive than **4.93**. **4.85** provided 1.4°C, 4.4°C, 8.2°C and 4.7°C stabilisation at 1 µM concentration against F21T, C-kit-1, C-kit-2 and Bcl-2 G-quadruplex sequences, respectively (**Table 2.50**). On the other hand, the molecule **4.86** (equivalent to **4.77**) provided much better interaction (i.e. 8.0°C, 9.9°C, 13.1°C and 8.5°C of stabilisation at 1 µM concentration against F21T, C-kit-1, C-kit-2 and Bcl-2 G-quadruplex sequences respectively) than **4.85** (**Table 2.49**).

This difference in melting temparature is possibly due to the formation of intramolecular hydrogen bonds between proximal amine and imine groups of the indazole at the middle and terminal positions of **4.85**. In contrast, in **4.86** the terminal building block is 5'-2' substituted rather than 5'-3' substitution as in **4.85**. This makes the amine and imine group of **4.86** too far away from each

other, so that these groups can only form hydrogen bonds with the guanine residues of G-quadruplex sequences rather making an intramolecular haydrogen bond as in **4.85.** Thus three other molecules including **4.119** (i.e. equivalent to the shape of 4.93 and capped with nitro indole), **4.118** (i.e. equivalent to the shape of **4.93** but with a second building block of indole and capped with nitro indole) and **4.88** (i.e. equivalent to the shape of **4.77** and capped with nitro indole) were synthesized.

The comparative FRET data analysis on **4.119, 4.118** and **4.93** showed that these molecules were significantly interactive towards G-quadruplex DNA types. As **4.119**, **4.118** and **4.93** provided 13.0°C, 11.1°C 16.4°C and 10.8°C stabilisation, 10.2°C, 10.7°C, 13.9°C and 12.2°C stabilisation and 12.6°C, 17.6°C, 11.4°C and 13.5 °C at 1 µM concentration against F21T, C-kit-1, C-kit-2 and Bcl-2 G-quadruplex sequences respectively (**Table 2.52**, **2.55** and **2.59**). This result suggests that replacement of the indazole unit with an indole unit in the middle and terminal positions of **4.118** and **4.119** makes the amine and imine groups far enough away from each other that these groups cannot participate in the formation of intramolecular hydrogen bonds. The overall data analysis of this library suggests that indole is a better building block for benzofused polyamides of three consecutive units than indazole. But it is also important to remember that indazole could be a better building block to make these compounds if these building blocks can be separated by an indole unit in such a way that they cannot form intramolecular hydrogen bonds.

Lastly, two sets of molecules (9 compounds in total) (**library-5)** with varying degrees of structural curvature were synthesized using commercially available 5-nitro-indole-3-carboxylic acid and 5-nitro-indazole-3-carboxylic acid building blocks by following the structural motif of lead molecule **4.93 (Figure 2.70)**. These molecules were synthesized with the aim of checking whether benzofused polyamides of three consecutive building blocks are better interactive ligands than benzofused polyamides of two consecutive building blocks. At the same time, the effect of electron-withdrawing and donating groups was also verified. FRET data analysis of **4.68** (molecule of two indole units with a nitro group at 5′ position of the second building block unit) and **4.122** (molecule of two indole units without a nitro group at 5′ position of the second building block unit) clearly showed an extra effect of the nitro group, as

4.68 provided 3.9°C, 7.3°C, 9.1°C and 5.9°C stabilisation, compared to 0.4°C, 1.6°C, 3.7°C and 1.3°C stabilisation from **4.122** (1 μM concentration against F21T, C-kit-1, C-kit-2 and Bcl-2 G-quadruplex sequences, respectively). This extra nitro group effect was further verified through observing exactly the same tendency in **4.83** (molecule of two indazole units with a nitro group at 5′ position of the second building block unit) versus **4.121** (molecule of two indazole units without a nitro group at 5′ position of the second building block unit) **(Table 2.59** and **2.62)**.

The ΔTm values of **4.21** (i.e. a molecule of (5′-2′)-(5′-2′) substitution), **4.64** (i.e. a molecule of (5′-3′)-(5′-2′) substitution) and **4.68** (i.e. a molecule of (5′-3′)-(5′-3′) substitution) showed that the linear-shaped **4.21** is less interactive than the relatively curved **4.64**. Furthermore, the most curved molecule **4.68** was found to show the most significant interaction. This suggests that interacting activity increases with the degree of curvature in ligand molecules. The molecules of equivalent curvature **4.122** (i.e. a molecule of (5′-3′)-(5′-2′) substitution) and **4.83** (i.e. a molecule of (5′-3′)-(5′-3′) substitution) also showed the same trend of interacting capacities as found for the benzofused polyamides of two consecutive indole units (**Table 2.62**). However, it is notable that **4.83** provided more significant stabilisation (i.e. 10.6°C, 11.8°C, 15.8°C and 12.8°C stabilisation at 1 μM concentration against F21T, C-kit-1, C-kit-2 and Bcl-2 G-quadruplex sequences, respectively) than **4.68.** This means that a third indazole unit, as in **4.85**, might be responsible for forming intramolecular hydrogen bonds and thereby reducing the stabilising capacity of ligand molecules.

The reduction of electron-withdrawing nitro groups to the electron-donating amino groups sharply decreased the interacting capacity of ligand molecules (**Tables 2.61** and **2.63**). These molecules, including **4.69** (reduced form of **4.68**) and **4.84** (reduced form of **4.83**) showed far less significant ΔTm values than their nitro group-containing parent molecules. Therefore, the data obtained from the **library-5** molecules were found to be totally supportive to the observations made from the previous libraries.

Conclusive remarks on overall FRET data analysis of all of the libraries-

- Benzofused polyamides (i.e. **library-1A** and **library-1B**) of three consecutive 5-nitro-indole-2-caboxylic acids, synthesised through three consecutive 5′-2′ substitutions (i.e. (5′-2′)-(5′-2′)-(5′-2′)), showed minimum G-quadruplex interactions against F21T, C-kit-1, C-kit-2 and Bcl-2 G-quadruplex sequences, respectively. These molecules (for example, **4.5**) do not cover the central core of the quadruplex interface and therefore cannot stack effectively upon it. Thus they produce few non-covalent interactions.

- It is evident from biophysical and molecular modelling studies that the introduction of a 5'-3' substituted moiety (i.e. **library-2** molecules of (5′-2′)-(5′-3′)-(5′-2′) substitutions) instead of a 5'-2'-substituted moiety, as in **library-2**, had a significant effect on the binding of benzofused polyamide molecules to quadruplex DNA. This introduction of a 5'-3' substituted benzofused molecule (for example, **4.52)** in the middle of the benzofused polyamides dramatically improved their interacting capacity towards G-quadruplex DNA.

- The inclusion of either a first or third 5'-3'-substituted benzofused moiety enhanced G-quadruplex stabilisation to a small degree compared to inclusion of a second substituted benzofused molecule.

- Introduction of 5-nitro-indole-3-carboxylic acid in place of 5-nitro-benzofused-2-carboxylic acid either at the first or third building block of the **library-2** molecules enhanced stabilisation of each quadruplex structure to a small degree. This likely occurs due to an enhanced shape-fit of the molecule within G-quadruplex DNA. However, the introduction of 5′-3′ substitution in the second of the three consecutive building blocks (i.e. (5′-2′)-(5′-3′)-(5′-2′)) is more critical to enhanced G-quadruplex stabilisation compared to the introduction of two 3′-5′ substitutions (i.e. (5′-3′)-(5′-3′)-(5′-2′) or (5′-2′)-(5′-3′)-(5′-3′)) as seen in **library-2** and **library-3,** respectively.

- The introduction of electron-withdrawing groups, especially nitro groups, at the 5’ position of the third benzofused building block significantly enhanced the interacting capacity of ligands. On the other hand, electron-donating groups, especially amino groups, significantly reduced the interacting capacity of ligands.

- Benzofused polyamides (for example **4.93**) with the highest degree of curvature (i.e. (5′-3′)-(5′-3′)-(5′-3′)) because of three consecutive 5′-3′ substitution of 5-nitro-indole-3-carboxylic acids (i.e. (5′-3′)-(5′-3′)-(5′-3′)) were found to show the most significant interaction towards G-quadruplex DNA.

- Benzofused polyamides of three consecutive building blocks (i.e. **4.93**) (i.e. (5′-3′)-(5′-3′)-(5′-3′)) were found to be more significantly interactive ligands than the benzofused polyamides (i.e. **4.68**) (i.e. (5′-3′)-(5′-3′)) of two consecutive building blocks.

- Indole was found to be the preferable building block for relatively significant interactive capacity of benzofused polyamide of three benzofused carboxylic acids.

- Indazole is a preferable building block for relatively significant interactive capacity of benzofused polyamides of two benzofused carboxylic acids.

- Indazole might be the preferable building block for benzofused polyamides of three units when they are substituted as first and second building blocks.

- The tertiary amine tail N1, N1-dimethylpropane-1,3-diamine was found to be better than any other tails at improving the interacting capacities of benzofused polyamides.

2.18 Cytotoxicity Test using the MTT Assay

The MTT assay was used to evaluate the cell-killing ability of the synthesised molecules. The IC_{50} (the concentration of compound at which 50% of cells die) of selected molecules was calculated over 96 hour incubation.

The newly synthesized compounds were evaluated in two human cancer cell lines, namely **MDA-MB-231**(triple negative breast cancer cell line) and **HeLa** (cervical cancer cell line).

In total, seventy compounds were evaluated for their cytotoxic efficacy in the **MDA-MB-231** cancer cell line through a preliminary MTT assay screen at a concentration of 25 µM. The nine molecules with the lowest IC_{50} were then selected for further cytotoxic studies in **HeLa** cell line. An upper limit of 50µM was set in the preliminary screen and compounds with IC_{50} values of 50 µM or more were considered to be poor leads for further analysis.

2.18.1 MTT Assay Results with the MDA-MB-231 Cell Line (Breast Cancer Cell Line) and HeLa cell Line.

According to the IC_{50} values described in **Tables 2.66** and **2.67,** the selected compounds (9 in total) from different libraries had the most significant cytotoxicity in the MDA-MB-231 cell line compared to the other molecules synthesized in different libraries. The compounds including **4.37**, **4.41**, **4.45**, **4.40**, **4.11**, **4.18** and **4.71** were found to show a significant cytotoxicity in significant cytotoxicity in the MDA-MB-231 cell line. On the other hand, four compounds including **4.45**, **4.40**, **4.11** and **4.18** were found to show a significant cytotoxicity in the HeLa cell line at different concentrations.

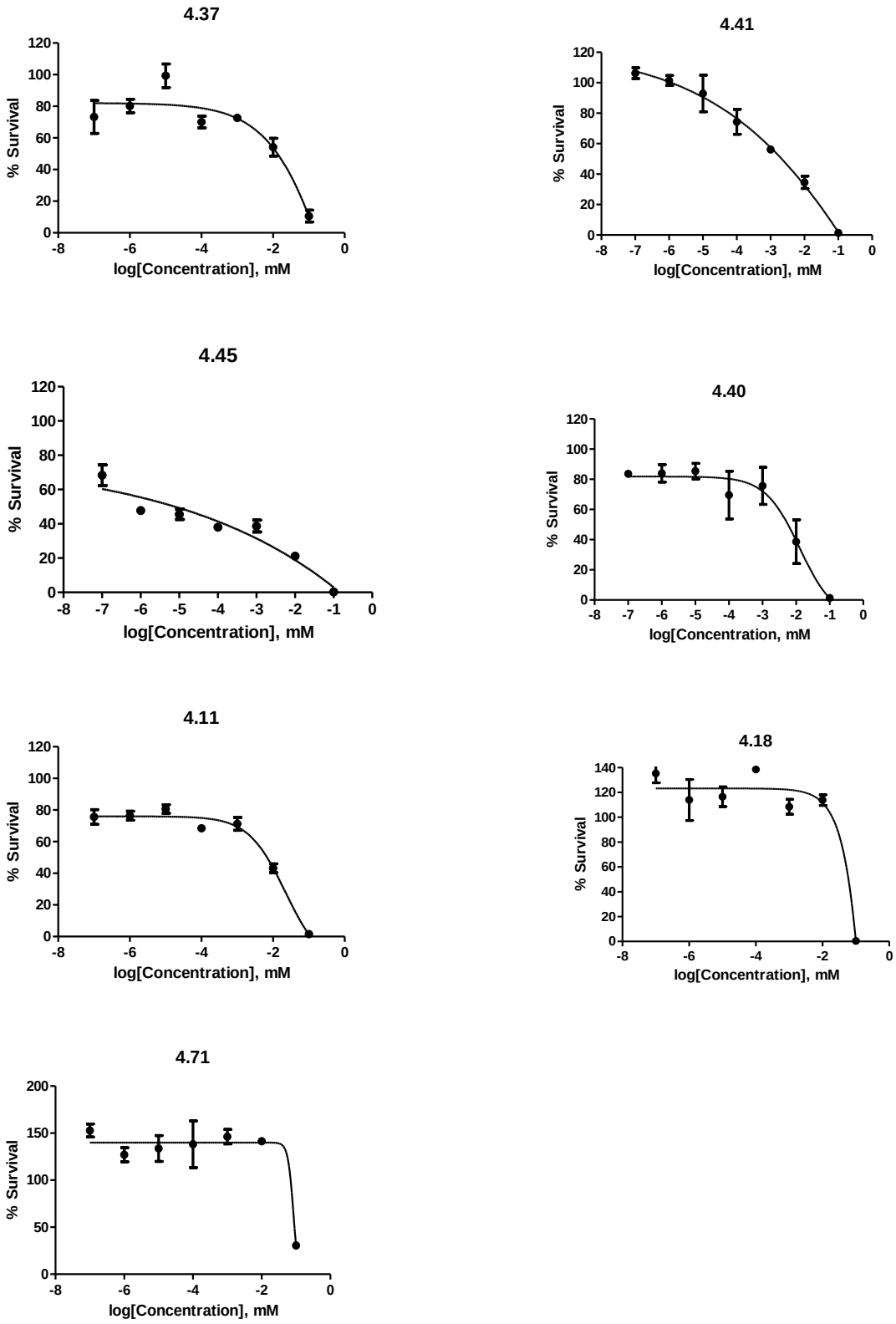

Figure 2.87: Dose Response Curves indicating the survival percentages of MDA-MB-231 cells at various concentrations of compounds **4.37**, **4.41**, **4.45**, **4.40**, **4.11**, **4.18** and **4.71** respectively.

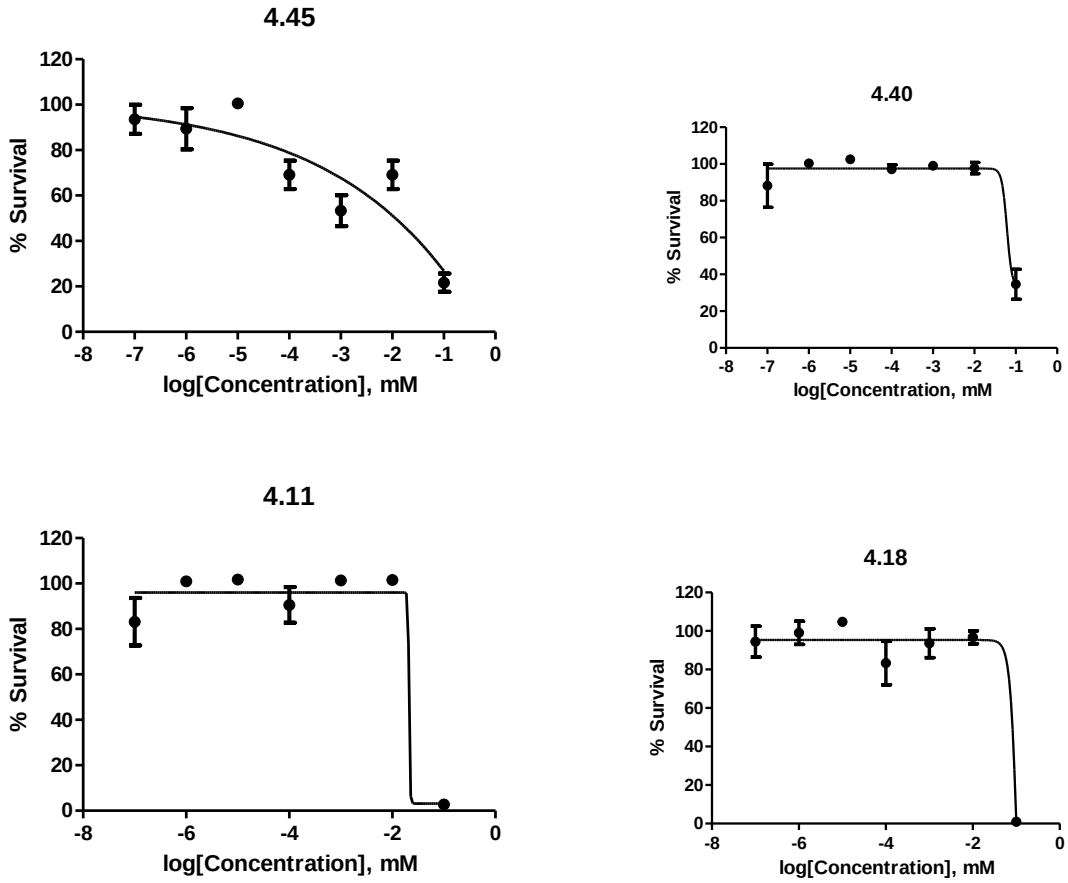

Figure 2.88: Dose Response Curves indicating the survival percentages of Hela cells at various concentrations of compounds **4.45**, **4.40**, **4.11** and **4.18** respectively.

Table 2.66: Cytotoxic effect of compounds with their IC_{50} concentrations in the MDA-MB-231 cell line (the data presented here are means of three technical repeats)

Library	Compound code	IC_{50} values (µM)± (s/d) Mean(n=3)	Standard Deviations
Library-1	4.37	58	11.01514
	4.41	9.12	2.940204
	4.45	0.040	1.980034
	4.40	12.75	3.085585
	4.11	21.82	6.838431
	4.18	86.75	10.87524
Library-3A	4.71	86.75	9.381942

Table 2.67: Cytotoxic effect of compounds with their IC_{50} concentrations in the HeLa cell line (the data presented here are means of three technical repeats)

Library	Compound code	IC_{50} values (μM)± (s/d) Mean(n=3)	Standard Deviations
Library-1	4.45	9.12	2.989671
	4.40	61.29	8.443619
	4.11	21.17	3.423395
	4.18	120	16.44182

It is noteworthy that **Library-2**, **3** and **4** molecules, all showed interactivity with G-quadruplex through biophysical studies (i.e. FRET based DNA melting assay). However, the FRET results did not correlate with cytotoxicities. A number of the least interactive molecules with the G-quadruplex exhibited the most potent cytotoxicities. For example, compound **4.45** possesses a cytotoxicity of 40nM, but biophysical studies suggest insignificant binding to the G-quadruplex (*i.e.,* ΔT_m values of 0.6°C, 1.3°C, 2.7°C and 1.5°C at 1 μM concentration against F21T, C-kit-1, C-kit-2 and Bcl-2 G-quadruplex sequences, respectively). This suggests a potential alternative mechanism of action to G-quadruplex stabilisation.

Compound **4.71,** on the other hand, was shown to be a potent quadruplex binding agent, with ΔTm values of 7.2°C, 15.1°C, 8.3°C and 5.9°C at 1 μM concentration against F21T, C-kit-1, C-kit-2 and Bcl-2 G-quadruplex sequences observed in FRET binding studies. However, this molecule showed insignificant cytotoxicity towards MDA-MB 231 (*i.e.,* IC_{50} values of 86.75 μM against MDA-MB 321 cell line).

In general, it is evident that increasing molecule curvature and enhancing G-quadruplex stabilisation does not result in enhanced cytotoxicity in the case of triaryl benzofused polyamides.

2.19 Conclusion Based on the MTT Assay Results for the Benzofused Polyamides (Libraries 1-5).

It is evident from the results of the cytotoxicity assay that there is a little correlation between the biophysical studies and the MTT assay results.

The most cytotoxic molecules have a similar 3-dimensional shape (i.e., three 5'/2'-substituted benzofused polyamide building blocks), suggesting that this particular shape may be associated with the cytotoxic effect. A similar cytotoxic effect is not observed for members of the other libraries which have different 3-dimensional shapes. For example, most of the cytotoxic molecules (i.e., **4.41**, **4.45** and **4.40**), possess a 3-(pyrrolidin-1-yl) propan-1-amine fragment as an amidic tail, suggesting that this component may play a role in the cytotoxicity of these molecules.

A degree of selectivity of the lead cytotoxic molecules between the MDA-MB-231 and HeLa cell lines is evident. For example, the lead cytotoxic molecule **4.45** has IC_{50} values of 0.040 µM and 9.12 µM for the MDA-MB-231 and HeLa cell lines, respectively.

It should be noted that the dose response curves obtained for the HeLa cell line were not optimal, and so accurate IC_{50}'s could not be obtained from these curves. Further cytotoxicity studies to improve the reliability of these results could not be carried out due to time constraints and technical issues relating to the cell culture facility in Britannnia House, so further studies will be undertaken in the future.

2.20 Future Work

Although a number of potent G-quadruplex stabilising agents have been generated during this study, a distinct lack of correlation between cytotoxicity and biophysical studies was observed. Therefore, in terms of a screening strategy, these results suggest that it is better to synthesize and test for cytotoxicity rather than undertake biophysical evaluation to aid selection of molecules for cytotoxicity testing. As such, in the case of the triaryl benzofused polyamides, a focused library should be generated around molecule **4.45** and a mechanism of action should be established. It is also necessary to modify the lead molecule structurally with the optimisation of amidic tail, functional group, benzofused building block types, solubility and other pharmacokinetic parameters. Different techniques such as gene expression studies, bio-physical studies (including circular dichroism or RT-PCR) may be undertaken in the future to understand how the molecule induces cell-killing. Once the mechanism of action is established, a suitable lead candidate should be selected for progression to human tumour xenograft mouse model study in an appropriate human cancer type.

It will also be necessary to study the mechanism of action of the cytotoxicity of **4.45** and related molecules in the WI 38 cell line (a known cell line of normal human tissue). Once the mechanism of action is established, a suitable lead candidate should be selected for progression to human tumour xenograft mouse model study in an appropriate human cancer type, which will further progress for phase-1 clinical trials.

Finally, a number of potent stabilisers of the G-quadruplex have been generated (*e.g.*, compounds **4.93**, **4.77**), and it may be possible for these molecules to be used as probes for the study of G-quadruplex structure and function.

Chapter 3: Materials and Methods

3.1 Chemical Sources

All the chemicals and reagents used in this project were purchased from commercial companies including Sigma-Aldrich, Fluorochem, Maybridge, Acros, Alfa Aesar, Fluka and Fisher Scientific.

3.2 Analytical Tools

The Liquid Chromatography-Mass Spectroscopy (LC-MS) technique was widely employed to monitor the reaction progression and identification of newly synthesized molecules. LC-MS was performed on a Waters Alliance 2695 with water and acetonitrile as the mobile phases. Formic acid (0.1%) was used with acetonitrile to maintain acidic conditions during the course of chromatographic analysis. The gradient conditions were acetonitrile/water (95%) for 2 minutes which was increased to 50% acetonitrile over 3 minutes. The gradient was then held at 50% acetonitrile for 1 minute and then increased to 95% acetonitrile over 1.5 minutes. The quantity of acetonitrile was then returned to 5% over 1.5 minutes and held for 0.5 minutes. The total duration of each run was 10 minutes. The flow rate was 1.5 mL/minute; 200µL was split *via* a zero dead volume T-piece which passed into the mass spectrometer. The wavelength range of the UV detector was 220-400 nm. A diode array (535 scans) was functionalised with the system. A monolithic (C-18, 50X4.60 mm) column was used in the system.

Proton NMR (^{1}H) and carbon NMR (^{13}C) experiments were carried out on a Bruker Avance 400 MHz spectrophotometer. Chemical shifts ($^{\delta}$H) were cited in ppm (parts per million) and referenced to deuterated dimethyl sulfoxide (DMSO-d_6, residual signal ^{1}Hδ=2.54, ^{13}Cδ=41.45) or deuterated methanol (MeOD, residual signal ^{1}Hδ=3.31, ^{13}Cδ=49.00). Multiplicities in ^{1}H NMR spectra are quoted as s=singlet, d= doublet, t=triplet, m=multiplet, dd= doublet of doublets, ddd (doublet of doublet of doublets, dt=doublet of triplets, td=triplet of doublets, sp=septet and br=broad. The code (0) in ^{13}C NMR spectra denotes the presence of quaternary carbon.

High Resolution Mass Spectrometry (HRMS) was carried out on a Thermo Navigator mass spectrometer coupled with liquid chromatography (LC) using electrospray ionisation (ES) and time-of-flight (TOF) mass spectrometry. Infra - red spectra (IR) were recorded on a Perkin Elmer spectrum 1000 instrument.

Every single reaction was checked by analytical thin layer chromatography (TLC) performed on E. Merck silica gel-60 F_{254} layered plates (0.25 mm). TLC plates were visualised under UV light (254 or 360 nm) and/or by staining the plates with vanillin spray or potassium permanganate solution followed by heating.

3.3 General Synthetic Scheme of Benzofused Polyamides

Initially, 5-amino benzofused-2-carboxylic acid was used to make a coupling reaction with a tertiary amine tail including 3-amino-N-methyl-N-methylenepropan-1-aminium, 2-(piperidin-1-yl) ethan-1amine and 4-(pyrrolidin-1-yl) butan-1-amine.

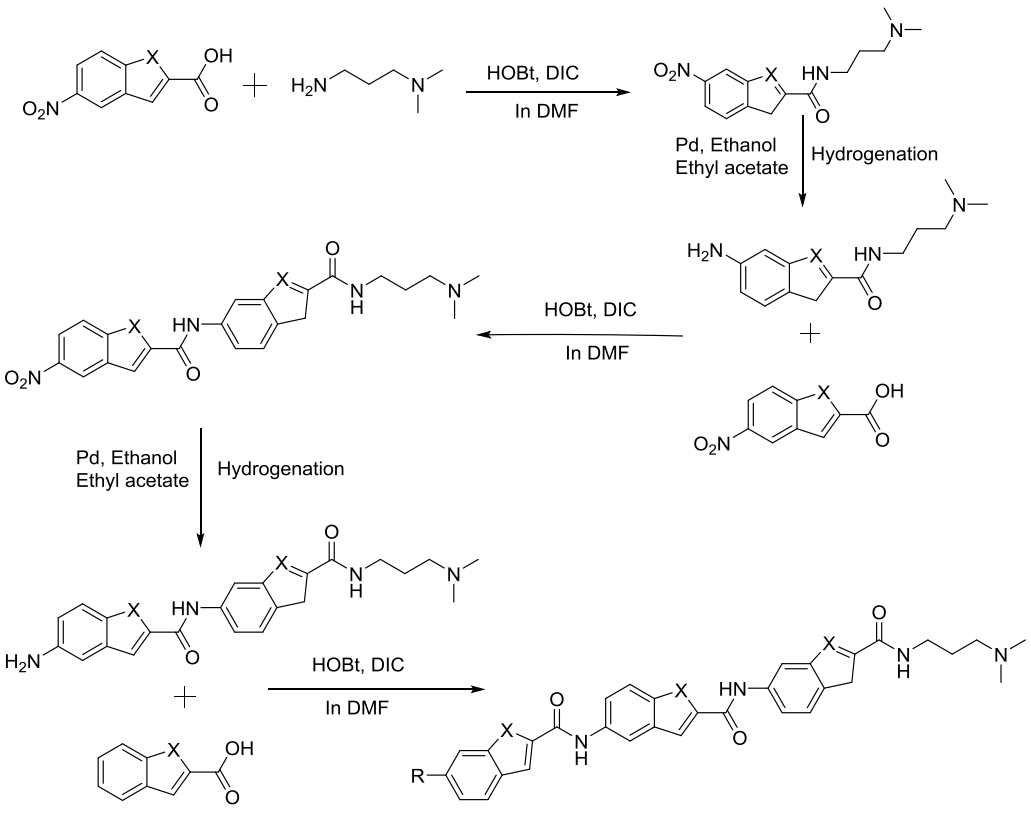

Figure 3.1: General reaction scheme for the ligands synthesized. Here X = O, S or N.

But this reaction did not work properly as the amino-benzofused carboxylic acid could couple with itself to make an aryl adduct. Thus in every reaction,

nitrobenzofused carboxylic acid was used in place of amino benzofused acid. Therefore, the synthesis involved the reduction of the nitro-group to an amino group through hydrogenation after each amide coupling reaction, so that subsequent coupling reactions had a free amino group to react with the next nitro benzofused carboxylic acid. A general reaction scheme using a N1,N1-dimethylpropane-1,3-diamine tail is shown above **(Figure 3.1)**.

3.4 Amide Formation through the Coupling Reaction

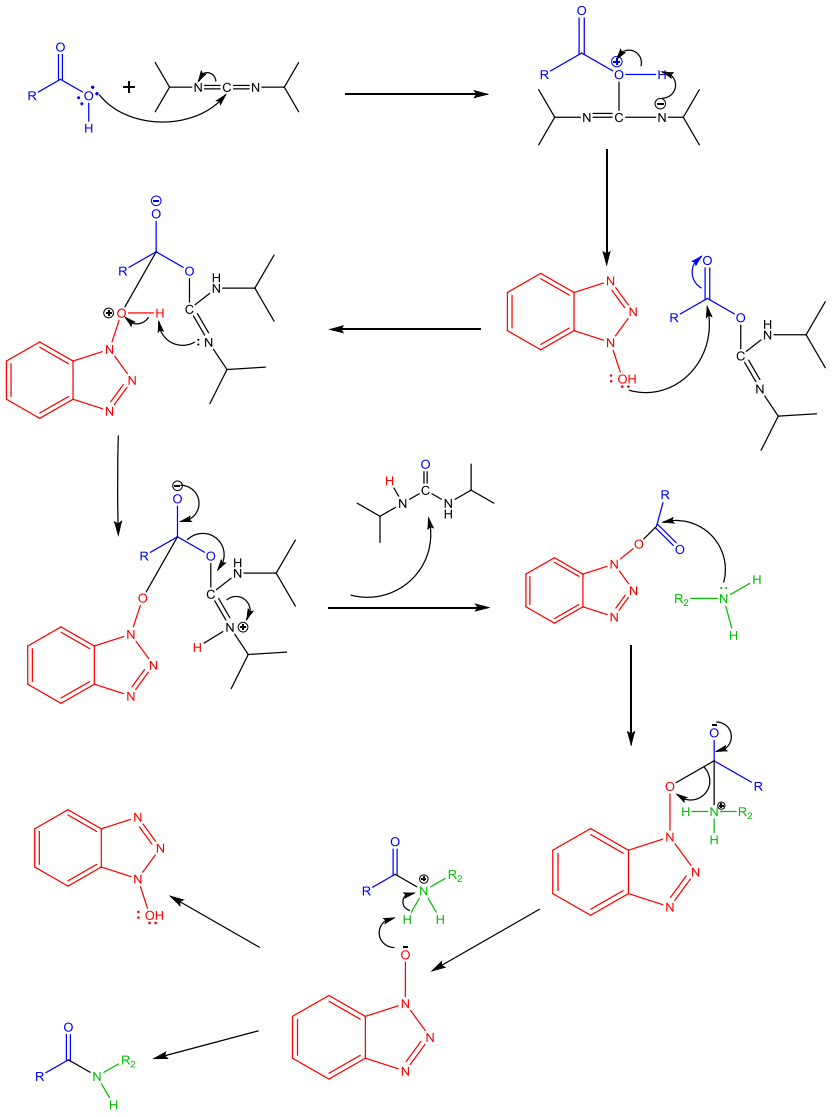

Figure 3.2: The mechanism for the HOBt-DIC-mediated amide coupling reaction.

DIC (Diisopropylcarbodiimide) and HOBt (Hydroxybenzotriazole) are commonly used amide coupling reagents. These reagents act together to accelerate amide

coupling by activating the carboxylic acid into an ester to enhance its reactivity towards amines **(Figure 3.2)**.

However, amide formation using DIC may lead to partial racemization of the acid. In addition to ester formation, HOBt helps to minimize side reactions.

Initially, the acid (1.2 eq.) was dissolved in DMF (5 mL for 100 mg of starting material) in a round bottom flask fitted with a magnetic stirrer. Then DIC (1.75 eq.) and HOBt (2.0 eq.) were added to the acid (1.0 eq.) and this mixture was allowed to stir at room temperature for formation of the ester from the acid. The amine (1 eq.) was added to the mixture and the mixture allowed to stir until the reaction was complete, as indicated by TLC or LCMS. Finally, the reaction mixture was applied to a conditioned SCX-2 cartridge and the resultant product was purified by the 'Catch and Release' method.

3.5 Purification by 'Catch and Release' Method

All reaction intermediates and final products containing tertiary amine tails were purified by the 'Catch and Release' method using SCX-2 cartridges. These are packed with silica-based sulfonic acid cationic exchange resins. Due to the presence of tertiary nitrogens in the products, they are retained in the cartridge. The SCX-2 cartridges were activated by washing under vacuum with DCM (2x) and methanol (2x), and the reaction mixture allowed to pass through the column under gravity. The cartridges were subsequently washed with DCM (3x), DMF (3x) and MeOH (2x) under vacuum to remove impurities. Finally the product is released from the cartridge using 2M NH_3 in MeOH. Excess MeOH was removed using a rotary evaporator. Structures of the synthesized compounds were confirmed by ^{1}H NMR and LCMS. The purity of compounds was established using LCMS, and the target purity for each compound prior to biological evaluation was 90% or greater.

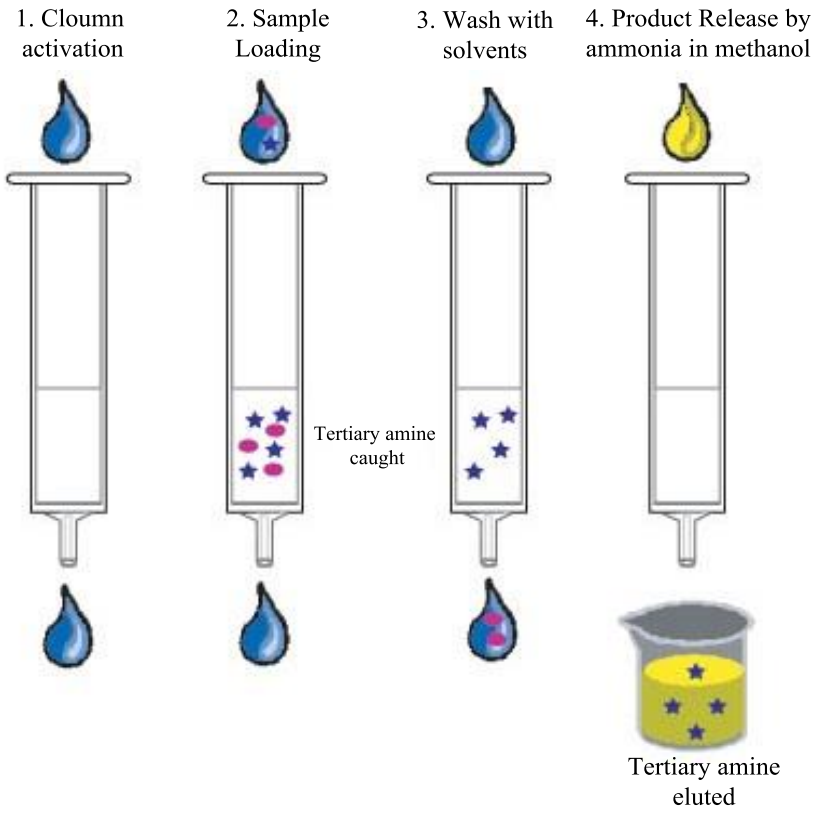

Figure 3.3: “Catch and Release” purification procedure using SCX-2 cartridge (Image courtesy: Silicycle, ultra-pure silica gels) [243].

3.6 Hydrogenation Reaction

The nitrobenzofused intermediate was dissolved in 20 mL of ethanol and added to a hydrogenation reaction bottle. 20 mg of 10% Pd (palladium on activated carbon) was added into the reaction vessel and mixed well. The reaction bottle was sealed and connected to a hydrogen reservoir. Air from the reaction bottle was removed by applying a vacuum, and was then flushed with hydrogen. Typically, a hydrogen pressure of approximately 40 psi was applied from the reservoir, and the bottle was then shaken vigorously to initiate the reaction. Progress of the reaction was monitored by TLC and LCMS, and on completion of the reaction the shaker was stopped, the bottle vented and the product recovered by means of filtration using Celite. Finally, the product is concentrated using a rotary evaporator.

3.7 Biological Evaluation of Synthesized Molecules

Preliminary assessment of G-quadruplex DNA stabilization was carried out with a FRET-based DNA melting assay using four different quadruplex sequences: human telomeric F21T, c-kit-1, c-kit-2 and Bcl-2 G-quadruplex sequences, and a hairpin duplex structure as a control.

Implicit solvent molecular dynamics simulations were conducted over a 10ns time-frame using the human telomeric G-quadruplex sequence (PDB ID: 3CDM) and results were assessed visually and through free energy of binding calculations. Finally, G-quadruplex ligands were evaluated biologically through cytotoxicity testing *via* MTT assays.

3.7.1 FRET-based DNA Melting Assay

Fluorescence Resonance Energy Transfer (FRET) technology is widely employed for the evaluation of ligands and their capacities to interact with specific secondary DNA structures like G-quadruplexes. It is measured through an increase in nucleic acid melting temperature (Δ**Tm**) [236]. The difference between the **Tm** of the ligand-bound DNA and the $\mathbf{T_m}$ of the unbound DNA is defined as the Δ**Tm** parameter [237]. One strand of an oligonucleotide is labelled with FAM (fluorescein) as a fluorescent donor and a complementary strand (or other end of heparin) is labelled with TAMRA as an acceptor [238]. The intensity of the FAM fluorescence upon excitation by heating is then measured as a function of temperature [239].

3.7.2 Materials and Methods for FRET Melting Assay

Quadruplex sequences used

F21T: FAM-d (G_3 $[TTAG_3]_3$-TAMRA)
C-kit-1: FAM-d ($G_3AG_3CGCTG_3AG_2AG_3$)-TAMRA.
C-kit-2: FAM-d ($G_3CG_3CGCGAG_3AG_4$)-TAMRA.
Bcl-2: FAM-d (G_3CGC-G_3-AG_3AA-TTG_3CG_3-TAMRA)
Duplex control: [FAM-$(TA)_2$ $GC(TA)_2T_6(TA)_2GC(TA)_2$-TAMRA]

3.7.3 FRET Buffer Preparation

Buffer solutions of 50 mM and 10 mM concentrations (500 mL each) were made with potassium hydroxide (1M) and potassium chloride (1M) and adjusted to pH 7.4 by the drop-wise addition of cacodylic acid. These were stored at -20 ^{o}C in a freezer.

3.7.4 DNA Annealing

100µM of fluorescence-labelled F21T, STAT3 and control DNA duplexes (Eurogentec) were diluted with sterile DEPC water (DNA Grade, Fisher Scientific) to provide 20 µM solutions. 400nM solutions of each sequence were prepared by serial dilution using FRET buffer. They were annealed by heating to 85 ^{o}C for 5 minutes followed by cooling to room temperature over 2-4 hours using a Grant Bio PCH-2 Dry Block Heating/Cooling System.

3.7.5 Ligand Solution

5mM of stock solution was prepared for each ligand in dimethyl sulfoxide (99.9%, A.C.S. spectrophotometric grade, Sigma-Aldrich). Working solutions of 100µM, 10µM, 4µM and 2µM were prepared by serially diluting with FRET buffer.

3.7.6 Plate Preparation

50µl of annealed sequence was added to each single well of a plate (Bio-Rad Laboratories), followed by 50µl of ligand solution. For each ligand of each concentration level, this process was repeated in triplicate. The same volume of pure FRET buffer was added to first line (A) of a 96 well plate to serve as a blank control. The plate was then processed in the DNA Engine Option (Continuous Fluorescence Detector, MJ Research) after 15 minutes of incubation at room temperature. The fluorescence measurement was made over a temperature range of 30 ^{o}C to 100 ^{o}C at intervals of 0.5 ^{o}C. The temperature was kept constant for 30 seconds before each measurement. The

incident radiation was set to 450-495 nm, and emitted radiation was measured at 515-545 nm.

3.7.7 Data Processing

The data was analysed using Scientific Graphing and Analysis Software (Version 7.0, Origin Lab Corp.). An increase in melting temperature (ΔTm) was determined by subtracting the value of the blank from the measured value for each sample. For each concentration of each ligand, an average ΔTm value was calculated from the three corresponding wells and plotted against the concentration of ligand.

3.8 Molecular Modelling and Molecular Dynamics (MD) Studies

Molecular Modelling is a combinatory method of both theoretical and computational studies which is widely used to design, model or study a chemical scaffold targeting specific sequences of DNA and proteins. In fact, it covers the areas of Computational Chemistry, Drug Design, Computational Biology and Material Sciences. This technique mainly helps to explain the molecular and binding nature of a chemical compound at an atomistic level. These methods also contribute to determining x-ray crystallographic structures with the help of NMR experiments.

Molecular Modelling and Molecular Dynamics (MD) Studies deal with the shape-fit of ligand molecules with their corresponding targets and thereby determines the binding affinity between the ligand and the receptor. Therefore, it is considered to be a competent method with which to study in detail the structure-activity relationships between libraries of novel ligand molecules synthesized in the field of drug discovery. Molecular docking calculations concern the use of static crystal structure, and are particularly useful in determining shape-fit in a receptor. On the other hand, the molecular dynamic simulation is based on the physical movement of individual atom in a molecule and of the molecule itself and the calculation involves the time-dependent behaviour of molecular scaffolds. Therefore, it provides valuable information on

the conformational changes of a molecular system (i.e. proteins or nucleic acids) as predicted over a certain time course.

Thus molecular modelling and molecular dynamics simulations are gaining more significance and expanding their field through technological advancement. The speed of computers has doubled every two years (Moor's Law [244]) for the past number of years, and the use of specialised GPUs and super computers has allowed the docking of large libraries of molecules and simulation of large macro molecules.

Molecular dynamic simulations provide the microscopic information including the positions of atoms and their velocities. Statistical mechanics convert the microscopic data to macroscopic variables such as pressure, energy and heat capacities. Statistical mechanics is able to calculate the changes of free energy for binding of a specific molecular system (i.e. ligand) and thereby determine the energetics and changes in the conformations. Thus the thermodynamic properties and the kinetics of a chemical scaffold can easily be determined using these techniques. In the field of drug discovery, the simulation of a chemical compound within its target receptor is supposed to provide the conformation of ligand-receptor complex with a lowest energy [245].

3.8.1 Receptor Preparation

The F21T quadruplex structure was downloaded from the Protein Data Bank (PDB ID: 3CDM). The quadruplex was then subjected to a number of steps of preparation in *Chimera,* including assignment of partial charges (AMBER ff98SB) and removal of hydrogens using the *DockPrep* module of AMBER, followed by writing to mol2 and pdb files. A molecular surface of the receptor was generated using *write dms*.

3.8.2 Ligand Preparation

All ligands were constructed and energy minimised using ChemBioOffice and exported in pdb format and converted into the Sybyl format mol2 using *Chimera* [246]. The *DockPrep* module in *Chimera* was then used to assign partial charges to each molecule (*AM1-BCC* charges in this instance), and atom types were

subsequently assigned *via* the AMBER GAFF force-field using ANTECHAMBER.

3.8.3 Docking

Docking experiments were undertaken using the DOCK6 software suite and the F21T quadruplex (PDB ID: 3CDM) was used in the study. In each case, the quadruplex interface was used as the receptor and the ligand used in the crystallography study was used as a guide for the docking site.

The receptor was prepared (outlined above) and a number of steps were undertaken in DOCK6 to isolate the binding pocket of interest. Firstly, spheres were generated around the surface of the molecule using *sphgen* and *Sphere_selector* was then used to filter results. Spheres within 15Å of the ligand were selected for further analysis. This resulted in the assessment of the full quadruplex.

Finally, every ligand was automatically positioned into the spheres with the maximum number of conformations set at a high level (500) to explore a large amount of conformational space, thus producing a docked ligand:DNA structure.

3.8.4 Evaluation of Ligand Binding

The ligand was evaluated based on the DOCK scoring function MMGBSA. During the docking process, a grid was created around the receptor. The grid was then used to allow rapid score evaluation in DOCK. Prior to scoring, orientations of the ligand which exhibited significant steric interactions with the receptor molecule were discarded using the *bump* filter.

In evaluating ligand-DNA interactions, two factors were considered crucial; shape-fit of the molecule to the DNA receptor, and positioning of the molecule on the DNA-binding interface. The latter was considered particularly relevant as in order to stabilise the quadruplex structure, it is known that ligands must bind to the G-tetrad.

3.9 Cytotoxicity Test with the MTT Assay

Cytotoxicity is the capacity of a drug or chemical compound to be toxic or growth inhibitory against a target cell line. Cytotoxicity studies are widely done to identify toxic compounds through the screening of a library of molecules. This tool is rationally designed to ensure that the newly synthesized molecules are toxic only to the desired cell line (for example, Breast Cancer Cell Line, MDA-MB-231) but non-toxic or safe for the normal healthy cells at the same time. Thus, this method provides information with which to help avoid any kind of adverse effect on a normal cell line.

A preliminary high-throughput screening was carried out to look for cytotoxic compounds which in turn aimed to develop more drug-like therapeutic agents through scrutinising and modifications. Therefore, this study defined the conditions to avoid any undesirable cytotoxic effect.

MTT assay is based on the reduction of an MTT dye named 3-(4, 5-dimethylthiazol-2-yl)-2,5-diphenyl-2H-tetrazolium bromide by the NAD(P)H dependent enzyme oxidoreductase. MTT is reduced due to the NADH formed by the metabolically active cells present. Therefore, this colorimetric reaction under certain conditions is correlated with viable cell potential as this enzyme reduces the MMT dye to an insoluble purple coloured formazan crystal which can easily be visible under a spectrophotometer (usually between 500 and 600 nm). This colour change directly reflects the number of viable cells present under cytotoxic conditions[247, 248].

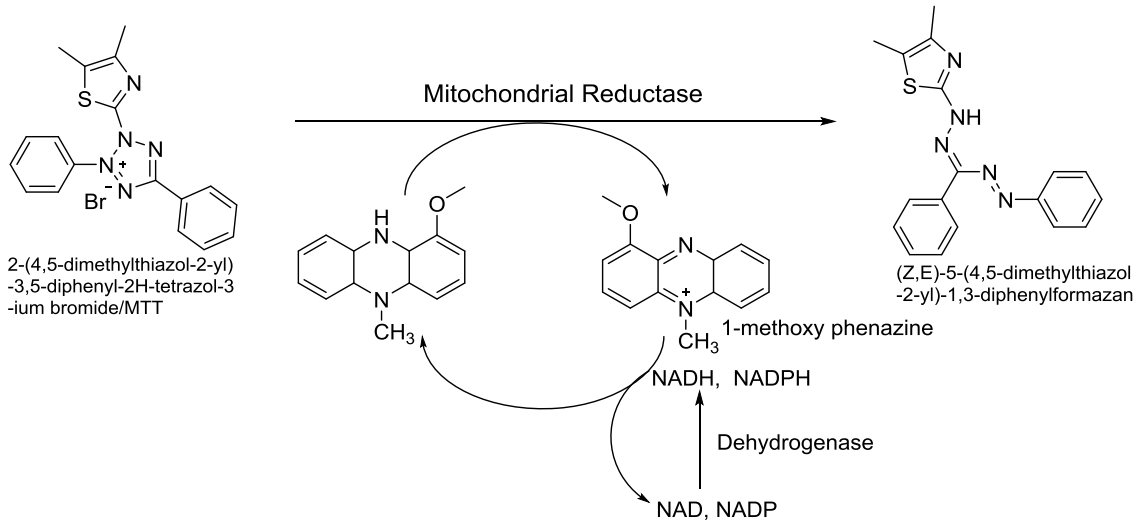

Figure 3.4: Schematic diagram showing the conversion of MTT to formazan in the presence of the electron acceptor 1-methoxy phenazine.

As MTT dye is sensitive to light, the assay is usually carried out in dark conditions. NAD (P)H is mostly formed within the mitochondria of the cell, thus 1-methoxy-phenazine methosulfate is used as an electron carrier to transfer the reduction equivalent from the mitochondrial matrix into the medium. However, the MTT assay can only detect the live cells because of its mechanism of action.

The assays using tetrazolium dye are used to assess cytotoxicity (loss of viable cells) or the cytostatic efficacy (modification from proliferation to latency of living cells) of prospective drug-like molecules and toxic materials.

3.9.1 Cell Lines Used for the MTT Assay

HeLa (Cervical cancer), MDA-MB-231 (triple negative breast cancer) and NCI H1975 (non-small cell lung cancer) cell lines were used in this assay, which were obtained from American Type Culture Collection (Manassas, VA).

3.9.2 Methods and Materials for MTT assay

The MTT assay is comprised of a number of crucial steps, from cell splitting to 96-well plate reading in a spectrophotometer. The following steps were followed to process the MTT assay for each type of cell line;

3.9.3Cell Culture

HeLa and MDA-MB-231 cell lines were cultivated in Dulbecco's modified eagle medium (DMEM) supplemented with 10% fetal bovine serum (FBS), 1% penicillin and streptomycin and 1% MEMNEAA (200x) non-essential amino acids. NCI H1975 cell lines were grown in RPMI-1640 supplemented with 10% fetal bovine serum (FBS) and 1% penicillin and streptomycin. These three cell lines were maintained in an incubator at 37°C with 5% CO_2.

3.9.4 Cell Passaging

Cell passaging or splitting is a procedure that allows cells to be kept alive and growing under cultured conditions for a prolonged period of time. Cells should be passaged when they are 90-100% confluent. In this process a small number of confluent cells are transferred into a new vessel since a high density of rapidly dividing cells is related to cells entering senescence. Suspension cultures can be simply split with a small amount of culture comprising a few cells diluted into a larger volume of fresh media. However, in the case of adherent culture, cells first need to be detached with trypsin, then a small number of detached cells can be used to seed a new culture.

70% ethanol was used to clean the fume hood, equipment, flasks, pipettes and other equipment before starting any process. DPBS (Dulbecco's Phosphate Buffered Saline) and DMEM (Dulbecco's Modified Eagle Medium) were taken out of the fridge ahead of time to become warm and ready to use. Cells contained in T-flasks were taken out from the incubator and checked under a microscope (dead cells floated and appeared round in shape whereas growing cells was attached to the bottom surface of the T-flask in a rod-shaped and

clustered fashion). Previous media was aspirated by using a vacuum pump (a sharp pointed pipette, 2 mL was used). 5 mL of DPBS was added to wash previous media fully and clean the T-flask, which was aspirated again to remove the floating dead cells. 1 mL of trypsin-EDTA was added to detach the growing cells and the flask was then incubated at 37°C in a 5% CO_2 incubator for 2 minutes. 10 mL of DMEM was added to inactivate the trypsin and the total cell suspension was then transferred into a falcon tube for centrifugation (2.5 minutes, 21 °C, 1.5 rpm). The supernatant medium was aspirated out, leaving the cells at the bottom of the falcon tube. Finally, 5 mL of DMEM was added and mixed properly and an appropriate amount of cell suspension was transferred into a newly labelled T-flask according to the next passage time. Furthermore, an appropriate amount of DMEM was added into the same T-flask to make a total volume of 15 mL (in general, 15 mL is considered to be an optimum volume for survival of cells in T-flask). Lastly, the new T-flask was returned to the incubator (37°C, 5% CO_2) for the next splitting schedule. Cells were passaged every 2 to 3 days.

3.9.5 Cell Count and Plate Preparation (Seeding of Cells)

Seeding is a process of spreading a defined amount (in volume or cell number) of a cell suspension onto a plate. 96-well polypropylene plates were used which are free of binding affinity for proteins or DNA, allowing complete sample recovery. This plate can withstand temperatures of -80 to +121°C. The following steps are used to seed the cells on to the plate:

1. 1 mL of DMEM was added to suspend the cells.

2. A haemocytometer was used to count cells, where a solution of cells was made with trypan blue stain (10 µL cells/ 90µL stain) to visualise the cells under an electron microscope.

3. An appropriate amount of cell suspension was taken to make a dilution of cells with DMEM to confirm ~ 10^6 cells per well.

4. A multichannel pipette was used to seed the cells on to the plate, which was then returned for incubation at 37°C in 5% CO_2 incubator (incubation time was varied from 24-72 hours).

3.9.6 Addition of Tested Samples

In this stage, the previous medium was aspirated out from every well by using sharp pipette tips and replaced with an equal amount (100 µL) of fresh medium and ligand of appropriate concentration, made from 5 mM stock solution by using DMSO, which were then added onto the cell seeded plate. Lastly, the plate was returned for further incubation at 37°C in a 5% CO_2 incubator. The incubation time was varied from 24 to 72 hours.

3.9.7 Plate Reading and Spectrometric Analysis

The final step involves the reading of data obtained from processed plates. Firstly, the old medium was aspirated out from each well after the predetermined incubation period and subsequently each well was washed with 100 µL of medium (high glucose content but without phenol red). Then all medium was aspirated out from each well and 100 µL of previously made MTT/medium phenol red-free solution was added into each well. A further 4 hours of incubation was done at 37°C in a 5% CO_2 incubator and the medium was then aspirated off from each well and 100µL of DMSO was added to dissolve the crystal formed. The plate was then incubated again for 5 minutes at 37°C in 5% CO_2 incubator and subsequently placed in shaker for 5 minutes (500 rpm) to remove all air bubbles.

Absorbance was then taken by an Infinite 200 Pro-plate reader at a wavelength of 570 nm and the data was processed with the help of Tecan i-control application software.

It is notable that the MTT solution was prepared in a 1:10 dilution with phenol red-free medium. The final solution was filtered through a 0.2 µm filter and stored in the dark at 4°C.

3.10 Standardisation of FRET Assay by using G-quadruplex Ligand TMPyP4

Cationic porphyrins like TMPyP4 **(Figure 2.10)** are commonly chosen to use as G-quadruplex ligands [134]. The ligand TMPyP4 was first reported to interact with DNA about 40 years ago; it has since been shown to be a G-quadruplex ligand [135, 136]. Since then the DNA-interacting capacity of this ligand has been widely assessed and it has been found to have a high level of affinity toward G-quadruplex DNA with poor selectivity [137-139]. However, sometimes it might be peculiar to show an extraordinary responses such as a unfolding of a quadruplexes in both d(CGG) repeats [140] or antithrombin aptamer[141] and RNA sequences (r(CGG) repeats[142]. Interestingly this ligand showed interactions with a wide variety of G-quadruplexes. Thus it is still extensively studied and analysed to investigate its interactive modes towards the different forms of DNA [146].

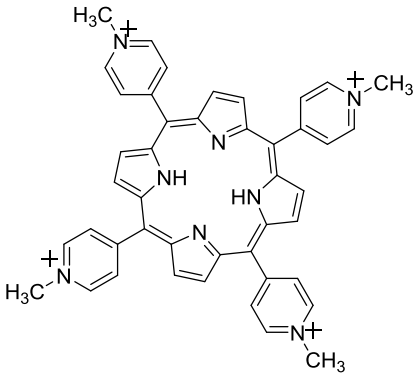

Figure 3.5: Structure of TMPyP4.

The FRET assay has been standardised by evaluating commercially available G-quadruplex ligand TMPyP4 in the same conditions as used for benzofused-polyamides. It is notable that TMPyP4 showed significantly higher interaction not only towards the G-quadruplex sequence types used but also with duplex DNA. None of the benzofused-polyamides show a minimum interaction with duplex DNA, indicating that benzofused-polyamides are specific towards G-quadruplex sequences.

Table 3.1: G-quadruplex and duplex DNA stabilization by TMPyP4 in FRET melting experiments at concentrations of 5, 2 and 1 µM respectively

Compounds	Quadruplex types	ΔT_m(°C)±(s/d)		
		5 µM	2 µM	1 µM
TMPyP4	F21T	35.3±0.43	35.3±0.11	35.3±0.26
	C-kit-1	40.0±0.22	41.0±0.34	40.5±0.13
	C-kit-2	33.4±0.31	31.7±0.20	32.1±0.15
	BCL-2	34.6±0.21	35.3±0.20	32.7±0.28
	Duplex DNA	38.0±0.42	38.0±0.14	29.0±0.07

FRET result showed that TMPyP4 provided a very high level of interaction with the different types of quadruplex sequences and duplex DNA as well. It provided stabilisation capacities of 35.3 °C, 40.5 °C, 32.1 °C, 32.7 °C and 28.7 °C against F21T, c-kit-1, c-kit-2 and Bcl-2 G-quadruplex sequences respectively, and also provided 29.0 °C of stabilisation against duplex DNA at 1 µM concentration. This is indicative of the non-specificity it exhibits towards binding sites.

3.10.1: Standardisation of FRET Assay by using DNA-Binding Ligand Distamycin A

Duplex DNA used here was checked by doing a FRET assay using distamycin, a well-known DNA minor groove binder.

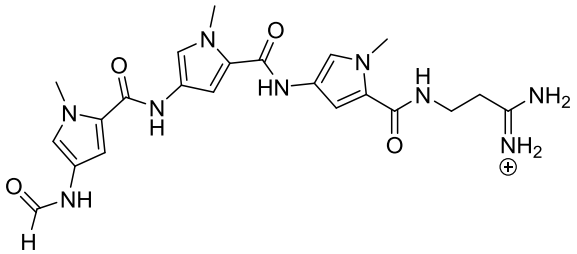

Figure 3.6: Structure of Distamycin A.

Table 3.2: Duplex DNA stabilization by distamycin in FRET melting experiments at concentrations of 5, 2 and 1 µM, respectively

Compounds	Quadruplex types	ΔT_m(°C)±(s/d)		
		5 µM	2 µM	1 µM
Distamycin	Duplex DNA	12.5±0.05	8.1±0.37	5.0±0.050

Distamycin A showed ΔTm values of 12.5 °C, 8.1 °C and 5.0 °C at 5 µM, 2 µM and 1 µM concentrations, respectively, against duplex DNA. This interacting capacity of distamycin A supports the notion that the FRET experiment worked well.

Chapter 4: Experimental (Chemistry)

4.1 Synthesis of 5-amino-N-(3-(dimethylamino)propyl)benzofuran-2-carboxamide (4.1)

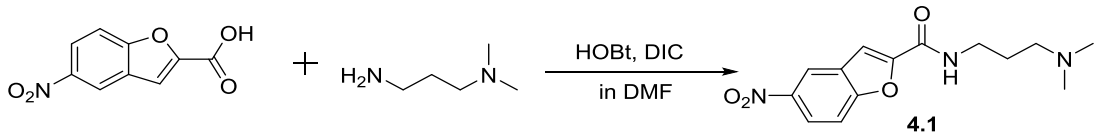

250 mg of 5-nitrobenzofuran-2-carboxylic acid (1.207 mmol, 1.2 eq.) was dissolved in 10 mL of DMF in a round bottom flask fitted with a magnetic stirrer. Then 105 µl of DIC (2.589 mmol, 1.75 eq.) and 2.0 equivalents of HOBt (326 mg, 2.405 mmol) were added to the acid (1.0 eq.). This mixture was stirred for at least 25 minutes at room temperature to ensure formation of the ester from the acid. Then 102.8 mg of N1, N1-dimethylpropane-1,3-diamine (1.0 mmol, 01 eq.) was added to the mixture and it was then stirred further for 6 hours at which point TLC and LCMS analysis showed the completion of reaction. Finally the reaction mixture was applied to a conditioned Isolute^{TM} SCX-2 cartridge and the product was purified by 'Catch and Release' method **(**described in the section **'Method and Materials'** of chapter 3**)**. A pale yellow solid was collected after drying under vacuum. Yield was 200mg, 60%.

Table 4.1: Characterisation data for compound **4.1**

4.1 Pale yellow solid	^{1}H NMR	^{1}H NMR (400 MHz, CD_3OD) $^{\delta}$H in ppm 8.56(d,*J*=2.0,1H),8.48(s,1H),8.25(dd,*J*=9.2,2.4,1H),7.66(d,*J*=8.4, 1H),7.44(s,1H),3.453.40(m,2H),2.40(t,*J*=6.4, 2H), 2.239(s, 6H), 1.74-1.70 (m, 2H).
	EIMS	Found 292.00$[M+H]^+$, Calculated for $C_{14}H_{17}N_3O_4$ 291.12 $[M]^+$

4.2 Synthesis of 5-amino-N-(3-(dimethylamino) propyl) benzofuran-2-carboxamide (4.2)

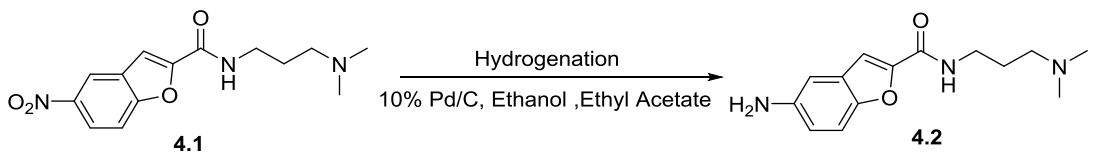

200 mg of **4.1** was dissolved in 20 mL of ethanol and 1 mL of ethyl acetate was added to a hydrogenation reaction bottle. 20 mg of 10% Pd (palladium on

activated carbon) was also added into the same reaction vessel and it was mixed well. The reaction bottle was sealed and connected to a hydrogen reservoir. Air within the reaction bottle was removed by applying vacuum, and flushed with hydrogen. Typically, a hydrogen pressure of approximately 40 psi was applied from the reservoir and the bottle was then shaken vigorously to initiate hydrogenation. Progress and completion of reaction was monitored by TLC and LCMS. The hydrogenation was completed by 5 hours at which point TLC and LCMS analysis showed the completion of reaction. The shaker was stopped, the bottle was vented. After this the product was recovered by means of filtration using Celite and was concentrated by using a rotary evaporator. A pale yellow solid was collected after drying under vacuum. Yield was 162 mg, 90%.

Table 34.2: Characterisation data for compound **4.2**

4.2 Pale yellow solid	^{1}H NMR	^{1}H NMR (400 MHz, CD_3OD) $^\delta$H in ppm 7.31(d,*J*=8.8,1H),7.28(s,1H),6.97(d,*J*=2.4,1H),6.91(dd,*J*=8.8,2.0,1 H),4.95(s,2H),2.34(s,6H),3.43(t,*J*=6.8,2H),2.54-2.50(m,2H), 1.84(t,*J*=6.8,2H).
	EIMS	Found 262.00$[M+H]^+$, Calculated for $C_{14}H_{19}N_3O_2$ 261.14 $[M]^+$

4.3 Synthesis of N-(3-(dimethylamino) propyl)-5-(5-nitrobenzofuran-2-carboxamido) benzofuran-2-carboxamide (4.3)

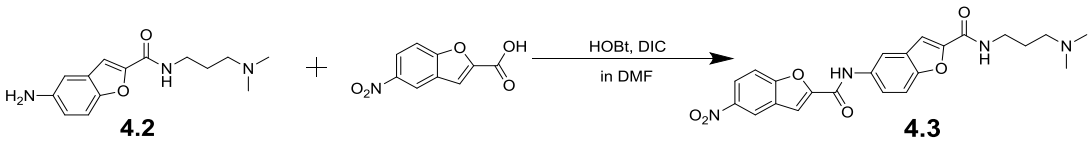

4.2 **4.3**

Initially, 144 mg of 5-nitrobenzofuran-2-carboxylic acid (0.697 mmol, 1.2 eq.) was dissolved in 10mL of DMF in a round bottom flask placed in a magnetic stirrer. Then DIC (188 µl, 1.21 mmol, 1.75 eq.) and HOBt (188.19 mg, 1.39 mmol, 2.0 eq.) were added to the acid solution (1.0 eq.). This mixture was allowed to stir at room temperature for 30 minutes to ensure the ester formation from the acid. Then amine **4.2** (130 mg, 0.498 mmol, 1 eq.) was added to that mixture, and it was allowed to stir for 8 hours at which point TLC and LCMS analysis showed the completion of reaction. The product was purified from the reaction mixture by 'Catch and Release' method using a conditioned Isolute^{TM}SCX-2 cartridge **(**described in the section **'Method and Materials'** of

chapter 3**)**. Lastly this product was then dried under vacuum and a pale yellow coloured solid was obtained. Yield=147mg, 66%.

Table 4.3: Characterisation data for compound **4.3**

4.3 Brown Solid	^{1}H NMR	^{1}HNMR(400MHz,$(CD_3)_2SO$) $^\delta$H in ppm 10.85(s,1H),8.80(t,*J*=8.4,2H),8.32(d,*J*=6.4, 1H),8.27(s,1H), 7.95(t,*J*=9.2,2H), 7.78(d,*J*=8.8,1H), 7.73(d,*J*=8.4,1H), 7.53 (s,1H), 3.17-3.12(m,2H), 2.28(t,*J*=6.0,2H), 2.15(s,6H), 1.67(t,*J*=6.8,2H).
	EIMS	Found 451.0 $[M+H]^+$, Calculated for $C_{23}H_{22}N_4O_6$, 450.15 $[M]^+$

4.4 Synthesis of 5-amino-N-(2-((3-(dimethyl amino) propyl) carbonyl) benzofuran5-yl) benzofuran-2-carboxamide (4.4).

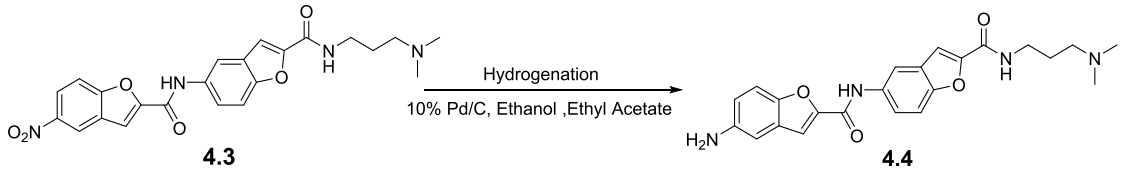

4.3 (147mg) was dissolved in 20 mL of ethanol and 1 mL of ethyl acetate was added to a hydrogenation reaction bottle. 20 mg of 10% Pd (palladium on activated carbon) 20 was added into the reaction vessel, and mixed well. The reaction bottle was sealed and connected to a hydrogen reservoir. Air from the reaction bottle was removed by applying vacuum, and was then by flushed with hydrogen. Typically, a hydrogen pressure of approximately 40 psi was applied from the reservoir, and the bottle was then shaken vigorously to initiate the reaction. Progress of the reaction was monitored by TLC and LCMS. The reaction required about 4.5 hours at which point TLC and LCMS analysis showed the completion of reaction. The shaker was stopped, the bottle vented, and the product was recovered by means of filtration using Celite. Finally, the product is concentrated by using a rotary evaporator. A pale yellow solid was obtained after drying under vacuum. Yield=80 mg, 51%.

Table 4.4: Characterisation data for compound **4.4**

4.4 Pale Yellow Solid	^{1}H NMR	(400MHz,$(CD_3)_2SO$) $^\delta$H in ppm 10.61(s,1H),8.84(t,*J*=5.6,1H),8.28(d,*J*=2,1H),7.79(dd,*J*=8.8,2.0, 1H),7.64(d,*J*=9.2,1H),7.55(d,*J*=3.6,2H),7.38(d,*J*=8.4,1H),6.83(d, *J*=2,1H),6.79(d,*J*=2.4,1H),2.51- 2.49 (m,2H), 2.25(t,*J*=6.8,2H), 2.13(s,6H), 1.68-1.62(m,2H).
	EIMS	Found 421.0 $[M+H]^+$, Calculated for $C_{23}H_{24}N_4O_4$, 420. $[M]^+$.

4.5 Synthesis of 5-(benzo[b]thiophene-2-carboxamido)-N-(2-((3-(dimethyl amino) propyl) carbonyl) benzofuran-5-yl) benzofuran-2-carboxamide (4.5).

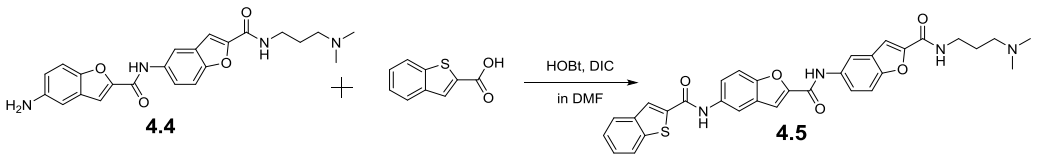

48 mg of benzo[b]thiophene-2-carboxylic acid (0.266 mmol, 1.2 eq.) was dissolved in 10mL of DMF in a round bottom flask. Then DIC (71.96 µl, 0.465 mmol, 1.75 eq.) and HOBt (71.82 mg, 0.532 mmol, 2.0 eq.) were added to the acid (1.0 eq.) and this mixture was allowed to stir at room temperature for 25 minutes to ensure the formation of ester from the acid. Then amine **4.4** (80 mg, 0.19 mmol, 1 eq.) was added to the mixture, and that mixture was allowed to stir for 5 hours at which point TLC and LCMS analysis showed the completion of reaction. Finally the reaction mixture was applied to a conditioned Isolute^{TM} SCX-2 cartridge and the product was purified by 'Catch and Release' method **(**described in the section **'Method and Materials'** of chapter 3**)**. A cream solid was obtained after drying under vacuum. Yield=34mg, 31%.

Table 4.5: Characterisation data for compound **4.5**

4.5 Cream Solid	^{1}H NMR	^{1}HNMR(400MHz,$(CD_3)_2SO$) $^{\delta}$H in ppm 10.69(d,*J*=7.8, 2H), 8.81(t,*J*=5.6,1H), 8.40(s,1H), 8.32(d,*J*=2,1H), 8.30(d,*J*=2,1H),8.09(d,*J*=1.6,1H),8.058.02(m,1H),7.82(t,*J*=2.8,2H), 7.79(d,*J*=2.8,1H),7.76(d,*J*=8.8,1H), 7.67(d,*J*=8.8,1H), 7.55(s,1H), 7.51-7.49 (m,2H), 2.51-2.49(m,2H), 2.27(t,*J*=6.8,2H), 2.15(s,6H), 1.67(t,*J*=6.8, 2H).
	^{13}C NMR	100MHz,$(CD_3)_2SO$); $^{\delta}$C in ppm 193.0, 191.0, 179.8, 158.2, 151.1, 140.1, 139.0, 137.9, 127.4, 125.7, 124.2, 123.3, 121.4, 120.4, 116.0, 114.0, 111.5, 109.6, 108.1, 106.6, 101.1, 94.9, 56.8, 45.1, 40.0, 39.8, 39.6, 39.4, 39.23, 39.0, 38.8, 35.9.
	EIMS	Found 581.8 $[M+H]^+$, Calculated for $C_{32}H_{28}N_4O_5S$, 580.17 $[M]^+$
	HRMS	*m/z* (+EI) Calc. for $C_{32}H_{28}N_4O_5S$ $[M]^+$, 580.1780, found 581.1851$[M+H]^+$.
	IR	(FTIR, V_{max}/'cm^{-1}): 3363, 1658, 1637, 1583, 1540, 1469, 1433, 1346, 1321, 1292, 1230, 1200, 1139, 1124, 1038, 941, 863, 838, 811, 786, 750, 736, 724, 625, 604, 577.

4.6 Synthesis of N-(2-((2-((3-(dimethylamino) propyl) carbamoyl) benzofuran-5-yl) carbamoyl) benzofuran-5-yl)-1H-benzo[d]imidazole-2-carboxamide (4.6).

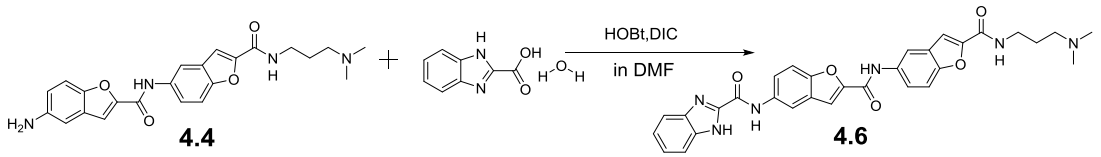

Initially, 30 mg of 1H-benzo[d]imidazole-2-carboxylic acid hydrate (0.166 mmol, 1.2 eq.) was dissolved in 5mL of DMF in a round bottom flask fitted with a magnetic stirrer. Then DIC (44.91 µl, 0.2905 mmol, 1.75 eq.) and HOBt (44.82 mg, 0.332 mmol, 2.0 eq.) were added to the acid (1.0 eq.). This mixture was allowed to stir at room temperature for 30 minutes to ensure the formation of ester from the acid. Then amine **4.4** (50.0 mg, 0.119 mmol, 1 eq.) was added to the mixture, and was allowed to stir for 5 hours at which point TLC and LCMS analysis showed the completion of reaction. Finally the product was purified by 'Catch and Release' method using conditioned Isolute^{TM} SCX-2 cartridge **(**described in the section **'Method and Materials'** of chapter 3**)**. A straw solid was obtained after drying in vacuum. Yield=12mg, 18 %.

Table 4.6: Characterisation data for compound **4.6**

4.6 Straw solid	^{1}H NMR	^{1}HNMR (400MHz,$(CD_3)_2SO$) $^{\delta}$H in ppm 11.0(s,1H), 10.66(s,1H), 8.80(t,*J*=5.2,1H), 8.46(s,1H), 8.30(s,1H), 8.00(d,*J*=8.8,1H), 7.82(s,2H), 7.75(d,*J*=8.8,2H), 7.66(d,*J*=8.8,2H), 7.54(s,1H), 7.35(s, 2H), 3.31(t,*J*=6.8,2H), 2.28(t, *J*=6.8,2H), 2.15(s,6H), 1.71-1.64(m ,2H).
	^{13}C NMR	(100MHz,$(CD_3)_2SO$); $^{\delta}$C in ppm 157.9, 157.3, 156.6, 151.2, 150.9, 150.0, 149.4, 145.5, 134.4, 134.2, 127.2, 127.1, 121.1, 120.6, 113.9, 111.9, 111.7, 110,9,109.4, 56.8, 45.0, 40.0, 39.8, 39.6, 39.4, 39.2, 39.0, 38.8, 37.2, 26.8.
	EIMS	Found 564.23 $[M+H]^+$, Calculated for $C_{31}H_{28}N_6O_5$, 563.21 $[M]^+$
	HRMS	*M/z* (+EI) Calc. for $C_{31}H_{28}N_6O_5$, 564.2121 $[M]^+$, found 565.2187$[M+H]^+$.
	IR	(FTIR), V_{max}/'cm^{-1}): 3265, 2939, 2219, 1705, 1631, 1533, 1475, 1437, 1361, 1331, 1308, 1221, 1159, 1097, 1039, 945, 886, 807, 770, 741, 715, 619.

4.7 Synthesis of N-(3-(dimethylamino) propyl)-5-nitrobenzo[b]thiophene-2-carboxamide (4.7).

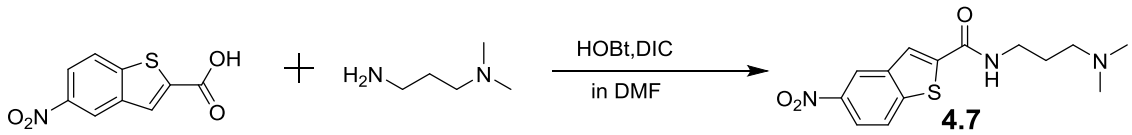

500 mg of 5-nitrobenzo[b]thiophene-2-carboxylic acid (2.24 mmol, 1.2 eq.) was dissolved in 15 mL of DMF in a round bottom flask. DIC (606 µl, 3.92 mmol, 1.75 eq.) and HOBt (608.8 mg, 4.48 mmol, 2.0 eq.) were added to the acid (1.0 eq.) and the mixture was allowed to stir at room temperature for 30 minutes to ensure the ester formation. 189.72 mg of N1, N1-dimethylpropane-1, 3-diamine (1.86 mmol, 1 eq.) was added into the same reaction mixture. Then this mixture was stirred for about 7 hours at which point TLC and LCMS analysis showed the completion of reaction. The reaction mixture was then applied to a conditioned Isolute^{TM} SCX-2 cartridge and the product was purified by 'Catch and Release' method **(**described in the section **'Method and Materials'** of chapter 3**)**. The product was dried under vacuum and A pale yellow solid was collected. Yield=350.0 mg, 51%.

Table 4.7: Characterisation data for compound **4.7**

4.7 Cream solid	^{1}H NMR	^{1}HNMR(400MHz,(CD_3OD) $^{\delta}$H in ppm 8.53(d,*J*=3.6,1H), 8.06(dd,*J*=8.8,2.4,1H), 7.93(d,*J*=9.2,1H), 7.86(s, 1H),3.41(t,*J*=6.8,2H),2.43(t,*J*=7.6,2H),2.73(s,6H),1.86(m,*J*=7.2,2H),
	EIMS	Found 308.0 $[M+H]^+$, Calculated for $C_{14}H_{17}N_3O_3S$, 307.09 $[M]^+$

4.8 Synthesis of 5-amino-N-(3-(dimethylamino) propyl) benzo[b]thiophene-2-carboxamide (4.8)

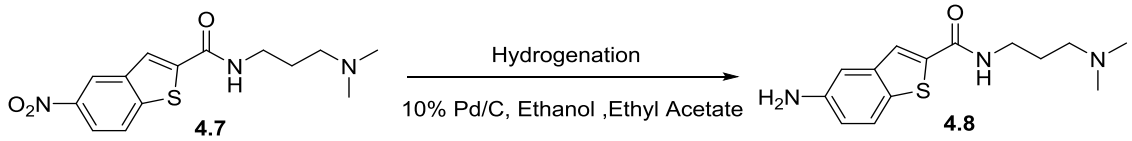

350 mg **4.7** was dissolved in 20 mL of ethanol and1 mL of ethyl acetate in a hydrogenation reaction bottle. 20 mg of 10% Pd (palladium on activated carbon) was added into the same bottle and mixed well. The bottle was sealed and connected to a hydrogen reservoir. Air within the reaction bottle was removed

under vacuum, and flushed with hydrogen. A hydrogen pressure of approximately 40 psi was applied from the reservoir, and the bottle was then shaken vigorously to initiate the reaction. Progress of the reaction was monitored by TLC and LCMS. The hydrogenation process took about 5 hours at which point TLC and LCMS analysis showed the completion of reaction. The bottle vented after stopping the shaker and the hydrogenated product has been recovered through filtration using Celite. Lastly the product was concentrated by the rotary evaporation. A cream solid was obtained after drying under vacuum. Yield was 310 mg, 98%.

Table 4.8: Characterisation data for compound **4.8**

4.8 Deep Brown solid	^{1}H NMR	^{1}HNMR (400MHz,(CD_3OD) $^\delta$H in ppm 7.69(s,1H),7.58(d,*J*=8.8,1H),7.14(d,*J*=2,1H), 6.93(dd,*J*=8.8, 2.4,1H), 3.44(t,*J*=6.8,2H),2.62(t,*J*=4.4,2H),2.43(s,6H),1.89-1.84(m,*J*=7.6,2H).
	EIMS	Found 278.0 $[M+H]^+$, Calculated for $C_{14}H_{19}N_3OS$, 277.12 $[M]^+$

4.9 Synthesis of N-(3-(dimethylamino)propyl)-5-(5-nitrobenzo[b]thiophene-2-carboxamido) benzo[b]thiophene-2-carboxamide (4.9).

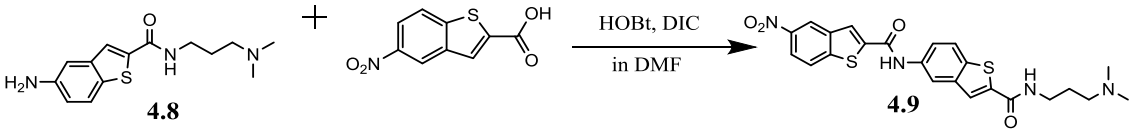

4.8 4.9

At the beginning, 5-nitrobenzo[b]thiophene-2-carboxylic acid (304 mg, 1.30 mmol, 1.2 eq.) was dissolved in 20 mL of DMF in a round bottom flask fitted with a magnetic stirrer. Then DIC (351 µl, 2.27 mmol, 1.75 eq.) and HOBt (351 mg, 2.60 mmol, 2.0 eq.) were added to the acid (1.0 eq.) solution and this mixture was stirred at room temperature for about 30 minutes to ensure the esterification of acid. Then amine (304 mg, 1.09 mmol, 1 eq.) was added to that mixture and it was allowed to stir for 7 hours at which point TLC and LCMS analysis showed the completion of reaction. Finally the product was purified from the reaction mixture by the Catch and Release' method using conditioned Isolute^{TM} SCX-2 cartridge **(**described in the section **'Method and Materials'** of chapter 3**)**. The product was concentrated and a pale yellow solid was obtained after drying in vacuum. Yield was 205mg, 39%.

Table 4.9: Characterisation data for compound **4.9**

4.9 Yellow solid	^{1}H NMR	^{1}HNMR(400MHz,($CD_3)_2SO$) $^\delta$H in ppm 10.95(s,1H), 8.42(s,1H), 8.88(d,*J*=2.4,1H), 8.83 (d, *J*=2.4,1H), 8.55(s,1H),8.41(d,*J*=2,1H),8.30(d,*J*=8.8,1H),8.25(s,1H),7.97(t,*J*=8.8, 1H),7.77(dd,*J*=9.2,2.4,1H),7.24-7.12(m,1H),3.34(d,*J*=6,2H),2.61 (t,*J*=7.6,2H), 2.39(s,6H), 1.793(t,*J*=7.2,2H).
	EIMS	Found 483.0 $[M+H]^+$, Calculated for $C_{23}H_{22}N_4O_4S_2$, 482.10 $[M]^+$

4.10 Synthesis of 5-amino-N-(2-((3-(dimethylamino) propyl) carbamoyl) benzo[b]thiophen-5-yl) benzo[b]thiophene-2-carboxamide (4.10).

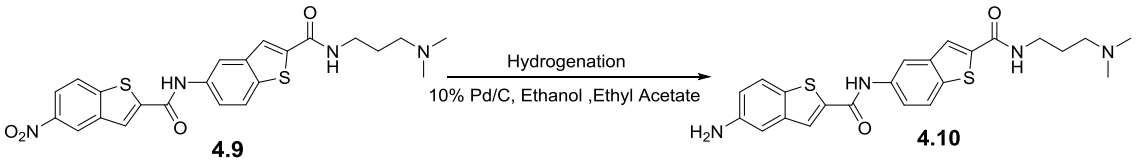

205 mg **of 4.9** was dissolved in 20 mL of ethanol and 1 mL of ethyl acetate in a hydrogenation reaction bottle. 20 mg of 10% Pd (palladium on activated carbon) was added into the reaction vessel and mixed well. The bottle was sealed and connected to a hydrogen reservoir. Air from the reaction bottle was removed by applying vacuum, and was then by flushed with hydrogen. Typically, approximately 40 psi of hydrogen pressure was applied from the reservoir, and the bottle was then shaken vigorously to initiate the reaction. Progress of the reaction was monitored by TLC and LCMS. A complete hydrogenation has taken 6 hours at which point TLC and LCMS analysis showed the completion of reaction. The shaker was stopped and the bottle was vented. The product was recovered by means of filtration using Celite. Finally, the product is concentrated by using a rotary evaporator. A yellow solid was obtained after drying in vacuum. Yield was 175 mg, 91%.

Table 4.10: Characterisation data for compound **4.10**

4.10 Yellow solid	^{1}H NMR	^{1}HNMR(400MHz,$(CD_3)_2SO$) $^\delta$H in ppm 10.69(s,1H),8.84(t,*J*=5.6,1H),8.44(d,*J*=2,1H),8.17(s,1H),8.05(s,1H), 7.96(d,*J*=8.8,2H),7.837.80(m,1H),7.64(d,*J*=8.8,1H),7.07(d,*J*=2.0,1H),6.87(dd,*J*=8.8,2.4,1H),5.21(s,2H),3.33-3.28(m,2H), 2.25(t,*J*=6.8,2H),2.12(s,6H),1.71-164(m,2H).
	EIMS	Found 453.0 $[M+H]^+$, Calculated for $C_{23}H_{24}N_4O_2S_2$, 452.13 $[M]^+$

4.11 Synthesis of N-(2-((2-((3-(dimethylamino) propyl) carbamoyl) benzo[b]thiophen-5-yl) carbamoyl) benzo[b]thiophen-5-yl) benzofuran-2-carboxamide (4.11).

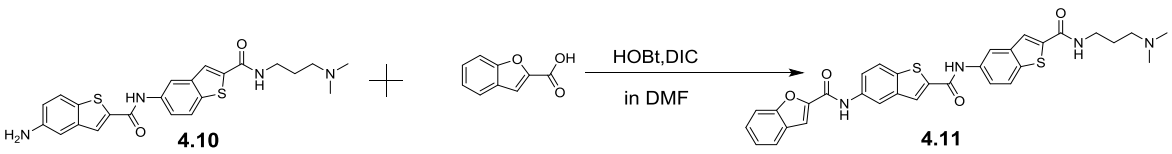

26 mg of benzofuran-2-carboxylic acid (0.158 mmol, 1.2 eq.) was dissolved in 5 mL of DMF in a round bottom flask fitted with a magnetic stirrer. Then DIC (43 µl, 0.276 mmol, 1.75 eq.) and HOBt (43 mg, 0.316 mmol, 2.0 eq.) were added to the acid (1.0 eq.) and this mixture was allowed to stir at room temperature for 30 minutes to ensure the formation of ester from the acid. Then amine **4.10** (60 mg, 0.132 mmol, 1 eq.) was added to the mixture and this mixture was allowed to stir for 5 at which point TLC and LCMS analysis showed the completion of reaction. Finally the reaction mixture was applied to a conditioned Isolute^{TM} SCX-2 cartridge and the product was purified by 'Catch and Release' method **(**described in the section **'Method and Materials'** of chapter 3**)**. An orange solid was obtained after drying in vacuum. Yield=28mg, 36%.

Table 4.11: Characterisation data for compound **4.11**

4.11 Orange solid	^{1}H NMR	^{1}HNMR(400MHz,$(CD_3)_2SO$) $^{\delta}$H in ppm 10.77(s,1H), 10.71(s,1H), 8.82(t,*J*=5.2,1H), 8.56(d,*J*=1.6,1H), 8.44(s,2H),8.06(d,*J*=7.6,2H),8.01(d,*J*=8.8,1H),7.92(dd,*J*=8.8,1.6,1 H), 7.85(d,*J*=5.2,2H), 7.82(dd,*J*=8.8,2.0,1H), 7.75(d,*J*=8.4,1H), 7.55-7.51(m,1H), 7.39 (t,*J*=7.6, 1H), 3.34-3.29(m,2H), 2.40 (t,*J*=7.2,2H), 2.24(s,6H), 1.76-1.69(m,2H).
	^{13}C NMR	(100MHz,$(CD_3)_2SO$); $^{\delta}$C in ppm 161.3, 160.3, 156.8, 154.4, 148.6,141.1, 140.8, 139.5, 139.4, 136.1, 135.9, 138.8, 135.6, 127.2, 127.1, 125.9, 124.5, 123.8, 123.0, 122.9, 120.6, 120.0, 116.1, 115.6, 111.95, 110.8, 56.4, 44.68, 40.0, 39.8, 39.2,26.6.
	EIMS	Found 597.3 $[M+H]^+$, Calculated for $C_{32}H_{28}N_4O_4S_2$, 596.15 $[M]^+$
	HRMS	*m/z* (+EI) Calc. for $C_{32}H_{28}N_4O_4S_2$, 596.1552 $[M]^+$, found 597.1625$[M+H]^+$.
	IR	(FTIR), V_{max}/'cm^{-1}): 3282, 2931, 2217, 1632, 1518, 1473, 1443, 1383, 1335, 1302, 1221, 1155, 1095, 1038, 951, 885, 807, 738, 720.

4.12 Synthesis of 5-(benzo[b]thiophene-2-carboxamido)-N-(2-((3-(dimethyl amino) propyl) carbamoyl) benzo[b]thiophen-5-yl) benzo[b]thiophene-2-carboxamide (4.12).

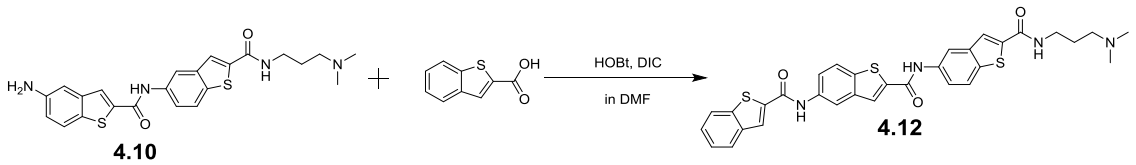

4.10 4.12

Initially, 28 mg of benzo[b]thiophene-2-carboxylic acid (0.158 mmol, 1.2 eq.) was dissolved in 10mL of DMF in a round bottom flask fitted with a magnetic stirrer. Then DIC (43 µl, 0.276 mmol, 1.75 eq.) and HOBt (43 mg, 0.316 mmol, 2.0 eq.) were added to the acid (1.0 eq.) and this mixture was allowed to stir at room temperature for 30 minutes to ensure the formation of ester from the acid. Then amine **4.10** (60 mg, 0.132 mmol, 1 eq.) was added to the same mixture and it was allowed to stir for 6 hours at which point TLC and LCMS analysis showed the completion of reaction. Finally the product was purified by 'Catch and Release' method using conditioned Isolute^{TM} SCX-2 cartridge **(**described in the section **'Method and Materials'** of chapter 3**)**. A pale yellow solid was collected after drying in vacuum. Yield=25 mg, 31%.

Table 4.12: Characterisation data for compound **4.12**

4.12 Light Yellow solid	^{1}H NMR	^{1}HNMR(400MHz,$(CD_3)_2SO$); $^{\delta}$H in ppm 10.79(s,1H), 10.73(s,1H), 8.81(t,*J*=5.2,1H), 8.53(d,*J*=1.6,1H), 8.47(s,1H), 8.44(s,2H), 8.08-8.04(m,3H), 8.01 (d,*J*=8.8,2H), 7.87(dd,*J*=8.8,2.0,1H), 7.82(dd,*J*=8.8,2.0,1H),7.53-7.47 (m, 2H), 3.34-3.27(m,2H), 2.34(t,*J*=7.2,2H), 2.19(s,6H), 1.74-1.67(m,2H).
	^{13}C NMR	(100MHz,$(CD_3)_2SO$); $^{\delta}$C in ppm 161.3, 160.5, 160.3, 141.2, 140.9, 140.4, 139.8, 139.5, 139.4, 139.1, 136.1, 135.98, 335.92, 135.6, 126.5, 125.9, 125.4, 125.0, 124.4, 123.0, 122.9, 122.8, 120.4, 120.0, 115.8, 115.7,56.5, 44.8,39.6, 39.2, 38.8,26.7.
	EIMS	Found 613.30 $[M+H]^+$, Calculated for $C_{32}H_{28}N_4O_3S_3$, 612.13 $[M]^+$
	HRMS	*M/z* (+EI) Calc. for $C_{32}H_{28}N_4O_3S_3$ 612.1324 $[M]^+$, found 613.1395$[M+H]^+$.
	IR	(FTIR), V_{max}/'cm^{-1}): 3302, 1634, 1575, 1526, 1445, 1339, 1300, 1271, 1231, 1154, 966, 874, 838, 803, 750, 715.

4.13 Synthesis of N-(2-((3-(dimethylamino) propyl) carbamoyl) benzo[b]thiophen-5-yl)-5-nitro benzofuran-2-carboxamide (4.13).

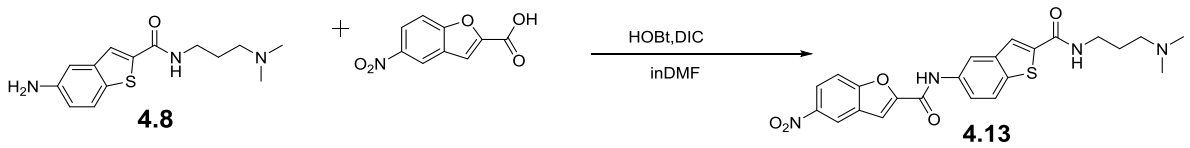

4.8 4.13

Initially, 5-nitrobenzofuran-2-carboxylic acid (143.48 mg, 0.693 mmol, 1.2 eq.) was dissolved in 20 mL of DMF in a round bottom flask which was placed on a magnetic stirrer. Then DIC (187.49 µl, 1.21 mmol, 1.75 eq.) and HOBt (187.11 mg, 1.386 mmol, 2.0 eq.) were added to the acid (1.0 eq.) and this mixture was allowed to stir at room temperature for 30 minutes for the esterification of acid. Then amine 4.8 (160 mg, 0.577 mmol, 1 eq.) was added to the mixture, and it was allowed to stir for 8 hours at which point TLC and LCMS analysis showed the completion of reaction. Finally the reaction mixture was applied to a conditioned Isolute^{TM} SCX-2 cartridge and the product was purified by 'Catch and Release' method **(**described in the section **'Method and Materials'** of chapter 3**)**. An orange solid was obtained after drying in vacuum. Yield=170mg, 65%.

Table 4.13: Characterisation data for compound **4.13**

4.13 Orange solid	^{1}H NMR	^{1}HNMR(400MHz,(CD_3OD); $^\delta$H in ppm 10.85(s,1H),8.79(d,*J*=2.0,2H),8.43(s,1H),8.05(s,1H),7.99(s,1H),7.95(t,*J*=8.0,2H),7.82(d,*J*=6.8,1H),3.30(t,*J*=6.0,2H),2.39(S,2H),2.23(s, 6H), 1.72(t,*J*=6.8,2H).
	EIMS	Found 567.10 $[M+H]^+$, Calculated for $C_{23}H_{22}N_4O_5S$, 466.13 $[M]^+$

4.14 Synthesis of 5-amino-N-(2-((3-(dimethylamino) propyl) carbamoyl) benzo[b]thiophen-5-yl) benzofuran-2-carboxamide (4.14).

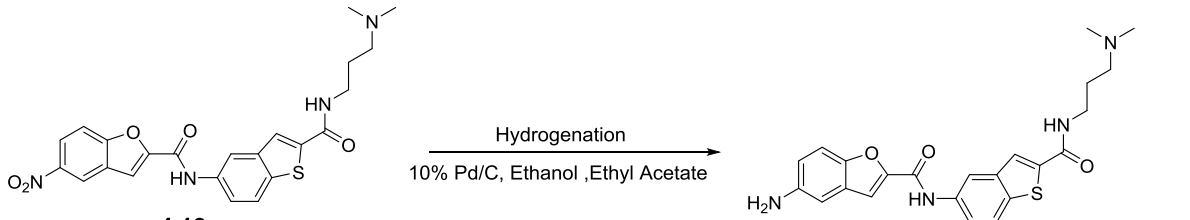

4.13 4.14

170 mg of **4.13** was dissolved in 20 mL of ethanol and 1 mL of ethyl acetate was added to a hydrogenation reaction bottle. 20 mg of 10% Pd (palladium on activated carbon) 20 was added into the same, and mixed well. The reaction bottle was sealed and connected to a hydrogen reservoir. Air from the reaction bottle was removed by means of vacuum, and was then by flushed with hydrogen. Approximately 40 psi of hydrogen pressure was applied from the reservoir, and the bottle was then shaken vigorously to initiate the reaction. Progress of the reaction was monitored by TLC and LCMS, and on completion of the reaction after 7 hours at which point TLC and LCMS analysis showed the completion of reaction.The shaker was stopped, the bottle vented. The product was recovered by means of filtration using Celite. Finally, the product is concentrated by using a rotary evaporator. A brown solid was obtained after drying in vacuum. Yield=145mg, 91%.

Table 4.14: Characterisation data for compound **4.14**

4.14 Brown solid	^{1}H NMR	^{1}HNMR(400MHz,$(CD_3)_2SO$); $^\delta$H in ppm 10.61(s,1H), 8.82(s,1H), 8.45(s,1H), 8.06(s,1H), 7.97(d,*J*=8.8,1H), 7.85(dd,*J*=8.8,2.0,1H),7.57(s,1H),7.39(d,*J*=8.8,1H),6.85-6.80(m,2H), 3.32-3.27(m,2H), 2.51-2.49(m,2H), 2.27(t,*J*=6.8,2H), 2.14(s,6H), 1.71-1.64(m,2H).
	EIMS	Found 437.0 $[M+H]^+$, Calculated for $C_{23}H_{24}N_4O_3S$, 436.15 $[M]^+$

4.15 Synthesis 5-(benzo[b]thiophene-2-carboxamido)-N-(2-((3-(dimethyl amino) propyl) carbamoyl) benzo[b]thiophen-5-yl) benzofuran-2-carboxamide (4.15).

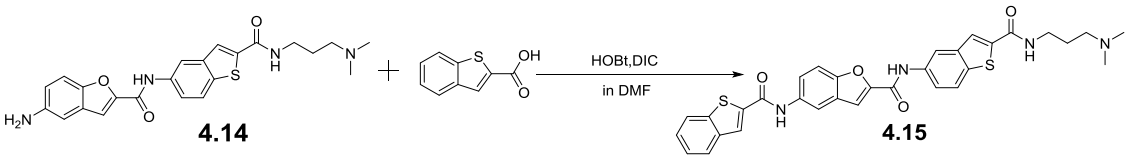

4.14 **4.15**

Initially, benzo[b]thiophene-2-carboxylic acid (40 mg, 0.224 mmol, 1.2 eq.) was dissolved in 10mL of DMF in a round bottom flask fitted with a magnetic stirrer. Then DIC (60 µl, 0.392 mmol, 1.75 eq.) and HOBt (60.48 mg, 0.448 mmol, 2.0 eq.) were added to the acid (1.0 eq.) and this mixture was allowed to stir at room temperature for 30 minutes to ensure the formation of ester from the acid. Then amine **4.14** (70 mg, 0.16 mmol, 1 eq.) was added to the same mixture and the mixture was allowed to stir for 5 hours at which point TLC and LCMS

analysis showed the completion of reaction. Finally the reaction mixture was applied to a conditioned Isolute^{TM} SCX-2 cartridge and the product was purified by 'Catch and Release' method **(**described in the section **'Method and Materials'** of chapter 3**)**. A pale yellow solid was obtained after drying in vacuum. Yield=28mg, 41%.

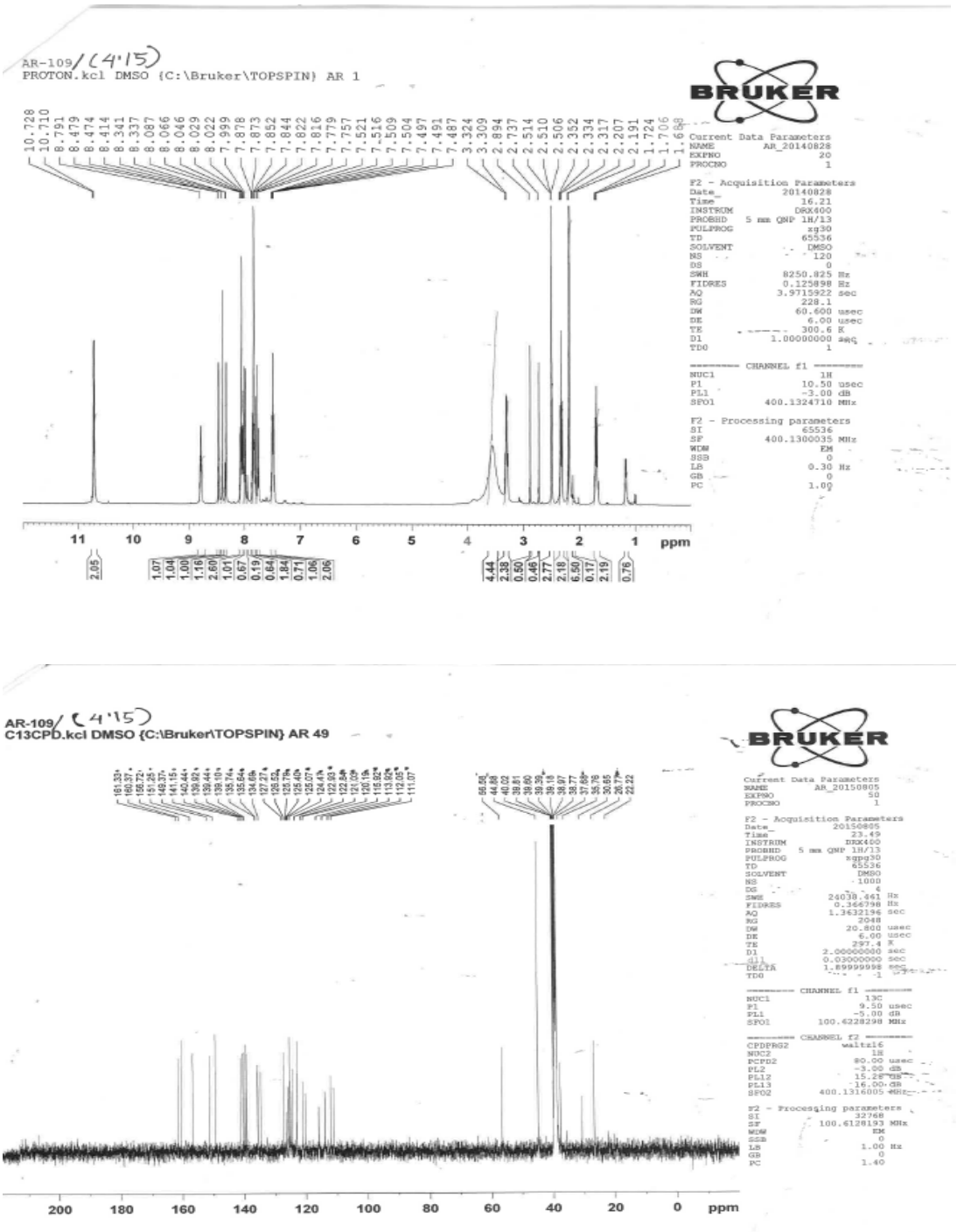

Figure 4.1: ^{1}H and ^{13}C NMR spectroscopic data of compound **4.15** as a representative of **library 1-A** compounds

Table 4.15: Characterisation data for compound **4.15**

4.15 Light Yellow solid	^{1}H NMR	^{1}HNMR(400MHz,$(CD_3)_2SO$); $^{\delta}$H in ppm 10.71(d,*J*=3.2,2H), 8.79(t,*J*=5.6,1H), 8.47(s,1H), 8.41(s,1H), 8.34(s,1H), 8.04(t,*J*=8.8,2H), 8.01(d,*J*=9.2,1H), 7.87(d,*J*=2,1H), 7.84(s,2H), 7.81(d,*J*=2.4,1H), 7.76(d,*J*=8.8,1H), 7.52-7.48 (m, 2H), 3.34-3.29(m,2H), 2.33 (t,*J*=7.2,2H), 2.20 (s,6H), 1.70(t,*J*=8.8,2H).
	^{13}C NMR	(100MHz,$(CD_3)_2SO$); $^{\delta}$C in ppm 161.3, 160.3, 156.7, 151.2, 149.3, 141.1, 140.4, 139.9,139.4, 139.1,135.7, 135.6,134.6, 127.2, 126.5, 125.7, 125.4, 125.0,124.4,122.9, 122.8, 121.0, 120.1, 115.9, 113.9, 112.0, 111.0, 56.5, 44.8, 39.3, 37.6,26.7.
	EIMS	Found 597.10 $[M+H]^+$, Calculated for $C_{32}H_{28}N_4O_4S_2$ 596.15 $[M]^+$
	HRMS	*m/z* (+EI) Calc. for $C_{32}H_{28}N_4O_4S_2$ 596.1552 $[M]^+$, found 597.1625$[M+H]^+$.
	IR	(FTIR, V_{max}/'cm^{-1}): 3285, 2936, 2762, 1741, 1660, 1634, 1585, 1539, 1470, 1447, 1427, 1343, 1297, 1273, 1232, 1207, 1142, 1126, 1040, 945, 893, 876, 847, 819, 809, 777, 755, 740, 720, 690.

4.16 Synthesis of N-(3-(dimethyl amino) propyl)-5-(5-nitro benzo [b]thiophene-2-carboxamido) benzofuran-2-carboxamide (4.16).

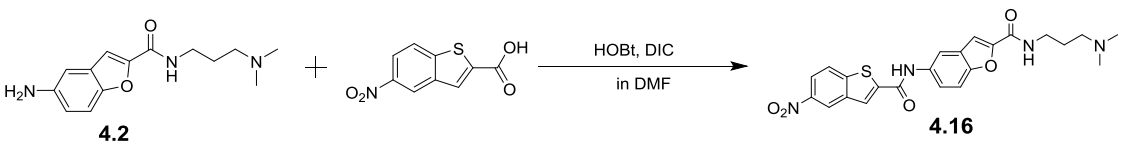

4.2 **4.16**

Initially, 118 mg of 5-nitrobenzo[b]thiophene-2-carboxylic acid (0.54 mmol, 1.2 eq.) was dissolved in 10mL of DMF in a round bottom flask fitted with a magnetic stirrer. Then DIC (146 µl, 0.945 mmol, 1.75 eq.) and HOBt (145.8 mg, 1.08 mmol, 2.0 eq.) were added to the acid (1.0 eq.) and this mixture was allowed to stir at room temperature for 30 minutes for the esterification of the acid. Then amine **4.2** (100.0 mg, 0.383 mmol, 1 eq.) was added to the mixture and the mixture was allowed to stir for 8 hours at which point TLC and LCMS analysis showed the completion of reaction. Finally the reaction mixture was applied to a conditioned Isolute^{TM} SCX-2 cartridge and the product was purified by 'Catch and Release' method **(**described in the section **'Method and Materials'** of chapter 3**)**. A deep brown solid was obtained after drying in vacuum. Yield=52 mg, 58%.

Table 4.16: Characterisation data for compound **4.16**

4.16 Deep Brown solid	^{1}H NMR	^{1}HNMR(400MHz,$(CD_3)_2SO$); $^\delta$H in ppm 10.87(s,1H), 8.87(d,*J*=5.2,2H), 8.38(s,1H), 8.27(dd,*J*=8.8,4.0,2H), 7.83(t,*J*=5.6,1H),7.66(dd,*J*=8.8,2.8,2H),7.45(s,1H),3.35(d,*J*=5.2,2 H), 2.51 (s,6H), 2.45(s,2H), 1.86(s,2H).
	EIMS	Found 467.10 $[M+H]^+$, Calculated for $C_{23}H_{22}N_4O_5S$, 466.13 $[M]^+$

4.17 Synthesis of 5-(5-aminobenzo[b]thiophene-2-carboxamido)-N-(3 (dimethylamino) propyl) benzofuran-2-carboxamide (4.17).

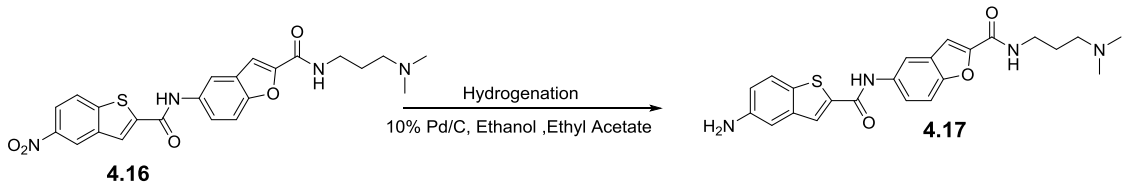

4.16 **4.17**

52 mg of **4.16** was dissolved in 20 mL of ethanol and 1 mL of ethyl acetate was added to a hydrogenation reaction bottle. 20 mg of 10% Pd (palladium on activated carbon) 20 was added into the reaction vessel, and mixed well. The reaction bottle was sealed and connected to a hydrogen reservoir. Air within the reaction bottle was removed by the application of vacuum, and was then by flushed with hydrogen. A hydrogen pressure of approximately 40 psi was applied from the reservoir, and the bottle was then shaken vigorously to initiate the reaction. Progress of the reaction was monitored by TLC and LCMS, and on completion of the reaction after 5 hours at which point TLC and LCMS analysis showed the completion of reaction. The shaker was stopped, the bottle vented, and the product was recovered by means of filtration using Celite. Finally, the product is concentrated by using a rotary evaporator. A light yellow solid was obtained after drying in vacuum. Yield=90 mg, 94%.

Table 4.17: Characterisation data for compound **4.17**

4.17 Light Yellow solid	^{1}H NMR	^{1}HNMR(400MHz,$(CD_3)_2SO$); $^{\delta}$H in ppm 10.59(s,1H),8.83(t,*J*=5.6,1H),8.24(d,*J*=2,1H),8.14(s,1H),7.807.75(m,1H),7.65(d,*J*=8.8,2H),7.54(s,1H),7.06(d,*J*=1.6,1H),6.86(dd,*J*=8.8,2.4,1H), 3.33-3.28(m,2H), 2.51(t,*J*=1.6,2H), 2.28-2.42 (m,2H), 2.14 (s,6H), 1.69-1.64(m,2H).
	EIMS	Found 536.10$[M+H]^+$, Calculated for $C_{23}H_{24}N_4O_3S$, 435.15 $[M]^+$

4.18 Synthesis of 5-(5-(benzofuran-2-carboxamido) benzo[b]thiophene-2-carboxamido)-N-(3-(dimethylamino) propyl) benzofuran-2-carboxamide (4.18).

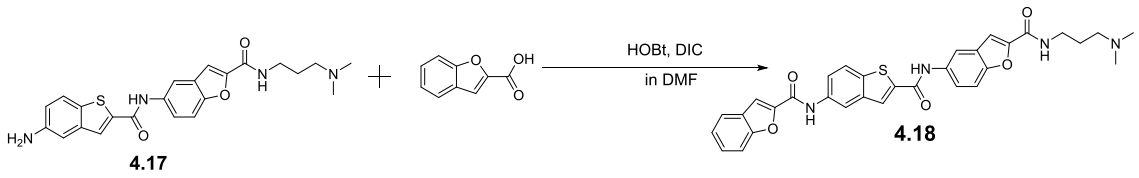

4.17 **4.18**

At the beginning, 46 mg of benzofuran-2-carboxylic acid (0.288 mmol, 1.2 eq.) was dissolved in 10mL of DMF in a round bottom flask fitted with a magnetic stirrer. Then DIC (77 µl, 0.504 mmol, 1.75 eq.) and HOBt (77 mg, 0.576 mmol, 2.0 eq.) were added to the acid (1.0 eq.) and this mixture was allowed to stir at room temperature for 30 minutes to ensure the ester formation. Then 90 mg of amine **4.17** (0.206 mmol, 1 eq.) was added to the mixture as, and the mixture was allowed to stir for 5 hours at which point TLC and LCMS analysis showed the completion of reaction. Lastly the reaction mixture was applied to a conditioned Isolute^{TM} SCX-2 cartridge and the product was purified by 'Catch and Release' method **(**described in the section **'Method and Materials'** of chapter 3**)**. A cream solid was obtained after drying in vacuum. Yield=42 mg, 36%.

Table 4.18: Characterisation data for compound **4.18**

4.18 Cream solid	^{1}H NMR	^{1}HNMR(400MHz,$(CD_3)_2SO$); $^{\delta}$H in ppm 10.77(s,1H),10.63(s,1H),8.83(s,1H),8.57(s,1H),8.39(s,1H), 8.27(s,1H),8.07(d,*J*=8.8,1H),7.94(d,*J*=7.2,1H),7.85(t,*J*=8,2H), 7.77(t,*J*=7.2,2H), 7.68 (d,*J*=8.8,1H), 7.53(t,*J*=7.6,2H), 7.39 (t,*J*=7.2, 1H), 3.32(t,*J*=6.8,2H), 2.27(t,*J*=6.4,2H), 2.21 (s,6H), 1.68(t,*J*=6.8,2H).
	^{13}C NMR	(100MHz,$(CD_3)_2SO$); $^{\delta}$C in ppm 160.2, 158.0, 156.8, 154.4, 150.9, 149.9, 148.5, 140.9, 139.3, 136.1,135.7, 134.3, 127.2, 127.0, 125.7, 123.9, 123.0, 122.9, 120.6, 116.1,113.9, 111.9, 111.8, 110.8, 109.4, 56.8, 45.0, 39.8, 39.2, 39.0, 37.3, 35.7.
	EIMS	Found 580.17 $[M+H]^+$, Calculated for $C_{32}H_{28}N_4O_5S$, 579.20 $[M]^+$
	HRMS	*M/z* (+EI) found 581.1851$[M+H]^+$.Calc. for $C_{32}H_{28}N_4O_5S$, 580.1780 $[M]^+$
	IR	(FTIR), V_{max}/'cm^{-1}): 3245, 2936, 1637, 1543, 1523, 1470, 1446, 1380, 1327, 1297, 1233, 1201, 1094, 1073, 1040, 964, 863, 806, 742, 714, 660.

4.19 Synthesis of N-(3-(dimethylamino) propyl)-5-nitro-1H-indole-2-carboxamide (4.19).

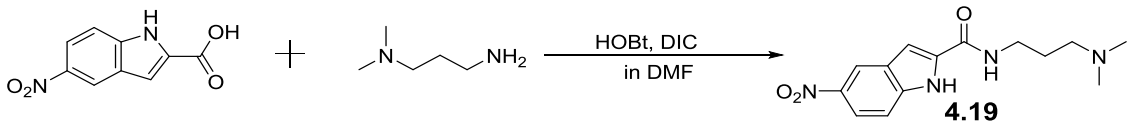

4.19

Initially, 400 mg of 5-nitro-1H-indole-2-carboxylic acid (1.94 mmol, 1.2 eq.) was dissolved in 10mL of DMF in a round bottom flask fitted with a magnetic stirrer. Then DIC (524 µl, 3.39 mmol, 1.75 eq.) and HOBt (523 mg, 3.88 mmol, 2.0 eq.) were added to the acid (1.0 eq.) and this mixture was allowed to stir at room temperature for 30 minutes to ensure the formation of ester from the acid. Then N1, N1-dimethylpropane-1, 3-diamine (160 µl, 1.56 mmol, 1 eq.) was added to the mixture and it was allowed to stir for about 7 hours at which point TLC and LCMS analysis showed the completion of reaction. At last the reaction mixture was applied to a conditioned Isolute^{TM} SCX-2 cartridge and the product was purified by 'Catch and Release' method **(**described in the section **'Method and Materials'** of chapter 3**)**. A yellow solid was obtained after drying in vacuum. Yield=300 mg, 54%.

Table 4.19: Characterisation data for compound **4.19**

4.19 Yellow solid	^{1}H NMR	^{1}HNMR(400MHz,$(CD_3)_2SO$); $^\delta$H in ppm 12.42(s,1H), 8.83(s,1H), 8.70(d,*J*=2,1H), 8.06(dd,*J*=8.8,2.0,1H), 7.56(d,*J*=9.2,1H), 7.37(s,1H), 3.34-3.30(m,2H), 2.27 (t,*J*=7.2,2H), 2.13 (s,4H), 1.67(t,2H).
	EIMS	Found 290.13 $[M+H]^+$, Calculated for $C_{14}H_{18}N_4O_3$, 289.10 $[M]^+$

4.20 Synthesis 5-amino-N-(3-(dimethylamino) propyl)-1H-indole-2-carboxamide (4.20).

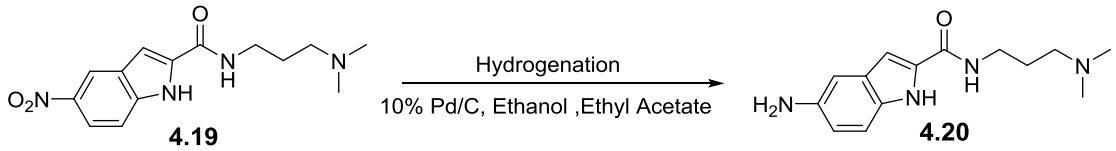

200mg of **4.19** was dissolved in 20 mL of ethanol and 1 mL of ethyl acetate was added to a hydrogenation reaction bottle. 20 mg of 10% Pd (palladium on activated carbon) 20 was added into the same, and mixed well. The reaction bottle was sealed and connected to a hydrogen reservoir. Air from the reaction bottle was removed under vacuum, and the reaction mixture was then flushed with hydrogen. Typically, a hydrogen pressure of approximately 40 psi was applied from the reservoir, and the bottle was then shaken vigorously to initiate the reaction. Progress of the reaction was monitored by TLC and LCMS, and the shaker was stopped on completion of the reaction after about 6 hours at which point TLC and LCMS analysis showed the completion of reaction. The product was recovered by means of filtration using Celite. Finally, the product is concentrated by using a rotary evaporator. An orange solid was obtained after drying in vacuum. Yield=250mg, 93%.

Table 4.20: Characterisation data for compound **4.20**

4.20 Orange solid	^{1}H NMR	^{1}HNMR(400MHz,$(CD_3)_2SO$); $^\delta$H in ppm 7.27(s,1H),7.25(s,1H),6.96(d,*J*=2,1H),6.87(s,1H),6.83(d,*J*=3.6,1H) , 6.80(d,*J*=2.0,1H), 3.40(t,*J*=6.8,2H), 3.33-3.32(m,2H), 2.44-2.41 (m,2H), 1.80 (t,*J*=7.2,4H), 1.11(d,*J*=6.8,2H).
	EIMS	Found 260.18 $[M+H]^+$, Calculated for $C_{14}H_{20}N_4O$, 260.16 $[M]^+$

4.21 Synthesis of N-(3-(dimethylamino) propyl)-5-(5-nitro-1H-indole-2-carboxamido)-1H-indole-2-carboxamide (4.21).

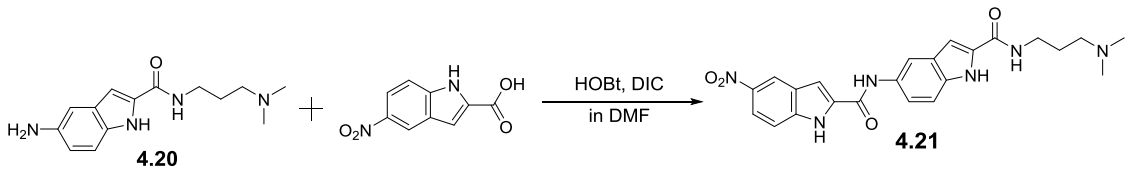

47 mg of 5-nitro-1H-indole-2-carboxylic acid (0.230 mmol, 1.2 eq.) was dissolved in 10mL of DMF in a round bottom flask and stirred. Then DIC (62 µl, 0.402 mmol, 1.75 eq.) and HOBt (62 mg, 0.460 mmol, 2.0 eq.) were added to the acid (1.0 eq.) and this mixture was allowed to stir at room temperature for 30 minutes to ensure the formation of ester from the acid.

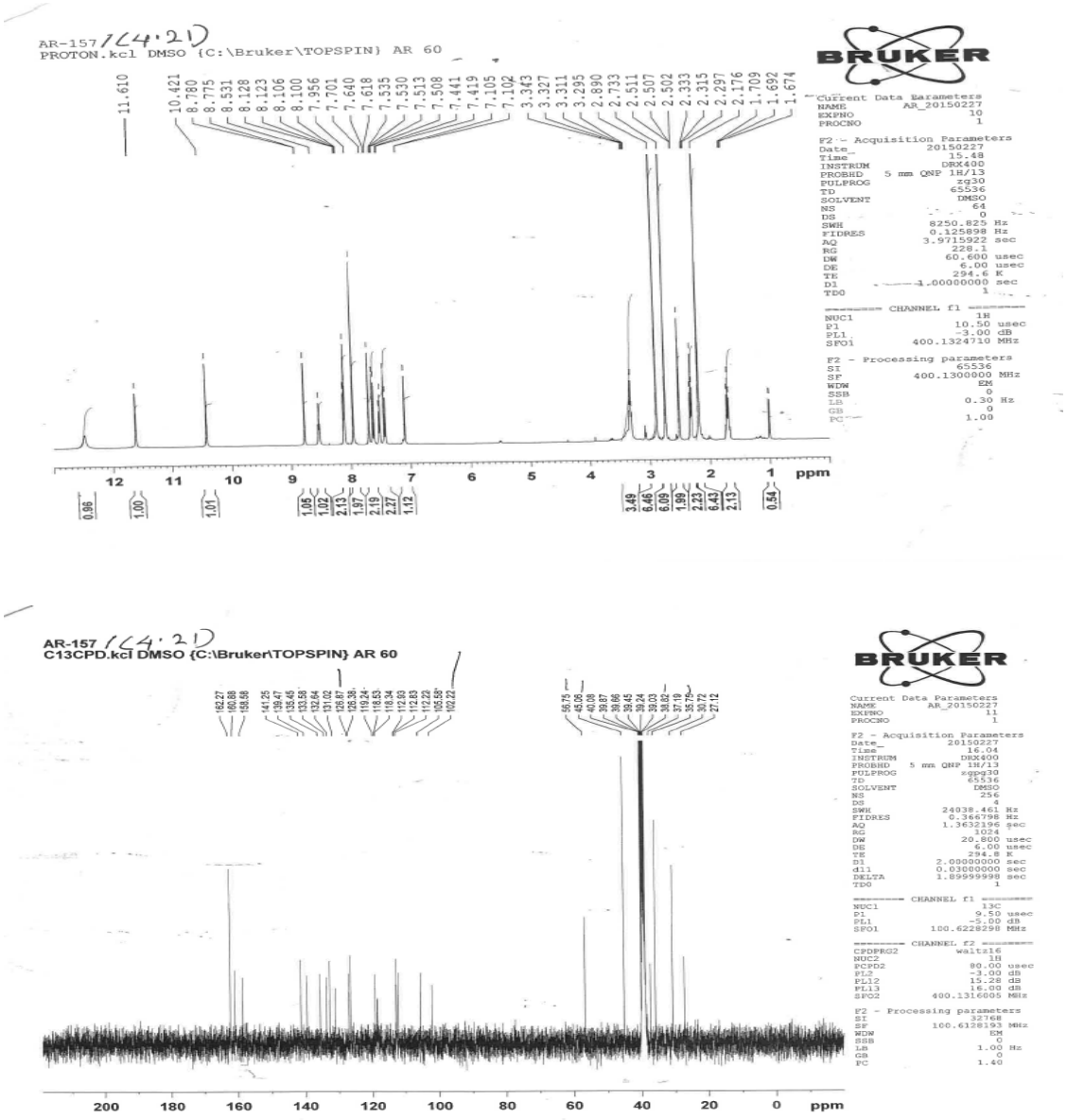

Figure 4.2: ^{1}H and ^{13}C NMR spectroscopic data of compound **4.21** as a representative of **library-5** compounds

Then amine **4.20** (50 mg, 0.192 mmol, 1 eq.) was added to the mixture and the mixture was allowed to stir for 8 hours at which point TLC and LCMS analysis showed the completion of reaction. Lastly the reaction mixture was applied to a conditioned Isolute^{TM} SCX-2 cartridge and the product was purified by 'Catch and Release' method **(**described in the section **'Method and Materials'** of chapter 3**)**. An orange solid was obtained after drying in vacuum. Yield=16mg, 19%.

Table 4.21: Characterisation data for compound **4.21**

4.21 Orange solid	^{1}H NMR	^{1}HNMR(400MHz,$(CD_3)_2SO$); $^{\delta}$H in ppm 12.47(s,1H),11.61(s,1H),10.42(s,1H),8.77(d,*J*=2.0,1H), 8.53(s,1H),8.11(dd,*J*=8.8,2.0,2H),7.70(s,1H),7.62(d,*J*=8.4,1H),7.52(dd,*J*=8.8,2.0,1H),7.10(s,1H),6.12(s,1H),3.34-3.29(m,2H), 2.50 (t,*J*=7.2,2H), 2.17 (s,6H), 1.69(t,*J*=6.8,2H).
	^{13}C NMR	(100MHz,$(CD_3)_2SO$); $^{\delta}$C in ppm 162.2, 160.8, 158.5, 141.2, 139.4, 135.4, 133.5, 132.6, 131.0, 126.8, 126.3, 119.2, 118.5, 118.3, 112.9, 112.8, 112.2, 105.5, 102.2, 56.7, 45.0, 38.8, 35.7.
	EIMS	Found 449.0 $[M+H]^+$, Calculated for $C_{23}H_{24}N_6O_4$, 448.18 $[M]^+$
	HRMS	*M/z* (+EI) Calc. for $C_{23}H_{24}N_6O_4$ $[M]^+$ 448.1859, found 449.1924$[M+H]^+$.
	IR	(FTIR), V_{max}/'cm^{-1}): 3270, 2970, 2301, 1738, 1611, 1536, 1536, 1468, 1439, 1365, 1342, 1312, 1236, 1209, 1169, 1128, 1094, 1039, 866, 802, 743, 683.

4.22 Synthesis of 5-amino-N-(2-((3-(dimethylamino) propyl) carbamoyl)-1H-indol-5-yl)-1H-indole-2-carboxamide (4.22).

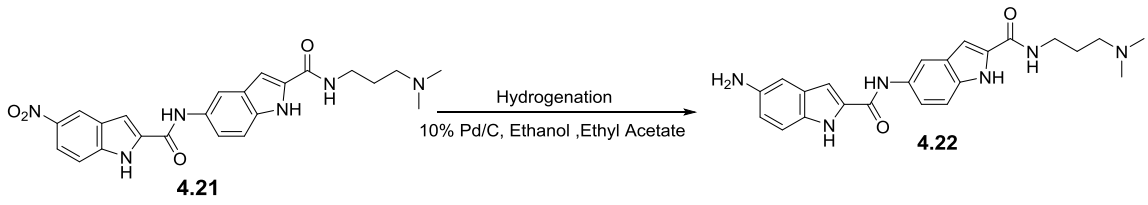

242 mg of **4.21** was dissolved in 20 mL of ethanol and 1mL of ethyl acetate was added to a hydrogenation reaction bottle. 20 mg of 10% Pd (palladium on activated carbon) 20 was added into the reaction vessel, and mixed well. The sealed reaction bottle was connected to a hydrogen reservoir. Air from the reaction bottle was removed by applying vacuum, and it was then by flushed with hydrogen. Typically, a hydrogen pressure of approximately 40 psi was applied from the reservoir, and the bottle was then shaken vigorously to initiate the reaction. Progress of the reaction was monitored by TLC and LCMS, and on

completion of the reaction after about 6 hours at which point TLC and LCMS analysis showed the completion of reaction.The shaker was stopped, the bottle vented, and the product was recovered by means of filtration using Celite. Finally, the product is concentrated by using a rotary evaporator. A yellow solid was obtained after drying in vacuum. Yield=210 mg, 93%.

Table 4.22: Characterisation data for compound **4.22**

4.22 Yellow solid	^{1}H NMR	^{1}HNMR(400MHz,$(CD_3)_2SO$); $^\delta$H in ppm 11.55(s,1H), 11.24(s,1H), 9.95(s,1H), 8.50(t,*J*=5.6,1H), 8.07(s,1H), 7.47(dd,*J*=8.8,1.6,1H), 7.37 (d,*J*=8.8,1H), 7.15(d,*J*=8.8,1H), 7.07(d,*J*=8.8,2H), 6.71(s,1H), 6.62(dd,*J*=8.8,2.0,1H), 3.31-3.26(m,2H), 2.25 (t,*J*=6.8,2H), 2.13(s,4H), 2.12 (s,2H), 1.67-1.61(m,2H).
	EIMS	Found 419.0 $[M+H]^+$, Calculated for $C_{23}H_{26}N_6O_2$, 418.21 $[M]^+$

4.23 Synthesis of 5-amino-N-(2-((3-(dimethylamino) propyl) carbamoyl)-1H-indol-5-yl)-1H-indole-2-carboxamide (4.23).

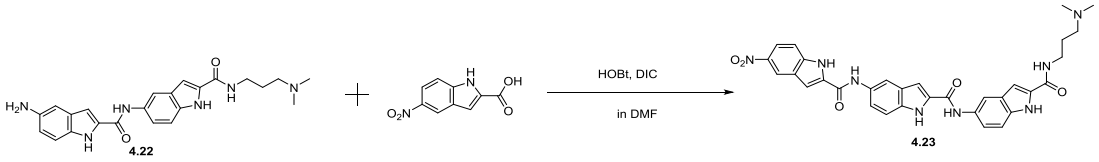

Initially, 50 mg of 5-nitro-1H-indole-2-carboxylic acid (0.186 mmol, 1.2 eq.) was dissolved in 10mL of DMF in a round bottom flask fitted with a magnetic stirrer. Then DIC (51 µl, 0.325 mmol, 1.75 eq.) and HOBt (50.8 mg, 0.372 mmol, 2.0 eq.) were added to the acid (1.0 eq.) and this mixture was allowed to stir at room temperature for 30 minutes to ensure the formation of ester from the acid. Then amine **4.22** (65 mg, 0.155 mmol, 1 eq.) was added and the mixture was allowed to stir for 5 hours at which point TLC and LCMS analysis showed the completion of reaction. Finally the reaction mixture was added to a conditioned Isolute^{TM} SCX-2 cartridge and the product was purified by 'Catch and Release' method **(**described in the section **'Method and Materials'** of chapter 3**)**. A pale yellow solid was obtained after drying in vacuum. Yield=27 mg, 29%.

Table 4.23: Characterisation data for compound **4.23**

4.23 Yellow solid	^{1}H NMR	^{1}HNMR(400MHz,$(CD_3)_2SO$); $^{\delta}$H in ppm 12.48(s,1H), 11.75(s,1H), 11.58(s,1H), 10.45(s,1H), 10.14(s,1H), 8.78(s,1H), 8.53(s,1H), 8.17(s,1H), 8.11(s,2H), 7.71(s,1H), 7.63(d,*J*=9.2,1H), 7.57(d,*J*=8.4,1H), 7.50 (t,*J*=9.6,2H), 7.43(s,2H), 7.10(s,1H), 3.34(d,*J*=7.2,2H), 2.35 (s,2H), 2.22 (s,4H), 1.71(d,*J*=6.4,2H).
	^{13}C NMR	(100MHz,$(CD_3)_2SO$); $^{\delta}$C in ppm 162.2, 160.9, 159.3, 158.6, 141.2, 139.4, 135.4, 133.9, 133.4, 132.6, 132.5, 131.3, 131.1, 126.9, 126.3, 119.2, 118.7, 118.5, 118.3, 1130, 112.8, 112.6, 112.3, 112.1, 105.6, 103.3, 102.2, 56.6, 44.9, 39.2, 35.7, 30.7.
	EIMS	Found 607.10 $[M+H]^+$, Calculated for $C_{32}H_{30}N_8O_5$, 606.23 $[M]^+$
	HRMS	*m/z* (+EI) Calc. for $C_{32}H_{30}N_8O_5$, 606.2339 $[M]^+$, found 607.2405$[M+H]^+$.
	IR	(FTIR), V_{max}/'cm^{-1}): 3242, 2938, 1660, 1634, 1585, 1545, 1519, 1471, 1445, 1417, 1382, 1328, 1295, 1250, 1230, 1126, 1096, 1067, 982, 870, 810, 740, 679, 661.

4.24 Synthesis of N-(3-(dimethylamino) propyl)-5-(5-(1-methyl-1H-indole-2-carboxamido)-1H-indole-2-carboxamido)-1H-indole-2-carboxamide (4.24)

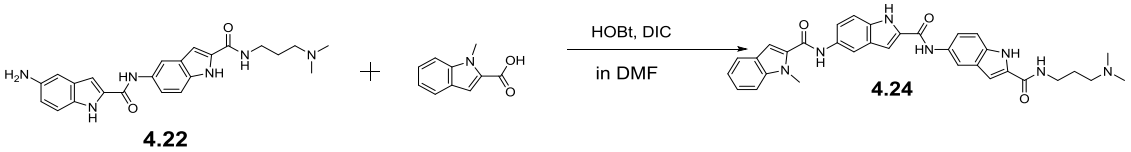

4.22 **4.24**

Initially, 21.87 mg of 1-methyl-1H-indole-2-carboxylic acid (0.125 mmol, 1.2 eq.) was dissolved in 10mL of DMF in a round bottom flask fitted with a magnetic stirrer. Then DIC (34 µl, 0.218 mmol, 1.75 eq.) and HOBt (34 mg, 0.250 mmol, 2.0 eq.) were added to the acid (1.0 eq.) and this mixture was allowed to stir at room temperature for 30 minutes for the formation of ester from the acid. Then amine **4.22** (50 mg, 0.104 mmol, 1 eq.) was added and the mixture was stirred for 6 hours at which point TLC and LCMS analysis showed the completion of reaction. At last the reaction mixture was applied to a conditioned Isolute^{TM} SCX-2 cartridge and the product was purified by 'Catch and Release' method **(**described in the section **'Method and Materials'** of chapter 3**)**. A yellow coloured solid was collected after drying in vacuum. Yield=10mg, 15%.

Table 4.24: Characterisation data for compound **4.24**

4.24 Yellow solid	^{1}H NMR	^{1}HNMR(400MHz,$(CD_3)_2SO$); $^{\delta}$H in ppm 11.76(s,1H),11.60(s,1H),10.27(s,1H),10.20(s,1H), 8.54(d,*J*=5.6,1H), 8.17(s,1H), 8.10(t,*J*=6.4,1H), 7.70(d,*J*=8.0,1H), 7.58(d,*J*=8.4,1H), 7.56-7.54(m,2H),7.44(t,*J*=8.8,2H),7.40(d,*J*=2.8,1H), 7.32(t,*J*=6.4,2H), 7.16(t,*J*=7.6,1H), 7.14(s,1H), 4.05(s,3H). 3.66-3.61(m, 2H), 3.08 (s, 2H), 2.73 (s, 4H), 2.15(s, 2H)**.**
	^{13}C NMR	(100MHz,$(CD_3)_2SO$); $^{\delta}$C in ppm 162.3, 161.2, 160.9, 160.2, 159.3, 156.8, 139.2, 138.5, 133.7, 133.4, 132.5, 132.4, 131.6, 131.3, 126.8, 125.5, 123.7, 121.6, 120.2, 118.4, 112.6, 112.2, 112.1, 110.5, 105.0, 56.8, 45.1, 39.4, 35.7, 31.4, 30.7, 28.9, 27.2.
	EIMS	Found 576.10 $[M+H]^+$, Calculated for $C_{33}H_{33}N_7O_3$, 575.26 $[M]^+$
	HRMS	*m/z* (+EI) Calc. for $C_{33}H_{33}N_7O_3$ $(M)^+$ 575.2645, found 576.2714$[M+H]^+$.
	IR	(FTIR), V_{max}/'cm^{-1}): 3268, 2968, 2343, 2300, 1738, 1616, 1536, 1467, 1438, 1368, 1341, 1313, 1236, 1211, 1168, 1128, 1087, 1038, 866, 804, 743, 683.

4.25 Synthesis of N-(2-((2-((3-(dimethylamino) propyl) carbamoyl) benzo[b]thiophen-5-yl) carbamoyl) benzofuran-5-yl)-1-methyl-1H-indole-2-carboxamide (4.25)

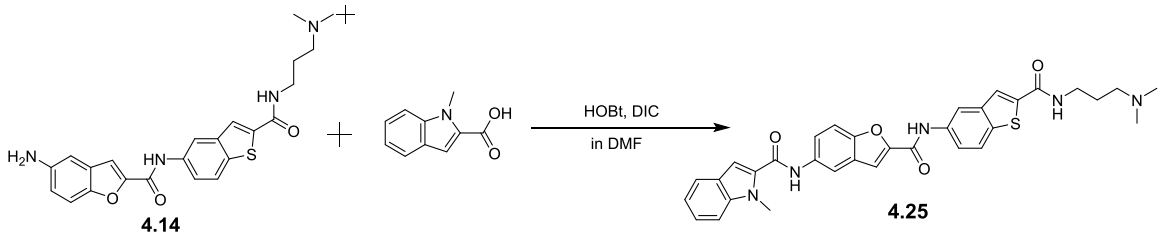

29 mg of 1-methyl-1H-indole-2-carboxylic acid (0.156 mmol, 1.2 eq.) was dissolved in 5 mL of DMF in a round bottom flask fitted with a magnetic stirrer. Then DIC (45 µl, 0.228 mmol, 1.75 eq.) and HOBt (45 mg, 0.330 mmol, 2.0 eq.) were added to the acid (1.0 eq.) and this mixture was allowed to stir at room temperature for 30 minutes to confirm esterification. Then amine **4.14** (60 mg, 0.137 mmol, 1 eq.) was added and the mixture was allowed to stir for 12 hours at which point TLC and LCMS analysis showed the completion of reaction. Finally the reaction mixture was applied to a conditioned Isolute^{TM} SCX-2 cartridge and the product was purified by 'Catch and Release' method

(described in the section **'Method and Materials'** of chapter 3**)**. A pale yellow solid was obtained after drying in vacuum. Yield=18mg, 23%.

Table 4.25: Characterisation data for compound **4.25**

4.25 Light Yellow solid	^{1}H NMR	^{1}HNMR(400MHz,$(CD_3)_2SO$); $^{\delta}$H in ppm 10.70(s,1H), 10.48(s,1H), 8.77(s,1H), 8.47(s,1H), 8.38(s,1H), 8.06(s,1H), 8.00(d,*J*=8.8,1H), 7.86(d,*J*=8.8,1H), 7.82(d,*J*=8.4,2H), 7.73(t,*J*=8.4,2H), 7.57(d,*J*=8.4,1H), 7.36(s,1H), 7.34(t,*J*=7.6,1H), 7.15(t,*J*=7.6, 1H), 4.05(s,3H), 3.32(t,*J*=6.8,2H), 2.28(t,*J*=6.8,2H), 2.15(s,6H), 1.69(t,*J*=7.2,2H).
	^{13}C NMR	(100MHz,$(CD_3)_2SO$); $^{\delta}$C in ppm 161.3, 160.5, 156.7, 151.0, 149.3, 141.1, 139.4, 138.6, 135.7, 135.6, 135.1, 131.9, 127.2, 125.4, 124.4, 123.9, 122.9, 121.7, 120.9, 120.3, 115.9, 113.5, 111.9, 111.0, 110.5, 105.5, 56.7, 45.0, 41.4, 39.6, 38.8,37.7, 31.4.
	EIMS	Found 594.2 $[M+H]^+$, Calculated for $C_{33}H_{31}N_5O_4S$, 593.2097 $[M]^+$
	HRMS	*M/z* (+EI) Calc. for $C_{33}H_{31}N_5O_4S$, 593.2097$[M]^+$, found 594.2169$[M+H]^+$.
	IR	(FTIR), V_{max}/'cm^{-1}): 3266, 2938, 2219, 1705, 1632, 1532, 1475, 1438, 1360, 1331, 1308, 1221, 1159, 1097, 1039, 945, 885, 807, 770, 741, 715, 619.

4.26 Synthesis of 5-nitro-N-(2-(piperidin-1-yl) ethyl) benzofuran-2-carboxamide (4.26)

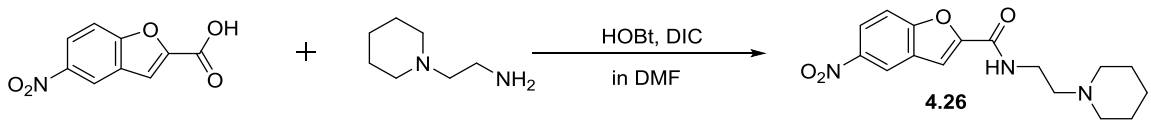

Initially, 200 mg of 5-nitrobenzofuran-2-carboxylic acid (0.966 mmol, 1.2 eq.) was dissolved in 10mL of DMF in a round bottom flask and it is stirred to mix well. Then DIC (260 µl, 1.69 mmol, 1.75 eq.) and HOBt (260 mg, 1.93 mmol, 2.0 eq.) were added to the acid (1.0 eq.) and this mixture was stirred at room temperature for at least 30 minutes to ensure the formation of ester from the acid. Then 2-(piperidin-1-yl) ethan-1-amine (104 mg, 0.805 mmol, 1 eq.) was added and the mixture was allowed to stir for 14 hours at which point TLC and LCMS analysis showed the completion of reaction. Finally the product was purified by 'Catch and Release' method using the conditioned Isolute^{TM} SCX-2 cartridge **(**described in the section **'Method and Materials'** of chapter 3**)**. A pale yellow solid was collected after drying in vacuum. Yield=160 mg, 66%.

Table 4.26: Characterisation data for compound **4.26**

4.26 Pale Yellow Solid	^{1}H NMR	^{1}H NMR(400MHz,CD_3OD); $^\delta$H in ppm 8.50(d,*J*=2.4,1H), 8.21(dd,*J*=6.8,2.4,1H), 7.60 (d,*J*=9.2,1H), 7.43(s,1H), 3.60(t,*J*=6.8,2H), 2.85-2.64(m,2H), 2.48(s,4H), 1.68-1.63(m,4H), 1.30(d,2H).
	EIMS	Found 318.0 $[M+H]^+$, Calculated for $C_{16}H_{19}N_3O_4$ 317.13 $[M]^+$

4.27 Synthesis of 5-amino-N-(2-(piperidin-1-yl) ethyl) benzofuran-2-carboxamide (4.27)

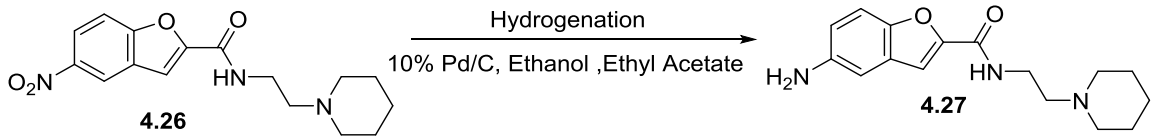

155 mg of **4.26** was dissolved in 20 mL of ethanol and 1 mL of ethyl acetate was added to a hydrogenation reaction bottle. 20 mg of 10% Pd (palladium on activated carbon) 20 was added into the same and mixed it well. The sealed reaction bottle was connected to a hydrogen reservoir and air from the reaction bottle was removed by applying vacuum. The mixture was then flushed with hydrogen. A hydrogen pressure of approximately 40 psi was applied from the reservoir, and the bottle was then shaken vigorously to initiate the reaction. Progress of the reaction was observed by TLC and LCMS. The shaker was stopped after about 6 hours at which point TLC and LCMS analysis showed the completion of reaction. The bottle was vented and the product was recovered by means of filtration using Celite. Finally, the product was concentrated by using a rotary evaporator. A pale yellow solid was obtained after drying in vacuum. Yield=136 mg, 96 %.

Table 4.27: Characterisation data for compound **4.27**

4.27 Yellow Solid	^{1}H NMR	^{1}H NMR(400MHz,CD_3OD); $^\delta$H in ppm 7.26(t,*J*=6.0,2H),6.95(d,*J*=2.0,1H),6.90(dd,*J*=8.8,2.4,1H),3.56(t, *J*=6.8,2H),2.64(t,*J*=6.8,2H), 2.55(s,4H), 1.64-1.58(m,4H), 1.45(d, 6.0,2H).
	EIMS	Found 288.0 $[M+H]^+$, Calculated for $C_{16}H_{21}N_3O_2$ 287.16 $[M]^+$

4.28 Synthesis of 5-nitro-N-(2-((2-(piperidin-1-yl) ethyl) carbamoyl) benzofuran-5-yl) benzofuran-2-carboxamide (4.28)

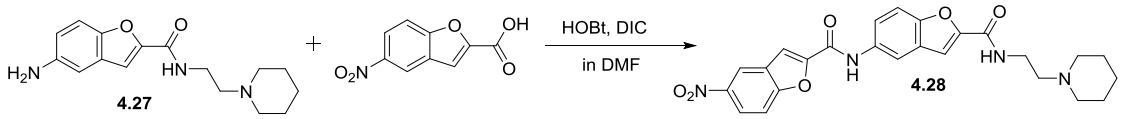

Initially, 60 mg of 5-nitrobenzofuran-2-carboxylic acid (0.208 mmol, 1.2 eq.) has been dissolved in 10mL of DMF in a round bottom flask placed into a magnetic stirrer. Then DIC (78.69 µl, 0.509 mmol, 1.75 eq.) and HOBt (78.57 mg, 0.582 mmol, 2.0 eq.) were added to the acid (1.0 eq.) and this mixture was allowed to stir at room temperature for 30 minutes to ensure the ester formation from the acid. The mixture was allowed to stir for 14 hours after addition of an amine **4.27** (60 mg, 0.208 mmol, 1 eq.), at which point TLC and LCMS analysis showed the completion of reaction. At last the reaction mixture was applied to a conditioned Isolute^{TM} SCX-2 cartridge and the product was purified by 'Catch and Release' method **(**described in the section **'Method and Materials'** of chapter 3**)**. A pale yellow colured solid was obtained after drying in vacuum. Yield=65mg, 65%.

Table 4.28: Characterisation data for compound **4.28**

4.28 Pale Yellow Solid	^{1}H NMR	^{1}HNMR(400MHz,$(CD_3)_2SO$); $^\delta$H in ppm 10.80(s,1H),8.81(d,*J*=2.40,1H),8.34(dd,*J*=9.2,2.4,1H),8.27(d,*J*= 2,1H),7.97-7.94(m,2H),7.78(dd,*J*=8.8,2.0,1H), 7.66(d,*J*=8.8,1H), 2.8(s, 2H), 2.43(t, *J*=6.8, 2H), 2.36(s, 4H), 1.51-1.45(m,4H), 1.37(d*J*=4.8,2H).
	EIMS	Found 477.0 $[M+H]^+$, Calculated for $C_{25}H_{24}N_4O_6$, 476.16 $[M]^+$

4.29 Synthesis of 5-amino-N-(2-((2-(piperidin-1-yl) ethyl) carbamoyl) benzofuran-5-yl) benzofuran-2-carboxamide (4.29)

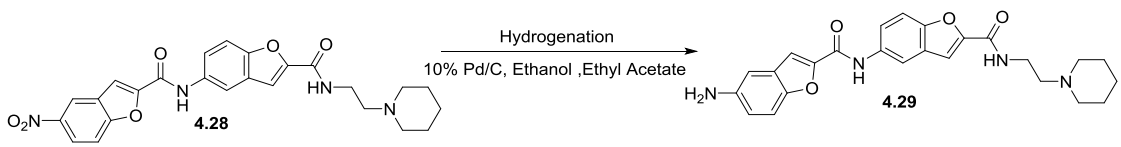

65 mg of **4.28** was dissolved in 20 mL of ethanol and 1 mL of ethyl acetate was added into a hydrogenation reaction bottle. 20 mg of 10% Pd (palladium on activated carbon) 20 was added into the same and mixed it well. The reaction bottle was sealed and connected to a hydrogen reservoir. Air of the bottle was removed by applying vacuum, and it was then flushed with hydrogen. Approximately 40 psi hydrogen pressure was applied from the reservoir, and the bottle was then shaken vigorously to initiate the reaction. Progress of the reaction was monitored by TLC and LCMS, and the shaker was stopped on completion of the reaction after 6 hours at which point TLC and LCMS analysis showed the completion of reaction. The bottle was vented and the product was recovered by means of filtration using Celite. Finally, the product was concentrated by using a rotary evaporator. A brown solid was obtained after drying in vacuum. Yield=52 mg, 85%.

Table 4.29: Characterisation data for compound **4.29**

4.29 Brown Solid	^{1}H NMR	^{1}HNMR(400MHz,$(CD_3)_2SO$); $^\delta$H in ppm 10.57(s,1H),8.60(t,*J*=6.0,1H),8.27(d,*J*=2,1H),7.94(t,*J*=4.0,1H), 7.79(dd,*J*=9.2,2.4,1H),7.63(d,*J*=9.2,1H),7.54(s,2H),7.37(d,*J*=8.8,1H) , 6.82(d,*J*=2,1H),6.80(d,*J*=2.4,1H),3.393.35(m,2H),3.16(s,2H),2.72(s, 2H),2.50-2.48(m,2H), 2.43(m,2H), 2.36(s,4H), 1.49-1.45(m,4H).
	EIMS	Found 447.0 $[M+H]^+$, Calculated for $C_{25}H_{26}N_4O_4$, 446.19 $[M]^+$

4.30 Synthesis of 5-(benzofuran-2-carboxamido)-N-(2-((2-(piperidin-1-yl) ethyl) carbonyl) benzofuran-5-yl) benzofuran-2-carboxamide (4.30)

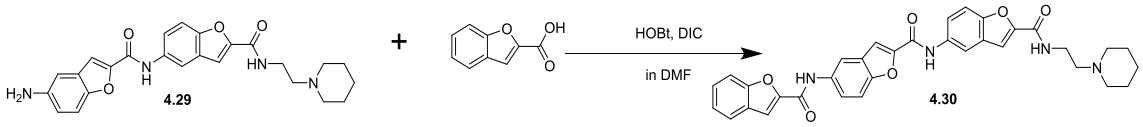

Initially, 23 mg of benzofuran-2-carboxylic acid (0.139 mmol, 1.2 eq.) was dissolved in 10mL of DMF in a round bottom flask fitted with a magnetic stirrer. Then DIC (38 µl, 0.243 mmol, 1.75 eq.) and HOBt (38 mg, 0.278 mmol, 2.0 eq.) were added to the acid (1.0 eq.) and this mixture was stirred at room temperature for at least 30 minutes to ensure the ester formation from the acid. Then amine **4.29** (52 mg, 0.116 mmol, 1 eq.) was and the mixture was allowed to stir for 7 hours at which point TLC and LCMS analysis showed the

completion of reaction. Finally the reaction mixture was applied to a conditioned Isolute^{TM} SCX-2 cartridge and the product was purified by 'Catch and Release' method **(**described in the section **'Method and Materials'** of chapter 3**)**. A pale yellow coloured solid was obtained after drying under vacuum. Total yield was12mg, 18%.

Table 4.30: Characterisation data for compound **4.30**

4.30 Pale Yellow Solid	^{1}H NMR	^{1}HNMR(400MHz,$(CD_3)_2SO$); $^{\delta}$H in ppm 10.73(s1H),10.69(s,1H),8.74(s,1H),8.35(d,*J*=2,1H),8.30(d,*J*=2, 1H),7.87(d,*J*=2,1H),7.85(d,*J*=6.8,1H),7.83-7.82(m,2H), 7.81-7.79(m,1H),7.76(d,*J*=2.8,1H),7.74(t,*J*=1.2,1H), 7.67(d,*J*=9.2,1H),7.54-7.50(m,1H),7.40-7.35(m,1H), 3.164(s,2H),2.72(d,*J*=0.8,4H),1.58(t,*J*=6.0,4H), 1.43(d,*J*=4,2H), 1.00(d,*J*=6.4,2H).
	^{13}C NMR	($100MHz,(CD_3)_2SO$); $^{\delta}$C in ppm 195.9, 194.7, 193.9, 184.0, 181.3, 162.6, 161.2, 155.8, 154.6, 150.5, 149.4, 138.9, 137.0, 130.8, 127.5, 123.5, 121.1, 116.1,112.2,110.7, 109.3,106.9, 98.7, 95.3, 75.9,66.7,59.3, 40.0, 39.87, 39.6, 39.2,39.0,38.8, 37.9.
	EIMS	Found 591.3 $[M+H]^+$, Calculated for $C_{34}H_{30}N_4O_6$, 590.21 $[M]^+$
	HRMS	*m/z* (+EI) Calc. for $C_{34}H_{30}N_4O_6$, 590.2165 $[M]^+$, found 591.2244$[M+H]^+$.
	IR	(FTIR), V_{max}/'cm^{-1}): 3351, 2925, 1658, 1583, 1538, 1473, 1358, 1297,1198, 1128, 1045, 942, 870, 802, 743, 609.

4.31 Synthesis of 5-(benzo[b]thiophene-2-carboxamido)-N-(2-((2-(piperidin-1-yl) ethyl) carbamoyl) benzofuran-5-yl) benzofuran-2-carboxamide (4.31)

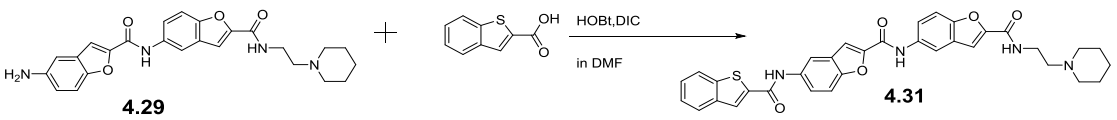

4.29 **4.31**

22 mg of benzo[b]thiophene-2-carboxylic acid (0.125 mmol, 1.2 eq.) was dissolved in 10mL of DMF in a round bottom flask placed at magnetic stirrer. Then DIC (33 µl, 0.218 mmol, 1.75 eq.) and HOBt (33mg, 0.25 mmol, 2.0 eq.) were added to the acid (1.0 eq.) and this mixture was allowed to stir at room temperature for 30 minutes to ensure the formation of ester from the acid. Then amine **4.29** (40 mg, 0.089 mmol, 1 eq.) was added and the mixture was allowed

to stir for 6 hours at which point TLC and LCMS analysis showed the completion of reaction. Lastly the product was purified by 'Catch and Release' method using a conditioned Isolute^{TM} SCX-2 cartridge **(**described in the section **'Method and Materials'** of chapter 3**)**. A white solid was obtained after drying in vacuum. Yield=8 mg, 15%.

Table 4.31: Characterisation data for compound **4.31**

4.31 White Solid	^{1}H NMR	^{1}HNMR(400MHz,$(CD_3)_2SO$); $^{\delta}$H in ppm 10.70(d,*J*=4,2H), 8.78(s,1H), 8.40(s,1H),8.32-8.30(m,2H), 8.07(d,*J*=7.6,1H), 8.04-8.02(m,1H), 7.95(s,1H), 7.83(d,*J*=4,1H) ,7.80(d,*J*=2,1H), 7.76(d,*J*=8.8,1H), 7.67(d,*J*=9.2,1H), 7.60(s,1H), 7.52-7.48(m,2H), 2.88(s,2H), 2.72(s,2H), 2.08(s,2H), 1.59(d,*J*=6.0,4H), 1.44(s,2H).
	^{13}C NMR	(100MHz,$(CD_3)_2SO$); $^{\delta}$C in ppm 179.7, 179.3, 176.3, 176.0, 174.4,174.2, 172.7, 166.7, 166.5, 166.1, 158.9, 158.6, 149.3, 139.8, 136.18, 134.7, 132.8, 131.2, 130.5, 125.8, 118.7, 116.0, 112.1, 108.0, 107.5, 106.2, 104.8, 47.2, 41.9, 40.0, 39.8, 39.6, 39.4, 39.2.
	EIMS	Found 607.0 $[M+H]^+$, Calculated for $C_{34}H_{30}N_4O_5S$ 606.1937 $[M]^+$
	HRMS	*m/z* (+EI) Calc. for $C_{34}H_{30}N_4O_5S$, 606.1937 $[M]^+$, found 607.2010 $[M+H]^+$.
	IR	(FTIR), V_{max}/'cm^{-1}): 3281, 2956, 1638, 1574, 1531, 1468, 1393, 1339, 1290, 1233, 1154, 1086, 1039, 952, 878, 809, 738, 716.

4.32 Synthesis of 5-nitro-N-(4-(pyrrolidin-1-yl) butyl) benzofuran-2-carboxamide (4.32)

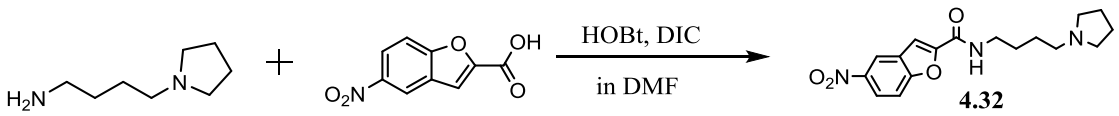

4.32

Initially, 500 mg of 5-nitrobenzofuran-2-carboxylic acid (2.41 mmol, 1.2 eq.) was dissolved in 10mL of DMF in a round bottom flask fitted with a magnetic stirrer. Then DIC (650.77 µl, 4.21 mmol, 1.75 eq.) and HOBt (650.7 mg, 4.82 mmol, 2.0 eq.) were added to the acid (1.0 eq.) and this mixture was allowed to stir at room temperature for 30 minutes to ensure the ester formation from the acid. Then 4-(pyrrolidin-1-yl) butan-1-amine (284 µl, 2.0 mmol, 1 eq.) was added and the mixture was stirred for 8 hours at which point TLC and LCMS analysis showed the completion of reaction. Finally the reaction mixture was applied to a

conditioned Isolute^{TM} SCX-2 cartridge and the product was purified by 'Catch and Release' method **(**described in the section **'Method and Materials'** of chapter 3**)**. A brown solid was obtained after drying in vacuum. Yield=545 mg, 82%.

Table 4.32: Characterisation data for compound **4.32**

4.32 Brown Solid	^{1}H NMR	^{1}HNMR(400MHz,(CD_3OD); $^{\delta}$H in ppm 8.51(d,*J*=2.4,1H),8.22(dd,*J*=9.2,2.4,1H),7.60(d,*J*=12.8,,1H), 7.44(s,1H), 3.37-3.32(m,2H), 2.51(s,2H), 2.48(s,2H), 2.45(s,2H), 1.72-1.69(m,4H), 1.67-1.61(m,4H).
	EIMS	Found 332.0 $[M+H]^+$, Calculated for $C_{17}H_{21}N_3O_4$, 331.15 $[M]^+$

4.33 Synthesis of 5-amino-N-(4-(pyrrolidin-1-yl) butyl) benzofuran-2-carboxamide (4.33)

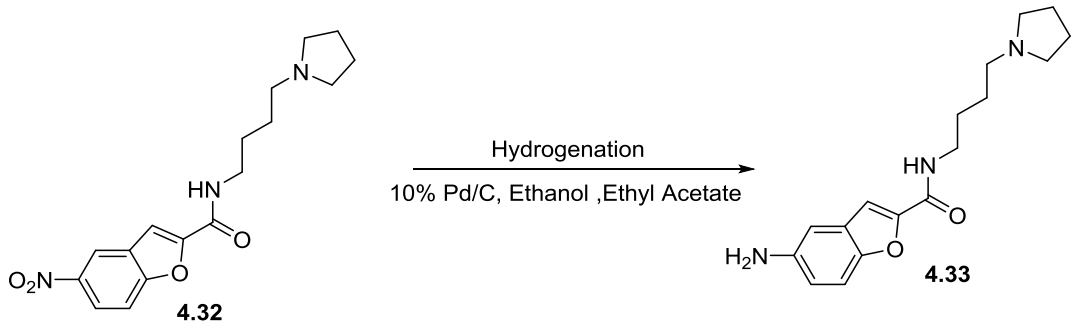

545 mg of **4.32** was dissolved in 20 mL of ethanol and 1 mL of ethyl acetate was added to a hydrogenation reaction bottle. 20 mg of 10% Pd (palladium on activated carbon) 20 was added into the reaction mixture and mixed it well. The sealed bottle has been connected to a hydrogen reservoir. Air from the reaction bottle was removed by applying vacuum, and it was then flushed with hydrogen. Typically, a hydrogen pressure of approximately 40 psi was applied from the reservoir and the bottle was then shaken vigorously to initiate the reaction. Progress of the reaction was monitored by TLC and LCMS. The reaction required about 6 hours at which point TLC and LCMS analysis showed the completion of reaction. The shaker was stopped, the bottle was vented, and the product was recovered by filtration using Celite. Finally, the product was concentrated by using a rotary evaporator. An orange solid was obtained after drying in vacuum. Yield=502 mg, 90 %.

Table 4.33: Characterisation data for compound **4.33**

4.33 Orange Solid	^{1}H NMR	^{1}HNMR(400MHz,(CD_3OD); $^\delta$H in ppm 8.29(s,1H),7.49(d,*J*=8.8,1H),7.45(s,1H),7.08(d,1H),7.08(d,*J*=2.0,1H),7.02(dd,*J*=8.4,2.0,1H),3.62-3.57(m,2H), 2.68-2.65(m,4H),2.62(d,*J*=7.6,2H),1.95-1.92(m,4H),1.86-1.80(m,2H),1.76(t,*J*=7.2,2H).
	EIMS	Found 302.1 $[M+H]^+$, Calculated for $C_{17}H_{23}N_3O_2$, 301.17 $[M]^+$

4.34 Synthesis of 5-nitro-N-(2-((4-(pyrrolidin-1-yl) butyl) carbamoyl) benzofuran-5-yl) benzofuran-2-carboxamide (4.34)

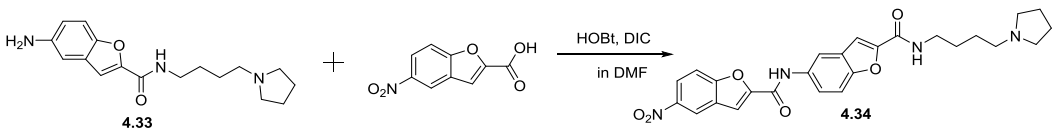

At first, 481 mg of 5-nitrobenzofuran-2-carboxylic acid (2.32 mmol, 1.2 eq.) was dissolved in 10mL of DMF in a round bottom flask fitted with a magnetic stirrer. Then DIC (627.68 µl, 4.06 mmol, 1.75 eq.) and HOBt (626.4 mg, 4.64 mmol, 2.0 eq.) were added to the acid (1.0 eq.) and this mixture was allowed to stir at room temperature for 30 minutes for esterification. Then amine (500 mg, 1.65 mmol, 1 eq.) was added and the mixture was allowed to stir for 13 hours at which point TLC and LCMS analysis showed the completion of reaction. Finally the reaction mixture separated by conditioned Isolute^{TM} SCX-2 cartridge and the product was purified by 'Catch and Release' method **(**described in the section **'Method and Materials'** of chapter 3**)**. A pale yellow solid was obtained after drying in vacuum. Yield=360 mg, 44%.

Table 34: Characterisation data for compound **4.34**

4.34 Pale Yellow Solid	^{1}H NMR	^{1}HNMR(400MHz,(CD_3OD); $^\delta$H in ppm 8.72(s,1H), 8.39(d,*J*=6.4,1H), 8.17(s,1H), 7.84(d,*J*=9.2,1H), 7.76 (t,*J*=1.2,1H), 7.68(t,*J*=1.2,1H), 7.59(d,*J*=4.8,1H), 7.46(s,1H), 7.27(d,*J*=4, 1H), 3.36(s,2H), 2.59(t, *J*=8.0,2H), 1.83(s,4H), 1.67(s,2H), 1.29-1.24(m,4H), 1.11(d ,*J*=6.4,2H).
	EIMS	Found 490.80 $[M+H]^+$, Calculated for $C_{26}H_{26}N_4O_6$, 490.18 $[M]^+$

4.35 Synthesis of 5-amino-N-(2-((4-(pyrrolidin-1-yl) butyl) carbamoyl) benzofuran-5-yl) benzofuran-2-carboxamide (4.35)

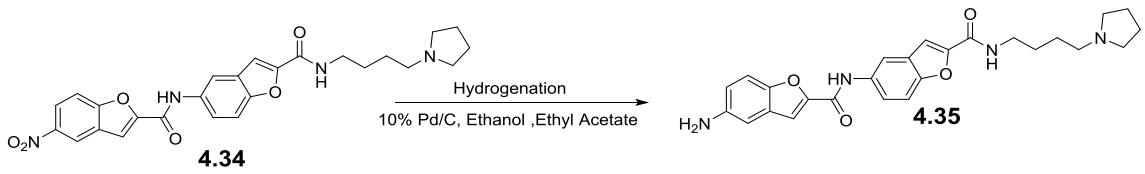

4.34 4.35

200mg of **4.34** was dissolved in 20 mL of ethanol and 1 mL of ethyl acetate was added to a hydrogenation reaction bottle. 20 mg of 10% Pd (palladium on activated carbon) 20 was added into the reaction mixture and mixed it well. The reaction bottle was sealed and connected to a hydrogen reservoir. Air from the reaction bottle was removed by applying vacuum, and it was flushed with hydrogen. A hydrogen pressure of approximately 40 psi was applied from the reservoir, and the bottle was then shaken vigorously to initiate the reaction. Progress of the reaction was monitored by TLC and LCMS and the shaker was stopped on completion of the reaction after 4 hour at which point TLC and LCMS analysis showed the completion of reaction. The bottle was vented, and the product was recovered by means of filtration using Celite. Lastly, the product is concentrated by using a rotary evaporator. A brown solid was obtained after drying in vacuum. Yield=160mg, 86%.

Table 4.35: Characterisation data for compound **4.35**

4.35 Brown Solid	^{1}H NMR	^{1}HNMR(400MHz,(CD_3OD); $^\delta$H in ppm 8.14(d,*J*=6.0,1H), 7.68(dd,*J*=5.2,1.6,1H), 7.52(d,*J*=14.4,1H), 7.41(s,2H), 7.41(s,1H), 6.99(d, *J*=4.8, 1H), 6.94(dd,*J*=8.8,2.0, 1H), 3.42(s,2H), 2.71(s,4H), 2.63(s,2H), 1.67(s,2H), 1.66(s,4H), 1.19(s,2H).
	EIMS	Found 460.21 $[M+H]^+$, Calculated for $C_{26}H_{28}N_4O_4$, 459.0 $[M]^+$

4.36 Synthesis of 5-(benzofuran-2-carboxamido)-N-(2-((4-(pyrrolidin-1-yl) butyl) carbamoyl) benzofuran-5-yl) benzofuran-2-carboxamide (4.36)

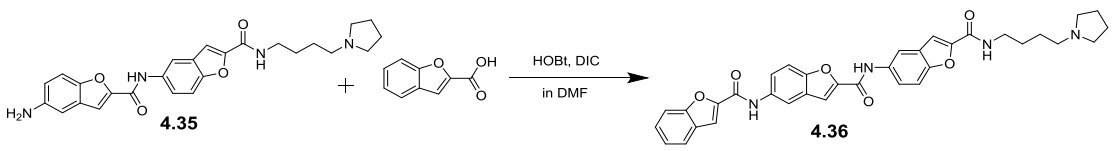

4.35 4.36

Initially, 29.58 mg of benzofuran-2-carboxylic acid (0.182 mmol, 1.2 eq.) was dissolved in 10mL of DMF in a round bottom flask placed at a magnetic stirrer.

Then DIC (50 µl, 0.3185 mmol, 1.75 eq.) and HOBt (50 mg, 0.364 mmol, 2.0 eq.) were added to the acid (1.0 eq.) and this mixture was allowed to stir at room temperature for 30 minutes to form ester. Then amine **4.35** (60 mg, 0.130 mmol, 1 eq.) was added and the mixture was allowed to stir for 6 hours at which point TLC and LCMS analysis showed the completion of reaction. Finally the reaction mixture was applied to a conditioned Isolute^{TM} SCX-2 cartridge and the product was purified by 'Catch and Release' method **(**described in the section **'Method and Materials'** of chapter 3**)**. A deep yellow solid was obtained after drying in vacuum. Yield=14mg, 18%.

Table 4.36: Characterisation data for compound **4.36**

4.36 Deep Yellow Solid	^{1}H NMR	^{1}HNMR(400MHz,$(CD_3)_2SO$); $^{\delta}$H in ppm 10.71(s,1H), 8.79(s,1H), 8.35(s,1H), 8.28(s,1H), 7.85(d,*J*=8.0, 1H),7.81(d,*J*=6.8,2H),7.79(s,1H),7.74(d,*J*=8.0,2H),7.71(d,*J*=14.4, 2H),7.65(d,*J*=9.2,1H),7.54-7.49(m,1H),7.37(t,*J*=7.6,1H), 2.03(s,2H),1.96(s,2H),1.80(s,4H),1.60-1.50(m,2H), 1.50(d,*J*=7.2,4H), 1.14-1.09(m,2H).
	^{13}C NMR	(100MHz,$(CD_3)_2SO$); $^{\delta}$C in ppm 171.4, 163.7, 157.7, 156.3, 153.1, 151.1,145.3, 139.9, 127.1, 123.0,120.9,114.2,111.9,111.0,109.3,99.1,92.2,90.8,69.7,55.3,53. 5,46.7,41.9,40.0, 39.8, 39.6, 39.4, 38.8,38.6, 31.8, 31.7, 30.6,30.1, 25.9, 23.0.
	EIMS	Found 605.1 $[M+H]^+$, Calculated for $C_{35}H_{32}N_4O_6$, 604.23 $[M]^+$
	HRMS	*m/z* (+EI) Calc. for $C_{35}H_{32}N_4O_6$, 604.2322 $[M]^+$, found 605.2401$[M+H]^+$.
	IR	(FTIR), V_{max}/'cm^{-1}): 3405, 2919, 1657, 1585, 1541, 1474, 1376, 1298, 1233, 941, 852, 801, 741.

4.37 Synthesis of 5-(benzo[b]thiophene-2-carboxamido)-N-(2-((4-(pyrrolidin-1-yl) butyl) carbamoyl) benzofuran-5-yl) benzofuran-2-carboxamide (4.37)

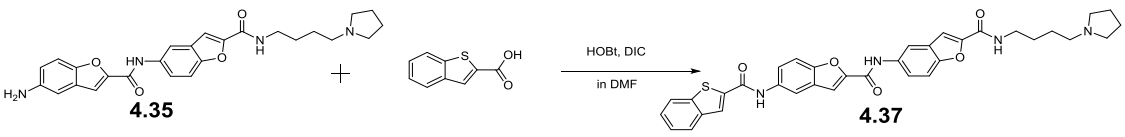

4.35 4.37

At first, 33 mg of benzo[b]thiophene-2-carboxylic acid (0.182 mmol, 1.2 eq.) was dissolved in 10mL of DMF in a round bottom flask fitted with a magnetic stirrer. Then DIC (49 µl, 0.318 mmol, 1.75 eq.) and HOBt (49 mg, 0.364 mmol, 2.0 eq.) were added to the acid (1.0 eq.) and this mixture was allowed to stir at room

temperature for 30 minutes to ensure the formation of ester. Then amine **4.35**(60 mg, 0.130 mmol, 1 eq.) was added and this mixture was allowed to stir for 6 hours at which point TLC and LCMS analysis showed the completion of reaction. The product was purified by 'Catch and Release' method using conditioned Isolute^{TM} SCX-2 cartridge **(**described in the section **'Method and Materials'** of chapter 3**)**. A deep yellow solid was obtained after drying in vacuum. Yield was 14mg, 18%.

Table 4.37: Characterisation data for compound **4.37**

4.37 Deep Yellow Solid	^{1}H NMR	^{1}HNMR(400MHz,$(CD_3)_2SO$); $^{\delta}$H in ppm 10.77(d,*J*=7.6,2H),8.86(s,1H),8.47(s,1H),8.38(d,*J*=10.4,2H), 8.11(dd,*J*=10.0,2.8,2H),7.88(d,*J*=10.0,3H),7.82(d,*J*=8.0,1H), 7.72(d,*J*=8.4,1H),7.62(s,1H),7.56(s,2H),3.35(d,*J*=4.0,2H),2. 57(S,2H),2.50(s,4H),2.15(s,2H),1.73(s,4H),1.62(d,*J*=5.6,2H) ,1.55(d,*J*=5.2,2H)
	^{13}C NMR	(100MHz,$(CD_3)_2SO$); $^{\delta}$C in ppm 162.2,160.3,157.9, 156.6, 151.2, 150.9, 150.0, 149.4, 140.4,139.9, 139.1, 134.6, 134.2, 127.2, 126.5, 125.7, 125.3, 125.0, 122.8, 120.9, 120.6, 113.9, 113.8, 112.0, 111.7, 110.9, 109.4, 55.1, 53.4, 40.0, 39.2, 30.7, 25.6, 23.9, 23.0.
	EIMS	Found 621.20 $[M+H]^+$, Calculated for $C_{35}H_{32}N_4O_5S$, 620.20 $[M]^+$
	HRMS	*m/z* (+EI) Calc. for $C_{35}H_{32}N_4O_5S$, 620.2093 $[M]^+$, found 621.2155$[M+H]^+$.
	IR	(FTIR), V_{max}/'cm^{-1}): 3312, 1656, 1585, 1535, 1471, 1434, 1231, 1198, 941, 870, 802, 752, 739, 620, 568.

4.38 Synthesis of 5-(5-nitrobenzo[b]thiophene-2-carboxamido)-N-(4-(pyrrolidin1-yl) butyl) benzofuran-2-carboxamide (4.38).

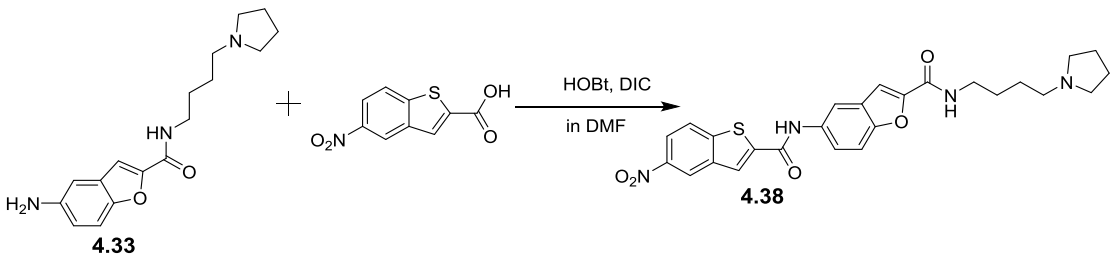

Initially, 153 mg of 5-nitrobenzo[b]thiophene-2-carboxylic acid (0.685 mmol, 1.2 eq.) was dissolved in 10mL of DMF in a round bottom flask fitted with a magnetic stirrer. Then DIC (184 µl, 1.19 mmol, 1.75 eq.) and HOBt (184 mg, 1.37 mmol, 2.0 eq.) were added to the acid (1.0 eq.) and this mixture was

allowed to stir at room temperature for 30 minutes to form ester from the acid. Then amine **4.33**(172 mg, 0.571 mmol, 1 eq.) was added and the mixture was allowed to stir for 7 hours at which point TLC and LCMS analysis showed the completion of reaction. Finally the reaction mixture was applied to a conditioned Isolute^{TM} SCX-2 cartridge and the product was purified by 'Catch and Release' method **(**described in the section **'Method and Materials'** of chapter 3**)**. A yellow coloured solid was obtained after drying in vacuum. Yield=145mg, 50%.

Table 4.38: Characterisation data for compound **4.38**

4.38 Yellow solid	^{1}H NMR	^{1}HNMR(400MHz,$(CD_3)_2SO$); $^\delta$H in ppm 10.85(s,1H),8.95(s,1H),8.75(t,*J*=5.6,1H),8.55(s,1H),8.35(d,*J*=8.8,1H), 8.28(dd,*J*=8.8,2.4, 1H), 7.76(dd,*J*=8.8, 2.0,1H), 8.23 (d,*J*=2,1H), 7.66(d,*J*=8,1H), 7.55(s, 1H), 3.31-3.26(m, 4H), 2.73(s,2H), 2.51-2.49(m,2H), 1.69-1.66(m,4H), 1.61-1.54(m,2H), 1.53-1.46(m,2H).
	EIMS	Found 507.10 $[M+H]^+$, Calculated for $C_{26}H_{26}N_4O_5S$,506.58 $[M]^+$

4.39 Synthesis of 5-(5-aminobenzo[b]thiophene-2-carboxamido)-N-(4-(pyrrolidin-1-yl) butyl) benzofuran-2-carboxamide (4.39)

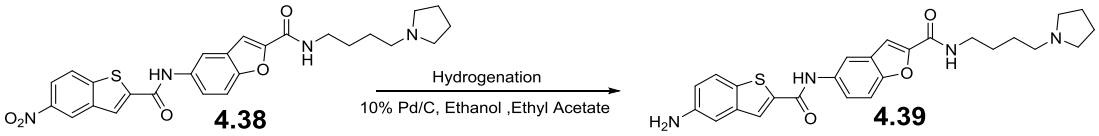

4.38 **4.39**

145 mg of **4.38** was dissolved in 20 mL of ethanol and1 mL of ethyl acetate was added to a hydrogenation reaction bottle. 20 mg of 10% Pd (palladium on activated carbon) 20 was added into the reaction vessel, and mixed that well. The reaction bottle was sealed and connected to a hydrogen reservoir. Air of the reaction bottle was removed by applying vacuum and it was flushed with hydrogen. Typically, approximately 40 psi of a hydrogen pressure was applied from the reservoir and the bottle was then shaken vigorously to initiate the reaction. Progress of the reaction was monitored by TLC and LCMS and the shaker was stopped after 5 hours at which point TLC and LCMS analysis showed the completion of reaction. The bottle was vented and the product was recovered by process of filtration using Celite. Finally the product was concentrated by using a rotary evaporator. A yellow solid was obtained after drying in vacuum. Yield was 96mg, 71%.

Table 4.39: Characterisation data for compound **4.39**

4.39 Yellow solid	^{1}H NMR	^{1}HNMR(400MHz,$(CD_3)_2SO$); $^\delta$H in ppm 10.67(s,1H),8.80(t,*J*=5.6,1H),8.24(d,*J*=2,1H),8.16(s,1H),7.78(dd,*J*=8.8,2.0,1H), 7.65-7.626(m,2H), 7.54(s,1H), 7.06(d,*J*=2,1H), 6.86(dd,*J*=8.8, 2.0,1H), 3.31-3.26(m, 4H), 2.73(s,2H), 2.51(s,2H), 1.61-1.54(m,2H), 1.22-1.13(m,4H), 1.05-0.99(m,2H).
	EIMS	Found 476.30 $[M+H]^+$, Calculated for $C_{26}H_{28}N_4O_3S$, 476.18 $[M]^+$

4.40 Synthesis of 5-(5-(benzo[b]thiophene-2-carboxamido) benzo [b]thiophene-2-carboxamido)-N-(4-(pyrrolidin-1-yl) butyl) benzofuran-2-carboxamide (4.40)

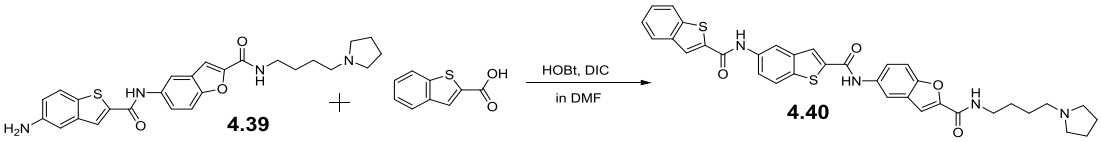

30 mg of benzo[b]thiophene-2-carboxylic acid (0.151 mmol, 1.2 eq.) was dissolved in 10mL of DMF in a round bottom flask fitted with a magnetic stirrer. Then DIC (41 µl, 0.264 mmol, 1.75 eq.) and HOBt (41 mg, 0.302 mmol, 2.0 eq.) were added to the acid (1.0 eq.) and this mixture was stirred at room temperature for 30 minutes to ensure the formation of ester from the acid. Then amine **4.39** (60 mg, 0.126 mmol, 1 eq.) was added and the mixture had been stirred for 6 hours at which point TLC and LCMS analysis showed the completion of reaction. Finally the reaction mixture was applied to a conditioned Isolute^{TM} SCX-2 cartridge and the product was purified by 'Catch and Release' method **(**described in the section **'Method and Materials'** of chapter 3**)**. A pale orange solid was obtained after drying in vacuum. Yield=10 mg, 13%.

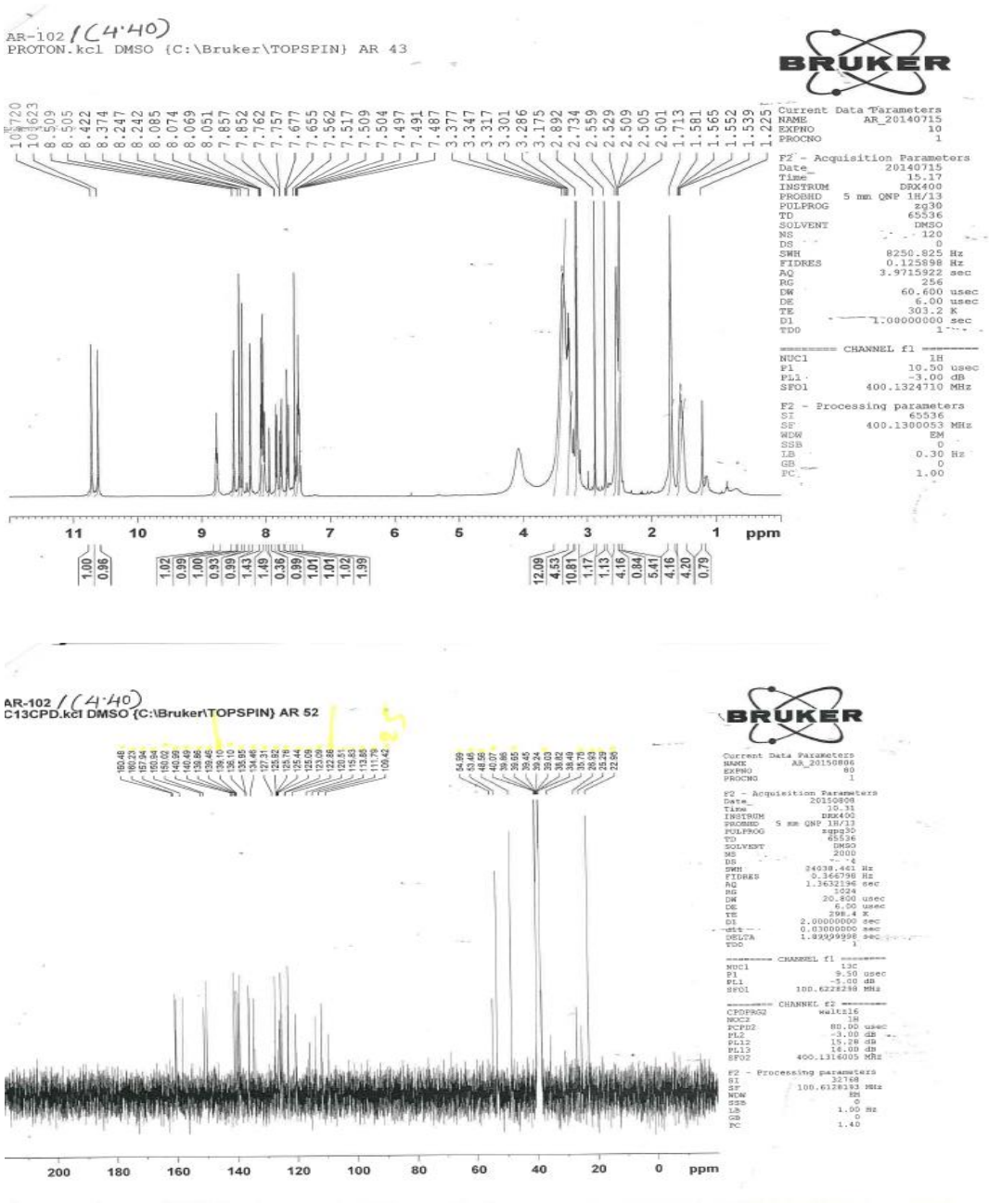

Figure 4.3: ^{1}H and ^{13}C NMR spectroscopic data of compound **4.40** as a representative of **library 1-B** compounds

Table 4.40: Characterisation data for compound **4.40**

4.40 Orange solid	^{1}H NMR	^{1}HNMR(400MHz,$(CD_3)_2SO$); $^{\delta}$H in ppm 10.72(s,1H), 10.62(s,1H), 8.77(s,1H), 8.50 (d,*J*=1.6,1H), 8.42(s,1H), 8.24(d,*J*=2,1H), 7.37 (s,1H), 8.08-8.05(m,2H), 7.95(s,1H), 7.84(dd,*J*=8.8,2.0,1H), 7.75(dd,*J*=8.8,2.0,1H), 7.66 (d,*J*=8.8,1H), 7.56(s,1H), 7.52-7.48 (m, 2H), 3.34-3.28(m,4H), 2.89(s,2H), 2.55(s,2H), 2.50 (s,2H), 1.71(s,4H), 1.58-1.53(m,2H).
	^{13}C NMR	(100MHz,$(CD_3)_2SO$); $^{\delta}$C in ppm 160.4, 160.2, 157.9, 150.9, 150.0, 140.9, 140.4, 139.8, 139.4, 139.1, 136.1, 135.9, 134.4, 127.3, 125.9, 125.7, 125.4, 125.0, 123.0, 122.8, 120.5, 115.8, 113.8, 111.7, 109.4, 54.9, 53.4, 48.5, 40.0, 39.6, 39.0, 35.7, 26.9, 25.2, 22.9.
	EIMS	Found 636.40 $[M+H]^+$, Calculated for $C_{35}H_{32}N_4O_4S_2$, 636.18 $[M]^+$
	HRMS	*m/z* (+EI) Calc. for $C_{35}H_{32}N_4O_4S_2$, 636.1865 $[M]^+$, found 637.1934$[M+H]^+$.
	IR	(FTIR), V_{max}/'cm^{-1}): 3299, 2939, 1635, 1590, 1574, 1528, 1469, 1446, 1432, 1343, 1298, 1275, 1236, 1198, 1153, 1035, 878, 845, 805, 753, 738, 715.

4.41 Synthesis of 1-methyl-N-(2-((2-((4-(pyrrolidin-1-yl) butyl) carbamoyl) benzofuran-5-yl) carbamoyl) benzofuran-5-yl)-1H-indole-2-carboxamide (4.41)

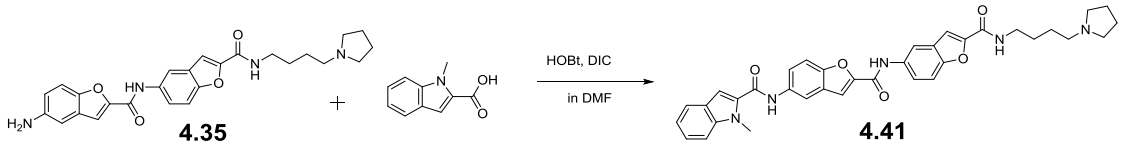

4.35 **4.41**

26.52 mg of 1-methyl-1H-indole-2-carboxylic acid (1.2 eq.) was dissolved in 10 mL of DMF in a round bottom flask fitted with a magnetic stirrer. Then DIC (40 µl, 0.262 mmol, 1.75 eq.) and HOBt (40 mg, 0.30 mmol, 2.0 eq.) were added to the acid (1.0 eq.) and this mixture was stirred at room temperature for 30 minutes to ensure the formation of ester. Then amine **4.35** (50 mg, 0.108 mmol, 1 eq.) was added and that mixture was allowed to stir for 8 hours at which point TLC and LCMS analysis showed the completion of reaction. Finally the reaction mixture was applied to a conditioned Isolute^{TM} SCX-2 cartridge and the product was purified by 'Catch and Release' method **(**described in the section **'Method and Materials'** of chapter 3**)**. A deep yellow solid was obtained after drying in vacuum. Yield=20 mg, 23%.

Table 4.41: Characterisation data for compound **4.41**

4.41 Deep Yellow Solid	^{1}H NMR	^{1}HNMR(400MHz,$(CD_3)_2SO$); $^{\delta}$H in ppm 10.69(s,1H), 10.50(s,1H), 8.81(t,*J*=5.6,1H), 8.38(s,1H), 8.30(s,1H), 7.81(d,*J*=9.2,3H),7.75(t,2H),7.67(d,*J*=8.8,1H),7.60(t,2H),7.36(d,*J*=6 ,1H), 7.33(d,*J*=7.6,1H), 7.17(t,1H), 4.05 (s,2H), 3.29(d,*J*=6,2H), 2.50(s,4H), 2.48(s,2H), 1.68(s,4H), 1.52(d,*J*=6.8,2H).
	^{13}C NMR	(100MHz,$(CD_3)_2SO$); $^{\delta}$C in ppm 179.4, 162.3, 160.5, 157.9, 156.6, 151.0, 150.9, 150.0, 149.3, 138.6, 135.1, 134.2, 132.0, 127.2, 127.2, 125.4, 123.9, 121.7, 120.9, 120.7, 120.2, 114.0, 113.5, 111.9, 111.7, 110.9, 110.5, 109.4, 105.5, 55.1, 53.4, 40.0, 39.2, 31.4, 30.6, 29.4.
	EIMS	Found 617.60 $[M+H]^+$, Calculated for $C_{36}H_{35}N_5O_5$, 617.26 $[M]^+$
	HRMS	*m/z* (+EI) Calc. for $C_{36}H_{35}N_5O_5$,617.2638 $[M]^+$, found 618.2708$[M+H]^+$.
	IR	(FTIR), V_{max}/'cm^{-1}): 2937, 2785, 1709, 1644, 1584, 1530, 1469, 1437, 1390, 1349, 1316, 1286, 1233, 1198, 1145, 1125, 1025, 1006, 944, 916, 878, 862, 803, 782, 748, 732, 637.

4.42 Synthesis of 3-methyl-N-(2-((2-((4-(pyrrolidin-1-yl) butyl) carbamoyl) benzofuran-5-yl) carbamoyl) benzofuran-5-yl) benzofuran-2-carboxamide (4.42)

4.35 **4.42**

Initially, 24 mg of 3-methylbenzofuran-2-carboxylic acid (0.130 mmol, 1.2 eq.) was dissolved in 5 mL of DMF in a round bottom flask fitted with a magnetic stirrer. Then DIC (35 µl, 0.2275 mmol, 1.75 eq.) and HOBt (35 mg, 0.260 mmol, 2.0 eq.) were added to the acid (1.0 eq.) and this mixture was allowed to stir at room temperature for 30 minutes to ensure the formation of ester from the acid.

Table 4.42: Characterisation data for compound **4.42**

4.42 Deep Yellow Solid	^{1}H NMR	^{1}HNMR(400MHz,$(CD_3)_2SO$); $^{\delta}$H in ppm 10.69(s,1H), 10.59(s,1H), 7.95(s,1H), 7.88(t, 2H), 7.82(s,2H), 7.80(s,1H), 7.72(t, *J*=9.2,2H), 7.68(t,*J*=9.2,2H), 7.54(t,*J*=7.6, 2H), 7.41(t,*J*=7.8,1H), 2.89(s,2H), 2.73(s,2H), 1.73(s,4H), 1.56(s,4H), 1.24(s,2H), 1.19(s,2H).
	^{13}C NMR	(100MHz,$(CD_3)_2SO$); $^{\delta}$C in ppm 162.2, 158.0, 157.9, 156.6, 152.7, 151.2, 150.9, 150.0, 149.3, 142.7, 134.4, 134.2, 130.6, 129.2, 127.4, 127.2, 127.1, 122.3, 121.2, 121.1, 120.6, 115.1, 114.1, 113.9, 111.8, 111.7, 110.9, 109.4, 54.8, 53.3, 40.0, 39.2, 35.7, 30.7, 26.8, 22.9.
	EIMS	Found 619.20 $[M+H]^+$, Calculated for $C_{36}H_{34}N_4O_6$, 618.24 $[M]^+$
	HRMS	*m/z* (+EI) Calc. for $C_{36}H_{34}N_4O_6$, 618.2478 $[M]^+$, found 619.2544$[M+H]^+$.
	IR	(FTIR), V_{max}/'cm^{-1}): 3305, 2948, 1639, 1582, 1533, 1470, 1433, 1345, 1296, 1233, 1198, 1129, 1085, 1041, 942, 874, 801, 738, 717.

Then amine **4.35**(50 mg, 0.108 mmol, 1 eq.) was added and the mixture was allowed to stir for 9 hours at which point TLC and LCMS analysis showed the completion of reaction. Finally the reaction mixture was applied to a conditioned Isolute^{TM} SCX-2 cartridge and the product was purified by 'Catch and Release' method **(**described in the section **'Method and Materials'** of chapter 3**)**. A deep yellow solid was obtained after drying in vacuum. Yield=12 mg, 18%.

4.43 Synthesis of 5-chloro-N-(2-((2-((4-(pyrrolidin-1yl) butyl) carbamoyl) benzofuran-5-yl) carbamoyl) benzofuran-5-yl) benzofuran-2-carboxamide (4.43).

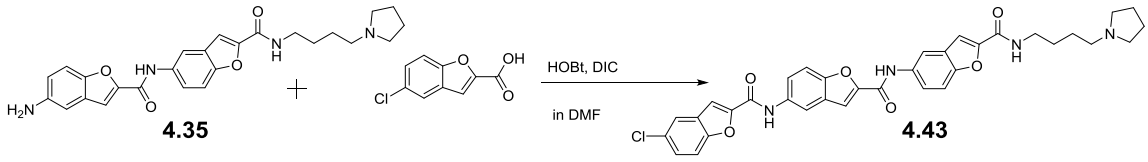

At first, the 5-chlorobenzofuran-2-carboxylic acid (36 mg, 0.1826 mmol, 1.2 eq.) was dissolved in 5 mL of DMF in a round bottom flask fitted with a magnetic stirrer. Then DIC (49.4 µl, 0.319 mmol, 1.75 eq.) and HOBt (49.30 mg, 0.3652 mmol, 2.0 eq.) were added to the acid (1.0 eq.) and this mixture was allowed to stir at room temperature for 30 minutes to ensure the formation of ester from the acid. Then amine **4.35**(60 mg, 0.13043 mmol, 1 eq.) was added and the mixture was allowed to stir for 12 hours at which point TLC and LCMS analysis showed the completion of reaction.

Table 4.43: Characterisation data for compound **4.43**

4.43 Deep Yellow Solid	^{1}H NMR	^{1}HNMR(400MHz,$(CD_3)_2SO$); $^{\delta}$H in ppm 10.83(s,1H),10.72(s,1H),8.80(t,*J*=5.6,1H),8.34(d,*J*=1.6,1H),8.29(d,*J*=1.6,1H),7.94(d,,*J*=2.0,1H),7.83(s,1H),7.80(d,*J*=6.4,2H),7.76(d,*J*=5.6,1H),7.65(d,*J*=9.2,1H),7.54(t,*J*=3.6,2H),7.04(d,*J*=8.4,1H),6.79(d,*J*=8.4,1H),3.69(d,*J*=4.8,2H),3.27(d,*J*=4.8,2H),2.40(d,*J*=5.6,4H),1.66(s,4H),1.58-1.53 (m,2H),1.47(t,*J*=6.4,2H), 1.09(d,*J*=6.4,2H).
	^{13}C NMR	(100MHz,$(CD_3)_2SO$); $^{\delta}$C in ppm 157.9, 156.6, 156.3, 152.9, 151.3, 150.9, 150.1, 150.0, 149.4, 134.28, 134.20, 128.7, 128.1, 127.2, 127.1, 122.2, 121.1, 120.6, 118.9, 114.1, 113.9, 113.6, 112.0, 111.7, 110.9, 110.1, 109.4, 55.2, 53.5, 40.0, 39.4, 38.8, 27.1, 25.8, 23.0.
	EIMS	Found 638.20 $[M+H]^+$, Calculated for $C_{35}H_{31}ClN_4O_6$, 638.19 $[M]^+$
	HRMS	*m/z* (+EI) Calc. for $C_{35}H_{31}ClN_4O_6$, 638.1932 $[M]^+$, found 629.2006$[M+H]^+$.
	IR	(FTIR), V_{max}/'cm^{-1}): 3336, 1656, 1582, 1542, 1476, 1435, 1357, 1296, 1231, 1197, 1170, 1144, 1087, 1064, 941, 890, 871, 801, 750, 739, 695, 629, 598.

Finally the reaction mixture was applied to a conditioned Isolute^{TM} SCX-2 cartridge and the product was purified by 'Catch and Release' method **(**described in the section **'Method and Materials'** of chapter 3**)**. A deep yellow solid was obtained after drying in vacuum. Yield=26 mg, 31%.

4.44 Synthesis of N-(2-((2-((4-(pyrrolidin-1-yl) butyl) carbamoyl) benzofuran-5-yl) carbamoyl) benzofuran-5-yl)-1H-benzo[d]imidazole-5-carboxamide (4.44).

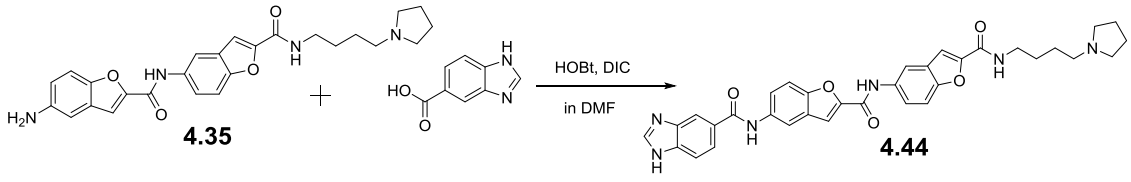

4.35 **4.44**

Initially, 29.58 mg of 1H-benzo[d]imidazole-5-carboxylic acid (0.182 mmol, 1.2 eq.) was dissolved in 10mL of DMF in a round bottom flask fitted with a magnetic stirrer. Then DIC (49.24 µl, 0.3185 mmol, 1.75 eq.) and HOBt (49.14 mg, 0.364 mmol, 2.0 eq.) were added to the acid (1.0 eq.) and this mixture was allowed to stir at room temperature for 30 minutes to ensure the ester formation. Then amine **4.35** (60 mg, 0.13043 mmol, 1 eq.) was added and the mixture was allowed to stir for 7 hours at which point TLC and LCMS analysis showed the

completion of reaction. Finally the reaction mixture was applied to a conditioned Isolute^{TM} SCX-2 cartridge and the product was purified by 'Catch and Release' method **(**described in the section **'Method and Materials'** of chapter 3**)**. A deep yellow solid was obtained after drying in vacuum. Yield=27mg, 34%.

Table 4.44: Characterisation data for compound **4.44**

4.44 Deep yellow Solid	^{1}H NMR	^{1}HNMR(400MHz,$(CD_3)_2SO$); $^{\delta}$H in ppm 10.43(s,1H),8.81(S,1H),8.38(s,2H),8.35(s,1H),8.31(s,1H),7.95(s,1H), 7.90(d,*J*=12,1H),7.81(s,2H),7.77(s,1H),7.72(t,*J*=5.6,2H),7.66(d,*J*=8.8 ,1H), 7.56(s,1H), 7.05(d,*J*=8,1H), 6.79(d,*J*=7.8,1H), 3.29(s,2H), 2.88(s,2H), 2.39(s,4H), 2.38(s,2H), 1.61(s,4H), 1.55(s,2H).
	^{13}C NMR	(100MHz,$(CD_3)_2SO$); $^{\delta}$C in ppm 166.0, 157.9, 156.6, 150.9, 150.0, 149.3, 144.2, 135.6, 134.2, 129.1, 128.3, 127.2, 127.1, 121.7, 121.1, 120.6, 113.9, 113.6, 113.5, 111.7, 110.9, 109.3, 55.3, 53.5, 41.6, 39.0, 38.6, 38.0, 36.8, 35.7, 27.1, 25.9, 23.3, 23.0.
	EIMS	Found 605.20 $[M+H]^+$, Calculated for $C_{34}H_{32}N_6O_5$, 604.24 $[M]^+$
	HRMS	*m/z* (+EI) Calc. for $C_{34}H_{32}N_6O_5$, 604.2434 $[M]^+$, found 605.2511$[M+H]^+$.
	IR	(FTIR, V_{max}/'cm^{-1}): 3305, 1638, 1586, 1523, 1473, 1433, 1338, 1292, 1238, 1199, 1144, 940, 871, 802, 738.

4.45 Synthesis of 1-methyl-N-(2-((2-((4-(pyrrolidin-1-yl) butyl) carbamoyl) benzofuran-5-yl) carbamoyl) benzo[b]thiophen-5-yl)-1H-indole-2-carboxamide (4.45)

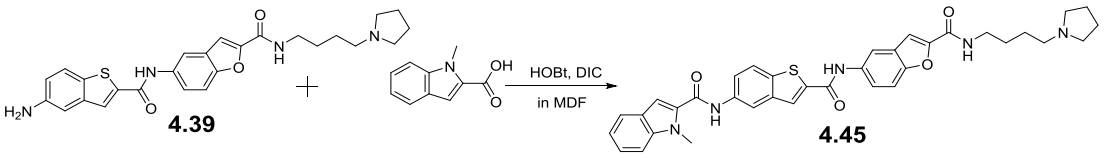

Initially, 23 mg of 1-methyl-1H-indole-2-carboxylic acid (0.126 mmol, 1.2 eq.) was dissolved in 10mL of DMF in a round bottom flask fitted with a magnetic stirrer. Then DIC (34 µl, 0.2205 mmol, 1.75 eq.) and HOBt (34 mg, 0.252 mmol, 2.0 eq.) were added to the acid (1.0 eq.) and this mixture was stirred at room temperature for at least 30 minutes to ensure the formation of ester from the acid. Then amine **4.39** (50 mg, 0.105 mmol,1 eq.) was added and the mixture was allowed to stir for 5 hours at which point TLC and LCMS analysis showed the completion of reaction. Finally the reaction mixture was applied to a conditioned Isolute^{TM} SCX-2 cartridge and the product was purified by 'Catch and Release' method **(**described in the section **'Method and Materials'** of

chapter 3**)**. A pale yellow solid was obtained after drying in vacuum. Yield=8 mg, 12%.

Table 4.45: Characterisation data for compound **4.45**

4.45 Orange solid	^{1}H NMR	^{1}HNMR(400MHz,$(CD_3)_2SO$); $^{\delta}$H in ppm 10.64(s,1H), 10.53(s,1H), 8.78(t,*J*=5.6,1H) 8.52(d,*J*=1.6,1H), 8.38 (s,1H),8.25(d,*J*=1.6,1H), 8.04(d,*J*=8.8,1H), 7.87(dd,*J*=8.8,2.0,1H), 7.78(dd,*J*=9.2,2.4,1H),7.72(d,*J*=7.6,1H),7.67(d,*J*=8.8,1H),7.58(t,*J* =8.4,2H),7.38(s,1H),7.32(t,*J*=7.2,1H),7.16(t,*J*=7.2,1H),3.31(t,*J*=5. 6,4H), 2.73(s,2H), 2.51(s,2H), 1.76(s,2H), 1.57(t,*J*=2.8,4H), 1.23(s,2H).
	^{13}C NMR	($100MHz,(CD_3)_2SO$); $^{\delta}$C in ppm 162.5, 160.6, 160.3, 159.8, 153.8, 151.7, 151.0, 150.0, 141.2, 139.4, 138.7, 136.9,136.4, 135.9,134.8, 131.8, 127.3, 124.2, 122.8, 120.7, 115.6, 113.8, 110.9, 109.5, 107.2, 106.0, 53.3, 40.0, 39.8,39.4, 39.2, 39.0, 31.4, 30.7, 26.7, 22.8.
	EIMS	Found 634.30 $[M+H]^+$, Calculated for $C_{36}H_{35}N_5O_4S$, 633.24 $[M]^+$
	HRMS	*m/z* (+EI) Calc. for $C_{36}H_{35}N_5O_4S$, 633.2410 $[M]^+$, found 634.2473$[M+H]^+$.
	IR	(FTIR), V_{max}/'cm^{-1}): 3287, 2947, 1638, 1591, 1574, 1530, 1468, 1447, 1432, 1392, 1340, 1292, 1233, 1201, 1154, 1038, 878, 810, 739, 716.

4.46 Synthesis of N-(2-((3-(dimethylamino) propyl) carbamoyl) benzo[b]thiophen-5-yl)-5-nitro-1H-indole-3-carboxamide (4.46).

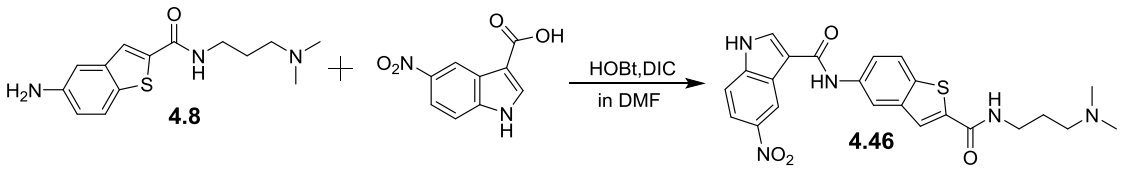

248 mg of 5-nitro-1H-indole-3-carboxylic acid (1.2096 mmol, 1.2 eq.) was dissolved in 10mL of DMF in a round bottom flask fitted with a magnetic stirrer. Then DIC (325 µl, 2.114 mmol, 1.75 eq.) and HOBt (325 mg, 2.4192 mmol, 2.0 eq.) were added to the acid (1.0 eq.) and this mixture was allowed to stir at room temperature for 30 minutes to ensure the formation of ester from the acid. Then amine **4.8** of 280 mg (1.008 mmol, 1 eq.) was added to the mixture and the mixture was allowed to stir for 14 hours at which point TLC and LCMS analysis showed the completion of reaction. Finally the reaction mixture was separated by conditioned Isolute^{TM} SCX-2 cartridge and the product was purified by 'Catch and Release' method **(**described in the section **'Method and Materials'** of chapter 3**)**. A yellow solid was obtained after drying in vacuum. Yield=245mg, 52%.

Table 4.46: Characterisation data for compound **4.46**

4.46 Yellow solid	^{1}H NMR	^{1}HNMR(400MHz,$(CD_3)_2SO$); $^\delta$H in ppm 12.15(s,1H),10.19(s,1H),9.17(d,*J*=2.4,1H),8.83(t,*J*=5.2,1H),8.64(s, 1H),8.49(d,*J*=1.6,1H),8.11(dd*J*=9.2,2.4,1H),8.04(s,1H),7.97(t,*J*=4. 8,2H),7.81(d,*J*=2,1H),7.79(d,*J*=2,1H),3.343.29(m,2H),2.342.30(m, *J*=6.8,2H), 2.18(s,6H), 1.70(t,*J*=7.2,2H).
	EIMS	Found 465.90 $[M+H]^+$, Calculated for $C_{23}H_{23}N_5O_4S$, 465.14 $[M]^+$

4.47 Synthesis of 5-amino-N-(2-((3-(dimethylamino) propyl) carbamoyl) benzo[b]thiophen-5-yl)-1H-indole-3-carboxamide (4.47).

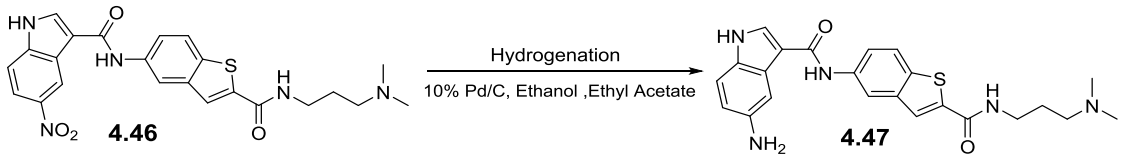

245 mg of **4.46** was dissolved in 20 mL of ethanol and 1 mL of ethyl acetate was added to a hydrogenation reaction bottle. 20 mg of 10% Pd (palladium on activated carbon) 20 was added into the reaction vessel, and mixed it well. The reaction bottle was sealed and connected to a hydrogen reservoir. Air from the reaction bottle was removed by applying vacuum, and was then by flushed with hydrogen. Typically, a hydrogen pressure of approximately 40 psi was applied from the reservoir, and the bottle was then shaken vigorously to initiate the reaction. Progress of the reaction was monitored by TLC and LCMS. The reaction required about 6 hours at which point TLC and LCMS analysis showed the completion of reaction. The shaker was stopped, the bottle was vented, and the product was recovered by the process of filtration using Celite. Finally, the product is concentrated by using a rotary evaporator. A deep brown solid was obtained after drying in vacuum. Yield was 196 mg, 86%.

Table 4.47: Characterisation data for compound **4.47**

4.47 Deep Brown solid	^{1}H NMR	^{1}HNMR(400MHz,$(CD_3)_2SO$); $^\delta$H in ppm 11.43(s,1H), 9.78(s,1H), 8.84(t,*J*=5.2,1H), 8.52 (s,1H), 8.22(s,1H), 8.07(s,1H),7.96(s,1H),7.83(d,*J*=8.8,1H), 7.53(s, 1H), 7.21(d,*J*=8.4, 1H),6.64(d,*J*=8.8,1H),3.38-3.33(m,2H),2.29(t,*J*=7.2,2H), 2.14(s,6H), 1.75-1.64(m,*J*=2H).
	EIMS	Found 435.50 $[M+H]^+$, Calculated for $C_{23}H_{25}N_5O_2S$, 435.00 $[M]^+$

4.48 Synthesis of 5-(benzofuran-2-carboxamido)-N-(2-((3-(dimethylamino) propyl) carbamoyl) benzo[b]thiophen-5-yl)-1H-indole-3-carboxamide (4.48).

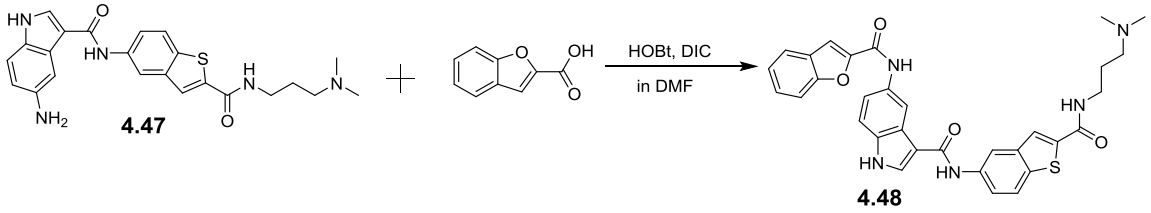

43 mg of benzofuran-2-carboxylic acid (0.262 mmol, 1.2 eq.) was dissolved in 10 mL of DMF in a round bottom flask placed at a magnetic stirrer. Then DIC (71 µl, 0.4585 mmol, 1.75 eq.) and HOBt (71 mg, 0.534 mmol, 2.0 eq.) were added to the acid (1.0 eq.) and this mixture was allowed to stir at room temperature for 30 minutes to ensure the formation of ester from the acid. Then amine **4.47** (95 mg, 0.218 mmol, 1 eq.) was added to the mixture and the mixture was allowed to stir for 6 hours at which point TLC and LCMS analysis showed the completion of reaction. At last the reaction mixture was applied to a conditioned Isolute^{TM} SCX-2 cartridge and the product was purified by 'Catch and Release' method **(**described in the section **'Method and Materials'** of chapter 3**)**. A cream solid was obtained after drying in vacuum. Yield=36.5 mg, 29 %.

Table 4.48: Characterisation data for compound **4.48**

4.48 Cream solid	^{1}H NMR	^{1}HNMR(400MHz,$(CD_3)_2SO$); $^{\delta}$H in ppm 11.85(d,*J*=2.4,1H), 10.51(s,1H), 9.93(s,1H), 8.87(t,*J*=5.2,1H), 8.66(d,*J*=2,1H), 8.49(d,*J*=1.6,1H), 8.36(d,*J*=2.8,1H), 8.31 (s,1H), 8.04(s,1H),8.97(s,1H),7.85-7.78(m,2H),7.74(d,*J*=8.4,1H),7.67(dd, *J*=8.8,2.0,1H),7.53-7.48(m,2H),7.37(t,*J*=7.2,1H),3.35-3.30(m,2H), 2.59(t,*J*=7.2,2H), 2.38(s,6H), 1.78(t,*J*=7.2,2H).
	^{13}C NMR	(100MHz,$(CD_3)_2SO$); $^{\delta}$C in ppm 164.5, 163.3, 162.2, 161.5, 156.4, 154.3, 149.2, 140.6, 139.5, 137.2, 134.3, 133.4, 131.8, 129.4, 127.2, 126.8, 126.3, 123.7, 122.7, 122.6, 119.8, 117.1, 113.5, 111.8, 111.7, 110.4, 109.9, 55.7, 43.8, 39.4, 35.7, 30.7.
	EIMS	Found 580.0 $[M+H]^+$, Calculated for $C_{32}H_{29}N_5O_4S$, 579.19 $[M]^+$
	HRMS	*m/z* (+EI) Calc. for $C_{32}H_{29}N_5O_4S$, 579.1940 $[M]^+$, found 580.2000$[M+H]^+$.
	IR	(FTIR), V_{max}/'cm^{-1}): 3259, 2937, 2219, 1705, 1631, 1532, 1474, 1436, 1386, 1361, 1330, 1308, 1247, 1221, 1160, 1097, 1038, 945, 885, 865, 807, 769,740, 715, 659, 618.

4.49 Synthesis 5-(benzo[b]thiophene-2-carboxamido)-N-(2-((3-(dimethyl amino) propyl) carbamoyl) benzo[b]thiophen-5-yl)-1H-indole-3-carboxamide (4.49).

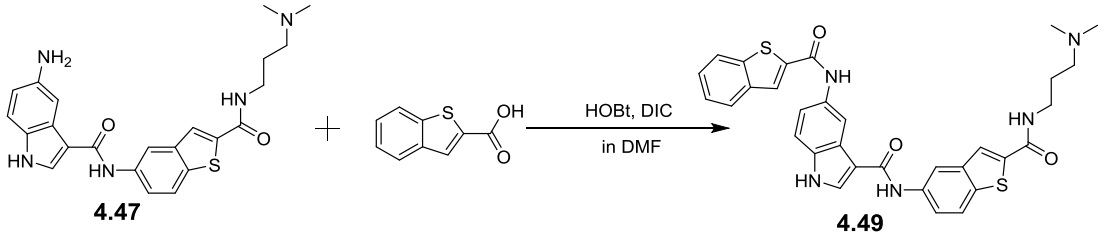

Initially, 44 mg of benzo[b]thiophene-2-carboxylic acid (0.248 mmol, 1.2 eq.) was dissolved in 10mL of DMF in a round bottom flask fitted with a magnetic stirrer. Then DIC (67 µl, 0.434 mmol, 1.75 eq.) and HOBt (67 mg, 0.496 mmol, 2.0 eq.) were added to the acid (1.0 eq.) and this mixture was allowed to stir at room temperature for 30 minutes to ensure the formation of ester from the acid. Then amine **4.47** (90 mg, 0.206 mmol, 1 eq.) was added to the mixture and the mixture was allowed to stir for 7 hours at which point TLC and LCMS analysis showed the completion of reaction. Finally the reaction mixture was applied to a conditioned Isolute^{TM} SCX-2 cartridge and the product was purified by 'Catch and Release' method **(**described in the section **'Method and Materials'** of chapter 3**)**. A cream solid was obtained after drying in vacuum. Yield=38mg, 31%.

Table 4.49: Characterisation data for compound **4.49**

4.49 Cream solid	^{1}H NMR	^{1}HNMR (400MHz,$(CD_3)_2SO$); $^{\delta}$H in ppm 11.82(s,1H),10.56(s,1H),9.92(s,1H),8.80(t,*J*=5.2,1H),8.62(d,*J*=1.6, 1H), 8.48(d,*J*=1.6,1H), 8.43 (s,1H), 8.37(s,1H), 8.07(t,*J*=6.4,1H), 8.02-7.98(m,2H),7.95(t,*J*=2.8,2H),7.81(dd,*J*=8.8,2.0,1H), 7.69(dd,*J*=8.8, 2.0,1H), 7.51-7.46(m,2H), 3.33-3.28(m,2H), 2.29(t,*J*=6.8,2H), 2.15(s,6H), 1.72-1.65(m,2H).
	^{13}C NMR	(100MHz,$(CD_3)_2SO$); $^{\delta}$C in ppm 163.2, 162.2, 161.3, 159.9, 140.8, 140.6, 140.3, 139.5, 139.2, 137.2, 134.3, 133.3, 132.1, 126.4, 126.2, 125.2, 124.9, 124.4, 122.7, 122.6, 119.8, 116.9, 114.7, 113.3, 111.7, 110.4, 56.8,45.1, 40.0, 39.2, 30.7, 27.0.
	EIMS	Found 596.20 $[M+H]^+$, Calculated for $C_{32}H_{29}N_5O_3S_2$, 595.17 $[M]^+$
	HRMS	*m/z* (+EI) Calc. for $C_{32}H_{29}N_5O_3S_2$, 595.1712 $[M]^+$, found 596.1771$[M+H]^+$.
	IR	(FTIR), V_{max}/'cm^{-1}): 3258, 2938, 2218, 1634, 1576, 1523, 1475, 1443, 1385, 1361, 1341, 1307, 1273, 1246, 1223, 1192, 1159, 1096, 1038, 951, 889, 864, 839, 809, 788, 771, 754, 740, 720, 687, 637.

4.50 Synthesis of N-(2-((3-(dimethylamino) propyl) carbamoyl) benzofuran-5-yl)-5-nitro-1H-indole-3-carboxamide (4.50).

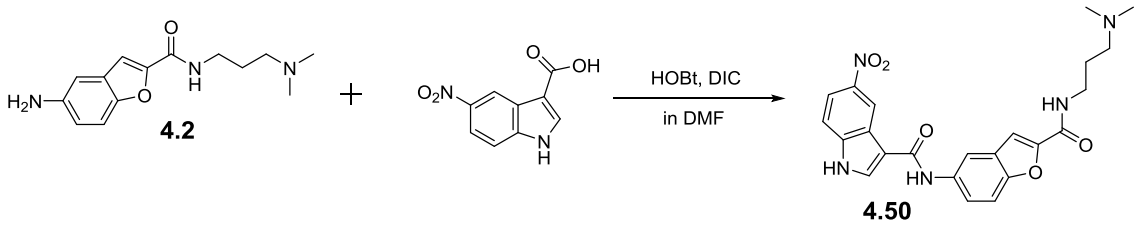

4.2 4.50

At the beginning 189.42 mg of 5-nitro-1H-indole-3-carboxylic acid (0.919 mmol, 1.2 eq.) was dissolved in 10mL of DMF in a round bottom flask fitted with a magnetic stirrer. Then DIC (248 µl, 1.60 mmol, 1.75 eq.) and HOBt (248 mg, 1.838 mmol, 2.0 eq.) were added to the acid (1.0 eq.) and this mixture was allowed to stir at room temperature for 30 minutes to ensure the formation of ester from the acid. Then amine **4.2** (200 mg, 0.766 mmol, 1 eq.) was added to the mixture and that mixture was allowed to stir for 11 at which point TLC and LCMS analysis showed the completion of reaction. Finally the reaction mixture was applied to a conditioned Isolute^{TM} SCX-2 cartridge and the product was purified by 'Catch and Release' method **(**described in the section **'Method and Materials'** of chapter 3**)**. A brown solid was obtained after drying in vacuum. Yield=162mg, 47%.

Table 4.50: Characterisation data for compound **4.50**

4.50 Brown solid	^{1}H NMR	^{1}HNMR(400MHz,$(CD_3)_2SO$); $^{\delta}$H in ppm 12.35(s,1H),10.11(s,1H),9.17(d,*J*=2,1H),8.82(t,*J*=5.6,1H),8.58(s,1H), 8.32(d,*J*=2,1H), 8.11(dd,*J*=8.8,2.4,1H), 7.74(dd,*J*=8.8,2.0,1H), 7.70 (d,*J*=5.2,1H), 7.65(d,*J*=8.8,1H), 7.55(s,1H), 3.34-3.29(m,2H), 2.28 (t,*J*=7.2,2H), 2.14 (s,6H), 1.70-1.65(m,2H).
	EIMS	Found 449.10 $[M+H]^+$, Calculated for $C_{23}H_{23}N_5O_5$, 449.16 $[M]^+$

4.51 Synthesis of 5-amino-N-(2-((3-(dimethylamino) propyl) carbamoyl) benzofuran-5-yl)-1H-indole-3-carboxamide (4.51).

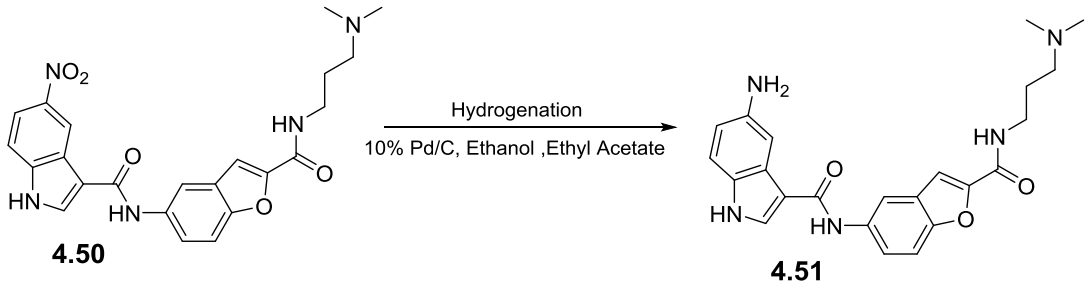

160 mg of **4.50** was dissolved in 20 mL of ethanol and 1 mL of ethyl acetate was added to a hydrogenation reaction bottle. 20 mg of 10% Pd (palladium on activated carbon) 20 was added into the reaction vessel, and mixed it well. The reaction bottle was sealed and connected to a hydrogen reservoir. Air from the reaction bottle was removed by applying vacuum, and was then by flushed with hydrogen. Typically, a hydrogen pressure of approximately 40 psi was applied from the reservoir, and the bottle was then shaken vigorously to initiate the reaction. Progress of the reaction was monitored by TLC and LCMS. Reaction required about 5 at which point TLC and LCMS analysis showed the completion of reaction. The shaker was stopped, the bottle was vented, and the product was recovered by means of filtration using Celite. Finally, the product is concentrated by using a rotary evaporator. A pale yellow solid was obtained after drying in vacuum. Yield=142 mg, 95%.

Table 4.51: Characterisation data for compound **4.51**

4.51 Yellow solid	^{1}H NMR	^{1}HNMR(400MHz,$(CD_3)_2SO$); $^\delta$H in ppm 11.39(s,1H), 9.72(s,1H), 8.85(t,*J*=5.6,1H), 8.27(d,*J*=2,1H), 8.13(s,1H), 7.75(d,*J*=3.6,1H), 7.73(d,*J*=2,1H), 7.53(s,1H), 7.45 (d,*J*=2,1H), 7.19(d,*J*=4.4,1H), 6.62-6.60 (m, 1H), 3.65(s,1H), 3.35-3.30(m,2H), 2.28 (t,*J*=6.8,2H), 2.14 (s,6H), 1.69(t,*J*=6.8,2H).
	EIMS	Found 419.20 $[M+H]^+$, Calculated for $C_{23}H_{25}N_5O_3$, 419.19 $[M]^+$

4.52 Synthesis 5-(benzofuran-2-carboxamido)-N-(2-((3-(dimethylamino) propyl) carbamoyl) benzofuran-5-yl)-1H-indole-3-carboxamide (4.52).

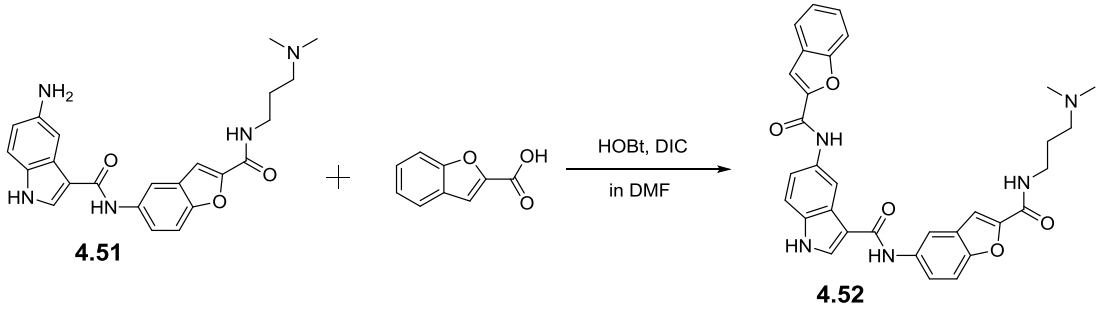

Initially, 43.30 mg of benzofuran-2-carboxylic acid (0.267 mmol, 1.2 eq.) was dissolved in 10mL of DMF in a round bottom flask fitted with a magnetic stirrer. Then DIC (72 µl, 0.467 mmol, 1.75 eq.) and HOBt (72.09 mg, 0.534 mmol, 2.0 eq.) were added to the acid (1.0 eq.) and this mixture was stirred at room temperature for at least 25 minutes to ensure the esterification. Then amine **4.51**(80 mg, 0.190 mmol, 1 eq.) was added and the mixture was allowed to stir for 6 hours at which point TLC and LCMS analysis showed the completion of reaction. Finally the reaction mixture was applied to a conditioned Isolute^{TM} SCX-2 cartridge and the product was purified by 'Catch and Release' method **(**described in the section **'Method and Materials'** of chapter 3**)**. A cream solid was obtained after drying in vacuum. Yield=37 mg, 35%.

Table 4.52: Characterisation data for compound **4.52**

4.52 Cream solid	^{1}H NMR	^{1}HNMR(400MHz,$(CD_3)_2SO$); $^{\delta}$H in ppm 11.93(s,1H),10.52(s,1H),9.94(d,*J*=8.8,1H),8.85(s,1H),8.68(dd,*J*= 6.0,1.6,1H), 8.36(s,1H), 8.32(d,*J*=2,1H), 7.83(t,*J*=8,2H), 7.78-7.74(m,1H), 7.72(s,1H), 7.66-7.61(m,2H), 7.53 (d,*J*=9.6,1H), 7.52-7.47(m,2H), 7.37 (t, *J*=7.6,1H), 3.87-3.80(m,2H), 3.39-3.32 (m,2H), 2.52 (s,6H), 1.76(t,*J*=7.2,2H).
	^{13}C NMR	(100MHz,$(CD_3)_2SO$); $^{\delta}$C in ppm 164.7, 163.3,158.5, 157.0, 156.6, 154.3, 150.4, 149.2, 149.0, 135.7, 133.4, 131.5, 127.1, 126.9, 126.3, 123.7, 122.7, 120.4, 113.0, 111.9, 111.5, 110.4, 110.0, 63.5, 52.2, 42.5, 39.5, 39.1, 38.9, 35.8, 23.1, 22,7.
	EIMS	Found 563.21 $[M+H]^+$, Calculated for $C_{32}H_{29}N_5O_5$, 562.30 $[M]^+$
	HRMS	*m/z*(+EI) Calc.for $C_{32}H_{29}N_5O_5$, 563.2169 $[M]^+$, found 564.2230 $[M+H]^+$.
	IR	(FTIR), V_{max}/'cm^{-1}): 3284, 2972, 1738, 1616, 1547, 1469, 1442, 1417, 1381, 1325, 1231, 1168, 1129, 1084, 1045, 875, 803, 736, 671.

4.53 Synthesis of N-(3-((2-((3-(dimethylamino) propyl) carbamoyl) benzo[b]thiophen-5-yl) carbamoyl)-1H-indol-5-yl)-1-methyl-1H-indole-2-carboxamide (4.53)

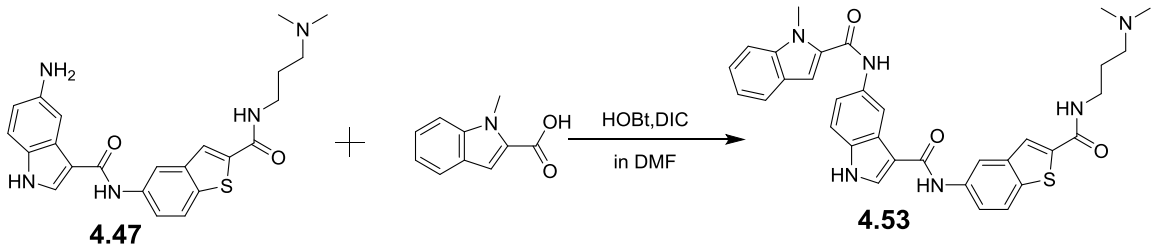

29 mg of 1-methyl-1H-indole-2-carboxylic acid (0.165 mmol, 1.2 eq.) was dissolved in 10mL of DMF in a round bottom flask fitted with a magnetic stirrer. Then DIC (45 µl, 0.2887 mmol, 1.75 eq.) and HOBt (45 mg, 0.330 mmol, 2.0 eq.) were added to the acid (1.0 eq.) and this mixture was allowed to stir at room temperature for 30 minutes to ensure the formation of ester from the acid. Then amine **4.47** (60 mg, 0.1379 mmol, 1 eq.) was added and the mixture was allowed to stir for 6 hours at which point TLC and LCMS analysis showed the completion of reaction. Finally the reaction mixture was applied to a conditioned Isolute^{TM} SCX-2 cartridge and the product was purified by 'Catch and Release' method **(**described in the section **'Method and Materials'** of chapter 3**)**. An orange solid was obtained after drying in vacuum. Yield=35mg, 43%.

Table 4.53: Characterisation data for compound **4.53**

4.53 Orange solid	^{1}H NMR	^{1}HNMR(400MHz,$(CD_3)_2SO$); $^{\delta}$H in ppm 11.84(s,1H), 10.30(s,1H), 9.92(s,1H), 8.81(s,1H), 8.67(s,1H), 8.46 (s,1H), 8.36(d,*J*=16,1H), 8.00(s,1H), 7.93(s,1H), 7.78(d,*J*=7.6,1H), 7.68(d,*J*=8,1H), 7.61-7.55(m,2H), 7.45(d,*J*=8.8,1H), 7.34 (s,1H), 7.30(t,*J*=7.6,1H), 7.12 (t,*J*=7.6,1H), 4.04(s,3H), 3.29(d,*J*=6.0,2H), 2.31 (t,*J*=6.8,2H), 2.17 (s,6H), 1.68(t,*J*=6.82H).
	^{13}C NMR	(100MHz,$(CD_3)_2SO$); $^{\delta}$C in ppm 163.3, 162.2, 161.5, 160.2, 156.7, 140.7, 139.6, 138.5, 137.2, 134.3, 133.1, 132.4, 126.4, 125.5, 124.4, 123.6, 122.8, 121.6, 120.1, 119.6, 117.1, 114.7, 113.1, 111.7, 110.5, 110.3, 105.0, 56.6, 44.9, 38.8, 35.7, 31.4, 30.7.
	EIMS	Found 592.22 $[M+H]^+$, Calculated for $C_{33}H_{32}N_6O_3S$, 591.40 $[M]^+$
	HRMS	*m/z* (+EI) Calc. for $C_{33}H_{32}N_6O_3S$ 592.2257 $[M]^+$, found 593.2314 $[M+H]^+$.
	IR	(FTIR), V_{max}/'cm^{-1}): 3257, 2932, 1647, 1575, 1548, 1521, 1476, 1435, 1386, 1359, 1338, 1308, 1246, 1224, 1169, 1149, 1096, 1037, 945, 915, 874, 806, 747, 717, 660.

4.54 Synthesis N-(3-((2-((3-(dimethylamino) propyl) carbamoyl) benzo[b]thiophen-5-yl) carbamoyl)-1H-indol-5-yl)-1H-benzo[d]imidazole-2-carboxamide (4.54).

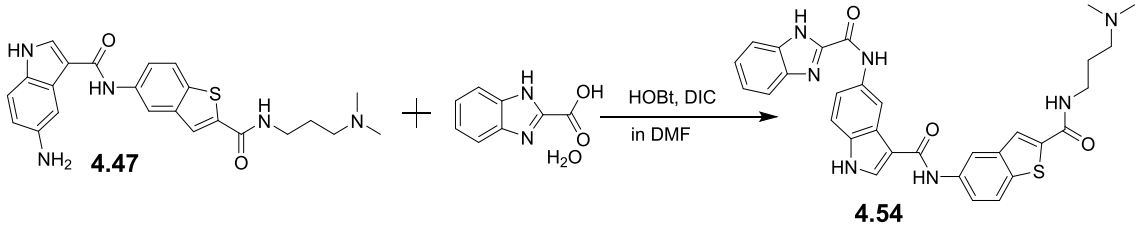

4.47 **4.54**

Initially, 30 mg of 1H-benzo[d]imidazole-2-carboxylic acid hydrate (0.165 mmol, 1.2 eq.) was dissolved in 10mL of DMF in a round bottom flask fitted with a magnetic stirrer.

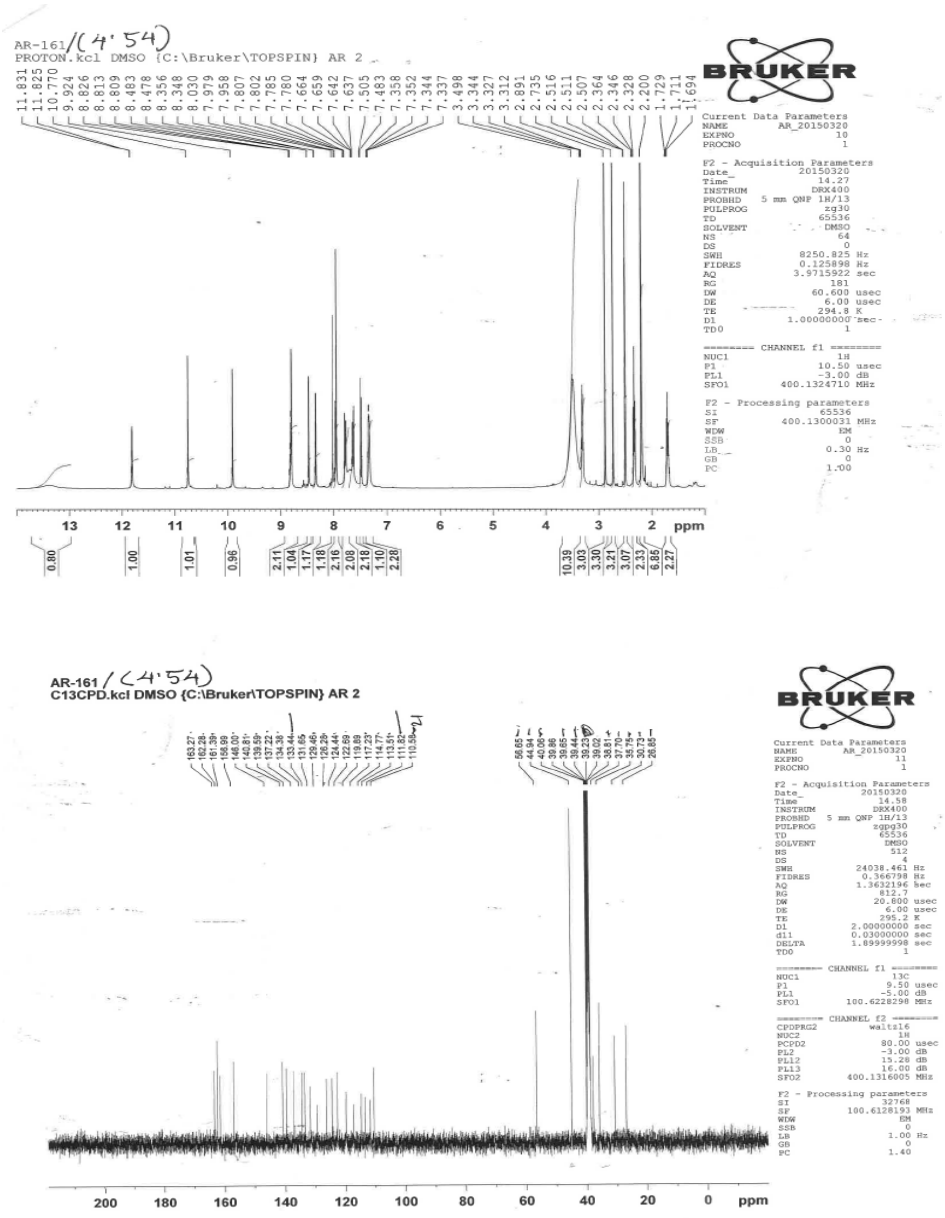

Figure 4.4: ^{1}H and ^{13}C NMR spectroscopic data of compound **4.54** as a representative of **library-2** compounds

Then DIC (45 µl, 0.228 mmol, 1.75 eq.) and HOBt (45 mg, 0.330 mmol, 2.0 eq.) were added to the acid (1.0 eq.) and this mixture was allowed to stir at room temperature for 30 minutes to ensure the esterification of the acid. Then amine **4.47** (60 mg, 0.137 mmol, 1 eq.) was added and the mixture was allowed to stir for 6 hours at which point TLC and LCMS analysis showed the completion of reaction. Finally the reaction mixture was applied to a conditioned Isolute^{TM} SCX-2 cartridge and the product was purified by 'Catch and Release' method **(**described in the section **'Method and Materials'** of chapter 3**)**. A deep brown solid was obtained after drying in vacuum. Yield was 30 mg, 38%.

Table 4.54: Characterisation data for compound **4.54**

4.54 Deep Brown solid	^{1}H NMR	^{1}HNMR(400MHz,$(CD_3)_2SO$); $^{\delta}$H in ppm 13.37(s,1H), 11.82(d,*J*=2.4,1H), 10.77(s,1H), 9.92(s,1H), 8.83-8.80(m,2H), 8.48(d,*J*=2,1H), 8.35(d,*J*=7.2,1H), 8.03(s,1H), 7.97(s,1H),7.79(dd,*J*=8.8,2.0,2H),7.65(dd,*J*=8.8,2.0,2H),7.49(d,*J*=8.8,1H), 7.35-7.33(m,2H), 3.34-3.29(m,2H), 2.34 (t,*J*=7.2,2H), 2.20 (s,4H), 1.71(t,*J*=7.2,2H).
	^{13}C NMR	(100MHz,$(CD_3)_2SO$); $^{\delta}$C in ppm 163.2, 162.2, 161.3, 156.9, 146.0, 140.8, 139.5, 137.2, 134.3, 133.4, 131.6, 129.4,126.2, 124.4, 122.6, 119.8, 117.2, 114.7, 113.5, 111.8, 110.5, 56.6, 44.9, 40.0, 39.6, 39.4, 38.8, 37.7, 35.7, 30.7, 26.8.
	EIMS	Found 580.20 $[M+H]^+$, Calculated for$C_{31}H_{29}N_7O_3S$, 579.20 $[M]^+$
	HRMS	*m/z* (+EI) Calc. for $C_{31}H_{29}N_7O_3S$, 579.2053 $[M]^+$, found 580.2113$[M+H]^+$.
	IR	(FTIR, V_{max}/'cm^{-1}): 3231, 2929, 1738, 1648, 1555, 1522, 1468, 1431, 1385, 1366, 1339, 1311, 1224, 1192, 1144, 1097, 1065, 1015, 869, 799, 736, 714, 660.

4.55 Synthesis of 5-(benzo[b]thiophene-2-carboxamido)-N-(2-((3-(dimethylamino) propyl) carbamoyl) benzofuran-5-yl)-1H-indole-3-carboxamide (4.55).

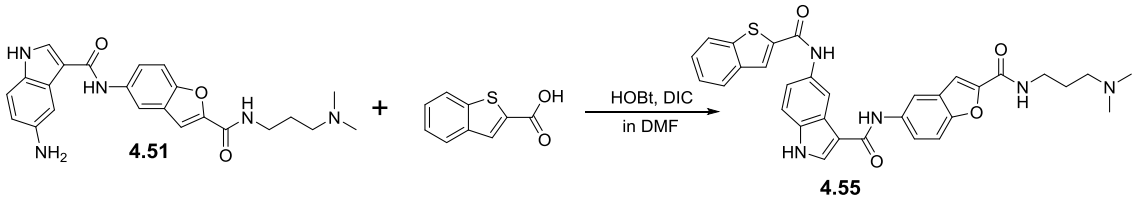

Initially, 27 mg of benzo[b]thiophene-2-carboxylic acid (0.148 mmol, 1.2 eq.) was dissolved in 5 mL of DMF in a round bottom flask fitted with a magnetic stirrer. Then DIC (40 µl, 0.259 mmol, 1.75 eq.) and HOBt (40 mg, 0.296 mmol,

2.0 eq.) were added to the acid (1.0 eq.) and this mixture was allowed to stir at room temperature for 30 minutes to ensure the formation of ester from the acid. Then amine **4.51**(52 mg, 0.124 mmol, 1 eq.) was added and the mixture was allowed to stir for 5 hours at which point TLC and LCMS analysis showed the completion of reaction. Finally the reaction mixture was applied to a conditioned Isolute^{TM} SCX-2 cartridge and the product was purified by 'Catch and Release' method **(**described in the section **'Method and Materials'** of chapter 3**)**. A light yellow solid was obtained after drying in vacuum. Yield=14 mg, 20%.

Table 4.55: Characterisation data for compound **4.55**

4.55 Light Yellow solid	^{1}H NMR	^{1}HNMR(400MHz,$(CD_3)_2SO$); $^{\delta}$H in ppm 11.76(s,1H), 10.53(s,1H), 9.86(s,1H), 8.79(s,1H), 8.59(s,1H), 8.40(s,1H),8.30(d,*J*=9.6,2H),8.04(dd,*J*=6.8,2.0,1H),7.98(t,*J*=6.8,1 H),7.72(d,*J*=2.0,1H),7.63-7.60(m,2H),7.51(s,1H),7.47(t,*J*=3.6,3H), 3.37(s,2H). 2.25 (t,*J*=6.8,2H), 2.13 (s,6H), 1.65(t,*J*=6.8,2H).
	^{13}C NMR	(100MHz,$(CD_3)_2SO$); $^{\delta}$C in ppm 163.1, 157.9, 150.3, 149.7, 140.6, 140.3, 139.2, 135.8, 133.3, 132.1, 127.2, 126.4, 126.2, 125.2, 124.9, 122.8, 120.0, 113.2, 112.7, 111.5, 110.4, 109.4, 56.8, 45.1, 40.0, 39.8, 39.6, 39.4, 39.0, 38.8, 37.3, 26.9.
	EIMS	Found580.20 $[M+H]^+$, Calculated for $C_{32}H_{29}N_5O_4S$, 579.19 $[M]^+$
	HRMS	*m/z* (+EI) Calc. for $C_{32}H_{29}N_5O_4S$, 579.1940 $[M]^+$, found 580.2003$[M+H]^+$.
	IR	(FTIR), V_{max}/'cm^{-1}): 3275, 2971, 2344, 2298, 1738, 1649, 1628, 1604, 1534, 1468, 1437, 1366, 1343, 1310, 1270, 1237, 1207, 1178, 1148, 1081, 1041, 938, 879, 792, 743, 722, 682, 662.

4.56 Synthesis of N-(3-((2-((3-(dimethylamino) propyl) carbamoyl) benzofuran-5-yl) carbamoyl)-1H-indol-5-yl)-1H-benzo[d]imidazole-2-carboxamide (4.56)

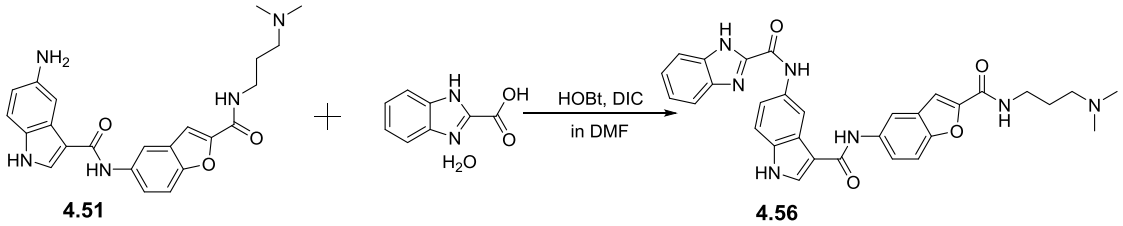

4.51 4.56

Initially, 30 mg of 1H-benzo[d]imidazole-2-carboxylic acid hydrate (0.186 mmol, 1.2 eq.) was dissolved in 10mL of DMF in a round bottom flask fitted with a magnetic stirrer. Then DIC (50 µl, 0.3255 mmol, 1.75 eq.) and HOBt (50 mg, 0.372 mmol, 2.0 eq.) were added to the acid (1.0 eq.) and this mixture was

allowed to stir at room temperature for 30 minutes to ensure the formation of ester from the acid. Then amine **4.51**(65 mg, 0.155 mmol, 1 eq.) was added and the mixture was allowed to stir for 5 hours at which point TLC and LCMS analysis showed the completion of reaction. At last the reaction mixture was taken to a conditioned Isolute^{TM} SCX-2 cartridge for purification and the product was purified by 'Catch and Release' method **(**described in the section **'Method and Materials'** of chapter 3**)**. A yellow solid was obtained after drying in vacuum. Yield=51 mg, 58%.

Table 4.56: Characterisation data for compound **4.56**

4.56 Yellow solid	^{1}H NMR	^{1}HNMR(400MHz,$(CD_3)_2SO$); $^{\delta}$H in ppm 13.45(s,1H), 11.82(s,1H), 10.74(s,1H), 9.87(s,1H), 8.82(s,2H), 8.33(s,2H), 7.73(t,*J*=9.3,2H), 7.63-7.58(m,2H), 7.54(d,*J*=4.0,1H), 7.48(dd,*J*=8.4,3.6,1H),7.33(s,2H),7.19-7.14(m,1H), 3.30(d,*J*=5.6,2H), 2.33(d,*J*=6.4,2H), 2.19(s,6H), 1.69(t,*J*=6.4,2H).
	^{13}C NMR	(100MHz,$(CD_3)_2SO$); $^{\delta}$C in ppm 163.2, 162.3, 158.0, 157.0, 150.3, 149.7, 146.0, 141.9, 135.8, 133.4, 131.6, 129.3, 127.2, 126.3, 123.4, 120.1, 119.6, 117.1, 113.5, 112.8, 111.8, 111.5, 110.6, 109.4, 56.7, 44.9, 40.1, 39.4, 38.8, 37.2, 26.7.
	EIMS	Found 563.30$[M+H]^+$, Calculated for $C_{31}H_{29}N_7O_4$, 563.22 $[M]^+$
	HRMS	*m/z* (+EI) Calc. for $C_{31}H_{29}N_7O_4$, 563.2281 $[M]^+$, found 564.2340 $[M+H]^+$.
	IR	(FTIR, V_{max}/'cm^{-1}): 3215, 2971, 1738, 1624, 1592, 1531, 1470, 1434, 1330, 1210, 1159, 1079, 945, 867, 766, 736.

4.57 Synthesis of N-(3-((2-((3-(dimethylamino) propyl) carbamoyl) benzofuran-5-yl) carbamoyl)-1H-indol-5-yl)-1-methyl-1H-indole-2-carboxamide (4.57)

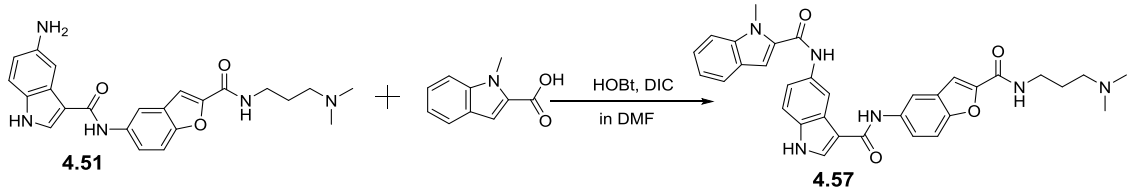

40 mg of 1-methyl-1H-indole-2-carboxylic acid (0.229 mmol, 1.2 eq.) was dissolved in 10mL of DMF in a round bottom flask fitted with a magnetic stirrer. Then DIC (62 µl, 0.400 mmol, 1.75 eq.) and HOBt (62 mg, 0.458 mmol, 2.0 eq.) were added to the acid (1.0 eq.) and this mixture was allowed to stir at room temperature for 30 minutes to ensure the formation of ester from the acid. Then amine **4.51** (80 mg, 0.190 mmol, 1 eq.) was added and the mixture was allowed

to stir for 7 hours at which point TLC and LCMS analysis showed the completion of reaction. Finally the reaction mixture was applied to a conditioned Isolute^{TM} SCX-2 cartridge and the product was purified by 'Catch and Release' method **(**described in the section **'Method and Materials'** of chapter 3**)**. An orange solid was obtained after drying in vacuum. Yield=82 mg, 75%.

Table 4.57: Characterisation data for compound **4.57**

4.57 Orange solid	^{1}H NMR	^{1}HNMR(400MHz,$(CD_3)_2SO$); $^{\delta}$H in ppm 11.80(s,1H),10.31(s,1H),9.88(s,1H),8.81(d,*J*=3.2,1H),8.72(d,*J*=2.0 ,1H),8.34(s,2H),7.77-7.74(m,1H),7.69(dd,*J*=8.0,2.8,1H), 7.62(d,*J*=8.8,2H), 7.55(t,*J*=6.0,2H), 7.48(dd,*J*=8.4,3.2,1H), 7.37 (d,*J*=2.8,1H), 7.31-7.29(m,1H), 7.17-7.11(m,1H), 3.50(s,3H), 3.30(t,*J*=6.0,2H), 2.28-2.24 (m,2H), 2.14(s,6H), 1.69-1.65(m,2H).
	^{13}C NMR	(100MHz,$(CD_3)_2SO$); $^{\delta}$C in ppm 163.2, 162.3, 160.2, 158.0, 150.3, 149.8, 138.5, 135.8, 133.2, 132.5, 129.1, 127.3, 126.4, 125.6, 123.6, 121.6, 120.1, 120.0, 117.0, 113.2, 112.7, 111.6, 111.5, 110.5, 109.4, 105.1, 56.9, 45.1, 40.0, 39.2, 37.3, 35.7, 31.4.
	EIMS	Found 576.30 $[M+H]^+$, Calculated for $C_{33}H_{32}N_6O_4$, 576.24 $[M]^+$
	HRMS	*m/z* (+EI) Calc. for $C_{33}H_{32}N_6O_4$, 576.2485 $[M]^+$, found 577.2544 $[M+H]^+$.
	IR	(FTIR), V_{max}/'cm^{-1}): 3197, 1705, 1626, 1535, 1469, 1435, 1359, 1333, 1215, 1181, 1148, 1077, 1048, 1024, 1005, 871, 809, 789, 769, 747, 622.

4.58 Synthesis of N-(3-(dimethylamino) propyl)-5-(5-nitro-1H-indole-3-carboxamido)-1H-indole-2-carboxamide (4.58).

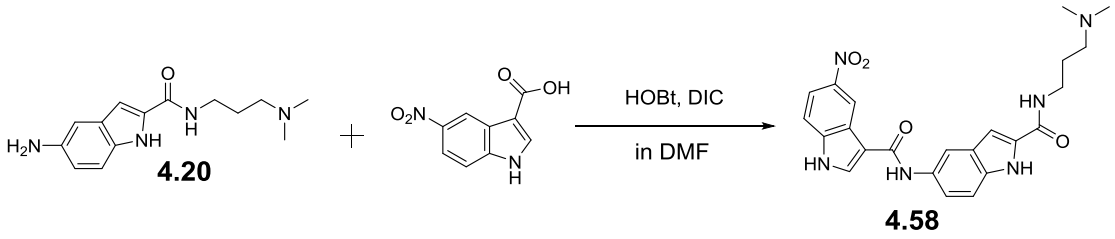

4.20 **4.58**

Initially, 171 mg of 5-nitro-1H-indole-3-carboxylic acid (0.830 mmol, 1.2 eq.) was dissolved in 10mL of DMF in a round bottom flask fitted with a magnetic stirrer. Then DIC (224 µl, 1.45 mmol, 1.75 eq.) and HOBt (224 mg, 1.66 mmol, 2.0 eq.) were added to the acid (1.0 eq.) and this mixture was allowed to stir at room temperature for 30 minutes to ensure the formation of ester from the acid. Then amine **4.20** (180 mg, 0.692 mmol, 1 eq.) was added and the mixture was

allowed to stir for about 7 hours at which point TLC and LCMS analysis showed the completion of reaction. Finally the reaction mixture was applied to a conditioned Isolute^{TM} SCX-2 cartridge and the product was purified by 'Catch and Release' method **(**described in the section **'Method and Materials'** of chapter 3**)**. A yellow solid was obtained after drying in vacuum. Yield=122mg, 40 %.

Table 4.58: Characterisation data for compound **4.58**

4.58 Yellow solid	^{1}H NMR	^{1}HNMR(400MHz,$(CD_3)_2SO$); $^\delta$H in ppm 11.55(s,1H), 9.89(s,1H), 9.18(d,*J*=2.4,1H), 8.55(d,*J*=7.8,2H), 8.15(t,*J*=4.0,1H),8.09(dd,*J*=9.2,2.4,1H),7.95(s,1H),7.68(d,*J*=8.8,1H), 7.48-7.40 (m,1H), 7.41(d,*J*=8.8,1H), 7.07(s,1H), 3.34-3.30(m,2H), 2.29 (t,*J*=7.2,2H), 2.16(s,6H), 1.69(t,*J*=6.8,2H).
	EIMS	Found 449.10$[M+H]^+$, Calculated for $C_{23}H_{24}N_6O_4$ 448.18 $[M]^+$

4.59 Synthesis of 5-(5-amino-1H-indole-3-carboxamido)-N-(3-(dimethyl amino) propyl)-1H-indole-2-carboxamide (4.59)

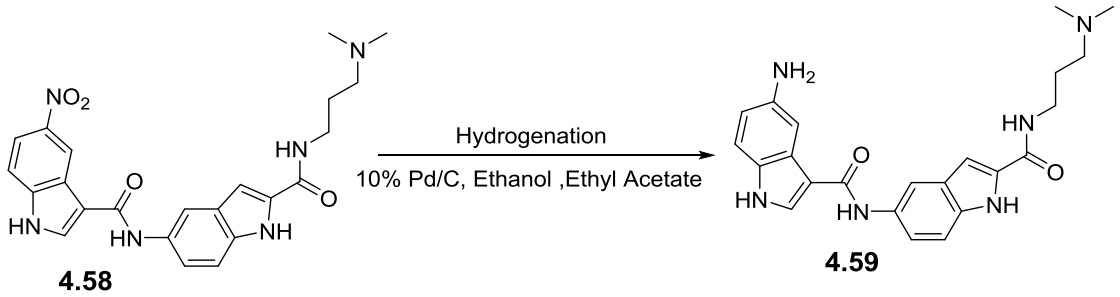

120 mg of **4.58** was dissolved in 20 mL of ethanol and 1 mL of ethyl acetate was added to a hydrogenation reaction bottle. 20 mg of 10% Pd (palladium on activated carbon) 20 was added into the reaction vessel, and mixed it well. The reaction bottle was sealed and connected to a hydrogen reservoir. Air from the reaction bottle was removed by applying vacuum, and was then by flushed with hydrogen. Typically, a hydrogen pressure of approximately 40 psi was applied from the reservoir, and the bottle was then shaken vigorously to initiate the reaction. Progress of the reaction was monitored by TLC and LCMS. The complete hydrogenation took about 6 hours at which point TLC and LCMS analysis showed the completion of reaction. The shaker was stopped, the bottle was vented, and the product was recovered by means of filtration using Celite.

Finally, the product is concentrated by using a rotary evaporator. A yellow solid was obtained after drying in vacuum. Yield=85mg, 77%.

Table 4.59: Characterisation data for compound **4.59**

4.59 Yellow solid	^{1}H NMR	^{1}HNMR(400MHz,$(CD_3)_2SO$); $^\delta$H in ppm 11.53(s,1H),11.32(s,1H), 9.46(s,1H), 8.55(t,*J*=5.2,1H), 8.11(s,2H), 7.48(t,*J*=8.4,2H), 7.39(d,*J*=8.8,1H), 7.16 (d,*J*=8.4,1H), 7.07(s,1H), 6.59-6.57(m,1H), 3.35-3.30(m,2H), 2.28 (t,*J*=7.2,2H), 2.15(s,6H), 1.72-1.65(m ,2H).
	EIMS	Found 419.20 $[M+H]^+$,Calculated for $C_{23}H_{26}N_6O_2$, 418.21 $[M]^+$

4.60 Synthesis of N-(3-(dimethyl amino) propyl)-5-(5-(5-nitro-1H-indole-2-carboxamido)-1H-indole-3-carboxamido)-1H-indole-2-carboxamide (4.60).

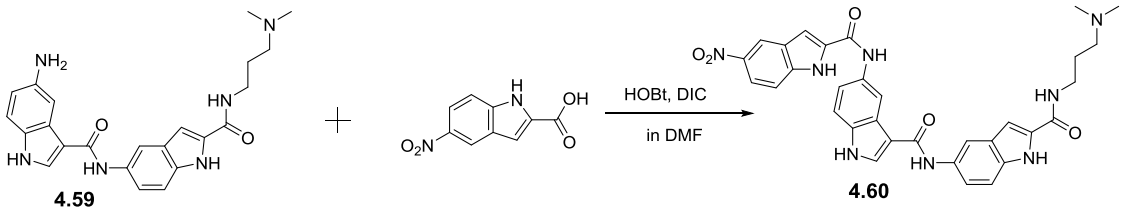

Initially, 41.23 mg of 5-nitro-1H-indole-2-carboxylic acid (0.20 mmol, 1.2 eq.) was dissolved in 5 mL of DMF in a round bottom flask fitted with a magnetic stirrer. Then DIC (54 µl, 0.35 mmol, 1.75 eq.) and HOBt (54 mg, 0.40 mmol, 2.0 eq.) were added to the acid (1.0 eq.) and this mixture was stirred at room temperature for 30 minutes to ensure the formation of ester from the acid. Then amine **4.59**(60 mg, 0.143 mmol, 1 eq.) was added and the mixture was allowed to stir for 7 hours at which point TLC and LCMS analysis showed the completion of reaction. Lastly the reaction mixture was purified by conditioned Isolute^{TM} SCX-2 cartridge and the product was purified by 'Catch and Release' method **(**described in the section **'Method and Materials'** of chapter 3**)**. A yellow solid was obtained after drying in vacuum. Yield=29 mg, 34%.

Table 4.60: Characterisation data for compound **4.60**

4.60 Yellow solid	^{1}H NMR	^{1}HNMR(400MHz,$(CD_3)_2SO$); $^{\delta}$H in ppm 12.46(s,1H), 11.72(s,1H), 11.49(s,1H), 10.49(s,1H), 9.65(s,1H), 8.77 (d,*J*=1.6,1H), 8.60(s,1H), 8.51(s,1H), 8.31(d,*J*=2.0,1H), 8.10(t,*J*=8.8,2H), 7.75(s,1H), 7.69(t,*J*=7.2,1H), 7.64(d,*J*=9.2,1H), 7.47 (t,*J*=8.8,2H), 7.38(d,*J*=8.8,1H), 7.06(s,1H), 3.33(m,2H), 2.30 (t,*J*=6.8,2H), 2.15(s,6H), 1.70(t,*J*=6.8,2H).
	^{13}C NMR	(100MHz,$(CD_3)_2SO$); $^{\delta}$C in ppm 163.0, 162.2, 160.9, 158.5, 141.2, 139.4, 135.5, 133.3, 133.0, 132.2, 131.9, 126.9, 126.47, 126.42,119.2, 118.2, 113.4, 112.8, 111.9, 111.6, 110.8, 105.6, 102.0, 56.8, 45.1, 39.6, 39.2, 38.7, 37.2, 35.7, 30.7, 27.2.
	EIMS	Found 606.40 $[M+H]^+$, Calculated for $C_{32}H_{30}N_8O$,606.23 $[M]^+$
	HRMS	*m/z* (+EI) Calc. for $C_{32}H_{30}N_8O_5$, 606.2339 $[M]^+$, found 607.2400 $[M+H]^+$.
	IR	(FTIR), V_{max}/'cm^{-1}): 3236, 1631, 1544, 1469, 1418, 1384, 1317, 1259, 1099, 1067, 806, 768, 743, 663.

4.61 Synthesis of 5-(5-(benzofuran-2-carboxamido)-1H-indole-3-carboxamido)-N-(3-(dimethylamino) propyl)-1H-indole-2-carboxamide (4.61).

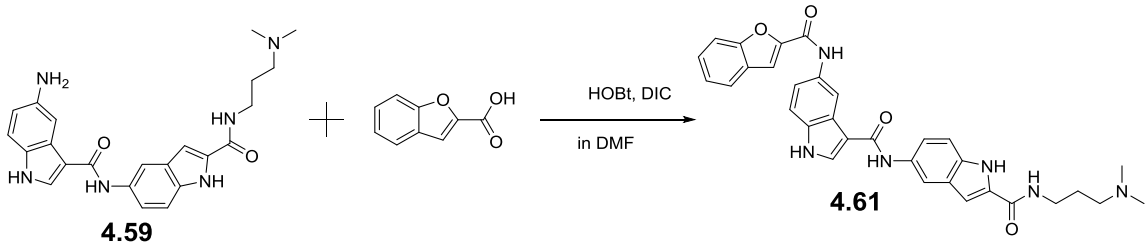

4.59 **4.61**

Initially, 33 mg of benzofuran-2-carboxylic acid (0.20 mmol, 1.2 eq.) was dissolved in 10mL of DMF in a round bottom flask fitted with a magnetic stirrer. Then DIC (54 µl, 0.35 mmol, 1.75 eq.) and HOBt (54 mg, 0.40 mmol, 2.0 eq.) were added to the acid (1.0 eq.) and this mixture was allowed to stir at room temperature for 30 minutes to ensure the formation of ester from the acid. Then amine **4.59**(85 mg, 0.143 mmol, 1 eq.) was added and the mixture was allowed to stir for 4 hours at which point TLC and LCMS analysis showed the completion of reaction. Finally the reaction mixture was applied to a conditioned Isolute^{TM} SCX-2 cartridge and the product was purified by 'Catch and Release' method **(**described in the section **'Method and Materials'** of chapter 3**)**. An orange solid was obtained after drying in vacuum. Yield=65 mg, 57%.

Table 4.61: Characterisation data for compound **4.61**

4.61 Orange solid	^{1}H NMR	^{1}HNMR(400MHz,$(CD_3)_2SO$); $^{\delta}$H in ppm 11.53(s,1H),10.52(s,1H),9.67(s,1H),8.68(d,*J*=2.0,1H),8.55(t,*J*=5.6, 1H),8.34(s,1H),8.16(s,1H),7.96(s,1H),7.83(t,*J*=8.0,2H),7.74(d,*J*=8. 4,1H), 7.66(dd,*J*=8.8,2.0,1H), 7.50 (t,*J*=7.2,3H), 7.42-7.35(m,2H), 7.09(s,1H), 3.35-3.30(m,2H), 2.28 (t,*J*=6.8,2H), 2.15(s,6H), 1.71-1.65(m,2H).
	^{13}C NMR	(100MHz,$(CD_3)_2SO$); $^{\delta}$C in ppm 163.0, 162.2, 160.9, 156.8, 156.4, 154.3, 149.2, 133.4, 133.0, 132.3, 131.6, 128.8, 127.2, 126.9, 126.8, 126.4, 123.7, 122.7, 118.2, 116.9, 113.6, 111.9, 111.8, 111.6, 110.8, 109.8, 102.1, 56.8, 45.1, 39.2, 35.7, 27.2.
	EIMS	Found 563.20 $[M+H]^+$, Calculated for $C_{32}H_{30}N_6O_4$, 562.23 $[M]^+$
	HRMS	*m/z* (+EI) Calc. for $C_{32}H_{30}N_6O_4$, 562.2329 $[M]^+$, found 563.2387$[M+H]^+$.
	IR	(FTIR), V_{max}/'cm^{-1}): 3261, 2973, 2255, 1635, 1590, 1540, 1470, 1447, 1355, 1309, 1258, 1231, 1176, 1047, 1023, 999, 866, 814, 744, 677, 614.

4.62 Synthesis of N-(3-(dimethylamino) propyl)-5-nitro-1H-indole-3-carboxamide (4.62).

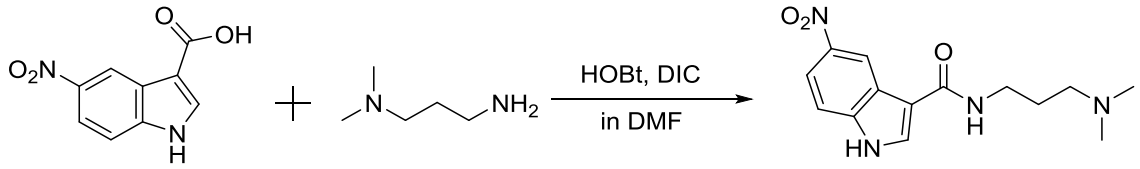

4.62

Initially, 300 mg of 5-nitro-1H-indole-3-carboxylic acid (1.45 mmol, 1.2 eq.) was dissolved in 10mL of DMF in a round bottom flask fitted with a magnetic stirrer. Then DIC (278 µl, 1.80 mmol, 1.75 eq.) and HOBt (278 mg, 2.06 mmol, 2.0 eq.) were added to the acid (1.0 eq.) and this mixture was allowed to stir at room temperature for 30 minutes to ensure the formation of ester from the acid. Then N1, N1-dimethylpropane-1, 3-diamine (106 mg, 1.04 mmol, 1 eq.) was added and the mixture was continued to stir for 9 hours at which point TLC and LCMS analysis showed the completion of reaction. Finally the reaction mixture was purified through conditioned Isolute^{TM} SCX-2 cartridge and the product was purified by 'Catch and Release' method **(**described in the section **'Method and Materials'** of chapter 3**)**. A pale yellow solid was obtained after drying in vacuum. Yield=210 mg, 50%.

Table 4.62: Characterisation data for compound **4.62**

4.62 Orange solid	^{1}H NMR	^{1}HNMR(400MHz,$(CD_3)_2SO$); $^\delta$H in ppm 12.54(s,1H),9.11(d,*J*=2.4,1H),8.278.25(m,2H),8.06(dd,*J*=9.2,2.4,1 H), 7.64 (d, *J*=9.2,1H), 3.34-3.29(m,2H), 2.33 (t,*J*=7.2,2H), 2.19 (s,6H), 1.70(t,*J*=6.8,2H).
	EIMS	Found 290.10 $[M+H]^+$, Calculated for $C_{14}H_{18}N_4O_3$, 290.13 $[M]^+$

4.63 Synthesis of 5-amino-N-(3-(dimethyl amino) propyl)-1H-indole-3-carboxamide (4.63).

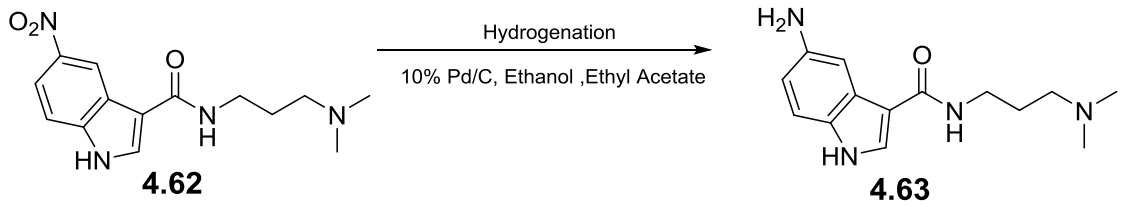

4.62 **4.63**

205 mg of **4.62** was dissolved in 20 mL of ethanol and added to a hydrogenation reaction bottle. 20 mg of 10% Pd (palladium on activated carbon) was added into the reaction vessel, and mixed well. The reaction bottle was sealed and connected to a hydrogen reservoir. Air within the bottle was removed by applying vacuum, and it ws flushed with hydrogen. A hydrogen pressure of approximately 40 psi was applied from the reservoir and the bottle was then shaken vigorously to initiate the reaction. Progress of the reaction was monitored by TLC and LCMS. The shaker was stopped upon the completion of the reaction after 5 hours at which point TLC and LCMS analysis showed the completion of reaction. The bottle was vented and the product was recovered by means of filtration using Celite. Finally, the product is concentrated by using a rotary evaporator. A deep brown solid was obtained after drying in vacuum. Yield=180 mg, 97%.

Table 4.63: Characterisation data for compound **4.63**

4.63 Deep Brown Solid	^{1}H NMR	^{1}HNMR(400MHz,$(CD_3)_2SO$); $^\delta$H in ppm 11.24(d,*J*=2,1H),7.83-7.79(m,2H),7.38(d,*J*=2,1H), 7.11(d,*J*=8.8,1H), 6.56-6.54 (m,1H), 4.56(s,2H), 3.29-3.24(m,2H), 2.31 (t,*J*=7.2,2H), 2.17 (s,6H), 1.66(t,*J*=7.2,2H).
	EIMS	Found 260.90 $[M+H]^+$, Calculated for$C_{14}H_{20}N_4O$, $[M]^+$

4.64 Synthesis of 5-amino-N-(3-(dimethylamino) propyl)-1H-indole-3-carboxamide (4.64).

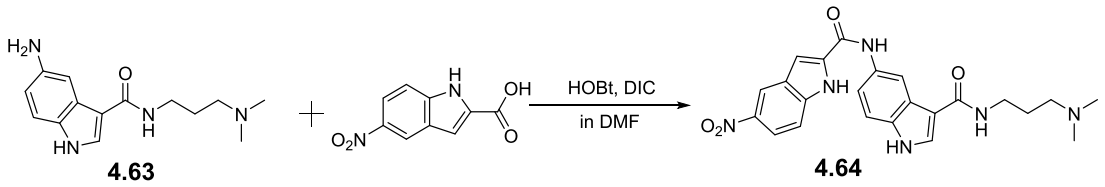

Initially, 95 mg of 5-nitro-1H-indole-2-carboxylic acid (0.461 mmol, 1.2 eq.) was dissolved in 10mL of DMF in a round bottom flask fitted with a magnetic stirrer. Then DIC (124 µl, 0.806 mmol, 1.75 eq.) and HOBt (124 mg, 0.922 mmol, 2.0 eq.) were added to the acid (1.0 eq.) and this mixture was allowed to stir at room temperature for 30 minutes to ensure the formation of ester from the acid. Then amine **4.63**(100 mg, 0.38 mmol, 1 eq.) was added and the mixture was allowed to stir for 7 hours at which point TLC and LCMS analysis showed the completion of reaction. Finally the reaction mixture was applied to a conditioned Isolute^{TM} SCX-2 cartridge and the product was purified by 'Catch and Release' method **(**described in the section **'Method and Materials'** of chapter 3**)**. A yellow solid was obtained after drying in vacuum. Yield=61mg, 36%.

Table 4.64: Characterisation data for compound **4.64**

4.64 Yellow solid	^{1}H NMR	^{1}HNMR(400MHz,$(CD_3)_2SO$); $^{\delta}$H in ppm 12.38(s,1H),11.50(s,1H),10.42(s,1H),8.74(d,*J*=2.0,1H),8.47(d,*J*=1.6,1H), 8.10(dd,*J*=9.2,2.4,1H), 7.98(d,*J*=2.4,1H), 7.89(t,*J*=7.2,1H), 7.71 (s,1H), 7.66-7.62(m,2H), 7.42(d,*J*=8.4,1H), 2.49(t,*J*=2.0,2H), 2.29(t,*J*=7.2,2H), 2.14(s,6H), 1.69-1.63(m,2H).
	^{13}C NMR	(100MHz,$(CD_3)_2SO$); $^{\delta}$C in ppm 164.4, 158.5, 141.2, 139.4, 135.5, 133.3, 131.6, 126.4, 126.1, 118.4, 111.4, 110.8, 57.0, 45.1, 39.9, 39.7, 39.5, 39.3, 39.0, 38.8, 36.9, 35.7, 27.5.
	EIMS	Found 449.10$[M+H]^+$, Calculated for $C_{23}H_{25}N_6O$, 448.18 $[M]^+$
	HRMS	*m/z* (+EI) Calc. for $C_{23}H_{25}N_6O_4$, 448.1859 $[M]^+$, found 449.1925 $[M+H]^+$.
	IR	(FTIR), V_{max}/'cm^{-1}): 3250, 2933, 1541, 1513, 1540, 1470, 1442, 1416, 1386, 1325, 1281, 1236, 1210, 1164, 1097, 1066, 1039, 990, 890, 867, 830, 812, 794, 763, 747, 727, 678, 661.

4.65 Synthesis of 5-amino-N-(3-((3-(dimethylamino) propyl) carbamoyl)-1H-indol-5-yl)-1H-indole-2-carboxamide (4.65).

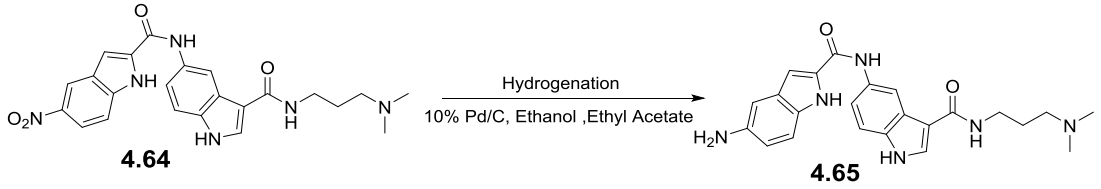

4.64 **4.65**

120 mg of **4.64** was dissolved in 20 mL of ethanol and 1 mL of ethyl acetate was added to a hydrogenation reaction bottle. 20 mg of 10% Pd (palladium on activated carbon) was added into the reaction vessel, and mixed this well. The reaction bottle was sealed and connected to a hydrogen reservoir. Air from the reaction bottle was removed by applying vacuum, and was then by flushed with hydrogen. Typically, a hydrogen pressure of approximately 40 psi was applied from the reservoir, and the bottle was then shaken vigorously to initiate the reaction. Progress of the reaction was monitored by TLC and LCMS analysis. The completion of the reaction required about 6 hours at which point TLC and LCMS analysis showed the completion of reaction. The shaker was stopped, the bottle was vented, and the product was recovered by the process of filtration using Celite. Finally, the product is concentrated by using a rotary evaporator. A yellow solid was obtained after drying in vacuum. Yield=82 mg, 74 %.

Table 4.65: Characterisation data for compound **4.65**

4.65 Yellow solid	^{1}H NMR	^{1}HNMR(400MHz,$(CD_3)_2SO$); $^\delta$H in ppm 11.47(s,1H),11.09(s,1H),9.93(s,1H),8.32(d,*J*=1.2,,1H),7.83(d,*J*=7.6,2H), 7.71(s,1H), 7.42(dd,*J*=8.4,1.2,1H), 7.34(d,*J*=8.8,1H), 7.05(d,*J*=8.4,1H), 6.98(s,1H), 6.49(dd,*J*=8.8,1H), 3.13-3.09(m,2H), 2.50(s,2H), 2.16(t,*J*=7.2,2H), 1.98(s,6H),1.53-1.46(m,2H).
	EIMS	Found 418.30 $[M+H]^+$, Calculated for $C_{23}H_{26}N_6O_2$, 418.21 $[M]^+$

4.66 Synthesis of N-(3-((3-(dimethylamino) propyl) carbamoyl)-1H-indol-5-yl)-5-(5-nitro-1H-indole-2-carboxamido)-1H-indole-2-carboxamide (4.66).

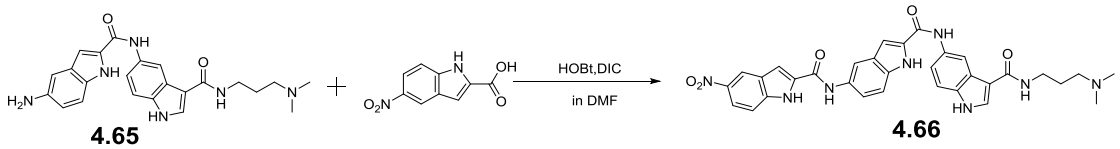

4.65 **4.66**

Initially, 57 mg of 5-nitro-1H-indole-2-carboxylic acid (0.278 mmol, 1.2 eq.) was dissolved in 10mL of DMF in a round bottom flask fitted with a magnetic stirrer.

Then DIC (75 µl, 0.488 mmol, 1.75 eq.) and HOBt (75 mg, 0.549 mmol, 2.0 eq.) were added to the acid (1.0 eq.) and this mixture was allowed to stir at room temperature for 30 minutes to ensure the formation of ester from the acid. Then amine **4.65**(82 mg, 0.196 mmol, 1 eq.) was added and the mixture was allowed to stir for 6 hours at which point TLC and LCMS analysis showed the completion of reaction. Finally the reaction mixture was applied to a conditioned Isolute^{TM} SCX-2 cartridge and the product was purified by 'Catch and Release' method **(**described in the section **'Method and Materials'** of chapter 3**)**. A yellow solid was obtained after drying in vacuum. Yield=64 mg, 54%.

Table 4.66: Characterisation data for compound **4.66**

4.66 Yellow solid	^{1}H NMR	^{1}HNMR(400MHz,$(CD_3)_2SO$); $^{\delta}$H in ppm 12.48(s,1H),11.71(s,1H),11.51(d,*J*=2.0,1H),10.43(s,1H),10.19(s,1H),8.78(d,*J*=2.4,1H),8.49(d,*J*=1.6,1H),8.18(s,1H),8.12(dd,*J*=9.2,2.0,1H),8.00(d,*J*=2.8,1H),7.95-7.90(m,1H),7.72(s,1H), 7.68(dd,*J*=8.8,1.6,1H), 7.64(d,*J*=9.2,1H), 7.58 (dd,*J*=8.8,1.6,1H), 7.51(s,1H), 6.78 (d,*J*=6.8,1H), 6.59 (d,*J*=6.8,1H), 3.32-3.27(m,2H), 2.28(t,*J*=7.2,2H), 2.15(s,6H), 1.67(t,*J*=6.8,2H).
	^{13}C NMR	(100MHz,$(CD_3)_2SO$); $^{\delta}$C in ppm 164.5, 159.2, 158.6, 141.2, 139.5, 135.4, 133.9, 133.1, 132.7, 131.9, 131.1, 127.9, 126.9, 126.4, 126.1, 119.2, 118.7, 118.5, 116.8, 113.2, 113.0, 112.8, 112.3, 111.4, 110.8, 105.6, 103.4, 57.0, 45.1, 39.0, 36.9, 27.5.
	EIMS	Found 606.40 $[M+H]^+$, Calculated for $C_{32}H_{30}N_8O_5$, 606.23 $[M]^+$
	HRMS	*m/z* (+EI) Calc. for $C_{32}H_{30}N_8O_5$, 606.2339 $[M]^+$, found 607.2398 $[M+H]^+$.
	IR	(FTIR), V_{max}/'cm^{-1}): 3252, 2921, 1646, 1616, 1587, 1554, 1519, 1471, 1417, 1372, 1324, 1286, 1248, 1216, 1166, 1135, 1099, 1069, 963, 943, 862, 802, 766, 743, 730, 681, 627.

4.67 Synthesis of N-(3-(dimethylamino) propyl)-5-(5-(5-nitro-1H-indole-3-carboxamido)-1H-indole-2-carboxamido)-1H-indole-2-carboxamide (4.67).

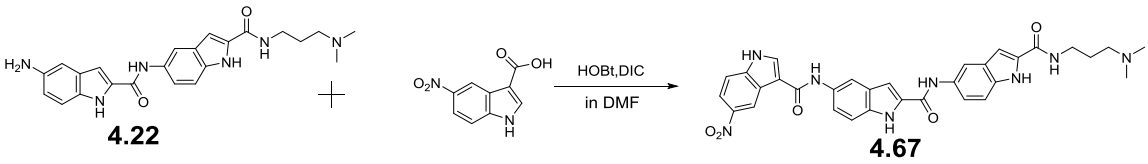

4.22 **4.67**

Initially, 53 mg of 5-nitro-1H-indole-3-carboxylic acid (0.258 mmol, 1.2 eq.) was dissolved in 5 mL of DMF in a round bottom flask fitted with a magnetic stirrer. Then DIC (70 µl, 0.451 mmol, 1.75 eq.) and HOBt (70 mg, 0.516 mmol, 2.0 eq.) were added to the acid (1.0 eq.) and this mixture was allowed to stir at room

temperature for 30 minutes to ensure the formation of ester from the acid. Then amine **4.22** (90 mg, 0.215 mmol, 1 eq.) was added and that mixture was allowed to stir for 4 hours at which point TLC and LCMS analysis showed the completion of reaction. Lastly the reaction mixture was applied to a conditioned Isolute^{TM} SCX-2 cartridge and the product was purified by 'Catch and Release' method **(**described in the section **'Method and Materials'** of chapter 3**)**. A deep brown solid was obtained after drying in vacuum. Yield=38 mg, 29%.

Table 4.67: Characterisation data for compound **4.67**

4.67 Deep Brown solid	^{1}H NMR	^{1}HNMR(400MHz,$(CD_3)_2SO$); $^{\delta}$H in ppm 12.45(s,1H), 11.68(s,1H), 11.57(s,1H), 10.15(s,1H), 9.93(s,1H), 9.18(d,*J*=1.8,1H), 8.57(s,1H), 8.52(s,1H), 8.19(s,1H), 8.11(s,1H), 8.09(d,*J*=2.4,1H), 7.69(d,*J*=9.2,1H), 7.54-7.50(m,2H), 7.47(s,1H), 7.44(d,*J*=5.6,1H), 7.41(d,*J*=3.2,1H), 7.10(d,*J*=1.2,1H), 3.34-3.29(m,2H), 2.30(t,*J*=7.2,2H), 2.16(s,6H), 1.69(t,*J*=6.8,2H).
	^{13}C NMR	(100MHz,$(CD_3)_2SO$); $^{\delta}$C in ppm 162.2, 162.1, 160.9, 159.4, 141.8, 139.3, 133.5, 133.4, 132.5, 132.4, 131.9, 131.6, 131.3, 127.0, 126.9, 125.9, 118.6, 118.4, 117.9, 117.4, 112.7, 112.4, 112.1, 103.2, 102.2, 56.8, 45.0, 38.8, 37.2, 35.7, 30.7, 27.1.
	EIMS	Found 607.20 $[M+H]^+$, Calculated for $C_{32}H_{30}N_8O_5$, 606.23 $[M]^+$
	HRMS	*m/z* (+EI) Calc. for $C_{32}H_{30}N_8O_5$, 606.2339 $[M]^+$, found 607.2399 $[M+H]^+$.
	IR	(FTIR), V_{max}/'cm^{-1}): 3242, 2934, 1638, 1543, 1522, 1471, 1419, 1380, 1323, 1298, 1251, 1228, 1201, 1130, 1094, 1072, 1040, 962, 869, 809, 790, 778, 744, 715, 691, 660.

4.68 Synthesis of N-(3-(dimethylamino) propyl)-5-(5-nitro-1H-indole-3-carboxamido)-1H-indole-3-carboxamide (4.68).

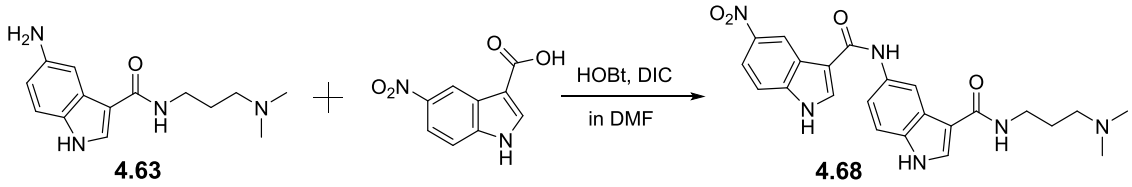

Initially, 200 mg of 5-nitro-1H-indole-3-carboxylic acid (0.968 mmol, 1.2 eq.) was dissolved in 5 mL of DMF in a round bottom flask fitted with a magnetic stirrer. Then DIC (261 µl, 1.69 mmol, 1.75 eq.) and HOBt (260 mg, 1.93 mmol, 2.0 eq.) were added to the acid (1.0 eq.) and this mixture was allowed to stir at room temperature for 30 minutes for esterification of acid. Then amine **4.63**

(180 mg, 0.692 mmol, 1 eq.) was added to the mixture and the mixture was allowed to stir for 15 hours at which point TLC and LCMS analysis showed the completion of reaction. Finally the reaction mixture purified by the help of conditioned Isolute^{TM} SCX-2 cartridge and the product was purified by 'Catch and Release' method **(**described in the section **'Method and Materials'** of chapter 3**)**. A deep brown solid was obtained after drying in vacuum. Yield=170 mg, 58%.

Table 4.68: Characterisation data for compound **4.68**

4.68 Cream Solid	^{1}H NMR	^{1}HNMR(400MHz,$(CD_3)_2SO$); $^{\delta}$H in ppm 11.48(s,1H),9.95(s,1H),9.18(d,*J*=2.4,1H),8.59(s,1H),8.45(d,*J*=2.4,1H),8.10(dd,*J*=8.8,2.4,1H),7.96(d,*J*=10,2H),7.92(t,*J*=5.6,1H),7.697.67(m,2H),7.40(d,*J*=8.8,1H),3.313.26(m,2H),2.29(t,*J*=7.2,2H), 2.15 (s,6H), 1.67 (t,*J*=6.8,2H).
	^{13}C NMR	(100MHz,$(CD_3)_2SO$); $^{\delta}$C in ppm 164.5, 162.0, 141.8, 139.2, 132.9, 132.3, 131.6, 127.7, 126.1, 125.9, 118.0, 117.3, 116.7, 112.8, 112.7, 112.6, 111.2, 110.7, 57.0, 45.1, 38.8, 36.8, 27.5.
	EIMS	Found 449.10 $[M+H]^+$, Calculated for$C_{23}H_{24}N_6O_4$, 448.18 $[M]^+$
	HRMS	*m/z* (+EI) Calc. for $C_{23}H_{24}N_6O_4$, 448.1859 $[M]^+$, found 449.1926$[M+H]^+$.
	IR	(FTIR), V_{max}/'cm^{-1}): 3265, 2971, 2344, 2297, 1738, 1604, 1533, 1468, 1437, 1367, 1342, 1311, 1270, 1208, 1178, 1148, 1072, 1038, 938, 882, 792, 744, 683, 662.

4.69 Synthesis of 5-amino-N-(3-((3-(dimethylamino) propyl) carbamoyl)-1H-indol-5-yl)-1H-indole-3-carboxamide (4.69).

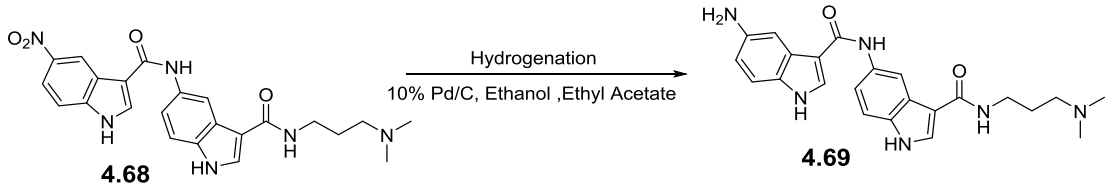

170 mg of **4.68** was dissolved in 20 mL of ethanol and 1 mL of ethyl acetate was added to a hydrogenation reaction bottle. 20 mg of 10% Pd (palladium on activated carbon) 20 was added into the reaction vessel, and mixed it well. The sealed reaction bottle was connected to a hydrogen reservoir. Air from the reaction bottle was removed by applying vacuum and it was flushed with hydrogen. Typically, a hydrogen pressure of approximately 40 psi was applied

from the reservoir, and the bottle was then shaken vigorously to initiate the reaction. Progress of the reaction was monitored by TLC and LCMS. The shaker was stopped after 4.5 hours at which point TLC and LCMS analysis showed the completion of reaction. The bottle was vented and the product was recovered by means of filtration using Celite. Finally, the product is concentrated by using a rotary evaporator. A deep brown solid was obtained after drying in vacuum. Yield=140 mg, 89%.

Table 4.69: Characterisation data for compound **4.69**

4.69 Deep Brown Solid	^{1}H NMR	^{1}HNMR(400MHz,$(CD_3)_2SO$); $^{\delta}$H in ppm 11.46(s,1H), 11.26(d,*J*=2.0,1H), 9.49(s,1H), 8.43(d,*J*=2.0,1H), 8.13(d,*J*=2.8,1H), 7.95(s,1H), 7.89(t,*J*=5.2,1H), 7.62(dd, *J*=8.8,2.0,1H), 7.47(d,*J*=2.0,1H), 7.35(d, *J*=8.4,1H), 7.14(d,*J*=8.4, 1H), 6.56(dd, *J*=8.4, 2.0,1H), 3.31-3.26(m,2H), 2.73(s,2H), 2.28(t, *J*=7.2, 2H), 2.15(s,6H), 1.69 (m,2H).
	^{13}C NMR	(100MHz,$(CD_3)_2SO$); $^{\delta}$C in ppm 164.6, 163.4, 162.2, 142.6, 133.1, 132.6, 129.6, 127.7, 127.6, 127.5, 126.1, 116.7, 112.5, 112.3, 111.7, 111.0, 110.6, 109.4, 104.4, 57.0, 45.2, 36.9, 35.7.
	EIMS	Found 418.10 $[M+H]^+$, Calculated for $C_{23}H_{26}N_6O_2$, 418.21 $[M]^+$
	HRMS	*m/z* (+EI) Calc. for $C_{23}H_{26}N_6O_2$, 418.2117 $[M]^+$, found 419.2182$[M+H]^+$.
	IR	(FTIR), V_{max}/'cm^{-1}): 3240, 2941, 2827, 1652, 1614, 1534, 1469, 1433, 1386, 1360, 1315, 1278, 1248, 1212, 1160, 1100, 1028, 933, 802, 768, 660, 612.

4.70 Synthesis of 5-(benzofuran-2-carboxamido)-N-(3-((3-(dimethylamino) propyl) carbamoyl)-1H-indol-5-yl)-1H-indole-3-carboxamide (4.70).

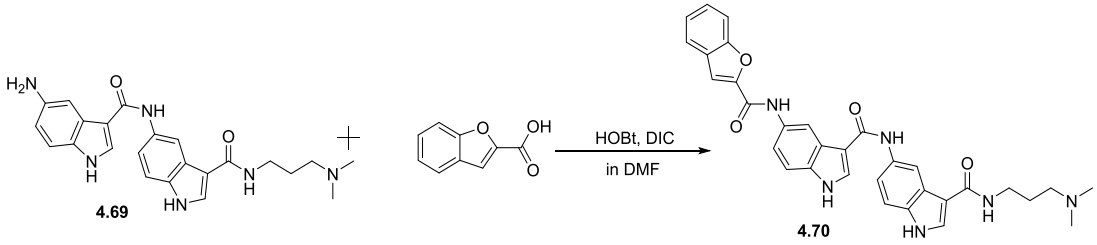

Initially, 33 mg of benzofuran-2-carboxylic acid (0.2002 mmol, 1.2 eq.) was dissolved in 5 mL of DMF in a round bottom flask fitted with a magnetic stirrer. Then DIC (54 µl, 0.35 mmol, 1.75 eq.) and HOBt (54 mg, 0.40 mmol, 2.0 eq.) were added to the acid (1.0 eq.) and this mixture was allowed to stir at room temperature for 30 minutes to ensure the formation of ester from the acid. Then amine **4.69**(60 mg, 0.143 mmol, 1 eq.) was added and the mixture was allowed to stir for 5 hours at which point TLC and LCMS analysis showed the

completion of reaction. Finally the reaction mixture was applied to a conditioned Isolute^{TM} SCX-2 cartridge and the product was purified by 'Catch and Release' method **(**described in the section **'Method and Materials'** of chapter 3**)**. A cream solid was obtained after drying in vacuum. Yield=12.5 mg, 16%.

Table 4.70: Characterisation data for compound **4.70**

4.70 Cream solid	^{1}H NMR	^{1}HNMR(400MHz,$(CD_3)_2SO$); $^{\delta}$H in ppm 8.45(s,1H),8.34(d,*J*=1.6,1H),8.14(d,*J*=1.6,1H),8.02(s,1H),7.76(s,1H), 7.64(d,*J*=7.6,1H),7.56(d,*J*=8,2H),7.51(s,2H),7.42(dd,*J*=8.8,2.0,1H), 7.37(s,1H), 7.36 (d,*J*=4,1H), 7.33(d,*J*=7.6,2H), 7.23 (t,*J*=7.2,2H), 3.33(t,*J*=6.8,2H), 2.38 (t,*J*=7.6,2H), 2.18 (s,6H), 1.76-1.70(m,2H).
	^{13}C NMR	(100MHz,$(CD_3)_2SO$); $^{\delta}$C in ppm 170.3, 168.4, 166.8, 159.5, 156.5, 150.3, 135.9, 135.4, 133.4,132.3, 130.3, 129.8, 128.9, 128.2, 127.7, 126.9, 124.9, 123.7, 119.5, 119.3, 115.7, 114.9, 112.9, 112.8, 112.4, 112.1, 111.8, 58.3, 49.6, 49.0, 45.4, 38.7.
	EIMS	Found 563.30 $[M+H]^+$, Calculated for $C_{32}H_{30}N_6O_4$, 562.23 $[M]^+$
	HRMS	*m/z* (+EI) Calc. for $C_{32}H_{30}N_6O_4$, 562.2329 $[M]^+$, found 563.2388$[M+H]^+$.
	IR	(FTIR), V_{max}/'cm^{-1}): 3214, 2970, 1740, 1623, 1592, 1538, 1474, 1437, 1359, 1313, 1258, 1216, 1177, 1156, 1092, 1047, 1023, 1001, 944, 805, 747, 627.

4.71 Synthesis of 5-(benzo[b]thiophene-2-carboxamido)-N-(3-((3-(dimethylamino) propyl) carbamoyl)-1H-indol-5-yl)-1H-indole-3-carboxamide (4.71).

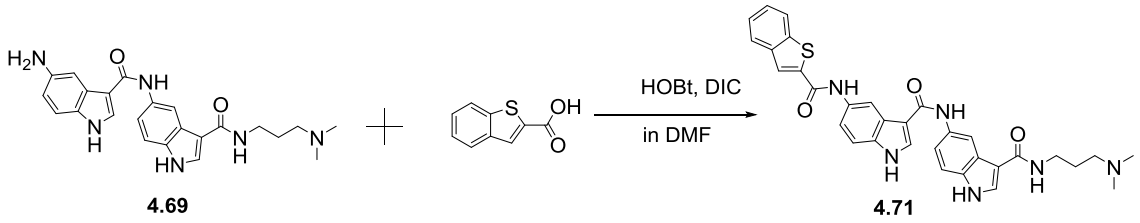

42 mg of benzo[b]thiophene-2-carboxylic acid (0.234 mmol, 1.2 eq.) was dissolved in 5 mL of DMF in a round bottom flask fitted with a magnetic stirrer. Then DIC (63.57 µl, 0.411 mmol, 1.75 eq.) and HOBt (63.45 mg, 0.46 mmol, 2.0 eq.) were added to the acid (1.0 eq.) and this mixture was allowed to stir at room temperature for at least 30 minutes for the esterification of acid. Then amine **4.67** (70 mg, 0.167 mmol, 1 eq.) was added and the mixture was allowed to stir for 4 hours at which point TLC and LCMS analysis showed the completion of reaction. Lastly the reaction mixture was applied to a conditioned

Isolute^{TM} SCX-2 cartridge and the product was purified by 'Catch and Release' method **(**described in the section **'Method and Materials'** of chapter 3**)**. A yellow solid was obtained after drying in vacuum. Yield=44 mg, 45%.

Table 4.71: Characterisation data for compound **4.71**

4.71 Yellow solid	^{1}H NMR	^{1}HNMR(400MHz,$(CD_3)_2SO$); $^{\delta}$H in ppm 11.70(s,1H),11.45(s,1H),10.53(s,1H),9.71(s,1H),8.61(d,*J*=1.6,1H), 8.47(d,*J*=1.6,1H),8.43(s,1H),8.35(d,*J*=6.4,1H),8.06(dd,*J*=6.8,2.4,1 H), 8.00(dd,*J*=6.4,2.4,1H), 7.96(s,1H), 7.90(t,*J*=5.6,1H), 7.72-7.66(m,2H), 7.49-7.46(m,3H), 7.39(d,*J*=8.8,1H), 3.31-3.26(m,2H), 2.28(t,*J*=7.2,2H), 2.14(s,6H), 1.67(t,*J*=6.8,2H).
	^{13}C NMR	(100MHz,$(CD_3)_2SO$); $^{\delta}$C in ppm 164.5, 162.9, 162.2, 159.9, 140.7, 140.3, 139.3, 133.3, 132.9, 132.6, 131.9, 128.8, 127.6, 126.6, 126.25, 126.20, 125.2, 124.9, 122.7, 116.6, 113.4, 112.6, 111.5, 111.1, 110.8, 110.6, 57.0, 45.2, 38.8, 36.9, 35.74, 30.7.
	EIMS	Found 579.10 $[M+H]^+$, Calculated for $C_{32}H_{30}N_6O_3S$, 578.21 $[M]^+$
	HRMS	*m/z* (+EI) Calc. for $C_{32}H_{30}N_6O_3S$, 578.2100 $[M]^+$, found 579.1430$[M+H]^+$.
	IR	(FTIR), V_{max}/'cm^{-1}): 3252, 2937, 1633, 1529, 1471, 1434, 1382, 1334, 1242, 1204, 1153, 1095, 1071, 868, 801, 765, 737, 715.

4.72 Synthesis of N-(3-((3-((3-(dimethylamino)propyl)carbamoyl)-1H-indol-5-yl)carbamoyl)-1H-indol-5-yl)-1-methyl-1H-indole-2-carboxamide (4.72).

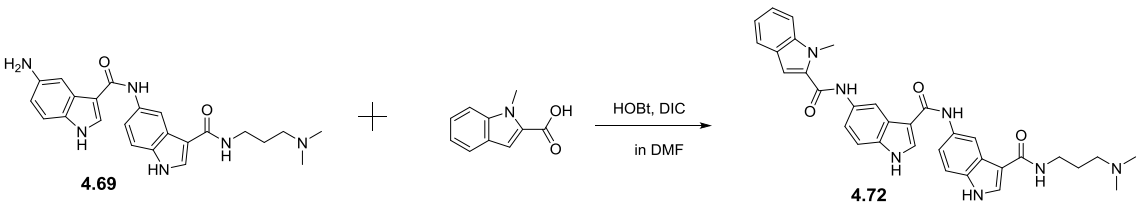

Initially, 38 mg of 1-methyl-1H-indole-2-carboxylic acid (0.217 mmol, 1.2 eq.) was dissolved in 5 mL of DMF in a round bottom flask fitted with a magnetic stirrer. Then DIC (58.59 µl, 0.379 mmol, 1.75 eq.) and HOBt (59 mg, 0.434 mmol, 2.0 eq.) were added to the acid (1.0 eq.) and this mixture was allowed to stir at room temperature for 30 minutes to ensure the formation of ester from the acid. Then 65 mg of amine **4.69** (0.155 mmol, 1 eq.) was added to the mixture and this mixture was stirred for 8 hours at which point TLC and LCMS analysis showed the completion of reaction. Finally the product of the reaction mixture was separated by using a conditioned Isolute^{TM} SCX-2 cartridge and the product was purified by 'Catch and Release' method **(**described in the section

'Method and Materials' of chapter 3**)**. An orange solid was obtained after drying in vacuum. Yield=27 mg, 30 %.

Table 4.72: Characterisation data for compound **4.72**

4.72 Orange solid	^{1}H NMR	^{1}HNMR(400MHz,$(CD_3)_2SO$); $^{\delta}$H in ppm 11.70(s,1H),11.49(s,1H),10.29(s,1H),9.70(s,1H),8.69(d,*J*=1.6,1H),8.49(d,*J*=1.6,1H),8.348.29(m,2H),7.97(d,*J*=2.4,2H),7.69(d,*J*=8.0,1H), 7.65-7.62(m,2H), 7.44(d,*J*=8.8,1H), 7.37 (d,*J*=4.4,2H), 7.29 (t,*J*=7.2,1H), 7.13 (t,*J*=7.6,1H), 4.05-4.00(m,3H), 3.32-3.27(m,2H), 2.54 (t,*J*=7.2,2H), 2.34 (s,6H), 1.78-1.71(m, 2H).
	^{13}C NMR	(100MHz,$(CD_3)_2SO$); $^{\delta}$C in ppm 164.7, 162.9, 162.2, 160.1, 138.5, 133.1, 132.9, 132.6, 132.5, 132.2, 127.7, 126.5, 126.1, 125.5, 123.6, 121.6, 120.1, 116.6, 113.3, 112.5, 111.4, 111.1, 110.8, 110.5, 110.4, 105.0, 56.1, 44.0, 40.0, 39.2, 36.4, 35.7, 31.4.
	EIMS	Found 575.40 $[M+H]^+$, Calculated for $C_{33}H_{33}N_7O_3$, 575.26 $[M]^+$
	HRMS	*m/z* (+EI) Calc. for $C_{33}H_{33}N_7O_3$, 575.2645 $[M]^+$, found 576.2703 $[M+H]^+$.
	IR	(FTIR), V_{max}/'cm^{-1}): 3257, 2972, 2342, 1739, 1649, 1601, 1537, 1471, 1435, 1363, 1309, 1251, 1214, 1152, 1085, 1044, 878, 803, 745, 682, 660.

4.73 Synthesis of N-(3-((3-((3-(dimethylamino) propyl) carbamoyl)-1H-indol-5-yl) carbamoyl)-1H-indol-5-yl)-1H-benzo[d]imidazole-2-carboxamide (4.73).

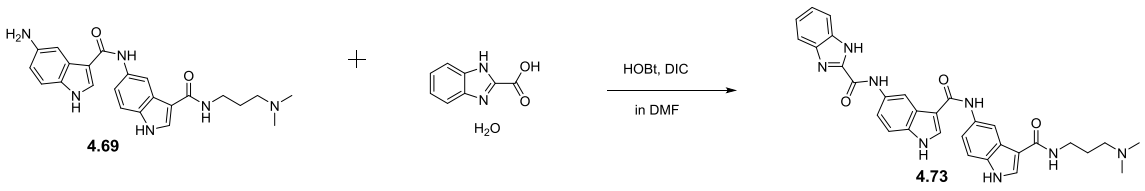

Initially, 34 mg of 1H-benzo[d]imidazole-2-carboxylic acid hydrate (0.186 mmol, 1.2 eq.) was dissolved in 10 mL of DMF in a round bottom flask fitted with a magnetic stirrer. Then DIC (51 µl, 0.3255 mmol, 1.75 eq.) and HOBt (51 mg, 0.372 mmol, 2.0 eq.) were added to the acid (1.0 eq.) and this mixture was allowed to stir at room temperature for 30 minutes to ensure the formation of ester from the acid. Then 65 mg of amine **4.69** (0.155 mmol, 1 eq.) was added and the mixture was allowed to stir for 6 hours at which point TLC and LCMS analysis showed the completion of reaction. Finally the reaction mixture was applied to a conditioned Isolute^{TM} SCX-2 cartridge and the product was purified by 'Catch and Release' method **(**described in the section **'Method and**

Materials' of chapter 3**)**. A light yellow solid was obtained after drying in vacuum. Yield=18 mg, 21%.

Table 4.73: Characterisation data for compound **4.73**

4.73 Light Yellow solid	^{1}H NMR	^{1}HNMR(400MHz,$(CD_3)_2SO$); $^{\delta}$H in ppm 11.72(d,*J*=2.4,1H), 11.49(d,*J*=2.4,1H), 10.73(s,1H), 9.71(s,1H), 8.81(d,*J*=2.0,1H), 8.50(d,*J*=1.6,1H), 8.32(d,*J*=2.8,1H), 8.02-7.95(m,2H), 7.64(d,*J*=2.0,1H), 7.62(t,*J*=2.4,1H), 7.60(d,*J*=2.0,1H), 7.46 (d,*J*=8.8,1H), 7.36(d,*J*=9.2,1H), 7.35-7.32(m,2H), 3.32-3.27(m,2H), 2.50-2.47 (m,2H), 2.30(s,6H), 1.77-1.70(m,2H).
	^{13}C NMR	(100MHz,$(CD_3)_2SO$); $^{\delta}$C in ppm 164.6, 162.9, 156.9, 146.0, 133.4, 132.9, 132.7, 131.3, 128.8, 127.7, 126.4, 126.1, 117.0, 116.8, 113.7, 112.6, 111.6, 111.2, 110.9, 110.5, 56.4, 44.4, 40.0, 39.8, 39.6, 39.4, 39.2, 39.0, 38.7, 36.5, 26.9.
	EIMS	Found 563.30 $[M+H]^+$, Calculated for $C_{31}H_{30}N_8O_3$, 562.24 $[M]^+$
	HRMS	*m/z* (+EI) Calc. for $C_{31}H_{30}N_8O_3$, 562.2441 $[M]^+$, found 563.2502 $[M+H]^+$.
	IR	(FTIR), V_{max}/'cm^{-1}): 3023, 2970, 1740, 1620, 1538, 1473, 1434, 1363, 1313, 1277, 1219, 1144, 1023, 1001, 894, 805, 769, 746, 622.

4.74 Synthesis of 5-(benzofuran-3-carboxamido)-N-(2-((3-(dimethylamino) propyl) carbamoyl) benzofuran-5-yl)-1H-indole-3-carboxamide (4.74).

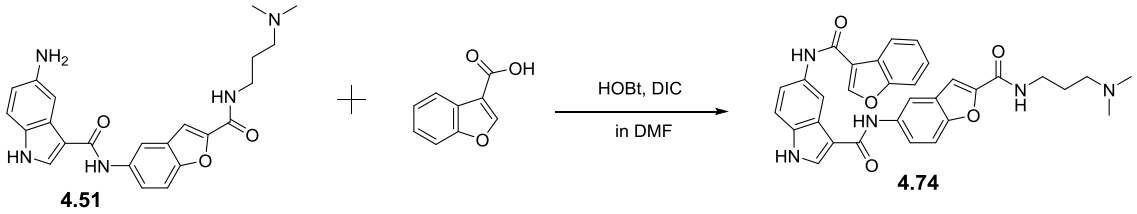

4.51 **4.74**

Initially, 37.91 mg of benzofuran-3-carboxylic acid (0.233 mmol, 1.2 eq.) was dissolved in 10 mL of DMF in a round bottom flask. Then DIC (63.03 µl, 0.407 mmol, 1.75 eq.) and HOBt (62.91 mg, 0.466 mmol, 2.0 eq.) were added to the acid (1.0 eq.) and this mixture was allowed to stir at room temperature for 30 minutes to ensure the formation of ester from the acid. Then amine **4.51**(70 mg, 0.166 mmol, 1 eq.) was added and the mixture was allowed to stir for 6 hours at which point TLC and LCMS analysis showed the completion of reaction. Finally the reaction mixture was applied to a conditioned Isolute^{TM} SCX-2 cartridge and the product was purified by 'Catch and Release' method **(**described in the chapter 3**)**. An orange solid was obtained after drying. Yield=38 mg, 40%.

Table 4.74: Characterisation data for compound **4.74**

4.74 Orange solid	^{1}H NMR	^{1}HNMR(400MHz,$(CD_3)_2SO$); $^{\delta}$H in ppm 8.52(d,*J*=6.8,2H), 8.44(d,*J*=1.6,1H), 8.13(s,1H), 8.08(t,*J*=2.8,1H), 7.97(s,1H), 7.70(dd,*J*=9.2,2.4,1H), 7.58(s,1H), 7.58-7.53(m,2H), 7.47(s,1H), 7.45(s,1H), 7.41 (dd,*J*=7.2,1.6,1H), 7.37(dd,*J*=4.0,1.6,1H), 7.34 (dd,*J*=7.2,1.2,1H), 3.50(t,*J*=6.4,2H), 3.19-3.15 (m,2H), 2.99 (s,6H), 2.06-1.98(m,2H).
	^{13}C NMR	(100MHz,$(CD_3)_2SO$); $^{\delta}$C in ppm 166.6, 163.9, 161.1, 156.8, 153.1, 150.7, 148.5, 136.4, 135.6, 133.1, 130.3, 128.9, 127.7, 126.6, 126.3, 124.9, 123.1, 122.8, 119.3, 118.9, 115.6, 115.3, 112.9, 112.7, 112.4, 112.1, 111.2, 58.2, 49.6, 49.0, 45.4, 38.7.
	EIMS	Found 563.50 $[M+H]^+$, Calculated for $C_{32}H_{29}N_5O_5$, 563.21 $[M]^+$
	HRMS	*m/z* (+EI) Calc. for $C_{32}H_{29}N_5O_5$, 563.2169 $[M]^+$, found 564.2228$[M+H]^+$.
	IR	(FTIR), V_{max}/'cm^{-1}): 3230, 2977, 2325, 1737, 1637, 1592, 1536, 1471, 1439, 1366, 1338, 1210, 1103, 1079, 1042, 858, 752.

4.75 Synthesis of 5-(benzo[b]thiophene-3-carboxamido)-N-(2-((3-(dimethyl amino) propyl) carbamoyl) benzofuran-5-yl)-1H-indole-3-carboxamide (4.75).

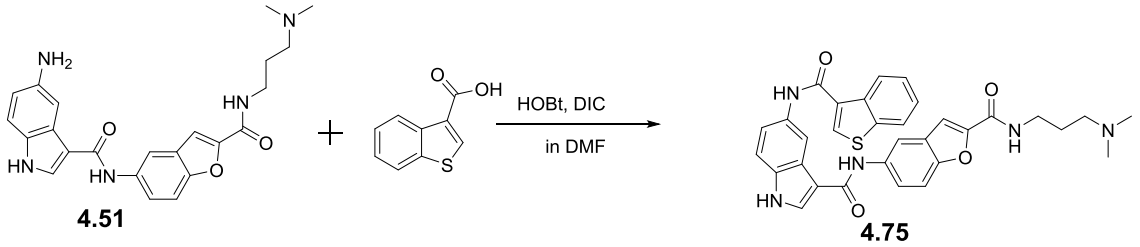

Initially, 41.28 mg of benzo[b]thiophene-3-carboxylic acid (0.266 mmol, 1.2 eq.) was dissolved in 10mL of DMF in a round bottom flask. DIC (71.88 µl, 0.465 mmol, 1.75 eq.) and HOBt (71.82 mg, 0.532 mmol, 2.0 eq.) were added to the acid (1.0 eq.) and this mixture was allowed to stir at room temperature for 30 minutes to ensure the formation of ester from the acid. Then amine **4.51** (80 mg, 0.190 mmol, 1 eq.) was added and the mixture was allowed to stir for 5 hours at which point TLC and LCMS analysis showed the completion of reaction. Finally the reaction mixture was applied to a conditioned Isolute^{TM} SCX-2 cartridge and the product was purified by 'Catch and Release' method **(**described in the chapter 3**)**. A yellow solid was obtained after drying. Yield=22 mg, 20%.

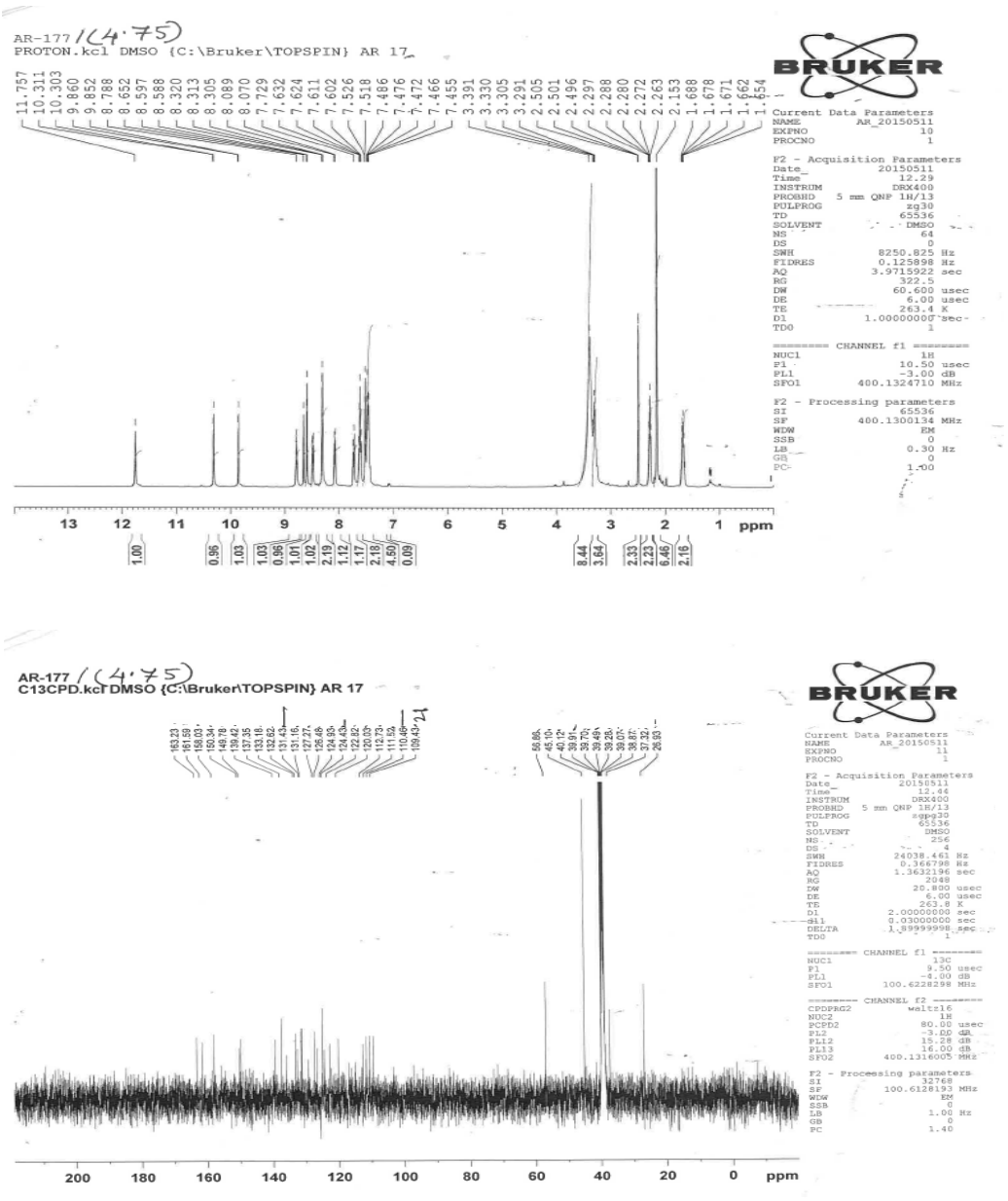

Figure 4.5: ^{1}H and ^{13}C NMR spectroscopic data of compound **4.75** as a representative of **library-3A** compounds

Table 4.75: Characterisation data for compound **4.75**

4.75 Yellow solid	^{1}H NMR	^{1}HNMR(400MHz,$(CD_3)_2SO$); $^{\delta}$H in ppm 11.75(s,1H),10.30(d,*J*=3.2,1H),9.85(d,*J*=3.2,1H),8.78(t,*J*=3.6,1 H),8.65(s,1H),8.59(d,*J*=3.6,1H),8.508.47(m,1H),8.31(t,*J*=2.8,2 H),8.07(t,*J*=5.2,1H),7.73(dd,*J*=8.8,2.4,1H),7.647.60(m,2H),7.52 (d,*J*=3.2,1H),7.49-7.45(m,3H),3.30(t,*J*=5.6,2H),2.29-2.26 (m,2H), 2.15(s,6H), 1.68-1.63(m,2H).
	^{13}C NMR	(100MHz,$(CD_3)_2SO$); $^{\delta}$C in ppm 163.2, 161.5, 158.0, 150.3, 149.7, 139.4, 137.3, 133.1, 132.6, 131.4, 131.1, 127.2, 126.4, 124.9, 124.4, 122.8, 120.0, 112.7, 111.5, 110.4, 109.4, 56.8, 45.1, 40.1, 39.9, 39.7, 39.4, 39.2, 39.0, 38.8, 37.3, 26.9.
	EIMS	Found 580.10 $[M+H]^+$, Calculated for $C_{32}H_{29}N_5O_4S$, 579.19 $[M]^+$
	HRMS	*m/z* (+EI) Calc. for $C_{32}H_{29}N_5O_4S$, 579.1940 $[M]^+$, found 580.2000 $[M+H]^+$.
	IR	(FTIR), V_{max}/'cm^{-1}): 3300, 2255, 1637, 1577, 1525, 1479, 1439, 1338, 1313, 1225, 1173, 1048, 1023, 999, 888, 859, 821, 759, 632.

4.76 Synthesis of N-(3-((2-((3-(dimethylamino) propyl) carbamoyl) benzofuran-5-yl) carbamoyl)-1H-indol-5-yl)-1H-indazole-3-carboxamide (4.76).

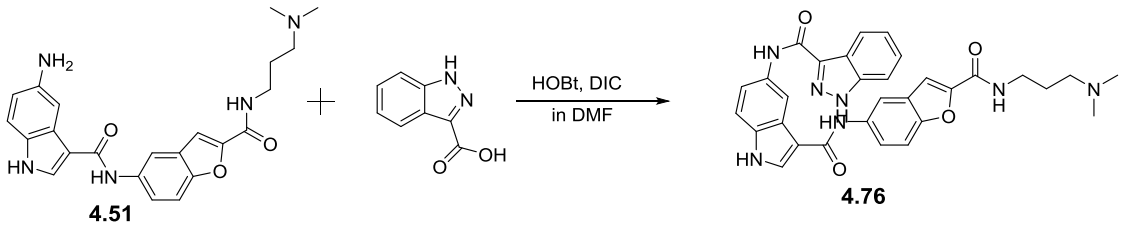

Initially, 47 mg of 1H-indazole-3-carboxylic acid (0.290 mmol, 1.2 eq.) was dissolved in 10 mL of DMF in a round bottom flask fitted with a magnetic stirrer. Then DIC (78 µl, 0.507 mmol, 1.75 eq.) and HOBt (78.3 mg, 0.58 mmol, 2.0 eq.) were added to the acid (1.0 eq.) and this mixture was allowed to stir at room temperature for 30 minutes to ensure the formation of ester from the acid. Then 87 mg of amine **4.51** (0.207 mmol, 1 eq.) was added and the mixture was allowed to stir for 6 hours at which point TLC and LCMS analysis showed the completion of reaction. Finally the reaction mixture was applied to a conditioned Isolute^{TM} SCX-2 cartridge and the product was purified by 'Catch and Release' method **(**described in the section **'Method and Materials'** of chapter 3**)**. A brown solid was obtained after drying in vacuum. Yield=13 mg, 13 %.

Table 4.76: Characterisation data for compound **4.76**

4.76 Brown solid	^{1}H NMR	^{1}HNMR(400MHz,$(CD_3)_2SO$); $^{\delta}$H in ppm 11.89(s,1H),10.16(s,1H), 9.85(d,*J*=9.2,1H),8.79(t,*J*=6.4,2H), 8.36-8.23(m,3H),7.74(t,*J*=6.4,1H),7.69-7.60(m,4H), 7.52(d,*J*=6.0,1H),7.45-7.39(m,2H),7.27-7.21(m,1H),3.66-3.58(m,2H), 2.25 (t,*J*=5.6,2H), 2.15(s,6H), 1.66(t,*J*=6.0,2H).
	^{13}C NMR	(100MHz,$(CD_3)_2SO$); $^{\delta}$C in ppm 163.2, 160.7, 158.0, 156.8, 150.3, 149.7, 141.8, 138.4, 135.7, 133.0, 132.3, 127.2, 126.3, 126.2, 123.1, 121.9, 121.8, 118.1, 112.8, 111.6, 111.5, 111.0, 110.4, 109.3, 56.8, 45.1, 40.65, 38.7, 37.3, 26.9, 24.8.
	EIMS	Found 564.0 $[M+H]^+$, Calculated for $C_{31}H_{29}N_7O_4$, 563.2281 $[M]^+$
	HRMS	*m/z* (+EI) Calc. for $C_{31}H_{29}N_7O_4$, 563.2281 $[M]^+$, found 564.2344 $[M+H]^+$.
	IR	(FTIR), V_{max}/'cm^{-1}): 3301, 2950, 1636, 1590, 1529, 1470, 1433, 1343, 1299, 1276, 1236, 1202, 1153, 1037, 879, 806, 753, 738, 716, 623.

4.77 Synthesis of N-(3-((3-((3-(dimethylamino) propyl) carbamoyl)-1H-indol-5-yl) carbamoyl)-1H-indol-5-yl)-5-nitro-1H-indole-2-carboxamide (4.77).

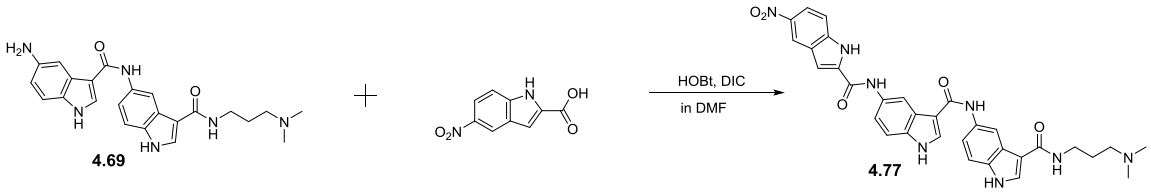

Initially, 43mg of 5-nitro-1H-indole-2-carboxylic acid (0.206 mmol, 1.2 eq.) was dissolved in 10 mL of DMF in a round bottom flask fitted with a magnetic stirrer. Then DIC (56 µl, 0.3605 mmol, 1.75 eq.) and HOBt (56 mg, 0.412 mmol, 2.0 eq.) were added to the acid (1.0 eq.) and this mixture was allowed to stir at room temperature for 30 minutes to ensure the formation of ester from the acid. Then 72 mg of amine **4.69** (0.172 mmol, 1 eq.) was added and the mixture was allowed to stir for 7 hours at which point TLC and LCMS analysis showed the completion of reaction. Finally the reaction mixture was applied to a conditioned Isolute^{TM} SCX-2 cartridge and the product was purified by 'Catch and Release' method **(**described in the section **'Method and Materials'** of chapter 3**)**. A

yellow solid was obtained after drying in vacuum. Yield=36 mg, 35%.

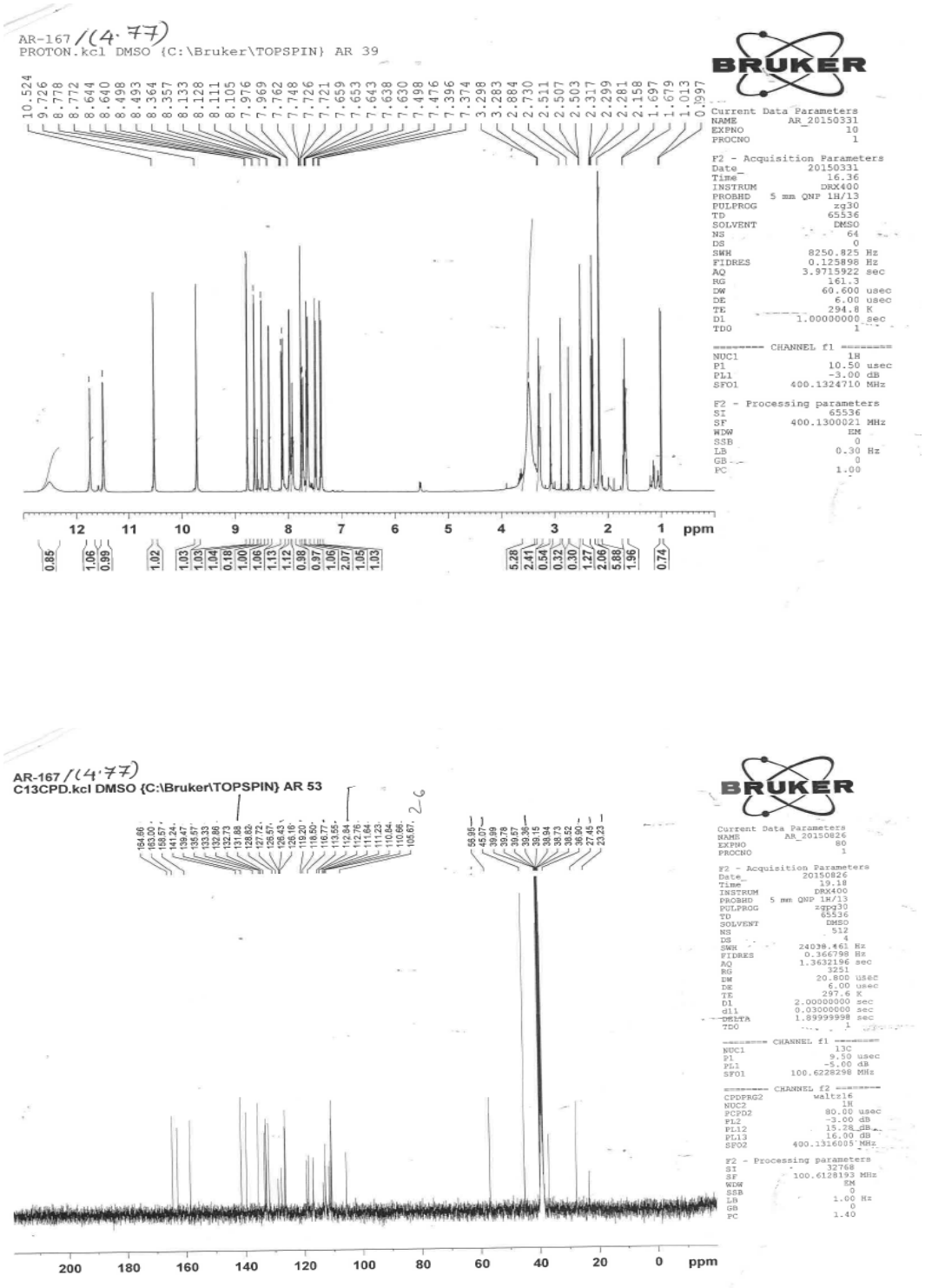

Figure 4.6: ^{1}H and ^{13}C NMR spectroscopic data of compound **4.77** as a representative of **library-3B** compounds

Table 4.77: Characterisation data for compound **4.77**

4.77 Yellow solid	^{1}H NMR	^{1}HNMR(400MHz,$(CD_3)_2SO$); $^{\delta}$H in ppm 12.52(s,1H), 11.74(d,*J*=2.4,1H), 11.48(d,*J*=2.4,1H), 10.52(s,1H), 9.72(s,1H),8.77(d,*J*=2.4,1H), 8.64 (d,*J*=1.6,1H), 8.49(d,*J*=2.0,1H), 8.36(d,*J*=2.8,1H),8.11(dd,*J*=8.8,2.0,1H),7.97(d,*J*=2.8,1H),7.92(t,*J*=6,1H), 7.76(s,1H), 7.73(dd,*J*=8.8,2.0,1H), 7.66-7.63 (m,2H), 7.48(d,*J*=8.8,1H), 7.38(d,*J*=8.8,1H), 3.31-3.26(m,2H), 2.29 (t,*J*=7.2,2H), 2.15(s,6H), 1.67(t,*J*=7.2,2H).
	^{13}C NMR	(100MHz,$(CD_3)_2SO$); $^{\delta}$C in ppm 164.6, 163.0, 158.5, 141.2, 139.4, 135.5, 133.3, 132.8, 132.7, 131.8, 128.8, 127.7, 126.5, 126.4, 126.1, 119.2, 118.5, 116.7, 113.5, 112.8, 112.7, 111.6, 111.2, 110.8, 110.8, 105.6, 56.9, 45.0, 39.3, 36.9, 27.4, 23.2.
	EIMS	Found 607.20 $[M+H]^+$, Calculated for $C_{32}H_{30}N_8O_5$, 606.23 $[M]^+$
	HRMS	*m/z* (+EI) Calc. for $C_{32}H_{30}N_8O_5$, 606.2339 $[M]^+$, found 607.2396 $[M+H]^+$.
	IR	(FTIR, V_{max}/'cm^{-1}): 3266, 2941, 2219, 1705, 1630, 1534, 1475, 1440, 1361, 1331, 1308, 1221, 1160, 1098, 1039, 945, 886, 807, 770, 741, 715, 619.

4.78 Synthesis of N-(3-(dimethylamino) propyl)-5-(5-(5-nitrobenzo[b]thiophene-2-carboxamido)-1H-indole-3-carboxamido)-1H-indole-3-carboxamide (4.78).

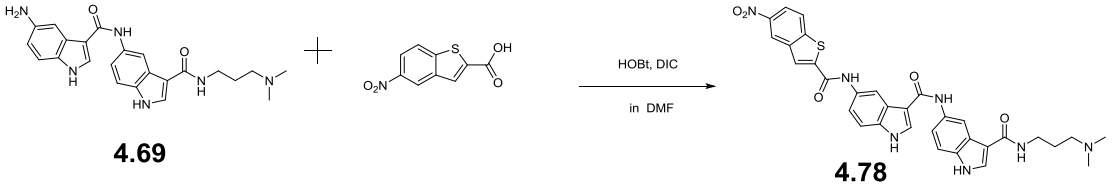

4.69 **4.78**

Initially, 67 mg of 5-nitrobenzo[b]thiophene-2-carboxylic acid (0.301 mmol, 1.4 eq.) was dissolved in 10mL of DMF in a round bottom flask fitted with a magnetic stirrer. Then DIC (81 µl, 0.526 mmol, 1.75 eq.) and HOBt (81 mg, 0.602 mmol, 2.0 eq.) were added to the acid (1.0 eq.) and this mixture was allowed to stir at room temperature for 30 minutes to ensure the formation of ester from the acid. Then amine **4.69**(90 mg, 0.215 mmol, 1 eq.) was added and the mixture was allowed to stir for 6 hours at which point TLC and LCMS analysis showed the completion of reaction. Finally the reaction mixture was applied to a conditioned Isolute^{TM} SCX-2 cartridge and the product was purified by 'Catch and Release' method **(**described in the section **'Method and Materials'** of chapter 3**)**. A deep yellow solid was obtained after drying in vacuum. Yield=20 mg, 15%.

Table 4.78: Characterisation data for compound **4.78**

4.78 Deep Yellow solid	^{1}H NMR	^{1}HNMR(400MHz,$(CD_3)_2SO$); $^{\delta}$H in ppm 11.72(d,*J*=2.4,1H), 11.45(d,*J*=2.4,1H), 10.75(s,1H), 9.71(s,1H), 8.94(t,*J*=2.0,1H), 8.64-8.60(m,2H), 8.47(d,*J*=1.6,1H), 8.37-8.33(m,2H), 8.29-8.27(m,1H), 7.96(s,1H), 7.90(t,*J*=5.6,1H), 7.70-7.64 (m,2H), 7.48(d,*J*=8.8,1H), 7.37(d,*J*=8.4,1H), 3.31-3.26(m,2H), 2.33 (t,*J*=6.8,2H), 2.18(s,6H), 1.72-1.65(m,2H).
	^{13}C NMR	(100MHz,$(CD_3)_2SO$); $^{\delta}$C in ppm 164.6, 162.9, 162.3, 159.2, 146.1, 145.3, 144.5, 139.1, 133.4, 132.9, 132.7, 131.6, 126.6, 126.1, 125.8, 124.1, 120.9, 119.9, 116.6, 113.6, 112.6, 110.8, 110.6, 56.9, 45.0, 40.0, 39.4, 39.2, 39.0, 38.8, 27.4, 23.2.
	EIMS	Found 623.20 $[M+H]^+$, Calculated for $C_{32}H_{29}N_7O_5S$, 623.19 $[M]^+$
	HRMS	*m/z* (+EI) Calc. for $C_{32}H_{29}N_7O_5S$, 623.1951 $[M]^+$, found 624.2017$[M+H]^+$.
	IR	(FTIR), V_{max}/'cm^{-1}): 3219, 1706, 1625, 1532, 1509, 1472, 1435, 1340, 1312, 1269, 1212, 1151, 1023, 1003, 945, 863, 803, 769, 736.

4.79 Synthesis of N-(3-(dimethylamino) propyl)-5-(5-(5-nitrobenzofuran-2-carboxamido)-1H-indole-3-carboxamido)-1H-indole-3-carboxamide (4.79).

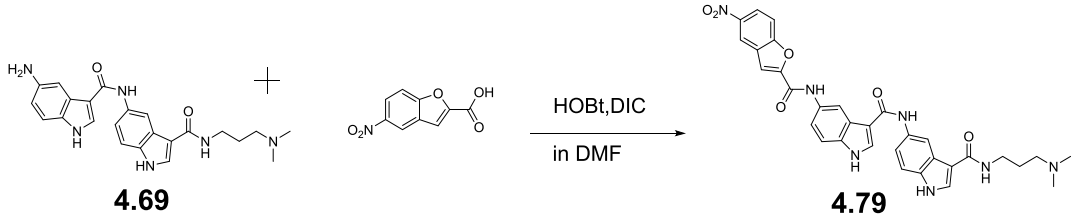

4.69 **4.79**

Initially, 52 mg of 5-nitrobenzofuran-2-carboxylic acid (0.251 mmol, 1.4 eq.) was dissolved in 10mL of DMF in a round bottom flask fitted with a magnetic stirrer. Then DIC (68 µl, 0.439 mmol, 1.75 eq.) and HOBt (68 mg, 0.502 mmol, 2.0 eq.) were added to the acid (1.0 eq.) and this mixture was allowed to stir at room temperature for 30 minutes to ensure the formation of ester from the acid. Then 75 mg of amine **4.69** (0.179 mmol, 1 eq.) was added to the mixture and that mixture was allowed to stir for 5 hours at which point TLC and LCMS analysis showed the completion of reaction. Lastly, the reaction mixture was applied to a conditioned Isolute^{TM} SCX-2 cartridge and the product was purified by 'Catch and Release' method **(**described in the section **'Method and Materials'** of chapter 3**)**. An orange solid was obtained after drying. Yield=29 mg, 27%.

Table 4.79: Characterisation data for compound **4.79**

4.79 Orange solid	^{1}H NMR	^{1}HNMR(400MHz,$(CD_3)_2SO$); $^{\delta}$H in ppm 11.73(s,1H),11.48(s,1H),10.67(s,1H),9.71(s,1H),8.84(d,*J*=2.4,1H), 8.65(d,*J*=1.2,1H), 8.48(s,1H), 8.36(dd,*J*=8.8,2.0,2H), 8.02(s,1H), 7.97(d,*J*=9.2,3H),7.697.63(m,2H),7.47(d,*J*=8.8,1H),7.38(d,*J*=8.4,1H), 3.69-3.59 (m,2H), 3.31(s,2H), 2.31(s,6H), 1.75(d,*J*=9.6,2H).
	^{13}C NMR	(100MHz,$(CD_3)_2SO$); $^{\delta}$C in ppm 164.7, 162.9, 157.0, 155.6, 152.0, 144.1, 133.4, 132.9, 132.7, 131.3, 127.8, 126.5, 126.1, 122.1, 119.5, 116.8, 112.9, 111.6, 111.1, 110.9, 110.5, 56.4, 44.4, 40.6, 39.8, 39.4, 39.2, 39.0, 38.4, 36.5, 26.8, 23.2.
	EIMS	Found 608.30 $[M+H]^+$, Calculated for $C_{32}H_{29}N_7O_6$, 607.21 $[M]^+$
	HRMS	*m/z* (+EI) Calc. for $C_{32}H_{29}N_7O_6$, 607.2179 $[M]^+$, found 608.2244$[M+H]^+$.
	IR	(FTIR), V_{max}/'cm^{-1}): 3276, 2972, 1739, 1649, 1606, 1530, 1464, 1435, 1367, 1311, 1211, 1148, 1067, 953, 884, 865, 792, 771, 744, 682.

4.80 Synthesis of N-(3-((3-((3-(dimethylamino) propyl) carbamoyl)-1H-indol-5-yl) carbamoyl)-1H-indol-5-yl)-5-nitro-1H-benzo[d]imidazole-2-carboxamide (4.80).

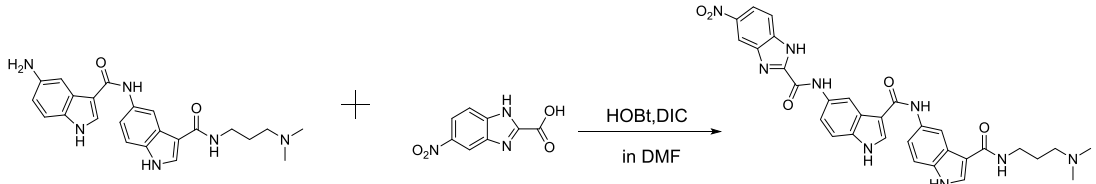

4.69 **4.80**

Initially, 59 mg of 5-nitro-1H-benzo[d]imidazole-2-carboxylic acid (0.284 mmol, 1.4 eq.) was dissolved in 10mL of DMF in a round bottom flask fitted with a magnetic stirrer. Then DIC (77 µl, 0.497 mmol, 1.75 eq.) and HOBt (77 mg, 0.568 mmol, 2.0 eq.) were added to the acid (1.0 eq.) and this mixture was stirred at room temperature for 30 minutes for complete esterification. Then amine **4.69** (85 mg, 0.203 mmol, 1 eq.) was added to the mixture and this mixture was allowed to stir for 4 hours at which point TLC and LCMS analysis showed the completion of reaction. Finally the reaction mixture was separated by using a conditioned Isolute^{TM} SCX-2 cartridge and the product was purified by 'Catch and Release' method **(**described in the section of chapter 3**)**. An orange solid was obtained after drying in vacuum. Yield was 7 mg, 6%.

Table 4.80: Characterisation data for compound **4.80**

4.80 Orange solid	^{1}H NMR	^{1}HNMR(400MHz,$(CD_3)_2SO$); $^{\delta}$H in ppm 11.68(d,*J*=2.4,1H), 11.43(d,*J*=2.4,1H), 10.89(s,1H), 9.67(s,1H), 8.79(d,*J*=1.6,1H),8.56(d,*J*=2.0,1H),8.43(d,*J*=2.0,1H),8.32(d,*J*=2.8, 1H), 8.20(dd,*J*=8.8,2.4,1H), 7.94(s,2H), 7.89(t,*J*=6.4,1H), 7.85-7.81(m,1H),7.64-7.59 (m,2H), 7.45(d,*J*=8.4,1H), 7.36(d,*J*=8.8,1H), 3.30-3.25(m,2H),2.36(t,*J*=7.2,2H), 2.20(s,6H), 1.72-1.65(m,2H).
	^{13}C NMR	(100MHz,$(CD_3)_2SO$); $^{\delta}$C in ppm 164.8, 162.9, 162.3, 156.9, 151.1, 146.2, 145.2, 143.2, 136.1, 133.8, 132.7, 132.5, 131.2, 126.4, 126.0, 123.8, 117.3, 117.1, 116.0, 113.7, 111.9, 111.2, 110.9, 110.6, 48.5, 44.7, 38.9, 38.7, 35.7, 30.7, 27.0.
	EIMS	Found 608.30 $[M+H]^+$, Calculated for $C_{31}H_{29}N_9O_5$, 607.22 $[M]^+$
	HRMS	*m/z* (+EI) Calc. for $C_{31}H_{29}N_9O_5$, 607.2292 $[M]^+$, found 608.2362$[M+H]^+$.
	IR	(FTIR), V_{max}/'cm^{-1}): 2970, 1740, 1638, 1537, 1479, 1366, 1228, 1217, 1154, 1024, 1004, 944, 887, 802, 778, 733.

4.81 Synthesis N-(3-(dimethylamino) propyl)-5-nitro-1H-indazole-3-carboxamide (4.81).

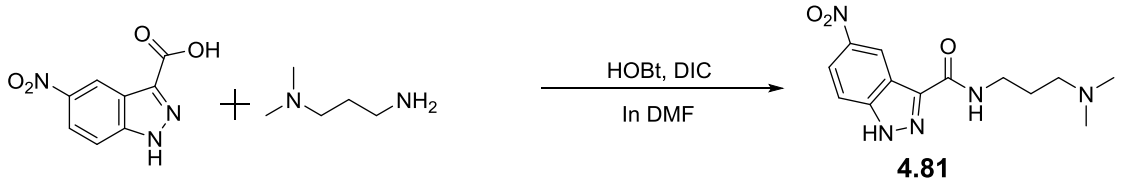

4.81

Initially, 250 mg of 5-nitro-1H-indazole-3-carboxylic acid (1.207 mmol, 1.2 eq.) was dissolved in 10mL of DMF in a round bottom flask fitted with a magnetic stirrer. Then DIC (326 µl, 2.11 mmol, 1.75 eq.) and HOBt (326 mg, 2.414 mmol, 2.0 eq.) were added to the acid (1.0 eq.) and this mixture was allowed to stir at room temperature for 30 minutes to ensure the formation of ester from the acid. Then 3-amino-N-methyl-N-methylenepropan-1-aminium (85 µl, 0.828 mmol, 1 eq.) was added and the mixture was allowed to stir for 7 hours at which point TLC and LCMS analysis showed the completion of reaction. Finally the reaction mixture was applied to a conditioned Isolute^{TM} SCX-2 cartridge and the product was purified by 'Catch and Release' method **(**described in the section **'Method and Materials'** of chapter 3**)**. A yellow solid was obtained after drying in vacuum. Yield=196 mg, 56%.

Table 4.81: Characterisation data for compound **4.81**

4.81 Yellow solid	^{1}H NMR	^{1}HNMR(400MHz,$(CD_3)_2SO$); $^\delta$H in ppm 9.04(d,*J*=2.4,1H),8.73(t,*J*=6.0,1H),8.22(dd,*J*=9.2,2.0,1H),7.81(d,*J*=9.2,1H),3.37-3.32(m,2H),2.32(t,*J*=6.4,2H),2.17(S,6H),1.71(t,*J*=7.2,2H).
	EIMS	Found 291.13 $[M+H]^+$, $C_{13}H_{17}N_5O_3$, 290.20 $[M]^+$

4.82 Synthesis 5-amino-N-(3-(dimethylamino) propyl)-1H-indazole-3-carboxamide (4.82).

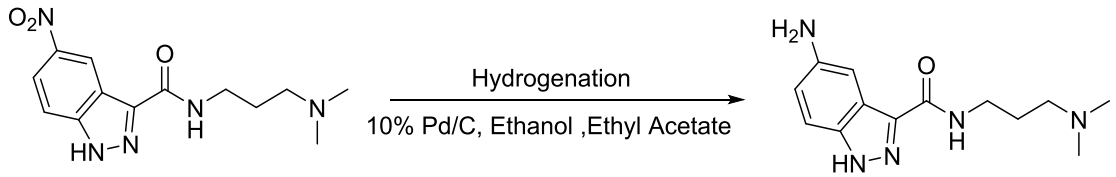

4.81 **4.82**

180 mg of **4.81** was dissolved in 20 mL of ethanol and 1 mL of ethyl acetate was added to a hydrogenation reaction bottle. 20 mg of 10% Pd (palladium on activated carbon) was added into the reaction vessel and it was mixed well. The reaction bottle was sealed and connected to a hydrogen reservoir. Air from the reaction bottle was removed by applying vacuum and it was then flushed with hydrogen. Typically, a hydrogen pressure of approximately 40 psi was applied from the reservoir and the bottle was then shaken vigorously to initiate the reaction. Progress of the reaction was monitored by TLC and LCMS. The shaker was stopped and the bottle was vented after 6 hours at which point TLC and LCMS analysis showed the completion of reaction. The product was recovered by means of filtration using Celite. Finally, the product is concentrated by using a rotary evaporator. A pale yellow solid was obtained after drying in vacuum. Yield=145 mg, 90 %.

Table 4.82: Characterisation data for compound **4.82**

4.82 Pale Yellow solid	^{1}H NMR	^{1}HNMR(400MHz,$(CD_3)_2SO$); $^\delta$H in ppm 8.21(t,*J*=6.0,1H),7.95(S,1H),7.337.29(m,2H),6.83(dd,*J*=8.8,2.4,1H),3.34-3.29(m,2H),2.26(t,*J*=6.8,2H),2.13(S,6H),2.10-2.06(m,2H),1.691.63(m,2H).
	EIMS	Found 262.0 $[M+H]^+$, Calculated for $C_{13}H_{19}N_5O$, 261.15 [M]

4.83 Synthesis of N-(3-(dimethylamino) propyl)-5-(5-nitro-1H-indazole-3-carboxamido)-1H-indazole-3-carboxamide (4.83).

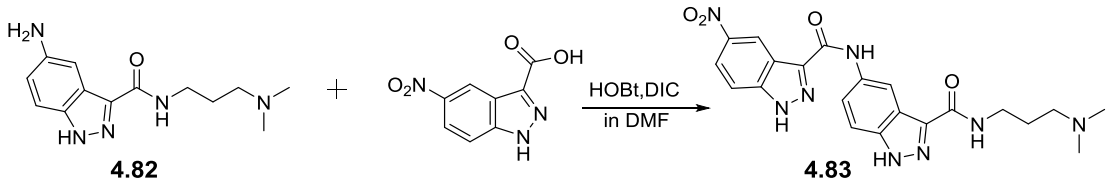

4.82 4.83

Initially, 155 mg of 5-nitro-1H-indazole-3-carboxylic acid (0.75 mmol, 1.4 eq.) was dissolved in 10mL of DMF in a round bottom flask fitted with a magnetic stirrer. Then 202 µl of DIC (1.313 mmol, 1.75 eq.) and HOBt (202 mg, 1.50 mmol, 2.0 eq.) were added to the acid (1.0 eq.) and this mixture was allowed to stir at room temperature for 30 minutes to ensure the formation of ester from the acid. Then 140 mg of **4.82** (0.536 mmol, 1 eq.) was added to the mixture and the mixture was allowed to stir for 7 hours at which point TLC and LCMS analysis showed the completion of reaction. Finally the reaction mixture was applied to a conditioned Isolute^{TM} SCX-2 cartridge and the product was purified by 'Catch and Release' method **(**described in the section **'Method and Materials'** of chapter 3**)**. A light yellow solid was obtained after drying in vacuum. Yield=109 mg, 45%.

Table 4.83: Characterisation data for compound **4.83**

4.83 Light Yellow	^{1}H NMR	^{1}HNMR(400MHz,$(CD_3)_2SO$); $^{\delta}$H in ppm 13.56(s,1H), 10.66(s,1H), 9.12(d,*J*=2.0,1H), 8.81(d*J*=1.6,1H), 8.43(t,*J*=5.6,1H), 8.26(dd,*J*=9.2,2.4,1H), 7.88-7.82(m,2H), 7.59(d,*J*=8.8,1H), 3.34(t,*J*=6.4,2H), 2.33(t,*J*=6.8,2H), 2.18(s,6H), 1.71(t,*J*=6.8,2H).
	^{13}C NMR	(100MHz,$(CD_3)_2SO$); $^{\delta}$C in ppm 162.1, 160.1, 143.7, 142.6, 140.9, 138.5, 138.2, 132.9, 121.9, 121.5, 121.0, 118.9, 112.4, 110.5, 57.0, 45.0, 39.2, 39.0, 38.8, 36.9, 27.1.
	EIMS	Found 451.0 $[M+H]^+$, Calculated for $C_{21}H_{22}N_8O_4$, 450.17 $[M]^+$
	HRMS	*M/z* (+EI) Calc. for $C_{21}H_{22}N_8O_4$, 450.1764 $[M]^+$, found 451.1826 $[M+H]^+$.
	IR	(FTIR), V_{max}/'cm^{-1}): 3376, 3201, 2923, 2818, 1655, 1638, 1597, 1531, 1481, 1335, 1318, 1252, 1152, 1100, 993, 891, 856, 842, 793, 767, 740, 727.

4.84 Synthesis of 5-amino-N-(3-((3-(dimethylamino) propyl) carbamoyl)-1H-indazol-5-yl)-1H-indazole-3-carboxamide (4.84).

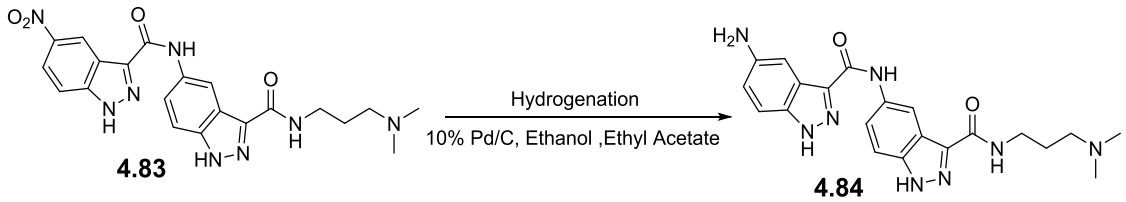

200 mg of **4.83** was dissolved in 20 mL of ethanol and 1 mL of ethyl acetate was added to a hydrogenation reaction bottle. 20 mg of 10% Pd (palladium on activated carbon) was added into the reaction vessel and it was mixed well. The reaction bottle was sealed and connected to a hydrogen reservoir. Air from the reaction bottle was removed by applying vacuum and it was flushed with hydrogen. Typically, a hydrogen pressure of approximately 40 psi was applied from the reservoir, and the bottle was then shaken vigorously to initiate the reaction. Progress of the reaction was monitored by TLC and LCMS. The shaker was stopped and the bottle was vented after 5 hours at which point TLC and LCMS analysis showed the completion of reaction. The product was recovered by means of filtration using Celite. Finally, the product was concentrated by using a rotary evaporator. A deep brown solid was obtained after drying in vacuum. Yield=140 mg, 75 %.

Table 4.84: Characterisation data for compound **4.84**

4.84 Deep Brown	^{1}H NMR	^{1}HNMR(400MHz,$(CD_3)_2SO$); $^{\delta}$H in ppm 13.67(s,2H), 10.15(s,1H), 8.77(d,*J*=1.2,1H), 8.39(t,*J*=6.0,1H), 7.78(dd,*J*=9.2,2.0,1H), 7.56(d,*J*=9.2,1H), 7.36(d,*J*=8.8,1H), 7.32(d,*J*=2.0,1H), 6.86(dd,*J*=8.8,2.0,1H), 3.35-3.30(m, 2H), 2.49(t,*J*=7.2,2H), 2.14(s,6H), 2.08(d,*J*=1.2,2H), 1.68(t,*J*=7.2,2H).
	^{13}C NMR	(100MHz,$(CD_3)_2SO$); $^{\delta}$C in ppm 162.2, 161.4, 152.5, 144.2, 138.3, 138.1, 136.9, 136.2, 135.9, 133.4, 123.4, 121.9, 121.2, 111.7, 110.9, 102.9, 57.1, 45.2, 38.5, 27.8, 22.5.
	EIMS	Found 421.10 $[M+H]^+$, calculated for $C_{21}H_{24}N_8O_2$, 420.20 $[M]^+$
	HRMS	*m/z* (+EI) Calc. for $C_{21}H_{24}N_8O_2$, 420.2022 $[M]^+$, found 421.2095 $[M+H]^+$.
	IR	(FTIR), V_{max}/'cm^{-1}): 3200, 2927, 1638, 1596, 1535, 1482, 1335, 1317, 1224, 1152, 1099, 1024, 994, 944, 891, 856, 841, 793, 739, 728, 637.

4.85 Synthesis N-(3-(dimethylamino) propyl)-5-(5-(5-nitro-1H-indazole-3-carboxamido)-1H-indazole-3-carboxamido)-1H-indazole-3-carboxamide (4.85).

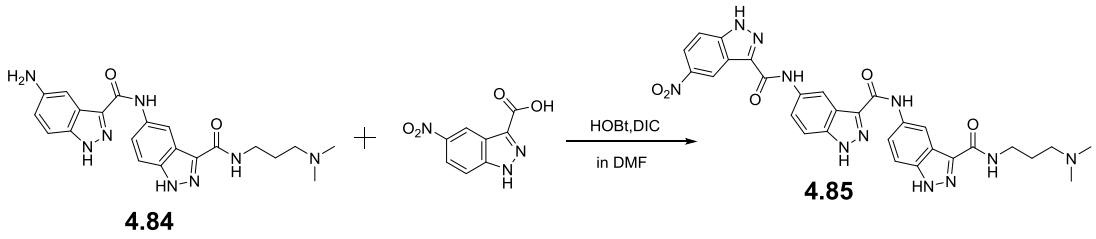

4.84 **4.85**

Initially, 49.5 mg of 5-nitro-1H-indazole-3-carboxylic acid (0.239 mmol, 1.4 eq.) was dissolved in 10 mL of DMF in a round bottom flask fitted with a magnetic stirrer. Then DIC (65 µl, 0.418 mmol, 1.75 eq.) and HOBt (65 mg, 0.478 mmol, 2.0 eq.) were added to the acid (1.0 eq.) and this mixture was stirred at room temperature for at least 30 minutes to ensure the formation of ester from the acid. Then 72 mg of amine **4.84** (0.171 mmol, 1 eq.) was added to the mixture and the mixture was allowed to stir for 5 hours at which point TLC and LCMS analysis showed the completion of reaction. Finally the reaction mixture was applied to a conditioned Isolute^{TM} SCX-2 cartridge and the product was purified by 'Catch and Release' method **(**described in the section **'Method and Materials'** of chapter 3**)**. A deep grey solid was obtained after drying in vacuum. Yield=14.4 mg, 15%.

Table 4.85: Characterisation data for compound **4.85**

4.85 Deep Grey	^{1}H NMR	^{1}HNMR(400MHz,$(CD_3)_2SO$); $^{\delta}$H in ppm 13.76(s,1H), 13.52(s,2H), 10.73(s,1H), 10.41(s,1H), 9.16(d,*J*=2.0,1H), 8.93(d,*J*=1.2,1H), 8.83(d,*J*=1.6,1H), 8.44(s,1H), 8.29(dd,*J*=9.2,2.4,1H), 7.91-7.87(m,2H), 7.85(dd,*J*=8.8,2.0,1H), 7.66(d,*J*=9.2,1H), 7.58(d,*J*=8.8,1H), 3.38-3.33(m,2H), 2.40(t,*J*=7.2,2H), 2.24(s,6H), 1.73(t,*J*=7.2, 2H).
	^{13}C NMR	(100MHz,$(CD_3)_2SO$); $^{\delta}$C in ppm 171.5, 162.2, 160.9, 160.0, 143.3, 142.8, 142.8, 140.9, 138.4, 138.3, 138.1, 136.9, 133.3, 131.4, 130.6, 127.5, 122.1, 121.9, 121.5, 121.0, 119.0, 112.2, 110.9, 56.7, 44.7, 39.2, 38.8, 36.7, 26.9.
	EIMS	Found 610.10 $[M+H]^+$, calculated for $C_{29}H_{27}N_{11}O_5$, 609.21 $[M]^+$
	HRMS	*m/z* (+EI) Calc. for $C_{29}H_{27}N_{11}O_5$, 609.2197 $[M]^+$, found 610.2264 $[M+H]^+$.
	IR	(FTIR), V_{max}/'cm^{-1}): 3200, 3013, 2970, 2945, 1740, 1651, 1594, 1540, 1478, 1366, 1343, 1317, 1228, 1217, 1150, 1090, 1023, 1000, 942, 897, 853, 792, 742, 625.

4.86 Synthesis of N-(3-(dimethylamino) propyl)-5-(5-(5-nitro-1H-benzo[d]imidazole-2-carboxamido)-1H-indazole-3-carboxamido)-1H-indazole-3-carboxamide (4.86).

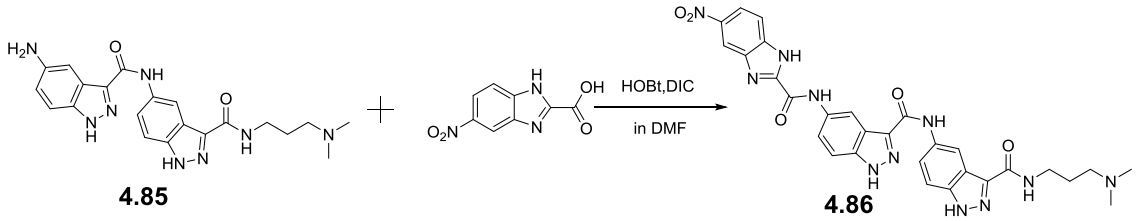

4.85 **4.86**

Initially, 52 mg of 5-nitro-1H-benzo[d]imidazole-2-carboxylic acid (0.253 mmol, 1.2 eq.) was dissolved in 10 mL of DMF in a round bottom flask fitted with a magnetic stirrer. Then 68 µl of DIC (0.442 mmol, 1.75 eq.) and HOBt (68 mg, 0.506 mmol, 2.0 eq.) were added to the acid (1.0 eq.) and this mixture was allowed to stir at room temperature for 30 minutes to ensure the esterification of acid. Then 76 mg of amine **4.85**(0.180 mmol, 1 eq.) was added to the mixture and the mixture was allowed to stir for 7 hours at which point TLC and LCMS analysis showed the completion of reaction. At last the reaction mixture was applied to a conditioned Isolute^{TM} SCX-2 cartridge and the product was purified by 'Catch and Release' method **(**described in the section **'Method and Materials'** of chapter 3**)**. A brown solid was obtained after drying in vacuum. Yield=14 mg, 13%.

Table 4.86: Characterisation data for compound **4.86**

4.86 Brown	^{1}H NMR	^{1}HNMR(400MHz,$(CD_3)_2SO$); $^{\delta}$H in ppm 13.82(s,1H),13.51(s,1H), 11.13(s,1H), 10.42(s,1H), 8.94(d,*J*=1.6,1H), 8.79(d,*J*=1.2,1H), 8.57(d,*J*=2.0,1H), 8.43(t,*J*=5.6,1H), 8.19(dd,*J*=8.8,2.0,1H), 7.95(s,1H), 7.90(dd,*J*=8.8,2.0,1H), 7.84(dd,*J*=8.8,2.4,2H), 7.69(d,*J*=8.8,1H), 7.58(d,*J*=8.8,1H), 3.38-3.33(m,2H), 2.35(t,*J*=7.2,2H), 2.20(s,6H), 1.72(t,*J*=6.8,2H).
	^{13}C NMR	(100MHz,$(CD_3)_2SO$); $^{\delta}$C in ppm 162.29, 162.23, 160.8, 157.3, 154.9, 149.6, 143.0, 142.7, 138.6, 138.4, 138.28, 138.20, 133.2, 132.9, 128.0, 121.9, 121.8, 121.5, 118.3, 113.8, 112.5, 112.2, 56.9, 44.9, 39.0, 36.8, 35.7, 30.7, 27.0.
	EIMS	Found 610.20 $[M+H]^+$, calculated for $C_{29}H_{27}N_{11}O_5$, 609.21 $[M]^+$
	HRMS	*m/z* (+EI) Calc. for $C_{29}H_{27}N_{11}O_5$, 609.2197 $[M]^+$, found 610.2258$[M+H]^+$.
	IR	(FTIR), V_{max}/'cm^{-1}): 3280, 2944, 1638, 1591, 1574, 1531, 1468, 1392,1 290, 1232, 1154, 1034, 953, 879, 809, 737, 716, 618.

4.87 Synthesis of 5-cyano-N-(3-((3-((3-(dimethylamino) propyl) carbamoyl)-1H-indol-5-yl) carbamoyl)-1H-indol-5-yl)-1H-indole-2-carboxamide (4.87).

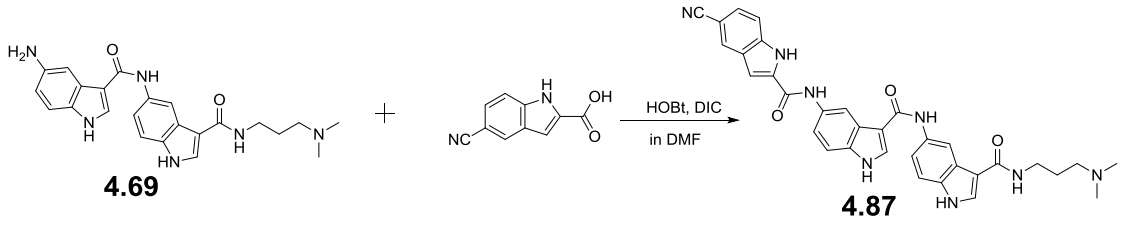

Initially 56 mg of 5-cyano-1H-indole-2-carboxylic acid (0.298 mmol, 1.2 eq.) was dissolved in 10 mL of DMF in a round bottom flask placed into a stirrer.

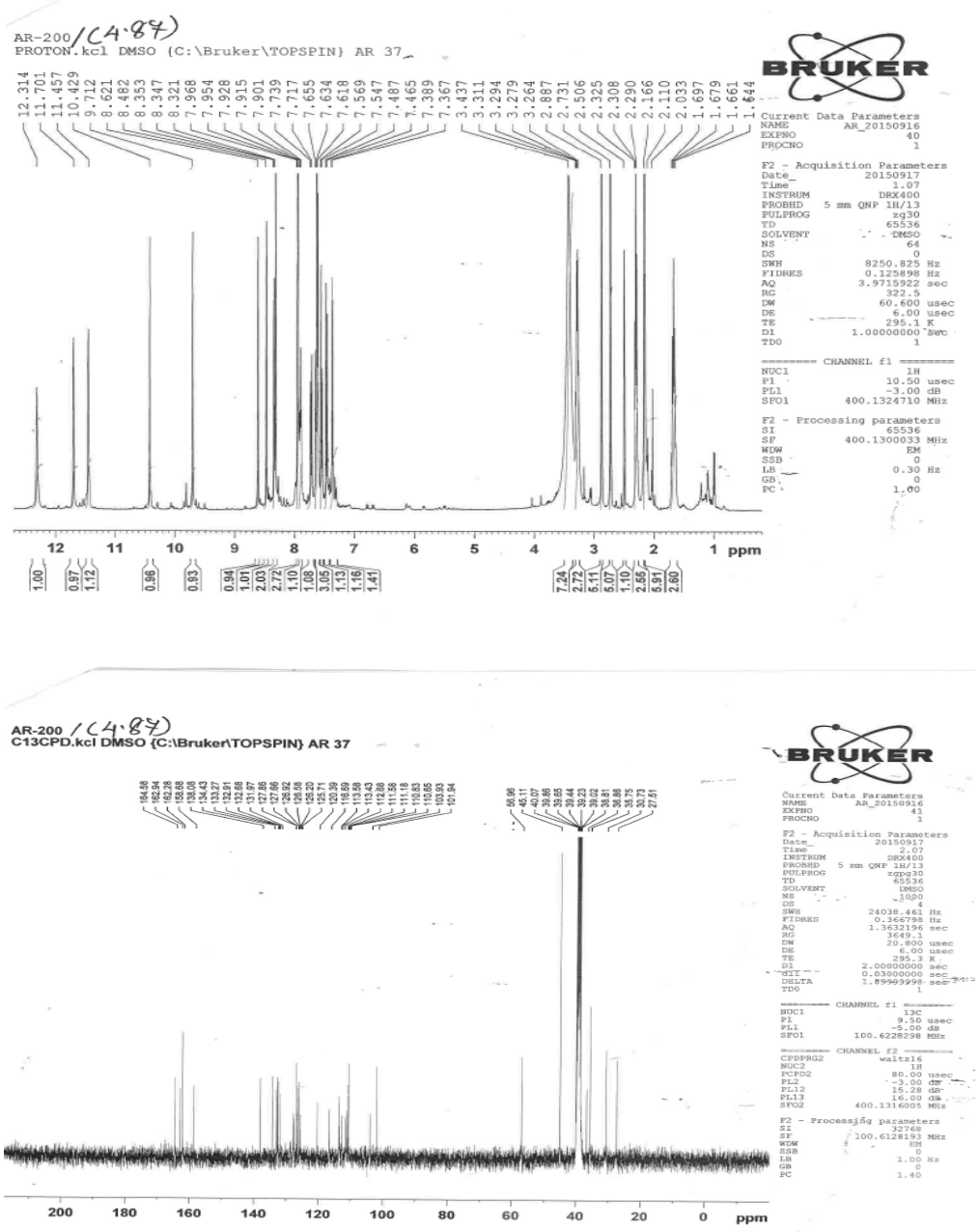

Figure 4.7: ^{1}H and ^{13}C NMR spectroscopic data of compound **4.87** as a representative of **library-4C** compounds

Then 80 µl of DIC (0.5215 mmol, 1.75 eq.) and HOBt (80 mg, 0.596 mmol, 2. 0eq.) were added to the acid (1.0 eq.) and mix it well and the mixture was allowed to stir at room temperature for 30 minutes to ensure the formation of ester from the acid. Then 104 mg of amine **4.69**(0.2488 mmol, 1 eq.) was added and the mixture was allowed to stir for 5 hours at which point TLC and LCMS analysis showed the completion of reaction. The reaction mixture was applied to a conditioned Isolute^{TM} SCX-2 cartridge and the product was purified by 'Catch and Release' method **(**described in the section **'Method and Materials'** of chapter 3**)**. An orange solid was obtained after drying in vacuum. Yield=75 mg, 51%.

Table 4.87: Characterisation data for compound **4.87**

4.87 Orange	^{1}H NMR	^{1}HNMR(400MHz,$(CD_3)_2SO$); $^{\delta}$H in ppm 12.31(s,1H),11.70(s,1H),11.45(s,1H),10.42(s,1H),9.71(s,1H),8.62(s,1H),8.48(s,1H),8.35(d,*J*=4.8,1H),8.32(s,2H),7.96(s,1H),7.91(t,*J*=5.2,1H),7.72(d,*J*=8.8,1H),7.63(t,*J*=8.4,2H),7.55(d,*J*=8.8,1H),7.47(d,*J*=8.8,1H),7.37(d,*J*=8.8,1H),3.313.26(m,2H),2.32(t,*J*=6.8,2H),2.16(s,6H),1.69(t,*J*=6.8,2H).
	^{13}C NMR	(100MHz,$(CD_3)_2SO$); $^{\delta}$C in ppm 164.5,162.9,162.2,158.6,138.0,134.4,133.2,132.9,132.6,131.9,127.8,127.6,126.9,126.5,126.2,125.7,120.9,116.6,113.5,113.4,112.6,111.5,111.1,110.8,110.6,103.9,101.9,56.9,45.1, 38.8,36.8,30.7,27.5.
	EIMS	Found 587.10 $[M+H]^+$, calculated for $C_{33}H_{30}N_8O_3$, 586.2441 [M]
	HRMS	*m/z* (+EI) Calc. for $C_{33}H_{30}N_8O_3$, 586.2441 $[M]^+$, found 587.2508 $[M+H]^+$.
	IR	(FTIR, V_{max}/'cm^{-1}): 3238, 2933, 2218, 1651, 1616, 1539, 1473, 1434, 1386, 1362, 1330, 1310, 1248, 1213, 1159, 1098, 1023, 1003, 944, 885, 805, 768, 737, 660, 618.

4.88 Synthesis of N-(3-(dimethylamino) propyl)-5-(5-(5-nitro-1H-indole-2-carboxamido)-1H-indazole-3-carboxamido)-1H-indazole-3-carboxamide (4.88)

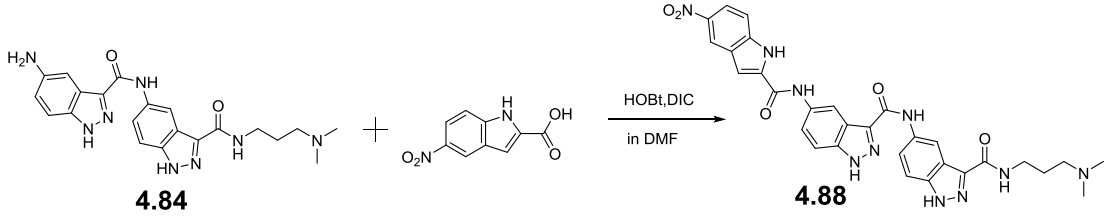

4.84 **4.88**

Initially, 36 mg of 5-nitro-1H-indole-2-carboxylic acid (0.171 mmol, 1.2 eq.) was dissolved in 10 mL of DMF in a round bottom flask fitted with a magnetic stirrer.

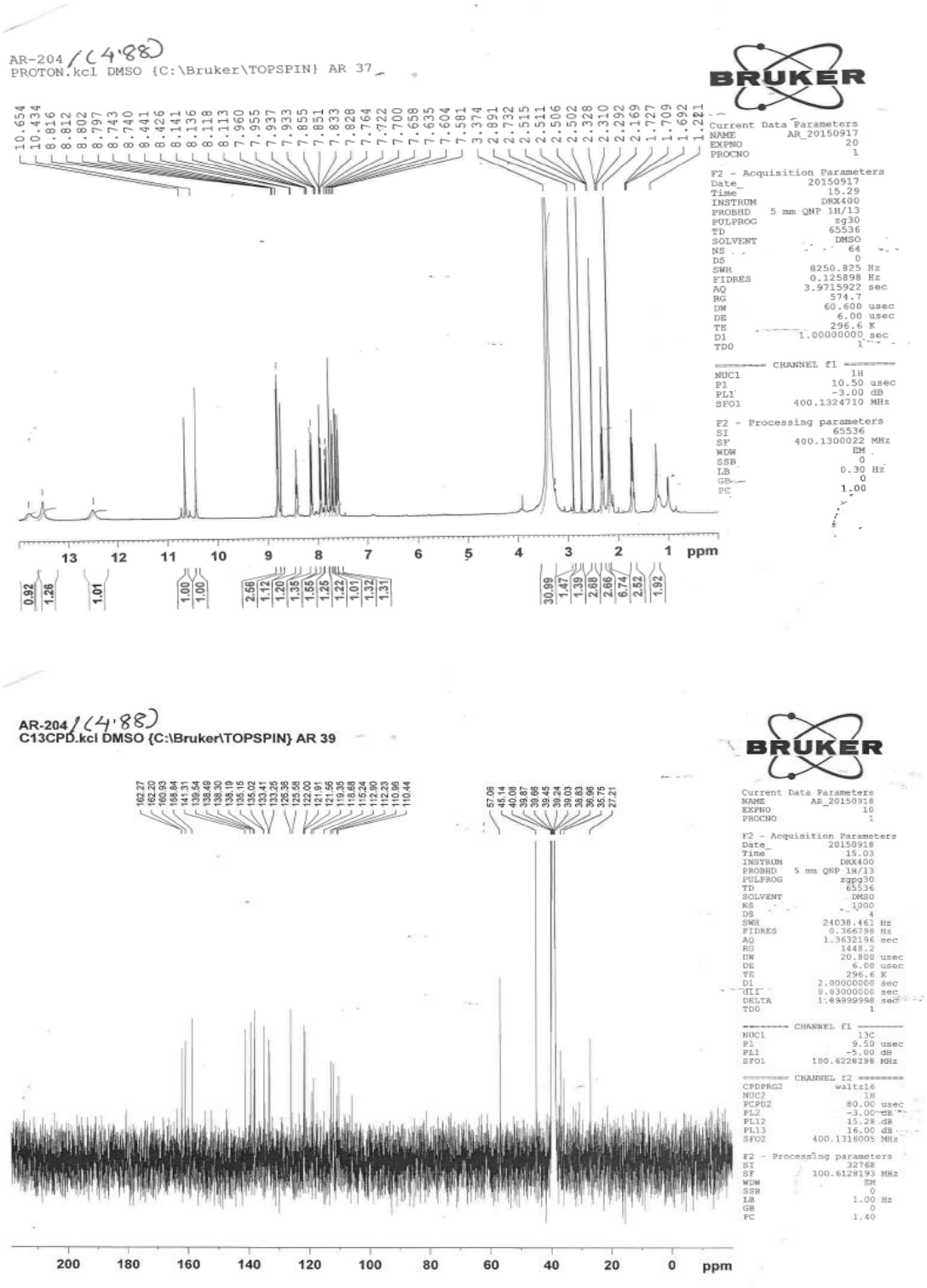

Figure 4.8: ^{1}H and ^{13}C NMR spectroscopic data of compound **4.88** as a representative of **library-4D** compounds

Then 46 µl of DIC (0.299 mmol, 1.75 eq.) and HOBt (46 mg, 0.342 mmol, 2.0 eq.) were added to the acid (1.0 eq.) and this mixture was allowed to stir at

room temperature for 30 minutes to ensure the formation of ester from the acid. Then 60 mg of amine **4.84**(0.142 mmol, 1 eq.) was added and the mixture was allowed to stir for 4 hours at which point TLC and LCMS analysis showed the completion of reaction. Finally the reaction mixture was applied to a conditioned Isolute^{TM} SCX-2 cartridge and the product was purified by 'Catch and Release' method **(**described in the section **'Method and Materials'** of chapter 3**)**. An orange solid was obtained after drying in vacuum. Yield=10 mg, 12%.

Table 4.88: Characterisation data for compound **4.88**

4.88 orange	^{1}H NMR	^{1}HNMR(400MHz,$(CD_3)_2SO$); $^{\delta}$H in ppm 13.76(s,1H),13.50(s,1H),12.48(s,1H),10.65(s,1H),10.43(s,1H),8.80 (dd,*J*=5.6,1.6,2H),8.74(d,*J*=1.2,1H),8.42(t,*J*=6.0,1H),8.12(dd,*J*=9.2, 2.0,1H),7.94(dd,*J*=9.2,2.0,1H),7.84(dd,*J*=8.8,2.0,1H),7.76(d,*J*=4.0, 1H),7.71(d,*J*=8.8,1H),7.64(d,*J*=9.2,1H),7.59(d,*J*=9.2,1H),2.51-2.50(m,2H),2.31(t,*J*=7.2,1H),2.16(s,6H),1.22(s,2H).
	^{13}C NMR	(100MHz,$(CD_3)_2SO$); $^{\delta}$C in ppm 162.2,160.9,158.8,141.3,139.5,138.4,138.3,138.1,135.1,133.4,133.2,126.3,121.9,121.5,118.6,112.9,112.2,110.4,57.0,45.1,40.0,39.8,39.6,39.4,39.2,39.0,38.8,36.9,35.7,27.2.
	EIMS	Found 608.20 $[M+H]^+$, calculated for $C_{30}H_{28}N_{10}O_5$, 608.2244 $[M]^+$
	HRMS	*m/z* (+EI) Calc. for $C_{30}H_{28}N_{10}O_5$, 608.2244 $[M]^+$, found 609.2317$[M+H]^+$.
	IR	(FTIR), V_{max}/'cm^{-1}): 3198, 2928, 1646, 1591, 1539, 1487, 1377, 1337, 1315, 1288, 1228, 1134, 1023, 998, 955, 883, 800, 779, 759, 732.

4.89 Synthesis of 5-(benzo[b]thiophene-3-carboxamido)-N-(3-((3-(dimethylamino) propyl) carbamoyl)-1H-indol-5-yl)-1H-indole-3-carboxamide (4.89).

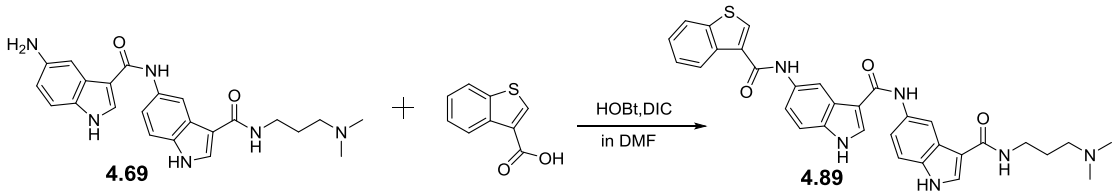

Initially, 30 mg of benzo[b]thiophene-3-carboxylic acid (0.167 mmol, 1.2 eq.) was dissolved in 5 mL of DMF in a round bottom flask fitted with a magnetic stirrer. Then 45 µl of DIC (0.29 mmol, 1.75 eq.) and HOBt (45 mg, 0.334 mmol, 2.0 eq.) were added to the acid (1.0 eq.) and this mixture was allowed to stir at room temperature for 30 minutes to ensure the formation of ester from the acid. Then 50 mg of amine **4.69** (0.119 mmol, 1 eq.) was added and the mixture was allowed to stir for 10 hours at which point TLC and LCMS analysis showed the

completion of reaction. Finally the reaction mixture was applied to a conditioned Isolute^{TM} SCX-2 cartridge and the product was purified by 'Catch and Release' method **(**described in the section **'Method and Materials'** of chapter 3**)**. A pale yellow solid was obtained after drying in vacuum. Yield=12 mg, 18 %.

Table 4.89: Characterisation data for compound

4.89 Pale yellow solid	^{1}H NMR	^{1}HNMR(400MHz,$(CD_3)_2SO$); $^{\delta}$H in ppm 11.72(dd,*J*=10.0,2.4,1H),11.48 (d,*J*=2.4,1H),) 10.30(s,1H), 9.71(s,1H), 8.64(d,*J*=8.8,1.6,1H), 8.60(d,*J*=2,1H), 8.49(dd,*J*=5.2,1.6,1H), 8.34(t,*J*=3.2,2H), 8.08(dd,*J*=5.6,1.2,1H), 7.98-7.93(m,2H), 7.67-7.63(m,1H), 7.58-7.54 (m,1H), 7.49-7.43(m,2H), 7.40-7.33 (m,2H), 3.34-3.26(m,2H), 2.41-2.21 (m,2H), 2.22 (s,6H), 1.70(t,*J*=7.2,2H).
	^{13}C NMR	(100MHz,$(CD_3)_2SO$); $^{\delta}$C in ppm 164.7, 164.6, 162.9, 161.5, 156.8, 139.9, 137.3, 133.1, 132.9, 132.6, 132.3, 131.3, 131.0, 128.6, 126.1, 124.8, 124.4, 122.7, 116.7, 116.6, 111.1, 110.8, 110.6, 56.6, 52.1, 44.6, 39.6, 39.0, 38.7, 36.6, 27.0, 23.2.
	EIMS	Found 578.50 $[M+H]^+$, calculated for $C_{32}H_{30}N_6O_3S$, 578.21 $[M]^+$
	HRMS	*m/z* (+EI) Calc. for $C_{32}H_{30}N_6O_3S$, 578.2100 $[M]^+$, found 579.2161 $[M+H]^+$.
	IR	(FTIR), V_{max}/'cm^{-1}): 3226, 2970, 1740, 1640, 1588, 1535, 1467, 1437, 1362, 1309, 1230, 1208, 1151, 1048, 1023, 1004, 946, 810, 766, 736, 626.

4.90 Synthesis of 5-(benzofuran-3-carboxamido)-N-(3-((3-(dimethylamino) propyl) carbamoyl)-1H-indol-5-yl)-1H-indole-3-carboxamide (4.90).

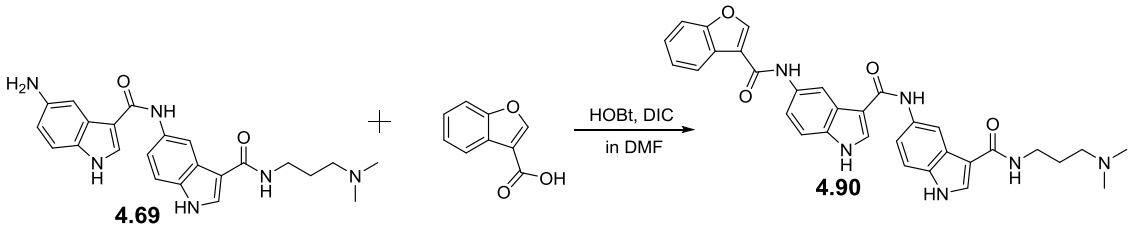

Initially, 33 mg of benzofuran-3-carboxylic acid (0.20 mmol, 1.2 eq.) was dissolved in 10 mL of DMF in a round bottom flask fitted with a magnetic stirrer. Then 55 µl of DIC (0.35 mmol, 1.75 eq.) and HOBt (55 mg, 0.40 mmol, 2.0 eq.) were added to the acid (1.0 eq.) and this mixture was allowed to stir at room temperature for 30 minutes to ensure the formation of ester from the acid. Then 60 mg of amine **4.69** (0.143 mmol, 1 eq.) was added and the mixture was allowed to stir for 7 hours at which point TLC and LCMS analysis showed the completion of reaction. Finally the reaction mixture was applied to a conditioned

Isolute^{TM} SCX-2 cartridge and the product was purified by 'Catch and Release' method **(**described in the section **'Method and Materials'** of chapter 3**)**. An orange solid was obtained after drying in vacuum. Yield=25 mg, 32%.

Table 4.90: Characterisation data for compound **4.90**

4.90 Orange solid	^{1}H NMR	^{1}HNMR(400MHz,$(CD_3)_2SO$); $^{\delta}$H in ppm 11.88(s,1H), 11.70(s,1H), 10.23(s,1H), 9.74(s,1H), 8.86 (s,1H), 8.64(s,1H), 8.59(s,1H), 8.50(d,*J*=8.0,1H), 8.36(s,1H), 8.19-8.16(m,2H), 8.01(s,1H), 7.69(d,*J*=7.2,1H), 7.62 (dd,*J*=8.8,2.0,2H), 7.43(d,*J*=10.0,1H), 7.38-7.36 (m,2H), 3.69-3.59(m,2H), 3.37-3.31 (m,2H), 2.51 (s,6H), 1.97(s,2H).
	^{13}C NMR	(100MHz,$(CD_3)_2SO$); $^{\delta}$C in ppm 168.3, 156.8, 156.1, 148.5, 135.7, 135.4, 133.4, 133.0, 130.2, 129.8, 127.7, 127.0, 126.7, 126.3, 124.9, 123.1, 119.6, 115.4, 115.0, 112.8, 112.4, 112.3, 112.1, 58.4, 53.9, 49.6, 49.4, 48.8, 42.7, 38.7, 28.5, 23.9.
	EIMS	Found 562.50 $[M+H]^+$, calculated for $C_{32}H_{30}N_6O_4$, 562.23 $[M]^+$
	HRMS	*m/z* (+EI) Calc. for $C_{32}H_{30}N_6O_4$, 562.2329 $[M]^+$, found 563.2388 $[M+H]^+$.
	IR	(FTIR), V_{max}/'cm^{-1}): 3245, 2969, 1617, 1542, 1473, 1377, 1328, 1221, 1170, 1127, 1077, 1040, 866, 805, 768, 741, 659.

4.91 Synthesis of N-(3-(dimethylamino) propyl)-5-(5-(1-methyl-1H-indole-3-carboxamido)-1H-indole-3-carboxamido)-1H-indole-3-carboxamide (4.91).

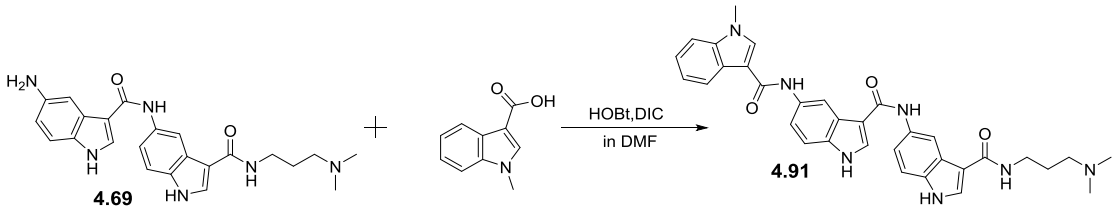

Initially, 31 mg of 1-methyl-1H-indole-3-carboxylic acid (0.177 mmol, 1.2 eq.) was dissolved in 10 mL of DMF in a round bottom flask fitted with a magnetic stirrer. Then 48 µl of DIC (0.311 mmol, 1.75 eq.) and HOBt (48 mg, 0.355 mmol, 2.0 eq.) were added to the acid (1.0 eq.) and this mixture was allowed to stir at room temperature for 30 minutes to ensure the formation of ester from the acid. Then 62 mg of amine **4.69** (0.148 mmol, 1 eq.) was added to the mixture and the mixture was allowed to stir for 6 hours at which point TLC and LCMS analysis showed the completion of reaction. At last the reaction mixture was applied to a conditioned Isolute^{TM} SCX-2 cartridge and the product was purified by 'Catch and Release' method **(**described in the section **'Method and**

Materials' of chapter 3**)**. An orange solid was obtained after drying in vacuum. Yield=18 mg, 21%.

Table 4.91: Characterisation data for compound **4.91**

4.91 Orange solid	^{1}H NMR	^{1}HNMR(400MHz,$(CD_3)_2SO$); $^{\delta}$H in ppm 11.60(s,*J*=2.4,1H), 11.44(s,1H), 9.72(s,1H), 9.67(s,1H), 8.55(d,*J*=1.6,1H), 8.47(d,*J*=1.6,1H), 8.40(dd,*J*=15.6,1.6,1H), 8.31(t,*J*=6.8,2H), 8.29-8.25(m,1H), 7.91(t,*J*=5.6,1H), 7.72 (dd,*J*=8.8,2.0,1H), 7.65(dd,*J*=8.8,2.0,1H), 7.53(d,*J*=8.0,1H), 7.41(d,*J*=8.8,1H), 7.36(dd,*J*=8.8,3.2,1H), 7.25(t,*J*=7.2,1H), 7.18(t,*J*=7.2,1H), 3.88(s,2H), 3.30-3.26(m,2H), 2.31 (t,*J*=7.2,2H), 2.16 (s,6H), 1.69-1.64(m, 2H).
	^{13}C NMR	(100MHz,$(CD_3)_2SO$); $^{\delta}$C in ppm 173.6, 164.5, 163.0, 162.6, 162.2, 143.1, 138.2, 133.2, 132.7, 132.6, 132.4, 132.1, 127.6, 126.9, 126.6, 126.4, 126.1, 120.9, 120.7, 116.6, 111.1, 110.6, 110.2,109.8, 56.9, 45.0, 40.0, 39.2, 36.8, 35.7, 33.0, 30.7, 27.4.
	EIMS	Found $[M+H]^+$ 576.40, Calculated for $C_{33}H_{33}N_7O_3$, 575.26 $[M]^+$
	HRMS	*m/z* (+EI) Calc. for $C_{33}H_{33}N_7O_3$, 575.2645 $[M]^+$, found 576.2703 $[M+H]^+$.
	IR	(FTIR), V_{max}/'cm^{-1}): 3294, 1631, 1526, 1446, 1339, 1300, 1235, 1155, 873, 838, 802, 750, 714.

4.92 Synthesis of N-(3-((3-((3-(dimethylamino) propyl) carbamoyl)-1H-indol-5-yl) carbamoyl)-1H-indol-5-yl)-1H-indazole-3-carboxamide (4.92).

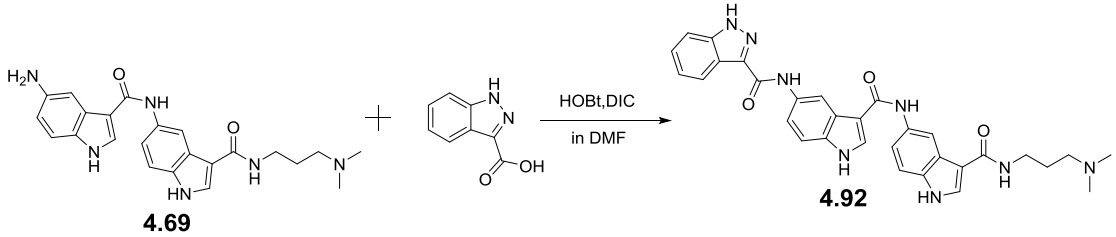

4.69 **4.92**

Initially, 48.80 mg of 1H-indazole-3-carboxylic acid (0.301 mmol, 1.4 eq.) was dissolved in 10 mL of DMF in a round bottom flask fitted with a magnetic stirrer. Then 58 µl of DIC (0.376 mmol, 1.75 eq.) and HOBt (58 mg, 0.43 mmol, 2.0 eq.) were added to the acid (1.0 eq.) and this mixture was allowed to stir at room temperature for 30 minutes to ensure the formation of ester from the acid. Then 90 mg of amine **4.69** (0.215 mmol, 1 eq.) was added and the mixture was allowed to stir for 7 hours at which point TLC and LCMS analysis showed the completion of reaction. Lastly the reaction mixture was applied to a conditioned Isolute^{TM} SCX-2 cartridge and the product was purified by 'Catch and Release'

method **(**described in the section **'Method and Materials'** of chapter 3**)**. A light yellow solid was obtained after drying in vacuum. Yield=32 mg, 27%.

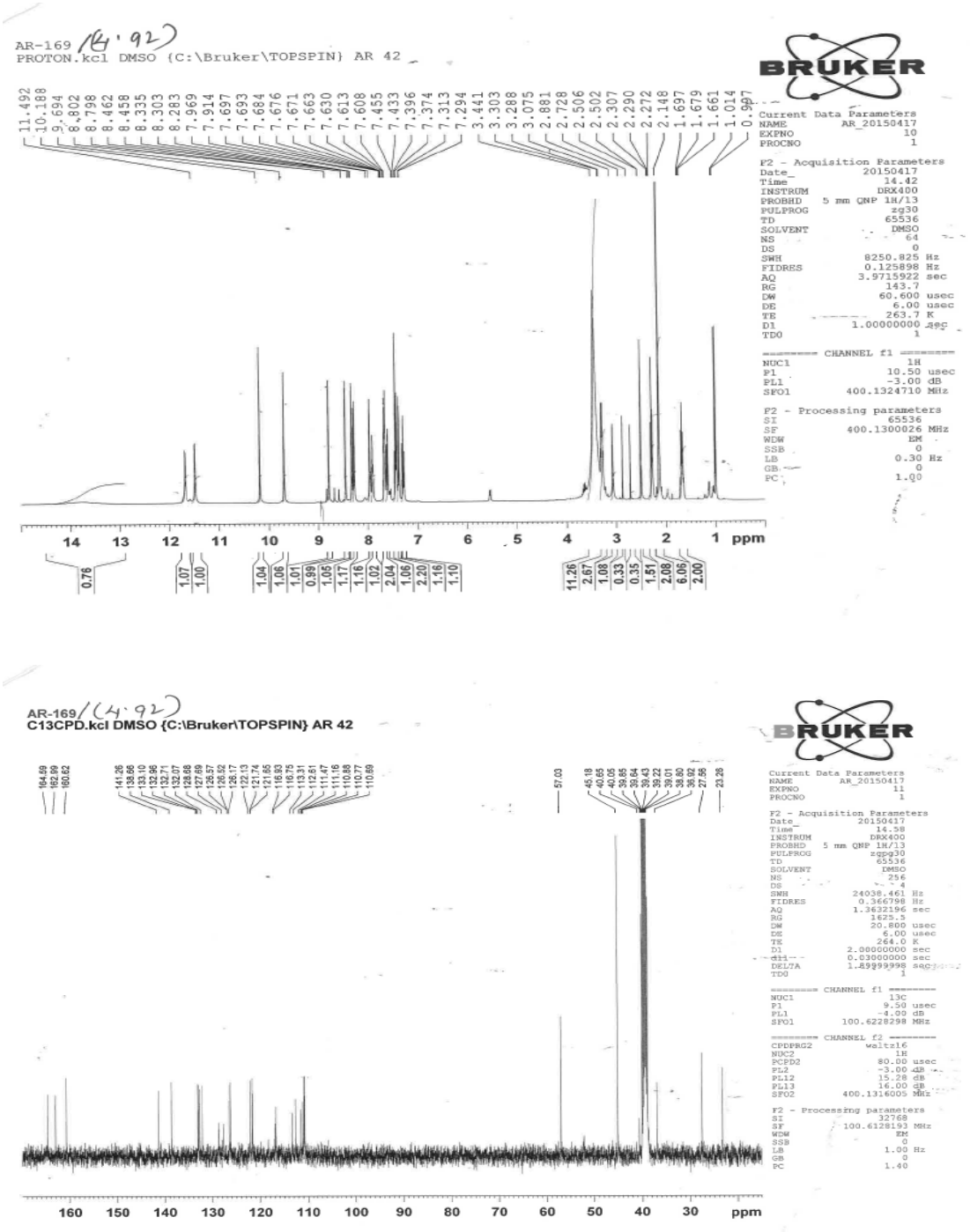

Figure 4.9: ^{1}H and ^{13}C NMR spectroscopic data of compound **4.92** as a representative of **library-4A** compounds

Table 4.92: Characterisation data for compound **4.92**

4.92 Light Yellow solid	^{1}H NMR	^{1}HNMR(400MHz,$(CD_3)_2SO$); $^{\delta}$H in ppm 13.89(s,1H), 11.82(s,1H), 11.49(s,1H), 10.18(s,1H), 9.69(s,1H), 8.80 (d,*J*=1.6,1H), 8.46(d,*J*=1.6,1H), 8.33(s,1H), 8.29(d,*J*=8.0,1H), 7.96(d,*J*=6.8,1H), 7.91(t,*J*=5.2,1H), 7.69-7.66(m,2H), 7.62(dd,*J*=8.8,2.0,1H), 7.45 (t,*J*=8.4,2H), 7.38(d,*J*=8.8,1H), 7.29(t,*J*=7.6,1H), 3.32-3.27(m,2H), 2.29 (t,*J*=6.8,2H), 2.14(s,6H), 1.69-166(m ,2H).
	^{13}C NMR	(100MHz,$(CD_3)_2SO$); $^{\delta}$C in ppm 164.5, 162.9, 160.6, 141.2, 138.6, 133.1, 132.9, 132.7, 132.0, 128.6, 127.6, 126.57, 126.52, 126.1, 122.1 121.7, 121.6, 116.9, 116.7, 113.3, 112.6, 111.4, 111.1, 110.8, 110.7, 110.6, 57.0, 45.1, 39.4, 27.5, 23.2.
	EIMS	Found 563.20 $[M+H]^+$,calculated for $C_{31}H_{30}N_8O_3$, 562.2441 [M]
	HRMS	*m/z* (+EI) Calc. for $C_{31}H_{30}N_8O_3$, 562.2441 $[M]^+$, found 563.2498 $[M+H]^+$.
	IR	(FTIR), V_{max}/'cm^{-1}): 3216, 2970, 2815, 1656, 1622, 1551, 1536, 1470, 1448, 1436, 1343, 1305, 1253, 1234, 1209, 1159, 1122, 1111, 1049, 1023, 1000, 907, 880, 818.

4.93 Synthesis of N-(3-(dimethylamino)propyl)-5-(5-(5-nitro-1H-indole-3-carboxamido)-1H-indole-3-carboxamido)-1H-indole-3-carboxamide (4.93).

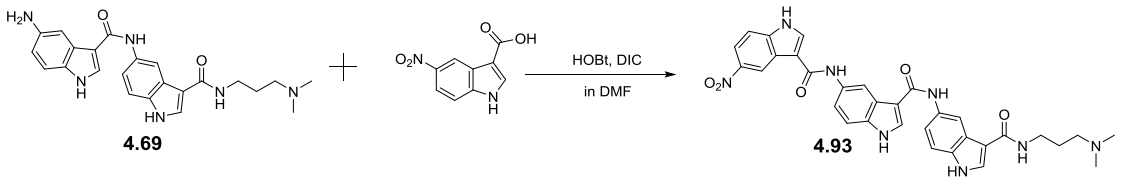

Initially, 30 mg of 5-nitro-1H-indole-3-carboxylic acid (0.143 mmol, 1.2 eq.) was dissolved in 10 mL of DMF in a round bottom flask fitted with a magnetic stirrer. Then 39 µl of DIC (0.250 mmol, 1.75 eq.) and HOBt (39 mg, 0.286 mmol, 2.0 eq.) were added to the acid (1.0 eq.) and this mixture was allowed to stir at room temperature for 30 minutes to ensure the formation of ester from the acid. Then 50 mg of amine **4.69** (0.119 mmol, 1 eq.) was added to the mixture and this mixture was allowed to stir for 6 hours at which point TLC and LCMS analysis showed the completion of reaction. Finally the reaction mixture was applied to a conditioned Isolute^{TM} SCX-2 cartridge and the product was purified by 'Catch and Release' method **(**described in the section **'Method and Materials'** of chapter 3**)**. A yellow solid was obtained after drying in vacuum. Yield=14mg, 20%.

Table 4.93: Characterisation data for compound **4.93**

4.93 Yellow solid	^{1}H NMR	^{1}HNMR(400MHz,$(CD_3)_2SO$); $^{\delta}$H in ppm 12.47(s,1H), 11.66(s,1H), 11.48(s,1H), 9.98(s,1H), 9.69(s,1H), 9.20 (s,1H), 8.59(d,*J*=14.4,2H), 8.50(s,1H), 8.33(t,*J*=3.6,2H), 8.09(dd,*J*=8.8,2.0,1H), 7.96(d,*J*=5.6,1H), 7.74(dd,*J*=8.8,1.6,1H), 7.69-7.63(m,2H), 7.44(d,*J*=8.8,1H), 7.37 (d,*J*=8.8,1H), 3.29(d,*J*=6,2H), 2.89(s,2H), 2.31 (s,6H), 1.74(d,*J*=6.0, 2H).
	^{13}C NMR	(100MHz,$(CD_3)_2SO$); $^{\delta}$C in ppm 164.8, 163.0, 162.3, 162.0, 158.4, 141.8, 140.4, 139.2, 138.8, 132.9, 132.6, 131.6, 127.8, 126.6, 126.1, 125.9, 120.0, 118.0, 116.7, 112.7, 112.65, 112.60, 110.7, 110.5, 561, 43.9, 39.1, 38.9, 38.7, 35.7, 30.7, 26.4.
	EIMS	Found $[M+H]^+$ 607.0, Calculated for $C_{32}H_{30}N_8O_5$, 606.23 $[M]^+$
	HRMS	*m/z* (+EI) Calc. for $C_{32}H_{30}N_8O_5$, 606.2339 $[M]^+$, found 607.2402 $[M+H]^+$.
	IR	(FTIR), V_{max}/'cm^{-1}): 3266, 2939, 2219, 1705, 1631, 1533, 1475, 1437, 1361, 1331, 1308, 1220, 1159, 1097, 1039, 945, 886, 807, 770, 741, 715, 619.

4.94 Synthesis of 5-nitro-N-(3-(piperidin-1-yl) propyl)-1H-indole-3-carboxamide (4.94).

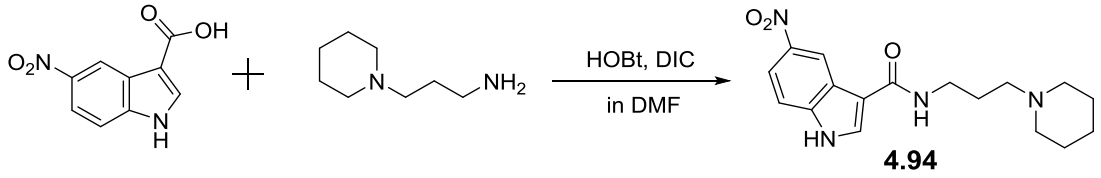

4.94

Initially, 200 mg of 5-nitro-1H-indole-3-carboxylic acid (0.970 mmol, 1.2 eq.) was dissolved in 10 mL of DMF in a round bottom flask fitted with a magnetic stirrer. Then 262.43 µl of DIC (1.69 mmol, 1.75 eq.) and HOBt (262 mg, 1.94 mmol, 2.0 eq.) were added to the acid (1.0 eq.) and this mixture was allowed to stir at room temperature for 30 minutes to ensure the formation of ester from the acid. Then 115.55 mg of 3-(piperidin-1-yl)propan-1-amine (0.809 mmol, 1 eq.) was added and the mixture was allowed to stir for 16 hours at which point TLC and LCMS analysis showed the completion of reaction. Finally the reaction mixture was applied to a conditioned Isolute^{TM} SCX-2 cartridge and the product was purified by 'Catch and Release' method. A yellow solid was obtained after drying in vacuum. Yield=165 mg, 52%.

Table 4.94: Characterisation data for compound **4.94**

4.94 Yellow solid	^{1}H NMR	^{1}HNMR(400MHz,$(CD_3)_2SO$); $^\delta$H in ppm 9.09 (s,1H), 8.38(s,1H), 8.22(t,*J*=5.6,1H), 8.05(dd,*J*=9.2,2.4,1H), 7.63(d,*J*=9.2,1H),3.32-3.27(m,2H),2.52-2.50(m,2H),2.37(t,*J*=6.4,4H),1.71(t,*J*=7.2,2H),1.53-1.48 (m,4H),1.38(d,*J*=4.4, 2H).
	EIMS	Found 331.10 $[M+H]^+$, calculated for $C_{17}H_{22}N_4O_3$, 330.16 $[M]^+$

4.95 Synthesis of 5-amino-N-(3-(piperidin-1-yl) propyl)-1H-indole-3-carboxamide (4.95).

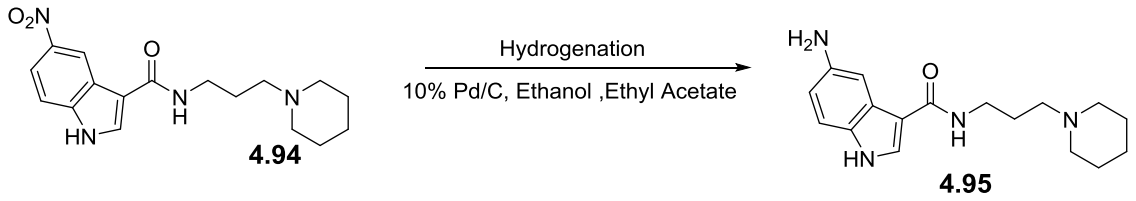

164 mg of **4.94** was dissolved in 20 mL of ethanol and added to a hydrogenation reaction bottle. 20 mg of 10% Pd (palladium on activated carbon) was added into the reaction vessel and it was mixed well. The reaction bottle was sealed and connected to a hydrogen reservoir. Air from the reaction bottle was removed by applying vacuum and it was then flushed with hydrogen. Typically, a hydrogen pressure of approximately 40 psi was applied from the reservoir, and the bottle was then shaken vigorously to initiate the reaction. Progress of the reaction was monitored by TLC and LCMS. The shaker was stopped and the bottle was vented after 5 hours at which point TLC and LCMS analysis showed the completion of reaction. The product was recovered by means of filtration using Celite. Lastly the product is concentrated by using a rotary evaporator. A yellow solid was obtained after drying in vacuum. Yield=145 mg, 97%.

Table 4.95: Characterisation data for compound **4.95**

4.95 Yellow solid	^{1}H NMR	^{1}HNMR(400MHz,$(CD_3)_2SO$); $^\delta$H in ppm 7.96(s,1H), 7.77(s,1H), 7.50(t,*J*=1.6,1H), 7.22(dd,*J*=5.6,0.8,1H), 6.75(dd,*J*=6.4,2.0,1H), 3.41-3.32(m,2H), 2.95(s,2H), 2.42-2.38(m,4H), 1.83-1.80 (m,2H), 1.611.55 (m,4H), 1.44(d,*J*=4.4, 2H).
	EIMS	Found 291.13 $[M+H]^+$, $C_{13}H_{17}N_5O_3$, 290.20 $[M]^+$

4.96 Synthesis of N-(3-(dimethylamino) propyl)-5-(5-nitro-1H-indole-3-carboxamido)-1H-indole-3-carboxamide (4.96).

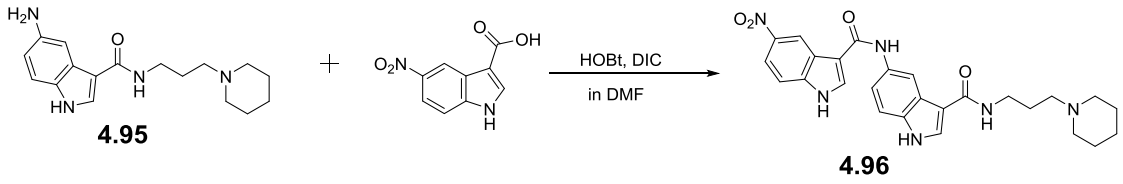

4.95 4.96

Initially, 117 mg of 5-nitro-1H-indole-3-carboxylic acid (0.568 mmol, 1.2 eq.) was dissolved in 10 mL of DMF in a round bottom flask fitted with a magnetic stirrer. Then 153 µl of DIC (0.994 mmol, 1.75 eq.) and HOBt (153 mg, 1.136 mmol, 2.0 eq.) were added to the acid (1.0 eq.) and this mixture was stirred at room temperature for 30 minutes to ensure the formation of ester from the acid. Then 142 mg of amine **4.95** (0.473 mmol, 1 eq.) was added and the mixture was allowed to stir for 8 hours at which point TLC and LCMS analysis showed the completion of reaction. Finally the reaction mixture was applied to a conditioned Isolute^{TM} SCX-2 cartridge and the product was purified by 'Catch and Release' method **(**described in the section **'Method and Materials'** of chapter 3**)**. A cream solid was obtained after drying in vacuum. Yield=136 mg, 59%.

Table 4.96: Characterisation data for compound **4.96**

4.96 Cream solid	^{1}H NMR	^{1}HNMR(400MHz,$(CD_3)_2SO$); $^\delta$H in ppm 12.35(s,1H), 11.48(s,1H), 9.95(s,1H), 9.18(d,*J*=3.6,1H), 8.58 (s,1H), 8.13-8.10(m,1H), 8.08(t,*J*=4.8,1H), 7.91-7.90(m,1H), 7.78-7.64 (m,2H), 7.24(d,*J*=8.4,1H), 3.37(s,2H), 3.30-3.25(m,2H), 2.51-2.49(m,4H), 1.72-1.65 (m,2H), 1.511.46 (m,4H), 1.37(d,*J*=4.8, 2H).
	EIMS	Found 301.20 $[M+H]^+$, $C_{17}H_{24}N_4O$, 300.19 $[M]^+$

4.97 Synthesis of 5-amino-N-(3-((3-(dimethylamino) propyl) carbamoyl)-1H-indol-5-yl)-1H-indole-3-carboxamide (4.97).

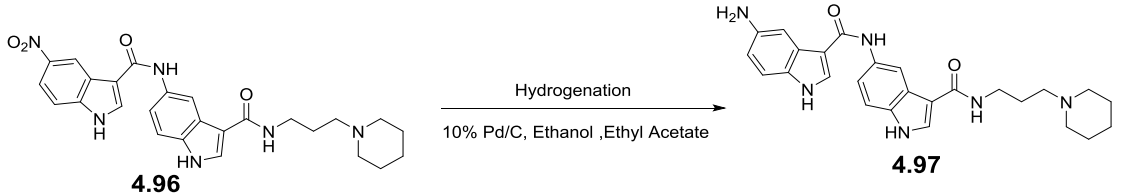

4.96 4.97

145 mg of **4.96** was dissolved in 20 mL of ethanol and1 mL of ethyl acetate was added to a hydrogenation reaction bottle. 20 mg of 10% Pd (palladium on activated carbon) was added into the reaction vessel, and mixed well. The reaction bottle was sealed and connected to a hydrogen reservoir. Air from the

reaction bottle was removed by applying vacuum, and was then by flushed with hydrogen. Typically, a hydrogen pressure of approximately 40 psi was applied from the reservoir, and the bottle was then shaken vigorously to initiate the reaction. Progress of the reaction was monitored by TLC and LCMS. The shaker was stopped and the bottle was vented after 5 hours at which point TLC and LCMS analysis showed the completion of reaction. The product was recovered by means of filtration using Celite. Finally, the product is concentrated by using a rotary evaporator. A deep brown solid was obtained after drying in vacuum. Yield=125 mg, 92%.

Table 4.97: Characterisation data for compound **4.97**

4.97 Deep Brown solid	^{1}H NMR	^{1}HNMR(400MHz,$(CD_3)_2SO$); $^\delta$H in ppm 8.59(s,1H), 8.27(d,*J*=1.6,1H), 8.01(s,1H), 7.97 (s,2H), 7.88(s,1H), 7.62(d,*J*=1.6,1H), 7.49(dd,*J*=7.2,2.0,1H), 7.42 (d,*J*=8.4,1H), 7.25(d,*J*=8.8,1H), 6.78(dd,*J*=8.4,2.0,1H), 3.67-3.41(m,2H), 3.33-3.32(m,2H), 2.57-2.53(m,4H), 1.87(t,*J*=7.6,2H), 1.63-1.58 (m,4H), 1.44-1.39 (m,2H), 1.30(t, *J*=4.8,2H).
	EIMS	Found 459.20 $[M+H]^+$, calculated for $C_{26}H_{30}N_6O_2$, 458.24 $[M]^+$

4.98 Synthesis of 5-nitro-N-(3-((3-((3-(piperidin-1-yl) propyl) carbamoyl)-1H-indol-5-yl) carbamoyl)-1H-indol-5-yl)-1H-indole-3-carboxamide (4.98).

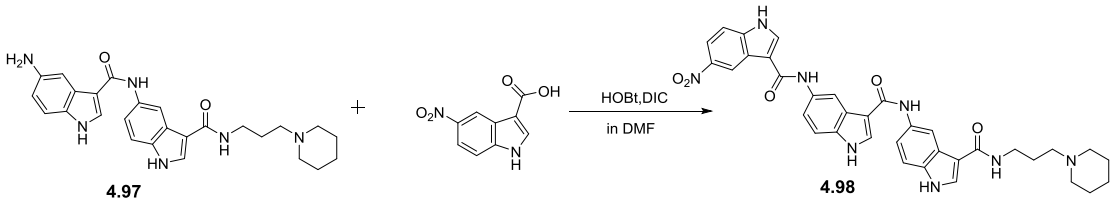

Initially, 36 mg of 5-nitro-1H-indole-3-carboxylic acid (0.175 mmol, 1.2 eq.) was dissolved in 10 mL of DMF in a round bottom flask fitted with a magnetic stirrer. Then 48 µl of DIC (0.307 mmol, 1.75 eq.) and HOBt (48 mg, 0.351 mmol, 2.0 eq.) were added to the acid (1.0 eq.) and this mixture was allowed to stir at room temperature for 30 minutes to ensure the formation of ester from the acid. Then 67 mg of amine **4.97**(0.146 mmol, 1 eq.) was added and the mixture was allowed to stir for 6 hours at which point TLC and LCMS analysis showed the completion of reaction. Finally the reaction mixture was separated by using a conditioned Isolute^{TM} SCX-2 cartridge and the product was purified by 'Catch and Release' method **(**described in the section **'Method and Materials'** of chapter 3**)**. A yellow solid was obtained after drying in vacuum. Yield=16.5 mg, 17%.

Table 4.98: Characterisation data for compound **4.98**

4.98 Yellow solid	^{1}H NMR	^{1}HNMR(400MHz,$(CD_3)_2SO$); $^{\delta}$H in ppm 12.42(s,1H),11.65(d,*J*=2.4,1H),11.47(d,*J*=2.0,1H),9.97(s,1H),9.69 (s,1H), 9.19 (d,*J*=2.4,1H), 8.59(t,*J*=6.8,2H), 8.51(d,*J*=2.0,1H), 8.32(d,*J*=3.2,2H),8.09(dd,*J*=8.8,2.4,1H),7.96(d,*J*=2.8,1H),7.71(dd, *J*=8.8,2.0,1H),7.69(s,1H),7.63(dd,*J*=8.8,2.0,1H),7.43(d,*J*=8.8,1H), 7.37(d,*J*=8.8,1H),3.313.26(m,2H),2.54(d,*J*=6.8,4H),1.75(t,*J*=7.2,2 H), 1.55 (t,*J*=5.2,4H), 1.39(s, 2H).
	^{13}C NMR	(100MHz,$(CD_3)_2SO$); $^{\delta}$C in ppm 164.7, 164.2, 162.9, 162.2, 162.0, 145.7, 141.8, 139.9, 139.3, 134.1,133.0, 132.9, 132.7, 132.6, 132.1, 131.6, 128.9, 126.8, 126.6, 126.1, 125.9, 125.8, 118.0, 117.3, 112.7, 111.1, 110.7, 110.5, 107.2, 55.7, 53.4, 39.2, 35.7,30.7, 24.6.
	EIMS	Found 647.40 $[M+H]^+$, calculated for $C_{35}H_{34}N_8O_5$, 646.26 $[M]^+$
	HRMS	*m/z*(+EI)Calc.for$C_{35}H_{34}N_8O_5$, 646.2652 $[M]^+$,found 647.2709 $[M+H]^+$.
	IR	(FTIR), V_{max}/'cm^{-1}): 3200, 2976, 1739, 1595, 1530, 1470, 1434, 1379, 1330, 1210, 1157, 1078, 945, 867, 790, 796, 733.

4.99 Synthesis of 1-methyl-N-(3-((3-((3-(piperidin-1-yl) propyl) carbamoyl)-1H-indol-5-yl) carbamoyl)-1H-indol-5-yl)-1H-indole-3-carboxamide (4.99).

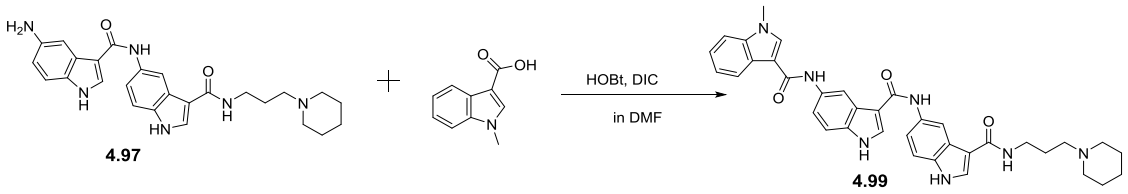

4.97 4.99

Initially, 29 mg of 1-methyl-1H-indole-3-carboxylic acid (0.135 mmol, 1.2 eq.) was dissolved in 10 mL of DMF in a round bottom flask fitted with a magnetic stirrer. Then 44 µl of DIC (0.2835 mmol, 1.75 eq.) and HOBt (44 mg, 0.324 mmol, 2.0 eq.) were added to the acid (1.0 eq.) and this mixture was allowed to stir at room temperature for 30 minutes to ensure the formation of ester from the acid. Then 62 mg of amine **4.97** (0.135 mmol, 1 eq.) was added and the mixture was allowed to stir for 6 hours at which point TLC and LCMS analysis showed the completion of reaction. Finally the reaction mixture was applied to a conditioned Isolute^{TM} SCX-2 cartridge and the product was purified by 'Catch and Release' method **(**described in the section **'Method and Materials'** of chapter 3**)**. A deep brown solid was obtained after drying in vacuum. Yield=15 mg, 18 %.

Table 4.99: Characterisation data for compound **4.99**

4.99 Deep Brown solid	^{1}H NMR	^{1}HNMR(400MHz,$(CD_3)_2SO$); $^{\delta}$H in ppm 11.61(s,1H),11.46(s,1H),9.72(s,1H),9.67(s,1H),8.56(d,*J*=1.6,1H), 8.48(d,*J*=1.6,1H),8.33-8.29(m,2H), 8.26(d,*J*=8.0,1H), 7.96(s,2H), 7.91(d,*J*-5.6,1H),7.70(dd,*J*=8.8,2.0,1H), 7.64(dd,*J*=8.8,2.0,1H),7.53(d,*J*=8.0,1H),7.41(d,*J*=8.8,2H),7.37(d,*J* =5.6,1H),7.25(t,*J*=6.8,1H),7.21(d,*J*=10.0,1),3.88(s,2H),3.31-3.26(m,2H),2.42(t,*J*=6.8,2H), 2.42(s,4H), 1.75-1.68 (m,2H), 1.53-1.38 (m,4H), 1.38(s, 2H).
	^{13}C NMR	(100MHz,$(CD_3)_2SO$); $^{\delta}$C in ppm 164.8, 164.6, 163.0, 162.6, 162.2, 147.2, 142.2, 136.7, 133.2, 133.0, 132.7, 132.6, 132.1, 126.9, 126.6, 126.1, 122.0, 121.3, 120.7, 116.5, 112.5, 110.66, 110.62, 109.8, 56.1, 53.7, 40.0, 39.4, 39.0, 38.8, 35.7, 33.0, 30.7, 26.4, 25.1, 23.7.
	EIMS	Found 616.40 $[M+H]^+$, Calc. for $C_{36}H_{37}N_7O_3$, 615.29 $[M]^+$
	HRMS	*m/z*(+EI)Calc.for$C_{36}H_{37}N_7O_3$, 615.2958 $[M]^+$,found 616.3023 $[M+H]^+$
	IR	(FTIR), V_{max}/'cm^{-1}): 3244, 2971, 1738, 1618, 1534, 1466, 1433, 1368, 1306, 1265, 1234, 1200, 1128, 1102, 1037, 946, 869, 800, 770, 746, 719, 660.

4.100 Synthesis of 5-nitro-N-(3-(pyrrolidin-1-yl) propyl)-1H-indole-3-carboxamide (4.100).

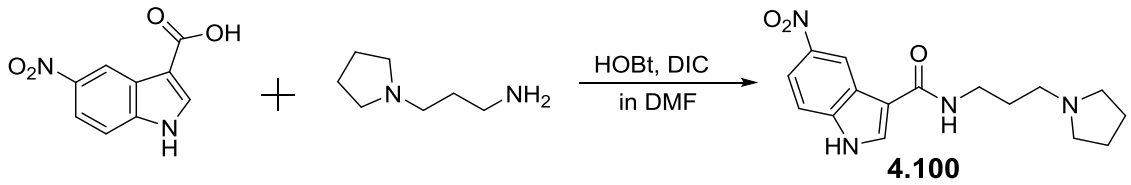

4.100

Initially, 150 mg of 5-nitro-1H-indole-3-carboxylic acid (0.728 mmol, 1.2 eq.) was dissolved in 10 mL of DMF in a round bottom flask fitted with a magnetic stirrer. Then 196 µl of DIC (1.27 mmol, 1.75 eq.) and HOBt (196 mg, 1.4 mmol, 2.0 eq.) were added to the acid (1.0 eq.) and this mixture was allowed to stir at room temperature for 30 minutes to ensure the formation of ester from the acid. Then 3-(pyrrolidin-1-yl) propan-1-amine (77 mg, 0.604 mmol, 1 eq.) was added and the mixture was allowed to stir for 8 hours at which point TLC and LCMS analysis showed the completion of reaction. Finally the reaction mixture was applied to a conditioned Isolute^{TM} SCX-2 cartridge and the product was purified by 'Catch and Release' method **(**described in the section **'Method and Materials'** of chapter 3**)**. A cream solid was obtained after drying in vacuum. Yield=160mg, 69%.

Table 4.100: Characterisation data for compound **4.100**

4.100 Cream solid	^{1}H NMR	^{1}HNMR(400MHz,$(CD_3)_2SO$); $^\delta$H in ppm 12.24(s,1H),9.09(d,*J*=3.6,1H), 8.23 (t,*J*=5.6,2H), 8.05(dd,*J*=9.2,2.4,1H), 7.63(d,*J*=8.8,1H), 3.34-3.29(m,2H), 2.56(s,2H), 2.45 (s,4H), 1.73 (t,*J*=7.2,2H), 1.65(s, 4H).
	EIMS	Found 317.10 $[M+H]^+$, Calc. for $C_{16}H_{20}N_4O_3$, 316.15 $[M]^+$

4.101 Synthesis of 5-amino-N-(3-(pyrrolidin-1-yl) propyl)-1H-indole-3-carboxamide (4.101).

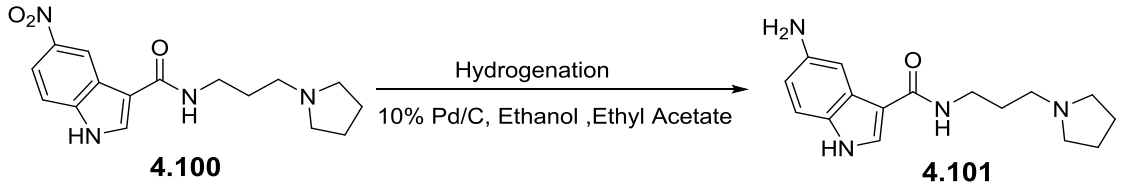

4.100 **4.101**

148 mg of **4.100** was dissolved in 20 mL of ethanol and added to a hydrogenation reaction bottle. 20 mg of 10% Pd (palladium on activated carbon) was added into the reaction vessel and it was mixed well. The reaction bottle was sealed and connected to a hydrogen reservoir. Air within the reaction bottle was removed under high vacuum and it was then flushed with hydrogen. Typically, a hydrogen pressure of approximately 40 psi was applied from the reservoir and the bottle was then shaken vigorously to initiate the reaction. Progress of the reaction was monitored by TLC and LCMS. The shaker was stopped and the bottle was vented on completion of the reaction after 4 hours at which point TLC and LCMS analysis showed the completion of reaction. Finally the product was recovered by means of filtration using Celite. Finally, the product is concentrated by using a rotary evaporator. A yellow solid was obtained after drying in vacuum. Yield=127 mg, 95%.

Table 4.101: Characterisation data for compound **4.101**

4.101 Yellow solid	^{1}H NMR	^{1}HNMR(400MHz,$(CD_3)_2SO$); $^\delta$H in ppm 11.30(s,1H), 7.87-7.82(m,2H), 7.37 (s,1H), 7.12(d,*J*=3.6,1H), 6.60(t,*J*=6.4,1H), 3.31-3.27(m,2H), 2.87(s,2H),2.73(s,2H), 2.57-2.52(m,4H), 1.76-1.71 (m,4H).
	EIMS	Found 287.00$[M+H]^+$, Calc. for $C_{16}H_{22}N_4O$, 286.17 $[M]^+$

4.102 Synthesis N-(3-(dimethylamino) propyl)-5-(5-nitro-1H-indole-3-carboxamido)-1H-indole-3-carboxamide (4.102).

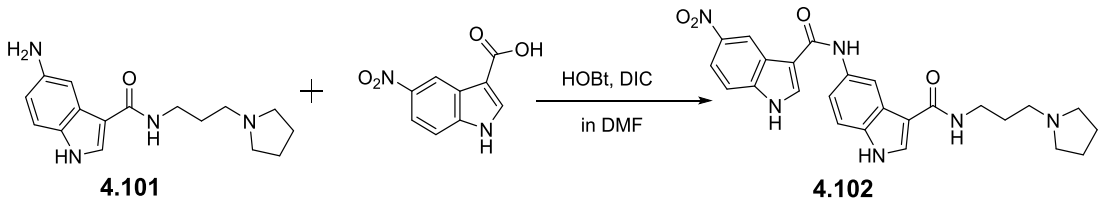

4.101 4.102

Initially, 109 mg of 5-nitro-1H-indole-3-carboxylic acid (0.528 mmol, 1.2 eq.) was dissolved in 10 mL of DMF in a round bottom flask fitted with a magnetic stirrer. Then 142 µl of DIC (0.24 mmol, 1.75 eq.) and HOBt (142 mg, 1.05 mmol, 2.0 eq.) were added to the acid (1.0 eq.) and this mixture was allowed to stir at room temperature for 30 minutes to ensure the formation of ester from the acid. Then 126 mg of amine **4.101**(0.440 mmol, 1 eq.) was added and the mixture was allowed to stir for 9 hours at which point TLC and LCMS analysis showed the completion of reaction. Finally the reaction mixture was separated by using a conditioned Isolute^{TM} SCX-2 cartridge and the product was purified by 'Catch and Release' method **(**described in the section **'Method and Materials'** of chapter 3**)**. A yellow solid was obtained after drying in vacuum. Yield=165 mg, 79%.

Table 4.102: Characterisation data for compound **4.102**

4.102 Yellow solid	^{1}H NMR	^{1}HNMR(400MHz,$(CD_3)_2SO$); $^\delta$H in ppm 11.56(s,1H), 9.98(s,1H), 9.21(s,1H), 8.62(s,1H), 8.50(s,1H), 8.17(s,1H), 8.00(d,*J*=3.6,1H), 7.96 (s,2H), 7.69(d,*J*=9.2,2H), 7.43(s,1H), 3.31(m,2H), 2.53-2.51(m,2H), 2.51 (s,4H), 1.71 (m,2H), 1.69(s, 4H).
	EIMS	Found 475.20 $[M+H]^+$, Calc. for $C_{25}H_{26}N_6O_4$, 474.20 $[M]^+$

4.103 Synthesis of 5-amino-N-(3-((3-(dimethylamino) propyl) carbamoyl)-1H-indol-5-yl)-1H-indole-3-carboxamide (4.103).

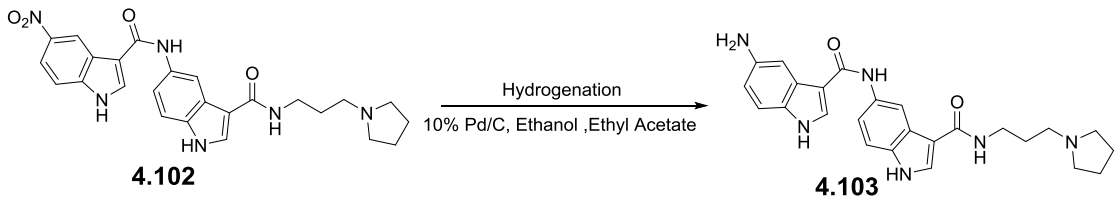

4.102 4.103

131 mg of **4.102** was dissolved in 20 mL of ethanol and 1 mL of ethyl acetate was added to a hydrogenation reaction bottle. 20 mg of 10% Pd (palladium on

activated carbon) was added into the reaction vessel and it was mixed well. The reaction bottle was sealed and connected to a hydrogen reservoir. Air from the reaction bottle was removed by applying vacuum and it was then flushed with hydrogen. Typically, a hydrogen pressure of approximately 40 psi was applied from the reservoir and the bottle was then shaken vigorously to initiate the reaction. Progress of the reaction was monitored by TLC and LCMS. The shaker was stopped and the bottle vented upon completion of the reaction after 6 hours at which point TLC and LCMS analysis showed the completion of reaction. The hydrogenated product was recovered by means of filtration using Celite. Finally, this product is concentrated by using a rotary evaporator. A deep brown solid was obtained after drying in vacuum. Yield=117mg, 95%.

Table 4.103: Characterisation data for compound **4.103**

4.103 Deep Brown solid	^{1}H NMR	^{1}HNMR(400MHz,$(CD_3)_2SO$); $^\delta$H in ppm 11.60(s,1H), 11.37(d,*J*=2.4,1H), 9.55(s,1H), 8.48(d,*J*=2.0,1H), 8.21-8.18(m,2H),8.07(d,*J*=2.8,1H),7.59(dd,*J*=8.8,2.0,1H), 7.48(d,*J*=2,1H),7.36(d,*J*=8.8,1H),7.16d,*J*=8.4,1H),6.59(d,*J*=2.4,1H) , 3.65(s,2H), 3.16(t,*J*=7.2,2H), 2.88(s, ,4H), 2.73 (s,4H), 2.51 (t,*J*=1.6,2H), 1.01(d, *J*=6.4,2H).
	EIMS	Found 445.30 $[M+H]^+$, Calc. for $C_{25}H_{28}N_6O_2$, 444.22 $[M]^+$

4.104 Synthesis of 5-nitro-N-(3-((3-((3-(pyrrolidin-1-yl) propyl) carbamoyl)-1H-indol-5-yl) carbamoyl)-1H-indol-5-yl)-1H-indole-3-carboxamide (4.104).

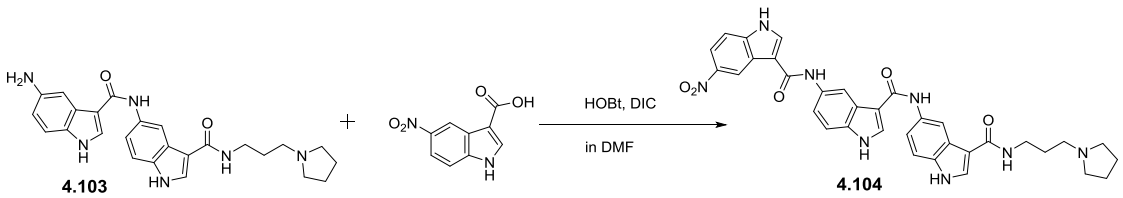

Initially, 34 mg of 5-nitro-1H-indole-3-carboxylic acid (0.162 mmol, 1.2 eq.) was dissolved in 10mL of DMF in a round bottom flask fitted with a magnetic stirrer. Then 44 µl of DIC (0.283 mmol, 1.75 eq.) and HOBt (44 mg, 0.324 mmol, 2.0 eq.) were added to the acid (1.0 eq.) and this mixture was stirred at room temperature for at least 30 minutes to ensure the formation of ester from the acid. Then 60 mg of amine **4.103** (0.136 mmol, 1 eq.) was added to the mixture and this mixture was allowed to stir for 8 hours at which point TLC and LCMS analysis showed the completion of reaction. Finally the reaction mixture was

separated by using a conditioned Isolute^{TM} SCX-2 cartridge and the product was purified by 'Catch and Release' method **(**described in the section **'Method and Materials'** of chapter 3**)**. A deep grey solid was obtained after drying in vacuum. Yield=18 mg, 21%.

Table 4.104: Characterisation data for compound **4.104**

4.104 Deep Grey solid	^{1}H NMR	^{1}HNMR(400MHz,$(CD_3)_2SO$); $^{\delta}$H in ppm 11.95(s,1H),11.67(s,1H),11.48(s,1H), 9.98(s,1H), 9.70(s,1H), 9.20(s,1H), 8.61(s,1H), 8.58(d,*J*=1.6,1H), 8.50(d,*J*=3.6,1H), 8.33(d,*J*=3.6,1H),8.09(dd,*J*=9.2,2.4,1H),7.95(s,3H),7.74(dd,*J*=8.8, 2.0,1H), 7.69-7.66(m,2H), 7.44(d,*J*=8.4,1H), 7.37(d,*J*=8.8,1H), 3.35(d,*J*=6.8,2H), 2.73(s, ,4H), 2.61 (s,2H), 1.72 (s,4H), 1.16(d, *J*=6,2H).
	^{13}C NMR	(100MHz,$(CD_3)_2SO$);$^{\delta}$C in ppm 164.7, 163.0, 162.3, 162.05, 162.0, 161.6, 156.1, 147.1, 141.8, 136.9, 132.98, 132.94, 132.68, 132.65, 128.5, 127.7, 126.6, 126.1, 125.9, 118.0, 117.3, 112.7, 111.2, 110.7, 110.6, 72.2, 53.3, 53.2, 39.2, 38.7, 35.7, 30.7, 28.1, 22.9.
	EIMS	Found 633.50 $[M+H]^+$, Calc. for $C_{34}H_{32}N_8O_5$, 632.24 $[M]^+$
	HRMS	*m/z* (+EI) Calc. for $C_{34}H_{32}N_8O_5$, 632.2496 $[M]^+$, found 633.2557 $[M+H]^+$.
	IR	(FTIR, V_{max}/'cm^{-1}): 3259, 2972, 2317, 1738, 1605, 1537, 1471, 1438, 1340, 1213, 1065, 865, 792, 771, 744, 682.

4.105 Synthesis of N-(3-morpholinopropyl)-5-nitro-1H-indole-3-carboxamide (4.105).

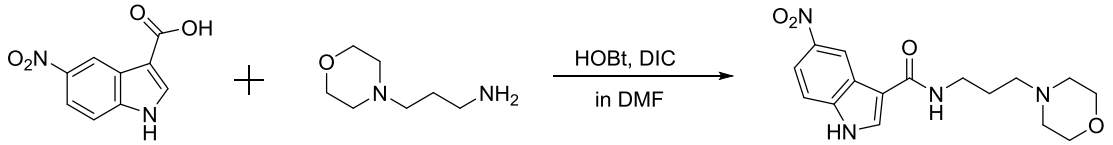

4.105

Initially, 150 mg of 5-nitro-1H-indole-3-carboxylic acid (0.728 mmol, 1.2 eq.) was dissolved in 10 mL of DMF in a round bottom flask placed in a magnetic stirrer. Then 196 µl of DIC (1.27 mmol, 1.75 eq.) and HOBt (196 mg, 1.4 mmol, 2.0 eq.) were added to the acid (1.0 eq.) and this mixture was allowed to stir at room temperature for 30 minutes to ensure the formation of ester from the acid. Then 87.36 mg of 3-morpholinopropan-1-amine (0.606 mmol, 1 eq.) was added and the mixture was allowed to stir for 7 hours at which point TLC and LCMS analysis showed the completion of reaction. Finally the reaction mixture was applied to a conditioned Isolute^{TM} SCX-2 cartridge and the product was purified by 'Catch and Release' method **(**described in the section **'Method and**

Materials' of chapter 3**)**. A yellow solid was obtained after drying in vacuum. Yield=169 mg, 70%.

Table 4.105: Characterisation data for compound **4.105**

4.105 Yellow solid	^{1}H NMR	^{1}HNMR(400MHz,$(CD_3)_2SO$); $^\delta$H in ppm 12.26(s,1H), 9.09(d,*J*=2.0,1H), 8.25(s,1H), 8.20 (t,*J*=5.6,1H), 8.05(dd,*J*=8.8,2.0,1H), 7.63(d,*J*=8.8,1H), 3.57(t,*J*=4.4,4H), 3.33-3.26(m,2H), 2.52-2.50(m,2H), 2.35 (t,*J*=6.8,4H), 1.73-1.66(m, 2H).
	EIMS	Found 333.20 $[M+H]^+$, Calc. for $C_{16}H_{20}N_4O_4$, 332.14 $[M]^+$

4.106 Synthesis of 5-amino-N-(3-morpholinopropyl)-1H-indole-3-carboxamide (4.106).

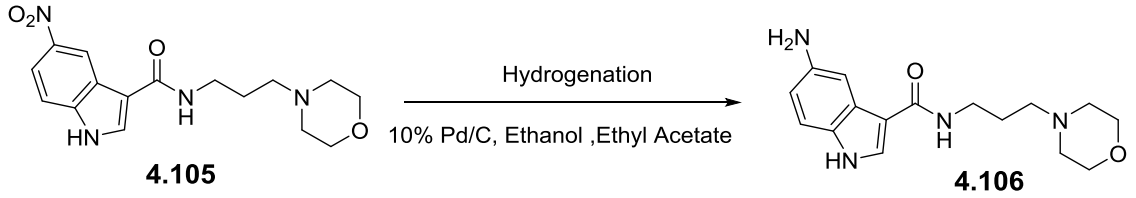

128 mg of **4.105** was dissolved in 20 mL of ethanol and added to a hydrogenation reaction bottle. 20 mg of 10% Pd (palladium on activated carbon) was added into the reaction vessel and it was mixed well. The reaction bottle was sealed and connected to a hydrogen reservoir. Air from the reaction bottle was removed by applying vacuum and it was then flushed with hydrogen. Typically, a hydrogen pressure of approximately 40 psi was applied from the reservoir and the bottle was then shaken vigorously to initiate the reaction. Progress of the reaction was monitored by TLC and LCMS. The shaker was stopped and vented on completion of the reaction after 7 hours at which point TLC and LCMS analysis showed the completion of reaction. The product was recovered by means of filtration using Celite. Finally, the product is concentrated by using a rotary evaporator. An orange solid was obtained after drying in vacuum. Yield=110 mg, 96%.

Table 4.106: Characterisation data for compound **4.106**

4.106 Orange solid	^{1}H NMR	^{1}HNMR(400MHz,$(CD_3)_2SO$); $^\delta$H in ppm 11.17(s,1H), 7.81(s,1H), 7.74(s,1H), 7.35 (s,1H), 7.10(d,*J*=8.4,1H), 6.55-6.53(m,1H), 3.79-3.70(m,2H), 3.56(s,4H), 3.293.19(m,2H), 2.50 (s,4H), 2.31 (t,*J*=6.8,2H), 1.70-1.63(m, 2H).
	EIMS	Found 303.20 $[M+H]^+$, Calc. for $C_{16}H_{22}N_4O_2$, 302.17 $[M]^+$

4.107 Synthesis of N-(3-(dimethylamino) propyl)-5-(5-nitro-1H-indole-3-carboxamido)-1H-indole-3-carboxamide (4.107).

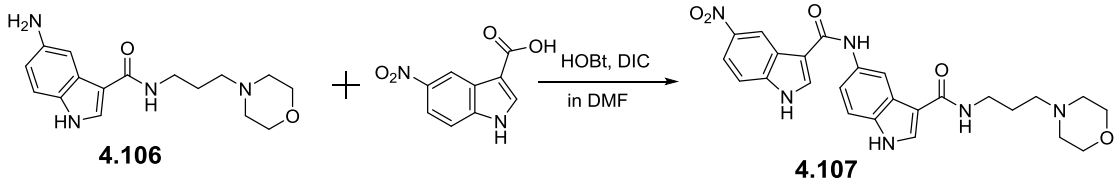

4.106 **4.107**

Initially, 82 mg of 5-nitro-1H-indole-3-carboxylic acid (0.397 mmol, 1.2 eq.) was dissolved in 10 mL of DMF in a round bottom flask fitted with a magnetic stirrer. Then 107 µl of DIC (0.694 mmol, 1.75 eq.) and HOBt (107 mg, 0.794 mmol, 2.0 eq.) were added to the acid (1.0 eq.) and this mixture was allowed to stir at room temperature for 30 minutes to ensure the formation of ester from the acid. Then 100 mg of amine **4.106**(0.331 mmol, 1 eq.) was added and the mixture was allowed to stir for 7 hours at which point TLC and LCMS analysis showed the completion of reaction. Finally the reaction mixture was applied to a conditioned Isolute^{TM} SCX-2 cartridge and the product was purified by 'Catch and Release' method **(**described in the section **'Method and Materials'** of chapter 3**)**. A yellow solid was obtained after drying in vacuum. Yield=94 mg, 58%.

Table 4.107: Characterisation data for compound **4.107**

4.107 Yellow solid	^{1}H NMR	^{1}HNMR(400MHz,$(CD_3)_2SO$); $^\delta$H in ppm 12.45(s,1H), 11.52(s,1H), 9.98(s,1H), 9.20(s,1H), 8.61(s,1H), 8.49(s,1H), 8.11(dd,*J*=9.2,2.4,1H), 8.01(s,1H), 7.96 (s,1H), 7.70-7.68(m,2H), 7.37(d,*J*=1.6,1H), 3.57(s,4H), 3.32(d,*J*=6.0,2H), 3.31 (d,*J*=6.0,2H), 2.38 (s,4H), 1.73(t, *J*=6.8,2H).
	EIMS	Found 491.20 $[M+H]^+$, Calc. for $C_{25}H_{26}N_6O_5$, 490.19 $[M]^+$

4.108 Synthesis of 5-amino-N-(3-((3-(dimethylamino) propyl) carbamoyl)-1H-indol-5-yl)-1H-indole-3-carboxamide (4.108).

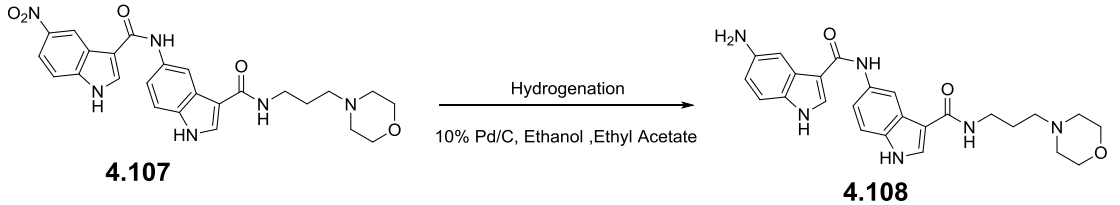

4.107 **4.108**

92 mg of **4.107** was dissolved in 20 mL of ethanol and 1 mL of ethyl acetate was added to a hydrogenation reaction bottle. 20 mg of 10% Pd (palladium on activated carbon) was added into the reaction vessel and mixed it well. The reaction bottle was sealed and connected to a hydrogen reservoir. Air from the reaction bottle was removed by applying vacuum and it was then flushed with hydrogen. Typically, a hydrogen pressure of approximately 40 psi was applied from the reservoir, and the bottle was then shaken vigorously to initiate the reaction. Progress of the reaction was monitored by TLC and LCMS. The shaker was stopped after 4.5 hours at which point TLC and LCMS analysis showed the completion of reaction.The bottle was vented and the product was recovered by means of filtration using Celite. Finally, the product is concentrated by using a rotary evaporator. A deep brown solid was obtained after drying in vacuum. Yield=81 mg, 94%.

Table 4.108: Characterisation data for compound **4.108**

4.108 Deep Brown solid	^{1}H NMR	^{1}HNMR(400MHz,$(CD_3)_2SO$); $^\delta$H in ppm, 11.47(s,1H), 11.27(s,1H), 8.44(s,1H), 8.13(d,*J*=2.8,1H), 8.00-7.95(m,2H),7.88(t,*J*=5.2,1H),7.60(dd,*J*=8.4,2.0,1H),7.46(d,*J*=2,1H), 7.33(d,*J*=8.4,1H), 7.12(d,*J*=8.4,1H), 6.55(dd,*J*=8.8,2.0,1H), 3.73(s,2H), 3.27(d,*J*=5.6,2H), 2.69(s,4H), 2.32(s ,2H), 1.69-1.64 (m,4H), 1.15-1.11 (m,2H).
	EIMS	Found 461.10 $[M+H]^+$, Calc. for $C_{25}H_{28}N_6O_3$, 460.22 $[M]^+$

4.109 Synthesis N-(3-morpholinopropyl)-5-(5-(5-nitro-1H-indole-3-carboxamido)-1H-indole-3-carboxamido)-1H-indole-3-carboxamide (4.109).

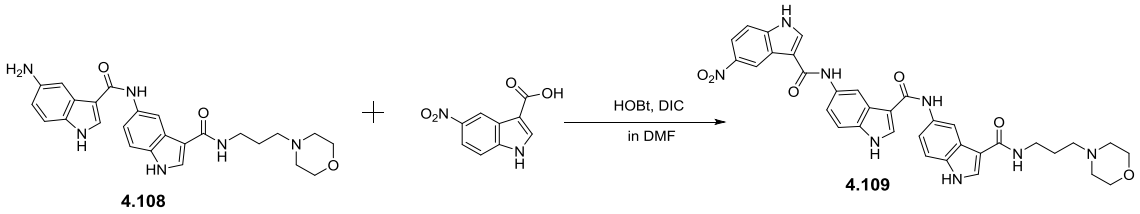

4.108 4.109

Initially, 31 mg of 5-nitro-1H-indole-3-carboxylic acid (0.148 mmol, 1.2 eq.) was dissolved in 10mL of DMF in a round bottom flask fitted with a magnetic stirrer. Then 40 µl of DIC (0.259 mmol, 1.75 eq.) and HOBt (40 mg, 0.297 mmol, 2.0 eq.) were added to the acid (1.0 eq.) and this mixture was allowed to stir at room temperature for 30 minutes to ensure the formation of ester from the acid. Then 57 mg of amine **4.108**(0.123 mmol, 1 eq.) was added to the same mixture

and it was stirred for 6 hours at which point TLC and LCMS analysis showed the completion of reaction. Finally the reaction mixture was separated by using a conditioned Isolute^{TM} SCX-2 cartridge and the product was purified by 'Catch and Release' method **(**described in the section **'Method and Materials'** of chapter 3**)**. An orange coloured solid was obtained after drying in vacuum. Yield=14 mg, 18%.

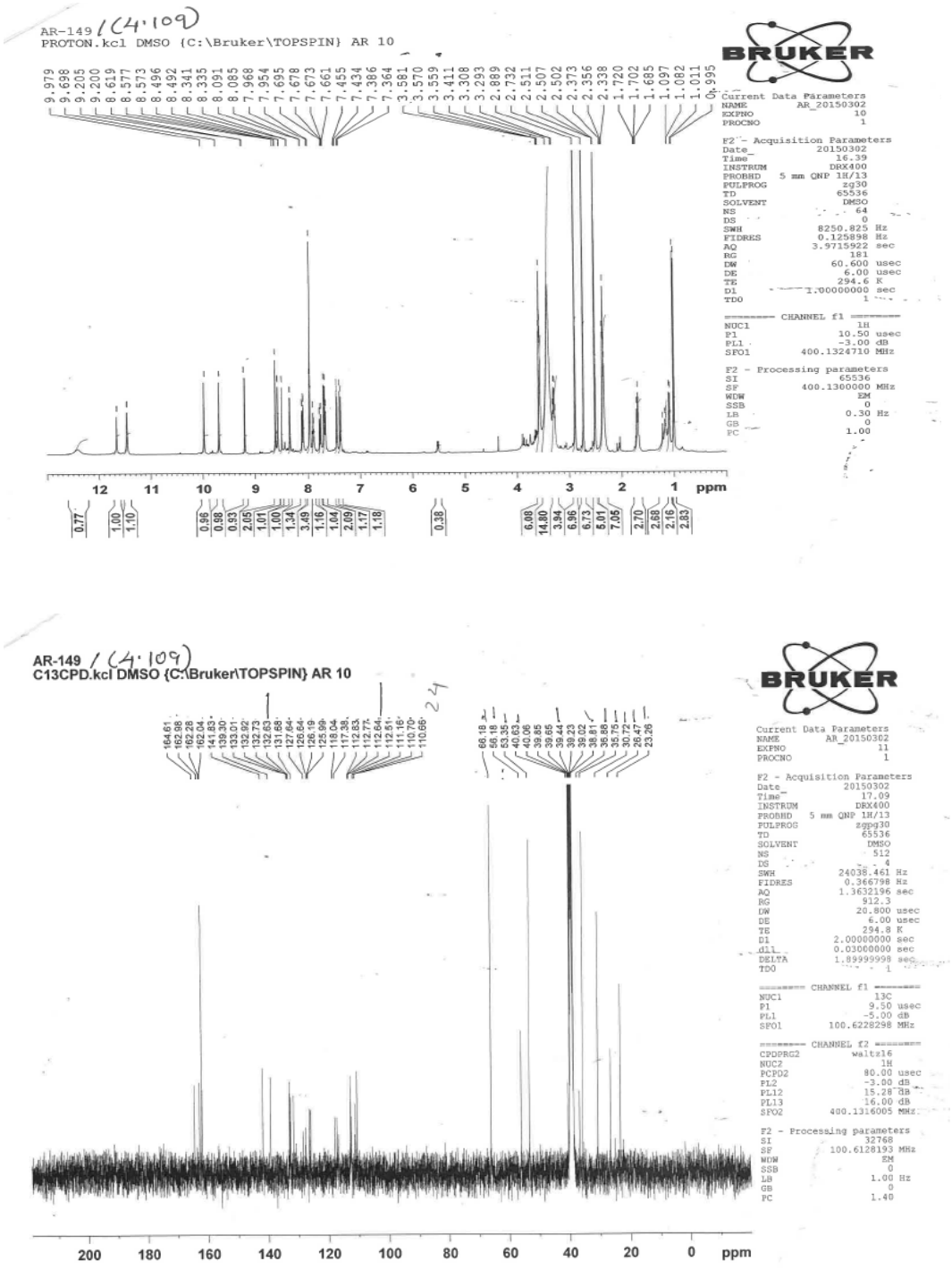

Figure 4.10: ^{1}H and ^{13}C NMR spectroscopic data of compound **4.109** as a representative of **library-4B** compounds

Table 4.109: Characterisation data for compound **4.109**

4.109 Orange solid	^{1}H NMR	^{1}HNMR(400MHz,$(CD_3)_2SO$); $^{\delta}$H in ppm 12.48(s,1H), 11.66(d,*J*=1.6,1H), 11.46(d,*J*=1.6,1H), 9.97(s,1H), 9.69(s,1H), 9.20(d,*J*=2.0,1H), 8.61(s,1H), 8.57(d,*J*=1.6,1H), 8.49(d,*J*=1.6,1H), 8.33(d,*J*=3.6,1H), 8.11(dd,*J*=8.8,2.4,1H), 7.96(s,1H), 7.88(d,*J*=6.0,1H), 7.76(dd,*J*=8.8,2.0,1H), 7.69-7.65(m,2H), 7.49(d,*J*=8.4,1H), 7.35(d,*J*=8.4,1H), 3.29(t,*J*=6.0,2H), 2.50(t, *J*=1.6,4H), 2.36 (t,*J*=6.8,4H), 1.70 (t,*J*=7.2,2H), 1.01(d, *J*=6.4,2H).
	^{13}C NMR	100MHz,$(CD_3)_2SO$); $^{\delta}$C in ppm 164.6, 162.9, 162.2, 162.0, 141.8, 139.3, 133.0, 132.9, 132.7, 132.6, 131.6, 127.6, 126.6, 126.1, 125.9, 118.0, 117.3, 112.8, 112.7, 112.6, 112.5, 111.1, 110.7, 110.6, 66.1, 56.1, 53.3, 40.6, 39.4, 36.8, 35.7, 30.7, 26.4, 23.3.
	EIMS	Found 649.20 $[M+H]^+$, Calculated for $C_{34}H_{32}N_8O_6$, 648.2445 $[M]^+$
	HRMS	*m/z* (+EI) Calc. for $C_{34}H_{32}N_8O_6$, 648.2445 $[M]^+$, found 649.2513 $[M+H]^+$.
	IR	(FTIR), V_{max}/'cm^{-1}): 3338, 2966, 1615, 1534, 1465, 1330, 1248, 1211, 1169, 1111, 1079, 1034, 863, 769, 747, 623, 585, 568, 557.

4.110 Synthesis of 5-amino-N-(3-((3-((3-(dimethylamino) propyl) carbamoyl)-1H-indol-5-yl) carbamoyl)-1H-indol-5-yl)-1H-indole-3-carboxamide (4.110).

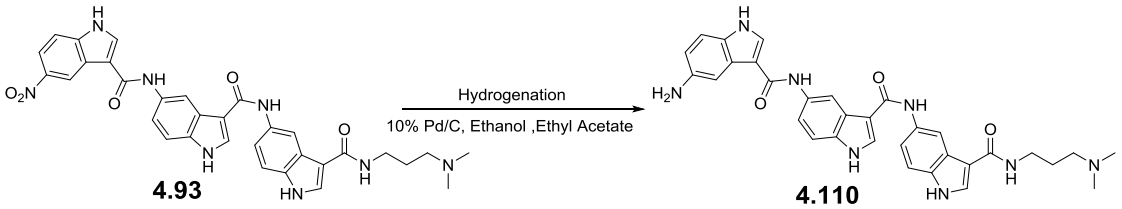

4.93 **4.110**

25 mg of **4.93** was dissolved in 20 mL of ethanol and 1 mL of ethyl acetate was added to a hydrogenation reaction bottle. 20 mg of 10% Pd (palladium on activated carbon) 20 was added into the reaction vessel. It was mixed well. The reaction bottle was sealed and connected to a hydrogen reservoir. Air from the reaction bottle was removed by applying vacuum, and was then by flushed with hydrogen. Typically, a hydrogen pressure of approximately 40 psi was applied from the reservoir. The bottle was then shaken vigorously to initiate the reaction. Progress of the reaction was monitored by TLC and LCMS. The shaker was stopped after 5.5 hours at which point TLC and LCMS analysis showed the completion of reaction. The bottle was then vented and the hydrogenated product was recovered by means of filtration using Celite. Finally,

the product is concentrated by using a rotary evaporator. A deep brown solid was obtained after drying in vacuum. Yield=14 mg, 61%.

Table 4.110: Characterisation data for compound **4.110**

4.110 Deep Brown solid	^{1}H NMR	^{1}HNMR(400MHz,$(CD_3)_2SO$); $^{\delta}$H in ppm 11.60(s,1H), 11.46(s,1H), 11.31(d,*J*=9.2,1H), 9.63(d,*J*=3.6,1H), 9.48(d,*J*=8.0,1H), 8.54(d,*J*=3.6,1H), 8.45(dd,*J*=6.41.6,,1H), 8.27(s,1H), 8.13(dd,*J*=7.2,2.4,1H), 7.92(s,1H), 7.87(t,*J*=5.2,1H), 7.67-7.63(m,2H), 7.45 (dd,*J*=2,1H), 7.35(t,*J*=8.8,2H), 7.15-7.09(m,1H), 6.57-6.50(m,1H), 3.63-3.52(m, ,2H), 2.25 (t,*J*=7.2,2H), 2.12 (s,4H), 1.64(t, *J*=6.8,2H).
	^{13}C NMR	($100MHz,(CD_3)_2SO$); $^{\delta}$C in ppm 164.4, 162.9, 159.7, 156.8, 156.3, 155.9, 154.7, 145.7, 144.6, 133.4, 132.9, 130.7, 129.6, 126.5, 126.1, 124.5, 119.6, 118.6, 115.2, 111.5, 111.1, 110.6, 107.8, 94.6, 66.2, 56.9, 45.1, 39.3, 39.1, 38.9, 38.7, 23.2,
	EIMS	Found 577.20 $[M+H]^+$, Calculated for $C_{32}H_{32}N_8O_3$, 576.2597 $[M]^+$
	HRMS	*m/z* (+EI) Calc. for $C_{32}H_{32}N_8O_3$, 576.2597 $[M]^+$, found 577.2668$[M+H]^+$.
	IR	(FTIR), V_{max}/'cm^{-1}): 3240, 2926, 1612, 1538, 1470, 1438, 1364, 1312, 1280, 1213, 1178, 1065, 1038, 991, 889, 792, 762, 745, 724, 677.

4.111 Synthesis of N-(3-(4-methylpiperazin-1-yl) propyl)-5-nitro-1H-indole-3-carboxamide (4.111).

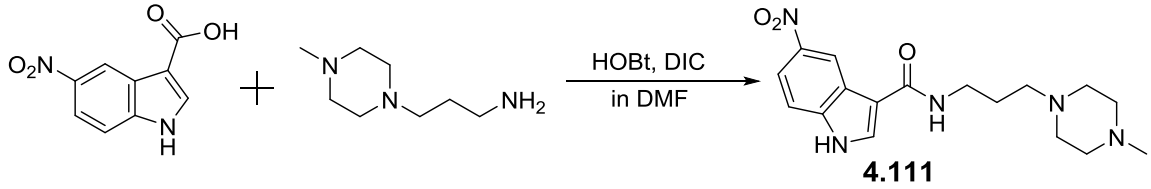

4.111

Initially, 250 mg of 5-nitro-1H-indole-3-carboxylic acid (1.207 mmol, 1.2 eq.) was dissolved in 10 mL of DMF in a round bottom flask fitted with a magnetic stirrer. Then DIC (324 µl, 2.10 mmol, 1.75 eq.) and HOBt (324 mg, 2.40 mmol, 2.0 eq.) were added to the acid (1.0 eq.) and this mixture was allowed to stir at room temperature for at least 20 minutes to ensure the formation of ester from the acid. Then 130 mg of 3-(4-methylpiperazin-1-yl) propan-1-amine (0.833 mmol, 1 eq.) was added and the mixture was allowed to stir for 8 hours at which point TLC and LCMS analysis showed the completion of reaction. Lastly the reaction mixture was separated by a conditioned Isolute^{TM} SCX-2 cartridge and the

product was purified by 'Catch and Release' method **(**described in the section **'Method and Materials'** of chapter 3**)**. A yellow solid was obtained after drying in vacuum. Yield=201 mg, 38%.

Table 4.111: Characterisation data for compound **4.111**

4.111 Yellow solid	^{1}H NMR	^{1}HNMR(400MHz,$(CD_3)_2SO$); $^\delta$H in ppm 12.26(s,1H), 9.07(d,*J*=2.4,1H), 8.23(s,1H), 8.17 (t,*J*=5.2,1H), 8.06-8.03(m,1H), 7.62(d,*J*=8.8,1H), 3.37(s,1H), 3.31-3.26(m,3H), 2.55 (s,2H), 2.33(t,*J*=6.8,8H), 1.71-1.64(m ,2H).
	EIMS	Found 346.10 $[M+H]^+$, Calculated for $C_{17}H_{23}N_5O_3$, 345.18 $[M]^+$

4.112 Synthesis of 5-amino-N-(3-(4-methylpiperazin-1-yl) propyl)-1H-indole-3-carboxamide (4.112).

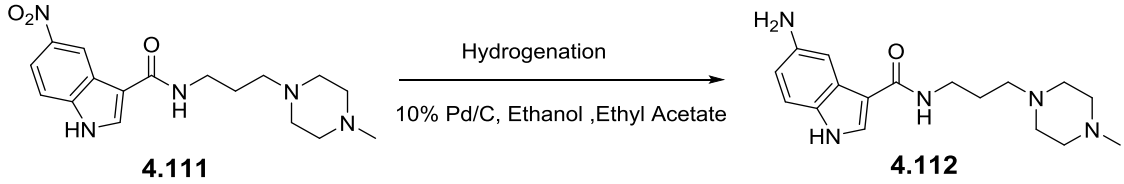

4.111 **4.112**

201 mg of **4.111** was dissolved in 20 mL of ethanol and added to a hydrogenation reaction bottle. 20 mg of 10% Pd (palladium on activated carbon) was added into the reaction vessel and it was mixed well. The sealed reaction bottle was connected to a hydrogen reservoir. Air within the reaction bottle was removed under vacuum and it was flushed with hydrogen. Approximately 40 psi of hydrogen pressure was applied from the reservoir and the bottle was then shaken vigorously to initiate the reaction. Progress of the reaction was monitored by TLC and LCMS and the shaker was stopped on completion of the reaction after 4 hours at which point TLC and LCMS analysis showed the completion of reaction. The bottle was vented and the product was recovered by using filtration using Celite. Finally the product is concentrated by using a rotary evaporator. An orange solid was obtained after drying in vacuum. Yield=176 mg, 95%.

Table 4.112: Characterisation data for compound **4.112**

4.112 Orange solid	^{1}H NMR	^{1}HNMR(400MHz,$(CD_3)_2SO$); $^\delta$H in ppm 11.22(s,1H), 7.58(s,1H), 7.38 (s,1H), 7.11 (d,*J*=8.4,1H), 6.54(d,*J*=8.8,1H), 3.94(s,2H), 3.26(d,*J*=6.0,2H), 2.50(s,1H), 2.13 (s,8H), 1.87(s,3H), 1.66(t,*J*=6.8,2H).
	EIMS	Found 316.10 $[M+H]^+$, Calculated for $C_{17}H_{25}N_5O$, 315.20 $[M]^+$

4.113 Synthesis of N-(3-(dimethylamino) propyl)-5-(5-nitro-1H-indole-3-carboxamido)-1H-indole-3-carboxamide (4.113).

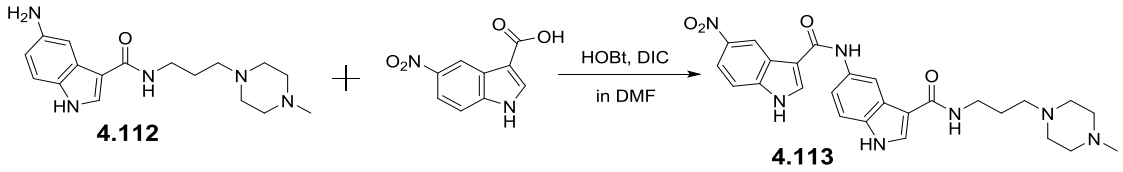

Initially, 144.9 mg of 5-nitro-1H-indole-3-carboxylic acid (0.70 mmol, 1.4 eq.) was dissolved in 15 mL of DMF in a round bottom flask fitted with a magnetic stirrer. Then 188.6 µl of DIC (1.22 mmol, 1.75 eq.) and HOBt (189 mg, 1.40 mmol, 2.0 eq.) were added to the acid (1.0 eq.). This mixture was allowed to stir at room temperature for 30 minutes to ensure the ester formation. Then 160 mg of amine **4.112** (0.50 mmol, 1 eq.) was added to the mixture and the mixture was allowed to stir for 6 hours at which point TLC and LCMS analysis showed the completion of reaction. Finally the reaction mixture was applied to a conditioned Isolute^{TM} SCX-2 cartridge and the product was purified by 'Catch and Release' method **(**described in the section **'Method and Materials'** of chapter 3**)**. A deep brown solid was obtained after drying in vacuum. Yield=135 mg, 58%.

Table 4.113: Characterisation data for compound **4.113**

4.113 Deep Brown solid	^{1}H NMR	^{1}HNMR(400MHz,$(CD_3)_2SO$); $^\delta$H in ppm 11.52(s,1H),9.97(s,1H),9.19(d,*J*=6.0,1H), 8.59(s,1H), 8.46(d,*J*=2.0,1H), 8.09(dd,*J*=9.2,2.4,1H), 7.98(s,1H), 7.94(s,1H), 9.92 (s,1H), 7.68-7.65(m,2H), 7.40(d,*J*=8.8,1H), 3.28(t,*J*=6.0,2H), 2.50(s,1H), 2.35-2.29 (m,8H), 2.11(s,3H), 1.68(t,*J*=7.2,2H).
	EIMS	Found 504.20 $[M+H]^+$, Calculated for $C_{26}H_{29}N_7O_4$, 503.22 $[M]^+$

4.114 Synthesis of 5-amino-N-(3-((3-(dimethylamino) propyl) carbamoyl)-1H-indol-5-yl)-1H-indole-3-carboxamide (4.114).

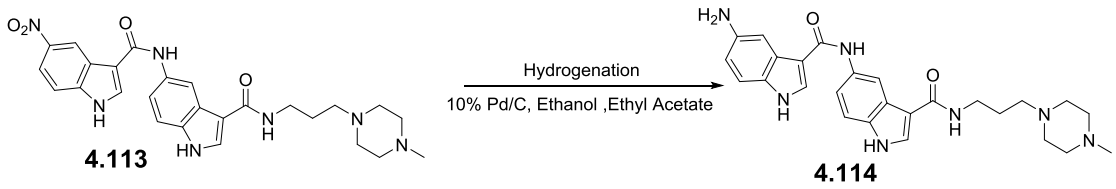

4.113 4.114

135 mg of **4.113** was dissolved in 20 mL of ethanol and 1 mL of ethyl acetate was added to a hydrogenation reaction bottle. 20 mg of 10% Pd (palladium on activated carbon) was added into the reaction vessel. This mixture was mixed well. The reaction bottle was sealed and connected to a hydrogen reservoir. Air from the reaction bottle was removed by applying vacuum and flushed with hydrogen. A hydrogen pressure of approximately 40 psi was applied from the reservoir and the bottle was then shaken vigorously to initiate the reaction. Progress of the reaction was monitored by TLC and LCMS analysis. The shaker was stopped after 6 hours at which point TLC and LCMS analysis showed the completion of reaction.The product was recovered by means of filtration using Celite. Finally, the product is concentrated by using a rotary evaporator. A deep brown solid was obtained after drying. Yield=107 mg, 84%.

Table 4.114: Characterisation data for compound **4.114**

4.114 Deep Brown solid	^{1}H NMR	^{1}HNMR(400MHz,$(CD_3)_2SO$); $^\delta$H in ppm 11.59(s,1H), 11.37(s,1H), 9.54(s,1H), 8.47(s,1H), 8.16(s,1H), 7.98(s,1H),7.93(t,*J*=5.6,1H),7.62(dd,*J*=8.8,1.6,1H),7.50(d,*J*=1.6,1H) , 7.37(d,*J*=8.8,1H), 7.16(d,*J*=8.8,1H), 6.60(dd,*J*=8.4,2.0,1H), 3.80(s,1H), 3.70-3.63(m,2H), 3.32-3.28(m,2H), 2.34 (t,*J*=6.8,8H), 2.12(s,3H), 1.72-1.65(m,2H).
	EIMS	Found 474.20 $[M+H]^+$, Calculated for $C_{26}H_{31}N_7O_2$, 473.25 $[M]^+$

4.115 Synthesis of N-(3-(4-methylpiperazin-1-yl)propyl)-5-(5-(5-nitro-1H-indole-3-carboxamido)-1H-indole-3-carboxamido)-1H-indole-3-carboxamide (4.115).

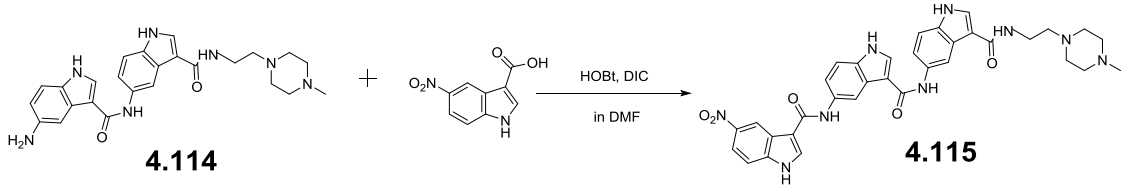

4.114 4.115

Initially, 45.5 mg of 5-nitro-1H-indole-3-carboxylic acid (0.221 mmol, 1.2 eq.) was dissolved in 10 mL of DMF in a round bottom flask placed at a magnetic stirrer. Then DIC (60 µl, 0.386 mmol, 1.75 eq.) and HOBt (60 mg, 0.442 mmol,

2.0 eq.) were added to the acid (1.0 eq.) and this mixture was allowed to stir at room temperature for 30 minutes to ensure the formation of ester from the acid. Then amine **4.114** (75 mg, 0.158m mol, 1 eq.) was added to the mixture and it was allowed to stir for 4 hours at which point TLC and LCMS analysis showed the completion of reaction. Lastly the reaction mixture was separated by using the conditioned Isolute^{TM} SCX-2 cartridge and the product was purified by 'Catch and Release' method **(**described in the section **'Method and Materials'** of chapter 3**)**. A yellow solid was obtained after drying in vacuum. Yield=12mg, 12%.

Table 4.115: Characterisation data for compound **4.115**

4.115 Yellow solid	^{1}H NMR	^{1}HNMR(400MHz,$(CD_3)_2SO$); $^{\delta}$H in ppm 12.36(s,1H),11.63(s,1H), 11.43(s,1H), 9.95(s,1H), 9.67(s,1H), 9.18(d,*J*=2.0,1H), 8.57(d,*J*=9.8,2H), 8.47(s,1H), 8.32(s,1H), 8.09(dd,*J*=8.8,2.0,1H), 7.94(s,1H), 7.85(t,*J*=5.2,1H),7.75(d,*J*=8.8,1H),7.68-7.64(m,2H), 7.42(d,*J*=8.8,1H), 7.35(d,*J*=8.8,1H), 3.35(s,1H), 3.28(t,*J*=6.4,2H), 2.33 (t,*J*=6.4,8H), 2.11(s,3H), 1.69-1.64(m,2H).
	^{13}C NMR	($100MHz,(CD_3)_2SO$); $^{\delta}$C in ppm 164.3, 163.0, 162.3, 162.0, 141.8, 139.2, 132.9, 132.6, 128.5, 127.5, 126.6, 126.1, 125.9, 118.0, 117.4, 116.7, 116.6, 113.3, 112.8, 112.7, 112.6, 112.4, 111.1, 110.7, 105.1, 55.7, 54.7, 52.6, 45.6, 39.3, 38.7, 35.7, 30.7, 26.7, 23.2.
	EIMS	Found 661.20 $[M+H]^+$, Calculated for $C_{35}H_{35}N_9O_5$, 661.27 $[M]^+$
	HRMS	*m/z* (+EI) Calc. for $C_{35}H_{35}N_9O_5$, 661.2761 $[M]^+$, found 662.2820$[M+H]^+$.
	IR	(FTIR, V_{max}/'cm^{-1}): 3160, 1621, 1583, 1538, 1470, 1434, 1361, 1331, 1310, 1269, 1241, 1213, 1180, 1147, 1120, 1076, 1047, 1022, 997, 943, 899, 870, 789, 767, 745, 692, 621.

4.116 Synthesis of N-(3-(dimethylamino) propyl)-5-(5-(5-methoxy-1H-indole-3-carboxamido)-1H-indole-3-carboxamido)-1H-indole-3-carboxamide (4.116).

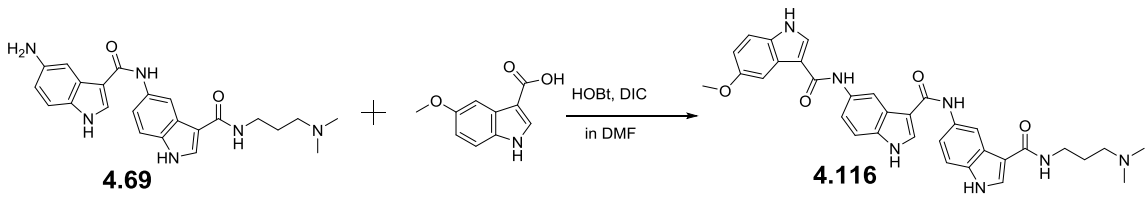

4.69 **4.116**

Initially, 40 mg of 5-methoxy-1H-indole-3-carboxylic acid (0.207 mmol, 1.2 eq.) was dissolved in 10 mL of DMF in a round bottom flask fitted with a magnetic stirrer. Then 56 µl of DIC (0.362 mmol, 1.75 eq.) and HOBt (56 mg, 0.415 mmol,

2.0 eq.) were added to the acid (1.0 eq.) and this mixture was stirred at room temperature for 30 minutes to ensure the ester formation. Then 62 mg of amine **4.69** (0.148 mmol, 1 eq.) was added and the mixture was allowed to stir for 5 hours at which point TLC and LCMS analysis showed the completion of reaction. Finally the reaction mixture was applied to a conditioned Isolute^{TM} SCX-2 cartridge and the product was purified by 'Catch and Release' method **(**described in the section **'Method and Materials'** of chapter 3**)**. A yellow solid was obtained after drying under vacuum. Yield=11mg, 13%.

Table 4.116: Characterisation data for compound **4.116**

4.116 Yellow solid	^{1}H NMR	^{1}HNMR(400MHz,$(CD_3)_2SO$); $^{\delta}$H in ppm 11.56(dd,*J*=11.6,2.8,1H), 11.42(d,*J*=2.4,1H), 9.65(d,*J*=4.0,2H), 8.58(d,*J*=2.0,1H),8.46(d,*J*=2.0,1H),8.31(t,*J*=3.2,2H),7.95(d,*J*=2.8, 1H), 7.89(t,*J*=5.6,1H), 7.79(d,*J*=2.4,1H), 7.70 (m,2H), 7.51(s,1H), 7.41-7.34(m,3H), 6.81(dd,*J*=8.8,2.4,1H), 3.27(t,*J*=6.8,2H), 2.51-2.49(m,3H), 2.30(t,*J*=6.8,2H), 2.16(s,6H), 1.69-1.64(m,2H).
	^{13}C NMR	(100MHz,$(CD_3)_2SO$); $^{\delta}$C in ppm 264.5, 163.1, 163.0, 154.3, 133.2, 133.0, 132.6, 131.0, 128.4, 127.6, 127.2, 126.6, 126.2, 126.1, 116.6, 112.5, 112.2, 111.1, 110.8, 110.6, 110.4, 102.5, 57.0, 55.1, 45.1, 39.8, 39.6, 39.4, 39.2, 39.0, 38.8, 36.8, 27.5.
	EIMS	Found 592.20 $[M+H]^+$, Calculated for $C_{33}H_{33}N_7O_4$, 591.25 $[M+H]^+$.
	HRMS	*m/z* (+EI) Calc. for $C_{33}H_{33}N_7O_4$, 591.2594 $[M]^+$, found 592.2662$[M+H]^+$.
	IR	(FTIR), V_{max}/'cm^{-1}): 3199, 2932, 1640, 1590, 1538, 1485, 1315, 1288, 1223, 1135, 1023, 1000, 956, 883, 801, 779, 759, 734.

4.117 Synthesis of 5-chloro-N-(3-((3-((3-(dimethylamino) propyl) carbamoyl)-1H-indol-5-yl) carbamoyl)-1H-indol-5-yl)-1H-indole-3-carboxamide (4.117).

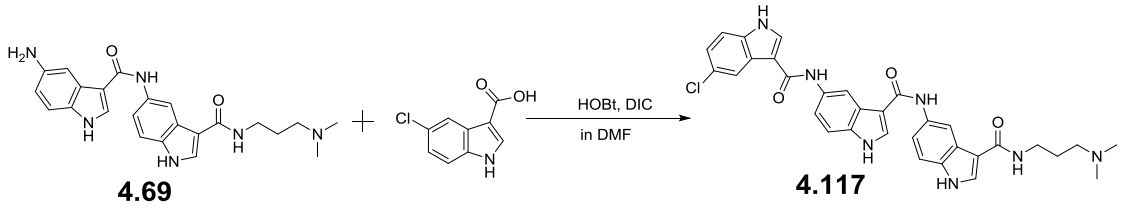

4.69 **4.117**

Initially, 58 mg of 5-chloro-1H-indole-3-carboxylic acid (0.298 mmol, 1.2 eq.) was dissolved in 10 mL of DMF in a round bottom flask fitted with a magnetic stirrer. Then 81 µl of DIC (0.521 mmol, 1.75 eq.) and HOBt (81 mg, 0.597 mmol, 2.0 eq.) were added to the acid (1.0 eq.) and this mixture was allowed to stir at room temperature for 30 minutes to ensure the esterification. Then 104 mg of amine **4.69**(0.248 mmol, 1 eq.) was added to the mixture and the mixture was allowed to stir for 4 hours at which point TLC and LCMS analysis showed the

completion of reaction. At last the reaction mixture was applied to a conditioned Isolute^{TM} SCX-2 cartridge and the product was purified by 'Catch and Release' method **(**described in the section **'Method and Materials'** of chapter 3**)**. An orange solid was obtained after drying in vacuum. Yield=22mg, 15%.

Table 4.117: Characterisation data for compound **4.117**

4.117 Orange solid	^{1}H NMR	^{1}HNMR(400MHz,$(CD_3)_2SO$); $^{\delta}$H in ppm 11.94(s,1H), 11.63(s,1H), 11.45(s,1H), 9.77(s,1H), 9.66(s,1H), 8.54(d,*J*=2.0,1H), 8.47(d,*J*=2.0,1H), 8.43(s,1H), 8.31(s,1H), 8.25(d,*J*=2.0,1H), 7.94(s,1H), 7.87(t,*J*=5.6,1H),7.71(dd,*J*=8.8,2.0,1H), 7.65(dd,*J*=8.8,2.0,1H),7.49(d,*J*=8.8,1H), 7.41(d,*J*=8.8,1H), 7.36(d,*J*=8.8,1H), 7.19(dd,*J*=8.4,2.0,1H), 3.30-3.25(m,2H), 2.27(t,*J*=7.2,2H), 2.14(s,6H), 1.70-1.63(m,2H).
	^{13}C NMR	(100MHz,$(CD_3)_2SO$);$^{\delta}$C in ppm 164.6, 162.7, 162.1, 155.7, 147.5, 134.8, 133.1, 132.8, 132.7, 129.6, 127.7, 127.4, 126.5, 125.2, 123.2, 121.9, 120.4, 119.7, 116.7, 111.1, 110.8, 110.4, 106.0, 45.2, 39.8, 39.6, 39.4, 39.2, 38.8, 35.7, 30.7, 27.5.
	EIMS	Found 596.10 $[M+H]^+$, Calculated for $C_{32}H_{30}ClN_7O_3$, 595.20 $[M]^+$
	HRMS	*m/z* (+EI) Calc. for $C_{32}H_{30}ClN_7O_3$, 595.2092 $[M]^+$, found 596.2165 $[M+H]^+$.
	IR	(FTIR), V_{max}/'cm^{-1}): 3284, 2972, 2302, 1737, 1639, 1594, 1570, 1527, 1469, 1333, 1233, 1208, 1161, 1088, 1046, 866, 794, 761, 731.

4.118 Synthesis of N-(3-((3-((3-(dimethylamino) propyl) carbamoyl)-1H-indol-5-yl) carbamoyl)-1H-indol-5-yl)-5-nitro-1H-indazole-3-carboxamide (4.118).

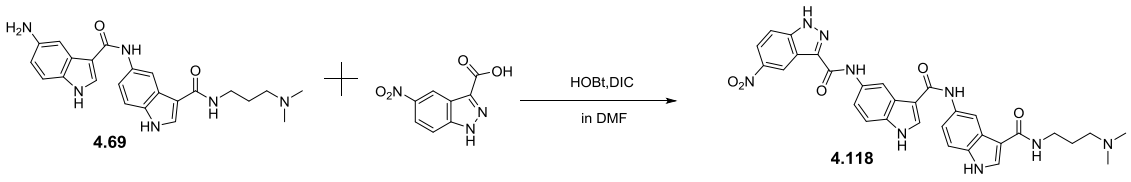

Initially, 118 mg of 5-nitro-1H-indazole-3-carboxylic acid (0.568 mmol, 1.2 eq.) was dissolved in 10 mL of DMF in a round bottom flask fitted with a magnetic stirrer. Then 153 µl of DIC (0.994 mmol, 1.75 eq.) and HOBt (153 mg, 1.136 mmol, 2.0 eq.) were added to the acid (1.0 eq.). This mixture was allowed to stir at room temperature for 30 minutes to ensure the formation of ester from the acid. Then 170 mg of amine **4.69**(0.406 mmol, 1 eq.) was added to the mixture and it was then allowed to stir for 6 hours at which point TLC and LCMS analysis showed the completion of reaction. Finally the reaction mixture was

applied to a conditioned Isolute^{TM} SCX-2 cartridge and the product was purified by 'Catch and Release' method **(**described in the section **'Method and Materials'** of chapter 3**)**. An orange solid was obtained after drying in vacuum. Yield=76mg, 31%.

Table 4.118: Characterisation data for compound **4.118**

4.118 Orange solid	^{1}H NMR	^{1}HNMR(400MHz,$(CD_3)_2SO$); $^{\delta}$H in ppm 11.69(d,*J*=2.0,1H), 11.45(d,*J*=2.0,1H), 10.45(s,1H), 9.7(s,1H), 9.16(d,*J*=3.6,1H), 8.81(d,*J*=1.6,1H), 8.48(d,*J*=1.6,1H), 8.35(d,*J*=2.8,1H), 8.27(dd,*J*=9.2,2.4,1H), 7.97(d,*J*=2.8,2H), 7.92(t,*J*=5.6,1H), 7.86(d,*J*=9.2,1H), 7.70-7.67(m,2H), 7.46(d,*J*=8.4,1H), 7.39(d,*J*=8.8,1H), 3.32-3.27 (m,2H), 2.36(t,*J*=7.2, 2H), 2.22(s,6H), 1.71-1.66(m,2H).
	^{13}C NMR	(100MHz,$(CD_3)_2SO$); $^{\delta}$C in ppm 164.6, 162.9, 162.2, 159.7, 143.4, 142.7, 141.2, 133.2, 132.9, 132.7, 131.7, 128.7, 127.7, 126.5, 126.1, 121.2, 121.0, 119.1, 117.0, 116.7, 113.7, 112.6, 112.1, 111.5, 111.1, 110.9, 110.6, 56.8, 44.9, 39.0, 36.8.
	EIMS	Found 608.20 $[M+H]^+$, Calculated for $C_{31}H_{29}N_9O_5$, 607.22 $[M]^{++}$.
	HRMS	*m/z* (+EI) Calc. for $C_{31}H_{29}N_9O_5$, 607.2292 $[M]^+$, found 608.2354 $[M+H]^+$.
	IR	(FTIR), V_{max}/'cm^{-1}): 3376, 3181, 2961, 2289, 1737, 1666, 1639, 1596, 1570, 1526, 1473, 1435, 1365, 1328, 1306, 1207, 1160, 1138, 1087, 938, 889, 855, 791, 763, 729.

4.119 Synthesis of N-(3-(dimethylamino) propyl)-5-(5-(5-nitro-1H-indole-3-carboxamido)-1H-indazole-3-carboxamido)-1H-indazole-3-carboxamide (4.119).

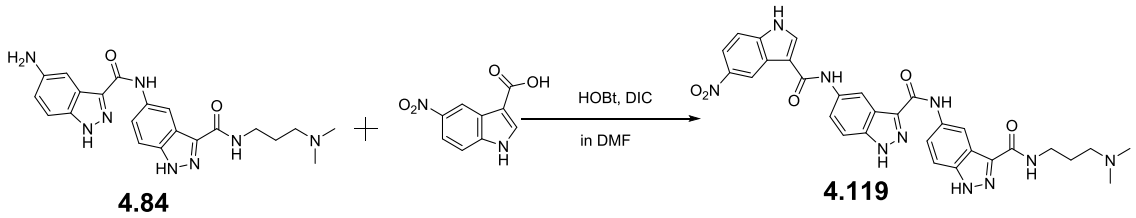

4.84 **4.119**

Initially, 36 mg of 5-nitro-1H-indole-3-carboxylic acid (0.171 mmol, 1.2 eq.) was dissolved in 10 mL of DMF in a round bottom flask fitted with a magnetic stirrer. Then 46 µl of DIC (0.299 mmol, 1.75 eq.) and HOBt (46 mg, 0.342 mmol, 2.0 eq.) were added to the acid (1.0 eq.) and this mixture was stirred at room temperature for at least 30 minutes to ensure the ester formation. Then amine **4.84**(60 mg, 0.142 mmol, 1 eq.) was added and the mixture was allowed to stir for 4 hours at which point TLC and LCMS analysis showed the completion of reaction. Finally the reaction mixture was separated by using conditioned Isolute^{TM} SCX-2 cartridge and the final product was purified by 'Catch and

Release' method **(**described in the section **'Method and Materials'** of chapter 3**)**. An orange solid was obtained after drying in vacuum. Yield=16 mg, 19%.

Table 4.119: Characterisation data for compound **4.119**

4.119 Orange solid	^{1}H NMR	^{1}HNMR(400MHz,$(CD_3)_2SO$); $^{\delta}$H in ppm 13.73(s,1H),13.50(s,1H),12.43(s,1H),10.40(s,1H),10.13(s,1H),9.18(d,*J*=2.4,1H),8.83(d,*J*=2.0,1H),8.69(d,*J*=1.6,1H),8.61(s,1H),8.42(t,*J*=5.2,1H),8.10(dd,*J*=7.2,2.0,1H),7.95(d,*J*=2.0,1H),7.94(S,1H),7.85(dd,*J*=8..8,2.0,1H),7.707.67(m,2H),7.58(d,*J*=8.8,1H),2.72(s,2H),2.37(t,*J*=7.2,2H),2.21(s,1H),1.72(t,*J*=7.2,2h).
	^{13}C NMR	(100MHz,$(CD_3)_2SO$);$^{\delta}$C in ppm 162.28,162.23,160.9,141.9,139.3,138.2,138.2,138.1,134.2,133.3,128.4,125.9,122.0,121.8,121.6,121.5,119.3,117.9,117.5,117.2,112.4,112.0,110.4,104.0,56.8,44.9,,36.8,35.7,30.7,27.0.
	EIMS	Found 609.10 $[M+H]^+$, Calculated for $C_{30}H_{28}N_{10}O_5$, 608.2244 $[M]^+$
	HRMS	*m/z* (+EI) Calc. for $C_{30}H_{28}N_{10}O_5$, 608.2244 $[M]^+$, found 609.2318$[M+H]^+$.
	IR	(FTIR, V_{max}/'cm^{-1}): 3266, 2940, 2219, 1705, 1630, 1533, 1475, 1439, 1360, 1331, 1308, 1220, 1159, 1098, 1039, 945, 886, 807, 770, 741, 714, 619.

4.120 Synthesis of N-(3-(dimethylamino) propyl)-5-(1H-indole-3-carboxamido)-1H-indole-3-carboxamide (4.120).

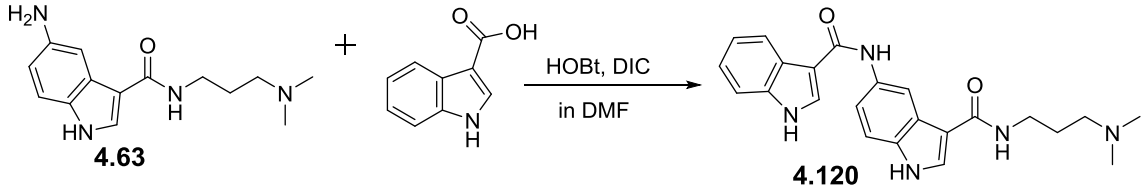

46 mg of 1H-indole-3-carboxylic acid (0.286 mmol, 1.2 eq.) was dissolved in 10 mL of DMF in a round bottom flask fitted with a magnetic stirrer. Then 77 µl of DIC (0.498 mmol, 1.75 eq.) and HOBt (77 mg, 0.572 mmol, 2.0 eq.) were added to the acid (1.0 eq.) and this mixture was allowed to stir at room temperature for 30 minutes to ensure the formation of ester from the acid. Then 62 mg of amine **4.63** (0.238 mmol, 1 eq.) was added to the mixture and the mixture was allowed to stir for 6 hours at which point TLC and LCMS analysis showed the completion of reaction. Finally the reaction mixture was applied to a conditioned Isolute^{TM} SCX-2 cartridge and the product was purified by 'Catch and Release' method **(**described in the section **'Method and Materials'** of chapter 3**)**. An orange solid was obtained after drying in vacuum. Yield=20 mg, 21%.

Table 4.120: Characterisation data for compound **4.120**

4.120 Orange solid	^{1}H NMR	^{1}HNMR(400MHz,$(CD_3)_2SO$); $^{\delta}$H in ppm 11.64(s,1H), 11.43(s,1H), 9.68(s,1H), 8.44(d,*J*=2.0,1H), 8.33(s,1H), 8.25(dd,*J*=6.8,1.2,1H), 7.96(s,1H), 7.89(d,*J*=5.6,1H), 7.64 (d,*J*=2.0,1H), 7.47(d,*J*=6.4,1H), 7.37(d,*J*=8.4,1H), 7.18-7.14(m,2H), 3.31-3.26(m,2H), 2.28(t,*J*=6.8,2H), 2.14(s,6H), 1.67(t,*J*=7.2,2H).
	^{13}C NMR	(100MHz,$(CD_3)_2SO$);$^{\delta}$C in ppm 164.5, 163.0, 136.1, 132.8, 132.7, 128.1, 127.6, 126.5, 126.1, 121.9, 121.1, 120.4, 116.8, 112.7, 111.8, 111.1, 110.8, 110.7, 57.0, 45.2, 38.8, 36.9, 27.5.
	EIMS	Found 404.10$[M+H]^+$, Calculated for $C_{23}H_{25}N_5O_2$, 403.20 $[M]^+$
	HRMS	*m/z* (+EI) Calc. for $C_{23}H_{25}N_5O_2$, 403.2008 $[M]^+$, found 404.2072 $[M+H]^+$.
	IR	(FTIR), V_{max}/'cm^{-1}): 2970, 2251, 2125, 1740, 1631, 1537, 1474, 1439, 1365, 1319, 1213, 1050, 1023, 1004, 819, 755, 619.

4.121 Synthesis of N-(3-(dimethylamino) propyl)-5-(1H-indazole-3-carboxamido)-1H-indazole-3-carboxamide (4.121).

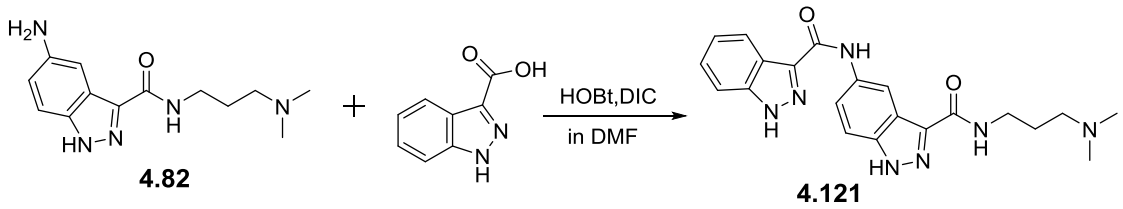

Initially, 49 mg of 1H-indazole-3-carboxylic acid (0.2988 mmol, 1.2 eq.) was dissolved in 10 mL of DMF in a round bottom flask placed in a magnetic stirrer. Then 81 µl of DIC (0.5229 mmol, 1.75 eq.) and HOBt (81 mg, 0.5976 mmol, 2.0 eq.) were added to the acid (1.0 eq.) and this mixture was allowed to stir at room temperature for at least 25 minutes for the esterification of the acid. Then amine **4.82** (65 mg, 0.249 mmol, 1 eq.) was added and the mixture was allowed to stir for 7 hours at which point TLC and LCMS analysis showed the completion of reaction. Finally the reaction mixture was separated by conditioned Isolute^{TM} SCX-2 cartridge and the product was purified by 'Catch and Release' method **(**described in the section **'Method and Materials'** of chapter 3**)**. An orange solid was collected after drying in vacuum. Yield=55mg, 54%.

Table 4.121: Characterisation data for compound **4.121**

4.121 Orange solid	^{1}H NMR	^{1}HNMR(400MHz,$(CD_3)_2SO$); $^{\delta}$H in ppm 13.61(s,2H),10.43(s,1H),8.84(s,1H),8.42(t,*J*=5.6,1H),8.27(d,*J*=8.0, 1H),7.82(d,*J*=8.8,1H),7.67(d,*J*=8.4,1H),7.58(d,*J*=9.2,1H),7.45(t,*J*= 7.2,1H),7.30(t,*J*=8.0,1H),3.37-3.32(m,2H),2.27(t,*J*=7.8,2H),2.13(s,6H),1.73(s,2H).
	^{13}C NMR	(100MHz,$(CD_3)_2SO$); $^{\delta}$C in ppm 162.2,160.9,141.2,138.4,138.3,138.2,133.2,126.6,122.2,121.9,12 1.7,121.5,112.1,110.8,110.4,57.1,45.1,40.0,38.8,37.0,27.2.
	EIMS	Found 405.10 $[M+H]^+$, Calculated for $C_{21}H_{23}N_7O_2$, 405.19 $[M]^+$
	HRMS	*m/z* (+EI) Calc. for $C_{21}H_{23}N_7O_2$, 405.1913 $[M]^+$, found 406.1980 $[M+H]^+$.
	IR	(FTIR), V_{max}/'cm^{-1}): 3263, 2972, 2302, 1739, 1635, 1606, 1532, 1470, 1437, 1368, 1345, 1313, 1211, 1150, 1118, 1073, 1039, 963, 868, 810, 798, 770, 749, 734.

4.122 Synthesis of N-methyl-N-methylene-3-(5-(5-nitro-1H-benzo[d]imidazole-2-carboxamido)-1H-indazole-3-carboxamido) propan-1-aminium (4.122).

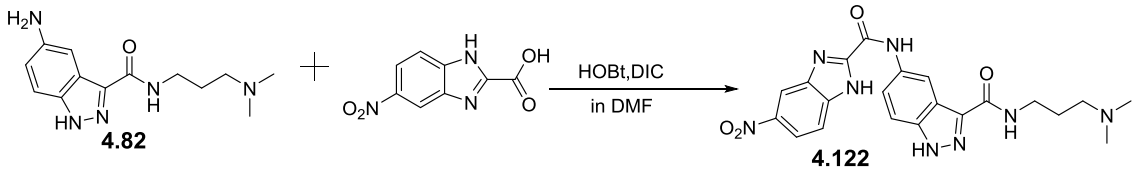

Initially, 50 mg of 5-nitro-1H-benzo[d]imidazole-2-carboxylic acid (0.24 mmol, 1.2 eq.) was dissolved in 10 mL of DMF in a round bottom flask fitted with a magnetic stirrer. Then 65 µl of DIC (0.42 mmol, 1.75 eq.) and HOBt (65 mg, 0.48 mmol, 2.0 eq.) were added to the acid (1.0 eq.) and this mixture was allowed to stir at room temperature for 30 minutes to ensure the formation of ester from the acid. Then 52 mg of amine **4.82** (0.20 mmol, 1 eq.) was added to the mixture and the mixture was allowed to stir for 4 hours at which point TLC and LCMS analysis showed the completion of reaction. Finally the reaction mixture was applied to a conditioned Isolute^{TM} SCX-2 cartridge and the product was purified by 'Catch and Release' method **(**described in the section **'Method and Materials'** of chapter 3**)**. An orange solid was obtained after drying under vacuum. Yield=7.25mg, 8%.

Table 4.122: Characterisation data for compound **4.122**

4.122 Orange solid	^{1}H NMR	^{1}HNMR(400MHz,$(CD_3)_2SO$); $^{\delta}$H in ppm 13.56(s,1H),11.12(s,1H),8.85(d,*J*=1.6,1H),8.56(d,*J*=2.0,1H),8.46 (t,*J*=5.6,1H),8.22(dd,*J*=8.8,2.4,1H),7.867.82(m,2H),7.62(d,*J*=9.2, 1H),3.37-3.32(m,2H),2.39(t,*J*=7.2,2H),2.23(s,7H),1.74-1.70(m,2H).
	^{13}C NMR	(100MHz,$(CD_3)_2SO$); $^{\delta}$C in ppm 163.2,162.1,156.8,150.8,143.2,138.4,138.3,132.4,121.9,121.4,1 18.6,116.0,112.7,110.7,105.4,56.8,44.8,40.0,38.8,36.8,26.9.
	EIMS	Found 450.0$[M+H]^+$, Calculated for $C_{21}H_{22}N_8O_4$, 450.1764 $[M]^+$
	HRMS	*m/z* (+EI) Calc. for $C_{21}H_{22}N_8O_4$, 450.1764 $[M]^+$, found 451.1835$[M+H]^+$.
	IR	(FTIR), V_{max}/'cm^{-1}): 3376, 3199, 2923, 1656, 1637, 1597, 1530, 1480, 1334, 1317, 1294, 1250, 1223, 1152, 1099, 1087, 1042, 993, 923, 891, 856, 841, 814, 792, 765, 739.

References:

[1] Gisele M. Hodges, C. R. (1994) *Developmental Biology and Cancer*, CRC Press Inc., United States of America.

[2] Schroeder, A., Jacks, T., and Anderson, D. G. (2012) Treating metastatic cancer with nanotechnology, *Nature Reviews Cancer 12*, 39-50.

[3] Hejmadi, M. (2010) *Introduction to Cancer Biology*, Ventus Publishing.

[4] Luo, J., Solimini, N. L., and Elledge, S. J. (2009) Principles of Cancer Therapy: Oncogene and Non-oncogene Addiction, *Cell 136*, 823-837.

[5] Alberts B, J. A., Lewis J (2002) *Molecular Biology of the Cell*, Garland Science, New York.

[6] Scott-Brown's (2008) *Otorhinolaryngology: Head and Neck Surgery* Vol. 3, 7

[7] Hurley, L. H. (2002) DNA and its associated processes as targets for cancer therapy, *Nature Reviews Cancer 2*, 188-200.

[8] Kazuo Nakamoto, M. T., Gary D. Strahan (2008) *Drug-DNA Interation Sructure and Spectra*, 1 st ed., Wiley publication.

[9] Clayden, J. (2005) *Organic Chemistry*, Vol. 1, Oxford University Press, New York.

[10] Sinden, R. R. (1994) *DNA Structure and Function,*Academic Press Inc. London.

[11] Weller, R. H. D. S. G. (1998) *The Gist of Genetics Guide to learning and Review*, Vol. 1, Jones and Bartlette Publisher International, London.

[12] Gilson, E., Giraud-Panis, M.-J., Pisano, S., Bennaroch, D., Ledu, M.-H., and Pei, B. (2013) One identity or more for telomeres ?, *Frontiers in Oncology 3*.

[13] Travers, A., Muskhelishvili, Georgi. (2015) DNA structure and function, *Federation of European Biochemical Societies 282*, 2205.

[14] Dey, I., and Rath, P. C. (2005) A novel rat genomic simple repeat DNA with RNA-homology shows triplex (H-DNA)-like structure and tissue-specific RNA expression, *Biochemical and Biophysical Research Communications 327*, 276-286.

[15] Schoonover, M., and Kerwin, S. M. (2012) G-quadruplex DNA cleavage preference and identification of a perylene diimide G-quadruplex photocleavage agent using a rapid fluorescent assay, *Bioorganic & Medicinal Chemistry 20*, 6904-6918.

[16] Han, H., and Hurley, L. H. (2000) G-quadruplex DNA: a potential target for anti-cancer drug design, *Trends in Pharmacological Sciences 21*, 136-142.

[17] Jissy, A. K., and Datta, A. (2012) Effect of external electric field on H-bonding and pi-stacking interactions in guanine aggregates, *European Journal of Chemical Physics and Physical Chemistry 13*, 4163-4172.

[18] Burge, S., Parkinson, G. N., Hazel, P., Todd, A. K., and Neidle, S. (2006) Quadruplex DNA: sequence, topology and structure, *Nucleic Acids Research 34*, 5402-5415.

[19] Črnugelj, M., Šket, P., and Plavec, J. (2003) Small Change in a G-Rich Sequence, a Dramatic Change in Topology: New Dimeric G-Quadruplex Folding Motif with Unique Loop Orientations, *Journal of the American Chemical Society 125*, 7866-7871.

[20] Balasubramanian, S., Hurley, L. H., and Neidle, S. (2011) Targeting G-quadruplexes in gene promoters: a novel anticancer strategy?, *Nature Reviews. Drug Discovery 10*, 261-275.
[21] Patel, D. J., Phan, A. T., and Kuryavyi, V. (2007) Human telomere, oncogenic promoter and 5′-UTR G-quadruplexes: diverse higher order DNA and RNA targets for cancer therapeutics, *Nucleic Acids Research 35*, 7429-7455.
[22] Parkinson, G. N., Lee, M. P. H., and Neidle, S. (2002) Crystal structure of parallel quadruplexes from human telomeric DNA, *Nature 417*, 876-880.
[23] Pascale Hazel , G. N. P., and Stephen Neidle (2006) Topology Variation and Loop Structural Homology in Crystal and Simulated Structures of a Bimolecular DNA Quadruplex, *Journal of the American Chemical Society 128 (16)*, pp 5480–5487.
[24] Smith, F. F. W. J. (1992) Quadruplex structure of Oxytricha telomeric DNA oligonucleotides, *Nature, 356*, 164-168.
[25] Zhang, N., Gorin, A., Majumdar, A., Chernichenko, N., and Skripkin, E. (2001) V-shaped scaffold: a new architectural motif identified in an A x (G x G x G x G) pentad-containing dimeric DNA quadruplex involving stacked G(anti) x G(anti) x G(anti) x G(syn) tetrads, *Journal of Molecular Biology . 311*, 1063-1079.
[26] Burge, S., Parkinson, G. N., Hazel, P., Todd, A. K., and Neidle, S. (2006) Quadruplex DNA: sequence, topology and structure, *Nucleic Acids Research 34*, 5402-5415.
[27] Kelly, J. A., Feigon, J., and Yeates, T. O. (1996) Reconciliation of the X-ray and NMR Structures of the Thrombin-Binding Aptamer d(GGTTGGTGTGGTTGG), *Journal of Molecular Biology, 256*, 417-422.
[28] Ma, D.-L., Ma, V. P.-Y., Leung, K.-H., Zhong, H.-J., and Leung, C.-H. (2013) *Structure-Based Approaches Targeting Oncogene Promoter G-Quadruplexes*.
[29] Nambiar, M., Srivastava, M., Gopalakrishnan, V., Sankaran, S. K., and Raghavan, S. C. (2013) G-Quadruplex Structures Formed at the HOX11 Breakpoint Region Contribute to Its Fragility during t(10;14) Translocation in T-Cell Leukemia, *Molecular and Cellular Biology 33*, 4266-4281.
[30] Dong, D. W., Pereira, F., Barrett, S. P., Kolesar, J. E., Cao, K., Damas, J., Yatsunyk, L. A., Johnson, F. B., and Kaufman, B. A. (2014) Association of G-quadruplex forming sequences with human mtDNA deletion breakpoints, *BMC Genomics 15*, 677.
[31] Neidle, S. (2012) 1 - Introduction: Quadruplexes and their Biology, In *Therapeutic Applications of Quadruplex Nucleic Acids* (Neidle, S., Ed.), pp 1-20, Academic Press, Boston.
[32] Kumari, S., Bugaut, A., Huppert, J. L., and Balasubramanian, S. (2007) An RNA G-quadruplex in the 5′ UTR of the NRAS proto-oncogene modulates translation, *Nature Chemical Biology 3*, 218-221.
[33] Gonzalez, V., Guo, K., Hurley, L., and Sun, D. (2009) Identification and characterization of nucleolin as a c-myc G-quadruplex-binding protein, *The Journal of Biological Chemistry 284*, 23622-23635.
[34] Postel, E. H., Berberich, S. J., Flint, S. J., and Ferrone, C. A. (1993) Human c-myc transcription factor PuF identified as nm23-H2 nucleoside diphosphate kinase, a candidate suppressor of tumor metastasis, *Science, 261*, 478-480.
[35] Bejugam, M., Sewitz, S., Shirude, P. S., Rodriguez, R., Shahid, R., and Balasubramanian, S. (2007) Trisubstituted isoalloxazines as a new class

of G-quadruplex binding ligands: small molecule regulation of c-kit oncogene expression, *Journal of the American Chemical Society. 129*, 12926-12927.
[36] Gunaratnam, M., Reszka, A. P., Schultes, C. M., Morjani, H., Riou, J. F., and Neidle, S. (2007) Mechanism of acridine-based telomerase inhibition and telomere shortening, *Biochemical Pharmacology 74*, 679-689.
[37] Tahara, H., Shin-Ya, K., Seimiya, H., Yamada, H., Tsuruo, T., and Ide, T. (2006) G-Quadruplex stabilization by telomestatin induces TRF2 protein dissociation from telomeres and anaphase bridge formation accompanied by loss of the 3' telomeric overhang in cancer cells, *Oncogene 25*, 1955-1966.
[38] Wong, L. S. M., van der Harst, P., de Boer, R. A., Huzen, J., van Gilst, W. H., and van Veldhuisen, D. J. (2010) Aging, telomeres and heart failure, *Heart Failure Reviews 15*, 479-486.
[39] Foundation, N. (2009) Telomere Copy Protection: Nobel Goes To Scientists Who Solved How Chromosome Ends Work, *Science Daily*.
[40] Wright, J. W. S. W. E. (2000) Hayflick, his limit, and cellular ageing, *Nature Reviews Molecular Cell Biology 1*, 72-76.
[41] Gurung, S. P., Schwarz, C., Hall, J. P., Cardin, C. J., and Brazier, J. A. (2015) The importance of loop length on the stability of i-motif structures Electronic supplementary information (ESI) available: Experimental details, UV melting curves at 295 nm, and CD spectra at pH 5 and 8. See DOI: 10.1039/c4cc07279k Click here for additional data file, *Chemical Communications, 51*, 5630-5632.
[42] Ambrus, A., Chen, D., Dai, J., Bialis, T., Jones, R. A., and Yang, D. (2006) Human telomeric sequence forms a hybrid-type intramolecular G-quadruplex structure with mixed parallel/antiparallel strands in potassium solution, *Nucleic Acids Research 34*, 2723-2735.
[43] de Lange, T. (2005) Shelterin: the protein complex that shapes and safeguards human telomeres, *Genes & Development 19*, 2100-2110.
[44] Phan, A. T., and Mergny, J. L. (2002) Human telomeric DNA: G-quadruplex, i-motif and Watson-Crick double helix, *Nucleic Acids Research 30*, 4618-4625.
[45] Ambrus, A., Chen, D., Dai, J., Jones, R. A., and Yang, D. (2005) Solution structure of the biologically relevant G-quadruplex element in the human c-MYC promoter. Implications for G-quadruplex stabilization, *Biochemistry 44*, 2048-2058.
[46] Smithfeigon, F. W. J. (1992) Quadruplex structure of Oxytricha telomeric DNA oligonucleotides, *Nature 356*, 164 - 168.
[47] Horvath, M. P., and Schultz, S. C. (2001) DNA G-quartets in a 1.86 Å resolution structure of an Oxytricha nova telomeric protein-DNA complex, *Journal of Molecular Biology 310*, 367-377.
[48] Biffi, G., Tannahill, D., McCafferty, J., and Balasubramanian, S. (2013) Quantitative visualization of DNA G-quadruplex structures in human cells, *Nature Chemistry 5*, 182-186.
[49] Henderson, A., Wu, Y., Huang, Y. C., Chavez, E. A., Platt, J., Johnson, F. B., Brosh, R. M., Sen, D., and Lansdorp, P. M. (2014) Detection of G-quadruplex DNA in mammalian cells, *Nucleic Acids Research 42*, 860-869.
[50] Blackburn, E. H. (1991) Structure and function of telomeres, *Nature 350*, 569-573.

[51] Siddiqui-Jain, A., Grand, C. L., Bearss, D. J., and Hurley, L. H. (2002) Direct evidence for a G-quadruplex in a promoter region and its targeting with a small molecule to repress c-MYC transcription, *Proceedings of the National Academy of Sciences of the United States of America 99*, 11593-11598.
[52] Rankin, S., Reszka, A. P., Todd, A. K., Ladame, S., Balasubramanian, S., and Neidle, S. (2005) Putative DNA quadruplex formation within the human c-kit oncogene, *Journal of the American Chemical Society 127*, 10584-10589.
[53] Cogoi, S., and Xodo, L. E. (2006) G-quadruplex formation within the promoter of the KRAS proto-oncogene and its effect on transcription, *Nucleic Acids Research 34*, 2536-2549.
[54] Dai, J., Chen, D., Jones, R. A., Hurley, L. H., and Yang, D. (2006) NMR solution structure of the major G-quadruplex structure formed in the human BCL2 promoter region, *Nucleic Acids Research 34*, 5133-5144.
[55] Jiang, F., and Kim, S. H. (1991) "Soft docking": matching of molecular surface cubes, *Journal of Molecular Biology. 219*, 79-102.
[56] Biffi, G., Tannahill, D., Miller, J., Howat, W. J., and Balasubramanian, S. (2014) Elevated Levels of G-Quadruplex Formation in Human Stomach and Liver Cancer Tissues, *PLoS ONE 9*, e102711.
[57] Huppert, J. L., and Balasubramanian, S. (2007) G-quadruplexes in promoters throughout the human genome, *Nucleic Acids Research 35*, 406-413.
[58] Shankar Balasubramanian, L. H. H., and Stephen Neidle. (2011) Targeting G-quadruplexes in gene promoters: a novel anticancer strategy?, *Nature Reviews Drug Discovery 10*, 261-275.
[59] Schonhoft, J. D., Bajracharya, R., Dhakal, S., Yu, Z., Mao, H., and Basu, S. (2009) Direct experimental evidence for quadruplex-quadruplex interaction within the human ILPR, *Nucleic Acids Research 37*, 3310-3320.
[60] Zhou, W., Brand, N. J., and Ying, L. (2011) G-quadruplexes-novel mediators of gene function, *Journal of Cardiovascular Translational Research 4*, 256-270.
[61] Phan, A. T., Modi, Y. S., and Patel, D. J. (2004) Propeller-type parallel-stranded G-quadruplexes in the human c-myc promoter, *Journal of the American Chemical Society. 126*, 8710-8716.
[62] Fernando, H., Reszka, A. P., Huppert, J., Ladame, S., Rankin, S., Venkitaraman, A. R., Neidle, S., and Balasubramanian, S. (2006) A conserved quadruplex motif located in a transcription activation site of the human c-kit oncogene, *Biochemistry 45*, 7854-7860.
[63] Phan, A. T., Kuryavyi, V., Burge, S., Neidle, S., and Patel, D. J. (2007) Structure of an unprecedented G-quadruplex scaffold in the human c-kit promoter, *Journal of the American Chemical Society 129*, 4386-4392.
[64] Neidle, S. (2009) The structures of quadruplex nucleic acids and their drug complexes, *Current Opinion in Sructural Biology 19*, 239-250.
[65] Hsu, S. T., Varnai, P., Bugaut, A., Reszka, A. P., Neidle, S., and Balasubramanian, S. (2009) A G-rich sequence within the c-kit oncogene promoter forms a parallel G-quadruplex having asymmetric G-tetrad dynamics, *Journal of the American Chemical Society 131*, 13399-13409.
[66] Ashman, L. K., Cambareri, A. C., To, L. B., Levinsky, R. J., and Juttner, C. A. (1991) Expression of the YB5.B8 antigen (c-kit proto-oncogene product) in normal human bone marrow, *Blood 78*, 30-37.

[67] Ronnstrand, L. (2004) Signal transduction via the stem cell factor receptor/c-Kit, *Cellular and Molecular Life Sciences : CMLS 61*, 2535-2548.
[68] Yamamoto, K., Tojo, A., Aoki, N., and Shibuya, M. (1993) Characterization of the promoter region of the human c-kit proto-oncogene, *Japanese Journal of Cancer Research 84*, 1136-1144.
[69] Bejugam, M., Gunaratnam, M., Müller, S., Sanders, D. A., Sewitz, S., Fletcher, J. A., Neidle, S., and Balasubramanian, S. (2010) Targeting the c-Kit Promoter G-quadruplexes with 6-Substituted Indenoisoquinolines, *ACS Medicinal Chemistry Letters 1*, 306-310.
[70] De Silva, C. M., and Reid, R. (2003) Gastrointestinal stromal tumors (GIST): C-kit mutations, CD117 expression, differential diagnosis and targeted cancer therapy with Imatinib, *Pathology Oncology Research 9*, 13-19.
[71] Howard, F. B., and Miles, H. T. (1982) Poly(inosinic acid) helices: essential chelation of alkali metal ions in the axial channel, *Biochemistry 21*, 6736-6745.
[72] Hardin, C. C., Henderson, E., Watson, T., and Prosser, J. K. (1991) Monovalent cation induced structural transitions in telomeric DNAs: G-DNA folding intermediates, *Biochemistry 30*, 4460-4472.
[73] Sen, D., and Gilbert, W. (1990) A sodium-potassium switch in the formation of four-stranded G4-DNA, *Nature 344*, 410-414.
[74] Ida, R., Kwan, I. C., and Wu, G. (2007) Direct 23Na NMR observation of mixed cations residing inside a G-quadruplex channel, *Chemical Communications*, 795-797.
[75] Olsen, C. M., Gmeiner, W. H., and Marky, L. A. (2006) Unfolding of G-quadruplexes: energetic, and ion and water contributions of G-quartet stacking, *The Journal of Physical Chemistry. B 110*, 6962-6969.
[76] Mergny, J. L., De Cian, A., Ghelab, A., Sacca, B., and Lacroix, L. (2005) Kinetics of tetramolecular quadruplexes, *Nucleic Acids Research 33*, 81-94.
[77] Yan, Y. Y., Lin, J., Ou, T. M., Tan, J. H., Li, D., Gu, L. Q., and Huang, Z. S. (2010) Selective recognition of oncogene promoter G-quadruplexes by Mg2+, *Biochemical and Biophysical Research Communications 402*, 614-618.
[78] Wei, D., Parkinson, G. N., Reszka, A. P., and Neidle, S. (2012) Crystal structure of a c-kit promoter quadruplex reveals the structural role of metal ions and water molecules in maintaining loop conformation, *Nucleic Acids Research 40*, 4691-4700.
[79] Wei, D., Husby, J., and Neidle, S. (2015) Flexibility and structural conservation in a c-KIT G-quadruplex, *Nucleic Acids Research 43*, 629-644.
[80] Yip, K. W., and Reed, J. C. (2008) Bcl-2 family proteins and cancer, *Oncogene 27*, 6398-6406.
[81] Juin, P., Geneste, O., Gautier, F., Depil, S., and Campone, M. (2013) Decoding and unlocking the BCL-2 dependency of cancer cells, *Nature Reviews Cancer 13*, 455-465.
[82] Sedlak, T. W., Oltvai, Z. N., Yang, E., Wang, K., Boise, L. H., Thompson, C. B., and Korsmeyer, S. J. (1995) Multiple Bcl-2 family members demonstrate selective dimerizations with Bax, *Proceedings of the National Academy of Sciences of the United States of America 92*, 7834-7838.

[83] Raghavan, S. C., Swanson, P. C., Wu, X., Hsieh, C. L., and Lieber, M. R. (2004) A non-B-DNA structure at the Bcl-2 major breakpoint region is cleaved by the RAG complex, *Nature 428*, 88-93.

[84] Zamzami, N., Brenner, C., Marzo, I., Susin, S. A., and Kroemer, G. (1998) Subcellular and submitochondrial mode of action of Bcl-2-like oncoproteins, *Oncogene 16*, 2265-2282.

[85] Hippenstiel, S., Schmeck, B., N'Guessan, P. D., Seybold, J., Krull, M., Preissner, K., Eichel-Streiber, C. V., and Suttorp, N. (2002) Rho protein inactivation induced apoptosis of cultured human endothelial cells, *American Journal of Physiology. Lung Cellular and Molecular Physiology 283*, L830-838.

[86] Chao, D. T., and Korsmeyer, S. J. (1998) BCL-2 family: regulators of cell death, *Annual Review of Immunology 16*, 395-419.

[87] Adams, J. M., and Cory, S. (1998) The Bcl-2 protein family: arbiters of cell survival, *Science, 281*, 1322-1326.

[88] Baretton, G. B., Diebold, J., Christoforis, G., Vogt, M., Muller, C., Dopfer, K., Schneiderbanger, K., Schmidt, M., and Lohrs, U. (1996) Apoptosis and immunohistochemical bcl-2 expression in colorectal adenomas and carcinomas. Aspects of carcinogenesis and prognostic significance, *Cancer 77*, 255-264.

[89] Dai, J., Dexheimer, T. S., Chen, D., Carver, M., Ambrus, A., Jones, R. A., and Yang, D. (2006) An intramolecular G-quadruplex structure with mixed parallel/antiparallel G-strands formed in the human BCL-2 promoter region in solution, *Journal of American Chemical Society 128*, 1096-1098.

[90] Luu, K. N., Phan, A. T., Kuryavyi, V., Lacroix, L., and Patel, D. J. (2006) Structure of the human telomere in K+ solution: an intramolecular (3 + 1) G-quadruplex scaffold, *Journal of the American Chemical Society 128*, 9963-9970.

[91] Aggarwal, B. B., Kunnumakkara, A. B., Harikumar, K. B., Gupta, S. R., Tharakan, S. T., Koca, C., Dey, S., and Sung, B. (2009) Signal Transducer and Activator of Transcription-3, Inflammation, and Cancer: How Intimate Is the Relationship?, *Annals of the New York Academy of Sciences 1171*, 59-76.

[92] Siveen, K. S., Sikka, S., Surana, R., Dai, X., Zhang, J., Kumar, A. P., Tan, B. K. H., Sethi, G., and Bishayee, A. (2014) Targeting the STAT3 signaling pathway in cancer: Role of synthetic and natural inhibitors, *Biochimica et Biophysica Acta (BBA) - Reviews on Cancer 1845*, 136-154.

[93] Lin, S., Xu, M., and Yuan, G. (2012) Study of STAT3 G-quadruplex folding patterns by CD spectroscopy and molecular modeling, *Chinese Chemical Letters 23*, 329-331.

[94] Dang, C. V. (January 1999) c-Myc Target Genes Involved in Cell Growth, Apoptosis, and Metabolism, *Molecular and Cell Biology 19*, 1-11.

[95] Hurley, L. H., Von Hoff, D. D., Siddiqui-Jain, A., and Yang, D. (2006) Drug Targeting of the c-MYC Promoter to Repress Gene Expression via a G-Quadruplex Silencer Element, *Seminars in Oncology 33*, 498-512.

[96] Raymond, E., Soria, J. C., Izbicka, E., Boussin, F., Hurley, L., and Von Hoff, D. D. (2000) DNA G-quadruplexes, telomere-specific proteins and telomere-associated enzymes as potential targets for new anticancer drugs, *Investigational New Drugs 18*, 123-137.

[97] Stella Pelengaris1, M. K. A. t. a. G. E. (2002) c-MYC: more than just a matter of life and death, *Nature Reviews Cancer 2*, 764-776
[98] Juin, P., Hueber, A. O., Littlewood, T., and Evan, G. (1999) c-Myc-induced sensitization to apoptosis is mediated through cytochrome c release, *Genes & Development 13*, 1367-1381.
[99] Soucie, E. L., Annis, M. G., Sedivy, J., Filmus, J., Leber, B., Andrews, D. W., and Penn, L. Z. (2001) Myc potentiates apoptosis by stimulating Bax activity at the mitochondria, *Molecular Cell Biology. 21*, 4725-4736.
[100] Juin, P., Hunt, A., Littlewood, T., Griffiths, B., Swigart, L. B., Korsmeyer, S., and Evan, G. (2002) c-Myc functionally cooperates with Bax to induce apoptosis, *Molecular Cell Biology 22*, 6158-6169.
[101] Martinou, J.-C., and Green, D. R. (2001) Breaking the mitochondrial barrier, *Nature Review Molecular Cell Biology 2*, 63-67.
[102] Green, D. R., and Evan, G. I. (2002) A matter of life and death, *Cancer Cell 1*, 19-30.
[103] Acehan, D., Jiang, X., Morgan, D. G., Heuser, J. E., Wang, X., and Akey, C. W. (2002) Three-dimensional structure of the apoptosome: implications for assembly, procaspase-9 binding, and activation, *Molecular Cell 9*, 423-432.
[104] Zindy, F., Eischen, C. M., Randle, D. H., Kamijo, T., Cleveland, J. L., Sherr, C. J., and Roussel, M. F. (1998) Myc signaling via the ARF tumor suppressor regulates p53-dependent apoptosis and immortalization, *Genes & Development 12*, 2424-2433.
[105] Kauffmann-Zeh, A., Rodriguez-Viciana, P., Ulrich, E., Gilbert, C., Coffer, P., Downward, J., and Evan, G. (1997) Suppression of c-Myc-induced apoptosis by Ras signalling through PI(3)K and PKB, *Nature 385*, 544-548.
[106] Zha, J., Harada, H., Yang, E., Jockel, J., and Korsmeyer, S. J. (1996) Serine phosphorylation of death agonist BAD in response to survival factor results in binding to 14-3-3 not BCL-X(L), *Cell 87*, 619-628.
[107] Pelengaris, S., Khan, M., and Evan, G. (2002) c-MYC: more than just a matter of life and death, *Nature Review of Cancer 2*, 764-776.
[108] Lam, E. Y., Beraldi, D., Tannahill, D., and Balasubramanian, S. (2013) G-quadruplex structures are stable and detectable in human genomic DNA, *Nature Communications 4*, 1796.
[109] Sun, D., Thompson, B., Jenkins, T. C., Neidle, S., and Hurley, L. H. (1997) Inhibition of human telomerase by a G-quadruplex-interactive compound, *Journal of Medicinal Chemistry 40*, 2113-2116.
[110] Perry, P. J., Reszka, A. P., Wood, A. A., Read, M. A., Gowan, S. M., Dosanjh, H. S., Trent, J. O., Jenkins, T. C., Kelland, L. R., and Neidle, S. (1998) Human telomerase inhibition by regioisomeric disubstituted amidoanthracene-9,10-diones, *Journal of Medicinal Chemistry 41*, 4873-4884.
[111] Perry, P. J., and Jenkins, T. C. (2001) DNA tetraplex-binding drugs: structure-selective targeting is critical for antitumour telomerase inhibition, *Mini Reviews in Medicinal Chemistry 1*, 31-41.
[112] Missailidis, S., Stanslas, J., Modi, C., Ellis, M. J., Robins, R. A., Laughton, C. A., and Stevens, M. F. (2002) Antitumor polycyclic acridines. Part 12. Physical and biological properties of 8,13-diethyl-6-methylquino[4,3,2-kl]acridinium iodide: a lead compound in anticancer drug design, *Oncology Research 13*, 175-189.

[113] Perry, P. J., Read, M. A., Davies, R. T., Gowan, S. M., Reszka, A. P., Wood, A. A., Kelland, L. R., and Neidle, S. (1999) 2,7-Disubstituted amidofluorenone derivatives as inhibitors of human telomerase, *Journal of Medicinal Chemistry 42*, 2679-2684.

[114] C. L Grand, H. H., R. M Muñoz, S Weitman, D. D Von Hoff, L. H Hurley. (2002) The Cationic Porphyrin TMPyP4 Down-Regulates c-MYC and Human Telomerase Reverse Transcriptase Expression and Inhibits Tumor Growth in Vivo 1 This research was supported by grants from the NIH and the Arizona Disease Control Research Commission, *Molecular Cancer Therapeutics 1*, 568.

[115] Ou, T. M., Lu, Y. J., Zhang, C., Huang, Z. S., Wang, X. D., Tan, J. H., Chen, Y., Ma, D. L., Wong, K. Y., Tang, J. C., Chan, A. S., and Gu, L. Q. (2007) Stabilization of G-quadruplex DNA and down-regulation of oncogene c-myc by quindoline derivatives, *Journal of Medicinal Chemistry 50*, 1465-1474.

[116] Mallesham Bejugam, S. S., Pravin S. Shirude, Raphaël Rodriguez, Ramla Shahid, and Shankar Balasubramanian. (October 05, 2007 () Trisubstituted Isoalloxazines as a New Class of G-Quadruplex Binding Ligands: Small Molecule Regulation of c-kit Oncogene Expression, *Journal of The American Chemical Society,129 (43)*, pp 12926–12927

[117] Rahman, K. M., Tizkova, K., Reszka, A. P., Neidle, S., and Thurston, D. E. (2012) Identification of novel telomeric G-quadruplex-targeting chemical scaffolds through screening of three NCI libraries, *Bioorganic & Medicinal Chemistry Letters 22*, 3006-3010.

[118] Cuenca, F., Nanjunda, R., Wilson, W. D., and Neidle, S. (2008) Tri- and tetra-substituted naphthalene diimides as potent G-quadruplex ligands, *Bioorganic Medicinal Chemistry Letters 18*, 1668-1673.

[119] Gunaratnam, M., Green, C., Moreira, J. B., Moorhouse, A. D., Kelland, L. R., Moses, J. E., and Neidle, S. (2009) G-quadruplex compounds and cis-platin act synergistically to inhibit cancer cell growth in vitro and in vivo, *Biochemical Pharmacology 78*, 115-122.

[120] Tofani, S., Barone, D., Berardelli, M., Berno, E., Cintorino, M., Foglia, L., Ossola, P., Ronchetto, F., Toso, E., and Eandi, M. (2003) Static and ELF magnetic fields enhance the in vivo anti-tumor efficacy of cis-platin against lewis lung carcinoma, but not of cyclophosphamide against B16 melanotic melanoma, *Pharmacological Research 48*, 83-90.

[121] Read, M., Harrison, R. J., Romagnoli, B., Tanious, F. A., Gowan, S. H., Reszka, A. P., Wilson, W. D., Kelland, L. R., and Neidle, S. (2001) Structure-based design of selective and potent G quadruplex-mediated telomerase inhibitors, *Proceedings of the National Academy of Sciences of the United States of America 98*, 4844-4849.

[122] Incles, C. M., Schultes, C. M., Kempski, H., Koehler, H., Kelland, L. R., and Neidle, S. (2004) A G-quadruplex telomere targeting agent produces p16-associated senescence and chromosomal fusions in human prostate cancer cells, *Molecular Cancer Therapy 3*, 1201-1206.

[123] Burger, A. M., Moore, M. J., Double, J. A., and Neidle, S. (2005) The G-quadruplex-interactive molecule BRACO-19 inhibits tumor growth, consistent with telomere targeting and interference with telomerase function, *Cancer Research 65*, 1489-1496.

[124] Taetz, S., Baldes, C., Klotz, U., and Lehr, C. M. (2006) Biopharmaceutical characterization of the telomerase inhibitor BRACO19, *Pharmaceutical Research 23*, 1031-1037.

[125] Moore, M. J., Tanious, F. A., Wilson, W. D., and Neidle, S. (2006) Trisubstituted acridines as G-quadruplex telomere targeting agents. Effects of extensions of the 3,6- and 9-side chains on quadruplex binding, telomerase activity, and cell proliferation, *Journal of Medicinal Chemistry 49*, 582-599.

[126] Schultes, C. M., Guyen, B., Cuesta, J., and Neidle, S. (2004) Synthesis, biophysical and biological evaluation of 3,6-bis-amidoacridines with extended 9-anilino substituents as potent G-quadruplex-binding telomerase inhibitors, *Bioorganic & Medicinal Chemistry Letters 14*, 4347-4351.

[127] Fedoroff, O. Y., Salazar, M., Han, H., Chemeris, V. V., Kerwin, S. M., and Hurley, L. H. (1998) NMR-Based model of a telomerase-inhibiting compound bound to G-quadruplex DNA, *Biochemistry 37*, 12367-12374.

[128] Martins, C., Gunaratnam, M., Stuart, J., Makwana, V., Greciano, O., Reszka, A. P., Kelland, L. R., and Neidle, S. (2007) Structure-based design of benzylamino-acridine compounds as G-quadruplex DNA telomere targeting agents, *Bioorganic & Medicinal Chemistry Letters 17*, 2293-2298.

[129] Mazzitelli, C. L., Brodbelt, J. S., Kern, J. T., Rodriguez, M., and Kerwin, S. M. (2006) Evaluation of binding of perylene diimide and benzannulated perylene diimide ligands to DNA by electrospray ionization mass spectrometry, *Journal of the American Society for Mass Spectrometry 17*, 593-604.

[130] Tuesuwan, B., Kern, J. T., David, W. M., and Kerwin, S. M. (2008) Simian virus 40 large T-antigen G-quadruplex DNA helicase inhibition by G-quadruplex DNA-interactive agents, *Biochemistry 47*, 1896-1909.

[131] Rossetti, L., Franceschin, M., Bianco, A., Ortaggi, G., and Savino, M. (2002) Perylene diimides with different side chains are selective in inducing different G-quadruplex DNA structures and in inhibiting telomerase, *Bioorganic & Medicinal Chemistry Letters,12*, 2527-2533.

[132] Zagotto, G., Neidle, S., and Palumbo, M. (2008) Aminoacyl-anthraquinone conjugates as telomerase inhibitors: synthesis, biophysical and biological evaluation, *Journal of Medicinal Chemistry 51*, 5566-5574.

[133] Franceschin, M., Schultes, C., and Neidle, S. (2006) Natural and synthetic G-quadruplex interactive berberine derivatives, *Bioorganic & Medicinal Chemistry Letters 16*, 1707-1711.

[134] Shi, D. F., Wheelhouse, R. T., Sun, D., and Hurley, L. H. (2001) Quadruplex-interactive agents as telomerase inhibitors: synthesis of porphyrins and structure-activity relationship for the inhibition of telomerase, *Journal of Medicinal Chemistry 44*, 4509-4523.

[135] Fiel, R. J., Howard, J. C., Mark, E. H., and Datta Gupta, N. (1979) Interaction of DNA with a porphyrin ligand: evidence for intercalation, *Nucleic Acids Research 6*, 3093-3118.

[136] Izbicka, E., Hurley, L. H., and Von Hoff, D. D. (1999) Effects of cationic porphyrins as G-quadruplex interactive agents in human tumor cells, *Cancer Research 59*, 639-644.

[137] De Cian, A., Guittat, L., Shin-ya, K., Riou, J. F., and Mergny, J. L. (2005) Affinity and selectivity of G4 ligands measured by FRET, *Nucleic Acids Symposium Series (2004)*, 235-236.

[138] Ren, J., and Chaires, J. B. (1999) Sequence and structural selectivity of nucleic acid binding ligands, *Biochemistry 38*, 16067-16075.
[139] Monchaud, D., Allain, C., and Teulade-Fichou, M.-P. (2006) Development of a fluorescent intercalator displacement assay (G4-FID) for establishing quadruplex-DNA affinity and selectivity of putative ligands, *Bioorganic & Medicinal Chemistry Letters 16*, 4842-4845.
[140] Weisman-Shomer, P., Cohen, E., Hershco, I., Khateb, S., Wolfovitz-Barchad, O., Hurley, L. H., and Fry, M. (2003) The cationic porphyrin TMPyP4 destabilizes the tetraplex form of the fragile X syndrome expanded sequence d(CGG)n, *Nucleic Acids Research 31*, 3963-3970.
[141] Joachimi, A., Mayer, G., and Hartig, J. S. (2007) A new anticoagulant-antidote pair: control of thrombin activity by aptamers and porphyrins, *J American Chemical Soc*iety,*129*, 3036-3037.
[142] Ofer, N., Weisman-Shomer, P., Shklover, J., and Fry, M. (2009) The quadruplex r(CGG)n destabilizing cationic porphyrin TMPyP4 cooperates with hnRNPs to increase the translation efficiency of fragile X premutation mRNA, *Nucleic Acids Research 37*, 2712-2722.
[143] Guliaev, A. B., and Leontis, N. B. (1999) Cationic 5,10,15,20-tetrakis(N-methylpyridinium-4-yl)porphyrin fully intercalates at 5'-CG-3' steps of duplex DNA in solution, *Biochemistry 38*, 15425-15437.
[144] Lee, Y. A., Kim, J. O., Cho, T. S., Song, R., and Kim, S. K. (2003) Binding of meso-tetrakis(N-methylpyridium-4-yl)porphyrin to triplex oligonucleotides: evidence for the porphyrin stacking in the major groove, *Journal of American Chemical Society 125*, 8106-8107.
[145] Uno, T., Hamasaki, K., Tanigawa, M., and Shimabayashi, S. (1997) Binding of meso-Tetrakis(N-methylpyridinium-4-yl)porphyrin to Double Helical RNA and DNA.RNA Hybrids, *Inorganic Chemistry 36*, 1676-1683.
[146] Wei, C., Jia, G., Yuan, J., Feng, Z., and Li, C. (2006) A spectroscopic study on the interactions of porphyrin with G-quadruplex DNAs, *Biochemistry 45*, 6681-6691.
[147] Parkinson, G. N., Cuenca, F., and Neidle, S. (2008) Topology conservation and loop flexibility in quadruplex-drug recognition: crystal structures of inter- and intramolecular telomeric DNA quadruplex-drug complexes, *Journal of Molecular Biology 381*, 1145-1156.
[148] Izbicka, E., Hurley, L. H., Wu, R. S., and Von Hoff, D. D. (1999) Telomere-interactive agents affect proliferation rates and induce chromosomal destabilization in sea urchin embryos, *Anti-cancer Drug Design 14*, 355-365.
[149] Shalaby, T., von Bueren, A. O., Hurlimann, M. L., Fiaschetti, G., Castelletti, D., Masayuki, T., Nagasawa, K., Arcaro, A., Jelesarov, I., Shin-ya, K., and Grotzer, M. (2010) Disabling c-Myc in childhood medulloblastoma and atypical teratoid/rhabdoid tumor cells by the potent G-quadruplex interactive agent S2T1-6OTD, *Molecular Cancer Therapy 9*, 167-179.
[150] Shin-ya, K., Wierzba, K., Matsuo, K., Ohtani, T., Yamada, Y., Furihata, K., Hayakawa, Y., and Seto, H. (2001) Telomestatin, a novel telomerase inhibitor from Streptomyces anulatus, *Journal of the American Chemical Society 123*, 1262-1263.
[151] De Cian, A., Cristofari, G., Reichenbach, P., De Lemos, E., Monchaud, D., Teulade-Fichou, M. P., Shin-Ya, K., Lacroix, L., Lingner, J., and Mergny, J. L. (2007) Reevaluation of telomerase inhibition by quadruplex ligands

and their mechanisms of action, *Proceedings of the National Academy of Sciences of the United States of America 104*, 17347-17352.
[152] Kim, M. Y., Vankayalapati, H., Shin-Ya, K., Wierzba, K., and Hurley, L. H. (2002) Telomestatin, a potent telomerase inhibitor that interacts quite specifically with the human telomeric intramolecular g-quadruplex, *J Journal of the American Chemical Society 124*, 2098-2099.
[153] Nakajima, A., Tauchi, T., Sashida, G., Sumi, M., Abe, K., Yamamoto, K., Ohyashiki, J. H., and Ohyashiki, K. (2003) Telomerase inhibition enhances apoptosis in human acute leukemia cells: possibility of antitelomerase therapy, *Leukemia 17*, 560-567.
[154] Sumi, M., Ohyashiki, J. H., and Ohyashiki, K. (2004) A G-quadruplex-interactive agent, telomestatin (SOT-095), induces telomere shortening with apoptosis and enhances chemosensitivity in acute myeloid leukemia, *International Journal of Oncology 24*, 1481-1487.
[155] Doi, T., Yoshida, M., Shin-ya, K., and Takahashi, T. (2006) Total synthesis of (R)-telomestatin, *Organic Letters 8*, 4165-4167.
[156] Jantos, K., Rodriguez, R., Ladame, S., Shirude, P. S., and Balasubramanian, S. (2006) Oxazole-based peptide macrocycles: a new class of G-quadruplex binding ligands, *Journal of the American Chemical Society 128*, 13662-13663.
[157] Gabelica, V., Baker, E. S., Teulade-Fichou, M. P., De Pauw, E., and Bowers, M. T. (2007) Stabilization and structure of telomeric and c-myc region intramolecular G-quadruplexes: the role of central cations and small planar ligands, *Journal of the American Chemical Society 129*, 895-904.
[158] Minhas, G. S., Pilch, D. S., Kerrigan, J. E., LaVoie, E. J., and Rice, J. E. (2006) Synthesis and G-quadruplex stabilizing properties of a series of oxazole-containing macrocycles, *Bioorganic & Medicinal Chemistry Letters 16*, 3891-3895.
[159] Gowan, S. M., Heald, R., Stevens, M. F., and Kelland, L. R. (2001) Potent inhibition of telomerase by small-molecule pentacyclic acridines capable of interacting with G-quadruplexes, *Molecular Pharmacology 60*, 981-988.
[160] Leonetti, C., Amodei, S., D'Angelo, C., Rizzo, A., Benassi, B., Antonelli, A., Elli, R., Stevens, M. F., D'Incalci, M., Zupi, G., and Biroccio, A. (2004) Biological activity of the G-quadruplex ligand RHPS4 (3,11-difluoro-6,8,13-trimethyl-8H-quino[4,3,2-kl]acridinium methosulfate) is associated with telomere capping alteration, *Molecular Pharmacology 66*, 1138-1146.
[161] Cookson, J. C., Laughton, C. A., Stevens, M. F., and Burger, A. M. (2005) Pharmacodynamics of the G-quadruplex-stabilizing telomerase inhibitor 3,11-difluoro-6,8,13-trimethyl-8H-quino[4,3,2-kl]acridinium methosulfate (RHPS4) in vitro: activity in human tumor cells correlates with telomere length and can be enhanced, or antagonized, with cytotoxic agents, *Molecular Pharmacology 68*, 1551-1558.
[162] Salvati, E., Zupi, G., and Biroccio, A. (2007) Telomere damage induced by the G-quadruplex ligand RHPS4 has an antitumor effect, *The Journal of Clinical Investigation 117*, 3236-3247.
[163] Phatak, P., Stevens, M. F., and Burger, A. M. (2007) Telomere uncapping by the G-quadruplex ligand RHPS4 inhibits clonogenic tumour cell growth in vitro and in vivo consistent with a cancer stem cell targeting mechanism, *British Journal of Cancer 96*, 1223-1233.

[164] Folini, M., Venturini, L., Cimino-Reale, G., and Zaffaroni, N. (2011) Telomeres as targets for anticancer therapies, *Expert Opinion on Therapeutic Targets 15*, 579-593.
[165] Duchler, M. (2012) G-quadruplexes: targets and tools in anticancer drug design, *Journal of Drug Targeting 20*, 389-400.
[166] Boer, D. R., Canals, A., and Coll, M. (2009) DNA-binding drugs caught in action: the latest 3D pictures of drug-DNA complexes, *Dalton Transactions (2003)*, 399-414.
[167] Lipinski, C. A., Lombardo, F., Dominy, B. W., and Feeney, P. J. (2001) Experimental and computational approaches to estimate solubility and permeability in drug discovery and development settings, *Advanced Drug Delivery Reviews 46*, 3-26.
[168] Doak, Bradley C., Over, B., Giordanetto, F., and Kihlberg, J. (2014) Oral Druggable Space beyond the Rule of 5: Insights from Drugs and Clinical Candidates, *Chemistry & Biology 21*, 1115-1142.
[169] Lipinski, C. A., Lombardo, F., Dominy, B. W., and Feeney, P. J. (1997) Experimental and computational approaches to estimate solubility and permeability in drug discovery and development settings, *Advanced Drug Delivery Reviews 23*, 3-25.
[170] Bidzinska, J., Cimino-Reale, G., Zaffaroni, N., and Folini, M. (2013) G-quadruplex structures in the human genome as novel therapeutic targets, *Molecules (Basel, Switzerland) 18*, 12368-12395.
[171] Frank Xiaoguang Han , R. T. W., and Laurence H. Hurley (1999) Interactions of TMPyP4 and TMPyP2 with Quadruplex DNA. Structural Basis for the Differential Effects on Telomerase Inhibition, *Journal of American Chemical Society 121 (15)*, 3561–3570.
[172] Brooks, T. A., and Hurley, L. H. (2010) Targeting MYC Expression through G-Quadruplexes, *Genes & Cancer 1*, 641-649.
[173] Drygin, D., Anderes, K., and Rice, W. G. (2009) Anticancer activity of CX-3543: a direct inhibitor of rRNA biogenesis, *Cancer Research 69*, 7653-7661.
[174] Riou, J. F., Guittat, L., Mailliet, P., Laoui, A., Renou, E., Petitgenet, O., Megnin-Chanet, F., Helene, C., and Mergny, J. L. (2002) Cell senescence and telomere shortening induced by a new series of specific G-quadruplex DNA ligands, *Proceedings of the National Academy of Sciences of the United States of America 99*, 2672-2677.
[175] Gomez, D., Aouali, N., Renaud, A., Douarre, C., Shin-Ya, K., Tazi, J., Martinez, S., Trentesaux, C., Morjani, H., and Riou, J. F. (2003) Resistance to senescence induction and telomere shortening by a G-quadruplex ligand inhibitor of telomerase, *Cancer Research 63*, 6149-6153.
[176] Pennarun, G., Granotier, C., Mailliet, P., and Boussin, F. D. (2005) Apoptosis related to telomere instability and cell cycle alterations in human glioma cells treated by new highly selective G-quadruplex ligands, *Oncogene 24*, 2917-2928.
[177] Granotier, C., Dutrillaux, B., and Boussin, F. D. (2005) Preferential binding of a G-quadruplex ligand to human chromosome ends, *Nucleic Acids Research 33*, 4182-4190.
[178] De Cian, A., Delemos, E., Mergny, J. L., Teulade-Fichou, M. P., and Monchaud, D. (2007) Highly efficient G-quadruplex recognition by bisquinolinium compounds, *Journal of the American Chemical Society 129*, 1856-1857.

[179] Yang, D., and Okamoto, K. (2010) Structural insights into G-quadruplexes: towards new anticancer drugs, *Future Medicinal Chemistry 2*, 619-646.
[180] Shalaby, T., Fiaschetti, G., Nagasawa, K., Shin-ya, K., Baumgartner, M., and Grotzer, M. (2013) G-quadruplexes as potential therapeutic targets for embryonal tumors, *Molecules (Basel, Switzerland) 18*, 12500-12537.
[181] Ou, T. M., Gu, L. Q., and Huang, Z. S. (2011) Inhibition of cell proliferation by quindoline derivative (SYUIQ-05) through its preferential interaction with c-myc promoter G-quadruplex, *Journal of Medicinal Chemistry 54*, 5671-5679.
[182] Ghosh, S., and Dasgupta, D. (2015) Quadruplex forming promoter region of c-myc oncogene as a potential target for a telomerase inhibitory plant alkaloid, chelerythrine, *Biochemical and Biophysical Research communications 459*, 75-80.
[183] Blackburn, E. H., Greider, C. W., and Szostak, J. W. (2006) Telomeres and telomerase: the path from maize, Tetrahymena and yeast to human cancer and aging, *Nature Medicine 12*, 1133-1138.
[184] Liu, J. N., Deng, R., Guo, J. F., Zhou, J. M., Feng, G. K., Huang, Z. S., Gu, L. Q., Zeng, Y. X., and Zhu, X. F. (2007) Inhibition of myc promoter and telomerase activity and induction of delayed apoptosis by SYUIQ-5, a novel G-quadruplex interactive agent in leukemia cells, *Leukemia 21*, 1300-1302.
[185] Zhou, J. M., Zhu, X. F., Lu, Y. J., Deng, R., Huang, Z. S., Mei, Y. P., Wang, Y., Huang, W. L., Liu, Z. C., Gu, L. Q., and Zeng, Y. X. (2006) Senescence and telomere shortening induced by novel potent G-quadruplex interactive agents, quindoline derivatives, in human cancer cell lines, *Oncogene, 25*, 503-511.
[186] Zhou, W. J., Deng, R., Zhang, X. Y., Feng, G. K., Gu, L. Q., and Zhu, X. F. (2009) G-quadruplex ligand SYUIQ-5 induces autophagy by telomere damage and TRF2 delocalization in cancer cells, *Molecular Cancer Therapeutics*. *8*, 3203-3213.
[187] Hampel, S. M., Sidibe, A., Gunaratnam, M., Riou, J. F., and Neidle, S. (2010) Tetrasubstituted naphthalene diimide ligands with selectivity for telomeric G-quadruplexes and cancer cells, *Bioorganic & Medicinal Chemistry Letters 20*, 6459-6463.
[188] Zaug, A. J., Podell, E. R., and Cech, T. R. (2005) Human POT1 disrupts telomeric G-quadruplexes allowing telomerase extension in vitro, *Proceedings of the National Academy of Sciences of the United States of America 102*, 10864-10869.
[189] Folini, M., Pivetta, C., Zaffaroni, N., and Sissi, C. (2010) Remarkable interference with telomeric function by a G-quadruplex selective bisantrene regioisomer, *Biochemical Pharmacology 79*, 1781-1790.
[190] Franceschin, M., Bianco, A., and Biroccio, A. (2012) Aromatic core extension in the series of N-cyclic bay-substituted perylene G-quadruplex ligands: increased telomere damage, antitumor activity, and strong selectivity for neoplastic over healthy cells, *ChemMedChem*. *7*, 2144-2154.
[191] Micheli, E., D'Ambrosio, D., Franceschin, M., and Savino, M. (2009) Water soluble cationic perylene derivatives as possible telomerase inhibitors: the search for selective G-quadruplex targeting, *Mini reviews in Medicinal Chemistry 9*, 1622-1632.
[192] Huang, H. S., Huang, F. C., and Lin, J. J. (2008) Synthesis, human telomerase inhibition and anti-proliferative studies of a series of 2,7-bis-

substituted amido-anthraquinone derivatives, *Bioorganic & Medicinal Chemistry 16*, 6976-6986.
[193] Rzuczek, S. G., Pilch, D. S., Liu, A., Liu, L., LaVoie, E. J., and Rice, J. E. (2010) Macrocyclic pyridyl polyoxazoles: selective RNA and DNA G-quadruplex ligands as antitumor agents, *Journal of Medicinal Chemistry 53*, 3632-3644.
[194] Satyanarayana, M., Rice, J. E., and LaVoie, E. J. (2010) Macrocyclic hexaoxazoles: Influence of aminoalkyl substituents on RNA and DNA G-quadruplex stabilization and cytotoxicity, *Bioorganic & Medicinal Chemistry Letters 20*, 3150-3154
[195] Liu, J., Guo, L., Yin, F., Zheng, X., Chen, G., and Wang, Y. (2008) Characterization and antitumor activity of triethylene tetramine, a novel telomerase inhibitor, *Biomedicine & pharmacotherapy, 62*, 480-485.
[196] Lixia, G., Fei, Y., Jiajia, J., and Jianhui, L. (2008) Triethylene tetramine, a novel ligand of G-quadruplex, induces senescence of MCF-7 cells, *Biotechnology Letters 30*, 47-53.
[197] Orlotti, N. I., Cimino-Reale, G., Borghini, E., Pennati, M., Sissi, C., Perrone, F., Palumbo, M., Daidone, M. G., Folini, M., and Zaffaroni, N. (2012) Autophagy acts as a safeguard mechanism against G-quadruplex ligand-mediated DNA damage, *Autophagy 8*, 1185-1196.
[198] Ohnmacht, S. A., Marchetti, C., Gunaratnam, M., Besser, R. J., Haider, S. M., Di Vita, G., Lowe, H. L., Mellinas-Gomez, M., Diocou, S., Robson, M., Šponer, J., Islam, B., Barbara Pedley, R., Hartley, J. A., and Neidle, S. (2015) A G-quadruplex-binding compound showing anti-tumour activity in an in vivo model for pancreatic cancer, *Scientific Reports 5*, 11385.
[199] Hiraku, Y., Oikawa, S., and Kawanishi, S. (2002) Distamycin A, a minor groove binder, changes enediyne-induced DNA cleavage sites and enhances apoptosis, *Nucleic Acids Symposium Series 2*, 95-96.
[200] Taylor, A., Webster, K., Gustafson, T., and Kedes, L. (1997) The anti-cancer agent distamycin A displaces essential transcription factors and selectively inhibits myogenic differentiation, *Molecular Cell Biology 169*, 61-72.
[201] Cocco, M. J., Hanakahi, L. A., Huber, M. D., and Maizels, N. (2003) Specific interactions of distamycin with G-quadruplex DNA, *Nucleic Acids Research 31*, 2944-2951.
[202] Moore, M. J. B., Cuenca, F., Searcey, M., and Neidle, S. (2006) Synthesis of distamycin A polyamides targeting G-quadruplex DNA, *Organic & Biomolecular Chemistry 4*, 3479-3488.
[203] Rahman, K. M., Reszka, A. P., Gunaratnam, M., Haider, S. M., Howard, P. W., Fox, K. R., Neidle, S., and Thurston, D. E. (2009) Biaryl polyamides as a new class of DNA quadruplex-binding ligands, *Chemical Communications*, 4097-4099.
[204] Drewe, W. C., Wilson, W. D., and Neidle, S. (2008) Rational design of substituted diarylureas: a scaffold for binding to G-quadruplex motifs, *Journal of Medicinal Chemistry 51*, 7751-7767.
[205] Latt, S. A., Stetten, G., Juergens, L. A., Willard, H. F., and Scher, C. D. (1975) Recent developments in the detection of deoxyribonucleic acid synthesis by 33258 Hoechst fluorescence, *The Journal of Histochemistry and Cytochemistry,23*, 493-505.
[206] Latt, S. A., and Stetten, G. (1976) Spectral studies on 33258 Hoechst and related bisbenzimidazole dyes useful for fluorescent detection of

deoxyribonucleic acid synthesis, *The Journal of Histochemistry and Cytochemistry, 24*, 24-33.
[207] Teng, M. K., Usman, N., Frederick, C. A., and Wang, A. H. (1988) The molecular structure of the complex of Hoechst 33258 and the DNA dodecamer d(CGCGAATTCGCG), *Nucleic Acids Research 16*, 2671-2690.
[208] Satz, A. L., and Bruice, T. C. (2001) Recognition of Nine Base Pairs in the Minor Groove of DNA by a Tripyrrole Peptide−Hoechst Conjugate, *Journal of American Chemical Society 123*, 2469-2477.
[209] Tanada, M., Tsujita, S., and Sasaki, S. (2006) Design of new bidentate ligands constructed of two Hoechst 33258 units for discrimination of the length of two A3T3 binding motifs, *The Journal of Organic Chemistry 71*, 125-134.
[210] Maji, B., and Bhattacharya, S. (2013) Molecular design of synthetic benzimidazoles for the switchover of the duplex to G-quadruplex DNA recognition, *Chimia 67*, 39-43.
[211] Dash, J., Shirude, P. S., and Balasubramanian, S. (2008) G-quadruplex recognition by bis-indole carboxamides, *Chemical Communications*, 3055-3057.
[212] Masutomi, K., and Hahn, W. C. (2003) Telomerase and tumorigenesis, *Cancer Letters 194*, 163-172.
[213] Brooks, T. A., Kendrick, S., and Hurley, L. (2010) Making sense of G-quadruplex and i-motif functions in oncogene promoters, *The FEBS Journal 277*, 3459-3469.
[214] Greenberg, R. A., O'Hagan, R. C., Deng, H., Xiao, Q., Hann, S. R., Adams, R. R., Lichtsteiner, S., Chin, L., Morin, G. B., and DePinho, R. A. (1999) Telomerase reverse transcriptase gene is a direct target of c-Myc but is not functionally equivalent in cellular transformation, *Oncogene 18*, 1219-1226.
[215] Wheelhouse, R. T., Sun, D., Han, H., Han, F. X., and Hurley, L. H. (1998) Cationic porphyrins as telomerase inhibitors: the interaction of tetra-(N-methyl-4-pyridyl) porphine with quadruplex DNA, *Journal of the American Chemical Society 120*, 3261-3262.
[216] Jaumot, J., and Gargallo, R. (2012) Experimental methods for studying the interactions between G-quadruplex structures and ligands, *Current Pharmaceutical Design 18*, 1900-1916.
[217] Paramasivan, S., Rujan, I., and Bolton, P. H. (2007) Circular dichroism of quadruplex DNAs: applications to structure, cation effects and ligand binding, *Methods 43*, 324-331.
[218] Bishop, G. R., and Chaires, J. B. (2003) Characterization of DNA structures by circular dichroism, *Current Protocols in Nucleic Acid Chemistry / edited by Serge L. Beaucage, Chapter 7*, Unit 7.11.
[219] Masiero, S., Trotta, R., Pieraccini, S., De Tito, S., Perone, R., Randazzo, A., and Spada, G. P. (2010) A non-empirical chromophoric interpretation of CD spectra of DNA G-quadruplex structures, *Organic & Biomolecular Chemistry 8*, 2683-2692.
[220] Cheng, M. K., Modi, C., Cookson, J. C., Hutchinson, I., Heald, R. A., McCarroll, A. J., Missailidis, S., Tanious, F., Wilson, W. D., Mergny, J. L., Laughton, C. A., and Stevens, M. F. (2008) Antitumor polycyclic acridines. 20. Search for DNA quadruplex binding selectivity in a series of 8,13-dimethylquino[4,3,2-kl]acridinium salts: telomere-targeted agents, *Journal of Medicinal Chemistry 51*, 963-975.

[221] Salim, N. N., and Feig, A. L. (2009) Isothermal titration calorimetry of RNA, *Methods 47*, 198-205.
[222] Arora, A., and Maiti, S. (2008) Effect of loop orientation on quadruplex-TMPyP4 interaction, *The Journal of Physical Chemistry. B 112*, 8151-8159.
[223] Bailly, C., Kluza, J., Martin, C., Ellis, T., and Waring, M. J. (2005) DNase I footprinting of small molecule binding sites on DNA, *Methods in Molecular Biology (Clifton, N.J.) 288*, 319-342.
[224] Chaires, J. B., and Mergny, J. L. (2008) Targeting DNA, *Biochimie 90*, 973-975.
[225] Ragazzon, P. A., Garbett, N. C., and Chaires, J. B. (2007) Competition dialysis: a method for the study of structural selective nucleic acid binding, *Methods 42*, 173-182.
[226] Webba De Silva, M. (2007) NMR methods for studying quadruplex nucleic acids, *Methods 43*, 264-277.
[227] Rosu, F., De Pauw, E., and Gabelica, V. (2008) Electrospray mass spectrometry to study drug-nucleic acids interactions, *Biochimie 90*, 1074-1087.
[228] Beck, J. L., Colgrave, M. L., Ralph, S. F., and Sheil, M. M. (2001) Electrospray ionization mass spectrometry of oligonucleotide complexes with drugs, metals, and proteins, *Mass Spectrometry Reviews 20*, 61-87.
[229] Brodbelt, J. S. (2010) Evaluation of DNA/Ligand interactions by electrospray ionization mass spectrometry, *Annual Review of Analytical Chemistry 3*, 67-87.
[230] Yuan, G., Zhang, Q., Zhou, J., and Li, H. (2011) Mass spectrometry of G-quadruplex DNA: formation, recognition, property, conversion, and conformation, *Mass Spectrometry Reviews 30*, 1121-1142.
[231] Aslanoglu, M., and Ayne, G. (2004) Voltammetric studies of the interaction of quinacrine with DNA, *Analytical and Bioanalytical Chemistry 380*, 658-663.
[232] Palecek, E. (2002) Past, present and future of nucleic acids electrochemistry, *Talanta 56*, 809-819.
[233] Lerman, L. S. (1961) Structural considerations in the interaction of DNA and acridines, *Journal of Molecular Biology 3*, 18-30.
[234] Veal, J. M., and Rill, R. L. (1991) Noncovalent DNA binding of bis(1,10-phenanthroline)copper(I) and related compounds, *Biochemistry 30*, 1132-1140.
[235] Rachwal, P. A., and Fox, K. R. (2007) Quadruplex melting, *Methods 43*, 291-301.
[236] De Cian, A., Guittat, L., Kaiser, M., Sacca, B., Amrane, S., Bourdoncle, A., Alberti, P., Teulade-Fichou, M. P., Lacroix, L., and Mergny, J. L. (2007) Fluorescence-based melting assays for studying quadruplex ligands, *Methods 42*, 183-195.
[237] Renčiuk, D., Zhou, J., Beaurepaire, L., Guédin, A., Bourdoncle, A., and Mergny, J.-L. (2012) A FRET-based screening assay for nucleic acid ligands, *Methods 57*, 122-128.
[238] Darby, R. A., Barton, C., Brown, T., and Fox, K. R. (2002) High throughput measurement of duplex, triplex and quadruplex melting curves using molecular beacons and a LightCycler, *Nucleic Acids Research 30*, e39.
[239] De Rache, A., and Mergny, J.-L. (2015) Assessment of selectivity of G-quadruplex ligands via an optimised FRET melting assay, *Biochimie 115*, 194-202.

[240] Mergny, J. L., and Maurizot, J. C. (2001) Fluorescence resonance energy transfer as a probe for G-quartet formation by a telomeric repeat, *European Journal of Chemical Biology 2*, 124-132.
[241] Juskowiak, B. (2006) Analytical potential of the quadruplex DNA-based FRET probes, *Analytica Chimica Acta 568*, 171-180.
[242] Dacres, H., Michie, M., Anderson, A., and Trowell, S. C. (2013) Advantages of substituting bioluminescence for fluorescence in a resonance energy transfer-based periplasmic binding protein biosensor, *Biosensors and Bioelectronics 41*, 459-464.
[243] Liang, J., Tsui, V., Van Abbema, A., Bao, L., Barrett, K., Beresini, M., Berezhkovskiy, L., Blair, W. S., Chang, C., Driscoll, J., Eigenbrot, C., Ghilardi, N., Gibbons, P., Halladay, J., Johnson, A., Kohli, P. B., Lai, Y., Liimatta, M., Mantik, P., Menghrajani, K., Murray, J., Sambrone, A., Xiao, Y., Shia, S., Shin, Y., Smith, J., Sohn, S., Stanley, M., Ultsch, M., Zhang, B., Wu, L. C., and Magnuson, S. (2013) Lead identification of novel and selective TYK2 inhibitors, *European Journal of Medicinal Chemistry 67*, 175-187.
[244] Moore, G. E. (2006) Cramming more components onto integrated circuits, Reprinted from Electronics, volume 38, number 8, April 19, 1965, pp.114 ff, *IEEE Solid-State Circuits Society Newsletter 11*, 33-35.
[245] Durrant, J. D., and McCammon, J. A. (2011) Molecular Dynamics Simulations and Drug Discovery, *9*, 1-9.
[246] Pettersen, E. F., Goddard, T. D., Huang, C. C., Couch, G. S., Greenblatt, D. M., Meng, E. C., and Ferrin, T. E. (2004) UCSF Chimera--a visualization system for exploratory research and analysis, *Journal* of *Computational Chemistry 25*, 1605-1612.
[247] Berridge, M. V., Herst, P. M., and Tan, A. S. (2005) Tetrazolium dyes as tools in cell biology: new insights into their cellular reduction, *Biotechnology Annual Review 11*, 127-152.
[248] Mosmann, T. (1983) Rapid colorimetric assay for cellular growth and survival: application to proliferation and cytotoxicity assays, *Journal of Immunological Methods 65*, 55-63.